Université de Montréal

Synthesis of Constrained Tricyclic Nucleosides and the Core of Nagilactone B

par
Robert D. Giacometti

Département de chimie
Faculté des arts et des sciences

Thèse présentée à la Faculté des études supérieures et postdoctorales
en vue de l'obtention du grade de
Philosophiæ Doctor (Ph. D.) en chimie

Août 2015

Résumé

Cette thèse décrit deux thèmes principaux: 1) la conception, la synthèse, et l'évaluation biophysique des nucléosides tricycliques, et 2) la synthèse de nagilactone B, un produit naturel norditerpenoïde dilactone de la famille de produits naturels “podolactone”.

Le premier chapitre décrit la stratégie de design rationnel des nucléosides nommé “restriction conformationnelle double” basée sur les études de modélisation structurales des duplex ADN–ARN modifiés. Cette stratégie implique un blocage du cycle furanose dans une configuration de type *N*- ou *S*, et une restriction de la rotation torsionelle autour de l’angle γ. La première contrainte a été incorporée avec un pont méthylène entre l’oxygène en position 2′ et le carbone 4′ du nucléoside. Cette stratégie a été inspirée par les acides nucléiques bloqués (ou “locked nucleic acid”, LNA). La deuxième contrainte a été réalisée en ajoutant un carbocycle supplémentaire dans l'échafaud de l’acide nucléique bloqué. Les défis synthétiques de la formation des nucléotides modifiés à partir des carbohydrates sont décrits ainsi que les améliorations aux stabilités thermiques qu’ils apportent aux duplex oligonucléïques dont ils font partie.

Chapitres deux et trois décrivent le développement de deux voies synthétiques complémentaires pour la formation du noyau de nagilactone B. Ce produit naturel a des implications pour le syndrome de Hutchinson–Gilford, à cause de son habilité de jouer le rôle de modulateur de l’épissage d’ARN pré-messager de lamine A. Ce produit naturel contient sept stereocentres différents, dont deux quaternaires et deux comprenant un *syn*-1,2-diol, ainsi que des lactones à cinq ou six membres, où le cycle à six ressemble à un groupement α-pyrone. La synthèse a débuté avec la cétone de Wieland-Miescher qui a permis d’adresser les défis structurels ainsi qu’explorer les fonctionnalisations des cycles A, B et D du noyau de nagilactone B.

Mots-clés: Thérapie antisens, acides nucléiques tricycliques, acides nucléiques bloqués, LNA, restriction conformationelle, nucléosides, oligonucléotides, acides nucléiques, de la conception basée sur la structure, la stabilité thermique des duplex, nagilactone B, podolactones, cétone de Wieland–Miescher, carbomethoxylation réductrice, oxydation allylique, trioxyde de chrome, l'oxydation Rubottom.

Abstract

The present thesis comprises two major themes: 1) the design, synthesis, and biophysical evaluation of conformationally restricted tricyclic nucleosides for antisense applications, and 2) strategic approaches for synthesizing the core of nagilactone B, a norditerpenoid dilactone from the podolactone family of natural products.

Guided by structural studies of modified DNA–RNA duplexes, Chapter One focuses on a proposed *dual-conformational-restriction strategy*, in which two modes of conformational restriction are incorporated into a single nucleotide modification: 1) locking the furanose ring in an *N*- or *S*-type configuration and 2) restricting rotation around backbone torsion angle γ. The first constraint was incorporated by way of a 2′,4′-anhydro bridge that is found in the scaffold of locked nucleic acid (LNA), while the second was realized by annealing an additional carbocyclic ring to the modified nucleoside. The synthetic challenges associated with preparing these highly constrained molecules from carbohydrate-derived starting materials are described, in addition to the corresponding improvements in duplex thermal stability they provide to oligonucleotide sequences containing them.

Chapters Two and Three describe complementary approaches for the synthesis of the core of nagilactone B, a natural product with implications for Hutchinson–Gilford progeria syndrome, as a consequence of its ability to act as a modulator of splicing events leading to lamin A. This natural product contains seven stereogenic centers overall, including a *syn*-1,2-diol moiety, a γ-lactone, and a pair of quaternary stereocenters, which are complemented by the presence of an α-pyrone moiety. To address the synthesis of these structural features, the utility of the Wieland–Miescher ketone was explored with an emphasis on synthesizing rings A, B, and D of the core of nagilactone B.

Keywords: Antisense therapy, tricyclic nucleic acids, locked nucleic acids, LNA, conformational restriction, nucleosides, oligonucleotides, nucleic acids, structure-based design, duplex thermal stability, nagilactone B, podolactones, Wieland–Miescher ketone, reductive carbomethoxylation, allylic oxidation, chromium trioxide, Rubottom oxidation.

Table of Contents

List of Tables

List of Schemes

List of Figures

List of Symbols and Abbreviations

>	greater than
>>	much greater than
α	stereochemical descriptor
$[\alpha]^t_D$	specific rotation at temperature *t* and wavelength of sodium D line
Å	angstrom
AC_{50}	concentration at which compound exhibits half-maximal efficacy
Ac	acetyl
AcO	acetate
aq	aqueous
β	stereochemical descriptor
Bn	benzyl
BOM	benzyloxymethyl
BSA	bis(trimethylsilyl)acetamide
Bu	butyl
Bx	general placeholder for a nucleobase
CDI	1,1′-carbonyldiimidazole
CPTS	collidinium *p*-toluenesulfonate
CSA	camphor-10-sulfonic acid
ΔT_m	difference in melting point between oligonucleotide containing the modification of interest duplexed with a complementary strand of RNA and the corresponding RNA–RNA duplex
d	day (for experimental details)
DBN	1,5-diazabicyclo[4.3.0]-5-nonene
DBU	1,8-diazabicyclo[5.4.0]undec-7-ene
DCE	dichloroethane (e.g., 1,2-DCE = 1,2-dichloroethane)
DDQ	2,3-dichloro-5,6-dicyano-1,4-benzoquinone
DMAP	4-dimethylaminopyridine
DME	1,2-dimethoxyethane
DMF	*N*,*N*-dimethylformamide
DMI	1,3-dimethyl-2-imidazolidinone
DMP	Dess–Martin periodinane
DNA	deoxyribonucleic acid
EDC	3-(ethyliminomethyleneamino)-*N*,*N*-dimethylpropan-1-amine
ent	enantiomer of the given compound that immediately follows the descriptor
ESI	electrospray ionization
Et	ethyl
h	hour(s) (for experimental details)

HATU	1-[bis(dimethylamino)methylene]-1*H*-1,2,3-triazolo[4,5-*b*]pyridinium 3-oxid hexafluorophosphate
HMPA	hexamethylphosphoramide
***h*ν**	indicates light; *h* is Planck's constant, and ν is the photon frequency
i	iso (as in *i*-Pr)
IBX	2-iodoxybenzoic acid
IC_{50}	half maximal inhibitory concentration
KHMDS	potassium bis(trimethylsilyl)amide
LDA	lithium diisopropylamide
Lev	levulinyl (i.e., 4-oxopentanoyl)
m	meta
***m*-CPBA**	3-chloroperoxybenzoic acid
M	molar (mol dm^{-3}, mol L^{-1})
Me	methyl
min	minutes (for experimental details)
mol	mole
mol %	mole percent
MOMCl	chloromethyl methyl ether (or chloro(methoxy)methane)
MPO	4-methoxypyridine-*N*-oxide
mRNA	messenger RNA
Ms	mesyl (methylsulfonyl)
MS	molecular sieves
m/z	mass-to-charge ratio
n	normal (as in *n*-butyl or *n*-Bu)
Nap	2-naphthylmethyl
NCS	*N*-chlorosuccinimide
NMR	nuclear magnetic resonance
OAc	acetate
OTf	triflate (as in trifluoromethanesulfonate)
%	percent
p	para
PCC	pyridinium chlorochromate
PDC	pyridinium dichromate
PG	protective group
pH	negative logarithm of hydrogen ion concentration
Piv	pivaloyl
Ph	phenyl (C_6H_5)
pNB	*para*-nitrobenzoyl
PPTS	pyridinium *p*-toluenesulfonate
Pr	propyl

q	quartet (spectra)
RNA	ribonucleic acid
RNase	ribonuclease
r.t.	room temperature (refers to ambient temperature of the surroundings)
s	singlet (spectra)
s	secondary (as in *s*-Bu)
t	triplet (spectra)
t	tertiary (as in *t*-Bu)
TMS	trimethylsilyl
TBAF	tetrabutylammonium fluoride
TBAI	tetrabutylammonium iodide
TBDPS	*tert*-butyldiphenylsilyl
TBS	*tert*-butyldimethylsily
TES	triethylsilyl
Tf	trifluoromethanesulfonyl
TFAA	trifluoroacetic anhydride
THF	tetrahydrofuran
T_m	melting temperature of oligonucleotide duplex: corresponds to the temperature at which 50% of a duplex is unwound into single strands
TMS	trimethylsilyl
tosyl	4-toluenesulfonyl (also Ts)
triflate	trifluoromethanesulfonate
Ts	tosyl (also 4-toluenesulfonyl)
v/v	volume per volume
w/v	weight per volume
w/w	weight per weight
wt	weight
wt %	weight percent

"Your time is limited, so don't waste it living someone else's life. Don't be trapped by dogma – which is living with the results of other people's thinking. Don't let the noise of others' opinions drown out your own inner voice. And most important, have the courage to follow your heart and intuition, they somehow already know what you truly want to become. Everything else is secondary."

Steve Jobs, 2005
Stanford Commencement Address

Acknowledgements

Thank you Professor Hanessian for accepting me into your research group at the University of Montreal and in particular, for providing me with an opportunity to work in collaboration with *Isis Pharmaceuticals* on the nucleoside projects. It's certainly inspiring to see the longevity you've had pursuing your passion for chemistry, and in that spirit I would like to thank you for giving me a great deal of perspective on life.

Professor Houk, I am incredibly grateful for the opportunity that you provided me to work with you and your group at UCLA for four months. Your mentorship and collaborative approach to tackling challenging problems were truly inspirational. I consider myself fortunate to have worked with you on so many diverse and interesting projects, which are not described in the present document. Moreover, I am indebted to all of the wonderful people in your group, who helped a synthetic organic chemist transition to the computational chemistry world and explore the American Southwest, particularly: Colin Lam, Stephen Lopez, Ashay Patel, Jessica Grandner, Mareike Holland, Hung Pham, Buck Taylor, Ilhan Yavuz, and Raghu Ramabhadran. The time I spent at UCLA was truly too short in duration.

A big thank you to Professor Collins and Professor Wuest for the guidance you have both provided during my studies, as members of my thesis committee. Your suggestions, critiques, and overall support are very much appreciated. Professor Collins, thank you for accepting me as an honorary member of your group (if only because of Anna) – and for the delicious pulled-pork sandwiches. I appreciate the advice you offered when times were tough and for the frank, but constructive criticisms you provided throughout my time at UdeM.

I am also grateful to all the members of the department who have helped make this research possible: the NMR group (Dr. Minh Tan Phan-Viet, Dr. Cédric Malveau, Silvie Bilodeau and Antoine Hamel), the Centre for Mass Spectral Analysis (Alexandra Furtos, Karine Venne, Marie-Christine Tang, and Christophe Camy), and the machine shop (Louis Beaumont, Yves Teasdale, Jean-François Myre). A big thank you to Michel Simard, Francine Bélanger-Gariépy, and Thierry Maris for taking the time (a lot of time!) to teach me how to acquire and analyze X-ray crystallographic data, as well as allowing me to use the instruments during the weekends – I truly appreciate it.

I was extremely fortunate to receive funding from the *National Sciences and Engineering Research Council of Canada, Université de Montréal*, and the *Schmeelk Canada Foundation* to support my studies, and I am truly grateful to all three organizations for their support.

I have been fortunate to be surrounded by many wonderful colleagues throughout my studies; it would take at least another volume to describe the positive impact each of you have had on my studies and life – either directly or otherwise – and your insights have hopefully made me a better scientist/colleague/friend/person. The following list is by no means exhaustive, and I sincerely apologize in advance for anyone that I have missed. A big thank you to: Etienne Chenard, Benoît Deschênes Simard, Stéphane Dorich, Eduardo Sánchez-Larios, William Bechara, Benjamin Schroeder, Jernej Wagger, Rebecca Fransson, Bradley Merner, Martin Bueschleb, Michael Perryman, Jean-Philippe Cusson, Benoît Sicard, Oscar M. Saavedra, Juan Carlos Salinas Hernandez, Lorena Rico, Miguel Vilchis-Reyes, Helge Menz, Thomas Jennequin, Eli Stoffman, Francesco Scorzelli, Vu Linh Ly, Bin Chen, Jérémie Tessier, Gabrielle St-Pierre, Phoebe Yap, Gwendal Grelier, Mike Mulholland, Anne-Catherine Bédard, André Bessette, Augusto Hernandez, Marie-Eve Mayer, Sylvain Petit #1, Sylvain Petit #2, Dominique Brossard, Alexandre Giguere, Shashidhar Jakkepalli, Sudip Pal, Amit Kumar Chattopadhyay, Laksiri Weerasinghe, all of the external collaborators at *Isis Pharmaceuticals*, particularly Punit Seth and Michael Østergaard, and of course to Michèle U. Ammouche, for your immeasurable ability to simply all of our lives so we can focus on our studies – and the delicious lunches!

A special thank you to my wonderful family and friends outside of chemistry, who have provided unwavering support throughout these past five years – and frankly, during the preceding undergraduate years as well. I have not been present nearly as frequently as I would have liked during these times, and I cannot thank you enough for the constant encouragement, inspiration, and perspective each of you have unceasingly provided, especially in the face of the rather bizarre hours and schedules that our time together often revolved around. I look forward to thanking each of you in person during the coming months and celebrating the start of a new chapter together.

Аня, большое спасибо за всё. I remember when we embarked on this graduate school adventure together (albeit, unknowingly at the time), and I am so very glad that you are here at the end of it. You really complement me in so many different ways and I cannot thank you enough for the love, support, and optimism you have continually provided. I look forward to many more adventures together.

To my mother and sister, I have not always vocalized my appreciation as much as I could, but your constant love and encouragement has truly sustained me through these years. Without you, none of the work described in this document would have been realized by my hands. This thesis is as much yours as it is mine.

Chapter 1:

Synthesis of Highly Constrained Tricyclic Nucleosides

1.1 Introduction

The first chapter describes the design, synthesis, and biophysical evaluation of highly constrained tricyclic nucleosides, which have particular relevance to the field of antisense therapeutics, and whose study was performed in collaboration with *Isis Pharmaceuticals*. Complementary to the traditional small-molecule approach to drug design, antisense therapeutics provide a promising platform for selectively targeting ribonucleic acid (RNA) and have, within the past three decades, emerged as a legitimate approach for selectively modulating gene expression. While traditional small molecule drugs inhibit disease-causing proteins based on the shape of the protein, antisense drugs inhibit the production of proteins based on the protein's mRNA and gene sequence. A brief description of the role of nucleic acids is given below, for the purpose of providing proper context for the potential application of the tricyclic nucleosides that were studied.

1.1.1 Nucleic Acids

Nucleic acids such as deoxyribonucleic acid (DNA) and ribonucleic acid (RNA) are polymeric macromolecules that are essential for life as we know it. They are comprised of monomeric subunits termed nucleotides (*Figure 1.1*), which contain a furanose sugar moiety,

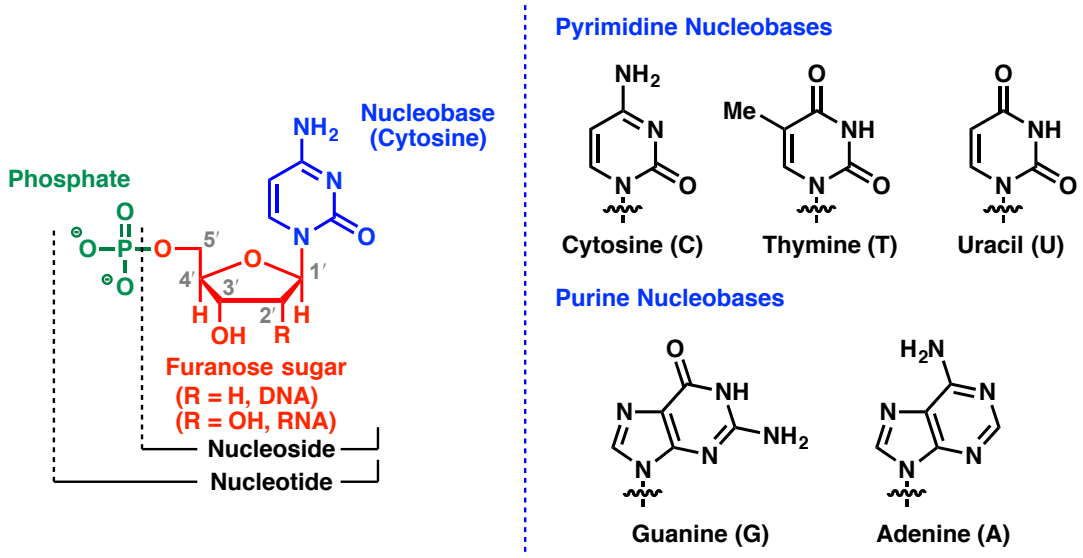

Figure 1.1 – Monomeric subunit of nucleic acids.

a phosphate group, and a nitrogenous heterocyclic base (nucleobase); devoid of the phosphate group, the subunit is referred to as a nucleoside. In the case of DNA, the pentose-derived sugar is deoxyribose, and the nucleobase is one of adenine, guanine, cytosine, or thymine, while natural RNA is comprised of a ribose-based monosaccharide and the same nucleobases, save for the substitution of thymine with its C5-demethylated analog, uracil.[1] The monomeric nucleotides in the nucleic acid scaffold are connected to one another through a phosphodiester linkage between the 3′ and 5′ position (i.e., the phosphorus atom attached to the C5′ oxygen atom is covalently bonded to the C3′ oxygen atom of the adjacent nucleotide); refer to *Figure 1.2* for an illustration.

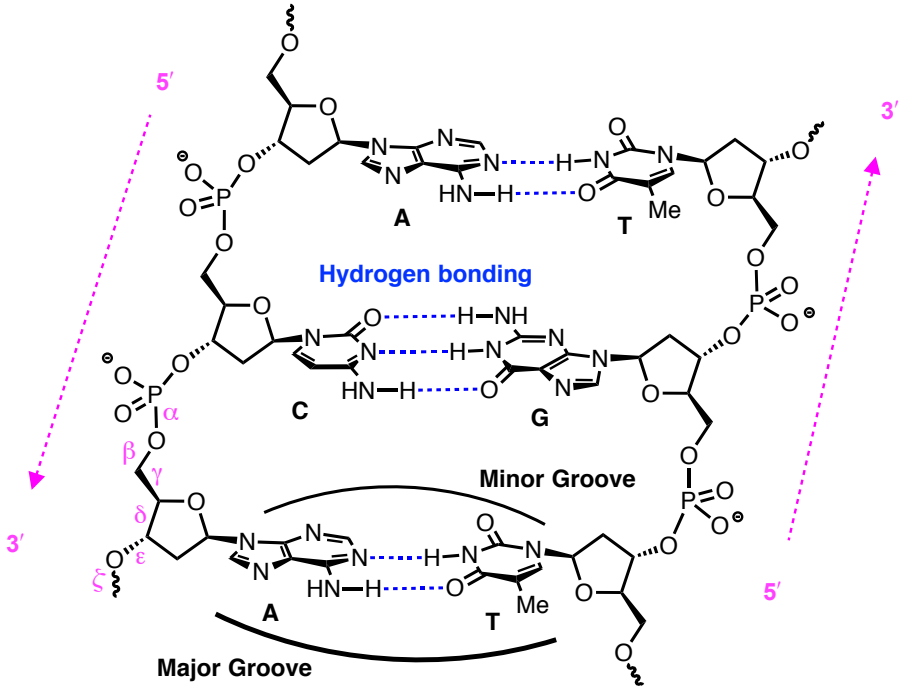

Figure 1.2 – Watson–Crick base pairing of DNA duplex.

As a consequence of the hydrogen-bonding donor and acceptor moieties present within each nucleobase, it is favourable for individual strands of DNA to pair up with one another (*Figure 1.2*). The strands are complementary and align in an antiparallel orientation, held together by a specific Watson–Crick base-paired hydrogen-bonding network*: adenine pairs with thymine and guanine pairs with cytosine, in agreement with the Chargraff group's base

* Base pairing that does not follow the Watson–Crick model is also known (i.e., Hoogstein hydrogen bonding), and the interested reader is directed elsewhere for a more thorough discussion.[2]

composition data.[3-5] Notably, guanine–cytosine pairs have three hydrogen bonds, while adenine–thymine pairs have only two, which results in extended regions of the former being more thermally stable than regions containing the latter. In addition to the antiparallel base-paired structure, the stereochemistry and conformation of the sugar moiety[6] (*Figure 1.4*, p. 5), as well as the torsional degrees of freedom along the backbone (i.e., along angles α through ζ, *Figure 1.2*) impart another structural feature – helicity.

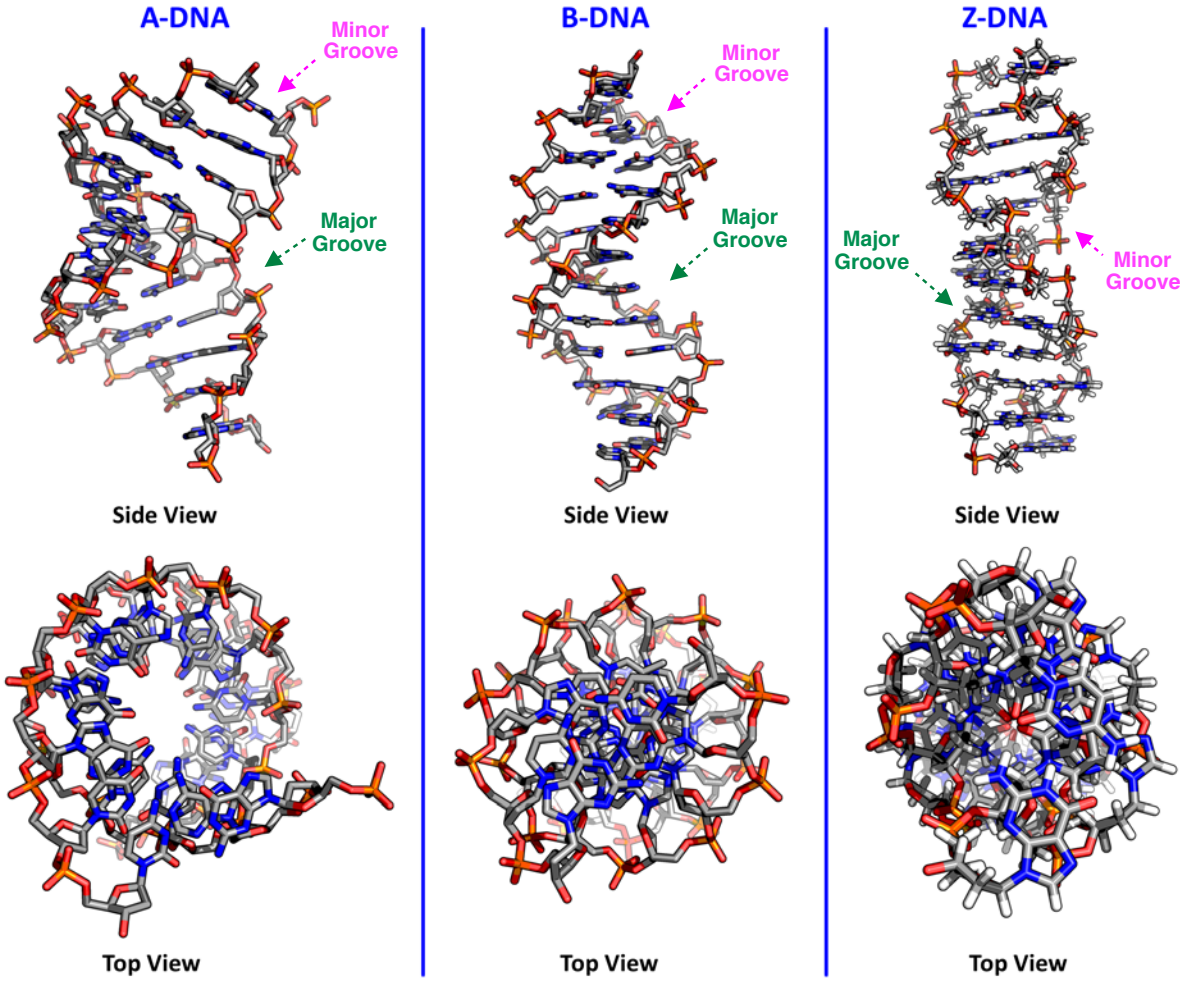

Figure 1.3 – Structures of A-, B- and Z-DNA.[7]

For DNA, three major helical structures have been observed with implications in biological processes: A-DNA, B-DNA, and Z-DNA (*Figure 1.3*).[2,8] The most commonly observed form of DNA under physiological conditions and *in vivo* is the right-handed B-DNA duplex, in which the deoxyribose sugar is found in an *S*-type sugar pucker (*Figure 1.4*) and the

base pairs are effectively perpendicular to and centered over the helical axis (top view, *Figure 1.3*). In contrast, A-type duplexes are characterized by a comparatively thicker right-handed helix, with a shorter distance between adjacent base pairs and a marked tilt and displacement of the base-pairs away from the helical axis (A-DNA, *Figure 1.4*). The A-type duplex contains a pentose sugar that is in an *N*-type sugar pucker (*Figure 1.4*), and it is commonly observed for dehydrated samples of DNA–DNA duplexes, as well as RNA–RNA and hybrid RNA–DNA duplexes. The remaining Z-DNA motif is a more significant departure from the other two motifs in that it is left-handed and is characterized by a zigzagging backbone as a consequence of the alternating sugar puckers for adjacent nucleosides; the sugar moiety of deoxyguanosine is found in an *N*-type sugar pucker, while those of thymidine, deoxycytidine, and deoxyadenosine are found in an *S*-type conformation. Furthermore, the guanine base is in a *syn*-conformation (i.e., its bulk extends over the pentose moiety rather than away from it), rather than the *anti*-conformation observed for A- and B-form nucleic acids. Z-DNA is less commonly observed in the cell, although it does occur in regions of alternating purine–pyrimidine sequences and has been observed as part of a junction within a strand of B-DNA, the so-called B-to-Z junction box, that is stabilized by Z-DNA-binding proteins.[9]

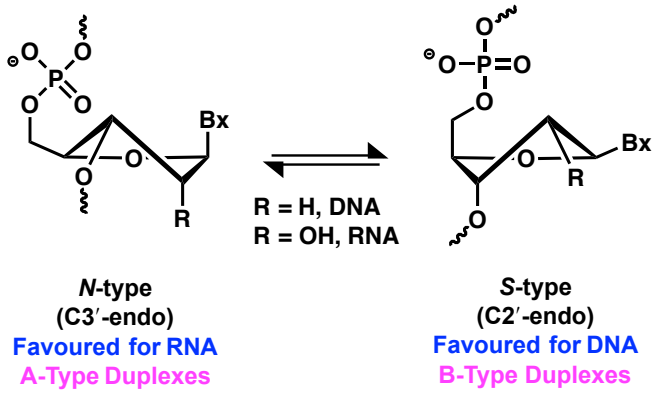

Figure 1.4 – Conformation of sugar moiety in nucleic acids.

Each duplex is also characterized by major and minor grooves that are adjacent to the base pairs and provide binding sites for proteins via hydrogen-bonding donor and acceptor motifs, as well as hydrophobic groups (i.e., methyl groups), where the latter is exclusive to the major groove.[10] Owing to the previously described conformational differences, the major groove of A-DNA is effectively deeper and narrower than the corresponding major groove of

B-DNA, while the minor groove is shallower and wider. Overall, the B-form of the duplex is considered to be universal, in the sense that it can accommodate any known sequence of naturally-occurring DNA and is stable under a broad variety of conditions.[2] Nevertheless, given that substantial variability in structural parameters (i.e., base pair tilt, rotation of helix per residue, pitch of the helix) has been observed with only mild changes to the environmental conditions, it would appear that the idealized structure of B-DNA does not represent a deep local energetic minimum.[2]

1.1.2 A Brief Overview of Protein Biosynthesis

The importance of nucleic acids, namely DNA and RNA, stems from their prominent role in encoding, transmitting, and expressing genetic information. This genetic information is used to direct the synthesis of proteins, which are macromolecular structures consisting of one or more chains of amino acid residues, that are ultimately responsible for performing a vast array of functions within living organisms, including transport, providing structural support, allowing movement, facilitating biochemical reactions as enzymes, and defending the body from antigens as antibodies. As such the collection of proteins within a cell will directly determine the function of a cell and is ultimately responsible for the overall health of an organism. Protein biosynthesis (*Figure 1.5*, p. 7) occurs through a highly-regulated sequence that may be conceptually separated into two major steps: transcription and translation. The former describes the flow of information from DNA to RNA, while the latter defines its propagation from RNA to protein. Interestingly, the movement of genetic material within biological systems follows the fundamental description put forth by Crick who stated that, *"[detailed residue-by-residue transfer of sequential] information cannot be transferred back from protein to either protein or nucleic acid."*[11,12] In other words, once the genetic information from DNA has been used to synthesize a protein, the same protein cannot be used to arrive back at DNA or RNA; this does not, however, rule out the reverse flow of information from RNA to DNA.

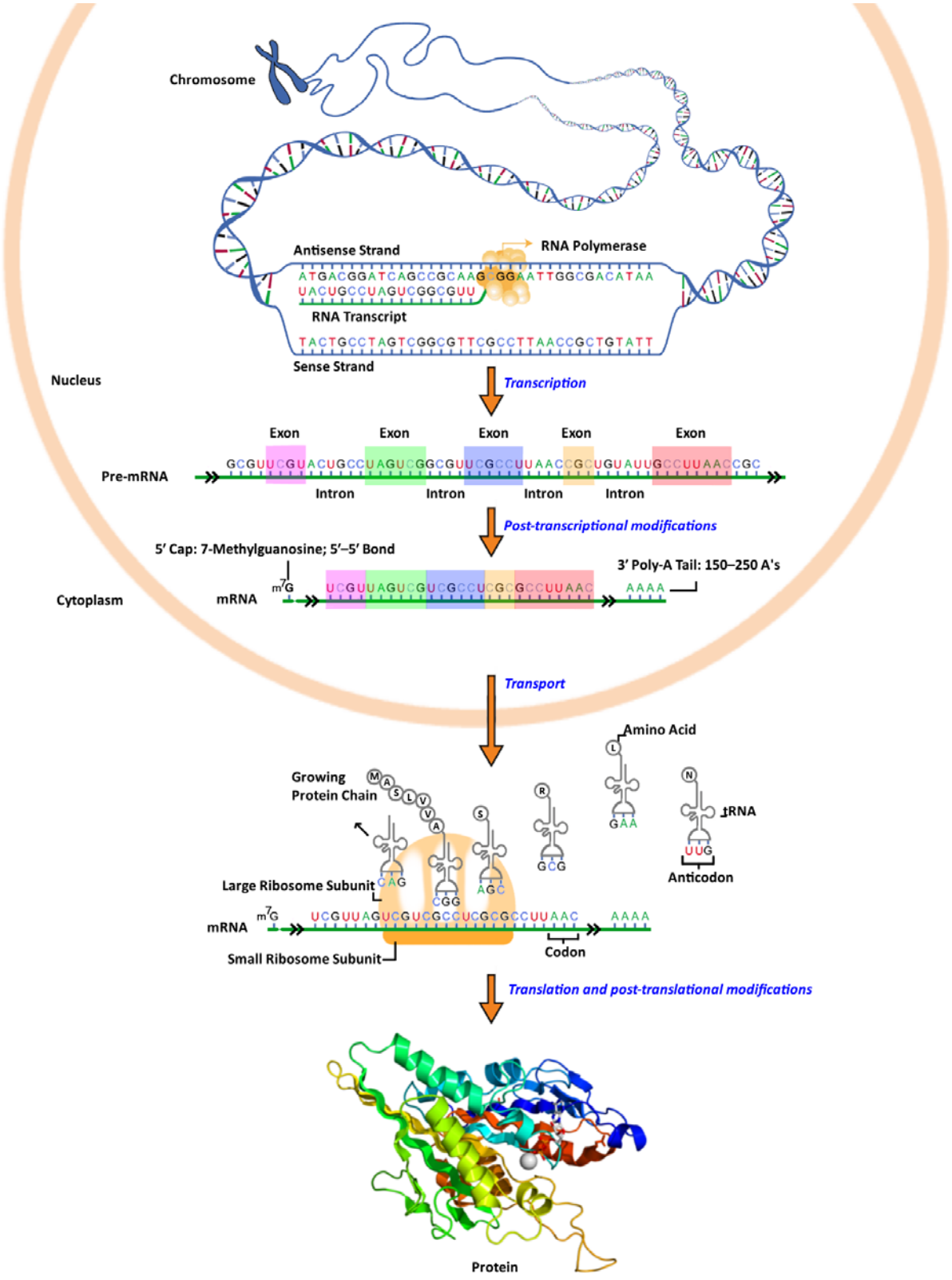

Figure 1.5 – A brief overview of protein biosynthesis.[13]

Transcription occurs in the nucleus of the cell and is mediated by a family of nucleotidyl transferase enzymes referred to as RNA polymerases (*Figure 1.5*, p. 7).[14] To initiate transcription in eukaryotic cells, well over 100 individual protein subunits must assemble in a promoter region along the DNA backbone. After initiation, the RNA polymerase is released from this large complex of proteins and moves stepwise along one strand of the unwound DNA backbone (i.e., the antisense strand) in the 5′ to 3′ direction at a pace of approximately 50 nucleotides per second.[1] As it moves along the antisense strand, RNA polymerase catalyzes the formation of phosphodiester bonds between nucleotides on the RNA transcript and incoming ribonucleotide triphosphates (i.e., ATP, CTP, UTP, and GTP).[1] Since the polymerase is only active in a segment of the gene in which the nucleobases are exposed and the helix unwound, as it moves along the DNA backbone, the RNA polymerase continues to unwind portions of the DNA double helix ahead of the polymerization active site in order to expose a new region of the template. Furthermore, the polymerase actively reforms the DNA double helix in the region behind the active site, by dynamically displacing the newly-formed RNA chain; in this way, only a small portion of a particular gene is unwound at any given time and the RNA transcript that forms is effectively single-stranded.

The RNA that forms is referred to as pre-messenger-RNA (pre-mRNA) because there are a number of post-transcriptional processing events that must occur in order to produce a mature mRNA molecule that can leave the nucleus and interact with the ribosomal machinery responsible for protein synthesis. Specifically, it is necessary to: 1) modify both ends of the pre-mRNA transcript, and 2) separate the sequence of nucleotides that codes for a protein (exons) from the intervening non-coding regions (introns) that are present. The first step is involves capping the 5′-end of the pre-mRNA transcript with a 7-methylguanosine moiety that is connected to the adjacent nucleoside through a 5′–5′ triphosphate linkage[15]; this is followed closely by polyadenylation of the 3′ end. Together, the capping and polyadenylation modifications assist the cell in discriminating between mRNA and other types of RNA, while serving as a way to verify that the mRNA produced is complete and the corresponding genetic information intact. The 5′-cap serves the additional role of assisting the cell in leaving the nucleus and plays an important role in the translation of mature mRNA into the corresponding protein.

The remaining post-transcriptional modification involves a series of splicing events, each of which effectively removes a single non-coding sequence (intron) through two sequential phosphoryl-transfer/transesterification reactions. Naturally, the process itself is significantly more intricate as a consequence of the need to effect splicing at specific sites. Accordingly, each splicing event is mediated by a RNA-protein complex (vis., the spliceosome), in which five additional RNA molecules and several hundred proteins are implicated.[16] Unlike the previously described transcription sequence, the key steps of the splicing sequence are actually performed by the RNA molecules, rather than proteins; in addition to being responsible for recognizing the sequences that specify the site of splicing, the RNA molecules also participate in the phosphoryl-transfer/transesterification reaction itself.

Following successful splicing events, the mature mRNA transcript is ready to be exported to the cytosol through nuclear pore complexes, where it may be translated into protein.[1] To ensure the mRNA has been properly processed, the cell can analyze the proteins that are bound to it, since it is expected that a characteristic presence (and corresponding absence) of certain proteins should be observed as a consequence of the sequence of processing the mRNA has gone through. The mRNA should only be released from the nucleus to the cytosol once the proteins bound to the mRNA collectively signal that transcription and the post-transcriptional modifications were successful.

To this point, the transfer of information is conceptually straightforward: since DNA and RNA are structurally and chemically similar, the former can serve as a template for the latter and direct the copying through complementary base pairing. In the case of protein synthesis, the information contained in RNA must effectively be translated into a different language, comprised of amino acids. Since there are only four unique nucleotides in mRNA and twenty different amino acids in a protein, a direct one-to-one translation of each "letter" is not possible. The rules that govern this translation are referred to as the genetic code and effectively state that the sequence of nucleotides in mRNA are read in consecutive groups of three, referred to as a codon. Each codon is recognized through the action of molecules known as transfer RNA (tRNA), which are precisely-folded single-stranded molecules of RNA, with a unique 3D structure. At one end of their scaffold, tRNA molecules can covalently bond with a single amino acid through an ester bond, while they simultaneously recognize and bond to

the nucleobases in each codon through complementary hydrogen-bonding base-pairing interactions that occur at another site (*Figure 1.2*, p. 3). Amino acids are covalently coupled to the appropriate tRNA molecule through the action of aminoacyl-tRNA synthetases, and it occurs through a two-step mechanism involving initial attachment of the amino acid and a subsequent discrimination step to ensure that the correct amino acid has been attached.

The mechanism by which amino-acid-carrying tRNA molecules link those amino acids together in a specific order to produce a protein – based on the sequence of codons in mRNA – is summarized in *Figure 1.5* (p. 7). The mRNA sequence is decoded within a well-studied structure known as the ribosome, which comprises two major subunits that are together composed of more than 50 different proteins and several strands of ribosomal RNA; there are also three major sites within the ribosome where each tRNA may be bound and specific reactions/events occur.[17-19] The small subunit provides a framework for the tRNA molecules to accurately pair with the strand of mRNA, while the large subunit catalyzes the formation of peptide bonds that link together amino acids in the forming polypeptide chain. Protein synthesis is initiated through a start codon, AUG, close to the 5′-end that codes for methionine and continues as the strand of mRNA is read in the 5′ to 3′ direction, with the individual amino acids added to the C-terminus of the growing polypeptide.[20] In general this occurs through a multistep process: 1) an incoming tRNA molecule will bind to the mRNA scaffold through hydrogen-bonding interactions with the codon, 2) the growing polypeptide is transferred to the adjacent tRNA molecule as a new peptide bond forms, and 3) the large and small ribosome subunits shift towards the 3′-end of the mRNA strand, creating space in the ribosome for another amino-acid-containing tRNA molecule, while ejecting the amino-acid-depleted tRNA molecule another from the 5′-end. This process continues until a stop codon is encountered, at which point the two ribosome subunits separate and the polypeptide chain is released. Next, the polypeptide chain must be correctly folded into its appropriate 3D conformation, bound to additional cofactors, and assembled with other protein subunits (if required).[21-25] It is only at this point that the protein is considered to be mature and functional.

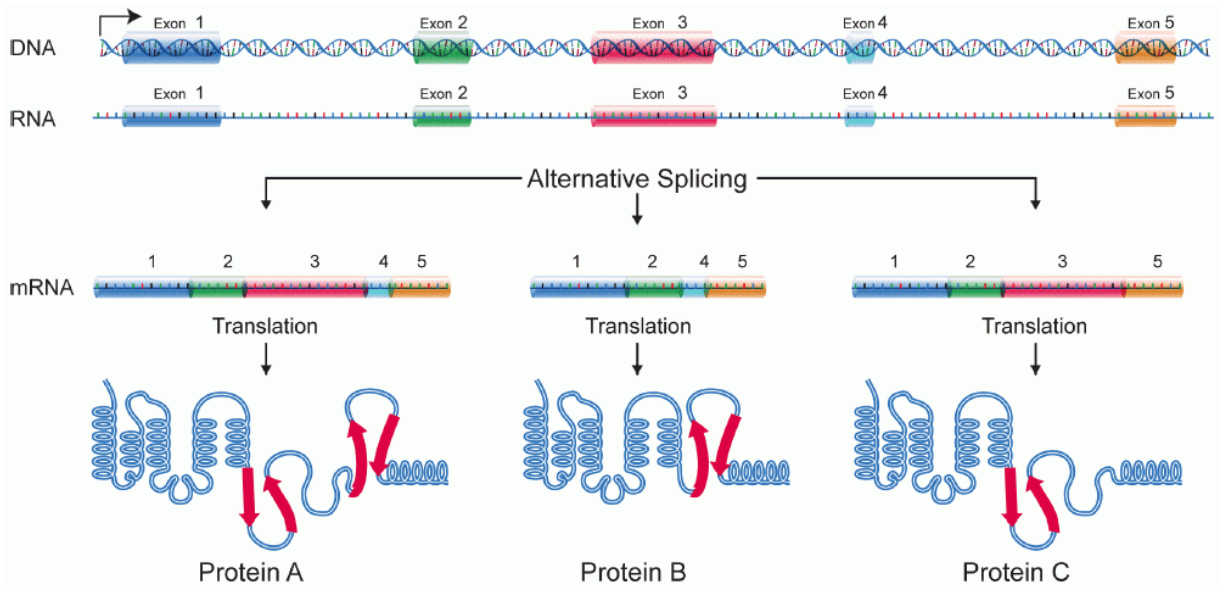

Figure 1.6 – Alternative splicing.[26]

The complexity of the biosynthetic sequence for protein synthesis is remarkable, yet despite the significant molecular machinery in place for error-checking, sometimes it does not proceed as expected. For example, aberrant splicing events (*Figure 1.6*) may lead to the production of protein isoforms that have different biological properties, particularly their ability to effect catalysis, their subcellular localization, and the protein–protein interactions they can participate in.[27] While the effects of the abnormal splicing events are difficult to predict, they become much more obvious when they lead to diseases; examples of diseases related to aberrant splicing events include spinal muscular dystrophy, Hutchinson–Gilford progeria syndrome, and Prader–Willi syndrome, amongst others.[27] Numerous studies have also shown that alternative splicing patterns are quite pervasive in cancerous cells.[28,29]

The following section describes a therapeutic approach for addressing these challenges as well as those associated with the regulation of gene expression.

1.1.3 Overview of the Antisense Approach

The pursuit of potential cures and treatments for diseases and challenges related to gene expression has frequently centered around developing small molecule therapeutics (molecular weight of less than 800 Daltons) that inhibit or increase the activity of proteins through the interactions of those small molecules with amino acid residues in binding pockets

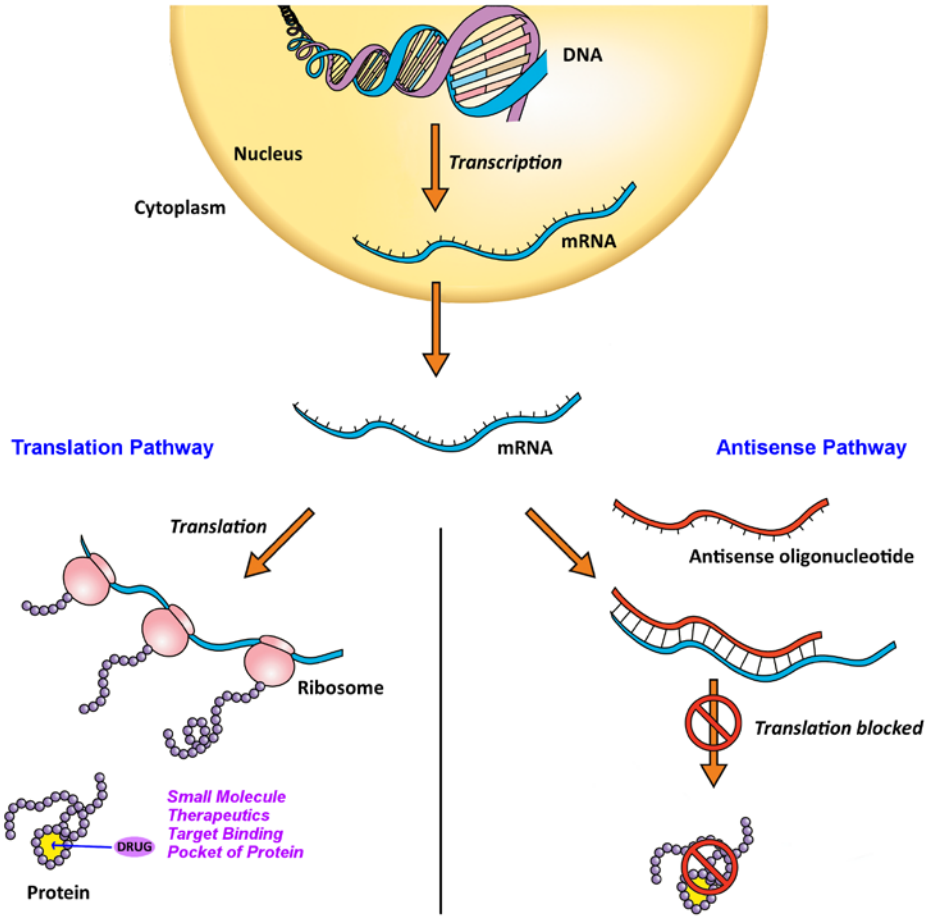

Figure 1.7 – Small molecule therapeutics versus antisense approach.[30]

of the protein; consequently, the interaction is based, at least partially, on shape complementarity with the protein (*Figure 1.7*). However, as additional information has surfaced on the biosynthetic pathways for gene expression (*Figure 1.5*, p. 7), a number of other targets began to emerge, including nucleic acids themselves. One such approach – referred to as the antisense approach* – is based on the premise that gene expression can be regulated by targeting RNA and gene sequences themselves, rather than proteins. In other words, while traditional small molecule therapeutics inhibit disease-causing proteins based on the shape of the protein, antisense therapeutics can directly inhibit the production of the protein itself by binding directly to the protein's mRNA and gene sequence through well-

* The term "antisense" is favoured since the nucleotide sequence of a particular therapeutic oligonucleotide is complementary to the corresponding target RNA; therefore it also has a sequence that is analogous to the DNA antisense strand that serves as the source code for a given protein (*Figure 1.5*, p. 7).

established Watson–Crick base-pairing interactions (*Figure 1.7*). The antisense oligonucleotides are typically 8 to >50 nucleotides in length, with an average length of 20 nucleotides, which corresponds to a molecular weight of roughly 7000 Daltons.

The appeal of the antisense approach is that there is significant potential to create gene-selective therapeutics using well-established concepts: base-pairing provides an opportunity for rational drug design based on hybridization (*Figure 1.2*, p. 3) and as our knowledge of the molecular biology of the cell increases, so too does the opportunity for rationally designing antisense oligonucleotides based on increasingly accurate models and validated RNA targets. For the purpose of modulating gene expression, RNA transcripts may be targeted by antisense oligonucleotides at many different points during protein biosynthesis; a number of examples are shown in *Figure 1.8* (p. 14). Following the binding of an antisense oligonucleotide to an RNA transcript, there are two primary mechanisms by which inhibition can occur: 1) interfere with the function of RNA, without promoting its degradation (i.e., modulation of RNA splicing, inhibition of translation or polyadenylation), or 2) promoting the degradation of RNA through endogenous enzymes (i.e., RNase H or RISC/Argonaute 2) by incorporating cleavage sequences that are directly designed into the antisense oligonucleotide. Notably, the mechanisms that result in degradation of the target RNA have been found to be more robust, particularly that of RNase H, which is a sequence-nonspecific endonuclease that cleaves RNA strands in RNA–DNA hybrids.[31]

The first explicit disclosure of a therapeutic antisense strategy that selectively targeted RNA was described in 1978 by Zamecnik and Stephenson, who demonstrated the ability of a synthesized 13-nucleotide-long oligodeoxyribonucleotide to inhibit the viral activity of Rous sarcoma virus 35S RNA, by binding to the viral RNA through complementary base-pairing.[32] At the time the synthesis itself was no small feat, and Zamecnik and Stephenson had the additional foresight to recognize the potential of this strategy for designing therapeutic agents; they proposed potential binding sites for the oligonucleotide in RNA, other targets (i.e., influenza, measles, and rabies), and even described practical approaches for stabilizing synthetic oligonucleotides through modifications to the 3′- and 5′-termini to protect against exonucleases that degrade nucleic acids.

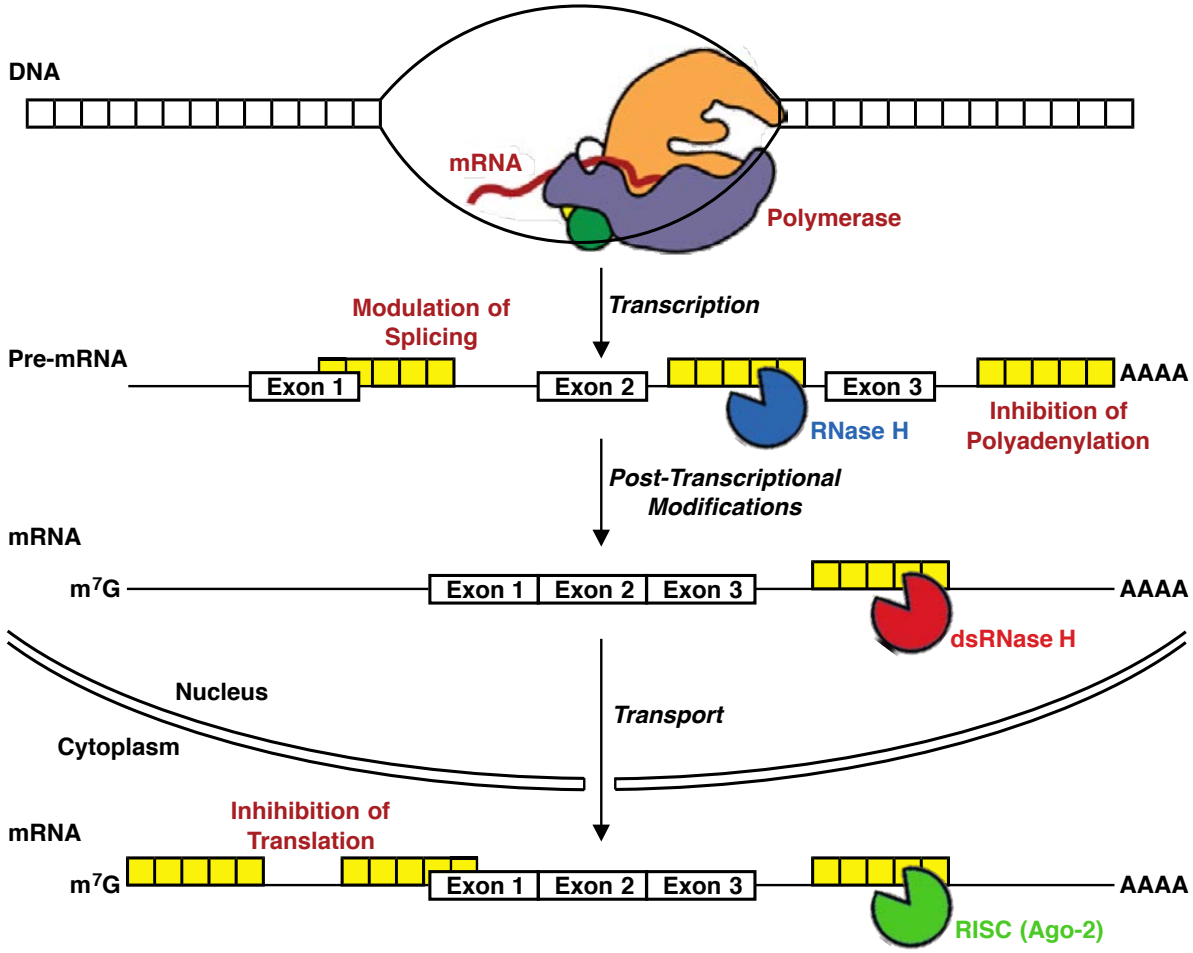

Figure 1.8 – Antisense mechanisms.[33]

Their attempts to improve the stability of oligonueotides were particularly insightful, since they further highlight one of the potential challenges associated with using antisense oligonucleotides to target RNA or DNA: unmodified RNA and DNA are inherently unstable molecules in biological systems. Despite the explicitly described potential for oligonucleotides reported by Zamecnik and Stephenson, essentially no medicinal chemistry research was performed on oligonucleotides to improve their therapeutic profile until the late 1980s. While significant strides have been made since that time, to date only two antisense drugs have been approved by the U.S. Food and Drug Administration: 1) formivirsen[34-36] for cytomegalovirus retinis (i.e., inflammation of the retina of the eye) and 2) mipomersen[37-40] for homozygous familial hypercholesterolemia (i.e., cholesterol). A brief description of modifications that have been made to oligonucleotides to improve their therapeutic potential is provided in Section 1.1.4, but it is apparent that a great deal remains to be discovered.

1.1.4 Modified Oligonucleotides

Unmodified oligonucleotides are not ideal therapeutic agents as a consequence of their instability within biological systems. In particular, they are susceptible to cleavage by ubiquitous nucleases and have rather poor pharmacokinetic properties; unmodified oligonucleotides are small enough to be filtered by the glomerulus and are only weakly bound to plasma proteins, which leads them to be rapidly filtered and excreted.[41] Furthermore, the ability of a strand of nucleic acid to discriminate between a natively complementary construct and a synthesized oligonucleotide is expected to be rather poor, since the base-pairing interactions in both cases are quite similar. Likewise, the affinity of DNA for RNA is lower than the affinity RNA has for itself,[42] which presents another challenge if one is targeting RNA using DNA-like antisense oligonucleotides to activate the robust RNase H pathway. Fortunately, the nucleic acid scaffold has a number of sites amenable to modification that can be used to improve the therapeutic profile of the antisense constructs, including the phosphodiester backbone, the nucleobase, and the sugar moiety (*Figure 1.9*, p. 16).

Thus far, the most useful modification has proven to be the substitution of a non-bridging oxygen atom in the phosphodiester backbone with a sulfur atom, forming a phosphorothioate backbone (**1.7**, *Figure 1.9*).[43] The introduction of the phosphorothioate linkage is particularly beneficial because: 1) it greatly increases the stability of the oligonucleotide to nucleolytic degradation, 2) it induces RNase H cleavage of the target RNA, and 3) it increases binding to plasma proteins, which prevents rapid excretion, while further facilitating binding to other acceptor sites.[44] Although the inclusion of the phosphorothioate linkage decreases the affinity of an antisense transcript for its intended RNA target ($\Delta T_m \approx -2$ °C/modification),[*] this drawback can be significantly attenuated by including modified nucleosides that increase the affinity of the antisense construct for its complementary strand. Overall, the benefits gained by including the phosphorothioate linkages greatly outweigh the downside, and for this reason they are generally included alongside other classes of

[*] T_m values refer to the midpoint on a curve of UV-absorption versus temperature, and are indicative of the point at which 50% of an oligonucleotide duplex has been unwound into the corresponding single strands.[45,46] The values provided in this chapter are given as the difference (ΔT_m) between DNA sequences containing the *modified* nucleotide and an analogous *unmodified* sequence of deoxyribonucleotides that serves as a control, when each is hybridized to complementary strands of DNA or RNA.

oligonucleotides in order to achieve the improved therapeutic properties required for use as a drug. Other modifications to the backbone have also been explored with varying levels of success and appeal, including boranophosphates,[47] phosphorodithioates, methylphosphonates, and phosphoramidates, amongst others.[48]

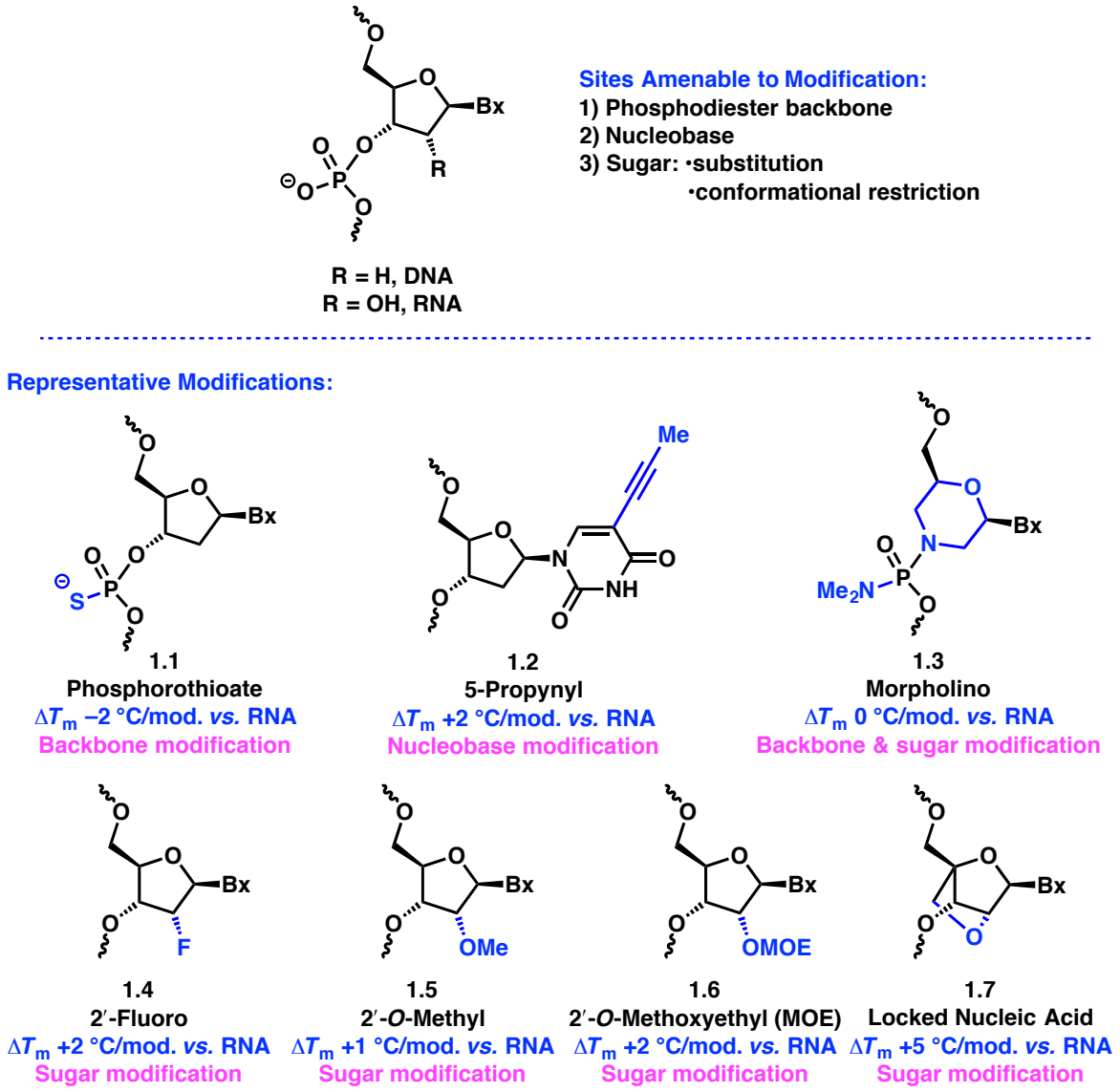

Figure 1.9 – Representative oligonucleotide modifications.

Another site that has been extensively modified within the nucleic acid scaffold is the nucleobase itself.[49,50] Typically, nucleobase modifications have focused on increasing the binding affinity for complementary nucleic acids, since the preservation of the Watson–Crick base-pairing interaction is crucial for the recognition of complementary nucleic acid targets.

Overall, as a consequence of the need to maintain comparable hydrogen bond donor–acceptor regions and accommodate the nucleobase, there are substantial restrictions on the portions of the nucleobase that may be productively modified. One prototypical example of a nucleobase modification is the inclusion of a propynyl moiety at the C5 position of the uracil (**1.2**, *Figure 1.9*), which results in an overall extension of the π-rich surface and an increase in the available hydrophobic surface.[51] This modification effects an overall increase in the stability of duplexes as a consequence of the enhancement of intrastrand stacking interactions between the nucleobases. Unfortunately, 5-propynyl-pyrimidine-containing oligodeoxynucleotides with a phosphorothioate backbone induce severe liver toxicity *in vivo*, which could not be attenuated through additional modifications.[52] Further changes to the nucleobase moiety have also been explored, including the incorporation of 5-thiazoylpyrimidines,[51] diaminopurines,[53] and phenoxazines,[54-57] but despite extensive efforts only modest progress has been made to address the ability of nucleobase modifications to support RNase H activity and to attenuate their often poor *in vivo* pharmacological profiles.

In contrast, modifications to the pentose sugar moiety of the nucleic acid scaffold have been markedly more successful overall. Interestingly, even complete substitution of the furanose sugar with a morpholine ring was found to be well-tolerated (**1.3**, *Figure 1.9*), affording scaffolds that have similar affinity to DNA–DNA duplexes and are also stable to nucleases as a consequence of the phosphoramidite bond.[58-61] The morpholino phosphoramidites do not, however, activate RNase H and are primarily used in steric blocking mechanisms (e.g., for alternative splicing or to prevent translation). Replacement of the sugar moiety with hydroxyproline or even peptides has also been explored, although many obstacles remain to be overcome for each.

By comparison, modifications to the C2′-position of the furanose ring have been much more successful than complete replacement of the sugar moiety, owing in part to the ability of substituents at that position to effectively pre-organize the pentose moiety into an *N*-type sugar pucker (*Figure 1.4*, p. 5) as a consequence of their electronegativity or steric bulk.[62] This results in an increase in binding affinity and also confers the additional benefit of nuclease resistance by virtue of the proximity of the C2′-substituent to the C3′-phosphodiester bond. Incorporating a (*R*)-configured fluorine atom at the C2′-position (**1.4,** *Figure 1.9*) favours the

N-type sugar conformation as a consequence of the electronegativity of the fluorine atom, while improving stability of the nucleoside relative to RNA. Although this modification does not activate RNase H or improve nuclease resistance beyond that displayed by DNA, the corresponding (*S*)-configured analogue was shown to activate RNase H.[63]

The incorporation of C2′-alkyl ethers (e.g., 2′-*O*-methyl **1.5** and 2′-*O*-methoxyethyl **1.6**, *Figure 1.9*) represents another group of modifications, which are particularly appealing in that they improve binding affinity, while also imparting on the corresponding antisense transcripts a substantial increase in resistance to degradation by nucleases. The 2′-*O*-methoxyethyl substitutent (**1.6**, *Figure 1.9*) is one of the most studied and oft-used of this class of modifications, and is often referred to as one of the representative modifications of second-generation antisense drugs since it is present in mipomersen; phosphorothioate linkages (**1.1**, *Figure 1.9*) exemplify the characteristic first-generation modification, and they are present in fomivirsen as well as mipomersen. Although RNase H activity is significantly attenuated for many nucleotides containing substituents at the C2′-position, a gapmer strategy can be used to address this limitation. The gapmer strategy involves including a sequence of unmodified deoxyribonucleotides (typically with a phosphorothioate backbone) between regions containing the modified nucleotides.[41] In this way, the central portion of the antisense oligonucleotide can recruit RNase H, while the flanking regions effectively improve nuclease resistance and increase affinity for complementary strands.

In contrast to incorporating discrete substituents at the C2′ position to confer nuclease resistance and a conformational bias to the sugar pucker, one can also imagine pursuing a complementary strategy for inducing the desired conformational bias: restricting rotation around torsional bonds along the nucleotide scaffold (*Figure 1.10*). Constraining the phosphodiester backbone (i.e., α,β-constrained nucleic acid **1.8**, *Figure 1.10*)[64] or torsion angles γ and δ (i.e., tricyclo-DNA **1.9,** *Figure 1.10*)[65,66] conferred a significant increase in duplex thermal stability ($\Delta T_m \approx +3$ °C/mod.). However, the most promising increase was observed when the furanose sugar was locked in an *N*-type sugar pucker by virtue of including a methylene tether between the C2′-oxygen atom and the C4′ position.[67-71] The resultant monomer, which has been dubbed Locked Nucleic Acid (LNA, **1.7**, *Figure 1.10*), has a sugar moiety that is effectively locked into the same conformation found in RNA, and as such,

oligonucleotides that incorporate LNA monomers tend to form A-type duplexes (*Figure 1.3*, p. 4). As a consequence of the constrained scaffold of LNA,[72-74] the oligonucleotides also display a remarkably high increase in affinity and specificity for the complementary strand relative to the corresponding DNA–RNA duplex.[75] Furthermore, oligonucleotides that include LNA monomers demonstrate high *in vivo* stability and a general lack of toxicity. While poly-LNA oligonucleotides do not inherently activate RNase H, implementation of a gapmer strategy has been successfully used to overcome this limitation.

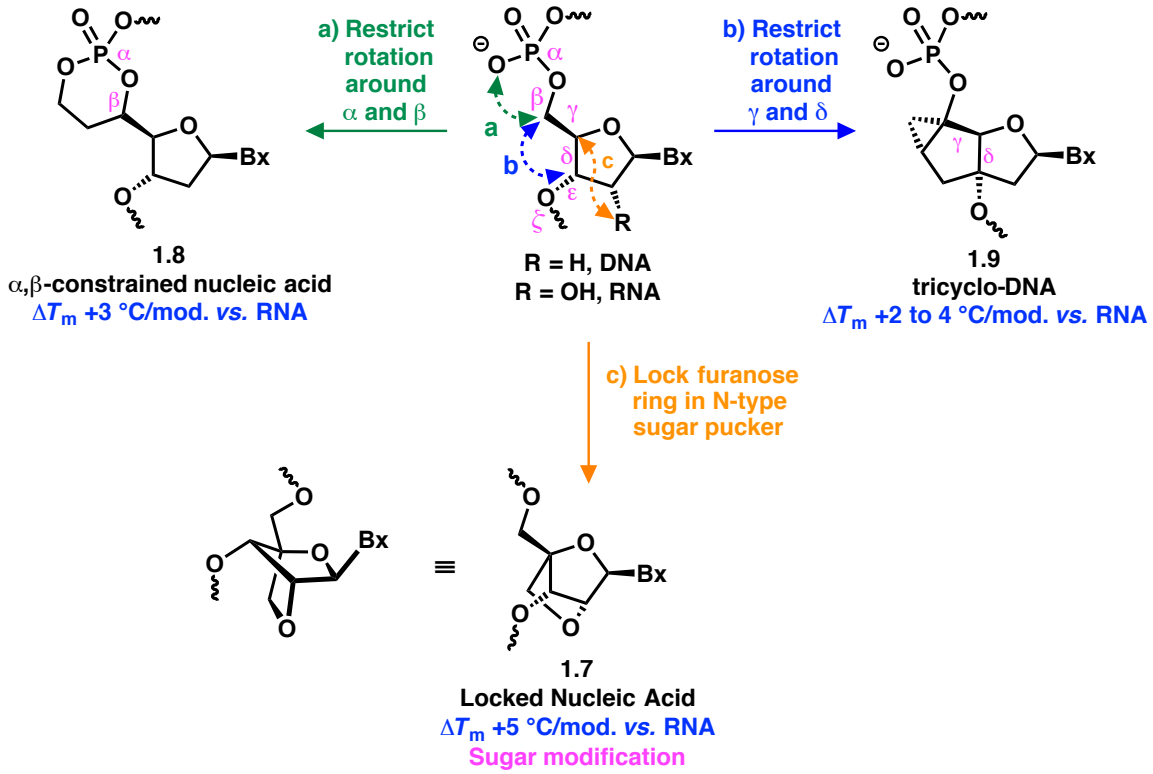

Figure 1.10 – Conformational restriction strategies.

Following their disclosure of the promising hybridization properties of LNA, the group of Wengel evaluated the seven other stereoisomers of this locked scaffold to determine whether the isomeric forms had comparable properties.[71] While all but two of the stereoisomers displayed similar binding affinity for complementary RNA relative to a DNA reference, the truly surprising observation came in the form of one of these stereoisomers exhibiting an increase in affinity for RNA that was comparable to the remarkably high value measured for LNA. This nucleoside was revealed to be the C1′ epimer of the enantiomer of

LNA, and as such was termed α-L-LNA. Intriguingly, when thymidine-based LNA (**1.10**, *Figure 1.11*) and α-L-LNA (**1.11**, *Figure 1.11*) are aligned in space, a number of key atoms overlay each other: N1 of the nucleobase, the C3′ hydroxy group, and the C5′ atom. While the high affinity observed for α-L-LNA is quite attractive in and of itself, further appeal may be found in its effective ability to act as a mimic of DNA, as a consequence of the conformational bias imposed on the scaffold by the bridging ether moiety. As such, oligodeoxynucleotides that incorporate monomers of α-L-LNA tend to form B-type duplexes when hybridized with DNA and duplexes that are intermediate between A- and B-type when hybridized with RNA, making them complementary to oligodeoxynucleotides that include monomers of LNA instead.

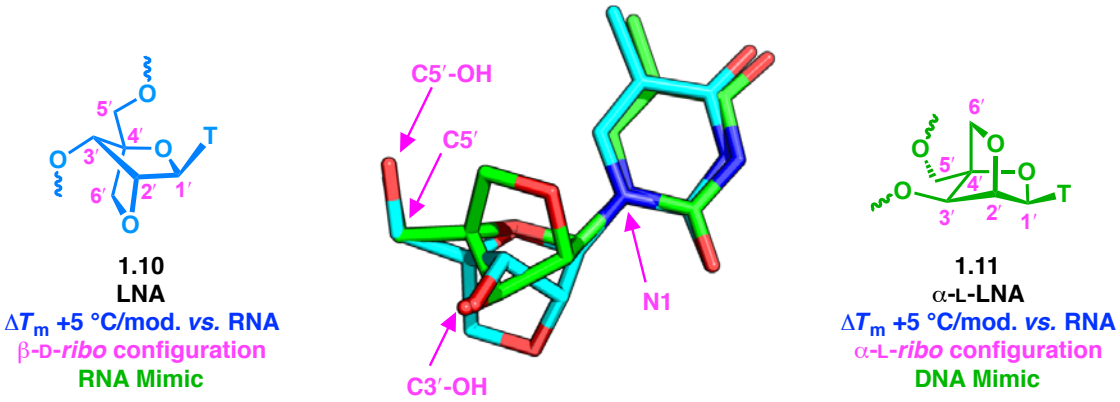

Figure 1.11 – Overlay of LNA and α-L-LNA.

As exemplified by LNA and α-L-LNA, nucleotide modifications that conformationally restrict rotation about the sugar–phosphate backbone have been very successful overall at improving the affinity of antisense constructs for their complementary strands. In part, this success stems from their ability to be used across a wide range of oligonucleotide sequences with predictable results, without interfering with the specificity of Watson–Crick base pairing. Consequently, while considering potential modifications to the nucleic acid scaffold that could further enhance their binding affinity for complementary strands of nucleic acid, strategies for further restricting the sugar-phosphate backbone were primarily considered. These endeavours are described in the following sections.

1.2 The Design of Tricyclic Nucleic Acid Analogues

The appealing hybridization properties of LNA and α-L-LNA provided a concrete starting point for further exploring additional ways to improve the duplex thermal stability of oligonucleotides through a conformational restriction strategy. While both LNA and α-L-LNA are, respectively, locked in an *N*- or *S*-type sugar pucker* by virtue of the methylene tether between the C2′-oxygen atom and the C4′ position of either, varying degrees of conformational flexibility are still possible along the sugar-phosphate backbone. This was highlighted by previous work at *Isis Pharmaceuticals* that described the influence of incorporating stereochemically-differentiated methyl groups on either bicyclic nucleoside scaffold at the C5′ position (*Figure 1.12*).[77,78]

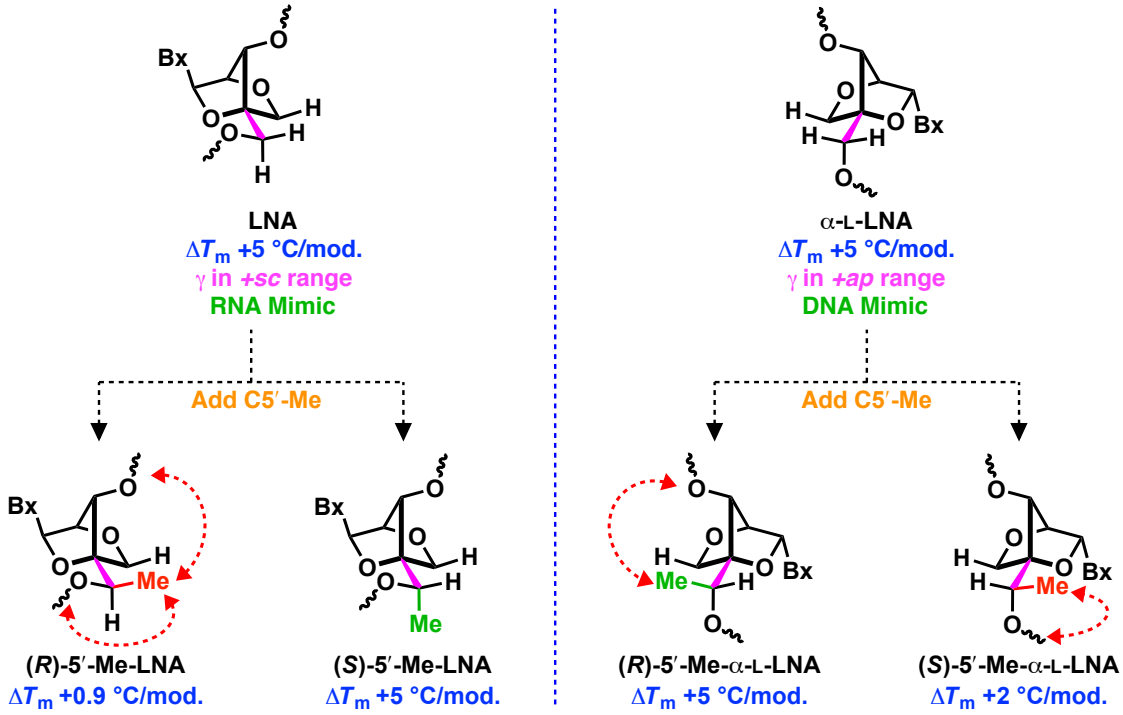

*ΔT_m values are reported *vs.* RNA; *sc* = synclinal; *ap* = antiperiplanar

Figure 1.12 – Incorporation of C5′-methyl group on constrained bicyclic scaffolds.

* Although the furanose conformation of α-L-LNA could alternatively be assigned as *N*-type (C3′-endo, ^3E) as a consequence of its L-configuration, for the purposes of directly comparing it with the conformations of DNA/RNA monomers and the parent LNA scaffold, the furanose conformation of an α-L-LNA monomer is referred to as being in an *S*-type conformation.[76]

In the case of LNA, the depicted conformer is preferred in duplexes because the C4′- and C5′-oyxgen atoms are in a gauche orientation and there is an additional stabilizing CH•••O interaction present in the form of an intramolecular hydrogen bond between the C5′-oxygen atom and the nucleobase[79] (i.e., H6 of pyrimidines or H8 of purines); the latter interaction is not possible in the trans/antiperiplanar orientation. The incorporation of an (*S*)-configured methyl group at the C5′ position of LNA (**1.14**, *Figure 1.12*) was well tolerated and did not markedly change the preferred conformation, since the methyl group effectively avoids unfavourable interactions with the charged phosphodiester backbone, while maintaining the stabilizing hydrogen-bonding interactions.[78] In contrast, when an (*R*)-configured methyl group was introduced (**1.13**, *Figure 1.12*), it was proposed – on the basis of NMR observations of the nucleoside monomer – that rotation around torsion angle γ took place to alleviate a repulsive 1,3-eclipsing interaction that would have otherwise occurred with the C3′-oxygen atom and corresponding charged phosphodiester backbone.[*,78,82] Notably, despite the disparity in their hybridization properties, both modified monomers were able to significantly increase the stability of oligonucleotides to exonucleases when they were incorporated in flanking positions using a gapmer strategy. Furthermore, the (*S*)-5′-methyl modification (**1.14**) showed promise in an animal model as a consequence of its ability to reduce hepatotoxicity and the inflammatory profile of LNA-containing antisense constructs.[78]

In comparison, the parent scaffold for the α-L-LNA series was found to have a conformation in which torsion angle γ is found in the +*ap* range. While the incorporation of a 5′-(*R*)-configured methyl group on the α-L-LNA scaffold led to a stabilizing influence (**1.15**, *Figure 1.12*), the corresponding 5′-(*S*)-configured methyl group (**1.16**, *Figure 1.12*) had a relative destabilizing effect.[77] This stands in direct contrast to the results observed for the analogous modification on the LNA scaffold, where the (*S*)-configured methyl group (**1.14**, *Figure 1.12*) was observed to be stabilizing and the (*R*)-configured methyl group (**1.13**, *Figure 1.12*) destabilizing. While it was proposed that the absence of an additional stabilizing CH•••O interaction (since the nucleobase is further away) in the α-L-LNA series could lead to similar energetic profiles for rotation around torsion angle γ, owing to a lack of crystal-structure data it difficult to ascribe the observations to a specific cause. Additional conformations along the

[*] Torsion angle γ corresponds to rotation around the magenta-coloured C4′-C5′ bond (*Figure 1.10*, p. 19).[80,81]

sugar-phosphate backbone are also possible and, as such, an accurate prediction of the distortions that would occur to torsion angles α and β as a consequence of a rotation around γ was not immediately apparent. Despite the apparent divergence in hybridization properties observed for the modified nucleosides of LNA and α-L-LNA, in each case, one of the diastereomeric pairs was found to be highly stabilizing relative to RNA and on par with the parent locked nucleic acid scaffold. Given the potential for rotation around torsion angle γ to play a fundamental role in further increasing (or decreasing) binding affinity, it was thought that the overall hybridization profile could be improved by restricting rotation about that angle through additional modifications to the bicyclic scaffold of the locked nucleic acids.

Previous work at *Isis Pharmaceuticals* also demonstrated that methyl groups incorporated at the C6′ position of LNA led to oligonucleotides that show LNA-like affinity for complementary RNA, in addition to their being significantly more resistant to degradation by nucleases (**1.17** and **1.18**, *Figure 1.13*).[83,84] This work was particularly promising in that it demonstrated that additional bulk at the C6′ position of LNA was tolerated, while imparting further benefits to its therapeutic profile. Accordingly, it was reasoned that it might be possible to restrict rotation around torsion angle γ in the LNA scaffold by effectively including multiple modifications in a single nucleoside. In essence, it was envisaged that methyl groups at the C5′ and C6′ positions could be tethered to one another through an annulation strategy in which a six-membered cyclohexane ring was effectively fused to the scaffold of LNA. The annulation would provide access to putative nucleoside monomers TriNA 1 (**1.19**, *Figure 1.13*) and TriNA 2 (**1.20**, *Figure 1.13*), which have been so-named in deference to their highly constrained tricyclic cores. Given the complementary hybridization characteristics observed for LNA and α-L-LNA – the former acts as a mimic of RNA, while the latter is a mimic of DNA – it was particularly attractive to pursue, in parallel, a related strategy for α-L-LNA (*Figure 1.14*).

Annulation of the (*R*)-configured methyl groups at the C5′ and C6′ position of the α-L-LNA scaffold could afford so-called α-L-TriNA 1 (**1.23**, *Figure 1.14*), in which the sugar pucker is locked and rotation around torsion angle γ is effectively restricted.[77,85] Alternatively, to conserve the alignment of torsion angle γ that is present in the parent α-L-LNA monomer, one can envision incorporating a cyclohexane ring between C3′ and C5′ to provide α-L-TriNA

2 (**1.24**, *Figure 1.14*);[77,86] this is analogous to locking the sugar pucker in a bicyclo-DNA scaffold, where rotation about γ is already restricted by virtue of the bicyclic core.[87]

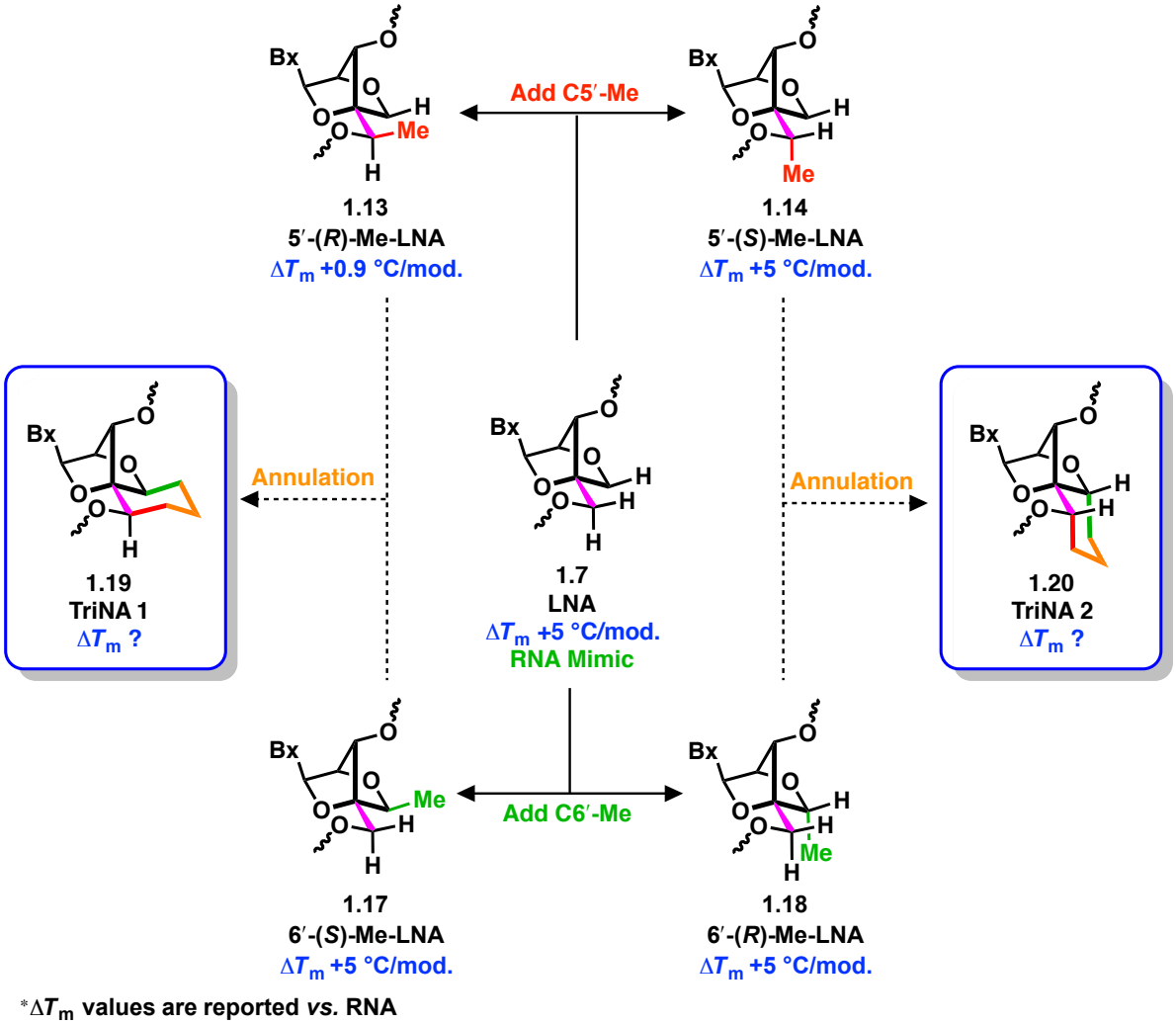

Figure 1.13 – Design of tricyclic nucleic acids from a LNA scaffold template.

Conceptually, the strategy effectively incorporates two modes of conformational restriction in a single nucleoside monomer: 1) locking the sugar moiety in an *N*-type sugar pucker by virtue of the C2′–C4′ anhydro bridge and 2) restricting rotation around torsion angle γ by fusing a six-membered cyclohexane ring to the scaffold. While each of these strategies have been explored individually, it was envisaged that their combined influence when incorporated into a single modified nucleoside could have an additive effect, resulting in increases in binding affinity that may not be possible using a single mode of constraint alone.

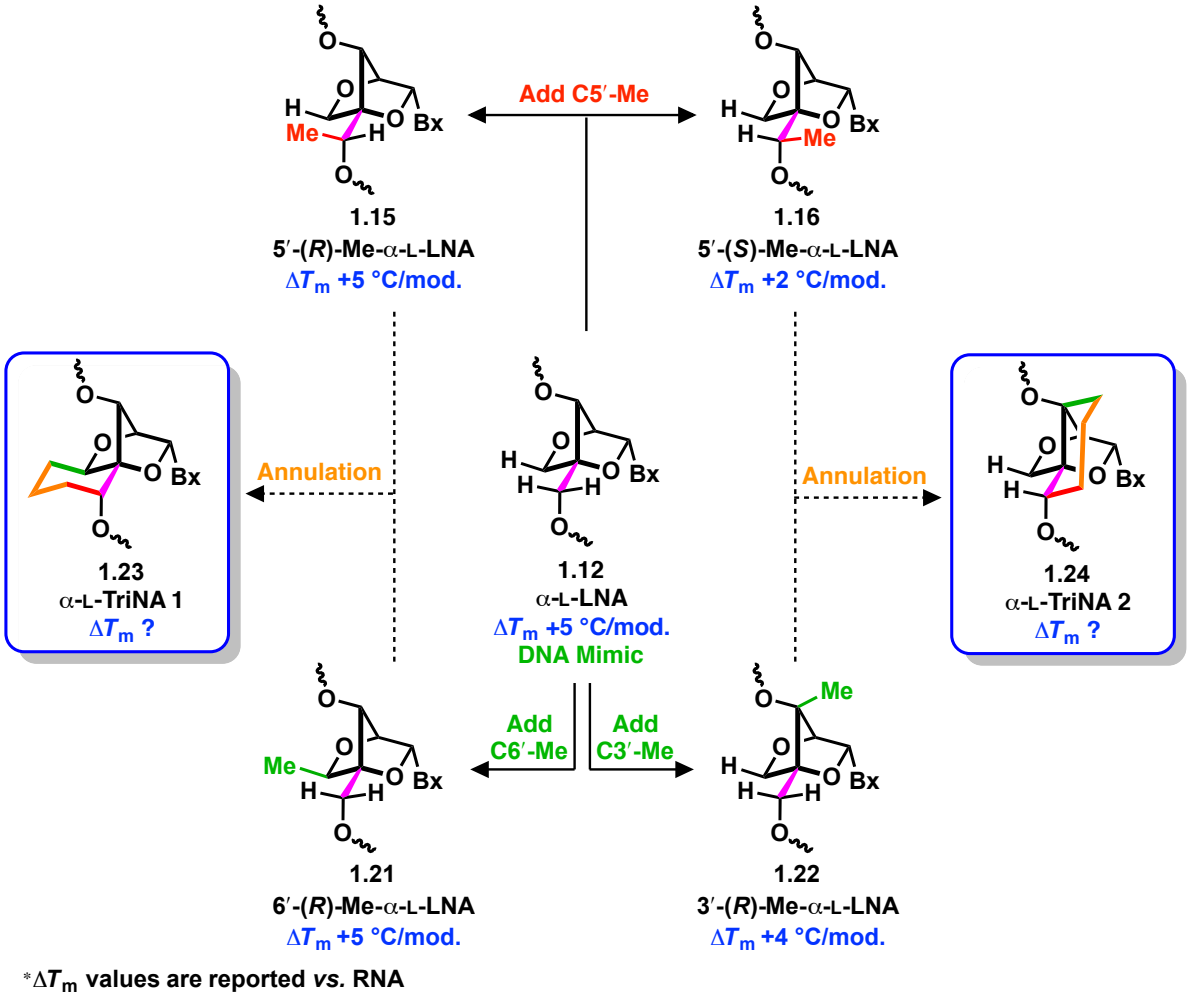

Figure 1.14 – Design of tricyclic nucleic acids based on α-L-LNA scaffold.

To screen for overt steric issues that could arise by appending the cyclohexane ring to the scaffold of the locked nucleic acids, the thymine-based nucleosides of the four previously described monomers – two based on the LNA scaffold (TriNA 1 and 2) and two derived from the α-L-LNA scaffold (α-L-TriNA 1 and 2) – were overlaid on the NMR or X-ray structure solutions of *S*-cEt- or α-L-LNA-modified duplexes (*Figure 1.15*). A cursory inspection of the models revealed that the appended six-membered cyclohexane ring could, in principle, be accommodated within the duplexes, if a similar conformation is favoured. However, it is apparent that the steric bulk of the cyclohexane ring will likely project into different regions of modified duplexes, which could lead to conformational changes in the phosphodiester backbone as a consequence of unfavourable steric interactions or a disruption of the spine of

hydration along the duplex.[42,88-91] Nevertheless, these changes would be difficult to predict *a priori* and consequently, the monomers were synthesized to provide a more concrete indication of their influence on the stability of oligonucleotide duplexes.

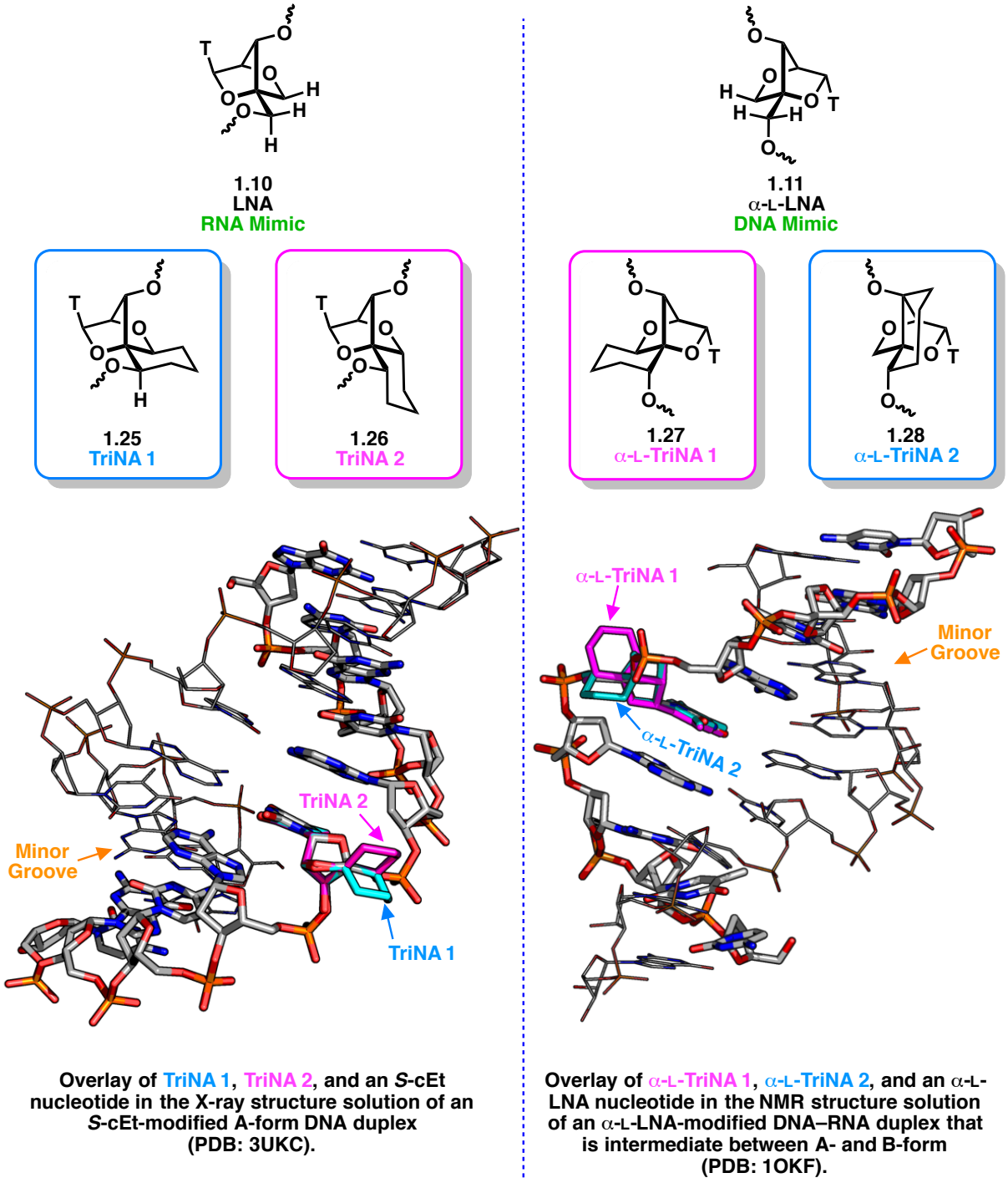

Figure 1.15 – Overlay of tricyclic nucleosides and NMR structure solutions.

The synthesis of the highly constrained tricyclic nucleoside monomers will be described in the following sections. Notably, these projects were the result of collaborative efforts within the Hanessian group (synthesis of the monomers) and with *Isis Pharmaceuticals* (preparation of oligonucleotides and duplex thermal stability measurements). Dr. Bradley Merner is acknowledged for his initial exploratory work related to the synthesis of TriNA 1 and 2. The synthesis of α-L-TriNA 2 was largely achieved through the efforts of a former postdoctoral research associate in the Hanessian group, Dr. Jernej Wagger, and the specific details of the synthesis will not be described in further detail here.[92]

1.3 Synthesis of α-L-TriNA 1

The synthesis of α-L-TriNA 1 was realized in collaboration with Dr. Benjamin Schroeder, a former postdoctoral research associate in the Hanessian group.[93] For the related synthesis of α-L-TriNA 2 please refer to the relevant publication that was recently disclosed by the Hanessian group.[92]

1.3.1 Retrosynthetic Analysis of α-L-TriNA 1

For the purpose of preparing a versatile α-L-TriNA 1 monomer that may be incorporated into oligonucleotides, we were cognizant that it would be advantageous to differentially protect the hydroxy groups at the C3′ and C5′ positions of its nucleoside scaffold (**1.29**, *Scheme 1.1*); the monomer could then be selectively deprotected and incorporated into an oligonucleotide using well-established phosphoramidite chemistry.[70,94,95] Consequently, orthogonally-protected nucleoside **1.29** was selected as the principle α-L-TriNA 1 target of interest. An analysis of the highly constrained structure of α-L-TriNA 1 precursor **1.29** revealed that stereocontrolled formation of the C2′–C4′ anhydro bridge would likely be one of the most challenging steps of the synthetic route. To overcome this hurdle, it was envisaged that intramolecular S_N2 displacement of an axial leaving group at C6′ on the scaffold of alcohol **1.30** would be feasible in the presence of an appropriately configured hydroxy group. This approach mirrors the oft-used strategy for the synthesis of α-L-LNA, although in that case the leaving group is located on a significantly less hindered primary carbon atom, rather than a secondary one that is surrounded by additional steric bulk.[96,97] Nevertheless, a secondary mesylate was successfully displaced to access 6′-(*R*)-methyl-α-L-LNA (**1.21**, *Figure 1.14*, p. 25)[85] and the analogous C6′-methylated LNA scaffolds (**1.17** and **1.18**, *Figure 1.13*, p. 24),[83] which provides additional support for this strategy.

To install the thymine nucleobase present in **1.31**, a robust glycosylation sequence described by Niedballa and Vorbrüggen was considered to be rather appealing.[98-100] The reaction would be performed on the corresponding 1,2-diacetyl-protected diol equivalent of **1.32**. A ring-closing metathesis reaction, conceivably mediated by the second-generation catalyst described by Grubbs' group, may be used to access the six-membered cyclohexene ring present in **1.32**.[101,102] The requisite vinylogous precursor (**1.33**) for the ring-closing

metathesis reaction may arise from addition of a vinyl-containing organometallic reagent (e.g., a Grignard reagent) to aldehyde **1.34**. Through a relatively straightforward sequence of reactions, the aldehyde may be prepared from primary alcohol **1.35**, which is itself accessible from diacetone-D-glucose (**1.36**) using a previously-disclosed sequence.[103-105]

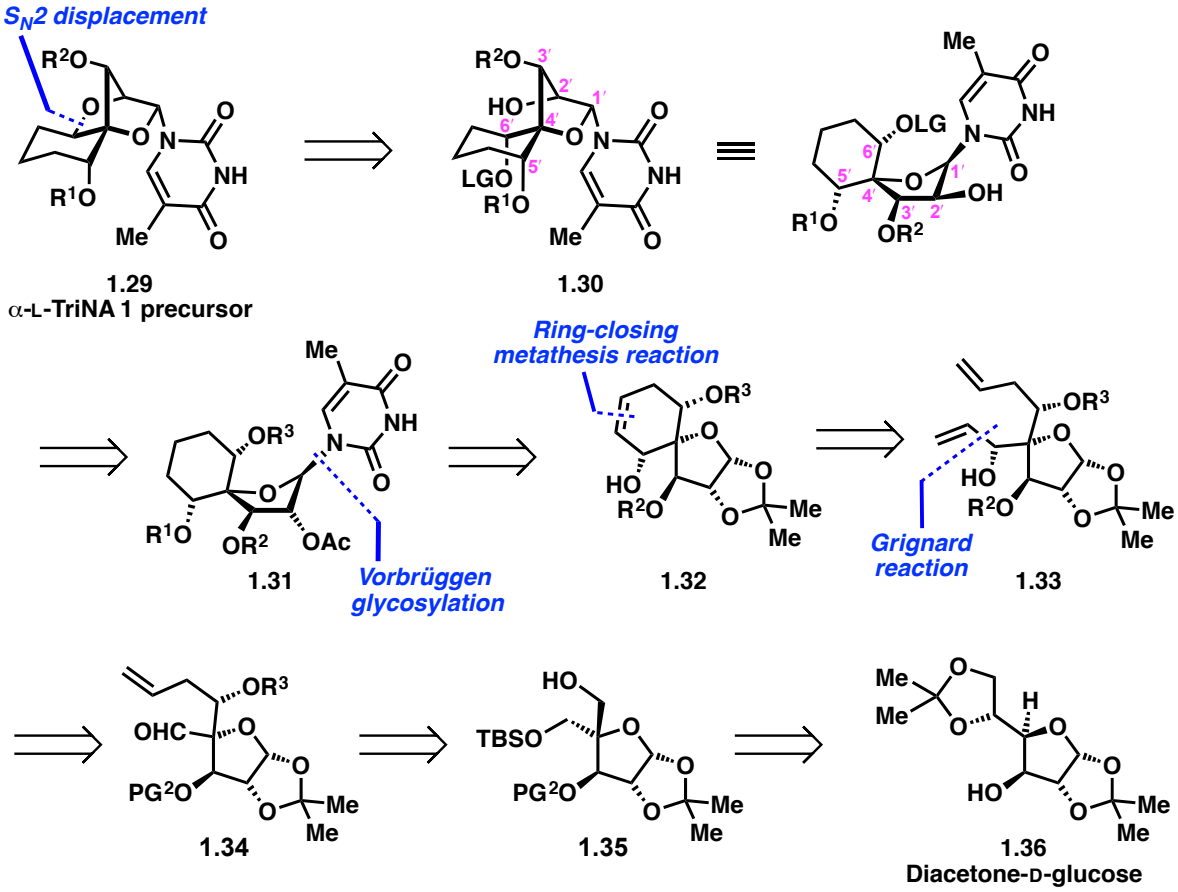

Scheme 1.1 – Retrosynthetic analysis for α-L-TriNA 1.

1.3.2 Synthesis of α-L-TriNA 1

The synthesis of α-L-TriNA 1 began with inexpensive carbohydrate-derived starting material, diacetone-D-glucose (**1.36**, *Scheme 1.2*). Protection of the free hydroxy group with benzyl bromide was followed by chemoselective acid-mediated deprotection of the less-substituted acetonide, and successive oxidation of the diol with sodium periodate to furnish aldehyde **1.37**.[104] A crossed-Cannizzaro aldol reaction in the presence of sodium hydroxide and formaldehyde was used to install the hydroxymethyl group with concomitant reduction of

the aldehyde to furnish diol **1.38**, with an overall yield of 64% over four steps.[106] Selective protection of the prochiral (*S*)-configured hydroxymethyl group with *tert*-butyldimethylsilyl chloride leads to a mixture of the desired monoprotected alcohol (**1.39**) alongside recovered starting material (i.e., diol **1.38**) and disilyl-protected material.[103] While this was not ideal, it was straightforward to recycle the recovered starting material and disilyl-protected material following fluoride-mediated deprotection of the latter.

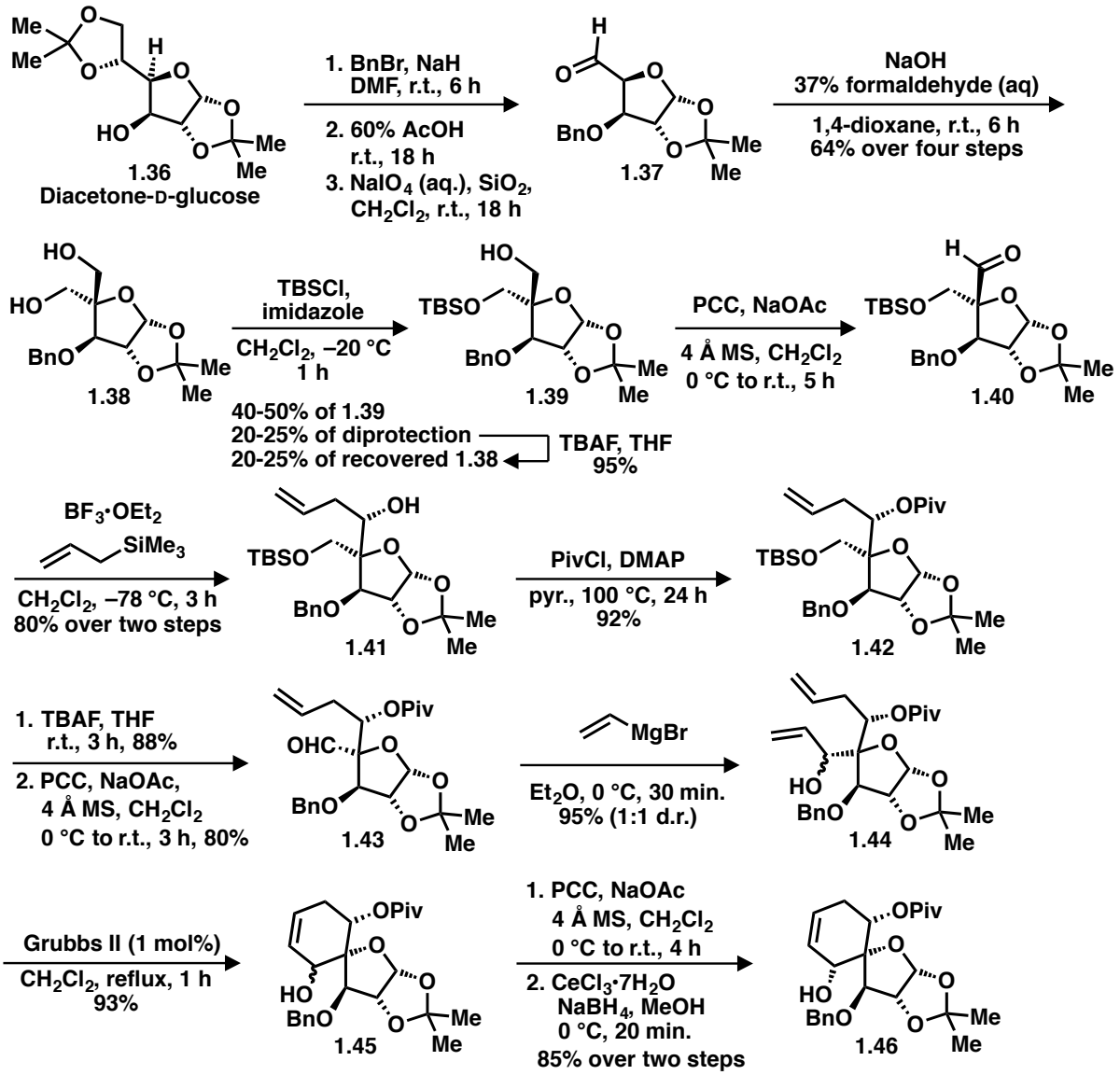

Scheme 1.2 – Synthesis of spirocyclic core of α-L-TriNA 1.

Oxidation of the primary hydroxy group with pyridinium chlorochromate and a subsequent Sakurai allylation reaction[107-110] afforded homoallylic alcohol **1.41**, which was protected as the corresponding pivaloyl ester (**1.42**). Tetrabutylammonium fluoride was used to deprotect the *tert*-butyldimethylsilyl protective group and the primary alcohol was oxidized to aldehyde **1.43** with pyridinium chlorochromate. Addition of vinylmagnesium bromide led to an inseparable 1:1 mixture of diastereomeric allylic alcohols (**1.44**), which were elaborated to the spirocyclic cyclohexene moiety in the presence of the Grubbs group's second-generation catalyst. At this stage it was possible to separate the diastereomeric alcohols (**1.45**) from one another, and the undesirable (*S*)-configured hydroxy epimer was inverted via an oxidation–reduction sequence to secure (*R*)-configured alcohol **1.46**, in which the C5′ stereocenter* was firmly established.

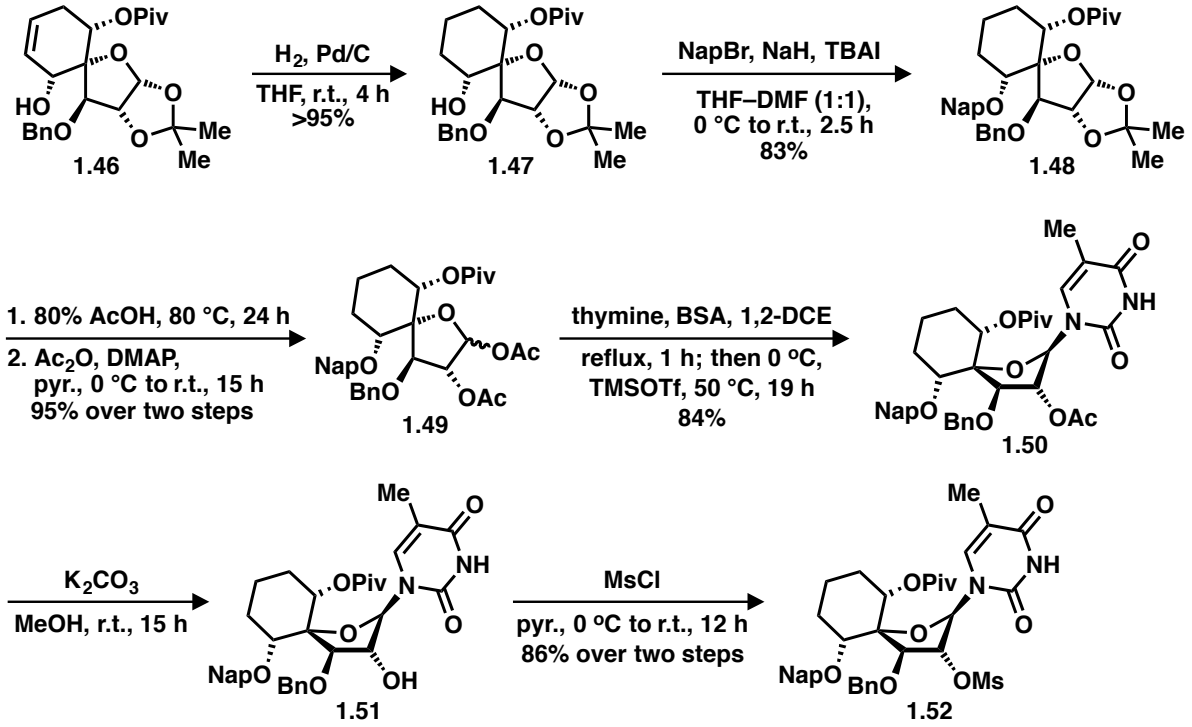

Scheme 1.3 – Synthesis of cyclization precursor en route to α-L-TriNA 1.

The alkene was then reduced under hydrogenation conditions and the secondary hydroxy group protected as a 2-naphthylmethyl ether to furnish spirocycle **1.48** (*Scheme 1.3*). A three-step sequence comprising deprotection of the acetonide, acetylation, and Vorbrüggen

* Nucleoside numbering.

glycosylation furnished nucleoside **1.50** with the thymine nucleobase, in 80% yield over the three steps. Selective hydrolysis of the C2′ acetyl ester and subsequent mesylation provided mesylate **1.52**.

It was initially conceived that the corresponding 2′,6′-dimesylate analogue of pivalyl-protected alcohol **1.52** (i.e., dimesylate **1.53**, *Scheme 1.4*) could, in the presence of a source of hydroxide, cyclize to form the desired 2′,4′-anhydro bridge in a single synthetic step,* but attempts by Dr. Benjamin Schroeder to do so resulted in the observation of a 1:1 mixture of 2,6′- and 2,2′-anhydronucleoside intermediates **1.54** and **1.55** instead (*Scheme 1.4*). This reactivity implied that it would likely be necessary to protect the imide nitrogen atom of the nucleobase before performing the key cyclization step; consequently, a multistep approach was pursued instead.

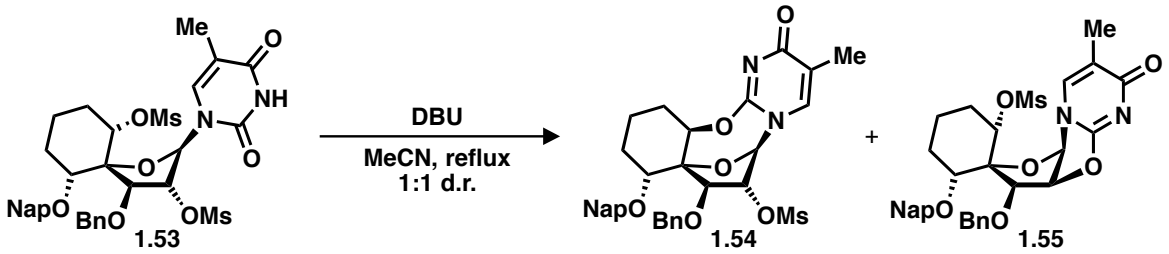

Scheme 1.4 – Formation of anhydronucleosides from a dimethanesulfonate ester.

For the purpose of forming the requisite 2′,4′-anhydro bridge found in the structure of α-L-TriNA 1, it was necessary to invert the C2′-hydroxy group present in alcohol **1.51** (*Scheme 1.3*). The prior observation of 2,2′-anhydronucleoside intermediate **1.55** (*Scheme 1.4*) was quite promising in that it effectively provided a synthetic option for accomplishing the task. Accordingly, a solution of thymine nucleobase **1.52** in acetonitrile was heated to reflux in the presence of a hindered base – 1,8-diazabicyclo[5.4.0]undec-7-ene – to effect displacement of the mesylate leaving group and formation of 2,2′-anhydronucleoside intermediate **1.56** (*Scheme 1.5*). Hydrolysis of the anhydronucleoside bridge as well as the pivaloyl ester furnished diol **1.57**, whose nucleobase was immediately protected in the presence of benzyl chloromethyl ether to afford diol **1.58**. Chemoselective activation of the C6′ hydroxy group was successfully accomplished in the presence of trifluoromethanesulfonic anhydride, which

* This approach has successfully been used to synthesize similar nucleosides.[85,96]

furnished triflate ester **1.59**, the key intermediate for the intramolecular cycloetherification reaction envisaged to establish the 2′,4′-anhydro bridge that restricts the conformation of the sugar moiety within the nucleoside scaffold.

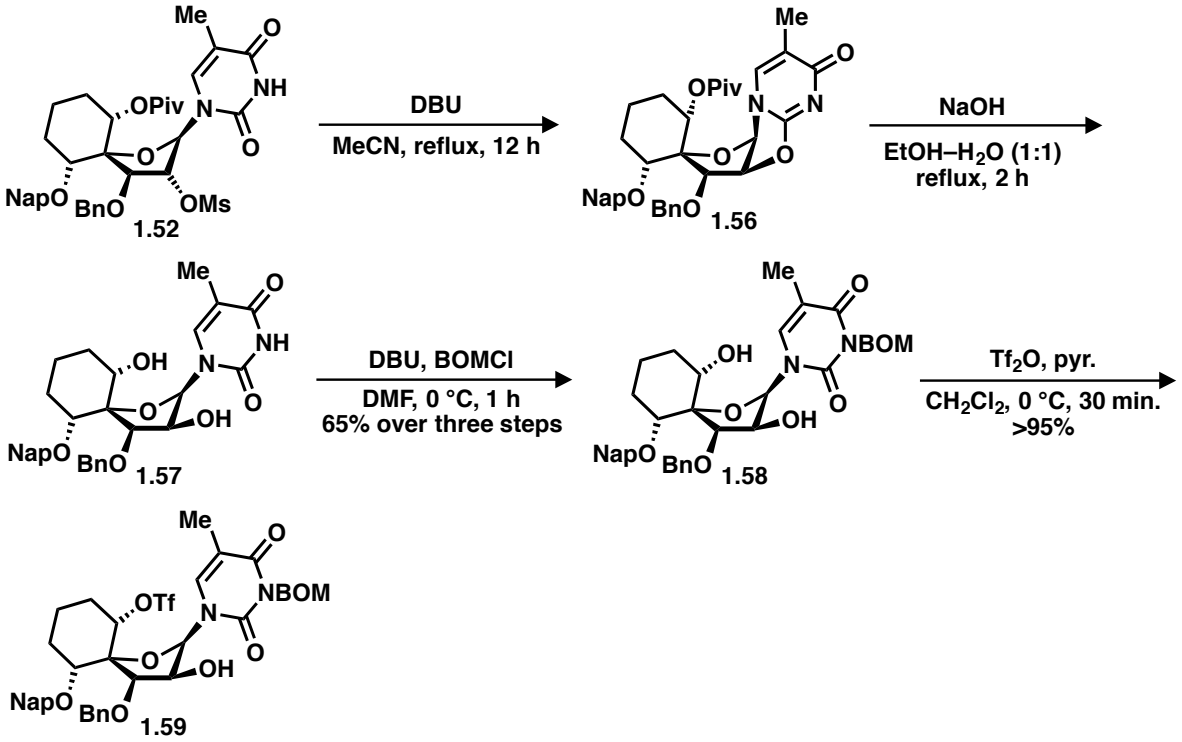

Scheme 1.5 – Synthesis of triflate for the key cycloetherification reaction.

The intramolecular cycloetherification reaction proved to be rather challenging, and under different conditions (*Table 1.1*, p. 34) varying quantities of three major products were observed: hydrolysis of the triflate (**1.58**), the desired tricyclic nucleic acid (**1.60**), and an apparent constitutional isomer of the tricyclic nucleic acid. Initial attempts to effect the cyclization with sodium hydroxide led to significant quantities of triflate hydrolysis (entry 1, *Table 1.1*), which could be recycled by reincorporating the triflate moiety. 1,8-Diazabicyclo[5.4.0]undec-7-ene and potassium carbonate were unreactive (entries 2–3, *Table 1.1*), while the use of pyridine led to displacement of the triflate moiety by the amine base itself (entry 4, *Table 1.1*). Caesium carbonate furnished minor quantities of the desired tricyclic nucleoside (entries 5–7, *Table 1.1*), but the major products were triflate hydrolysis and another product that appeared to be a constitutional isomer of the tricyclic nucleoside on the basis of its identical molecular weight. When sodium hydride was used, a significantly

higher quantity of the desired tricyclic nucleoside was observed, but the reaction was rather capricious and the yields were inconsistent (entry 8, *Table 1.1*). Higher and more consistent yields of the tricyclic nucleoside were observed when sodium amide was used (entry 9, *Table 1.1*), but the yield did not exceed 60% as a consequence of the presence of significant quantities of the constitutional isomer. Furthermore, it was necessary that the reaction be closely monitored to limit further reactivity of the products, and it was essential that sodium amide was added to a preheated solution of triflate **1.59**, rather than warming the solution once the base was added. While the yields obtained for the intramolecular cycloetherification were not ideal, the reaction was nevertheless robust, even when gram-scale quantities of triflate **1.59** were used.

Table 1.1 – Intramolecular cycloetherification to prepare the 2′,4′-anhydro bridge.

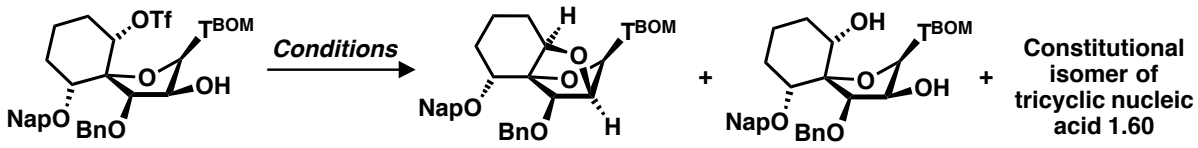

1.59 | **1.60** Tricyclic nucleic acid | **1.58** Hydrolysis

Entry	Conditions	Observation
1	$NaOH_{(aq.)}$, various solvents, heat	Mostly **1.58**
2	DBU, CH_3CN, heat	No reaction
3	K_2CO_3, MeOH, heat	No reaction
4	pyridine, heat	Pyridine displaced triflate
5	Cs_2CO_3, 1,2-DCE, 80 ºC	**1.60** (~20%) + **1.58**
6	Cs_2CO_3, 4 Å MS, DMF, 55 ºC	**1.60** (~15%) + **1.58** (~15%) + Isomer (>50%)
7	Cs_2CO_3, DMF, 55 ºC	**1.60** (~15%) + **1.58** (~25%) + Isomer (~25%)
8	NaH, DMF, 55 ºC	**1.60** (~30–50%) + **1.58** + Isomer
9	$NaNH_2$, DMF, 55 ºC	**1.60** (~55%) + Isomer (~38%)

*Other strong bases (i.e., NaHMDS, NaH and 18-crown-6) were unreactive or led to a mixture of hydrolysis and isomer.

While further optimization was certainly possible, it was clear that prior identification of the constitutional isomer could provide further guidance on the most appropriate way to tackle that challenge. Initial attempts to isolate the constitutional isomer were hindered by its apparent instability, but the identity of this product was eventually realized through X-ray crystallographic analysis of its *para*-nitrobenzoate diester analogue (**1.62**, *Scheme 1.6*). Surprisingly, the constitutional isomer was identified as benzyl enol ether **1.61**, in which the

secondary C2′-hydroxy group was effectively eliminated with concurrent hydrolysis of the triflate moiety. Although β-elimination of the triflate ester was previously considered as a potential deterrent for pursuing an intramolecular cycloetherification strategy, it was seemed more likely that the β-elimination would have occurred within the cyclohexane ring instead of the ribose portion of the spirocyclic nucleoside. In fact, in some ways, it is surprising that the desired cycloetherification reaction prevailed by such a considerable margin over the alternative reaction pathway where the triflate is eliminated from the cyclohexane moiety.

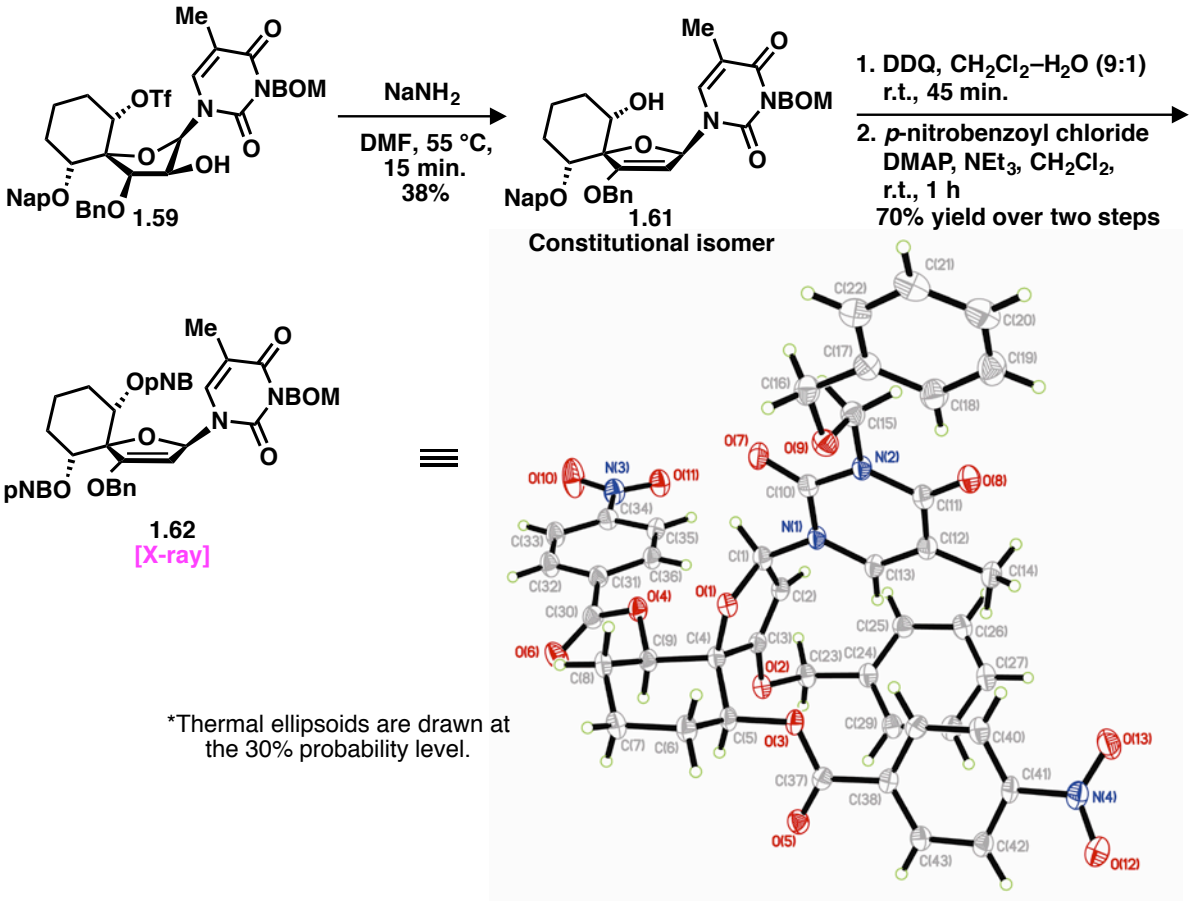

Scheme 1.6 – Structure elucidation of the constitutional isomer.

A closer inspection of triflate-containing nucleoside **1.59** revealed that the favoured selectivity of the site of elimination may stem from the conformational preference of the cyclohexane ring and a transient intramolecular migration of the triflate group (Scheme 1.7, p. 36). It was proposed that initial deprotonation of the C2′-hydroxy group with sodium amide leads to an anion in which the cyclohexane moiety could be equilibrated between two different

conformers: one in which the triflate is in an axial orientation (**1.63**, Scheme 1.7) and another where it is effectively equatorial (**1.64**, Scheme 1.7). While intramolecular S_N2 displacement of an axially-configured triflate leaving group by the C2′-alkoxide moiety was expected to lead to the desired tricyclic nucleoside (**1.60**), it appeared likely that an equatorially-oriented triflate group could undergo a *trans*-sulfonylation reaction (**1.64** to **1.65**) as a consequence of its close proximity to the alkoxide moiety in that conformation. Following triflyl migration, the observed benzyl enol ether would then arise through subsequent elimination of the triflate from the pentose-derived moiety of the nucleoside (**1.65** to **1.61**). While further optimization could potentially supress the formation of side product **1.61** – with concomitant increase in yield of the desired tricyclic nucleoside – we were cognizant that successful formation of the tricyclic core made it essential that α-L-TriNA 1 itself be first incorporated into an oligonucleotide for the purpose of evaluating its impact on the thermal stability of duplexes.

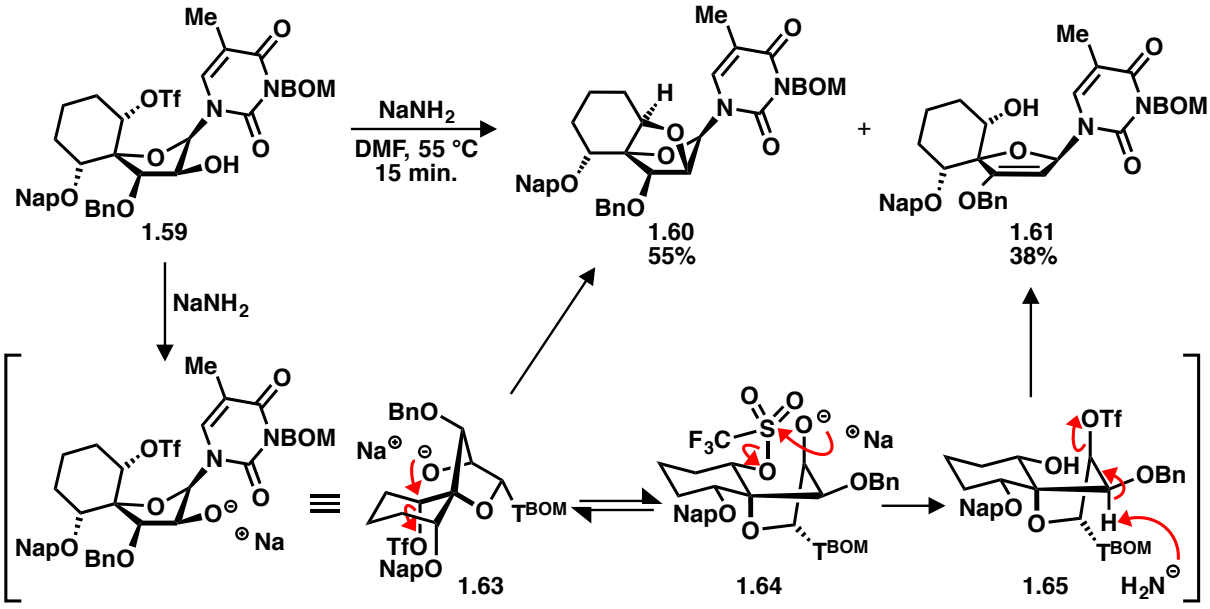

Scheme 1.7 – Proposed mechanism for the cycloetherification reaction.

To facilitate the incorporation of the α-L-TriNA 1 monomer in an oligonucleotide with the use of well-established phosphoramidite chemistry,[70,94,95] it was initially envisaged that the C5′-oxygen atom of **1.60** (*Scheme 1.8*) could be protected with the dimethoxytrityl protective group, following removal of the naphthyl ether. 2,3-Dichloro-5,6-dicyano-1,4-benzoquinone was used to chemoselectively deprotect the naphthyl ether moiety on the C5′-oxygen atom to afford alcohol **1.66**, and the hydroxy group was reprotected with acetic anhydride.

Hydrogenolysis was used to deprotect the C5′-benzyl ether as well as the N3-benzyloxymethyl ether and afforded alcohol **1.68** in excellent yield. Protection of the C5′-hydroxy group as the triethylsilyl ether afforded the desired orthogonally-protected α-L-TriNA 1 monomer (**1.69**) that was envisaged to be incorporated into oligonucleotide sequence. The overall yield for the 30-step synthetic sequence was approximately one percent, but the robustness allowed a sufficient quantity of the nucleoside to be prepared and sent to our collaborators at *Isis Pharmaceuticals* for biophysical evaluation.

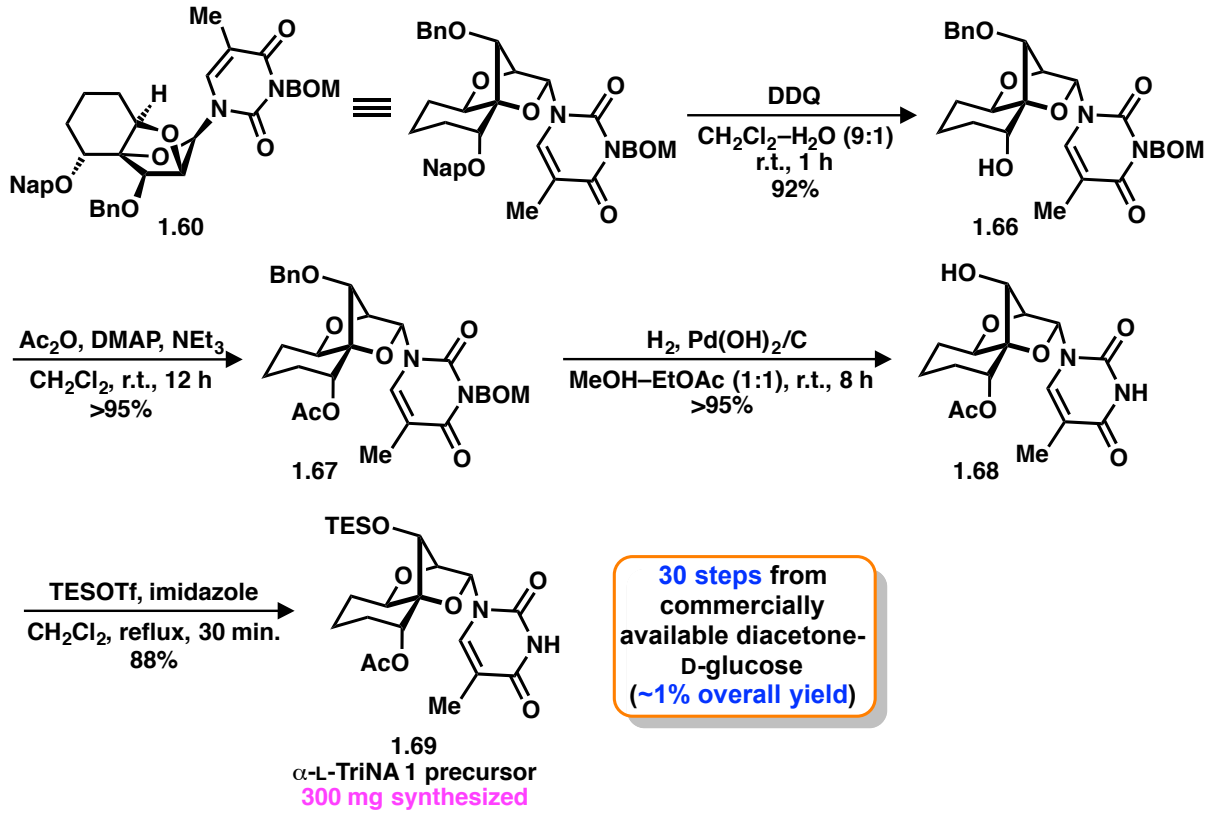

Scheme 1.8 – Synthesis of triethylsilyl and acetyl-protected α-L-TriNA 1.

Definitive evidence that the desired tricyclic core of the nucleoside had been prepared was secured in the form of a X-ray crystal structure of *para*-nitrobenzoate ester **1.70** (*Figure 1.16*). In addition to further substantiating the tricyclic core of the nucleoside, the stereochemical orientations of the protected hydroxy groups at C3′ and C5′ were firmly established.

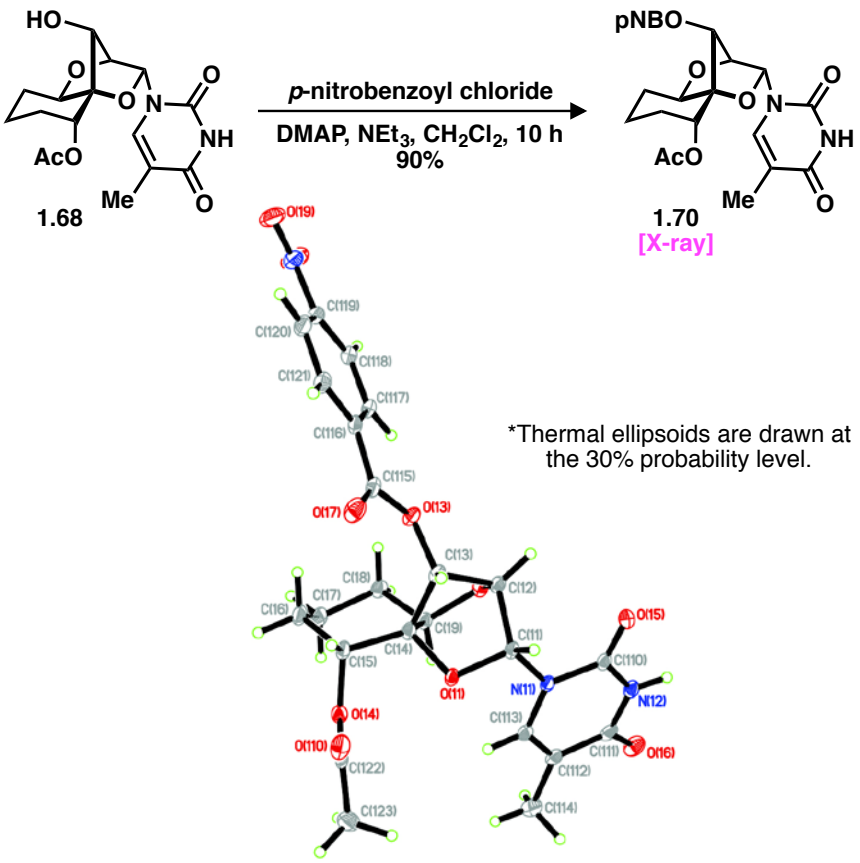

Figure 1.16 – X-ray crystallographic evidence for the tricyclic nucleic acid core.

Unfortunately, chemoselective deprotection of the acetyl-protected C5′-hydroxy group was not as straightforward as was originally anticipated (*Scheme 1.9*, p. 39). Initial attempts at *Isis Pharmaceuticals* to effect the deprotection with ammonia in methanol led to a mixture of the starting material (**1.69**) and differentially deprotected products. While the desired alcohol (**1.71**) was the major product, it was only isolated in 44% yield. Our own attempt with a mixture of potassium carbonate in methanol was more effective on smaller quantities of material, but the reaction itself was nevertheless not particularly robust overall. With the hope of recovering some of the isolated diol (**1.72**), a bid was made to selectively protect the C3′ or C5′ hydroxy groups, but initial efforts were not promising. Moreover, all attempts to protect

the C5′-hydroxy group in **1.71** as the corresponding dimethoxytrityl ether* were also unproductive, likely as a consequence of the significantly hindered nature of this position.

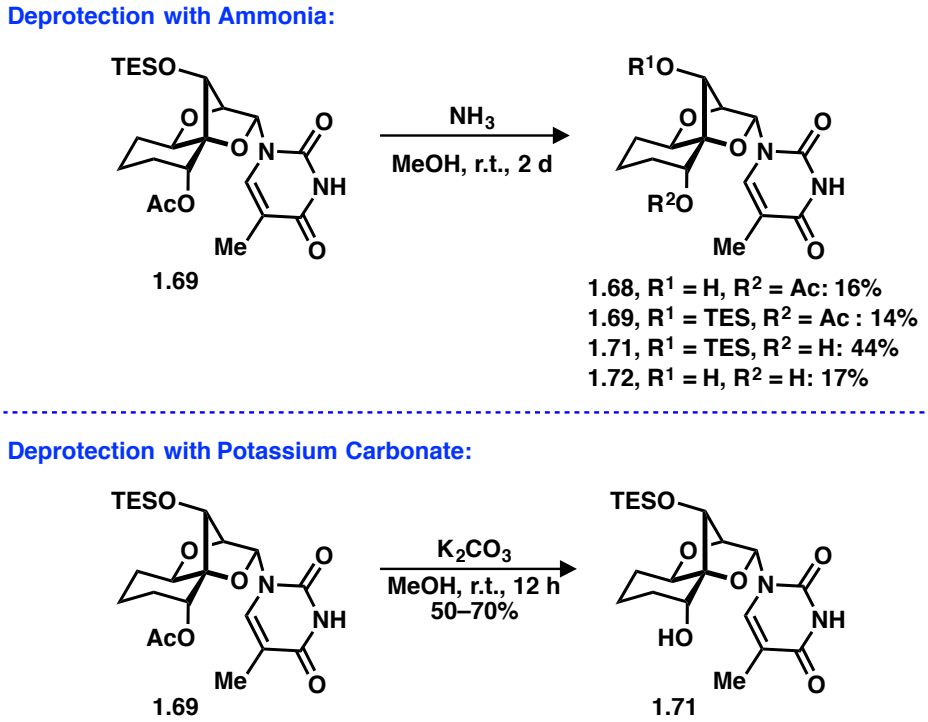

Scheme 1.9 – Attempted chemoselective deprotection of acetyl-protected C5′-OH.

Consequently, nucleoside monomer **1.71** was manually coupled with a commercially-available DMTr-protected thymidine phosphoramidite instead (*Scheme 1.10*, p. 40). Following the initial coupling reaction, the intermediate phosphite ester was oxidized to a diastereomeric mixture of phosphate esters with *tert*-butyl hydroperoxide,[111] which yielded silyl-protected dimer **1.73**. Chemoselective removal of the triethlysilyl ether proceeded without incident, but the ensuring phosphitylation of the C5′-hydroxy group was very low-yielding; although the conversion appeared to be excellent by thin-layer-chromatographic analysis, the subsequent isolation and recovery was drastically lower. Overall, 66 mg of phosphoramidite **1.74** was prepared, which was sufficient for its incorporation in a pair of oligonucleotides.

* Initial attempts focused on using DMTrOTf or DMTrCl in the presence of *N*,*N*-diisopropylethylamine or 2,6-lutidine, with pyridine as the solvent, but no reaction was observed, even upon heating.

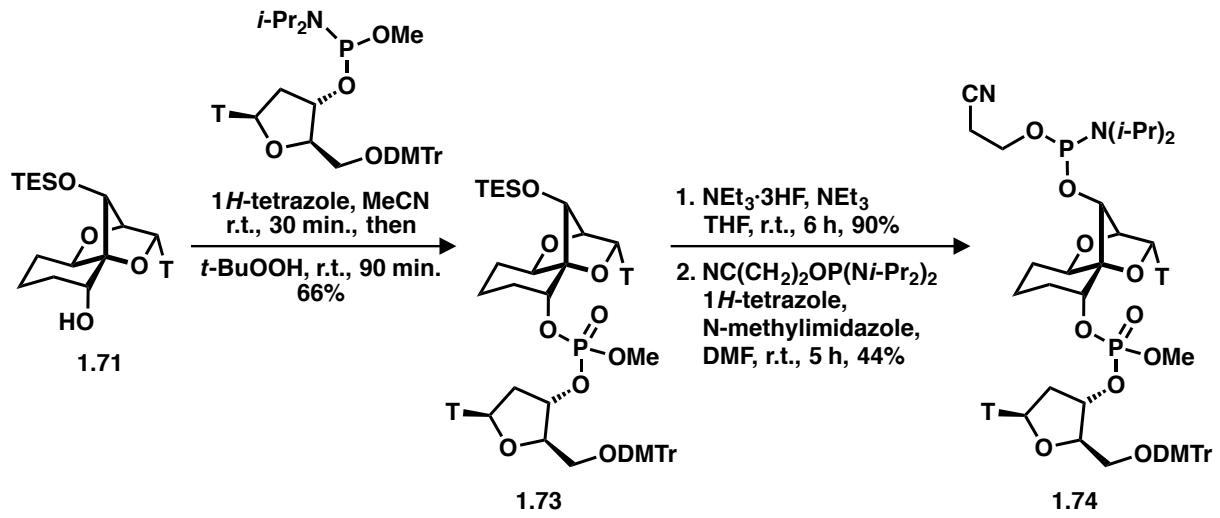

Scheme 1.10 – Synthesis of phosporamidite for solid-phase oligonucleotide synthesis.

To address the challenges associated with the instability of the triethylsilyl protective group and overall difficulty in chemoselectively removing the acetyl ester in its presence, a decision was made to prepare a levulinyl ester instead.[112,113] Consequently, protection of the C5′-hydroxy group in **1.66** with acetic anhydride was set aside in favour of an esterification reaction with 1-ethyl-3-(3-dimethylaminopropyl)carbodiimide-activated levulinic acid that furnished orthogonally-protected nucleoside **1.75** (*Scheme 1.11*). Hydrogenolysis in the presence of palladium(II) hydroxide proceeded without incident and provided access to alcohol **1.76**, the key α-L-TriNA 1 precursor that was sent to *Isis Phamaceuticals* for biophysical evaluation. Phosphitylation of the free C3′-hydroxy group provided phosphoramidite **1.77**, which was manually incorporated into oligonucleotide sequences. Removal of the levulinyl protective group was carried out with hydrazine in a mixture of pyridine and acetic acid, which allowed the oligonucleotide sequence to be elaborated from free C5′-hydroxy group.[112,113]

Duplex thermal stability measurements of oligonucleotides that include α-L-TriNA 1 monomers are described in Section 1.5 on page 52.[93]

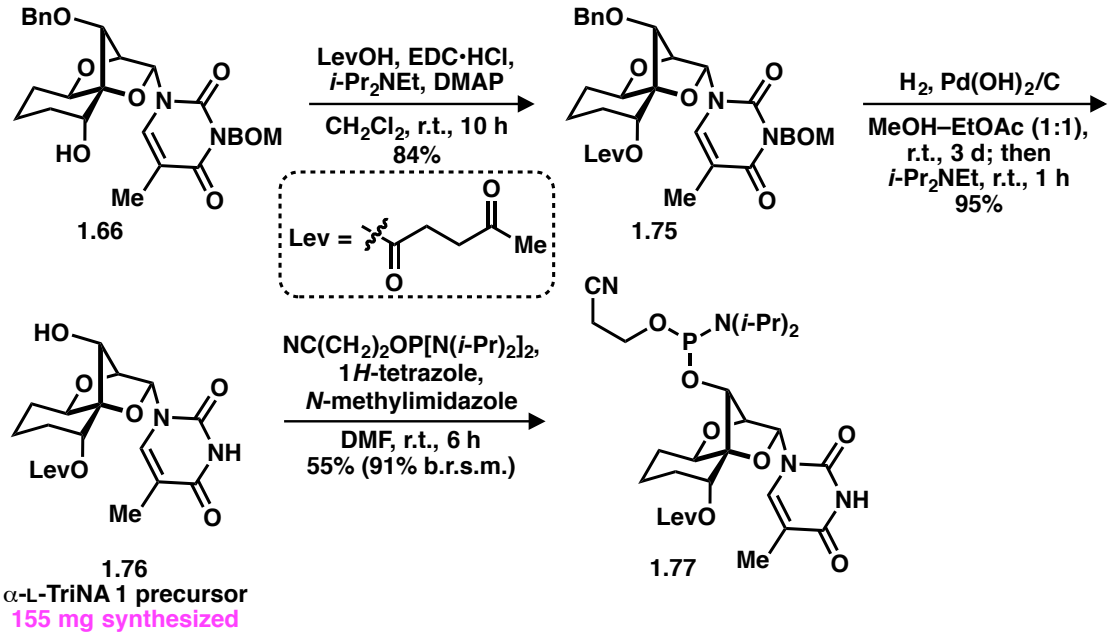

Scheme 1.11 – Preparation of the α-L-TriNA 1 phosphoramidite monomer.

1.4 Synthesis of TriNA 1

1.4.1 Retrosynthesis of TriNA 1

Similar to the route realized for the synthesis of α-L-TriNA 1, it was envisaged that the requisite TriNA 1 monomer (**1.78**, *Scheme 1.12*) with orthogonal protective groups could be synthesized from a carbohydrate precursor. The initial synthetic route was designed such that both TriNA 1 and TriNA 2 (**1.19** and **1.20**, *Figure 1.13*, p. 24) could be prepared from the same carbohydrate precursor, using an identical synthetic sequence – save for very minor differences in each route that would establish the correct stereochemical configurations at C5′ and C6′ within the monomers. As a consequence of the challenges encountered to form the C2′–C4′ anhydro bridge on a cyclohexane scaffold during the synthesis of α-L-TriNA 1 (*Table 1.1*, p. 34), an attempt was made to address the efficiency of the cyclization by performing it earlier in the synthetic sequence.

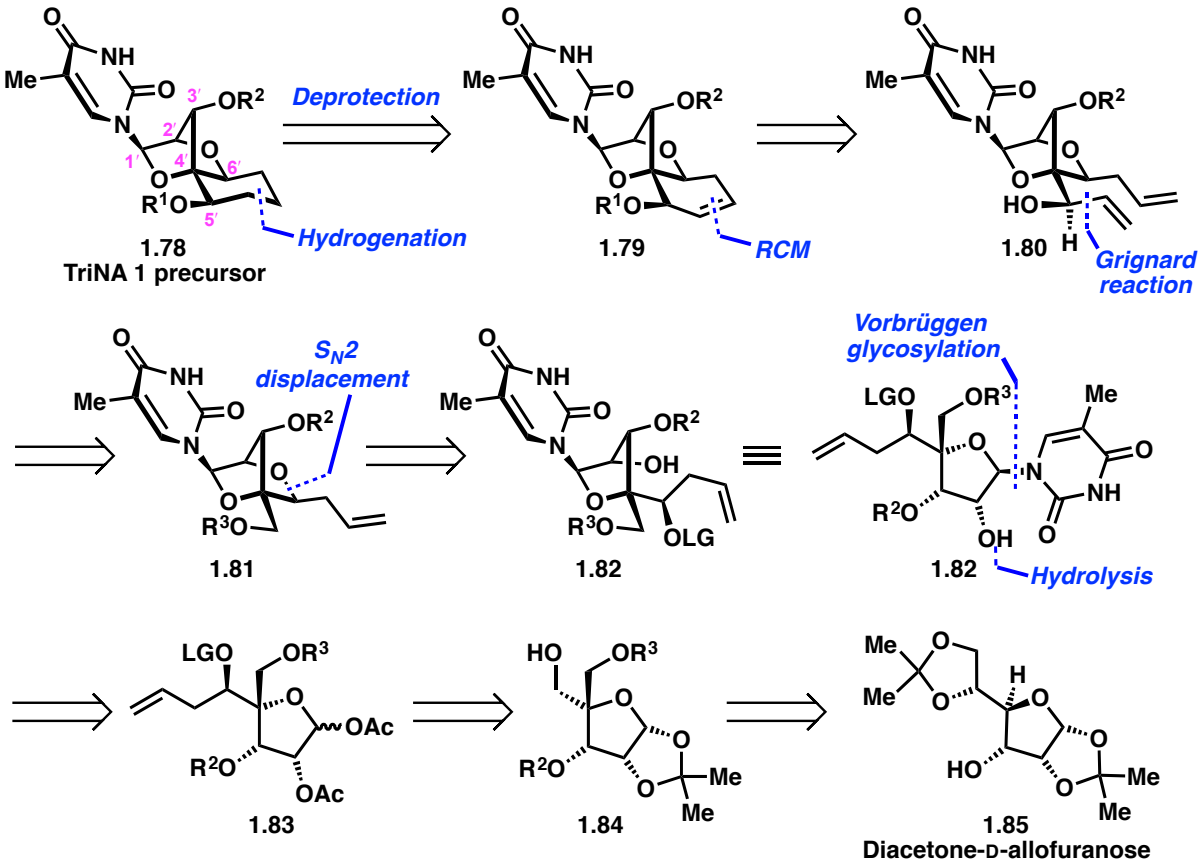

Scheme 1.12 – Retrosynthetic analysis for TriNA 1.

For the synthesis of the TriNA 1 monomer (**1.78**, *Scheme 1.12*), it was planned that the crucial fused cyclohexane ring in **1.79** would be installed through a ring-closing metathesis reaction from **1.80**. A Grignard reaction on the corresponding C5′ aldehyde of **1.81** would provide access to the diene precursor (**1.80**) that was anticipated to participate in the ring-closing metathesis reaction. Notably, the addition of an organometallic reagent to the corresponding aldehyde of **1.81** effectively establishes the stereocenter at C5′; consequently it is one of the two steps in the proposed sequence that differentiates TriNA 1 and TriNA 2. The pivotal cyclization reaction to form the C2′–C4′ anhydro bridge is the other step that allows for differentiation between the two sequences. The tricyclic core of **1.81** was envisaged to arise through an intramolecular S_N2 displacement of an appropriate leaving group from **1.82**, similar to the previously-disclosed approach for the synthesis of the C6′-methyl analogues of LNA (**1.17** and **1.18**, *Figure 1.13*, p. 24).[83] Accordingly, by using a (*R*)- or (*S*)-configured leaving group, it was envisaged that the scaffolds of both TriNA 1 and 2 could be established using a very similar synthetic sequence.

The cyclization precursor **1.82** may itself arise from diacetate **1.83** by way of a Vorbrüggen glycosylation sequence,[98-100] which incorporates the thymine nucleobase into the scaffold. Establishing the stereochemistry of the leaving group was planned to take place through an allylation reaction on the corresponding aldehyde of **1.84**, which may itself be prepared from commercially-available diacetone-D-allofuranose* (**1.85**) through an established sequence.[83]

1.4.2 Synthesis of TriNA 1

The synthesis of TriNA 1 began with readily-available diacetone-D-allofuranose (**1.85**, *Scheme 1.13*, p. 44). Protection of the free secondary hydroxy group with 2-naphthyl bromide was followed by acid-catalyzed hydrolysis of the less-substituted acetonide moiety and subsequent sodium-periodate-mediated cleavage of the intermediate 1,2-diol to afford aldehyde **1.86**. A crossed-Cannizzaro aldol reaction with formaldehyde was used to install the hydroxymethyl group and reduce the aldehyde moiety in a single synthetic operation, which

* Diacetone-D-allofuranose is commercially available, but it may also be prepared from diacetone-D-glucofuranose (**1**, *Scheme 1.2*, p. 29) through a well-established oxidation–reduction sequence.[114]

yielded diol **1.87**.[106] Selective protection of the pro-(*R*)-hydroxymethyl group with *tert*-butyldiphenylsilyl chloride furnished 60% of primary alcohol **1.88**, alongside approximately 20% of the epimeric mono-silyl-protected product; as was previously described, the former is a crystalline solid, while the latter is an oil at ambient temperature, which greatly facilitates its isolation.[83] Oxidation of the primary alcohol with pyridinium chlorochromate delivered aldehyde **1.89**, which was envisaged to provide stereochemically-differentiated homoallylic alcohols that would provide an opportunity to synthesize both TriNA 1 and 2 from a common intermediate, using a similar synthetic sequence (*Scheme 1.12*, p. 42).

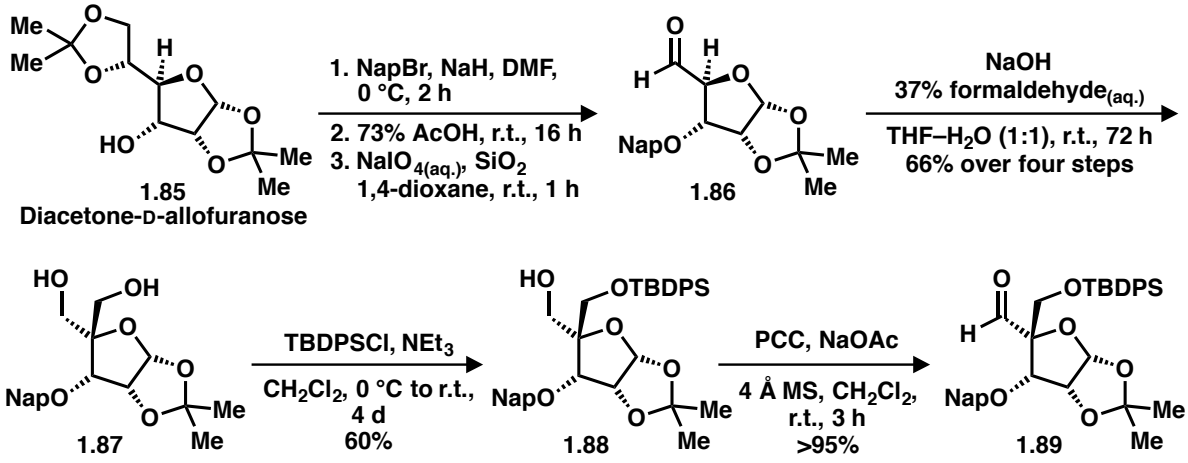

Scheme 1.13 – Synthesis of precursor for allylation reaction.

In collaboration with Dr. Jernej Wagger, a number of conditions were screened for the purpose of effecting the allylation reaction in a stereospecific manner (*Table 1.2*, p. 45). Overall, under the conditions that were attempted, the homoallylic alcohol with a (*R*)-configured hydroxy group (**1.91**) was favoured in each instance. This stereochemical configuration corresponds to that required for the synthesis of TriNA 2, while the (*S*)-configured epimer (**1.90**) was needed for the synthesis of TriNA 1. Compared with the other Lewis acids screened, the use of $MgBr_2 \bullet Et_2O$ (entries 3–4, *Table 1.2*) increased the amount of (*S*)-configured diastereomer **1.90**, but this isomer nevertheless did not made up more than 40% of the mixture of products, and $BF_3 \bullet Et_2O$ was still more convenient to work with on larger quantities of material.

Table 1.2 – Attempted conditions for allylation reaction.

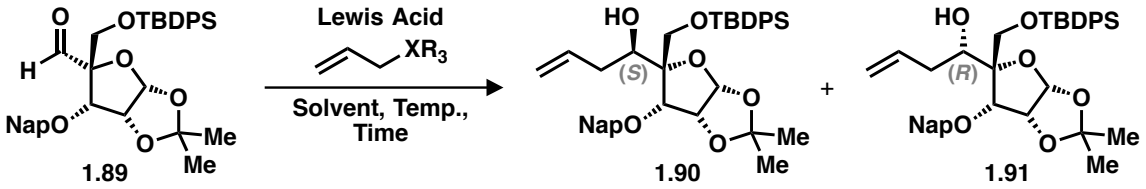

Entry	XR_3	Lewis Acid	Solvent	Temperature	Time	Yield/Conv.	Ratio of 1.90 to 1.91
1	$SiMe_3$	$BF_3{\cdot}Et_2O$	CH_2Cl_2	–40 °C	1 h	90%[a]	0 : 1
2	$SiMe_3$	$MgBr_2{\cdot}Et_2O$	CH_2Cl_2	–40 °C	24 h	–	–
3	$SnBu_3$	$MgBr_2{\cdot}Et_2O$	CH_2Cl_2	–40 °C	5 h	>95%[b]	1 : 3.5
4	$SnBu_3$	$MgBr_2{\cdot}Et_2O$	CH_2Cl_2	–10 °C	25 min.	>95%[b]	1 : 1.5
5	$SnBu_3$	$MgBr_2{\cdot}Et_2O$	Toluene	r.t.	20 min.	>95%[b]	1 : 1.6
6	$SnBu_3$	$MgBr_2{\cdot}Et_2O$	THF	r.t.	26 h	>95%[b]	0 : 1
7	$SnBu_3$	$TiCl_4$	CH_2Cl_2	–78 °C	12 min.	>95%[b]	0 : 1
8	$SnBu_3$	$SnCl_4$	CH_2Cl_2	–40 °C	25 min.	>95%[b]	0 : 1
9	$SnBu_3$	$AlCl_3$	CH_2Cl_2	–78 °C to r.t.	17 h	53%[b]	0 : 1

[a] Isolated yield; [b] Determined by NMR.

To overcome the initial difficulty in directly preparing the (*S*)-configured homoallylic alcohol with the allylation strategy, an oxidation–reduction sequence was pursued instead. Homoallylic alcohol **1.91** (*Scheme 1.14*) was oxidized to the corresponding ketone (**1.92**) with Dess–Martin periodinane and the ketone was subsequently reduced in the presence of different hydride-based reducing reagents (*Table 1.3*, p. 46).

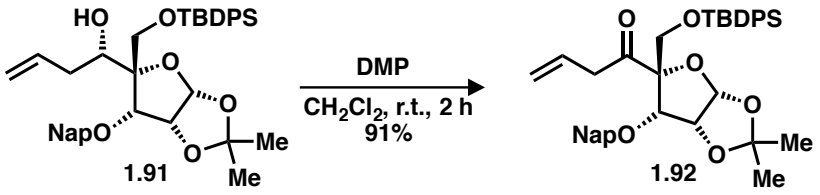

Scheme 1.14 – Oxidation of homoallylic alcohol.

While initial attempts to reduce ketone **1.92** with sodium borohydride (entry 2, *Table 1.3*, p. 46) and lithium triethylborohydride (entry 5, *Table 1.3*, p. 46) favoured the formation of the desired (*S*)-configured homoallylic alcohol (**1.90**), the observed selectivities were rather low. Interesting, when cerium trichloride heptahydrate was used as an additive in the presence of sodium borohydride, the selectivity shifted significantly in favour of the (*R*)-configured

alcohol (**1.91**) instead (entry 3, *Table 1.3*). Fortunately, the use of lithium aluminum hydride as the reducing agent at –78 °C led to a substantial increase in stereoselectivity, with (*S*)-configured homoallylic alcohol **1.90** favoured by a wide margin (entry 1, *Table 1.3*).

Table 1.3 – Ketone reduction with various sources of hydride.

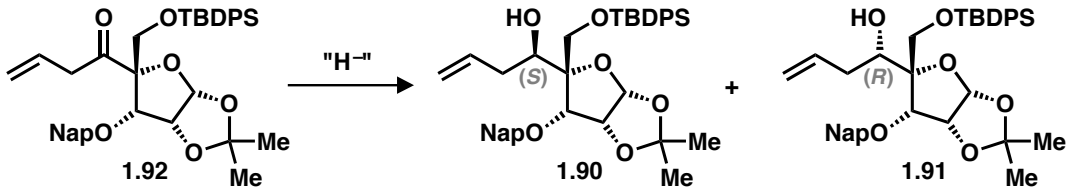

Entry	"H⁻"	Additive	Solvent	Temperature	Time	Ratio of 1.90 to 1.91[a]
1	$LiAlH_4$	–	THF	–78 °C	10 min.	> 20 : 1
2	$NaBH_4$	–	MeOH	0 °C to r.t.	40 min.	4 : 1
3	$NaBH_4$	$CeCl_3 \cdot 7H_2O$	MeOH	r.t.	10 min.	1 : 8
4	$NaBH(OAc)_3$	–	MeOH	r.t.	24 h	–
5	$LiEt_3BH$	–	THF	–40 °C	10 min.	2 : 1

[a] Reactions performed on TLC scale.

When carried out on larger quantities of material, the reduction with lithium aluminium hydride remained stereoselective and was high yielding, but a longer reaction time was needed for full conversion of the ketone (*Scheme 1.15*, p. 47). The secondary hydroxy group was then converted to the corresponding mesylate (**1.93**), before a three-step sequence was used to install the thymine nucleobase. Iron(III) chloride hexahydrate[115] was used to remove the acetonide protecting group in the presence of the mesylate and the intermediate 1,2-diol was acetylated with acetic anhydride to furnish diacetate **1.94**. Although the iron-mediated deprotection was effective – even when carried out on gram-scale quantities of material – the use of fresh iron(III) chloride hexahydrate was vital for ensuring that the yield of the 1,2-diol was high and the number of side-products minimized.* Following acetylation, the thymine nucleobase was incorporated into the scaffold via a Vorbrüggen glycosylation sequence,[98-100] which furnished the key intermediate (**1.95**) for the intramolecular S_N2 displacement that was envisaged to deliver the requisite anhydro bridge.

* If iron(III) chloride hexahydrate of lesser quality was used, the reaction mixture would become very dark upon addition of the reagent and a significant amount of highly-polar material formed. The yield of 60% over three steps (i.e., **1.93** to **1.95**) is ~10% higher if the reaction is carried out on milligram quantities of **1.93** and in the presence of higher-quality iron(III) chloride hexahydrate.

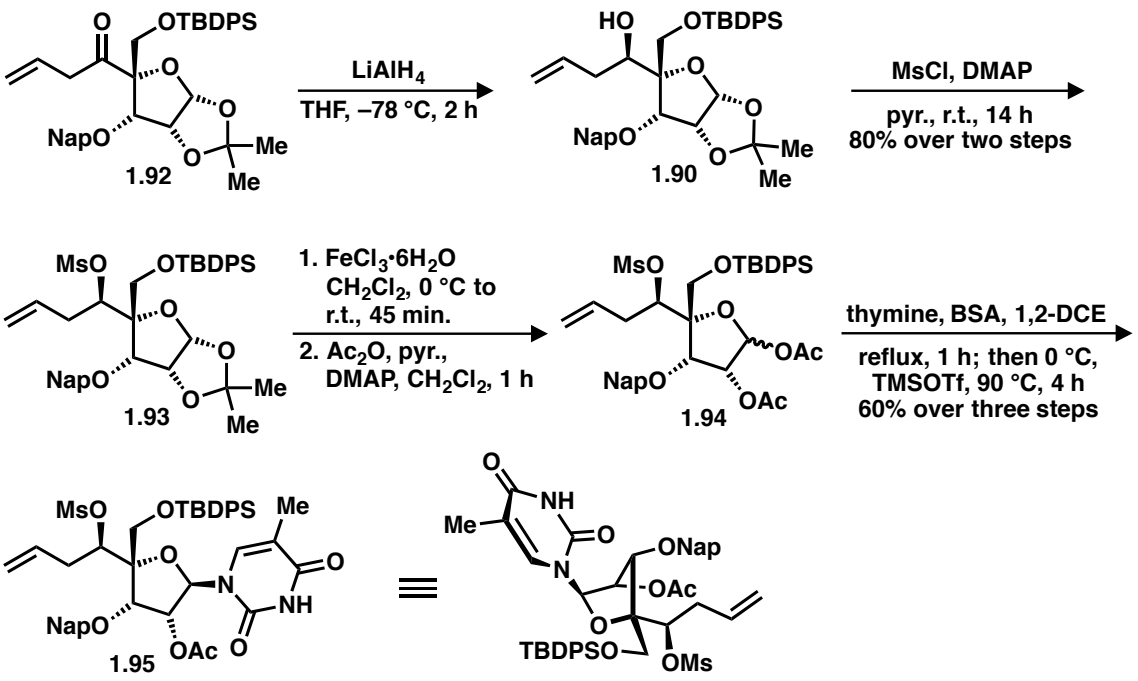

Scheme 1.15 – Installation of the nucleobase and synthesis of the cyclization precursor.

Potassium carbonate was used to effect a one-pot deprotection–cyclization sequence, whereby the acetyl ester at the C2′ position of nucleoside **1.95** was hydrolyzed and the resultant transient alkoxide intermediate (**1.96**) displaced the homoallylic mesylate leaving group via an intramolecular S_N2 reaction (*Scheme 1.16*).[83] This sequence was quite effective and, notably, did not lead to appreciable quantities of elimination products that may also feasibly arise under the conditions of the reaction. The intramolecular cycloetherification reaction furnished the key C2′-C4′ oxacyclic bridge, which is present in LNA and was appropriately substituted to allow for further elaboration to the corresponding six-membered ring embedded in the tricyclic scaffold of TriNA 1.

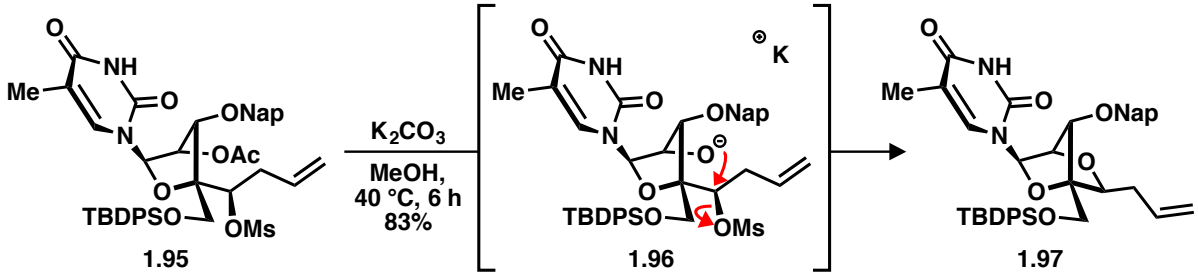

Scheme 1.16 – Intramolecular S_N2 displacement to form anhydro bridge of TriNA 1.

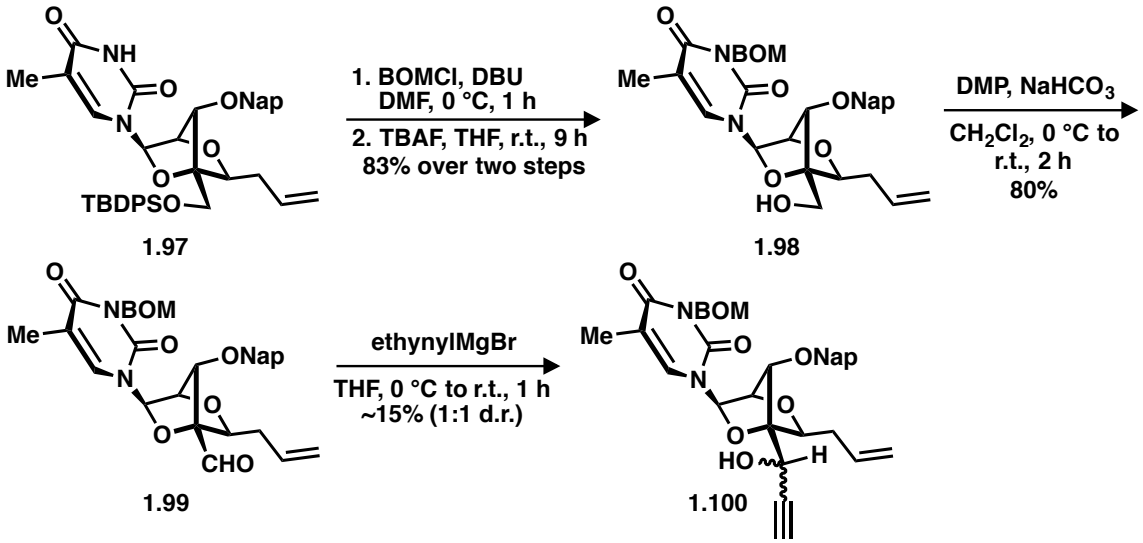

Scheme 1.17 – Synthesis of alkynyl alcohol.

At this point in the synthesis, it was envisaged that an alkene moiety could be installed at the C5′ position to provide a functional group handle, from which the six-membered cyclohexane ring could be formed through a ring-closing metathesis reaction (*Scheme 1.12*, p. 42). To avoid undesirable side-reactions and improve its solubility during the ensuing synthetic sequence, nucleoside **1.97** was first protected as its *N*-benzyloxymethyl derivative, before the tert-butyldiphenylsilyl protective group was removed to provide primary alcohol **1.98** (*Scheme 1.17*). Oxidation of primary alcohol **1.98** with Dess–Martin periodinane was initially quite unreliable, but the inclusion of solid sodium bicarbonate in the reaction mixture addressed that issue and ensured that consistent yields were realized. Originally, it was reasoned that the addition of alkenyl- or alkynyl-derived organometallic reagents to aldehyde **1.99** could stereoselectively furnish the C5′ hydroxy group in one step, but after numerous attempts,* even the highest-yielding and most consistent result with ethynylmagnesium bromide only afforded 15% of a 1:1 mixture of diastereomeric alcohols (**1.100**), which was far from practical. To overcome this hurdle, an alternative approach involving addition of an organometallic reagent to a Weinreb–Nahm amide was pursued instead (*Scheme 1.18*).

* Numerous conditions were tried, including: slow/fast/inverse addition, addition at temperatures as low as –78 °C, use of BOM-free aldehyde, diethyl ether rather than tetrahydrofuran, different Grignard reagents (i.e., vinyl, propenyl, propynyl), organolithium reagents, and copper(I) iodide as an additive.

Accordingly, alcohol **1.98** (*Scheme 1.18*) was oxidized to the corresponding carboxylic acid with chromic acid (the product of chromium trioxide mixed with sulfuric acid),[116] which was subsequently converted to Weinreb–Nahm amide **1.101**.[117] Although the chromium-mediated oxidation was consistent on quantities of up to ~0.5 g of alcohol **1.98**, the conditions were harshly acidic, and further increasing the scale of the reaction resulted in significantly lower yields. Recently, a related oxidation was performed on the analogous C6′ epimer of **1.98** – for the purpose of preparing TriNA 2 – and revealed that the oxidation may be more reliable under neutral conditions using pyridinium dichromate in *N*,*N*-dimethylformamide.[118-120] Although nucleophilic addition of alkenyl-based Grignard reagents (i.e., vinylmagnesium bromide or 1-propenylmagnesium bromide) to Weinreb–Nahm amide **1.101** did not work well, the corresponding alkynyl-derived Grignard reagents (i.e., 1-propynylmagnesium bromide or ethynylmagnesium bromide) added as anticipated to furnish ketone **1.102**. Consequently, it was necessary to chemoselectively reduce the alkyne moiety to the corresponding alkene in order to access diene **1.103** for the ring-closing metathesis reaction. Inspired by conditions reported by the process chemistry group at *Merck*,[121] we performed the semihydrogenation of alkyne **1.102** with Lindlar's catalyst[122,123] in the presence of 1,10-phenanthroline, with *N*,*N*,-dimethylformamide as the solvent. The use of a highly polar aprotic solvent such as *N*,*N*,-dimethylformamide was crucial, as noted by the observation of significant quantities of over-reduced alkane products when comparatively less-polar ethyl acetate was used in its place. The ensuing ring-closing metathesis reaction catalyzed by the second-generation catalyst reported by the Grubbs group was successful and provided access to cyclohexene **1.104**, which contained the tricyclic core of TriNA 1.

Chemo- and stereoselective 1,2-reduction of enone **1.104** with sodium borohydride in the presence of cerium(III) chloride heptahydrate firmly established the requisite stereochemistry of the C5′-hydroxy group in **1.105**.[*] Given the success realized with the levulinyl ester for α-L-TriNA 1 (*Scheme 1.11*, p. 41), the C5′-hydroxy group in **1.106** was also protected as the corresponding levulinate.[112,113] Reduction of the alkene moiety and concomitant hydrogenolysis of the benzyloxymethyl ether furnished the key TriNA 1

[*] It was also possible to chemoselectively hydrogenate the alkene moiety first (H_2, 6 mol% Pd/C, EtOAc, r.t., 75%), before stereoselectively reducing the ketone under Luche's conditions.

monomer (**1.107**) that was phosphitylated (**1.108**) and subsequently incorporated into oligonucleotides for biophysical evaluation.

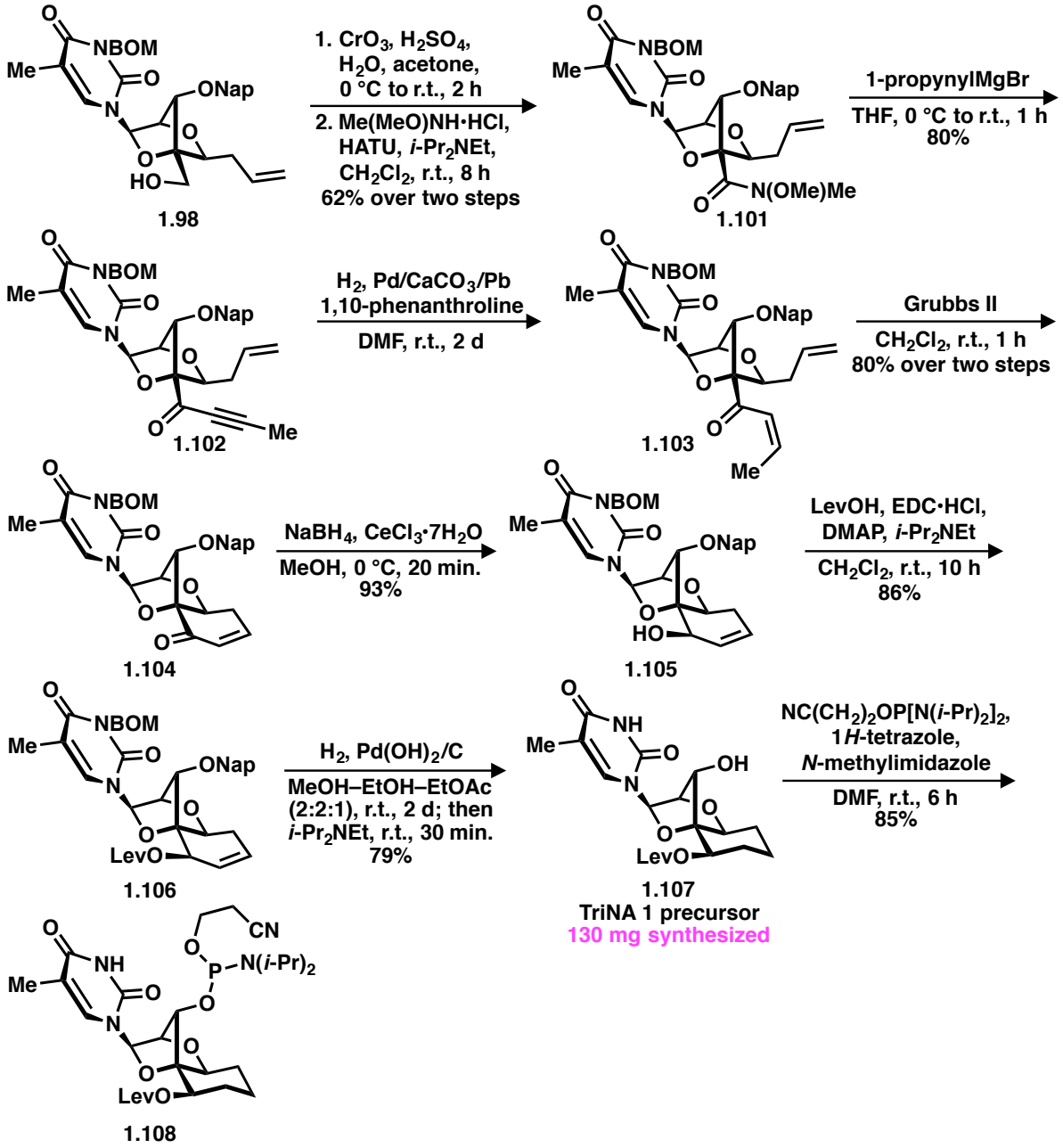

Scheme 1.18 – Completion of the synthesis of a TriNA 1 monomer.

By protecting the C5′-hydroxy group in **1.106** as the corresponding *p*-nitrobenzoate ester instead (**1.109**, *Figure 1.17*, p. 51), a crystalline compound was obtained, which allowed

the stereochemistry of the tricyclic nucleoside to be further substantiated through X-ray crystallographic analysis.

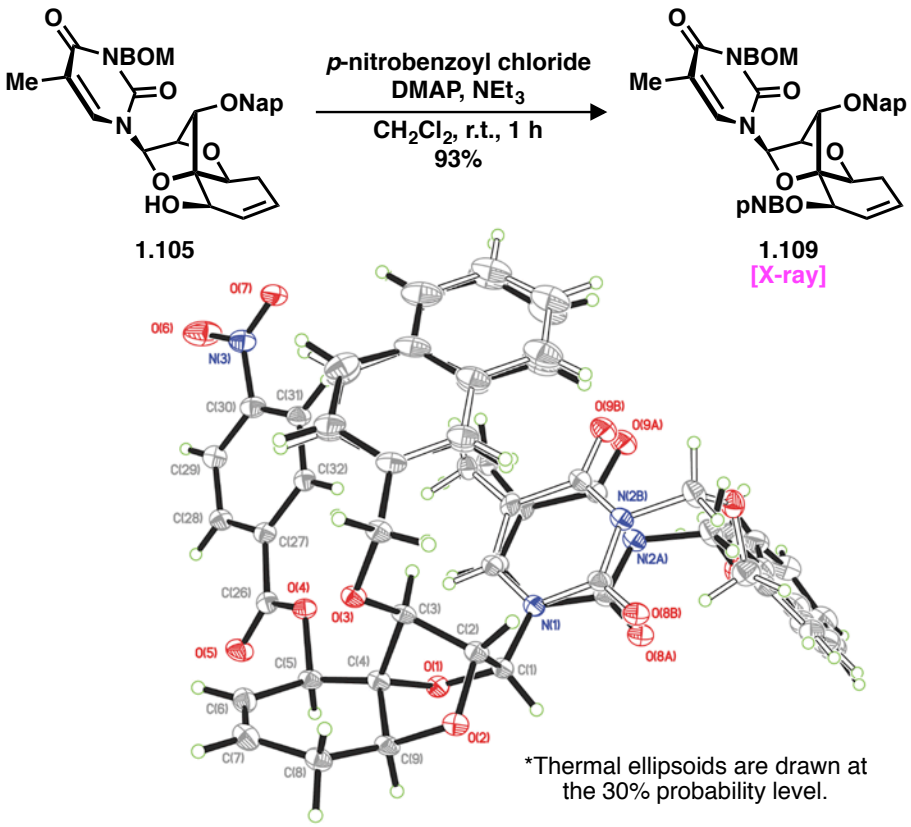

Figure 1.17 – Verification of the tricyclic scaffold of TriNA 1.

1.5 Duplex Thermal Stability Measurements

The synthesized tricyclic nucleosides were ultimately evaluated in T_m studies to determine the stability bestowed upon oligonucleotide duplexes by virtue of incorporating locked nucleic acid monomers in which torsion angle γ had been further constrained. Measured values of T_m refer to the midpoint on a curve of UV absorption versus temperature, and are indicative of the point at which 50% of an oligonucleotide duplex has been unwound into the corresponding single strands;[45,46] as such, the measured values correlate with the stability of oligonucleotide duplexes. The T_m measurements provided in the following sections are reported relative to an unmodified sequence of DNA that was hybridized to complementary DNA or RNA, and as such they are shown as the difference (ΔT_m). Consequently, positive values are indicative of a stabilizing influence relative to the control, while negative values reveal a destabilizing influence.

1.5.1 Duplex Thermal Stability Measurements for α-L-TriNA 1 and 2

Monomers of α-L-TriNA 1 and 2 were incorporated into two previously-described oligodeoxynucleotide sequences[124,125] for the purpose of evaluating their influence on the stability of DNA–DNA or DNA–RNA duplexes, as compared to the unmodified sequences (*Table 1.4*). Relative to the unmodified DNA sequence, incorporation of the α-L-TriNA 1 monomer (**1.27**, *Table 1.4*) in a stretch of deoxythymidine residues was found to be quite stabilizing when it was hybridized to complementary strands of DNA (ΔT_m +2.6 °C/mod., entry 1, *Table 1.4*) or RNA (ΔT_m +7.1 °C/mod., entry 1, *Table 1.4*). In line with our initial objective, α-L-TriNA 1 (**1.27**, *Table 1.4*) was also found to be further stabilizing relative to the α-L-LNA scaffold (**1.11**, *Table 1.4*): the measured T_m values for an oligodeoxynucleotide (entry 1, *Table 1.4*) containing α-L-TriNA 1 were 1.2 °C higher than those containing α-L-LNA when hybridized to DNA, and 1.4 °C greater when hybridized to complementary RNA. To provide a sequence-dependent context, the α-L-TriNA 1 monomer was incorporated in a mixed purine–pyrimidine sequence (entries 2–4, *Table 1.4*), which further confirmed the stabilizing influence conferred by α-L-TriNA 1. On average, oligonucleotides containing α-L-TriNA 1 showed duplex thermal stabilities that were 0.4 °C higher than those containing α-L-LNA when hybridized to DNA, and 0.9 °C greater when hybridized to complementary RNA.

In fact, in one instance (entry 3, *Table 1.4*), the inclusion of α-L-TriNA 1 in an oligodeoxynucleotide led to a T_m increase of 8.3 °C vs. RNA, as compared with the unmodified DNA sequence, and an increase of 2 °C compared with the corresponding α-L-LNA-modified oligodeoxynucleotide. This increase in duplex thermal stability was highly encouraging, and provided a firm endorsement for the potential that the dual-conformational-restriction strategy holds for stabilizing DNA–DNA and DNA–RNA duplexes.

Table 1.4 – Duplex thermal stability of α-L-TriNA-modified oligonucleotides.

1.11
α-L-LNA

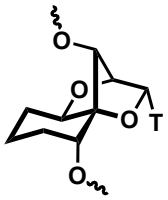

1.27
α-L-TriNA 1

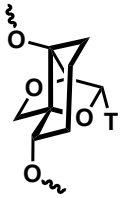

1.28
α-L-TriNA 2

		ΔT_m / Mod. versus DNA (°C)[b]			**ΔT_m / Mod. versus RNA (°C)**		
Entry	**Sequence (5′ to 3′)[a]**	**α-L-LNA**	**α-L-TriNA 1**	**α-L-TriNA 2**	**α-L-LNA**	**α-L-TriNA 1**	**α-L-TriNA 2**
1	d(GCGTT**T**TTTGCT)	+1.4	+2.6	–2.6	+5.7	+7.1	+1.2
2	d(CCAG**T**GATATGC)	+3.8	+3.0	-	+5.6	+5.3	-
3	d(CCAGTGA**T**ATGC)	+6.5	+7.4	+2.3	+6.3	+8.3	+4.4
4	d(CCAGTGATA**T**GC)	+4.4	+4.4	-	+4.5	+4.7	-
Average ΔT_m / Modification		**+4.0**	**+4.4**	**–0.2**	**+5.5**	**+6.4**	**+2.8**

[a]Red boldface letters indicates modified nucleotide, base code: T = thymine, U = uracil, C = cytosine, A = adenine and G = guanine; [b]T_m values were measured in 10 mM sodium phosphate buffer (pH 7.2) containing 100 mM NaCl and 0.1 mM EDTA. Sequence of DNA complements: 5′-d(AGCAAAAAACGC)-3′ for entry 1 and 5′-d(GCATATCACTGG)-3′ for entries 2–4. Sequence of RNA complements: 5′-r(AGCAAAAAACGC)-3′ for entry 1 and 5′-r(GCAUAUCACUGG)-3′ for entries 2–4. An unmodified sequence of DNA was hybridized to complementary DNA or RNA as a control and the tabular values are reported relative to that reference: T_m = 49.1 °C vs. DNA and 46.0 °C vs. RNA for entry 1 (d(GCGTTTTTTGCT)); and 47.3 °C vs. DNA and 43 °C vs. RNA for entries 2–4 (d(CCAGTGATATGC)).

Conversely, it was established that on average, oligodeoxynucleotides modified with α-L-TriNA 2 monomers (**1.28**) did not have a stabilizing influence on DNA–DNA duplexes and in one instance its inclusion was found to be significantly destabilizing (entry 1, *Table 1.4*). When hybridized with RNA, α-L-TriNA-2-containing duplexes were stabilizing relative to unmodified DNA sequences (average ΔT_m +2.8 °C/mod., *Table 1.4*), but only by half the amount conferred by the more readily accessible α-L-LNA modification (**1.11**). This mirrors the previous observation for the incorporation of (*R*)- or (*S*)-configured methyl groups at the C5′ position of α-L-LNA, where 5′-(*R*)-methyl analogue **1.15** was found to provide a

stabilization on par with α-L-LNA (**1.12**) and 5′-(*S*)-analogue **1.16** was comparatively less-stabilizing (*Figure 1.12*, p. 21).[77] Nevertheless, although the α-L-TriNA 2 modification was less stabilizing compared with either α-L-LNA or α-L-TriNA 2, its study underscored the importance of the C2′–C4′ anhydro bridge. A previously-synthesized bicyclic analogue of α-L-TriNA 2,[87] which lacks the anhydro bridge (i.e., *cis*-α-L-[4.3.0]bicyclo-DNA), was found to be highly destabilizing when incorporated in oligodeoxynucleotides and hybridized to DNA (ΔT_m –8.8 °C/mod., with same site of modification as entry 1 in *Table 1.4*) or RNA (ΔT_m –3.7 °C/mod., with same site of modification as entry 1 in *Table 1.4*). Consequently, it appears that locking the conformation of the sugar backbone with the anhydro bridge imparts a significant advantage compared to restricting torsion angle γ alone.

Table 1.5 – Mismatch discrimination properties of α-L-TriNA-modified oligonucleotides.

		ΔT_m / Mod. versus RNA (°C)[a]			
		Match (°C)	Mismatch Discrimination[b] [T_m(mismatch) – T_m(match)] (°C)		
Entry	**Modification**	**X = A**	**X = G**	**X = C**	**X = U**
1	DNA	0.0[c]	–4.1	–13.0	–13.2
2	α-L-LNA (**1.10**)	+5.7	–4.7	–14.8	–13.5
3	α-L-TriNA 1 (**1.27**)	+7.1	–5.5	–16.7	–17.0
4	α-L-TriNA 2 (**1.28**)	+1.2	–5.7	–14.3	–12.1

[a] T_m values were measured in 10 mM sodium phosphate buffer (pH 7.2) containing 100 mM NaCl and 0.1 mM EDTA using 5′-d(GCGTT**T**TTTGCT)-3′, where the bold and underlined nucleotide indicates the site of modification; the complementary sequence of RNA was 5′-r(AGCAAA**X**AACGC)-3′. Base code: T = thymine, U = uracil, C = cytosine, A = adenine and G = guanine; [b] Mismatch discrimination values were calculated by subtracting the T_m measured versus the mismatched RNA complement (X = G, C, or U) from the T_m measured versus the matched RNA complement (X = A) for each modification; [c] T_m of unmodified DNA control used as reference was 49.1 °C vs. RNA.

Since the ability of an antisense transcript to discriminate between complementary strands of RNA is quite important when designing an antisense therapeutic,[41] the ability of α-L-TriNA 1 and 2 to discriminate between mismatched complements of RNA was also determined (*Table 1.5*). Monomers of α-L-LNA, α-L-TriNA 1, and α-L-TriNA 2 were incorporated at the bold and underlined position of the 5′-d(GCGTT**T**TTTGCT)-3′ oligodeoxyribonucleotide sequence and hybridized to a complementary strand of RNA, 5′-r(AGCAAA**X**AACGC)-3′, in which the site indicated by **X** includes a different nucleobase on the nucleoside scaffold. Both α-L-TriNA 1 and 2 exhibited excellent mismatch discrimination properties, with the values observed for α-L-TriNA 1 (entry 3, *Table 1.5*) being particularly

impressive in that they provided an additional improvement over α-L-LNA (entry 2, *Table 1.5*).

To address the origin of the differences in duplex thermal stability observed between α-L-TriNA 1 and 2, as compared with the parent α-L-LNA scaffold, a closer examination of the structures of the monomers overlaid on the NMR structure solution of an α-L-LNA-modified DNA–RNA duplex was made (*Figure 1.18*). While the bulk of the cyclohexane moiety in α-L-TriNA 1 is expected to lie on and extend into the major groove of the modified duplex, the added bulk of the six-membered ring in α-L-TriNA 2 appears to be directed into the minor groove. As a consequence of these orientations, in the initial model for α-L-TriNA 2, there is likely a pair of close contacts between the methylene moieties of the cyclohexane ring and the

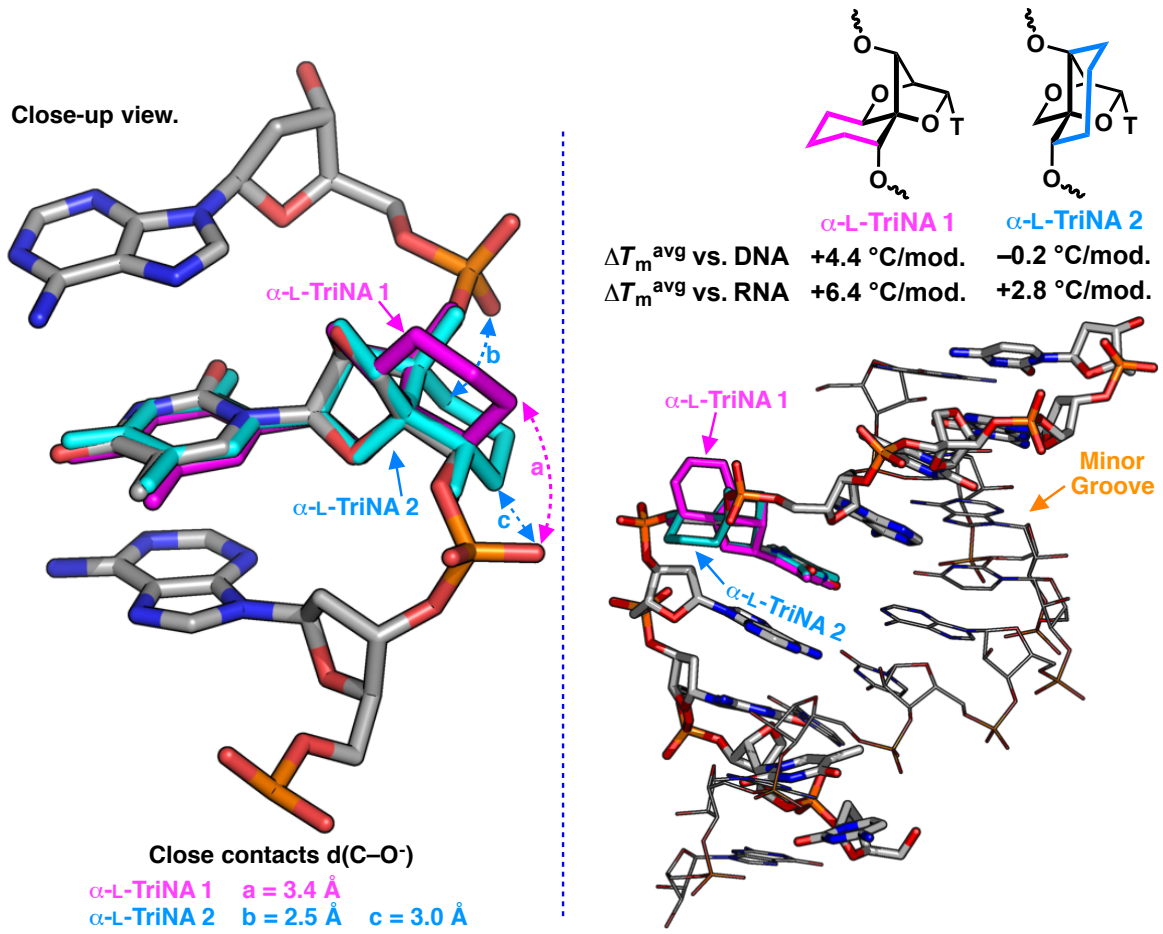

Overlay of α-L-TriNA 1, α-L-TriNA 2, and an α-L-LNA nucleotide in the NMR structure solution of an α-L-LNA-modified DNA–RNA duplex that is intermediate between A- and B-form (PDB: 1OKF).

Figure 1.18 – Overlay of α-L-TriNA 1 and 2 on an α-L-LNA-modified DNA–RNA duplex.

charged, non-bridging oxygen atoms of the phosphodiester backbone; the expected distances are ~2.5 Å and ~3.0 Å, with the former likely having a larger influence on the destabilization.

While this interaction may, in principle, be partially alleviated through additional rotations along the phosphodiester backbone, it would likely lead to less-ideal torsion angles along the rest of the backbone and the added bulk of the cyclohexane ring may nevertheless further disrupt the network of water molecules that typically lines the sugar–phosphate backbone.[72,90,91] In the case of α-L-TriNA 1, the closest contact between the cyclohexane moiety and a non-bridging oxygen atom is further away (~3.4 Å) and the additional interaction is not present, which is one potential explanation for the observed differences in duplex thermal stability between α-L-TriNA 1 and 2.

1.5.2 Duplex Thermal Stability Measurements for TriNA 1 and 2

Similar to the approach taken for α-L-TriNA 1 and 2, monomers of TriNA 1 and 2 were incorporated into a previously-described oligodeoxynucleotide sequence[126] for the purpose of evaluating their influence on the stability of DNA–RNA duplexes, as compared to the unmodified sequences (*Table 1.6*). For comparison, the tricyclic analogues were evaluated against LNA, as well as the corresponding 6′-(*S*)- and 6′-(*R*)-methyl-LNA analogues – *S*-cEt (**1.110**) and *R*-cEt (**1.111**), respectively. Furthermore, the positional dependence of the incorporated monomers was explored by measuring T_m values for sequences in which the precise location of the monomer along the oligodeoxyribonucleotide sequence varied.

Overall, TriNA 1 and 2 were found to have a stabilizing influence on DNA–RNA duplexes, when the monomers were incorporated into oligodeoxyribonucleotides at various positions along the sequence, as compared against an unmodified DNA control sequence (entries 1–4, *Table 1.6*). Regardless of the position of the modification, TriNA 2 (**1.26**) was more stabilizing than TriNA 1 (**1.25**), with average ΔT_m values of +6.2 °C and +4.4 °C, respectively. By comparison, the average ΔT_m values measured for oligodeoxynucleotides modified with LNA, *S*-cEt, or *R*-cEt monomers was +6 °C. In a sense, the increased stability imparted by TriNA 2 compared with TriNA 1 mirrors the trend observed for the incorporation of (*S*)- or (*R*)-configured methyl groups at the C5′ position of LNA (*Figure 1.12*, p. 21): the former (**1.14**) was highly-stabilizing – on par with LNA – and latter (**1.13**) comparatively less-

stabilizing.[48] In that system, 5′-(*R*)-methyl-LNA analogue **1.13** was proposed to be less-stabilizing as a consequence of a potential rotation around in torsion angle γ brought about by the presence of the added methyl group. In the TriNA 1 modification, rotation about this torsion angle is limited by virtue of the cyclohexane moiety, and accordingly it reveals that restricting rotation around torsion angle γ has an overall positive influence on duplex thermal stability in this scaffold. Furthermore, it appears that the additional bulk of the cyclohexane ring is actually well tolerated as compared against the methyl group in 5′-(*R*)-methyl-LNA analogue **1.13**.

Table 1.6 – Duplex thermal stability of TriNA-modified oligonucleotides.

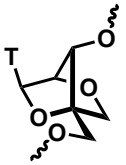

1.10
LNA

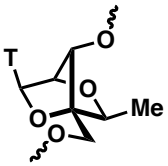

1.110
***S*-cEt**

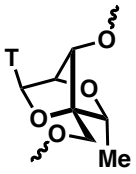

1.111
***R*-cEt**

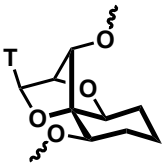

1.25
TriNA 1

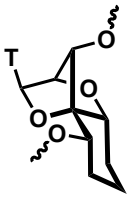

1.26
TriNA 2

		ΔT_m / Mod. versus RNA (°C)[b]				
Entry	**Sequence (5′ to 3′)[a]**	**LNA**	***S*-cEt**	***R*-cEt**	**TriNA 1**	**TriNA 2**
1	d(GGA**T**GTTCTCGA)	6.3	6.3	6.6	5.3	6.8
2	d(GGATG**T**TCTCGA)	5.6	5.1	5.6	4.0	6.1
3	d(GGATGT**T**CTCGA)	7.0	6.9	7.0	4.5	6.4
4	d(GGATGTTC**T**CGA)	5.0	4.7	4.6	3.6	5.5
Average ΔT_m / Modification		**6.0**	**5.8**	**6.0**	**4.4**	**6.2**

[a]Red boldface letters indicate site of modified nucleotide, base code: T = thymine, U = uracil, C = cytosine, A = adenine and G = guanine; [b]T_m values were measured in 10 mM sodium phosphate buffer (pH 7.2) containing 100 mM NaCl and 0.1 mM EDTA and the modified sequences were hybridized to complementary RNA, 5′-r(UCGAGAACAUCC)-3′. An unmodified DNA sequence was hybridized to complementary RNA as a control and the duplex had a T_m of 49.3 °C.

Although TriNA 2 displayed stabilization properties that were on par with those for LNA and the 6′-methyl analogues of LNA (i.e., *S*-cEt and *R*-cEt), a more pronounced increase in duplex thermal stabilization over those scaffolds was not observed, as was analogously noted for α-L-TriNA 1 over α-L-LNA (*Table 1.4*, p. 53). For additional insight into the influence of fusing a cyclohexane ring to the scaffold of LNA, the monomeric units of TriNA 1 and 2 were overlaid on the X-ray structure solution of an *S*-cEt-modified DNA duplex (*Figure 1.19*, p. 58). An inspection of the structural overlay reveals that the added bulk of the six-membered ring in TriNA 2 is expected to lie at the edge of and extend towards the minor

groove of the modified duplex, whereas it lies at and is directed towards the major groove in TriNA 1. Consequently, the cyclohexane moiety of TriNA 1 is expected to come into closer contact with one of the charged, non-bridging oxygen atoms in the phosphodiester backbone at the 5′-end of the monomer. Explicitly, visual analysis of the structures suggested that the TriNA 1 may experience a tight contact between one of the non-bridging oxygen atoms of the 5′-phosphodiester linkage and the (*R*)-5′-methylene group of the carbocyclic ring (~2.7 Å). In contrast, the analogous distance for TriNA 2 is ~3.2 Å, and the tightest contact (~2.9 Å) is likely between the (*S*)-5′-methylene group and the uncharged 3′-oxygen atom of the 3′-adjacent nucleotide.

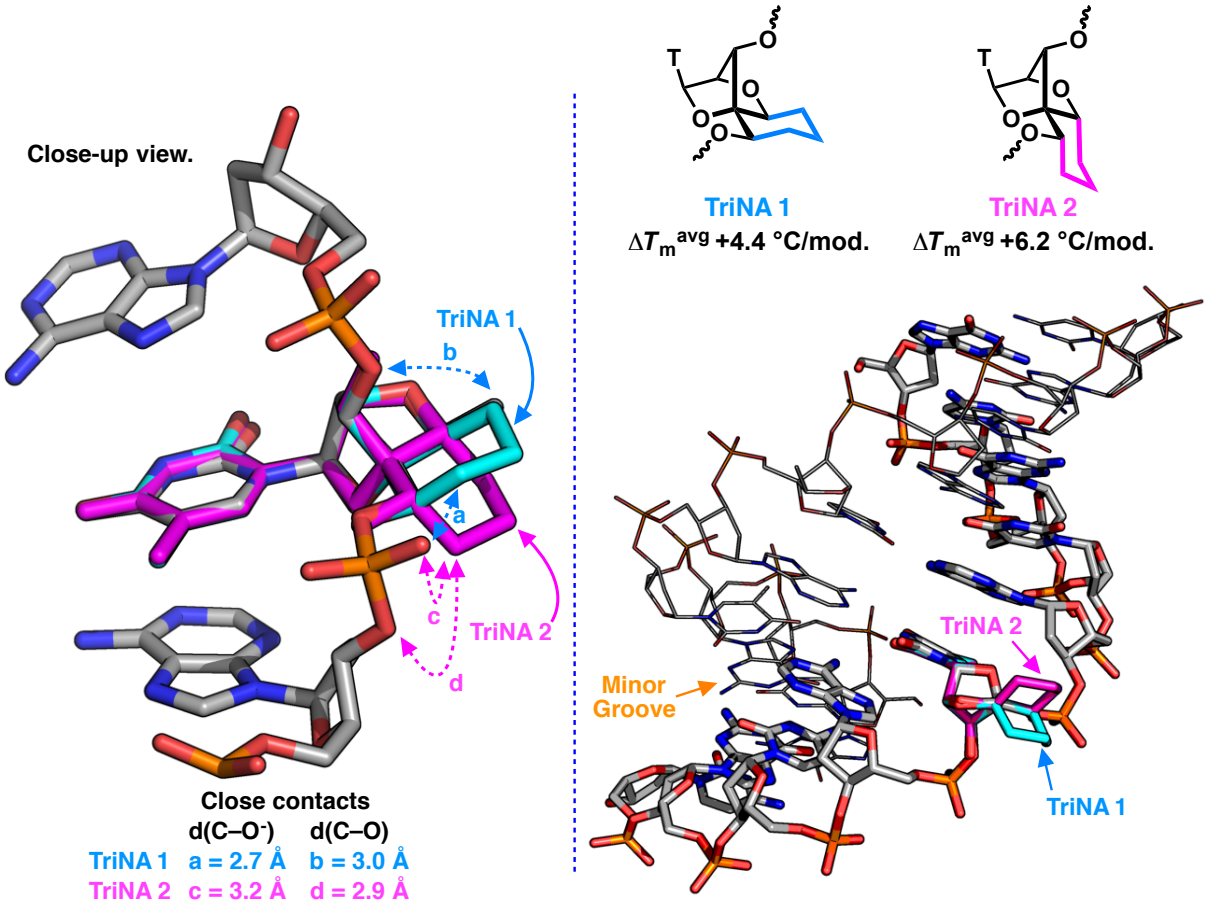

Figure 1.19 – Overlay of TriNA 1 and 2 on an *S*-cEt-modified DNA–DNA duplex.

Although partial alleviation of this destabilizing interaction may be possible through additional rotations along the phosphodiester backbone, it would lead to altered torsional

angles along the rest of the backbone. Furthermore, given the differences in hydration of the sugar–phosphate backbone between duplexes with dissimilar structures (i.e., A-form vs. B-form), the added bulk of the cyclohexane ring may also disrupt the water molecules that bridge successive anionic oxygen atoms in the phosphate groups that line the backbone of the A-form duplex expected to be present for mimics of RNA.[72,90,91] In the case of TriNA 2, the closest contact is with a bridging oxygen atom at the same phosphodiester linkage, although another similar interaction is also present with TriNA 1. This provides one possible rationale for the observed differences in the ability of TriNA 1 and 2 to improve the stability of DNA–RNA duplexes through further conformational restriction of LNA.

1.6 Conclusions and Perspectives

Overall, the strategy of dual conformational restriction appears to be quite useful for stabilizing oligonucleotide duplexes, and the results of our study provide a firm endorsement of it (*Figure 1.20*). By incorporating two modes of conformational restriction – locking the furanose ring in an *N*- or *S*-type sugar pucker and further restricting rotation about torsional angle γ – it was possible to appreciably increase the stability of duplexes relative to their unmodified constructs to levels that were on par with, or better than, their contemporary locked nucleic acid analog standards (i.e. LNA and α-L-LNA). Significant improvements in the duplex-stabilizing properties of α-L-TriNA 1 (**1.27**, *Figure 1.20*) over the α-L-LNA scaffold (**1.11**) were particularly impressive, given that previous attempts to increase duplex thermostability by appending six-membered rings to restrict conformational freedom of the nucleoside furanose ring were unsuccessful.[127-130]

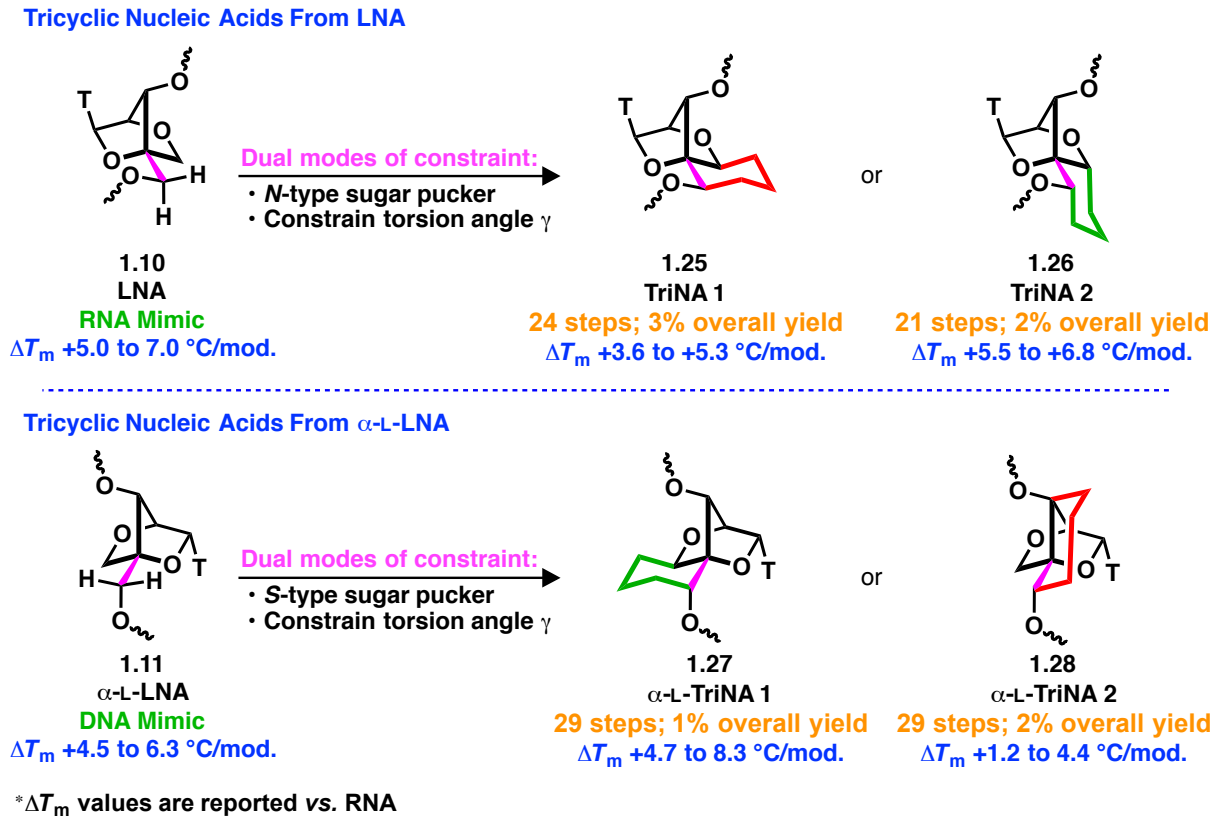

Figure 1.20 – Summary of the dual-conformational-restriction strategy.

Importantly, the studies described in this document provide additional confirmation that further limiting the degrees of freedom of a single nucleobase within an oligodeoxynucleotide can improve duplex thermal stability beyond the levels that have already been achieved. Furthermore, given that the locked nucleic acid scaffold can tolerate additional steric bulk in the form of a cyclohexane ring, it is conceivable that the properties of these tricyclic nucleic acids could be further improved by introducing other functional groups along the carbocyclic ring. The tricyclic analogues synthesized in the present thesis enhance hydrophobicity/lipophilicity along the major or the minor groove of oligonucleotide duplexes, but the incorporation of heteroatoms or other polar functional groups may also be used to augment the hydration network along the sugar–phosphate backbone, as well as further improve binding affinity, nuclease stability, and other properties of interest. Although further studies are required to elucidate the specific combination of factors responsible for the increase in thermal stability observed for the tricyclic nucleic acid analogues (i.e., enthalpy vs. entropy), [75] the implications of the current study are highly encouraging and provide a basis for further improvements to the properties of antisense oligonucleotides.

While the synthetic sequences used to access the tricyclic nucleosides are rather lengthy overall – 21 to 29 synthetic steps in total – they provided an excellent opportunity to validate the concept of *dual conformational constraint*. Moreover, given that the nucleobase is incorporated towards the midpoint of the synthetic sequences and there are multiple functional group handles en route to the six-membered cyclohexane ring, it would appear that the sequences themselves could be amenable to preparing additional analogues of interest. The low yields for the first-generation syntheses (1 to 3% overall) certainly highlight one of the major challenges associated with preparing highly-constrained tricyclic nucleic acid analogues, but they also provide new synthetic opportunities. By validating the concept that inspired our study of these tricyclic nucleosides, it is now much more appealing for future synthetic endeavours to focus on developing progressively more efficient and robust routes to access these unique scaffolds.

Chapter 2:

First-Generation Strategy for Synthesizing the Core of Nagilactone B

2.1 Introduction

The podolactone family of natural products comprises a number of unique truncated diterpenoids (**2.1**–**2.3**, *Figure 2.1*), whose scaffold incorporates a characteristic γ-lactone between C19 and C6 (ring D), and a δ-lactone between C12 and C14 (ring C).[131-133] Interest in this family of natural products stems, in part, from its broad spectrum of biological activity, which includes *in vivo* and *in vitro* antitumor,[134-138] anti-inflammatory,[139] antifeedant,[140,141] antifungal,[142,143] and plant growth regulatory activity,[144-146] as either an inhibitor or stimulant for the latter. A few examples of podolactones (**2.4**–**2.9**) and their reported biological activity are shown in *Figure 2.2*.

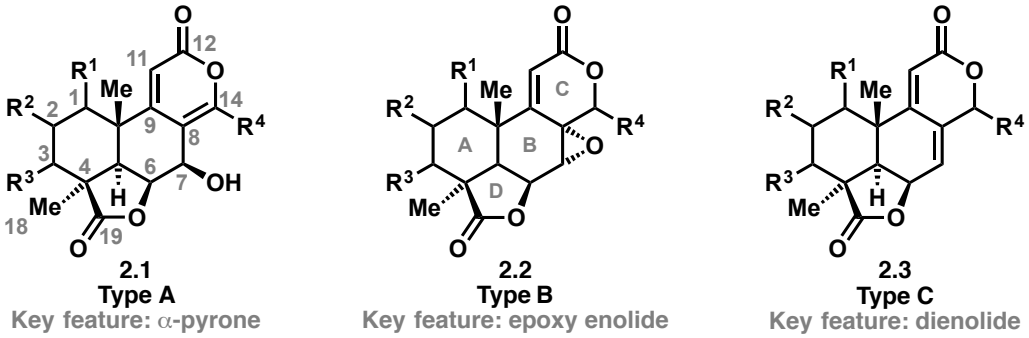

Figure 2.1 – General scaffold of podolactones.

Remarkably, members of the podolactone family of natural products have been isolated from two unique sources – plants related to the genus *Podocarpus* and filamentous fungi – with a unique biosynthetic origin proposed for compounds derived from each source.[147-149] Evidence in favour of two distinct biosynthetic pathways can be found in the fact that plant-based podolactones have a nor- or bisnorditerpenoid scaffold, while those isolated from fungal sources tend to have a tetranorditerpenoid core, in which four carbon atoms are absent from the parent diterpene precursor.

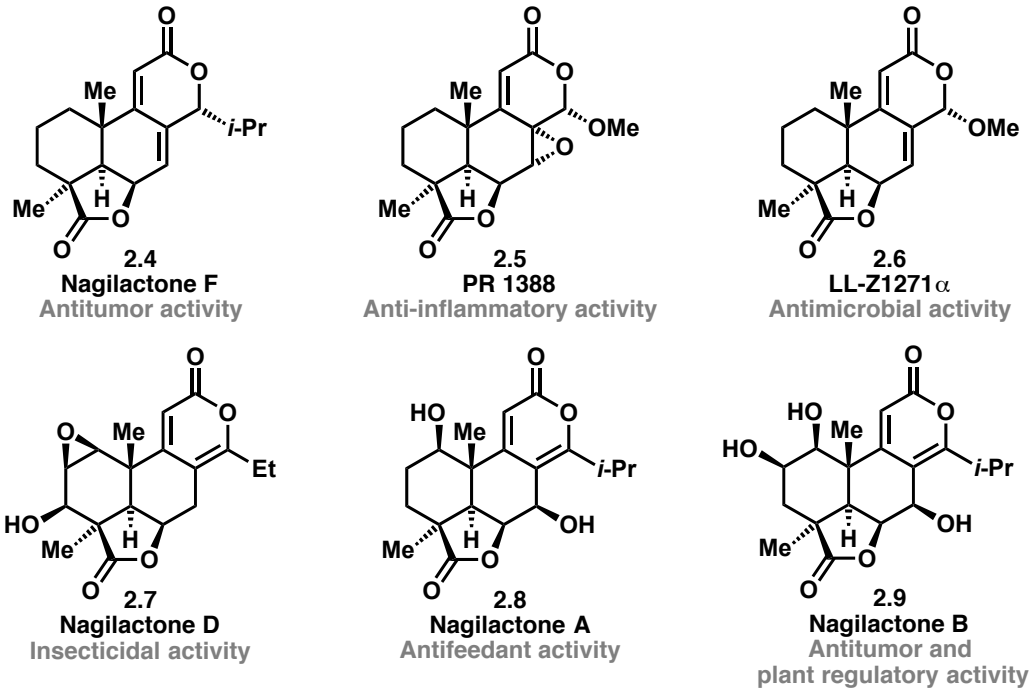

Figure 2.2 – Reported biological activity of select podolactones.

On the basis of previously isolated totarane diterpenes from the same plant that furnished the podolactones, a team of researchers from Osaka City University, led by Hayashi, proposed one possible biogenetic pathway for the plant-derived podolactones (*Scheme 2.1*).[147] The proposed biosynthesis begins with a *meta*-pyrocatechase-type fission of 12-hydroxytotarol-derived scaffolds (**2.10** to **2.11**), followed by ring closure and subsequent decarbonylation to afford the characteristic α-pyrone moiety found in A-type podolactones (**2.1**, *Figure 2.1*, p. 63). Support for the proposal is found in the fact that *meta*-pyrocatechase fission has been well documented to occur with other catechols, and hydroxy-acid intermediates have also been established as precursors for α-pyrones.[150-152]

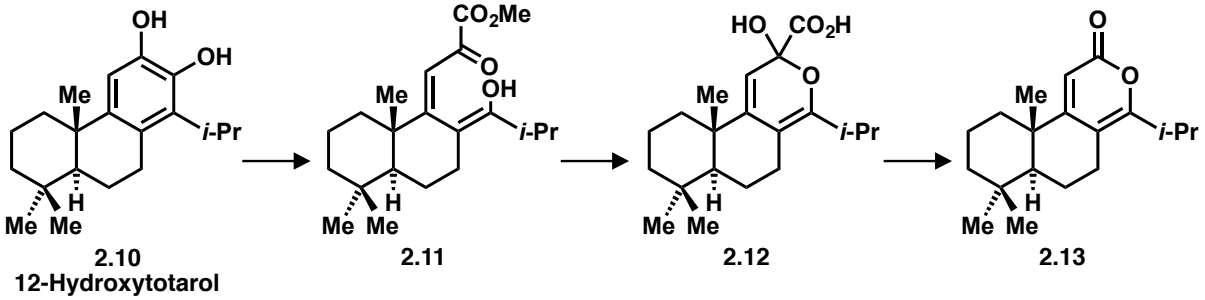

Scheme 2.1 – Proposed biosynthetic pathway for plant-derived podolactones.

In contrast, tetranorditerpenoid podolactones isolated from fungal sources are proposed, on the basis of isotope labelling experiments, to originate from *cis*/*trans*-communic acid (**2.14**) and its related diterpenes (*Scheme 2.2*).[148,149] Oxidative cleavage of the trisubstituted alkene in communic acid, followed by overall intramolecular cyclization of the carboxylic acids onto a pair of alkenes, establishes the dilactone core of **2.20**. Recent work by the group of Barrero, in which allylic alcohol **2.16** was converted directly to dilactone **2.20** by way of a bislactonization reaction, provides further evidence for the feasibility of the biosynthetic proposal.[143,153]

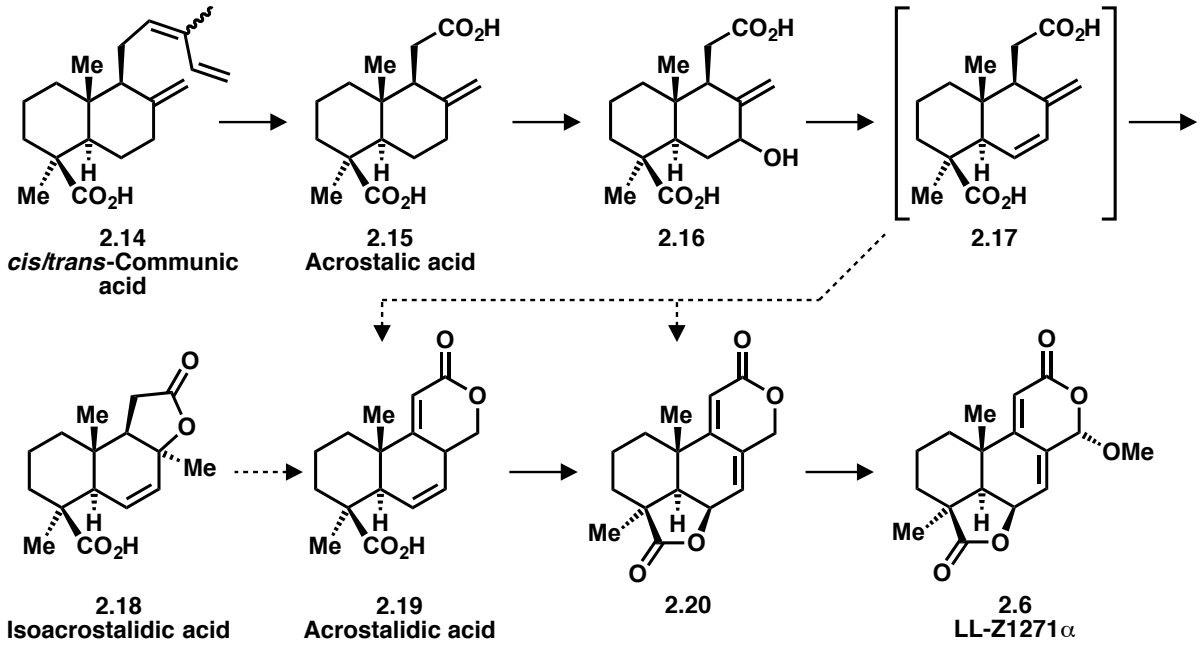

Scheme 2.2 – Proposed biosynthesis for fungi-derived podolactones.

Notably, both biosynthetic proposals have served as inspiration for strategies aimed at synthesizing members of the podolactone family of natural products. Key challenges for synthesizing podolactones include γ-lactonization to prepare the D ring, δ-lactonization for ring C, and the bislactonization oxidations required to incorporate the alcohol, epoxide, and alkene functional groups that decorate the underlying tetracyclic scaffold. A number of relevant examples are discussed in Section 2.2.

2.2 Previous Syntheses of Podolactones

Initial work on podolactones focused on their inherent reactivity, often for the purpose of preparing derivatives that could be compared with dilactones whose stereochemistry and structure had previously been established. The initial studies were incredibly insightful and revealed a striking stability that many podolactones had to common reagents, as a consequence of stereochemical shielding of the functional groups and their poor solubility in organic solvents.[154] The preliminary reports were likewise beneficial in that they led to the discovery of standard sequences for converting the more abundant A- and B-type podolactones into the less available C-type scaffold.[155] These breakthroughs were an immediate consequence of the unexpected reactivity certain scaffolds displayed towards standard chemical transformations (*Scheme 2.3*).[131,147,156-158] Building on these studies, a number of groups have since tackled the synthetic challenges associated with the podolactones.[131,143,145,159-166]

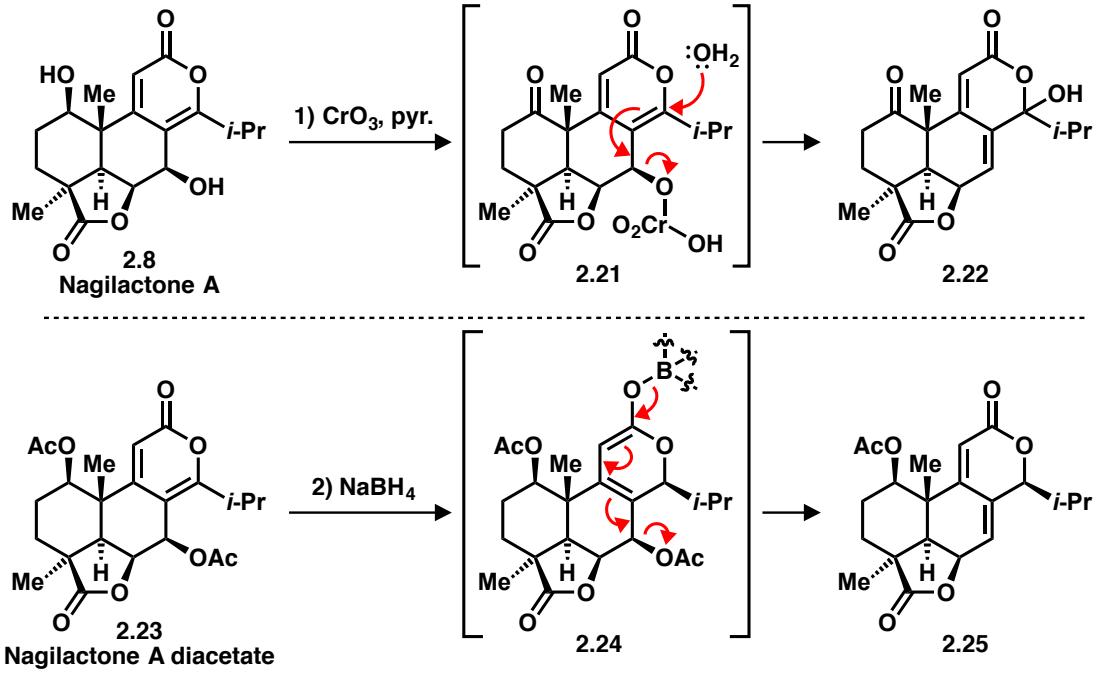

Scheme 2.3 – Unexpected reactivity of nagilactone A and nagilactone A diacetate.[147]

Despite many years of study, the structures of compounds within this family of natural products are still being confirmed and revised.[167] The following subsections describe a number of synthetic strategies that have been explored for this family of natural products.

2.2.1 Adinolfi Group's Synthesis of LL-Z1271α (1972)

The first synthesis of a podolactone was reported in 1972 by a group of researchers led by Adinolfi (*Scheme 2.4*).[159] This group successfully prepared the antibiotic LL-Z1271α (**2.6**) by using a known degradation product of marrubiin (**2.26**), a diterpene containing the A, B, and D rings of the intended target, and one which was previously synthesized by the authors.[168-170] By developing a synthesis around a degradation product (**2.27**), the team led by Adinolfi ultimately focused on installing ring C of the podolactone core.

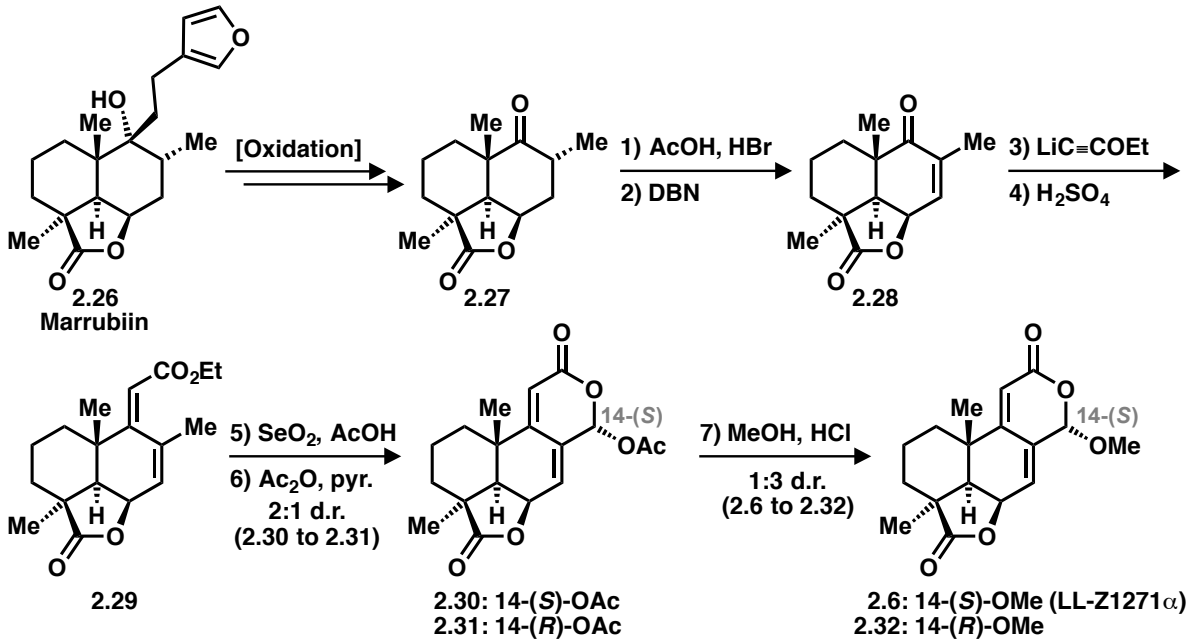

Scheme 2.4 – Synthesis of LL-Z1271α via degradation of marrubiin.[159]

To this end, they converted ketone **2.27** to the corresponding enone with a bromination-elimination sequence. Enone **2.28** was then treated with lithium ethoxyacetylide to furnish a tertiary propargylic alcohol, which underwent a Meyer-Schuster rearrangement[171] in the presence of a catalytic amount of concentrated sulfuric acid, to yield dienoic ester **2.29**. Selenium-dioxide-facilitated oxidation furnished a lactol, which could be acetylated in the presence of acetic anhydride and pyridine. Exposing acetates **2.30** and **2.31**, individually or as

a mixture of epimers, to hydrochloric acid in methanol gave a 1:3 mixture of LL-Z1271α (**2.6**) and its C14 epimer (**2.32**).

2.2.2 Welch Group's Synthesis of LL-Z1271α (1977)

In 1977 Welch's group reported the synthesis of racemic LL-Z1271α ((±)-**2.6**),[160] starting from (±)-Wieland–Miescher ketone **2.33**, which became accessible in larger quantities as a result of earlier efforts by Ramachandran and Newman.[172] The key features of the Welch group's approach include stereoselective methylation to establish the quaternary centre at C4, bromolactonization to form the γ-lactone, and an improvement on the acid-catalyzed Meyer-Schuster rearrangement[171] used by Adinolfi's group, which resulted in a more favourable anomeric ratio (*Scheme 2.5*).

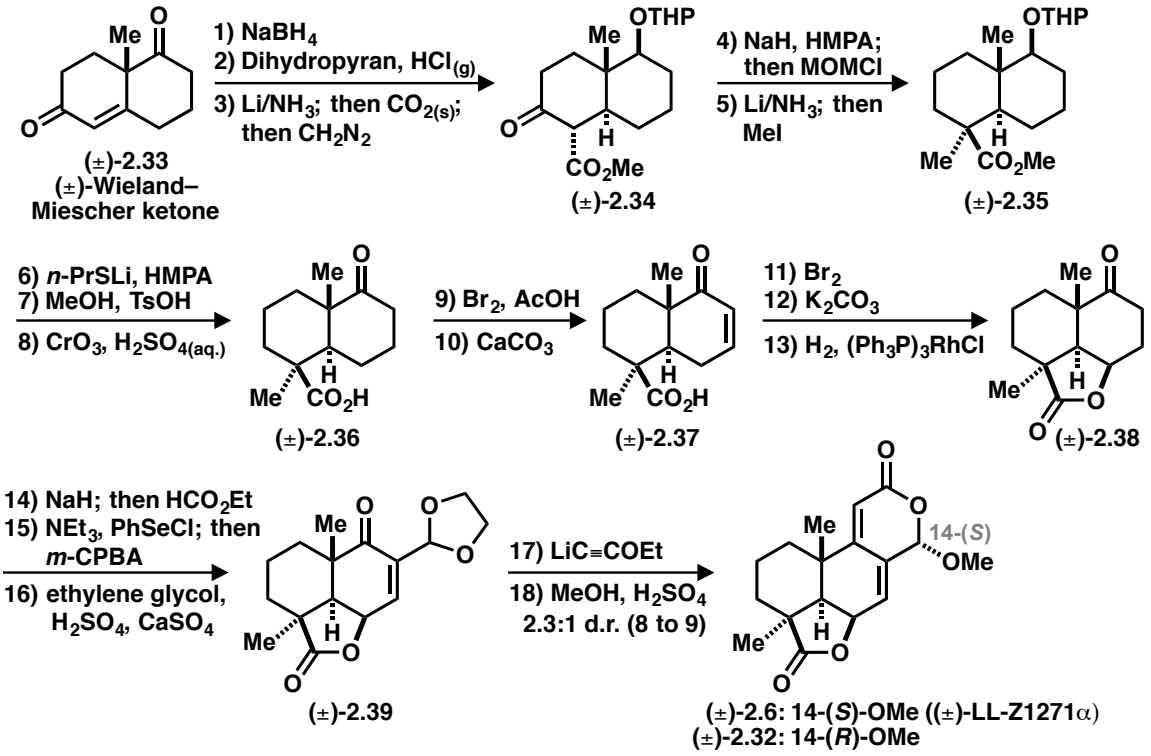

Scheme 2.5 –Synthesis of racemic LL-Z1271α from the Wieland–Miescher ketone.[160]

Reports from the Spencer group shed light on the first three steps of the synthesis (reduction with sodium borohydride, protection, and reductive carbomethoxylation), and provided access to β-keto ester (±)-**2.34**.[173] Unfortunately, direct methylation of the enolate of β-keto ester (±)-**2.34** is known to proceed from the β-face of the enolate, which would result in

abietic-type stereochemistry,[174,175] rather than the desired podocarpic stereochemistry.[176] To circumvent this challenge, Welch group's developed a novel elimination-alkylation reaction based on the work of Coates and Shaw,[177] which effected deoxygenation and stereoselective methylation in a single step, to furnish (±)-**2.35**. This sequence was an effective way to set the quaternary centre with the desired stereochemistry and concomitantly remove the ketone functional group. However, despite its appeal for the synthesis of LL-Z1271α, the advantage of the elimination-alkylation reaction is actually detrimental to the preparation of A-ring analogues, where the ketone may act as a functional group handle for further diversification.

The next crucial stage in the synthesis of (±)-LL-Z1271α revolved around the incorporation of the γ-lactone component into the scaffold. Welch's team initially envisaged that the carboxylic acid moiety in (±)-**2.37** could displace an allylic bromide that had been installed at C6, in the presence of potassium carbonate. While the desired lactone formed as expected, examination of the spectroscopic data of isolable intermediates revealed that allylic bromination had not taken place; instead, dibromide (±)-**2.40** (*Scheme 2.6*) arose through *trans*-diaxial ring opening of a bromonium ion intermediate. Nevertheless, in the presence of potassium carbonate, dibromide (±)-**2.40** was converted directly to lactone (±)-**2.42** through a sequence comprising *trans*-diaxial elimination of the bromide at C7 ((±)-**2.40** to (±)-**2.41**) and subsequent intramolecular S_N2' displacement of the bromide leaving group at C8, as a consequence of the close proximity and orientation of the carboxylate anion with respect to the alkene of the allylic bromide moiety.[178]

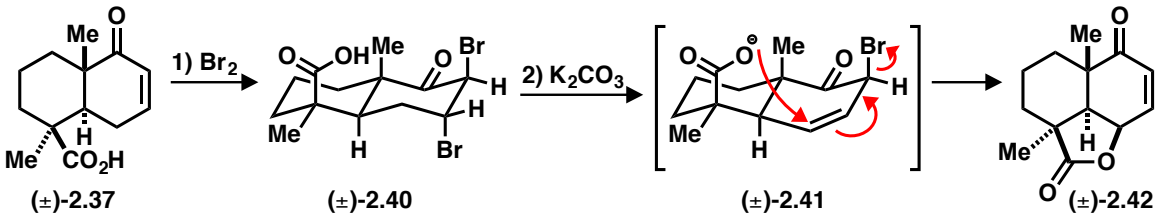

Scheme 2.6 – Bromolactonization of the carboxylic acid enone.

Finally, following a sequence of reactions that resulted in the incorporation of the acetal-protected aldehyde in (±)-**2.39**, the Welch group capped their synthesis of (±)-LL-Z1271α with a strategy reminiscent of that reported by Adinolfi's team five years earlier. Notably, the Welch group's judicious decision to include an acetal moiety allowed (±)-LL-Z1271α to be prepared directly via the Meyer-Schuster rearrangement strategy,[171] without the

need to proceed through an intermediate lactol. The consequence of their decision was a more favourable C14 anomeric ratio of (±)-**2.6** to (±)-**2.32** (*Scheme 2.5*), albeit still with significant opportunity for improvement.

2.2.3 Hayashi Group's Synthesis of Nagilactone F (1982)

Inspired by the proposed biosynthesis for plant-derived podolactones (*Scheme 2.1*, p. 64) and the extensive efforts they continually devoted to this family of natural products, the group of Hayashi successfully pursued and completed the first total synthesis of a norditerpenoid dilactone, nagilactone F (**2.4**).[161] Although the lack of functional group handles in ring A of nagilactone F (or podocarpic acid) certainly hampers the potential application of their synthetic approach to the preparation of ring-A analogues, the significant anticancer activity observed for nagilactone F, compared to its congeners, made it a particularly relevant target.[131,138] The key features of the Hayashi group's synthesis include the transformation of a phenolic ring into a δ-lactone, photochemical cyclization of a dienoic acid to install the δ-lactone, and radical-mediated lactonization to furnish the γ-lactone (*Scheme 2.7*).

The synthesis began with (*S*)-(+)-podocarpic acid (**2.43**), a natural product whose structure and absolute configuration were previously established.[179-181] Birch reduction of the phenolic ring and subsequent esterification of the acid furnished C9–C11-unsaturated-enone **2.44** (*Scheme 2.7*), which was reduced under catalytic hydrogenation conditions. The desired C13–C14-unsaturated enone was incorporated by way of a selenium-mediated *syn*-oxidation sequence,[182] which was inspired by work disclosed by the group of Spencer.[173] Lithium diisopropylcuprate was used to install the isopropyl side chain via conjugate addition, and the resultant enolate was directly trapped with phenylselenyl chloride and successively oxidized to enone **2.45**. Ozonolysis and Jones oxidation furnished ketoacid **2.46**. Notably, the group of Hayashi initially envisioned transforming ketoacid **2.46** into an α-pyrone and then converting it to a C-type scaffold using the previously established reactivity of the A-type podolactones (*Scheme 2.3*, p. 66).[147,155] Unfortunately, although the α-pyrone moiety was successfully incorporated into the scaffold (*Scheme 2.8*), attempts to install an appropriate leaving group at C7 did not bear fruit, and the strategy was eventually abandoned.

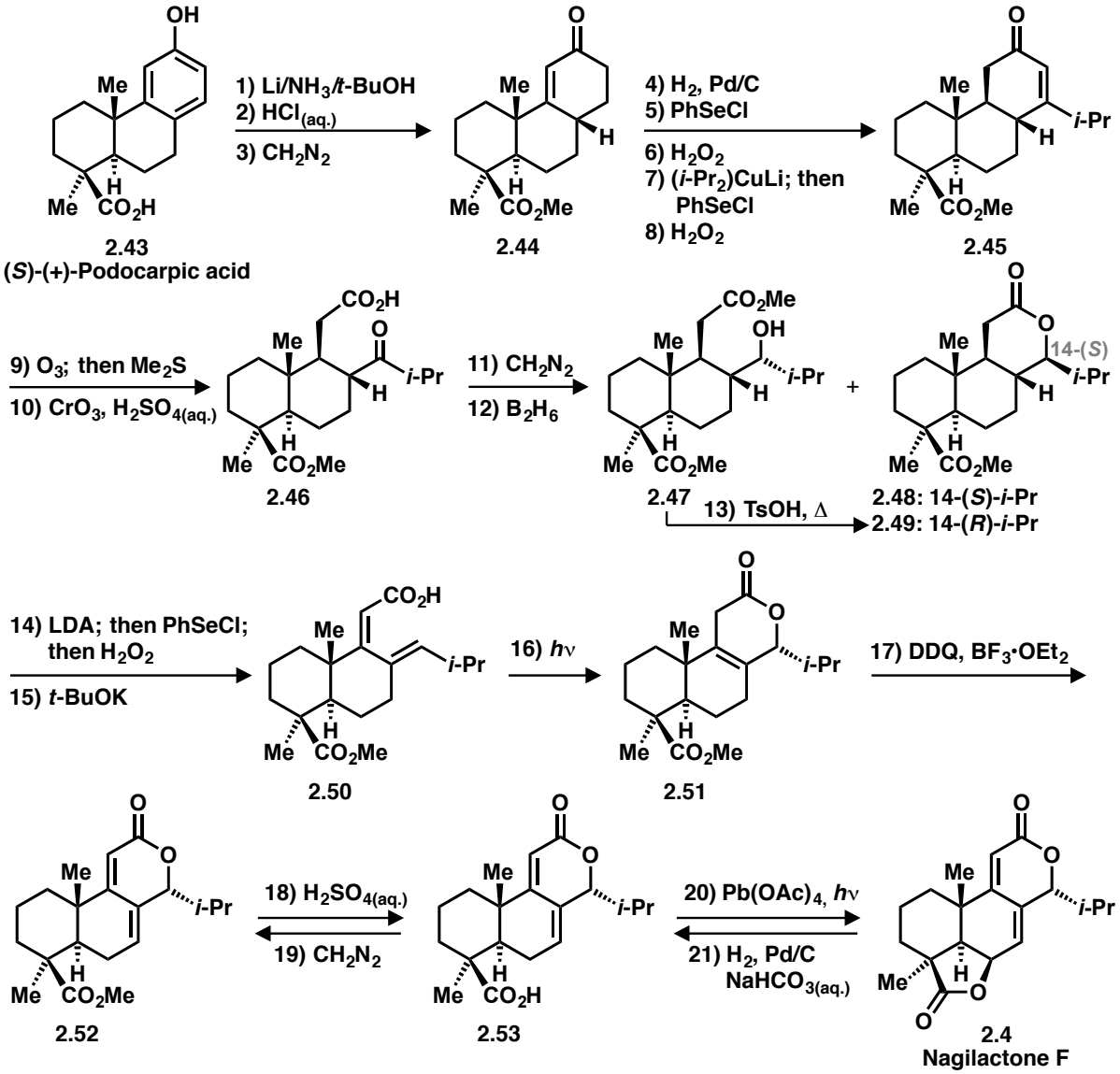

Scheme 2.7 – Synthesis of nagilactone F by Hayashi's group.[161]

Following the difficulties they encountered oxidizing α-pyrone **2.54** at C7, the Hayashi group focused their efforts on cyclizing ketoacid **2.46** (*Scheme 2.7*) to epimeric lactones **2.48** and **2.49**, following esterification and diborane reduction of the ketone. Although lactonization of hydroxy acid **2.47** (*Scheme 2.7*) required more forcing conditions, both lactones could be elaborated to the same intermediate – carboxylic acid **2.50** – with another selenium-mediated *syn*-oxidation sequence and successive elimination using potassium *tert*-butoxide. Irradiation of carboxylic acid **2.50** in ethanol with a medium-pressure mercury lamp gave exclusively lactone **2.51**, which was oxidized to the corresponding C7–

C8,C9–C11-unsaturated dienolide **2.52** with 2,3-dichloro-5,6-dicyano-1,4-benzoquinone in the presence of boron trifluoride. Hydrolysis of the methyl ester proved to be rather difficult under basic conditions, but was eventually realized in the presence of concentrated sulfuric acid, which provided access to the penultimate product. The Hayashi group's synthesis of nagilactone F was successfully realized through an allylic lactonization reaction, carried out by refluxing carboxylic acid diene **11** with lead(IV) acetate in benzene under a 15 W fluorescent lamp.

Despite the prominent reliance on selenium-mediated dehydrogenation sequences, Hayashi's group presented a rather elegant solution for establishing the stereochemistry of the C14 isopropyl group. Since that time, the intriguing properties of nagilactone F have inspired a number of improvements and complementary synthetic strategies for preparing members of the podolactone family of natural products.[145,162,163]

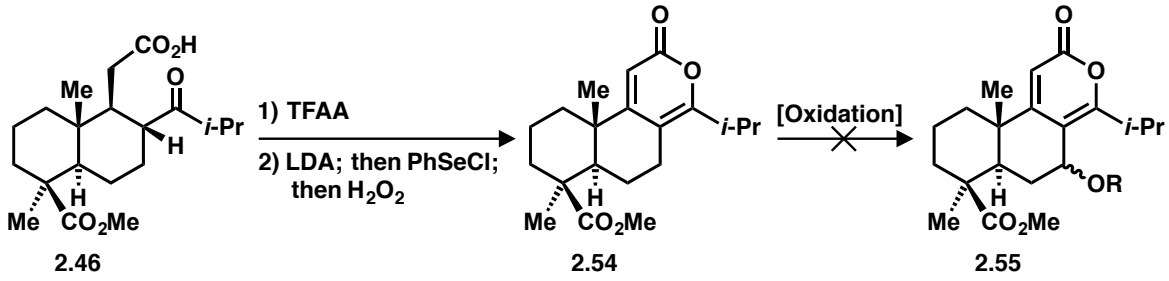

Scheme 2.8 – Alternative strategy studied by Hayashi's group.

2.2.4 Barrero Group's Synthetic Endeavours (1999–2002)

Similar to Hayashi's team, the Barrero group has also devoted a significant amount of effort to the synthesis of podolactones, as evidenced by the substantial number of articles they have published on this topic.[143,145,146,153,164] This subsection will focus on two of their synthetic strategies, one starting with communic acid and the other stemming from geraniol.

With communic acid, the proposed biosynthetic precursor for fungi-derived podolactones, as their starting material of choice, the Barrero group tackled the synthesis of several podolactones with a strategy that was complementary to that disclosed by Hayashi's team.[143,145] The key steps of the Barrero group's sequence include selective ozonolysis of *trans*-communic acid and an elegant palladium-catalyzed bislactonization reaction that was

used to incorporate the γ- and δ-lactone in one step (*Scheme 2.9*).[143,153] The regioselective ozonolysis reaction was accomplished at low temperatures, with a noticeable improvement in the yield[183] and practicality made possible by the availability of pure *trans*-communic acid from a conifer in Southern Spain (*Cupressus sempervirens*); previous syntheses required a difficult separation of *mirceo*-communic acid from its *cis*- and *trans*-isomers using silver-nitrate-impregnated silica gel.[145] Jones oxidation, diesterification, and selenium-mediated oxidation provided access to allylic alcohol **2.56**. The most efficient strategy for allylic elimination of the secondary hydroxy group was through a the corresponding triflate in the presence of tetrakis(triphenylphosphine)palladium(0). Subsequent demethylation of both esters afforded key dienoic diacid **2.17**, the dilactone precursor.

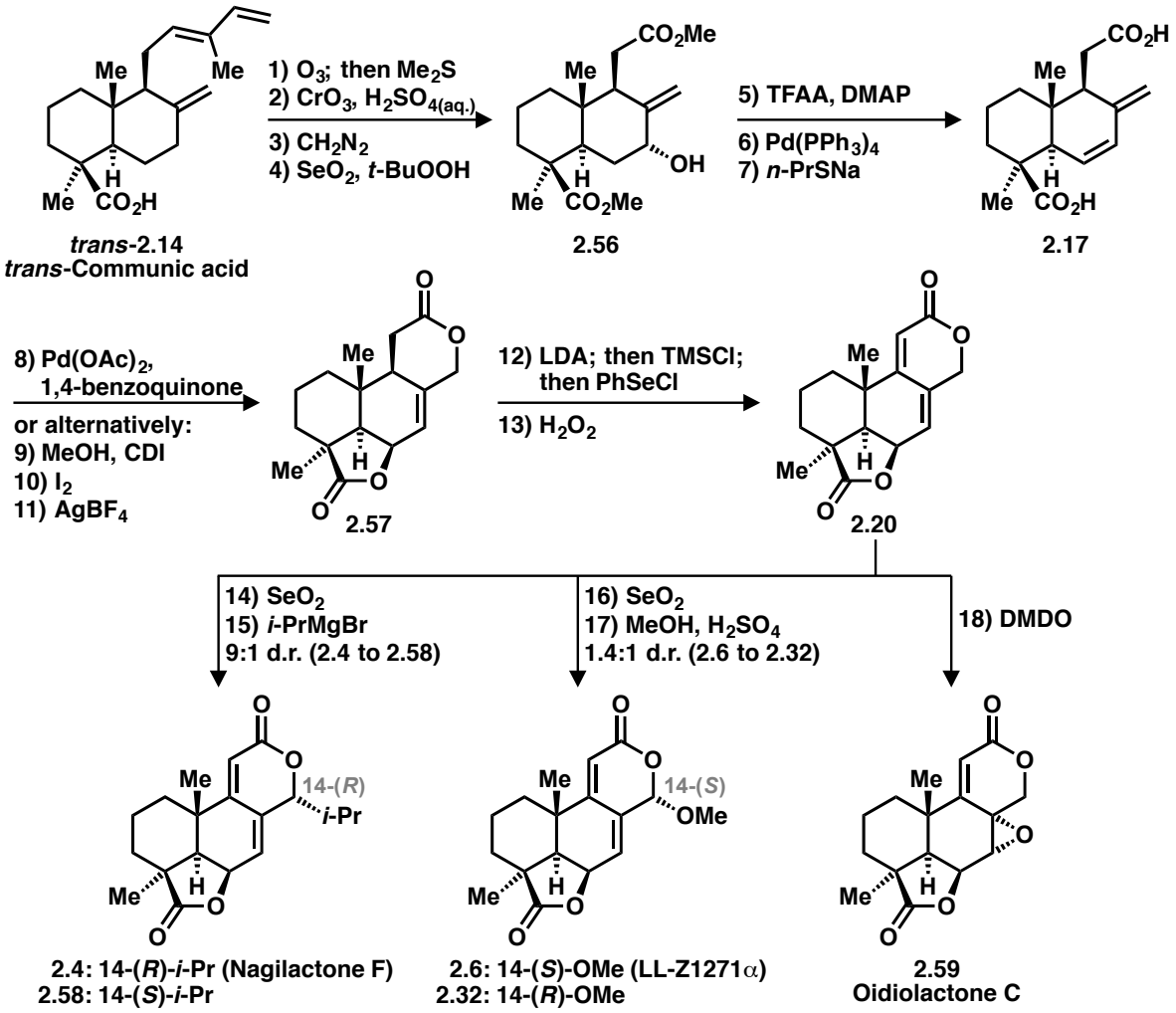

Scheme 2.9 - Synthesis of podolactones from *trans*-communic acid.[143,145]

The pivotal palladium-catalyzed 1,4-regioselective bislactonization reaction proceeded smoothly in the presence of 1,4-benzoquinone, efficiently installing both the γ- and δ-lactone in one step (**2.17** to **2.57**).[153] Although an intramolecular carboxylate-mediated lactonization reaction had been used in the past to construct a bicyclic scaffold in the presence of a palladium catalyst,[184,185] the disclosure by Barrero's group was the first example of an intramolecular dilactonization of a conjugated diene. Oxidation to the diene, using the typical selenium-mediated conditions, provided access to a key synthetic intermediate (**2.20**) that could be elaborated to a diverse group of podolactones. Epoxidation of diene **2.20** with dimethyldioxirane gave the B-type scaffold in oidiolactone C (**2.59**), while oxidation to the lactol with selenium generated a versatile intermediate that could be converted to LL-Z1271α (**2.6**) with methanol and sulfuric acid, or exposed to a Grignard reagent to access related alkyl analogues such as nagilactone F (**2.4**). Overall, the Barrero group's route was more efficient than those that came before it and it allowed for a greater degree of late-stage diversification, compared with the route disclosed by Hayashi's group.

As was alluded to during the description of the Welch group's synthesis of (±)-LL-Z1271α (*Scheme 2.5*, p. 68), one of the significant limitations with contemporary synthetic routes is their overall neglect of incorporating functional groups in ring A. The groups of de Groot[162,186] and Barrero[164] attempted to address these shortcomings through their respective syntheses of (±)-3β-hydroxynagilactone F and its 14-desisopropyl analogue (±)-**2.68**, the latter of which is described below in *Scheme 2.10*. Although the Barrero group intended to prepare the originally-reported structure of wentilactone B (**2.68**),[187] their diligence ultimately led to a structural revision of that natural product when they realized that the synthesized compound ((±)-**2.68**) was actually the 3β-OH regioisomer of naturally-occurring wentilactone B.* Their approach features two key steps: radical cyclization to generate the bicyclic decalone core and the previously described palladium-catalyzed bislactonization sequence.

Starting with geraniol (**2.60**), standard transformations led to a 4:1 mixture of homologated diol **2.61** and its *E*/*Z*-isomer, which could be separated. Regioselective

* Wentilactone B was assigned, on the basis of a comparison of its ^{1}H NMR spectrum with that of 2α-hydroxynagilactone F, to be the regioisomer of **2.68**, in which the hydroxy group has been transposed to the 2α-position instead.[164]

chlorination of the allylic alcohol and subsequent alkylation with the dianion of ethyl 2-methylacetoacetate afforded acyclic diene **2.62**, the starting material for the intended radical cyclization reaction. Inspired by work from Zoretic's group, Barrero's group effected oxidative free-radical cyclization of the acyclic precursor (**2.62**) using a 2:1 molar ratio of $Mn(OAc)_3$ to $Cu(OAc)_2$, which led to the previously-reported racemic bicyclic scaffold with the desired relative stereochemistry and an exocyclic alkene moiety ((±)-**2.63**).[188-190] Interestingly, asymmetric versions of this versatile reaction that make use of (–)-8-phenylmenthyl esters have been explored as well, with favourable diastereoselectivities observed.[190,191]

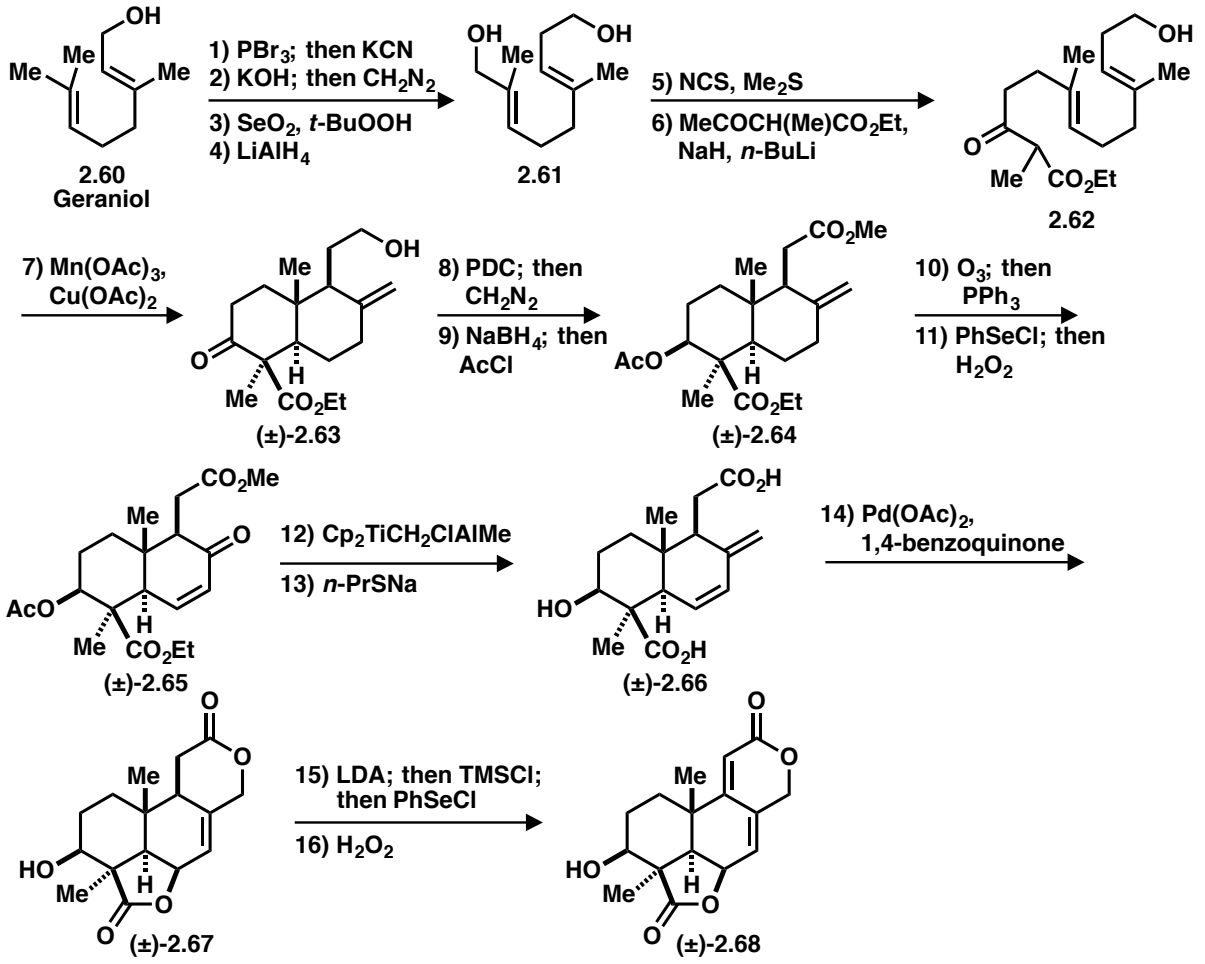

Scheme 2.10 – Racemic synthesis of the 3β-hydroxy regioisomer of wentilactone B.[164]

Oxidation of the primary alcohol, esterification, and a reduction–protection sequence led to diester (±)-**2.64** (*Scheme 2.10*). Ozonolysis and selenium-mediated dehydrogenation

afforded enone (±)-**2.65**, which paved the way for access to the corresponding diene with the Tebbe reagent.[192] Attempts to deprotect the ester led to a mixture of diacid (±)-**2.66** and the corresponding monoethyl ester; however, they were separable and the latter could be recycled. Regioselective bislactonization proceeded smoothly in the presence of palladium(II) acetate and 1,4-benzoquinone, using the same conditions reported for the Barrero group's synthesis of podolactones from *trans*-communic acid (*Scheme 2.9*, p. 73).[143] Oxidation to the diene, using phenylselenium chloride and hydrogen peroxide, afforded the dilactone diene product ((±)-**2.68**). Although the synthesis afforded an unnatural* and racemic product, it led to the structural revision of wentilactone B and ultimately unveiled a unique way to access podolactone scaffolds, including those that may contain functional groups in ring A.

2.2.5 Hanessian Group's Synthetic Approach to Podolactones (2009)

The Hanessian group's interest in podolactones can be traced back to work by Dr. Nicolas Boyer, who successfully developed a strategy to synthesize dilactones of type B and C,[165] using a route that was adapted from the Welch group's previously-disclosed synthesis of (±)-LL-Z1271α (*Scheme 2.5*, p. 68).[160] Notably, Hanessian and Boyer made a number of practical improvements to the Welch group's synthetic sequence, and they were ultimately able to modify the late-stage strategy in order to access seven different podolactones enantioselectively. More recently, the Hanessian group has also prepared analogues of type A podolactones, culminating in the synthesis of a ring A aromatic congener of urbalactone.[166] Key steps for the Hanessian–Boyer approach include reductive carbomethoxylation, bromolactonization, a Morita-Baylis-Hillman reaction, and an intermolecular Reformatsky-type reaction to access a versatile intermediate that was elaborated to a diverse group of podolactones (*Scheme 2.11*).[165]

The synthesis began with enantiopure (+)-Wieland–Miescher ketone ((+)-**2.33**), which was protected as the corresponding monoketal and subjected to a reductive carbomethoxylation in the presence of Mander's reagent (i.e., methyl cyanoformate) to furnish methyl ester **2.69**.[193-195] The ketone functional group was removed in two steps: conversion to its enol triflate and subsequent palladium-catalyzed reduction in the presence of tributyltin

* Unnatural with respect to the podolactones that have been isolated to date.

hydride.[196] Diastereoselective reduction of α,β-unsaturated ester **2.70** with magnesium turnings in methanol afforded the corresponding saturated ester in excellent yield.[197,198] Stereoselective methylation yielded α-branched methyl ester **2.71**, in which the quaternary stereocenters were effectively set. Although the four-step sequence (**2.69** to **2.71**) used to remove the ketone and set the quaternary centre was two steps longer than the Welch group's approach (*Scheme 2.5*, p. 68) – and the analogous reaction reported by the Theodorakis group[199] – it was significantly more robust and boasted a higher yield (79% versus less than 60%).

With the quaternary centre set, the focus of the synthesis shifted to incorporating the lactones, starting with the D ring γ-lactone. Deprotection of ketal **2.71** under acidic conditions, followed by IBX-mediated oxidation[200] furnished the C7–C8-unsaturated enone, whose ester functional group was hydrolyzed to the corresponding carboxylic acid with sulfuric acid. Hydroxymethylation at C8 was accomplished with an efficient Morita–Baylis–Hillman reaction[201] in the presence of aqueous formaldehyde and dimethylphenylphosphine and provided alcohol **2.27**. This was a notable improvement over the tactics used by Welch's group, and was made possible through the significant amount of research that was performed on the Morita–Baylis–Hillman reaction since the initial work by Welch's group.[202,203]

A bromolactonization reaction to incorporate the γ-lactone was successfully realized using the procedure reported by the Welch group (*Scheme 2.6*, p. 69). Protection of the primary alcohol as the triethylsilyl ether and a catalytic intramolecular Reformatsky-type reaction with ethyl iodoacetate in the presence of bis(triphenylphosphine)nickel(II) dichloride and diethylzinc furnished tertiary alcohol **2.74**. This alcohol was the critical intermediate used to prepare LL-Z1271α, nagilactone F, and a number of additional oidiolactones of interest, through a similar set of reaction conditions that were applied in a different sequence for each.

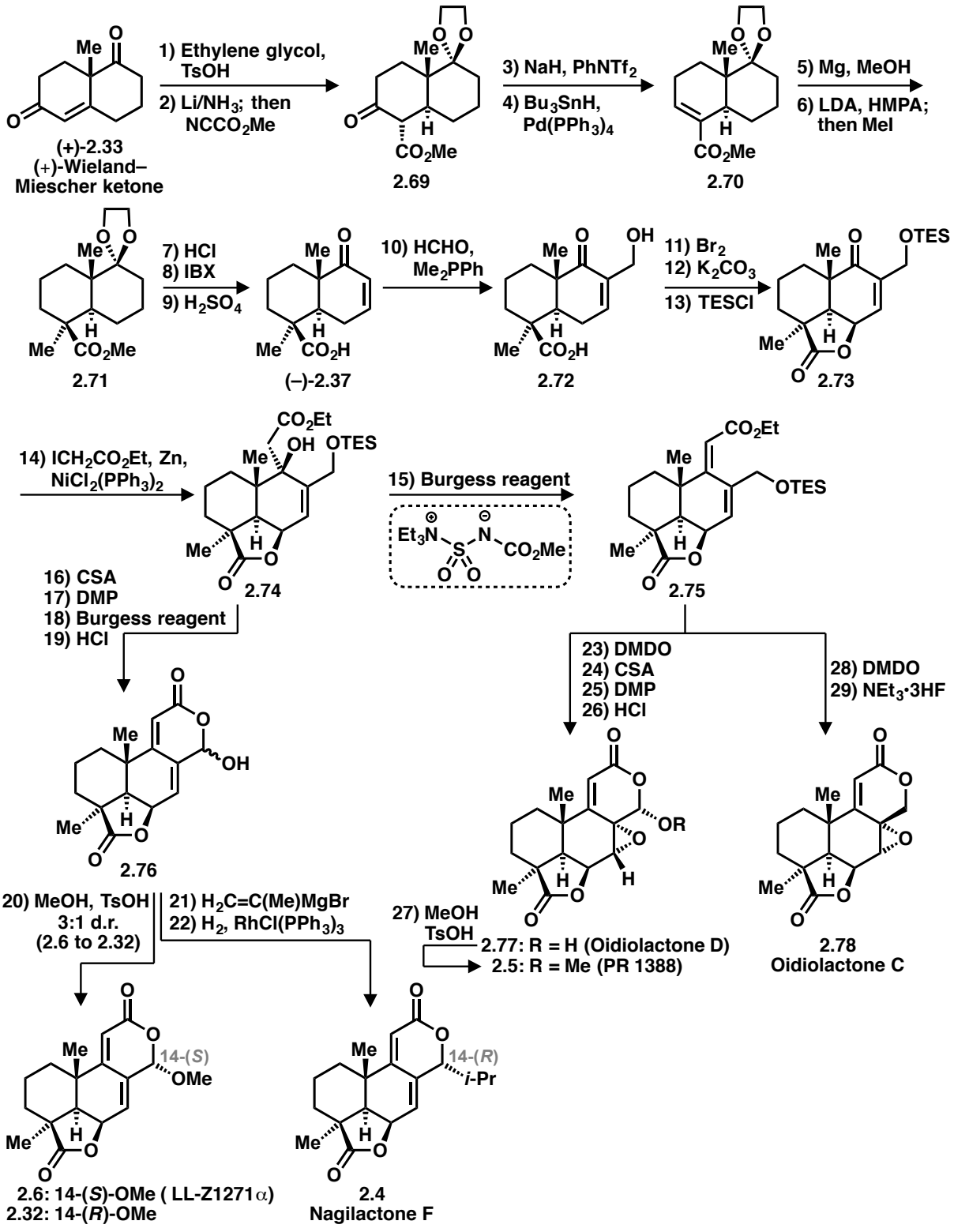

Scheme 2.11 – Hanessian and Boyer's synthesis of podolactones.[165]

For the purpose of preparing PR 1388 and oidiolactones C and D, tertiary alcohol **2.74** was dehydrated in the presence of the Burgess reagent,[204] to afford dienoic ester **2.75**. Subsequent epoxidation with dimethyldioxirane occurred from the sterically more accessibly face of the bicyclic scaffold. Triethylamine-trihydrofluoride-mediated deprotection of the triethylsilyl ether led to concomitant lactonization via a transient intermediate alkoxide, which effectively installed the δ-lactone moiety and furnished oidiolactone C (**2.78**) in one step. Alternatively triethylsilyl ether deprotection with camphor-10-sulfonic acid, followed by oxidation of the primary alcohol to an aldehyde with Dess–Martin periodinane, and ensuing protic-acid-catalyzed lactonization provided oidiolactone D (**2.77**) in excellent yield. Further exposure of oidiolactone D to a catalytic amount of 4-toluenesulfonic acid in methanol led to the corresponding *O*-methylated natural product, PR 1388 (**2.5**)

Alternatively, to synthesize nagilactone F and LL-Z1271α, the triethylsilyl ether protective group of **2.74** was first deprotected with camphor-10-sulfonic acid and the corresponding primary alcohol oxidized with Dess–Martin periodinane. Dehydration of the tertiary hydroxy group with the Burgess reagent and hydrochloric-acid-catalyzed lactonization yielded lactol **2.76**, an intermediate previously disclosed by Barrero's group (*Scheme 2.9*, p. 73). LL-Z1271α was prepared directly from lactol **2.76** with a combination of methanol and 4-toluenesulfonic acid, which resulted in incremental increases to the yield and stereoselectivity compared with the previously-reported syntheses. Lastly, nagilactone F (**2.4**) was prepared using a two-step sequence involving nucleophilic addition of isopropenylmagnesium bromide and subsequent hydrogenation of the alkene in the presence of Wilkinson's catalyst.

2.3 A Brief Introduction to Nagilactone B

Following the Hanessian group's interest in synthesizing naturally-occurring podolactones (refer to Section 2.2.5, p. 76),[165] as well developing novel approaches to non-natural analogs,[166] it became appealing to consider the synthesis of another member of the podolactone family of natural products, nagilactone B (**2.9**, *Figure 2.3*). Nagilactone B is a norditerpenoid dilactone, which was isolated in 1968 from the leaves and seeds of *Podocarpus nagi* (Thunberg) Kuntze* by the group of Hayashi in Osaka, Japan.[147] Since its isolation, nagilactone B has been the focus of only a few studies aimed at evaluating its biological activity.[137,138,205,206] In particular, the antitumor activity of nagilactone B was evaluated in an *in vitro* assay against Yoshida sarcoma cells, revealing a modest IC_{50} of 1.72 μM,[137,138] while its ability to stimulate the growth of lettuce seedling roots was the highest observed amongst eight different podolactones at a concentration of 21 μM.[205]

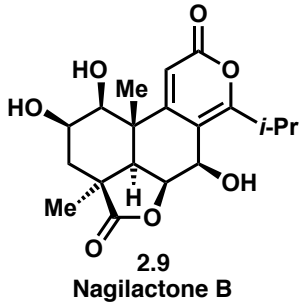

Figure 2.3 – Nagilactone B.

More recently, our interest in nagilactone B was roused by a PubChem assay (AID: 1498),[207] describing the potential of nagilactone B to act as a modulator of splicing events leading to lamin A (AC_{50} = 16 μM), a protein responsible for providing structural support to the nucleus of cells. This finding was particularly encouraging in light of a recent breakthrough by a team led by Lévy who discovered that a single point mutation in the gene coding for lamin A can drastically alter the normal course of splicing and consequently translation (mRNA to protein), causing Hutchinson–Gilford progeria syndrome, a premature aging disease.[208] In particular, an abnormal splicing event leads to a truncated version of

* This was found to be the appropriate name of the plant and was used in place of "*P. nagi* Zoll. & Moritzi", which was described in the original publication.

prelamin A protein (i.e., progerin), which cannot properly integrate into the nuclear envelope, resulting in severe abnormalities to the nucleus' shape and, ultimately, limiting the cell's ability to function and divide. The aforementioned assay was particularly striking in that HeLa S3 cells treated with nagilactone B showed a robust reduction in levels of progerin RNA, which is a significant step towards stabilizing and inhibiting the production of progerin, with the eventual goal of correcting the abnormal splicing event responsible for Hutchinson–Gilford progeria syndrome.[209,210] Additional disclosures in the literature also provide evidence that progerin may play a role in the normal course of mammalian aging, which has even wider implications for medicine and human health.[211,212]

Despite the promising therapeutic properties displayed by a number of naturally-occurring podolactones, additional studies have the potential to provide access to even more favourable properties and a better understanding of their origin. In particular, the lack of synthetic approaches to podolactones that place an emphasis on functionalizing ring A of the scaffold further encouraged us to tackle the synthesis of nagilactone B. Although nagilactone B has not been synthesized to date, a thesis submitted by Liu in 1980 describes initial efforts made in Wheeler's group to prepare ring A and B of this natural product using a Diels–Alder-type strategy.[213] Ultimately Liu and Wheeler were unable to prepare the bicyclic scaffold and the route was largely abandoned, in favour of pursuing Diels–Alder reactions of related molecules, rather than directing efforts towards the synthesis of nagilactone B.[213]

The following section extends the history of our foray into the podolactone family of natural products and describes a first-generation strategy for synthesizing the core of a type A podolactone, nagilactone B, with a particular emphasis on rings A, B, and D.

2.4 First-Generation Strategy

An analysis of the structure of nagilactone B (**2.9**, *Figure 2.4*), revealed that the key challenges in preparing this molecule would likely be associated with installing the 1,2-diol moiety, the quaternary centres at C4 and C10, and both the γ- and δ-lactones. Similar to the previous synthetic strategies, it was deemed advantageous to install the quaternary centres early on, especially given the challenges associated with their formation in organic synthesis.[181,214,215] An examination of the core of nagilactone B, coupled with knowledge from the previous approach that was taken in the Hanessian group (*Scheme 2.11*, p. 78),[165] led to the decision that the synthetic approach should start with (+)-Wieland–Miescher ketone ((+)-2.33, *Scheme 2.12*), a well-established and versatile scaffold that unambiguously establishes the C10 quaternary centre. The versatility of the Wieland–Miescher ketone, which has been reviewed elsewhere,[216] revealed that for the purpose of synthesizing nagilactone B, the use of its well-established core would provide an opportunity to focus on incorporating the 1,2-diol moiety and C4 quaternary centre towards the beginning of the synthesis, while ring C could be prepared through adjustments to the sequences described in Section 2.2.

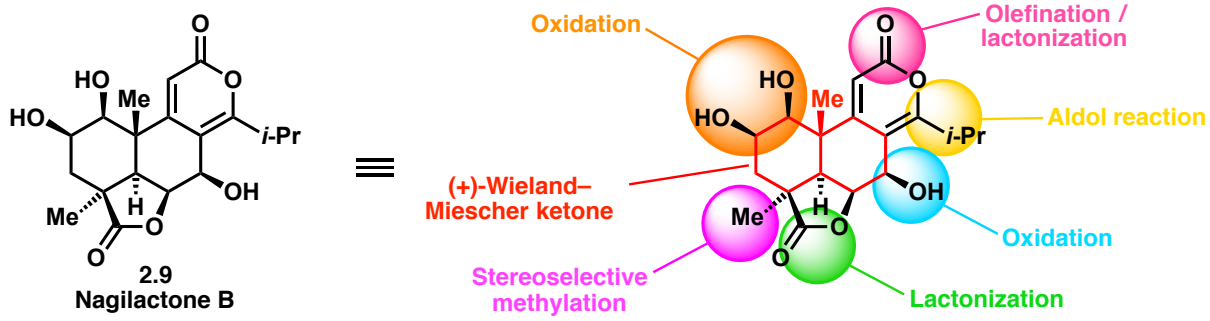

Figure 2.4 – General analysis of the structure of nagilactone B.

A retrosynthetic analysis for the first-generation route is given below in *Scheme 2.12*. Establishing the α-pyrone moiety in **2.79** was envisioned to take place towards the end of the synthesis through an intramolecular cyclization, based loosely on the lactonization reported by Hayashi's group (*Scheme 2.8*, p. 72). The ester moiety in **2.80** could be incorporated using an olefination reaction, or alternatively through a catalytic intermolecular Reformatsky-type reaction, with subsequent elimination of the tertiary alcohol.[165] Following allylic oxidation to access **2.83**,[217-221] the isobutyryl side chain of **2.82** may be integrated into the scaffold using an

aldol reaction. The previously described bromolactonization reaction would establish the γ-lactone in **2.84**, while the diol moiety in **2.86** may be synthesized by oxidizing the scaffold of **2.88**.[160] Alkylative transposition was envisaged as the key step at the beginning of the synthesis, whereby the quaternary centre of **2.88** was set through α-methylation of α,β-unsaturated ester **2.70**, with concomitant transposition of the alkene.[222,223]

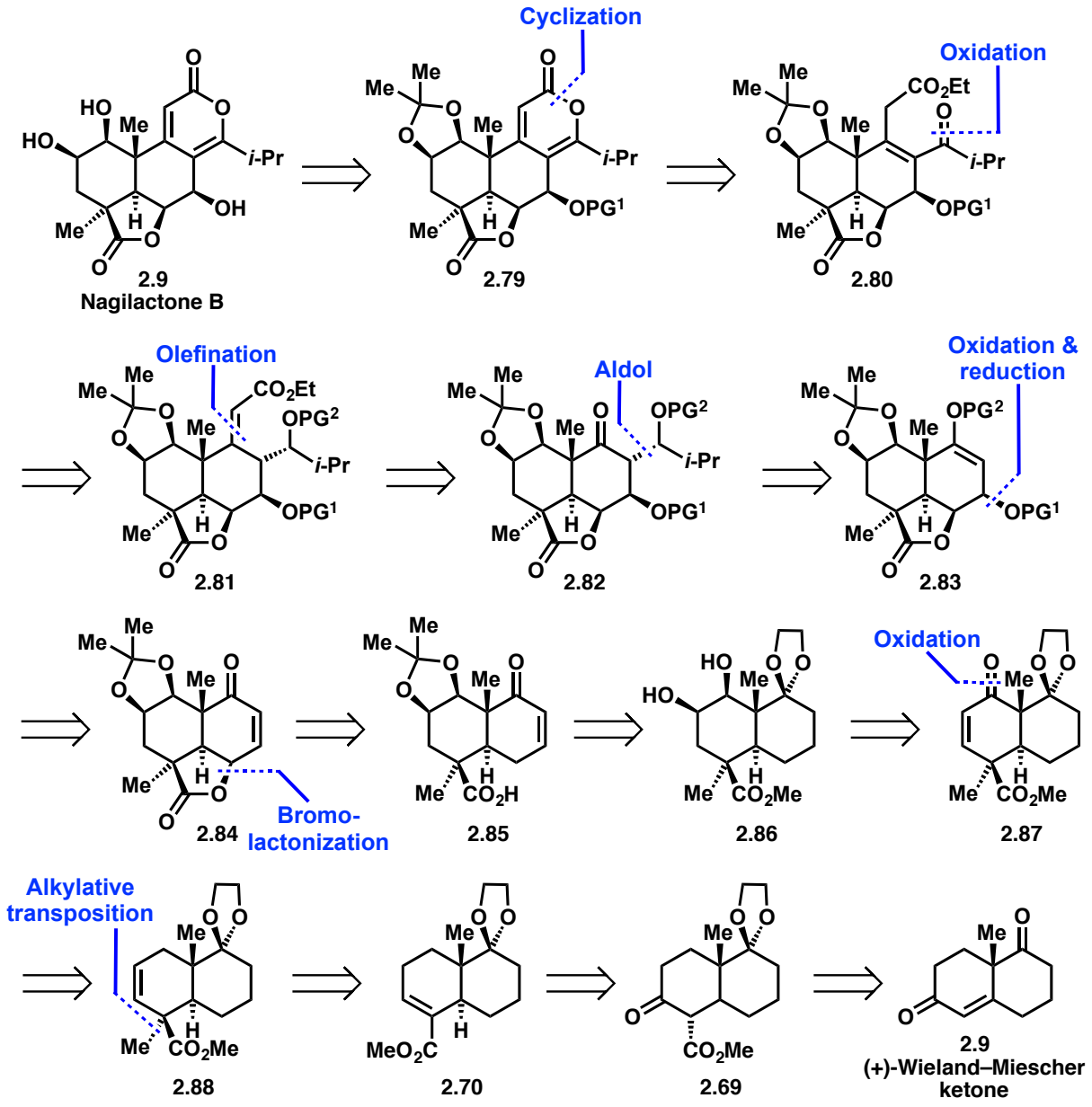

Scheme 2.12 – First-generation retrosynthetic analysis for nagilactone B.

The alkene of **2.88** may be functionalized to afford the diol or a number of other ring A analogues of interest, which is why it was initially selected as a key intermediate.[224] α,β-Unsaturated ester **2.70** (*Scheme 2.12*) may itself be prepared from the Wieland–Miescher ketone using a sequence established by Danishefsky's group[225] that was also used during Hanessian and Boyer's synthesis of numerous podolactones (*Scheme 2.11*, p. 78). For the purpose of providing context and practical advice regarding the synthesis of the Wieland–Miescher ketone, Section 2.4.1 briefly describes its history, before the first-generation synthesis of the core of nagilactone B is described in Section 2.4.2.

2.4.1 Wieland–Miescher Ketone

The first-generation synthetic strategy for preparing nagilactone B began with (+)-Wieland–Miescher ketone ((+)-**2.33**, *Figure 2.5*), a versatile scaffold which has found wide application[216] for the synthesis of many biologically-active natural products since its initial racemic disclosure in 1950 by two industrial chemists, Peter Wieland and Karl Miescher, who

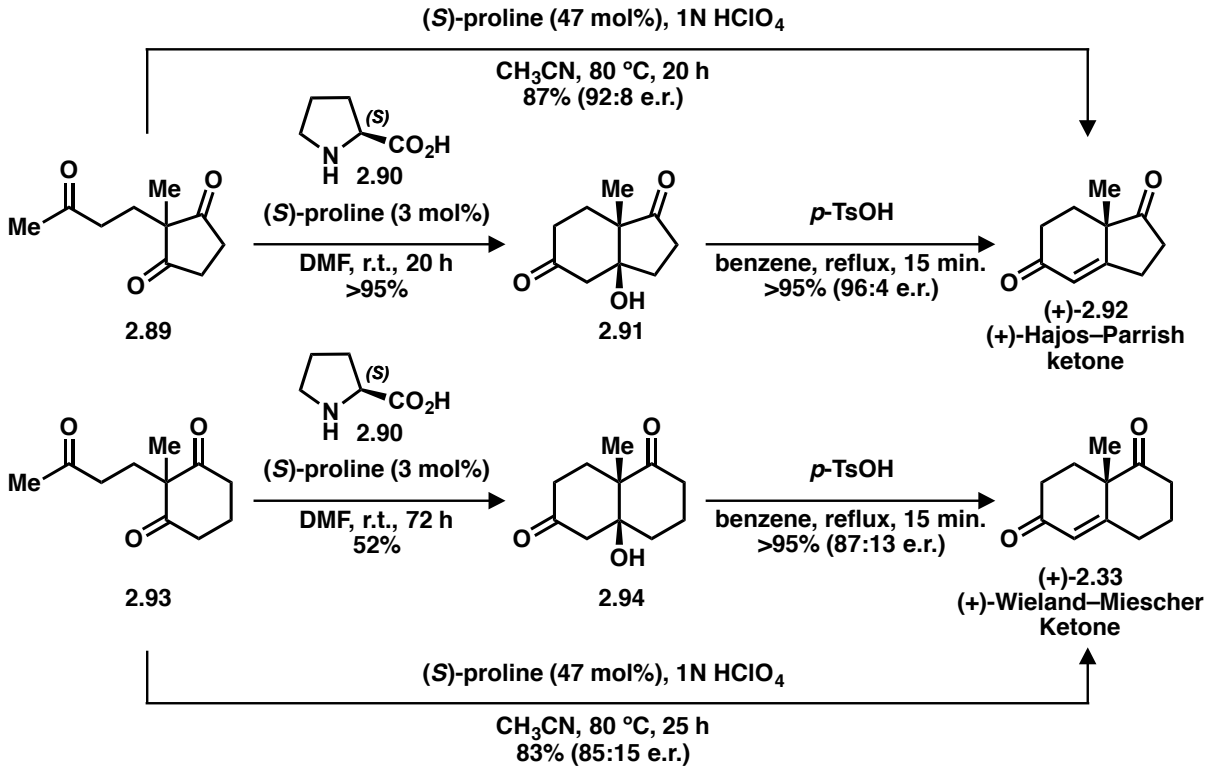

Figure 2.5 – First enantioselective syntheses of (+)-Wieland–Miescher ketone.

were working at *Ciba Geigy*.[226] A method for directly preparing the enantiopure version of this building block and the related (+)-Hajos–Parrish ketone ((+)-**2.92**) was not unveiled until the early 1970s, when two groups of industrial chemists, Hajos and Parrish at *Hoffmann La Roche*, and Eder, Sauer, and Wiechert at *Schering AG*, independently disclosed that (*S*)-proline (**2.90**, *Figure 2.7*) was capable of effecting the desired transformation enantioselectively. While Hajos and Parrish developed a two-step procedure, where they could isolate intermediate aldol products before effecting an acid-catalyzed dehydration (i.e., **2.89** to **2.91** to **2.92**), the conditions reported by the team of Eder, Sauer, and Wiechert led directly to the aldol condensation product (i.e., **2.89** to **2.92**, *Figure 2.5*). Notably, this was also the first disclosure of an asymmetric organocatalytic reaction, nearly 30 years before publications by List, Lerner, and Barbas,[227] as well as the group of MacMillan,[228] sparked a surge of interest in the field that would become known as asymmetric organocatalysis.

However, despite the potential of the Wieland–Miescher ketone, the use of this scaffold in asymmetric synthesis was still hindered by significant practical challenges associated with producing it in the quantities often required for endeavours in the field of total synthesis (>25 g) or industrial environments (>>100 g). In particular its application to many synthetic endeavours was limited by the requirement to use solvents with high boiling points for the reaction, large volumes of silica gel and solvents for an initial purification, and multiple capricious recrystallizations to improve the enantiopurity of the final product, which is nevertheless obtained in low yield alongside significant quantities of industrial waste. An industrial team led by Fürst eventually described an improved procedure, which became the *de facto* standard for its preparation on multigram-scale for more than 30 years, yet even that procedure was still far from ideal.[229,230] Other groups have attempted to refine the procedure as well, resorting to studies of recrystallizations in different solvent systems[231] or on chemical derivatives,[232,233] as well as kinetic resolutions with baker's yeast.[234] Despite their attempts, the lack of a clear mechanistic understanding for the role of proline as a catalyst in this reaction was a major reason substantial progress towards directly addressing the enantioselectivity of this reaction was not realized until after 2000.

Building on numerous mechanistic studies, a transition state proposal was eventually put forth by Houk's group at UCLA, in which proline acts as a bifunctional catalyst by

activating the donor carbonyl component through enamine formation, while also forming a hydrogen bond between the carboxylic acid moiety and the electrophilic carbonyl group (*Figure 2.6*, transition structures leading to the Hajos–Parrish ketone is depicted).[235,236] Two Zimmerman–Traxler-like transition states are possible: *syn* and *anti*, where those terms refer to the orientation of the enamine with respect to the carboxylic acid; *anti* transition state **TS-2.1** leads to the experimentally observed major product when (*S*)-proline is used as the catalyst. Many refinements have been reported since that initial disclosure,[237-240] and the mechanistic details for related reactions are still passionately debated in the literature.[241,242]

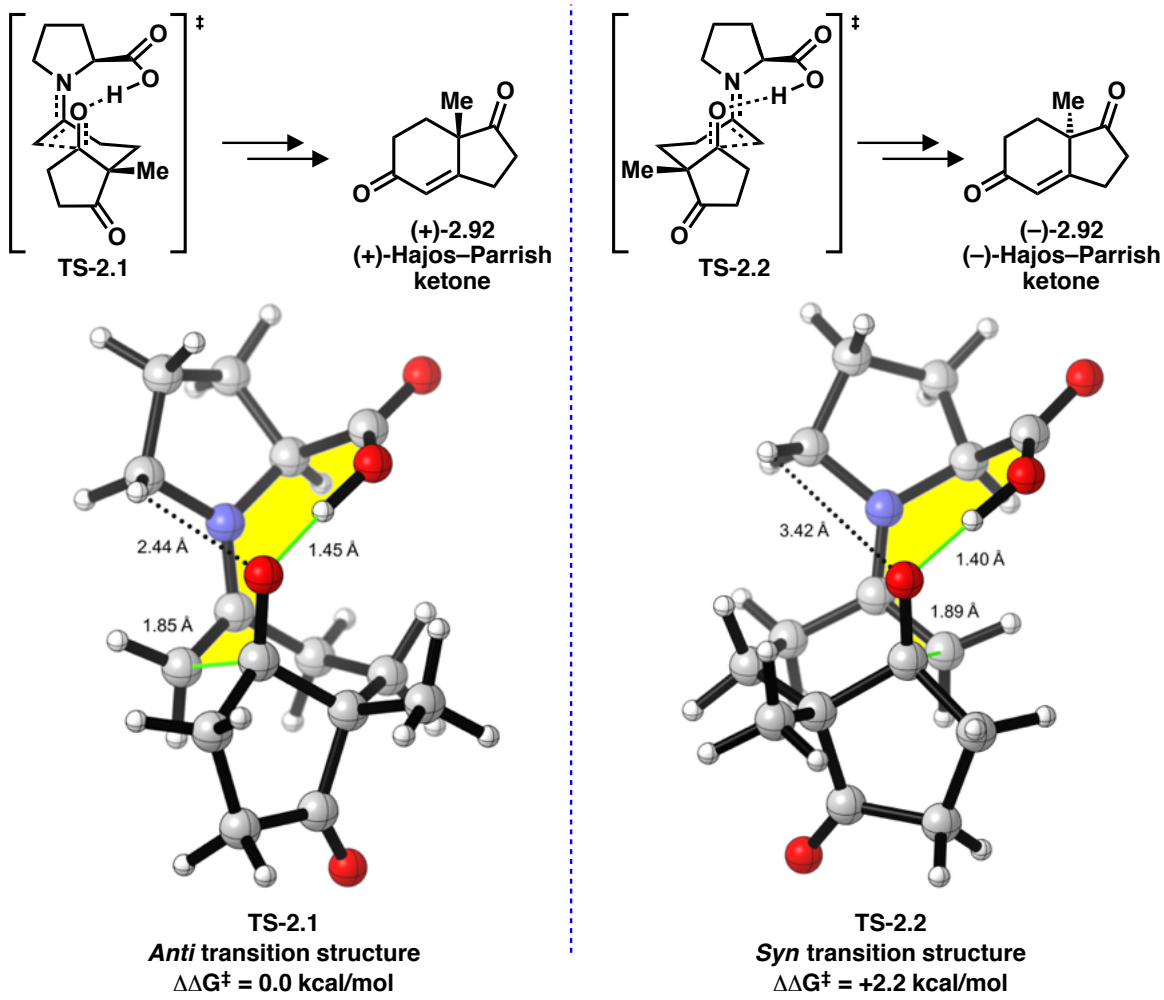

Figure 2.6 – Computed transition structures for proline-catalyzed aldol reaction.[240,243]

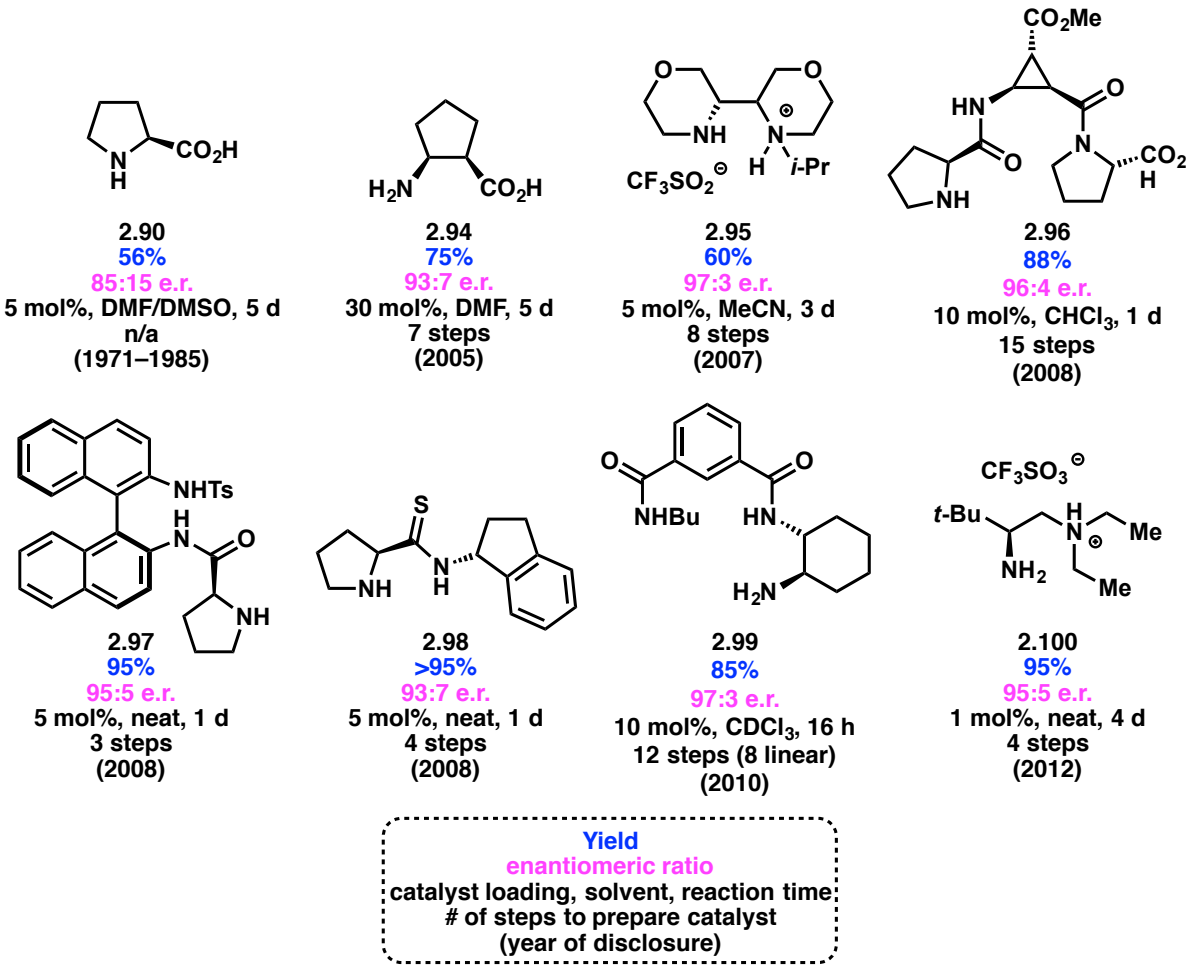

Figure 2.7 – Catalysts used to synthesize the Wieland–Miescher ketone.*

Shortly after publications by the groups of Houk, List, Barbas, and McMillan, a number of other teams began publishing their own efforts towards identifying organocatalysts capable of producing the Wieland–Miescher ketone in enantiopure form, without recourse to gruelling purifications or concession steps. Examples of organocatalysts with diverse scaffolds that have been used to synthesize the Wieland–Miescher ketone with varying levels of enantioselectivity and overall efficiency are shown in *Figure 2.7*. Initial improvements were found in the Davies group's disclosure of β-amino acid **2.94**[244], but it was not until 2007 with the disclosures of bimorpholine catalyst **2.95**[245] and tripeptide **2.96**[246], that small molecules were reported as being capable of achieving enantiomeric ratios in excess of 95:5. Despite an

* As drawn, catalysts **2.90**, **2.95**–**2.99** are used to synthesize (+)-Wieland–Miescher ketone, while catalysts **2.94** and **2.100** afford (–)-Wieland–Miescher ketone.

increase in the number of steps required to obtain each catalyst, the significant improvements in enantioselectivity and yield were very encouraging. Binam-based sulfonamide **2.97**[247] and prolinethioamide **2.98**[248] were published by the group of Nájera, while cyclohexane-1,2-diamine-based **2.99**[249] and *tert*-leucine-derived **2.100**[250] were reported by the groups of Morán and Luo, respectively.

Of all the catalysts disclosed to date, sulfonamide **2.97** and *tert*-leucine-derived **2.100** appeared the most promising, as both catalysts may be prepared quickly, and their corresponding ability to catalyze the formation of the Wieland–Miescher ketone was marked by high yields and enantioselectivities, low catalyst loadings, solvent-free conditions, and a straightforward workup and recrystallization. Furthermore, subsequent refinements with both catalysts led to robust and practical protocols for preparing the Wieland–Miescher ketone on multigram scale with either **2.97**[251] or **2.100**[252]. The procedure for synthesizing (+)-Wieland–Miescher ketone with catalyst **2.97** was available upon embarking on the synthesis of nagilactone B, and although the *Organic Syntheses* preparation[251] describes the reaction on 15 g, it was possible to routinely scale it up to over 75 g, without any significant complications.

2.4.2 Reductive Carbomethoxylation (Ketal Protective Group)

The synthesis of nagilactone B (**2.9**, *Figure 2.3*) started with 2-methyl-1,3-cyclohexanedione (**2.101**), which was elaborated to the (+)-Wieland–Miescher ketone ((+)-**2.33**) using a two-step procedure that made use of binam-derived sulfonamide catalyst **2.97**.[251] The unconjugated ketone was selectively protected as the corresponding ketal using ethylene glycol and one equivalent of p-toluenesulfonic acid, using a robust procedure described by Demnitz and Ciceri.[253] This method is particularly effective in that monoketal **2.102** may be purified by recrystallization, rather than resorting to column chromatography, which is a significant advantage when working with large quantities of material. A minor amount of Wieland–Miescher ketone starting material often remained at the end of the reaction (~5–7%), but it could readily be recycled. Following ketal protection, enone **2.102** was subjected to dissolving metal reduction (lithium–ammonia) to establish the *trans*-fused ring junction and the intermediate lithium enolate was diastereoselectively carbomethoxylated with Mander's reagent (methyl cyanoformate) to yield methyl ester **2.69**.[193,199,225,254]

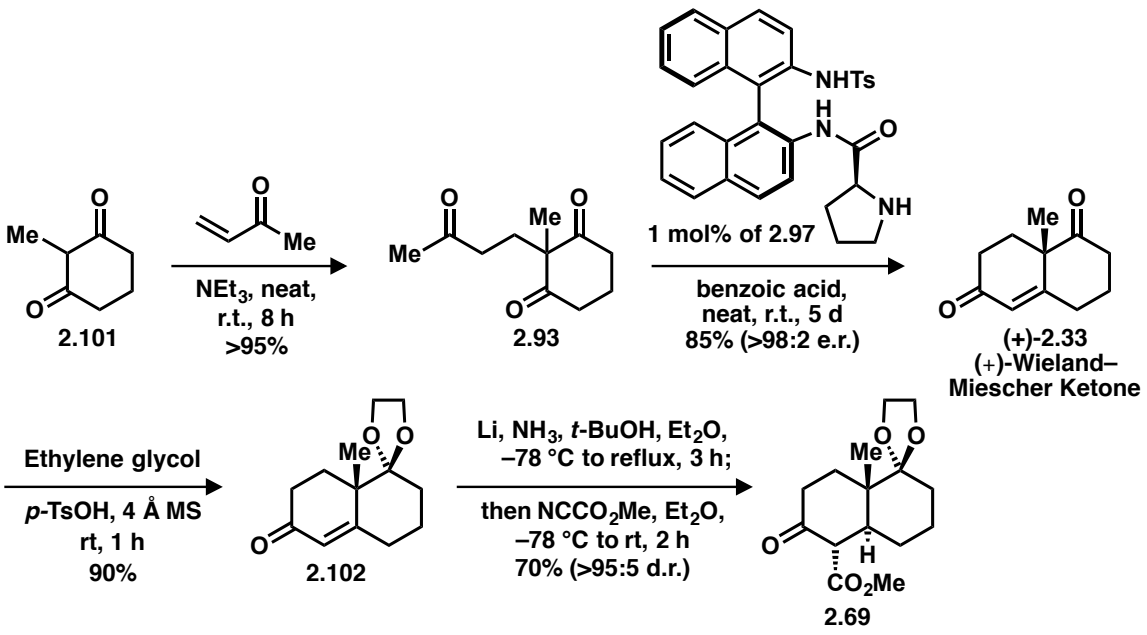

Scheme 2.13 – 2-Methyl-1,3-cyclohexanedione to β-keto ester.

Attempted dissolution of β-ketoester **2.69** in a minimal volume of 1:1 diethyl ether–hexanes, while preparing to purify the material by flash column chromatography, led to a significant quantity of colourless solid precipitating out of the solution, leaving an orange supernatant. Filtration and washing of the solid with cold 1:1 diethyl ether–hexanes revealed that the solid was in fact β-ketoester **2.69**. Furthermore, it was sufficiently pure that column chromatography of the bulk material was rendered superfluous. This was a fortuitous discovery and significantly increased the practicality of the sequence used by Danishefsky's group.[225]

A number of groups have studied the stereoselectivity of dissolving metal reductions, which has resulted in a multitude of mechanistic proposals, albeit with many consistent themes.[255-258] The currently accepted mechanistic proposal,[255] as it relates to the synthesis, is shown in *Scheme 2.14*. One-electron reduction of enone **2.102** affords 1,4-radical anion **2.103**, which preferentially adopts a conformation that allows for significant orbital overlap with the enolate system, while simultaneously reducing the number of unfavourable diaxial interactions. Furthermore, the singly-occupied molecular orbital at the ring junction adopts a slightly pyramidalized geometry that is quasiaxial with respect to both rings, with an extended (i.e., larger) orbital lobe on the α-face.[259] This pyrimidalization stems from favourable σ-

donation interactions with bonding orbitals in the adjacent ring, which are absent in other conformations. Consequently, addition of a second electron occurs predominantly from the α-face of the bicyclic scaffold, where the orbital coefficient is significantly larger. This preferentially affords configurationally stable dianion **2.104**, which is rapidly protonated in the presence of *tert*-butanol to give enolate **2.105**, with a *trans*-fused ring junction. This enolate was isolated and dried under vacuum before it was used in the following carbomethoxylation reaction.

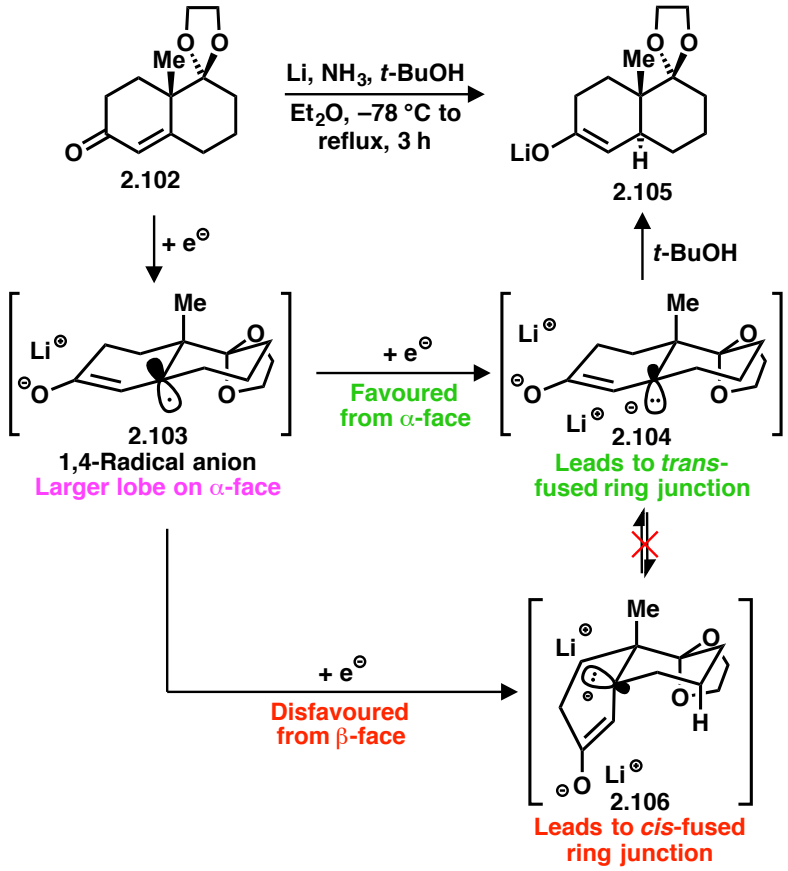

Scheme 2.14 – Dissolving metal reduction mechanism.[255]

Carbomethoxylation of lithium enolate **2.105** was carried out in tetrahydrofuran with Mander's reagent at –78 °C and provided access to β-ketoester **2.69** (*Scheme 2.15*). The presence of an axial methyl group at the C10 position rendered axial approach of methyl cyanoformate from the β-face of the bicyclic scaffold as unfavourable, owing to the 1,3-diaxial interactions it would experience from that trajectory; this unfavourable approach is depicted in chair-like transition structure **TS-2.3**. Instead, to avoid steric interactions with the

methyl group and satisfy stereochemical requirements,[260] the decalone-derived enolate adopts a twist-boat conformation, which permits the reagent to approach along an axial-like trajectory, as shown in transition structure **TS-2.4**. Although this introduces considerable torsional strain compared with the corresponding chair-like transition state, alleviating 1,3-diaxial interactions with the C10 methyl group appears to be favoured overall.[261]

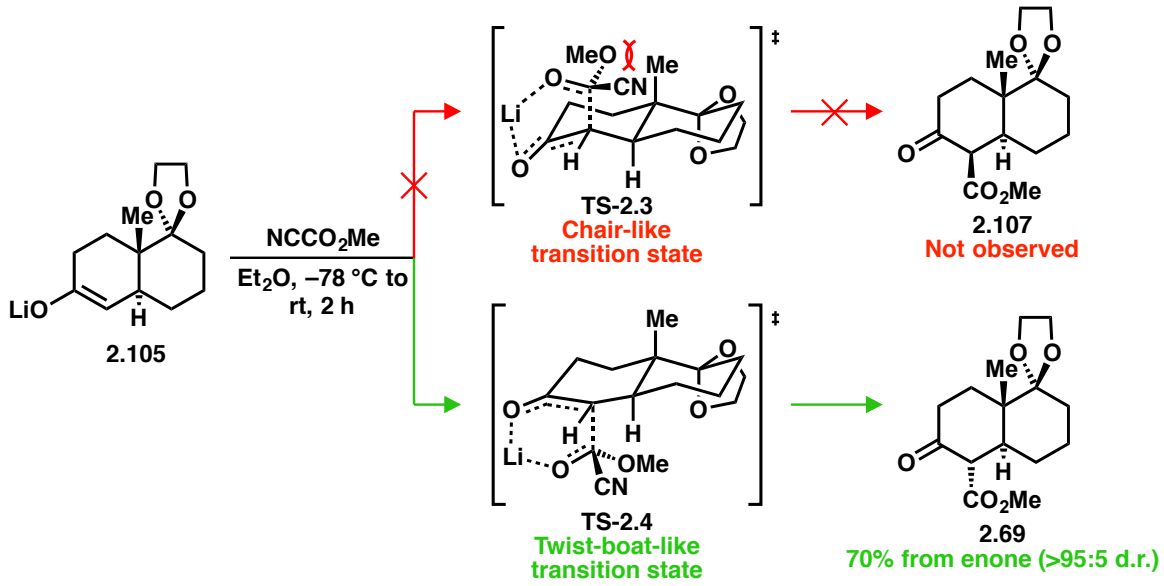

Scheme 2.15 – Carbomethoxylation of lithium enolate with Mander's reagent.

2.4.3 Alkylation (Ketal Protective Group)

For the purpose of directly accessing the quaternary centre while preserving the ketone moiety, which could serve as a handle for functionalizing ring A, an effort to directly methylate the anion of β-ketoester **2.69** in the presence of methyl iodide was pursued. It was initially thought that significant 1,3-diaxial steric interactions between the C10 axial methyl group and an incoming electrophile would direct the latter to the α-face of the bicyclic scaffold, as was previously observed during the carbomethoxylation reaction (*Scheme 2.15*). Unfortunately, although conversion for the methylation of β-ketoester **2.69** was ≥70%, a 1:1 mixture of epimeric diastereomers **2.108** and **2.109** was observed (*Scheme 2.16*).

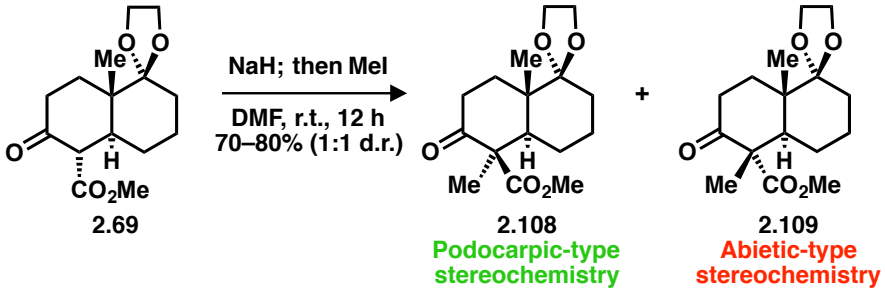

Scheme 2.16 – Direct alkylation of β-ketoester.

Initial attempts to improve this ratio by screening different bases (and correspondingly counterions) as well as solvents, led to a surprising result: the diastereomeric ratio increasingly favoured the abietic-type stereochemistry found in **2.109**, rather than the desired podocarpic-type scaffold (*Table 2.1*). In other words, trajectories along the same face as the C10 methyl group became more favourable for an incoming electrophile. Attempts to perform the methylation with methyl triflate and with lithium-containing bases such as lithium diisopropylamide and lithium bis(trimethylsilyl)amide, as well as in the presence of hexamethylphosphoramide, did not lead to any significant changes to the diastereomeric ratio.

Table 2.1 – Alkylation of β-ketoester with methyl iodide.

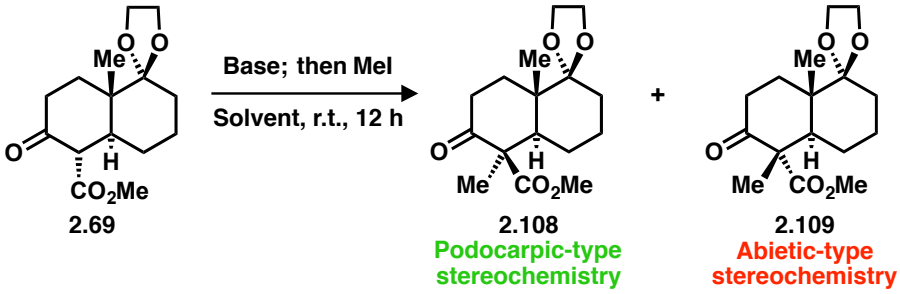

Entry*	Base	Solvent	Ratio of 2.108 to 2.109
1	NaH	DMF	1 : 1
2	NaH	THF	1 : 2
3	KHMDS	THF	1 : 2
4	KHMDS	DMF	1 : 4

*Reactions performed on TLC scale

Further increasing the bulk of the nucleophile was briefly considered as an alternative option, but a more thorough search of the chemical literature revealed that these efforts would not likely have a very high probability of overall success, as a consequence of the nature of the

enolate salt being more important than the size of the alkylating agent in this system.[174,176] Specifically, it appears that for this system the energetic consequences of steric 1,3-diaxial interactions between the axial C10 methyl group and an incoming electrophile on the β-face (**TS-2.6**) are comparable to those arising from torsional strain as the ester moiety passes across the centre of mass of the C5–C6 bond during alkylation from the α-face (**TS-2.5**). The apparent minimal energy difference between these two sources of strain is effectively highlighted by the indiscriminate nature of the alkylation. Notably, this result stands in contrast to analogous alkylation reactions that have been observed with a nitrile moiety in place of the methyl ester, which further highlights the importance of the enolate salt.[262,263]

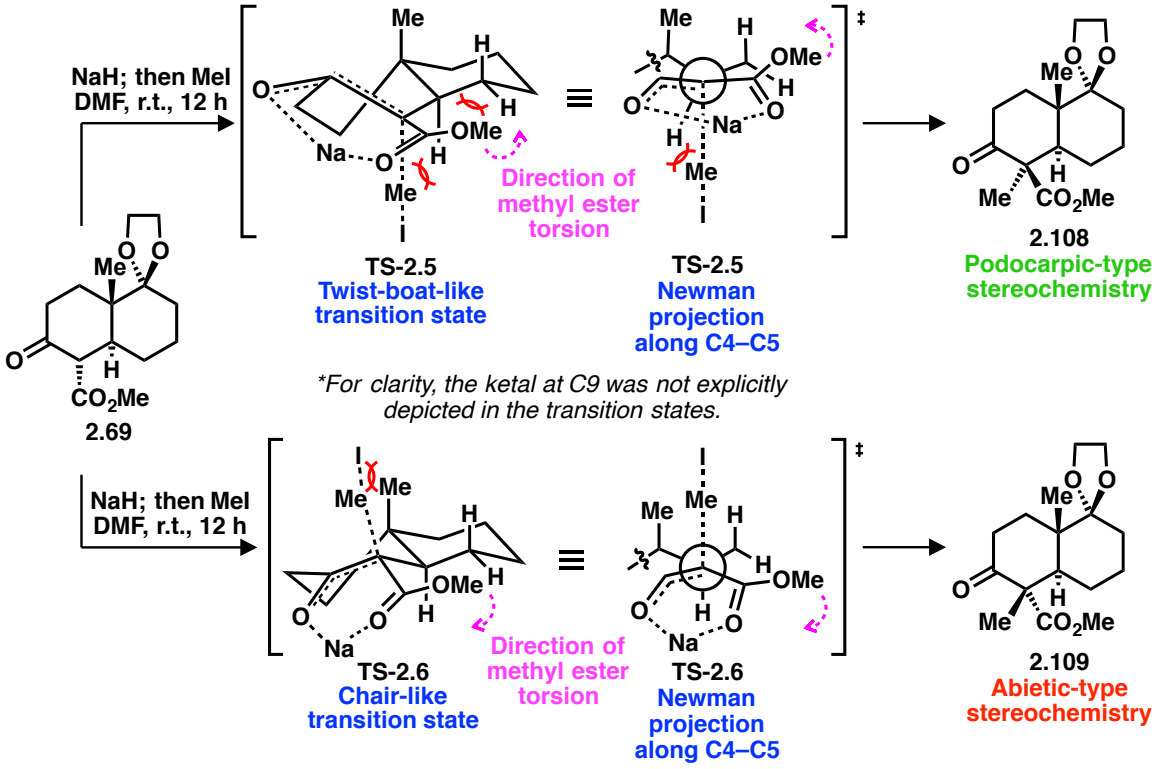

Scheme 2.17 – Comparison of transition states for methylation of β-ketoester.

Comparing the attempted diastereoselective methylation of β-keto ester **2.69** (*Scheme 2.17*) to similar reactions in the chemical literature led to the realization that it may be possible to address the stereoselectivity by ensuring that the enolate anion is effectively exocyclic, because alkylations on those systems tend to occur with an equatorial trajectory.[264-270] A pair of notable examples which inspired this approach are shown below in *Scheme 2.18*.[264,270] The

disclosure of Hutt and Mander was particularly interesting, as they demonstrated the feasibility of performing the alkylation on an unsaturated system (**2.113**), with concomitant transposition of the alkene moiety during the course of the alkylation to yield methyl ester **2.115**. While the additional bulk of the methoxymethyl ether protective group is certainly expected to influence the facial selectivity through steric interactions with the incoming electrophile, it would also be instructive to evaluate whether the same selectivity is observed in the presence of an axial methyl group for the purpose of synthesizing ring A substituted podolactones.

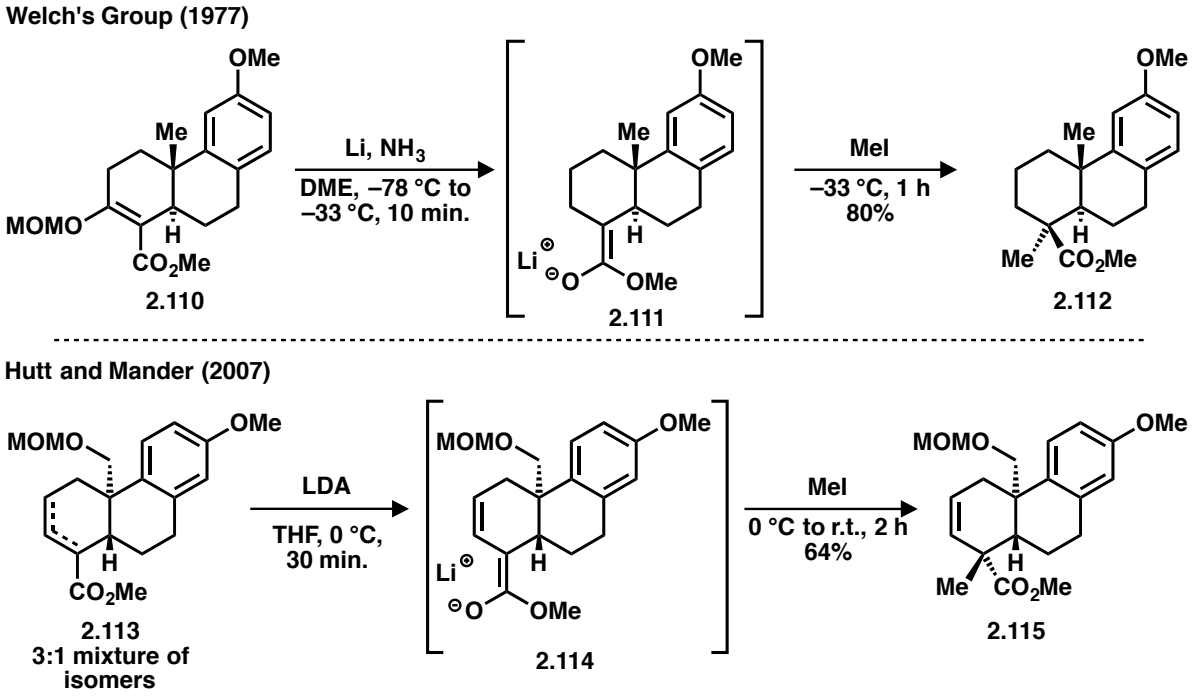

Scheme 2.18 – Alkylation via exocyclic enolate to set quaternary centre.[264,270]

Consequently, the focus was shifted towards preparing α,β-unsaturated ester **2.70** (*Scheme 2.19*), which was envisaged to undergo diastereoselective methylation, while also avoiding the oft-observed difficulties associated with methylating non-enolic β-keto esters.[271] Unsaturated ester **2.70** was synthesized using a two-step sequence that involved conversion of β-keto ester **2.69** to enol triflate **2.116**, followed by hydride reduction in the presence of tetrakis(triphenylphosphine)palladium(0) and tributyltin hydride.[196]

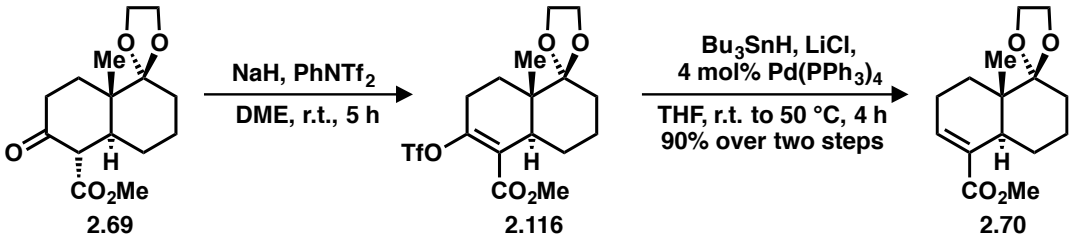

Scheme 2.19 – Synthesis of α,β-unsaturated ester.

With lithium diisopropylamide as the base, alkylative transposition of α,β-unsaturated ester **2.70** was attempted with methyl iodide and methyl triflate in the presence or absence of highly-polar coordinating additives (*Table 2.2*). Encouragingly, the diastereomeric ratio shifted to 2:1 in favour of the desired podocarpic-type methyl ester (**2.88**), as compared with the analogous alkylation reaction that was performed on β-keto ester **2.69** (*Table 2.1*). Unfortunately, further attempts to improve the ratio of **2.88** to **2.117** by incorporating coordinating additives or changing the electrophile and temperature were wholly unsuccessful. Although low overall yields and poor diastereoselectivity were discouraging for the alkylation reaction, success was found in another option: allylic oxidation.

Table 2.2 – Alkylative transposition of α,β-unsaturated ester.

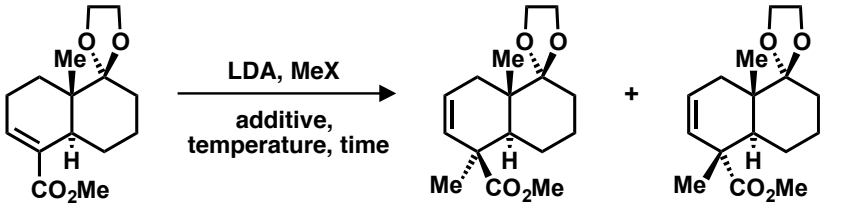

Entry*	Base (equiv.)	Additive	MeX	Temperature	Time	Ratio of 2.88 to 2.117
1	LDA (6.0 eq.)	DMI	MeI	–78 °C	3 h	2 : 1
2	LDA (6.0 eq.)	DMI	MeOTf	–78 °C	3 h	2 : 1**
3	LDA (6.0 eq.)	–	MeOTf	–78 °C	4 h	2 : 1
4	LDA (6.0 eq.)	HMPA	MeI	–78 °C to r.t.	4 h	2 : 1
5	LDA (4.0 eq.)	–	MeI	0 °C	4 h	2 : 1

* Reactions performed on TLC scale; ** 50% isolated yield when performed on 50 mg scale.

2.4.4 Allylic Oxidation (Ketal Protective Group)

In conjunction with pursuit of an alkylative transposition approach to the quaternary centre, attempts were made to functionalize ring A directly using an allylic oxidation reaction (*Scheme 2.20*). It was envisaged that allylic oxidation at C2 of α,β-unsaturated ester **2.70** would provide access to a versatile γ-keto-α,β-unsaturated ester (**2.118**, *Scheme 2.20*) that could be used to install the 1,2-diol moiety of nagilactone B, as well as serve as a handle to prepare ring A analogues of other podolactones that are oxidized at C2 (e.g., 2β-hydroxynagilactone F,[167] nagilactone I,[167] and salignone M[272]). One of the key challenges of oxidizing this scaffold stems from the regioselectivity of the oxidation reaction. Given the distinct possibility of oxidizing the tertiary centre instead of C2, it could also be feasible to access enone **2.119** through an ensuing rearrangement as well, depending on the energetic landscape of the oxidation pathway. Owing to the disclosure of similar oxidations on comparable scaffolds in the chemical literature (*Scheme 2.21*), initial attempts focused on performing the allylic oxidation with the use of chromium trioxide in the presence of 3,5-dimethylpyrazole, as well as contemporary methods utilizing manganese and rhodium catalysts in the presence of *tert*-butyl hydroperoxide.

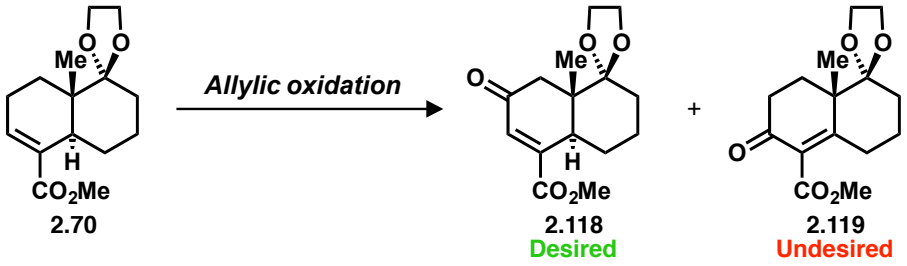

Scheme 2.20 – Allylic oxidation to functionalize ring A.

During their synthesis of manzamine A, Martin's group used an optimized version of an allylic oxidation method reported by the group of Salmond, which involved a ten to twenty-fold stoichiometric excess of chromium trioxide and 3,5-dimethylpyrazole at temperatures between –25 and –10 °C (**2.120** to **2.121**).[273,274] Despite the large excess of chromium trioxide required, this procedure was particularly appealing in that it involved a similar α,β-unsaturated ester (**2.120**) and was successfully carried out on 18 g (119 mmol) of the ester. In stark contrast to the superstoichiometric quantities of chromium trioxide required by that method,

the corresponding Uemura–Doyle oxidation (**2.112** to **2.123**) offered significant appeal in that it could be carried out with only 0.1 mol% of dirhodium tetracaprolactamate in the presence of *tert*-butyl hydroperoxide.[275] A related oxidation with 10% manganese(III) acetate dihydrate was also promising, in that it highlighted a potential opportunity to use a mild, efficient, chemoselective, and regioselective oxidant to functionalize a complex alkene (**2.124** to **2.125**).[276]

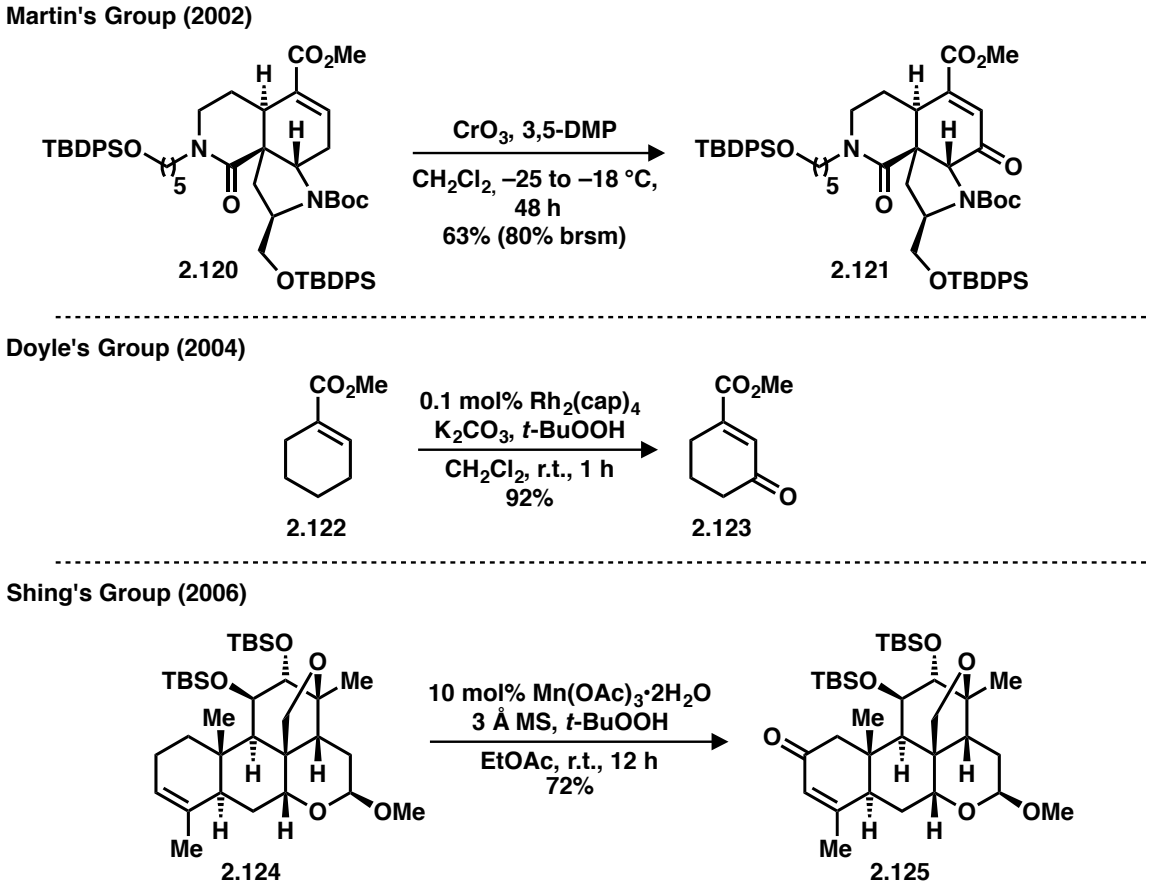

Scheme 2.21 – Allylic oxidation of similar scaffolds.

Initial experiments with chromium trioxide and 3,5-dimethylpyrazole were encouraging and afforded enone **2.118** in 48% yield (73% b.r.s.m.), even when carried out on multigram scale (entry 1, *Table 2.3*). The major side product in this case arose from apparent oxidation of the ketal moiety, which was the first evidence that using a different protective group in future routes might be better. Although significant quantities of the originally considered side product arising from oxidation at the tertiary center (**2.119**) were not observed

with the ketal protective group, it was later found to be the major side product when the ketal moiety was switched in favour of the *tert*-butyldimethylsilyl protective group (*Scheme 2.27*, p. 104).

Table 2.3 – Allylic oxidation of α,β-unsaturated ester.

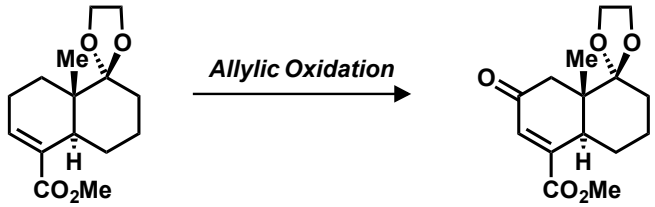

2.70 **2.118**

Entry	Oxidant	Additive(s)	Solvent	Temperature	Time	Result
1	CrO_3 (15 eq.), 3,5-DMP	–	CH_2Cl_2	–25 to –15 °C	6 h	48% (73% b.r.s.m.)†
2	$Mn(OAc)_3$* (0.15 eq.), *t*-$BuOOH_{(dec.)}$	3 Å MS	EtOAc	r.t.	36 h	**2.70** : **2.118** = 7 : 1
3	$Mn(OAc)_3$* (0.15 eq.), *t*-$BuOOH_{(dec.)}$	3 Å MS, O_2,	EtOAc	r.t.	36 h	**2.70** : **2.118** = 1 : 2
4	$Rh_2(cap)_4$ (0.02 eq.), *t*-$BuOOH_{(dec.)}$	K_2CO_3	CH_2Cl_2	r.t.	32 h	**2.70** : **2.118** = 1 : 6
5	$Rh_2(cap)_4$ (0.02 eq.), *t*-$BuOOH_{(aq.)}$	–	1,2-DCE	r.t.	32 h	**2.70** : **2.118** = 1 : 20
6	$Rh_2(cap)_4$ (0.02 eq.), *t*-$BuOOH_{(aq.)}$	–	1,2-DCE	40 °C	16 h	72%†

*$Mn(OAc)_3 \cdot 2H_2O$; † Yield of after chromatography.

In addition to the use of chromium trioxide, an attempt to use manganese(III) acetate dihydrate was also made, which initially resulted in rather low conversion and the recovery of a significant amount of starting material (entry 2, *Table 2.3*). This was partially addressed by performing the reaction under an atmosphere of oxygen gas, which improved conversion in favour of the intended enone (entry 3, *Table 2.3*). The use of dirhodium tetracaprolactamate was particularly favourable and immediately resulted in overall excellent conversion to the anticipated product on milligram scale (entries 4–5, *Table 2.3*). A brief optimization resulted in an overall isolated yield of 72% when the reaction was carried out with dirhodium tetracaprolactamate at 40 °C in 1,2-dichloromethane (entry 6, *Table 2.3*). Unfortunately, although the reaction worked well with quantities of up to 0.10 g (~0.37 mmol) of α,β-unsaturated ester **2.70**, increasing the amount further had a deleterious influence on the yield, which was reduced by half when carried out on ~0.5 g of the same material.

2.4.5 Incorporation of 1,2-*syn*-Diol (Ketal Protective Group)

With the enone in hand, attempts were made to prepare a 1,2-diketone, which was envisaged to be a direct precursor to the 1,2-diol moiety present in nagilactone B, by way of hydride reduction. Selenium-dioxide-mediated oxidation reactions were successful on smaller scale (*Scheme 2.22*), but the yields varied considerably once the reaction was scaled up. This was initially attributed to either: a) the potential of selenium dioxide to perform an allylic oxidation at the tertiary position, or b) the stability of the product under the reaction conditions. In an attempt to evaluate the two possibilities, a two-step oxidation sequence was pursued, involving hydroxylation followed by oxidation to the ketone.

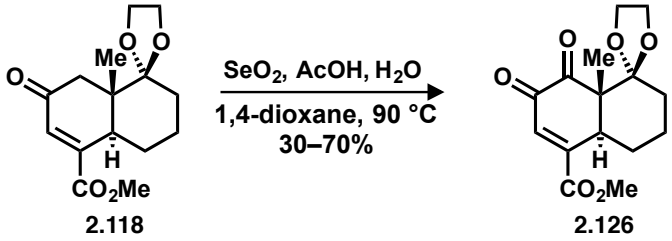

Scheme 2.22 – Selenium-dioxide-mediated oxidation to access 1,2-diketone.

In the presence of potassium bis(trimethylsilyl)amide, Davis' oxaziridine was used to effect hydroxylation at –78 °C, which led to α-hydroxy ketone **2.127** (*Scheme 2.23*).[277,278] Despite the use of potassium as the counterion, minor amounts of an imino–aldol side product (**2.128**) were observed; this side product and the benzenesulfonamide by-product eluted very close to α-hydroxy ketone **2.127**, which resulted in a rather arduous purification by column chromatography. While camphor-based oxaziridines are known to eliminate the presence of imino–aldol side products,[277] the conversion of starting material to product with camphor-based oxaziridines was significantly lower (~5–10% overall conversion) than with the corresponding (±)-2-(phenylsulfonyl)-3-phenyloxaziridine. The presence of a ketal moiety appeared to sufficiently increase steric bulk on the α-face of the scaffold, such that the camphor-based oxaziridines were unable to interact with the enolate, while the axial methyl group simultaneously shielded the β-face. Given this premise, it seemed reasonable that eliminating some of the steric bulk of the ketal moiety could increase the yield, while simultaneously reducing the amount of imino–aldol side product for the hydroxylation

reaction with (±)-2-(phenylsulfonyl)-3-phenyloxaziridine. This is described in Section 2.4.6, starting on page 102.

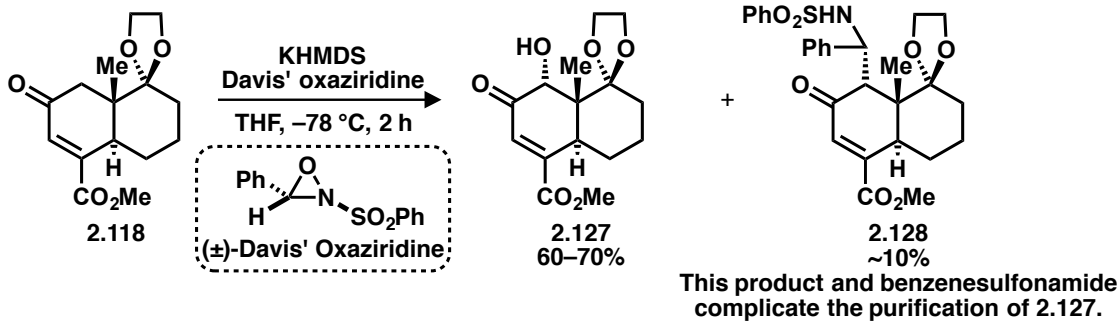

Scheme 2.23 – Preparation of α-hydroxy ketone.

Although oxidation of α-hydroxy ketone **2.127** was possible with Dess–Martin periodinane (*Scheme 2.24*), it quickly became apparent that the resultant 1,2-diketone was not very stable.[279] In retrospect, this is not particularly surprising given the highly-electrophilic nature of the 1,2-diketone moiety coupled with the electrophilicity of the unsaturated ester. On milligram scale, the diketone could be directly reduced to a *syn*-1,2-diol with sodium borohydride and protected as the corresponding ketal (**2.129**), without concomitant reduction of the alkene. Although the sequence was not amenable to scale-up as a consequence of the instability of diketone **2.126**, it did allow for a preliminary confirmation of the *syn*-1,2-diol moiety and consequently provided minor validation for the synthetic route.

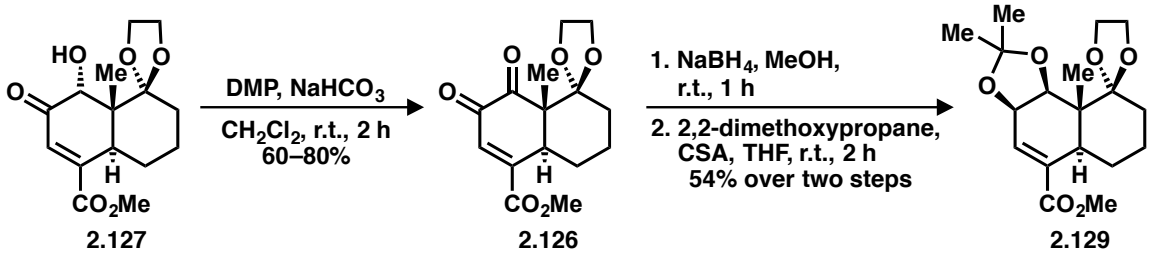

Scheme 2.24 – Preparation of 1,2-diol.

For the purpose of improving the stability of 1,2-diketone **2.126**, it was reasoned that the alkene should be directly reduced after the hydroxylation step, before the ensuing oxidation. The driving force behind that idea was the concept that the saturated ring would provide an opportunity for the diketone to exist in its tautomeric form, which is expected to be more stable.[280,281] This worked rather well, with hydrogenation of α-hydroxy ketone **2.127**

yielding a separable mixture of epimeric esters, which could readily be oxidized with Dess–Martin periodinane to the corresponding mixture of diketones (**2.131**, *Scheme 2.25*). Notably, the diketones, which existed in the mono-enol tautomeric form, were significantly more stable than the corresponding unsaturated analogues. Reduction with sodium borohydride led to a mixture of α-hydroxy ketone **2.132** and diol **2.133**, of which the former could be reduced to diol **2.133** with sodium borohydride in the presence of cerium(III) chloride under conditions initially described by Luche.[282] The stereochemistry of the (4*S*)-configured methyl ester of α-hydroxy ketone **2.135** was confirmed by X-ray crystallographic analysis, which allowed for verification of the facial selectivity of the initial hydride reduction (*Figure 2.8*). Protection of the 1,2-diol moiety with 2,2-dimethoxypropane afforded acetonide **2.134**.

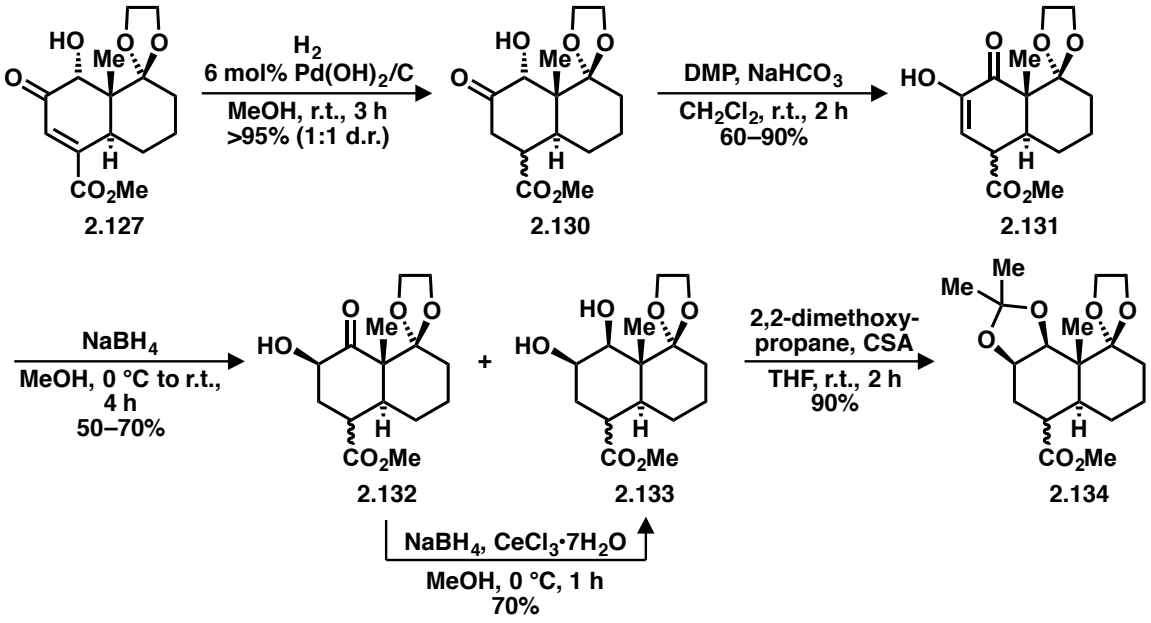

Scheme 2.25 – Synthesis of protected 1,2-diol via enol ketone.

Despite the promise of this route, the possibility of using a *tert*-butyldimethylsilyl protective group in place of the ketal at C9 became increasingly appealing for the preparation of additional material, especially given the difficulties encountered purifying α-hydroxy ketone **2.127** (*Scheme 2.25*) and the apparent ketal oxidation side product observed during the allylic oxidation reaction.

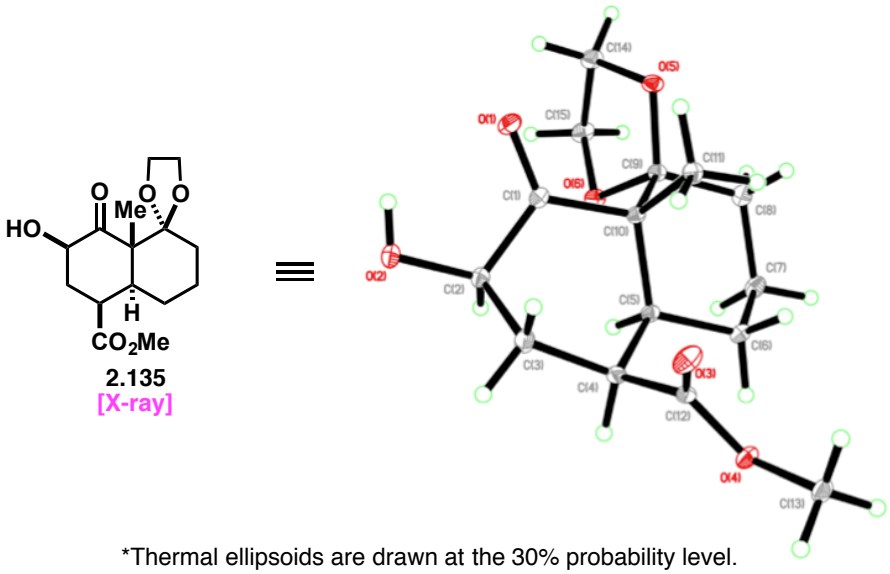

*Thermal ellipsoids are drawn at the 30% probability level.

Figure 2.8 – X-ray crystallographic structure of α-hydroxy ketone.*

2.4.6 Preparing the 1,2-*syn*-Diol (*tert*-Butyldimethylsilyl Protective Group)

For the purpose of evaluating whether the challenging purifications associated with the Davis'-oxaziridine-mediated α-hydroxylation reaction with could be addressed purely by swapping protective groups, an initial effort was made with an advanced intermediate that was readily available (*Scheme 2.26*). The ketal protective group of **2.118** was removed in the presence of indium(III) trifluoromethanesulfonate and acetone under transketalization conditions,[283] before the resulting diketone (**2.136**) was chemo- and stereoselectively reduced with sodium borohydride using conditions reported by Ward's group.[284] Protection of the secondary alcohol as a *tert*-butyldimethylsilyl ether provided a potential precursor to the α-hydroxy ketone.[285] Under the same conditions previously described for the ketal-protected precursor (*Scheme 2.23*, p. 100), α-hydroxylation of ketone **2.138** was carried out with Davis' oxaziridine as the electrophile. This approach proved to be effective and afforded a modest increase in yield of the desired α-hydroxy ketone (**2.139**), with a corresponding improvement in the associated purification since none of the undesirable imino–aldol side product was observed in the reaction mixture.

* Obtained with racemic material that was used for very preliminary explorations of the synthesis; useful for verifying relative stereochemistry.

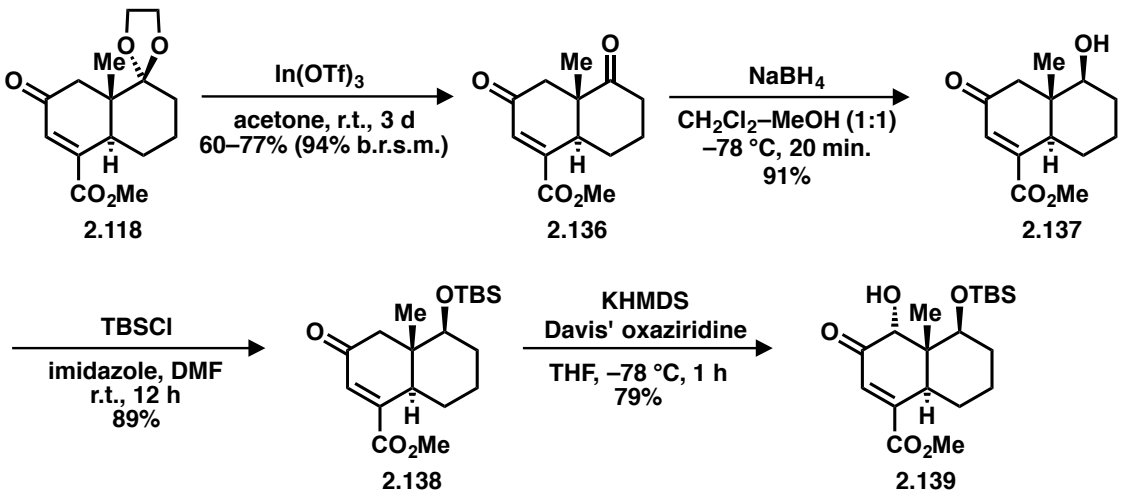

Scheme 2.26 – Improvement of α-hydroxylation reaction with TBS protective group.

With a more desirable option in hand, additional α-hydroxy ketone **2.139** was prepared using the previously described chemistry, in the presence of a *tert*-butyldimethylsilyl protective group rather than the ketal (*Scheme 2.27*).[286,287] The overall robustness of this sequence, even on multigram scale, was demonstrated by the fact that the reactions proceeded without any significant deviations from the previous sequence, with yields that were on par with or better than those of the previous route. It was only in the case of the allylic oxidation reaction that a minor difference was noted, whereby the major side product was observed to be **2.144**. This side product likely arises from initial oxidation at C5, and effectively resulted in elimination of the previously installed stereocenter at C5, with simultaneous reinstallation of the ketone at C3. The structure was verified by X-ray crystallographic analysis (*Figure 2.9*).

While scaling up the route depicted in *Scheme 2.27*, we quickly noted that the chromium-trioxide–3,5-dimethylpyrazole-mediated allylic oxidation (**2.143** to **2.138**, *Scheme 2.27*) was especially difficult to perform on multigram quantities of α,β-unsaturated ester **2.143**. In part, this stemmed from the need to use >10 molar equivalents of chromium trioxide for each equivalent of alkene, with an equivalent amount of 3,5-dimethylpyrazole. This prompted a second evaluation of some of the transition metal catalysts previously screened for the corresponding ketal (*Table 2.3*, p. 98). In particular, the allylic oxidation was attempted with $Rh_2(cap)_4$,[275] $Mn(OAc)_2•2H_2O$,[276] $Pd(OH)_2$,[288] CuI,[289] *N*-hydroxysuccinimide,[290] *N*-hydroxyphthalimide,[290,291] pyridinium dichromate,[292] and pyridinium chlorochromate,[290]along

with with *tert*-butyl hydroperoxide as a solution in water or decanes. Disappointingly, these attempts were not successful with respect to preparing enone **2.138** in larger quantities, and the chromium-trioxide–3,5-dimethylpyrazole-mediated allylic oxidation remained the most promising from the perspective of yield. As was previously observed for the analogous ketal-protected scaffold, $Rh_2(cap)_4$ provided favourable conversions when used on smaller quantities of α,β-unsaturated ester **2.143**, but led to poor reaction outcomes on larger scale. Notably, the combination of *N*-hydroxysuccinimide or *N*-hydroxyphthalimide with chromium-based oxidants led to significantly larger quantities of the undesired side product (**2.144)**. In fact, in the presence of pyridinium chlorochromate (PCC) and *N*-hydroxysuccinimide (NHS), enone **2.144** was isolated as the major product with a yield of 91% (*Scheme 2.28*).

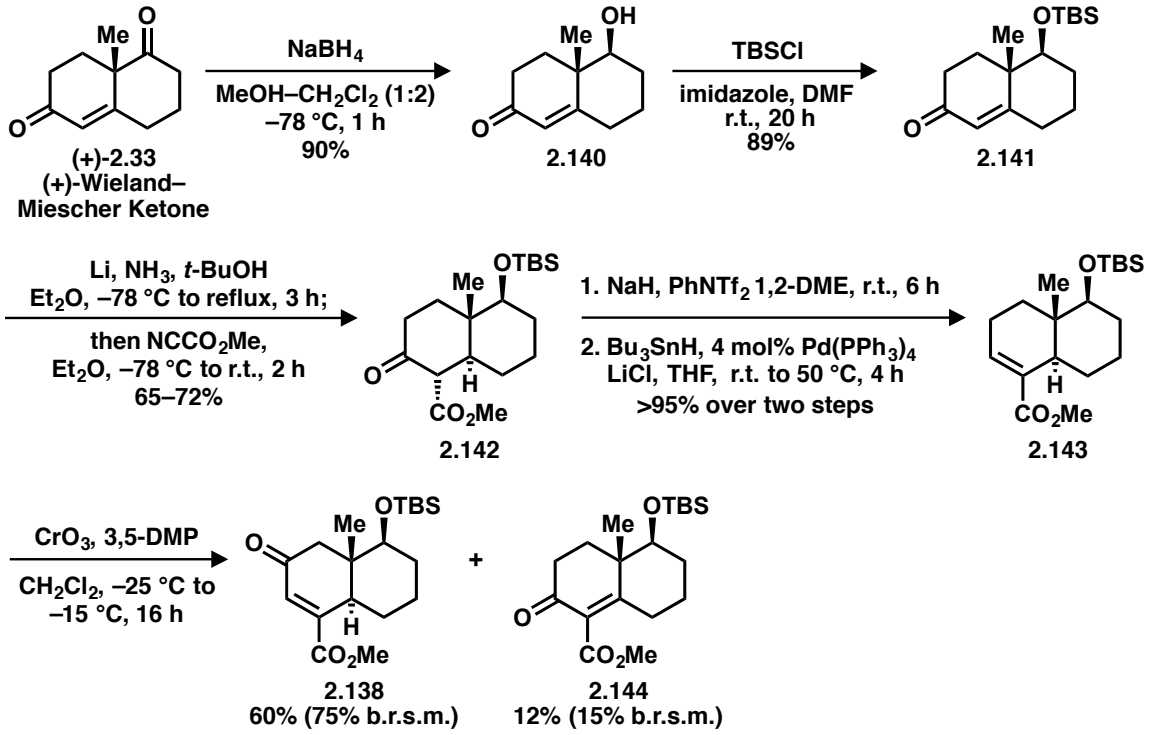

Scheme 2.27 – (+)-Wieland–Miescher ketone to γ-keto-α,β-unsaturated ester.

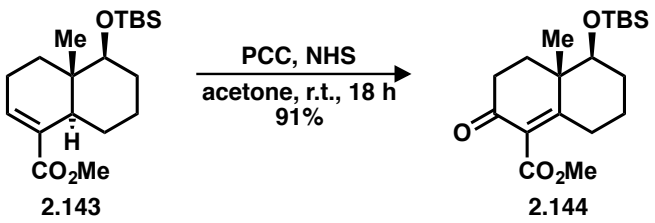

Scheme 2.28 – Oxidation of α,β-unsaturated ester with PCC and NHS.

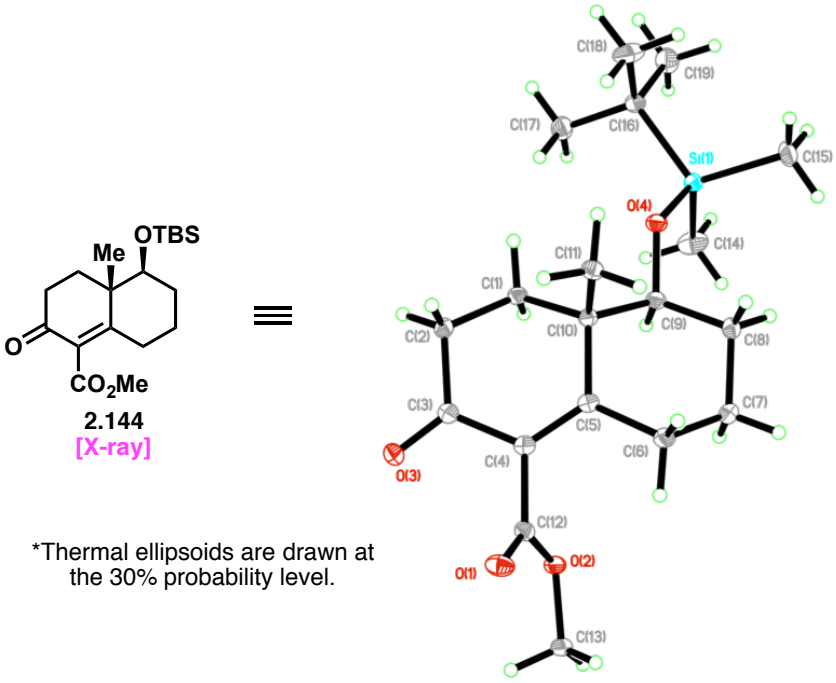

Figure 2.9 – X-ray crystallographic structure of enone.

α-Hydroxy ketone **2.139** was prepared using the established α-hydroxylation reaction with Davis' oxaziridine (*Scheme 2.26*, p. 103), and the enone was subsequently reduced to a 2.4:1 mixture of epimeric diastereomers (i.e., **2.145** and **2.146**) in the presence of hydrogen gas and $Pd(OH)_2/C$ (*Scheme 2.29*). The structure of (4*S*)-configured methyl ester **2.145** was unambiguously assigned through X-ray crystallographic analysis (*Figure 2.10*). Given the stereoselectivity of an analogous reduction with magnesium in methanol that was performed on a similar scaffold by Dr. Boyer (*Scheme 2.11*, p. 78),[165] an attempt was also made to do the same with enone **2.139** in order to suppress the formation of one of the stereoisomers.[197,198] While this could also facilitate purification, it was done with the intention of exclusively forming the (4*S*)-configured methyl ester in anticipation of the potential need to circumvent

challenges Dr. Boyer had with deprotonating a similar (4*R*)-configured methyl ester during the synthesis of the related podolactones (*Scheme 2.11*, p. 78).[165] Unfortunately, reducing the enone with magnesium in methanol actually provided more of the undesirable (4*R*)-configured methyl ester (**2.146**), so the hydrogenation conditions were used instead.

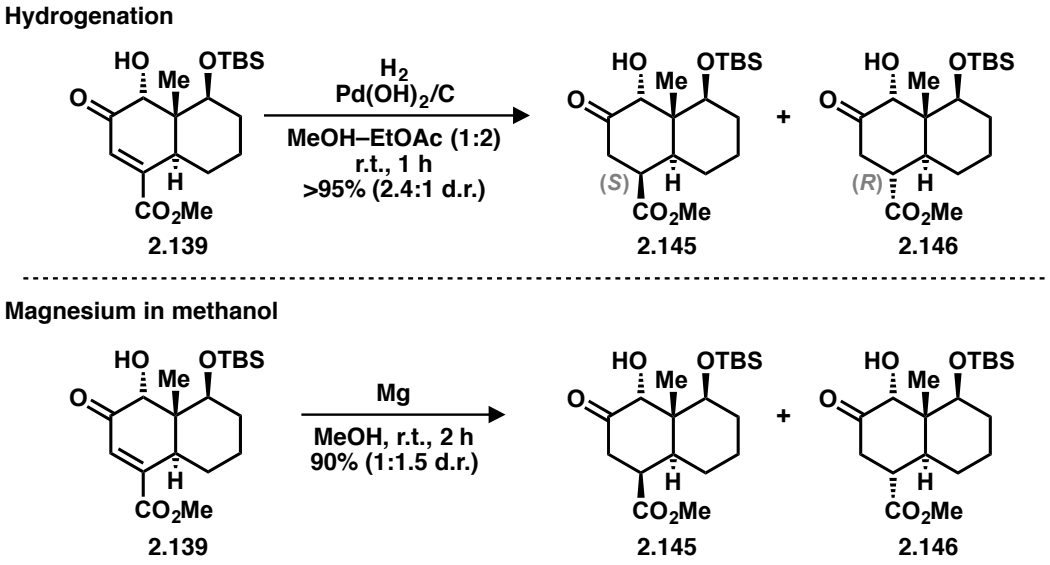

Scheme 2.29 – Reduction of α,β-unsaturated ester.

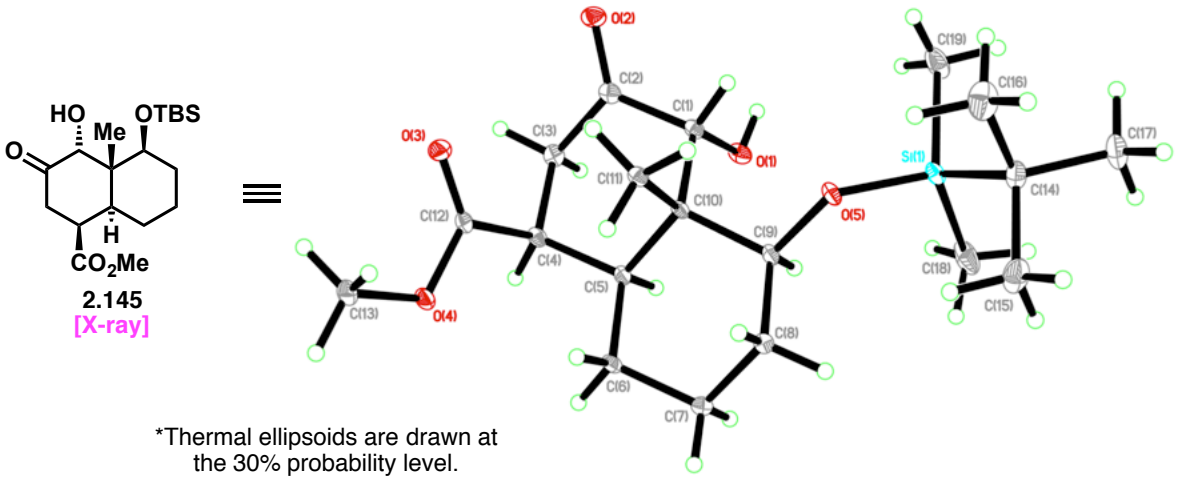

Figure 2.10 – X-ray crystallographic structure of enone.*

* Obtained with racemic material that was used for very preliminary explorations of the synthesis. The structure was useful for verifying the relative stereochemistry, and the enantiopure version was later synthesized.

Following reduction of α,β-unsaturated ester **2.139**, the isolated α-hydroxy ketones were individually oxidized to the corresponding 1,2-diketones (*Scheme 2.30*). Initially Dess–Martin periodinane was used to oxidize (4*S*)-configured methyl ester **2.145**, but inconsistent yields on >100 mg scale led to a search for a more robust oxidation method. Swern oxidations that made use of oxalyl chloride or acetic anhydride were also rather ineffective, but the corresponding Omura–Sharma–Swern variation with trifluoroacetic anhydride was quite robust and furnished the diketone, which was present in its tautomeric form (*Scheme 2.30*).[293] Under the reaction conditions, the Omura–Sharma–Swern variation actually resulted in the epimerization of the methyl ester to the more favourable configuration (i.e., **2.145** to **2.148**). Practically speaking this was rather advantageous, since the epimeric mixture of methyl ethers produced after hydrogenation converged to the same product (**2.148**) following oxidation. However, whether the deprotonation of the α-configured methyl ester would prove challenging, as observed by Dr. Boyer, remained to be seen.

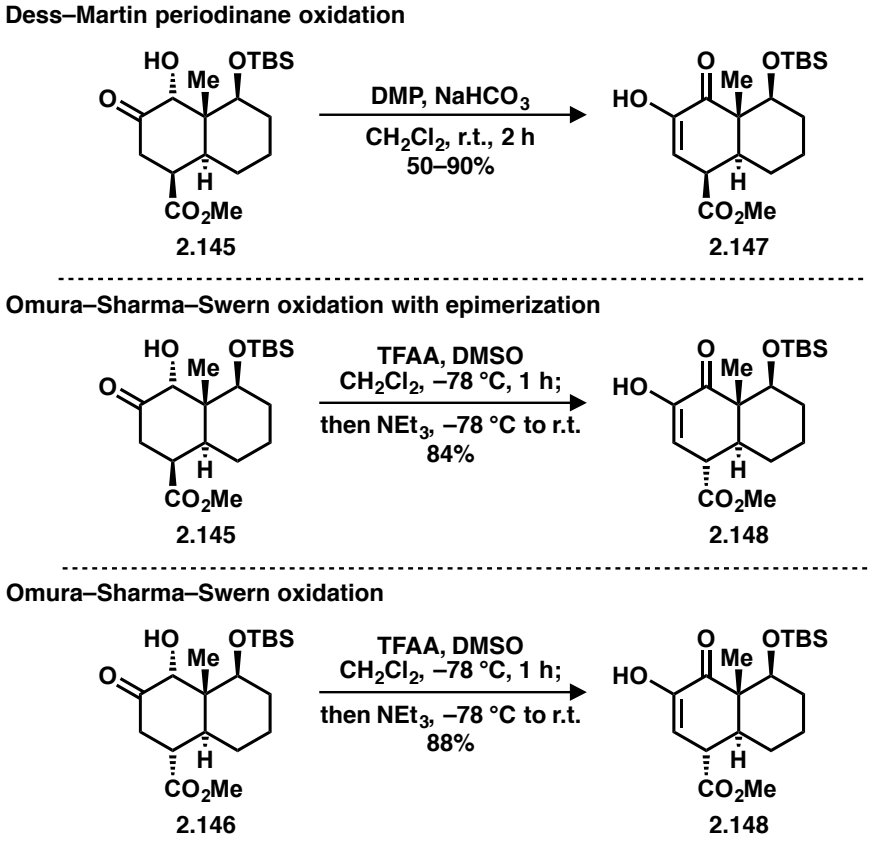

Scheme 2.30 – Oxidation to 1,2-diketone.

Following Omura–Sharma–Swern oxidation, the resultant diketone (**2.148**) was reduced directly to the 1,2-diol with sodium borohydride in the presence of cerium(III) chloride (*Scheme 2.31*). Initially, bulkier hydride sources (e.g., lithium tri-*sec*-butylborohydride) and those with an axial preference for hydride delivery were also screened (e.g., *tert*-butylamine borane[294]), but the former typically resulted in incomplete reduction, as was also observed for the analogous sequence with the ketal series (*Scheme 2.25*, p. 101). With the protected diol in hand, the methylation was attempted in order to set the quaternary centre with the desired podocarpic-type stereochemistry.

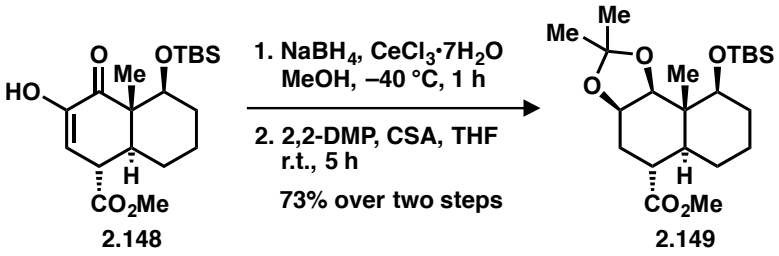

Scheme 2.31 – Synthesis of 1,2-diol.

2.4.7 Alkylation and Incorrect Stereochemistry of Quaternary Centre

α-Methylation of the corresponding ester enolate of **2.149** (*Scheme 2.32*) was carried out in the presence of methyl iodide at –78 °C, but unfortunately it was the undesired (*R*)-configured quaternary stereocenter (abietic-type stereochemistry) that was produced in excellent yield and with complete selectivity, rather than the requisite (*S*)-configured podocarpic-type stereocenter. The stereochemistry of methyl ester **2.150** was unambiguously assigned by X-ray crystallographic analysis (*Figure 2.11*), following removal of the *tert*-butyldimethylsilyl ether protective group and oxidation of secondary alcohol **2.151** to the corresponding ketone (**2.152**, *Scheme 2.32*). Removal of the *tert*-butyldimethylsilyl ether protective group was rather sluggish overall at ambient temperature with a variety of fluoride sources, including pyridine hydrofluoride and triethylamine trihydrofluoride (*Scheme 2.32*). Tetrabutylammonium fluoride could also effect the deprotection, but the reaction mixture had to be heated at 50 °C and the conversion was highly dependent on the quality of the reagent, as was analogously observed during the total synthesis of decaturin C.[287]

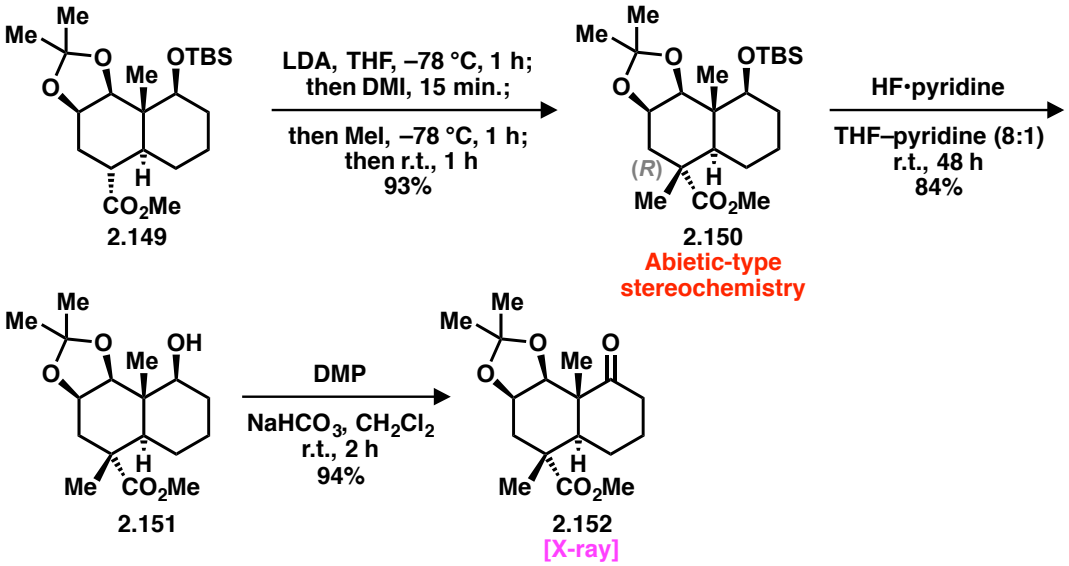

Scheme 2.32 – α-Methylation of ester afforded abietic-type stereochemistry.

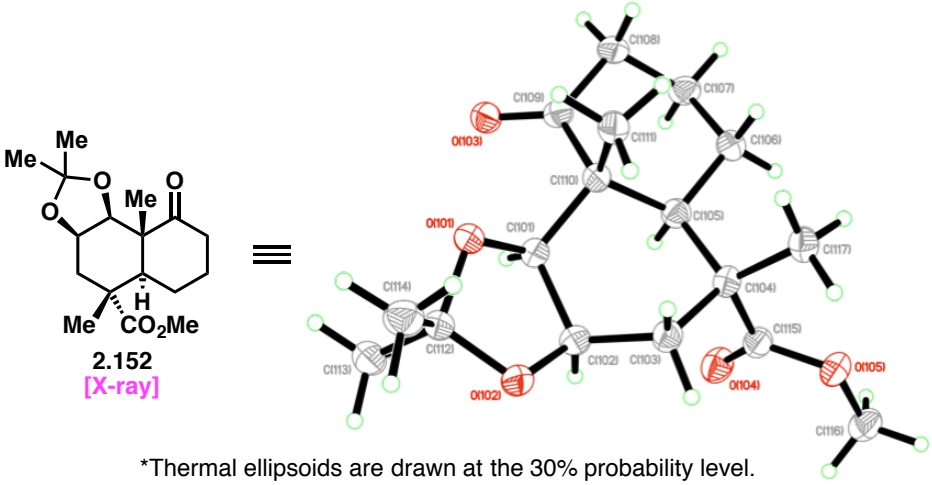

*Thermal ellipsoids are drawn at the 30% probability level.

Figure 2.11 – X-ray crystallographic structure of ketone.

Although the stereochemical outcome of the alkylation was not ideal, it was nevertheless appropriate to explore the possibility of installing an enone in ring B, which could eventually be used to form the γ-lactone through the envisaged bromolactonization reaction (*Scheme 2.12*, p. 83). Owing to the success previously observed for the synthesis of related podolactones,[165] the first attempt to install the enone was with 2-iodoxybenzoic acid directly (entries 1–2, *Table 2.4*).[200] Unfortunately, there was no significant conversion to the enone under those conditions, and ketone **2.152** was recovered; attempts with selenium-based

methods[287] were equally ineffective. Although an initial attempt with palladium(II) trifluoroacetate in ethyl acetate (entry 3, *Table 2.4*), using the method reported by Stahl's group,[295] was similar to that for 2-iodoxybenzoic acid, changing the solvent to 1,4-dioxane (entry 4, *Table 2.4*) was quite promising and led to a higher conversion of ketone **2.152** to enone **2.153**. The exclusive use of dimethyl sulfoxide as the solvent (entry 5, *Table 2.4*) led to complete consumption of ketone **2.152** and the formation of enone **2.154**, in which the acetonide protective group was no longer present. Although deprotection was partially alleviated with the addition of sodium carbonate (entry 6, *Table 2.4*), it was also possible to immediately re-protect *syn*-1,2-diol **2.154** as acetonide **2.153** (*Scheme 2.33*), which had the additional benefit of facilitating the subsequent purification by column chromatography.

Table 2.4 – Oxidation of ring B ketone to enone.

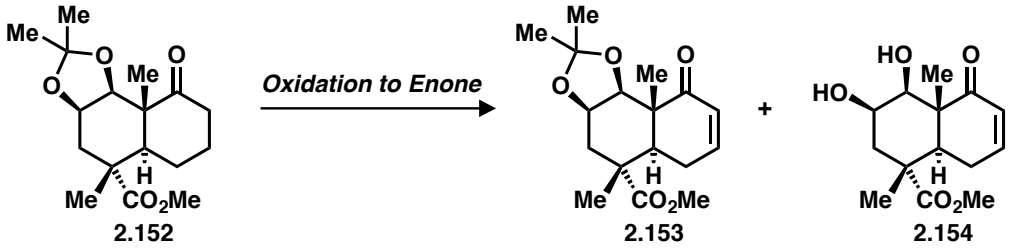

Entry	Oxidant	Additive	Solvent	Temp.	Time	Conv.[a]	Ratio of 2.152 : 2.153 : 2.154[a]
1	IBX	-	DMSO–toluene (1:3)	80 °C	24 h	10%	9 : 1 : 0
2	IBX	-	DMSO–HFB (1:2)[b]	80 °C	24 h	10%	9 : 1 : 0
3	$Pd(TFA)_2$,[c] O_2	40% DMSO	EtOAc	60 °C	16 h	10%	9 : 1 : 0
4	$Pd(TFA)_2$,[c] O_2	40% DMSO	1,4-dioxane	80 °C	16 h	40%	6 : 4 : 0
5	$Pd(TFA)_2$,[d] O_2	-	DMSO	80 °C	16 h	>90%	0 : 0 : 1
6	$Pd(TFA)_2$,[d] O_2	0.1 eq. Na_2CO_3	DMSO	80 °C	16 h	>90%	0 : 1 : 1
7	$Pd(OAc)_2$,[d] O_2	0.1 eq. Na_2CO_3	DMSO	80 °C	16 h	40%	6 : 4 : 0

[a] Determined by ^1H NMR; [b] HFB = hexafluorobenzene; [c] 20 mol% $Pd(TFA)_2$; [d] 100 mol% $Pd(TFA)_2$

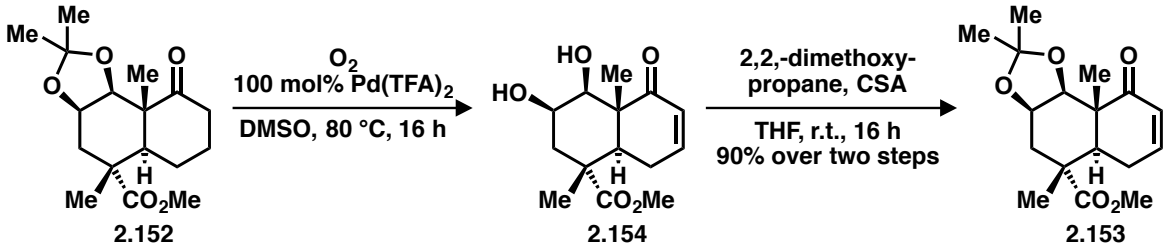

Scheme 2.33 – Oxidation to enone and re-protection of 1,2-diol.

To explore possible opportunities for overcoming the undesirable outcome of the α-methylation reaction, transition state structures were explored with an appropriate model system (*Figure 2.12*). For the model system, the trimethylsilyl protective group was used in place of the *tert*-butyldimethylsilyl group in order to reduce the number of possible conformers, given that the silyl ether protective group at C9 is not expected to have a significant influence on the facial selectivity of the alkylation reaction. Furthermore, methyl chloride was used in place of methyl iodide to reduce the computational cost of the calculations as well, since it is not expected to have a significant influence on the selectivity of the reaction given the overriding restriction in conformational flexibility of the scaffold imposed by the presence of the acetonide-protected 1,2-diol.[296-298]

Quantum chemical computations were performed with *Gaussian 09*. To identify the lowest energy conformers for the bicyclic enolate, Monte Carlo conformational searches were performed with Macromodel 9.9[299] and the corresponding conformers were then optimized at the B3LYP[300-303]/6-31+G(d,p) level in conjunction with the IEF-PCM implicit solvation model[304] to account for the influence of tetrahydrofuran, the solvent used experimentally. Transition state searches were performed in the presence of methyl chloride at the same level, and additional single-point energies of the optimized transition states were evaluated at the B3LYP-D3(BJ)[305-309] and M06-2X[310] levels with the polarized, triple-ζ valence quality def2-TZVPP basis set of Weigend and Ahlrichs[311] within the IEF-PCM model for tetrahydrofuran. Thermal corrections evaluated from unscaled vibrational frequencies at the B3LYP/6-31+G(d,p) level on optimized geometries were added to the single point electronic energies to obtain the free energies. The free energy corrections were calculated using Truhlar's quasiharmonic approximation.[312,313]

The lowest-energy transition structures leading to each diastereomer are shown in *Figure 2.12*. Consistent with the experimental observation of the major isomer having a (*R*)-configured quaternary centre, alkylation from the *si* face of the ester enolate (β face of the trans-fused scaffold) was calculated to be more favourable than the corresponding transition state leading to the (*S*)-configured quaternary centre by 1.3 kcal/mol. Inspection of the lowest energy transition structure (**TS-2.7**) reveals that ring A is in a boat-type conformation, with the ester enolate pointed towards the β face, effectively avoiding steric interactions with the axial C10 methyl group and minimizing strain with respect to the C6 methylene group. As the C–C

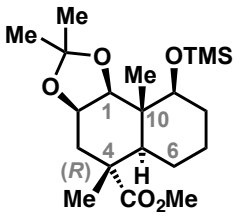

2.155
Abietic-type stereochemistry

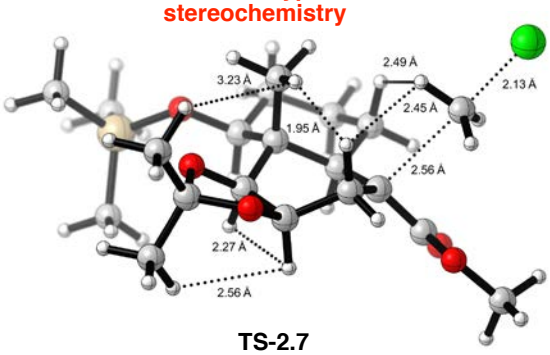

TS-2.7
Boat transition structure
Leads to (*R*)-Configuration
ΔG‡ = +16.5 (+12.1, +16.7) kcal/mol
ΔΔG‡ = 0.0 (0.0, 0.0) kcal/mol

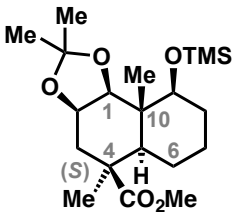

2.156
Podocarpic-type stereochemistry

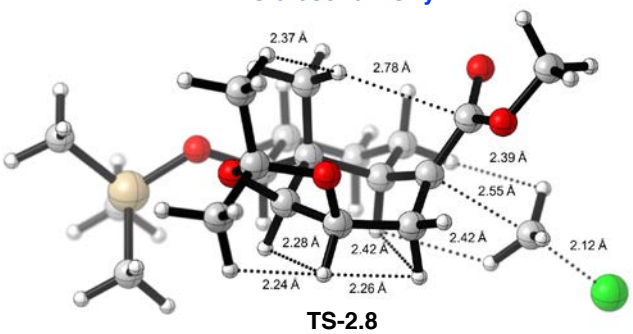

TS-2.8
Half-chair-like transition structure
Leads to (*S*)-Configuration
ΔG‡ = +17.8 (+13.0, +17.4) kcal/mol
ΔΔG‡ = +1.3 (+0.9, +0.7) kcal/mol

B3LYP/6-31+G(d,p)-IEF-PCM(tetrahydrofuran) geometries, frequencies, and energies are shown. The corresponding values for the B3LYP-D3(BJ)/def2-TZVPP-IEF-PCM(tetrahydrofuran)//B3LYP/6-31+G(d,p)-IEF-PCM(tetrahydrofuran) and M06-2X/def2-TZVPP-IEF-PCM(tetrahydrofuran)//B3LYP/6-31+G(d,p)-IEF-PCM(tetrahydrofuran) levels are provided sequentially in parentheses.

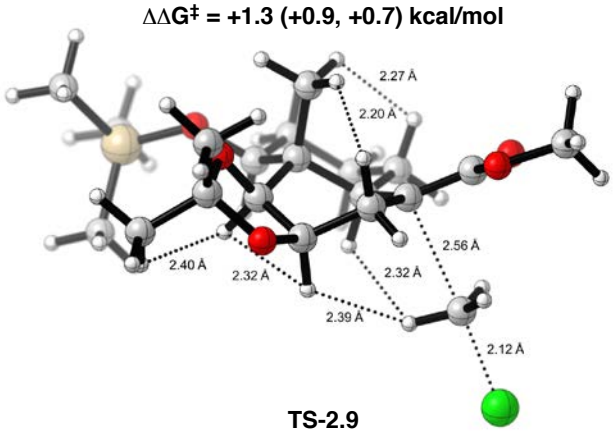

TS-2.9
Twist-boat transition structure
Leads to (*S*)-Configuration
ΔΔG‡ = +18.0 (+13.9, +18.3) kcal/mol
ΔΔG‡ = +1.5 (+1.8, +1.6) kcal/mol

Figure 2.12 – Transition structures for α-methylation of ester enolate.

bond forms, the conformation of ring A moves towards a twist-boat-like conformation, which relieves some strain between the axial methyl group and the axial hydrogen atom at C3. Although this conformation ensures that the methyl substituents of the acetonide protective group avoid coming into close contact with the C10 axial methyl group, it comes at the expense of a close contact between the axial hydrogen atoms at C1 and C2 (2.27 Å), as well as

between the axial methyl group and the axial hydrogen atom at C3 (1.95 Å). In the next-highest-energy transition structure (**TS-2.8**), which leads to the (*S*)-configured quaternary centre, ring A is in a higher energy half-chair-like conformation, effectively placing the ester enolate into a conformation that brings it closer to the C10 axial methyl group (2.78 Å) as well as the methylene group at C10. Close contacts are also observed between hydrogen atoms located at C1, C2, and C3, while the pro-(*R*)-methyl group of the acetonide protective group moves significantly closer to the axial methyl group at C10 (2.37 Å), as a consequence of the half-chair-like geometry adopted by ring A. Although the incoming electrophile in **TS-2.8** avoids steric interactions with the axial methyl group that are present in **TS-2.7**, these interactions are overshadowed by the unfavourable intramolecular interactions that arise from the conformational restrictions imposed by the acetonide protective group. Notably, another transition state leading to the (*S*)-configured quaternary centre was also located in which ring A was in a twist-boat-like conformation (**TS-2.9**), but it was also found to be higher in energy than **TS-2.7**. In this last transition state, the electrophile also passes into closer contact with the hydrogen atoms at C2 and C5 as a consequence of the geometry adopted by the scaffold.

To overcome this challenge of stereoselectivity, it was reasoned that a non-cyclic protective group would be better, since it would allow both rings to effectively adopt a chair conformation, which has been shown to favour alkylation from the correct face of the bicyclic scaffold.[165,199] A dimethyl ether derivative was selected to be the model system, since it was the smallest group available to protect the alcohol in an efficient manner. Consequently, diol **2.157** (*Scheme 2.34*) was converted into the corresponding dimethyl ether derivative in excellent yield, and stereoselective alkylation was attempted for the purpose of synthesizing **2.159**. Unfortunately, deprotonation of methyl ester **2.158** at C4 was exceptionally difficult with lithium diisopropylamide and lithium bis(trimethylsilyl)amide, even at ambient temperature in the presence of polar additives, such as hexamethylphosphoramide or 1,3-dimethyl-2-imidazolidinone. To ensure that the difficulty did not lie with the electrophile, an attempt was made to quench the potential enolate with deuterium oxide, but the absence of incorporated deuterium was strong evidence that the enolate had not formed.

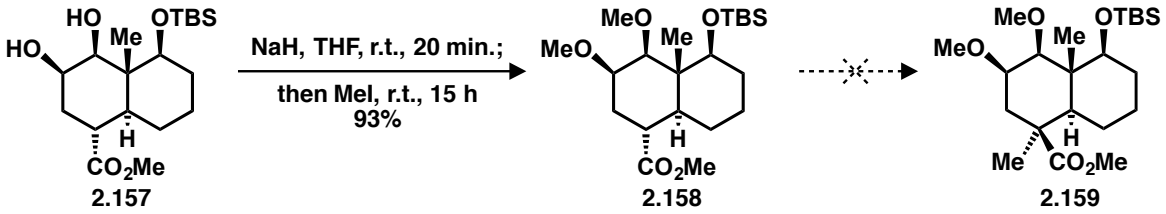

Scheme 2.34 – Attempted alkylation with a more flexible scaffold.

The inability to conveniently deprotonate a related α-configured methyl ester was noted in passing by Dr. Boyer during his synthesis of similar podolactones,[165] and was one reason initial attempts were made to exclusively prepare the α configured methyl ester instead during the current route (*Scheme 2.29*, p. 106). It appears that the preferred conformation of ring A places the hydrogen atom at C4 into a sterically encumbered orientation which precludes it from attaining proper orbital alignment with an incoming base, which is necessary for proton transfer to occur. Fortunately, the presence of the acetonide places the same hydrogen atom into a less encumbered environment and allowed the corresponding ester enolate to be generated, even if the same acetonide was responsible for the undesirable stereochemical outcome of the subsequent alkylation. For this reason, a decision was made to exploit the inherent selectivity of the alkylation and synthesize a standard with the desired configuration at the quaternary centre using a circuitous sequence of reactions instead.

2.4.8 Alkylation and Stereochemistry of Quaternary Centre

As a consequence of the conformational restrictions imposed by the acetonide protective group, alkylation of the ester enolate of **2.149** favours approaches from the *si* face – *syn* to the C10 axial methyl group. To properly configure the quaternary stereocenter, it was reasoned that the ester could be reduced to the methyl group, while a judiciously selected electrophile could be oxidized to the corresponding acid (or ester) – effectively establishing the desired podocarpic-type stereochemistry through an indirect, albeit potentially effective route (*Scheme 2.35*). To this end, benzyl chloromethyl ether was selected as the electrophile, since it represents a protected primary alcohol that could, in principle, be oxidized to the desired acid or ester, following reduction of the original methyl ester group.

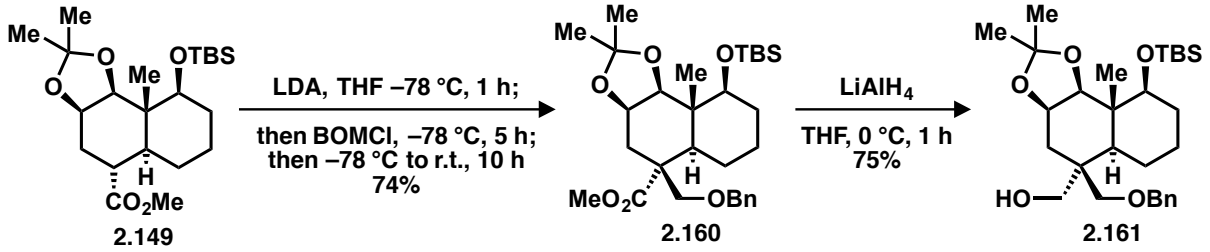

Scheme 2.35 – Alkylation with benzyl chloromethyl ether to set quaternary stereocenter.

Alkylation with benzyl chloromethyl ether proceeded with a modest yield of 74% to provide benzyl-protected hydroxymethyl-branched ester **2.160**, with the expected stereochemistry. Reduction of methyl ester **2.160** proceeded smoothly in the presence of lithium aluminum hydride and furnished the primary, albeit neopentylic, hydroxy group in **2.161**.[314,315] Reduction of the primary hydroxy group to the analogous methyl moiety was envisaged to occur through a two-step procedure: 1) activation, and 2) hydride-mediated displacement of a leaving group. Initial forays into this sequence began with mesylation/tosylation of the primary alcohol and either direct hydride-mediated reduction, or reduction through an intermediate iodide.

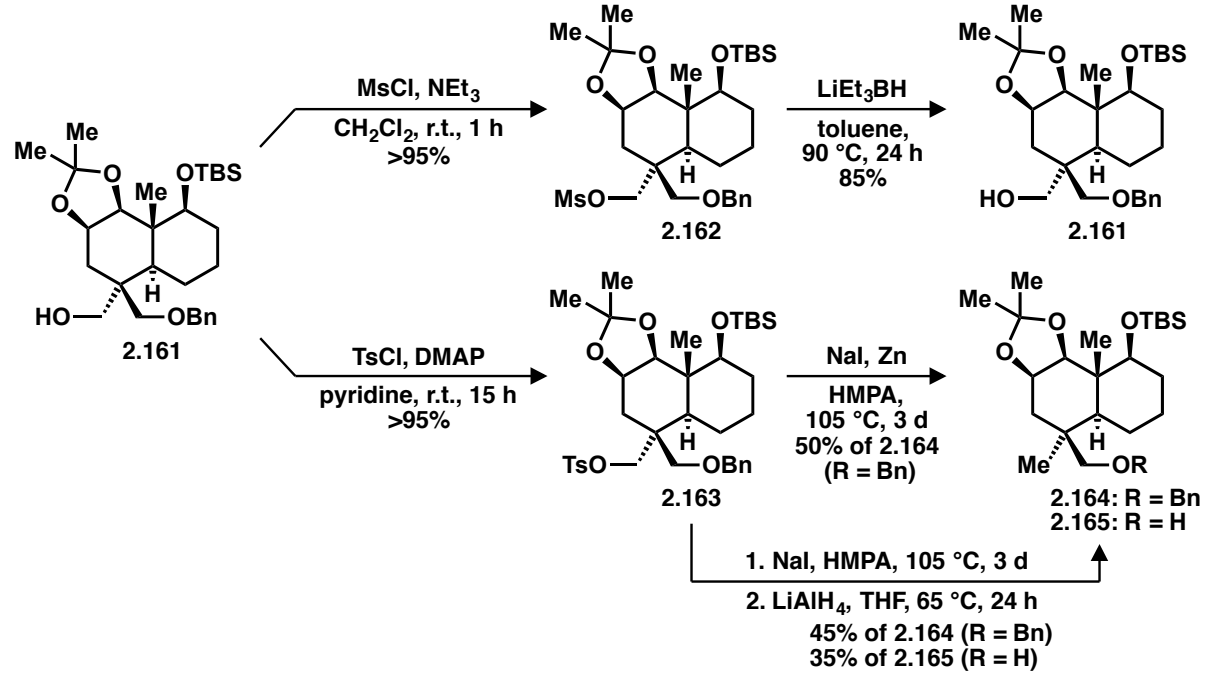

Scheme 2.36 – Reduction of primary alcohol via mesylate or tosylate.

Mesylation and tosylation furnished the corresponding sulfonate esters (i.e., **2.162** and **2.163**) in excellent yield, with the former reaction proceeding more quickly than the latter (*Scheme 2.36*). Attempted reduction of mesylate ester **2.162** with lithium triethylborohydride was unproductive, in that the initial primary alcohol precursor (**2.161**) was recovered unchanged, likely as a result of the sterically demanding nature of the neopentylic alcohol. This is perhaps emphasized by the relatively high temperature required for the reduction and the lack of reactivity – as observed by thin-layer chromatographic analysis – below 65 °C, where it was quite sluggish. Reduction of the tosylate ester with zinc in the presence of sodium iodide was more successful in effecting the desired course of reduction, but the yield was rather low (**2.163** to **2.164**).[314,316,317] Since this reduction likely proceeds through an intermediate alkyl iodide, a two-step procedure involving displacement of the tosylate ester, followed by reduction of the alkyl iodide was also pursued, with lithium aluminum hydride as the reducing agent.[318] This last sequence was more efficient overall, affording a mixture of benzyloxymethyl ether **2.164** and deprotected primary alcohol **2.165** in 80% overall yield.

Importantly, successful reduction of the alkyl iodide effectively unveiled a more streamlined approach for reducing primary alcohol **2.161**, in which the intermediate sulfonate esters were rendered superfluous, and the probability of avoiding the use of hexamethylphosphoramide as a solvent increased. Accordingly, neopentylic alcohol **2.161** was converted directly to alkyl iodide **2.166** in the presence of iodine, triphenylphosphine, and imidazole (*Scheme 2.37*), using a method initially reported by Garegg's group during their work on carbohydrates.[319,320] The alkyl iodide could then be reduced in excellent yield to a mixture of benzyloxymethyl ether **2.164** and deprotected primary alcohol **2.165** in the presence of sodium borohydride in dimethylsulfoxide, or chemoselectively reduced to benzyloxymethyl ether **2.164** with lithium triethylborohydride (*Scheme 2.37*). While the overall yields were identical for the two options, reductions with lithium triethylborohydride in toluene were favoured as they tended to be more convenient to work with and the need to isolate only one product significantly simplified the associated purification.

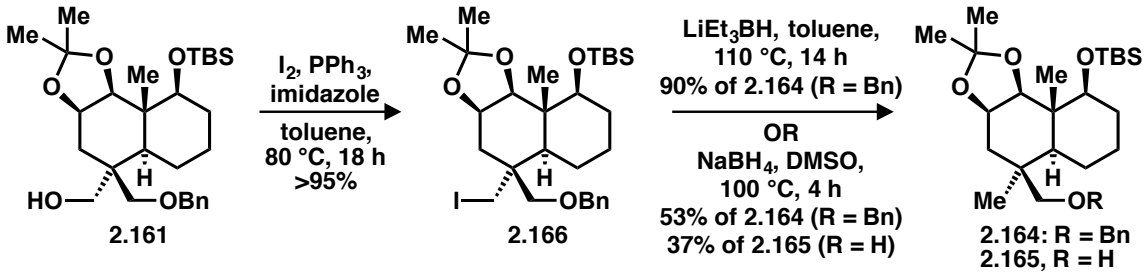

Scheme 2.37 - Reduction of neopentylic alcohol to establish quaternary stereocenter.

Regardless of the method used to reduce the alkyl iodide, the benzyloxymethyl ether was converged to primary alcohol **2.165** with hydrogen and palladium(II) hydroxide on carbon (*Scheme 2.38*). A three-step sequence was used to prepare methyl ester **2.168**: Dess–Martin-periodinane-mediated oxidation of primary alcohol **2.165**, followed by Pinnick oxidation of aldehyde **2.167**,[321,322] and subsequent methylation of the carboxylic acid with trimethylsilyldiazomethane.[323] Similar to the sequence explored for the epimeric quaternary centre (*Scheme 2.32*, p. 109), the *tert*-butyldimethylsilyl protective group was removed with a source of fluoride and the resultant secondary alcohol oxidized with Dess–Martin periodinane to provide ketone **2.169**. For this sequence, triethylamine trihydrofluoride was used in place of pyridine hydrofluoride because it was found to be more robust overall.

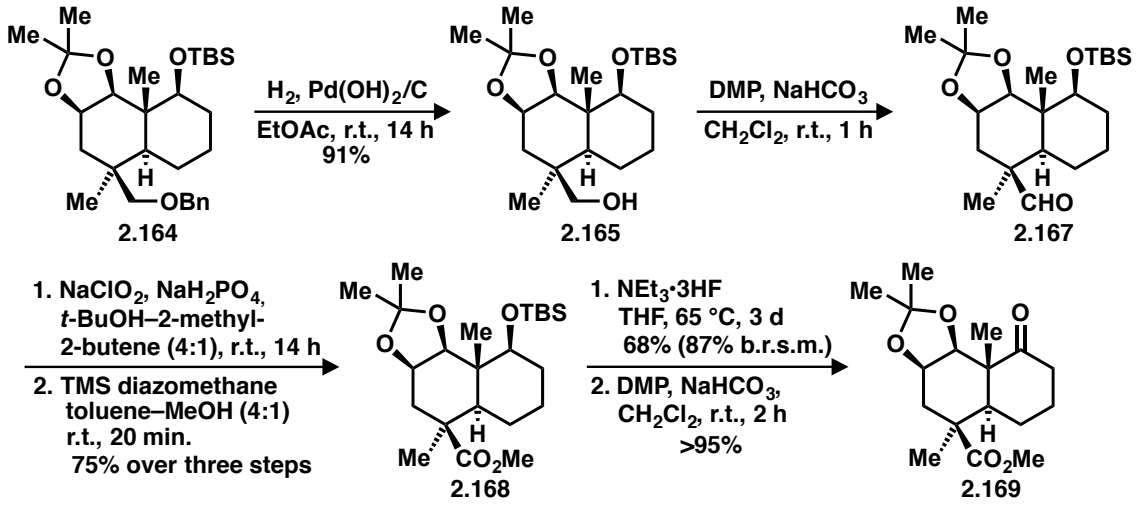

Scheme 2.38 – Oxidation to methyl ester and deprotection of silyl ether.

Notably, during an attempt to oxidize aldehyde **2.167** with Oxone®,[324] both the *tert*-butyldimethylsilyl group and the acetonide were effectively removed (*Scheme 2.39*). Cleavage

of the silyl ether under the reaction conditions was particularly surprising, given the challenge associated with removing it in the presence of fluoride sources – as well as Oxone® being previously established as a method for selectively deprotecting primary *tert*-butyldimethylsilyl protective groups in the presence of secondary ones.[325] In any case, acetal **2** was a highly crystalline solid and allowed the absolute configuration of the quaternary stereocenter to be verified with X-ray crystallography (*Figure 2.13*).

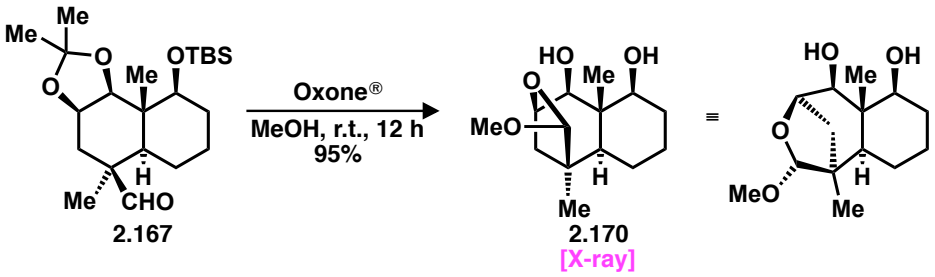

Scheme 2.39 – Oxidation with Oxone®.

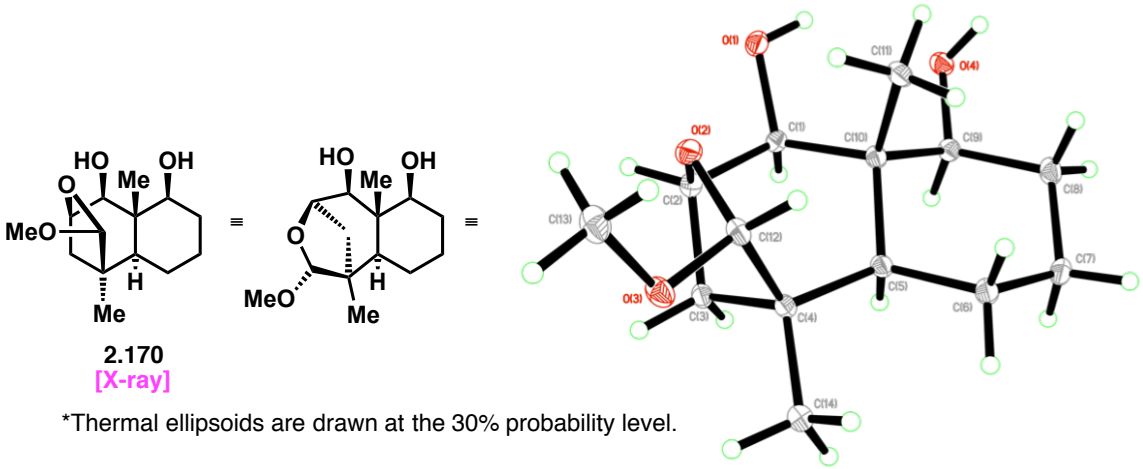

*Thermal ellipsoids are drawn at the 30% probability level.

Figure 2.13 – X-ray crystallographic structure of diol from Oxone®-mediated-oxidation.

2.4.9 Overview of the First-Generation Sequence

At this point, it was necessary to begin another scale-up for the purpose of preparing significantly larger quantities of material that would likely be necessary to complete the synthesis of nagilactone B. A summary of the synthetic sequence to this point is provided on page 120 in *Scheme 2.40*. The overall yield for the 21-step synthetic sequence from (+)-Wieland–Miescher ketone (+)-**2.33** to ketone **2.169** is approximately 3%, with 12 silica-based

purifications. The key steps for the synthesis include regioselective allylic oxidation, reduction of a 1,2-diketone to afford a *syn*-1,2-diol, and a multi-step sequence for establishing the quaternary centre. Although the presence of the acetonide protective group necessitates using a circuitous sequence of reactions to set the quaternary stereocenter, the advantage of this approach is that both podocarpic- and adiabatic-type scaffolds are readily accessible from a common intermediate (**2.149**).

Nevertheless, while it was putatively feasible to prepare sufficient material to continue the synthesis (10 g of Wieland–Miescher ketone would optimistically provide 0.5 g of ketone **2.169**, if the yields of the latter reactions in the synthesis remain consistent on larger scale), it was also apparent that there were many technical challenges associated with doing so. In particular, two major bottlenecks for the synthesis include the initial reductive carbomethoxylation reaction and the crucial allylic oxidation with chromium trioxide. The former required significant care and necessitated condensing large volumes of ammonia on multigram scale, while the latter required ≥12 molar equivalents of chromium trioxide for the allylic oxidation to be efficient. To put this in perspective, for every 10 g of α,β-unsaturated ester intended to be oxidized, more than 35 g of chromium trioxide is required. Even putting aside for a moment the significant toxicity associated with this inorganic material, its use in such quantities makes for particularly difficult purifications as a consequence of the large quantities of chromium salts that are generated, and the presence of emulsions that make it difficult to pinpoint the interface between the nearly opaque aqueous and organic phases.

It was also very clear that a number of significant challenges remained for completing the synthesis: formation of the γ-lactone, oxidation at C7, and preparing the α-pyrone moiety with an isopropyl group (*Scheme 2.12*, p. 83). Optimistically, following a traditional sequence[165] more than more than 12 additional steps would be required, many of which were expected to be synthetically challenging. Despite the possibilty of completing the first-generation synthesis given enough time and resources,[326-332] a second-generation approach began to take priority as concurrent studies on the latter approach showed significant potential. The second-generation approach is described in Chapter 3.

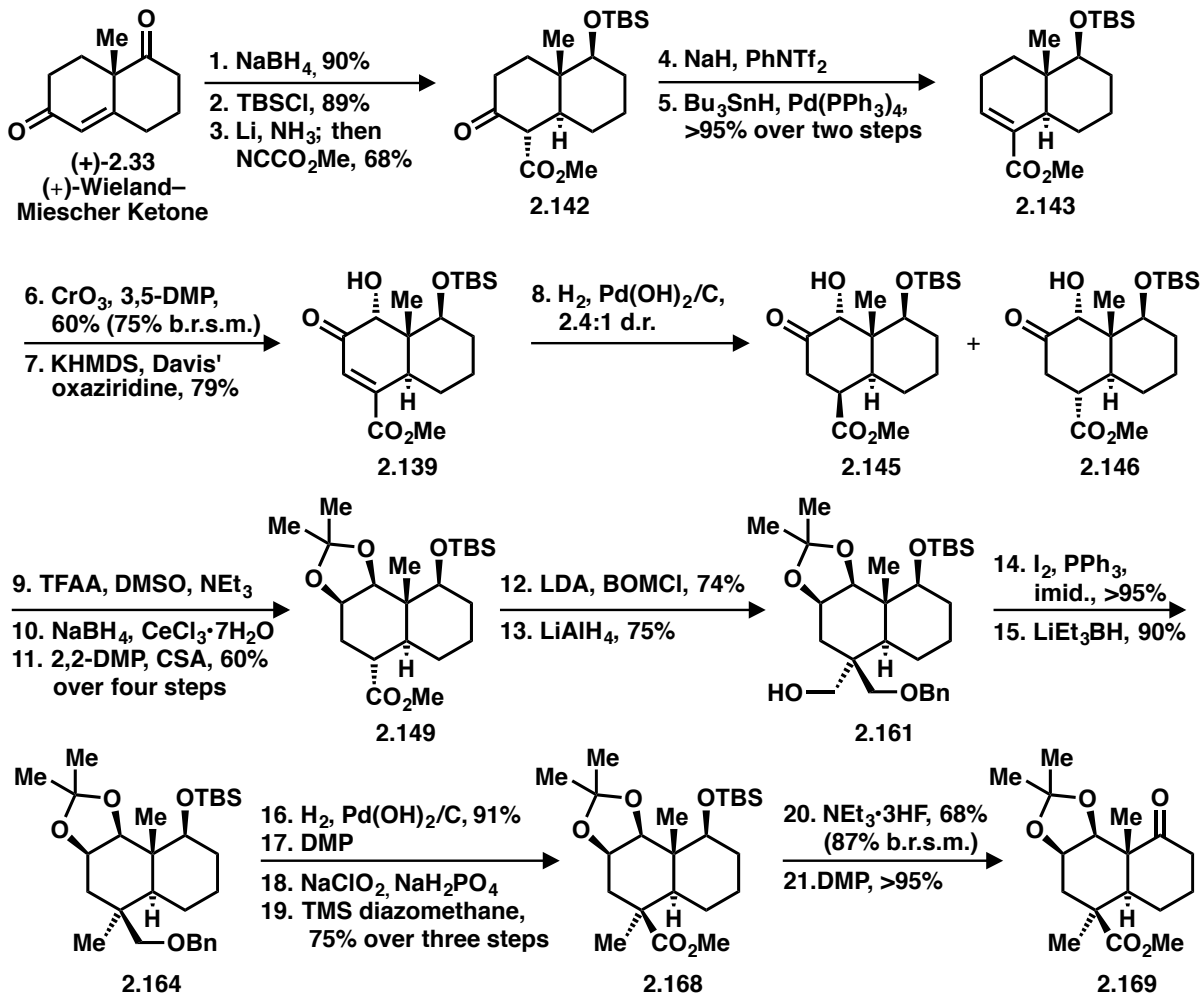

Overall: 21 steps, 14 purifications with silica, ~3% overall yield

Reagents and Conditions: 1. $NaBH_4$, MeOH–CH_2Cl_2 (1:2), –78 °C, 1 h, 90%; **2.** TBSCl, imidazole, DMF, r.t., 20 h, 89%; **3.** Li, NH_3, *t*-BuOH, Et_2O, –78 °C to reflux, 3 h; then $NCCO_2Me$, Et_2O, –78 °C to r.t., 2 h, 68%; **4.** NaH, $PhNTf_2$,1,2-DME, r.t., 6 h; **5.** Bu_3SnH, 4 mol% $Pd(PPh_3)_4$, LiCl, THF, r.t. to 50 °C, 4 h, >95% over two steps; **6.** CrO_3, 3,5-DMP, CH_2Cl_2, –25 to –15 °C, 16 h, 60% (75% b.r.s.m.); **7.** KHMDS, Davis' oxaziridine, THF, –78 °C, 1 h, 79%; **8.** H_2, 4 mol% $Pd(OH)_2$/C, MeOH–EtOAc (1:2), r.t., 20 h, 2.4:1 d.r. (**5** to **6**); **9.** TFAA, DMSO, CH_2Cl_2, –78 °C, 1 h; then NEt_3, –78 °C to r.t, 30 min.; **10.** $NaBH_4$, $CeCl_3$•$7H_2O$, MeOH, –40 °C, 1 h; **11.** 2,2-DMP, CSA, THF, r.t. , 5 h, 60% over four steps; **12.** LDA, THF, –78 °C, 1 h; then BOMCl, –78 °C, 5 h; then –78 °C to r.t., 10 h, 74%; **13.** $LiAlH_4$, THF, 0 °C, 1 h, 75%; **14.** I_2, PPh_3, imidazole, toluene, 80 °C, 18 h, >95%; **15.** $LiEt_3BH$, toluene, 110 °C, 14 h, 90%; **16.** H_2, 5 mol% $Pd(OH)_2$/C, EtOAc, r.t., 14 h, 91%; **17.** DMP, $NaHCO_3$, CH_2Cl_2, r.t.,1 h; **18.** $NaClO_2$, NaH_2PO_4, *t*-BuOH–2-methyl-2 butene (4:1), r.t., 14 h; **19.** TMS diazomethane, MeOH–toluene (1:4), r.t., 20 min., 75% over three steps; **20.** NEt_3•3HF, THF, 65 °C, 3 d, 68% (87% b.r.s.m.); **21.** DMP, $NaHCO_3$, CH_2Cl_2, r.t., 2 h, >95%.

Scheme 2.40 – First-generation sequence for synthesizing the core of nagilactone B.

2.5 Future Work, Conclusions, and Perspective

Although the first-generation synthesis holds significant promise, to truly improve the efficiency of that route for the purpose of preparing nagilactone B, it is imperative that a scalable alternative to the use of chromium trioxide be found for the regioselective allylic oxidation reaction (*Scheme 2.27*). The potential demonstrated by dirhodium tetracaprolactamate[275] on milligram quantities of material (*Table 2.3*, p. 98) is particularly appealing and would serve as a good starting point.

Another avenue to explore involves directly functionalizing γ-keto-α,β-unsaturated ester **2.138** or its hydroxylated derivate (**2.139**, (*Scheme 2.41*); if the quaternary centre can be established through a regio- and stereoselective conjugate addition reaction it would significantly streamline the sequence by effectively eliminating eight synthetic steps, thereby avoiding the indirect route for setting the quaternary centre. A method reported by the group of Hoveyda, which makes use of catalytic quantities of N-heterocyclic carbene copper complexes has significant potential for addressing this challenge and should be explored in subsequent studies on this particular approach.[333,334] Notably, this reaction could be optimized at one of two different stages: 1) with unsubstituted γ-keto-α,β-unsaturated ester **2.138**, or 2) with the C1-substituted α-hydroxy ketone **2.139**, which could direct alkylation through coordination to the secondary hydroxy group. The former approach would be more broadly applicable, but for the synthesis of nagilactone B, the latter approach provides an alternative option that may be more effective.

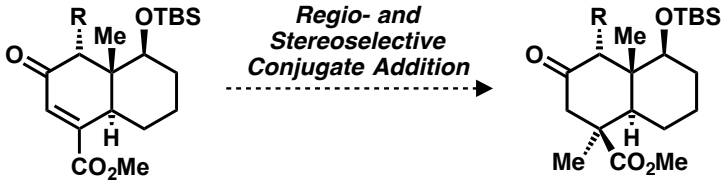

2.138: R = H
2.139: R = OH

2.171: R = H
2.172: R = OH

Scheme 2.41 – Conjugate addition to establish quaternary stereocenter.

Indeed, a serious effort to optimize the crucial allylic oxidation and conjugate addition reaction would significantly increase the applicability of this approach[335] for the synthesis of

nagilactone B, as well as analogues that are oxidized at C2, such as 2β-hydroxynagilactone F,[167] nagilactone I,[167] and salignone M.[272]

With knowledge gained from the first-generation strategy, the goal of synthesizing nagilactone B was guided towards a second-generation approach, which began to show significant promise. Chapter 3 focuses on the second-generation strategy for synthesizing the core of nagilactone B.

Chapter 3:

Second-Generation Strategy for Synthesizing the Core of Nagilactone B

3.1 Introduction

Please refer to Chapter 2 for an introduction to the podolactone family of natural products (Section 2.1, p. 63), including previous syntheses (Section 2.2, p. 66) and a brief description of nagilactone B (Section 2.3, p. 80).

Experiences with the first-generation sequence for synthesizing the core of nagilactone B, as described in Chapter 2, reinforced the challenges associated with synthesizing the *syn*-1,2-diol moiety and establishing the quaternary centre. A cursory analysis of that route (*Scheme 2.40*, p. 120) exposed the fact that many of those issues are a direct consequence of using (+)-Wieland–Miescher ketone as the starting material. Comparing the scaffold of (+)-Wieland–Miescher with that of nagilactone B reveals that although the C10 axial methyl group and the bicyclic scaffold are conserved overall, a significant amount of manipulation is likely needed to convert (+)-Wieland–Miescher ketone to nagilactone B (*Figure 3.1*).

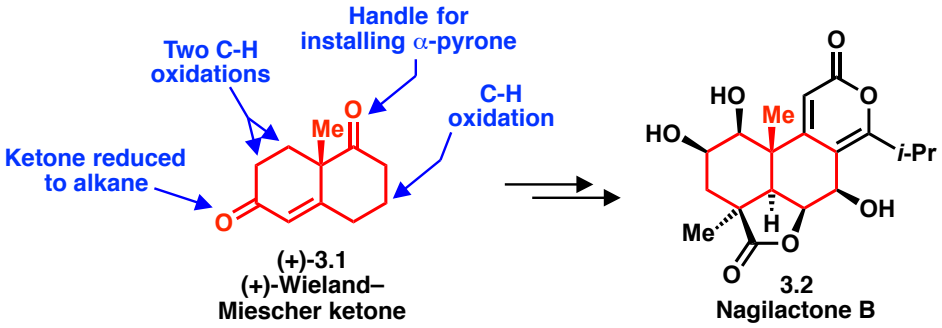

Figure 3.1 – Overview of first-generation approach for synthesizing nagilactone B.

Specifically, although the enone may be used as a handle for installing the *syn*-1,2-diol moiety and the C4 quaternary stereocenter of nagilactone B, it comes at the expense of synthetic efficiency since its presence actually hinders the stereoselectivity of the alkylation at C4 to set the quaternary centre (*Scheme 2.16*, p. 92). Furthermore the ketone at C3 must eventually be reduced to the corresponding alkane, given that it is not present in the scaffold of the norditerpenoid dilactone natural product. For the purpose of preparing nagilactone B, it is also necessary to effect formal C-H oxidations at C1 and C2, which must either occur stereoselectively on the same face as the axial C10 methyl group or, more likely, through oxidation–reduction sequences. Using (+)-Wieland–Miescher ketone also necessitates

performing two remote C-H oxidations at C1 and C7, of which neither position is directly activated by virtue of being next to a conveniently manipulable functional group. Taken together, these concessions truly diminish the overall efficiency of the first-generation approach and led to the pursuit of alternative strategy in its place.[335-338]

Inspiration for the complementary second-generation strategy arose when options for preparing the (+)-Wieland–Miescher ketone in larger quantities were taken into consideration. In particular, the reported efficiency of the *tert*-leucine-derived catalyst described by Luo's group (**2.100**, *Figure 2.7*, p. 87) was especially intriguing and a new procedure disclosed around that time prompted a closer look at its use for the scale up.[250,252] Notably, the reported L-*tert*-leucine-derived catalyst was actually used to prepare enantiomeric (–)-Wieland–Miescher ketone ((–)-**3.1**), in part because it is synthesized from the less expensive enantiomer of *tert*-leucine.[339] Perhaps as a consequence of the ongoing struggles with chromium-based allylic oxidation reactions or the overall challenges associated with the first-generation synthesis, the structure of (–)-Wieland–Miescher ketone immediately stood out as a potential precursor for the synthesis of nagilactone B, and ring-A-functionalized podolactones in general. A conceptual comparison of these two approaches, in which the core is highlighted in an effort to demonstrate the utility of each enantiomer to the synthesis of nagilactone B, is provided in *Figure 3.2*.

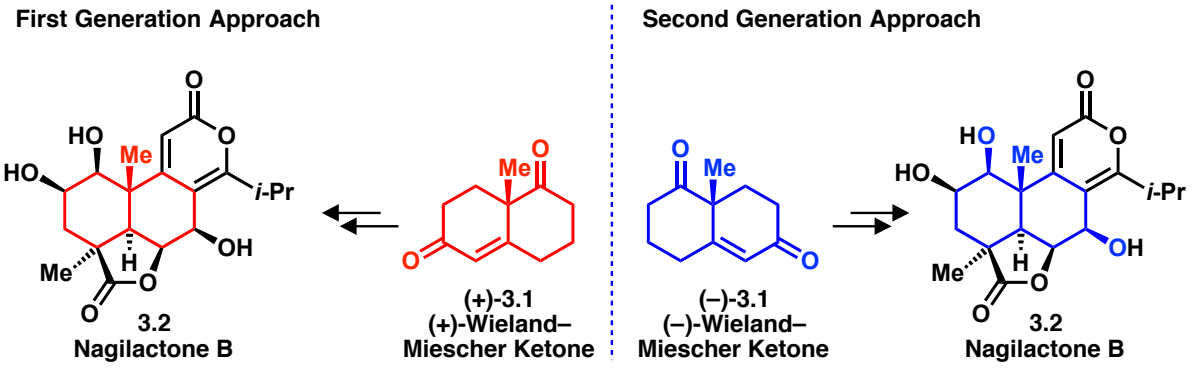

Figure 3.2 – Applying the Wieland–Miescher ketone to the synthesis of nagilactone B.

The advantages of pursuing such a strategy were immediately evident: the ketone moieties could serve as handles for installing the key functional groups, while also being incorporated into the scaffold as secondary alcohols without recourse to conciliatory

oxidation–reduction sequences. For nagilactone B, the diol moiety could potentially be installed early in the synthesis, without involving chromium-mediated allylic oxidation reactions, lengthy oxidation–reduction sequences, or late-stage oxidations to install the C7 hydroxy group. Moreover, for the purposes of preparing ring A analogues, it was envisaged that the C1 ketone could be protected and serve as a functional group handle for diversification towards the end of the synthesis, depending on the synthetic target of interest. Lastly, a practical advantage of working with the Wieland–Miescher ketone, was that it was readily available as a consequence of the first-generation sequence, which made it significantly more convenient to perform exploratory reactions for the second approach, while simultaneously working on the first-generation sequence.

Of course, despite this route's appeal in that it could potentially address oxidations at C2 and C7, it was likewise apparent that the overall success would rely upon the ability to prepare the quaternary centre and the γ- and δ-lactone moieties – both challenges in their own right. A brief description of related work that has been disclosed for similar scaffolds, which served as inspiration for initial investigations is provided in Section 3.3 (p. 129).

3.2 Synthetic Strategy for Second-Generation Synthesis

Re-examination of the first-generation sequence for synthesizing nagilactone B (*Figure 2.4*, p. 82), led to an updated strategy that used (–)-Wieland-Miescher ketone as the starting material (*Figure 3.3*). While the challenges associated with preparing the γ- and δ-lactones did not significantly change, those related to incorporating the *syn*-1,2-diol and C7 hydroxy group appeared to be significantly alleviated. For the purpose of synthesizing nagilactone B, the *syn*-1,2-diol moiety was intended to be installed early on in the synthesis, followed closely by the quaternary stereocenter, and then the lactone moieties.

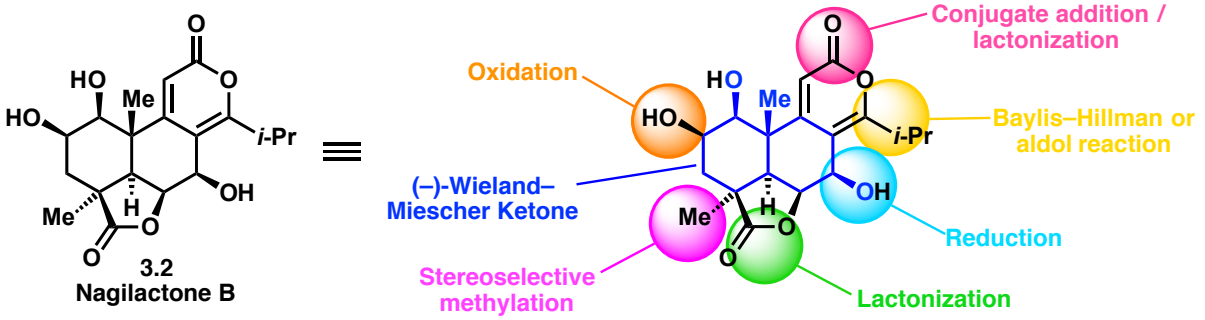

Figure 3.3 – Updated analysis of the structure of nagilactone B.

A retrosynthetic analysis for the second-generation route is given in *Scheme 3.1*. Similar to the first-generation sequence, synthesizing the α-pyrone moiety was envisaged to occur towards the end of the synthetic sequence. Conjugate addition of an appropriate nucleophile on an activated diketone such as **3.4**, would lead to a precursor that could undergo intramolecular cyclization under conditions similar to those previously reported by Hayashi (*Scheme 2.8*, p. 72); perhaps this could even occur spontaneously under the reaction conditions. Alternatively, conjugate addition on an unsubstituted enone (e.g., **3.5**) with an appropriate silyl ketene acetal,[340-342] followed by an aldol reaction could also furnish the desired lactone.[343] The ring D γ-lactone in **3.5** may be prepared by displacing an appropriate leaving group directly with the ester (or alternatively with a carboxylic acid); potential candidates for leaving groups include halides[344] and sulfonate esters (e.g., mesylate, tosylate, triflate, etc.).[345-347] The C4 quaternary stereocenter of **3.6** would be established by stereoselectively alkylating the corresponding enolate of an ester or nitrile such as **3.7**,[263] depending on the efficiency of the sequences used to functionalize enone **3.8** at the allylic

position of the enone. Correspondingly, enone **7** (*Scheme 3.1*) could be prepared from (–)-Wieland–Miescher ketone ((–)-**3.1**) by oxidizing the bicyclic scaffold at C2.[348]

For the purposes of synthesizing nagilactone B, enone **3.8** was initially targeted as the key synthetic intermediate, since the versatility of that structure appeared to provide multiple options for exploring the synthesis. A secondary benefit of targeting enone **3.8** was that this intermediate could also be useful for the synthesis of other natural products with a *syn*-1,2-diol moiety – especially if it could be incorporated into the scaffold with relative ease.[349-358] A brief description of previously disclosed synthetic sequences with relevance for this route is provided in Section 3.3.

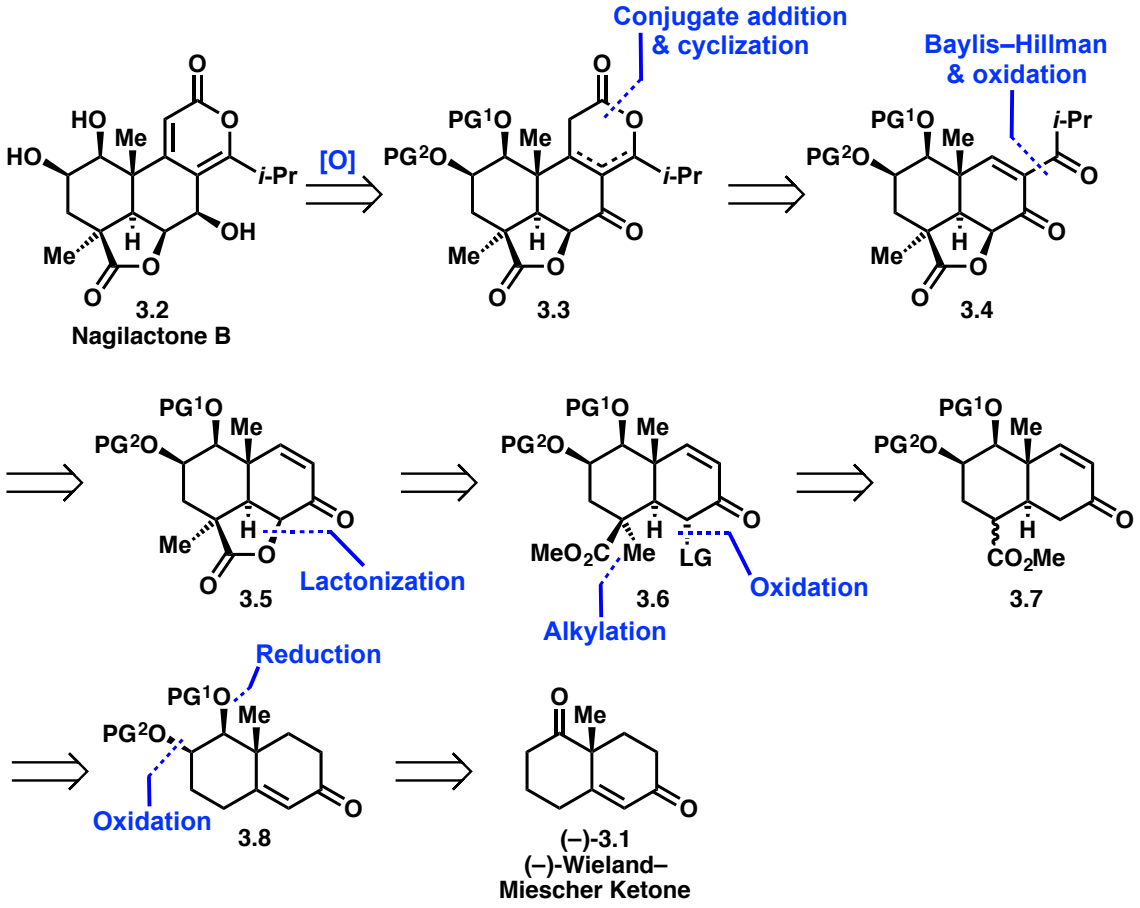

Scheme 3.1 – Second-generation retrosynthetic analysis for nagilactone B.

3.3 Pertinent Synthetic Work from the Literature

3.3.1 Rubottom Oxidation for *syn*-1,2-Diol: *Meiji Seika Kaisha* (1999)

A search of the chemical literature delivered a particularly promising option for incorporating the *syn*-1,2-diol moiety, based primarily on previous research performed at *Meija Seika Kaisha*, where the synthesis and properties of non-steroidal progesterone receptor ligands had been studied (*Scheme 3.2*).[348] The key step with applicability to the synthesis of nagilactone B was a Rubottom oxidation of trimethylsilyl enol ether **3.9**,[359] in which the secondary alcohol was directly incorporated on the same face as the axial C10 methyl group with favourable facial selectivity. Even more promising was the fact that a number of subsequent steps were described, including the ensuing reduction, which was reported to occur stereoselectively to afford alcohol **3.11** with the desired *syn*-1,2-diol moiety – a key structural feature in nagilactone B. It should be noted that although this sequence was quite promising, it was also the only example in which a *syn*-1,2-diol at this position was prepared directly from the Wieland–Miescher ketone and explicit experimental procedures were absent from the publication.

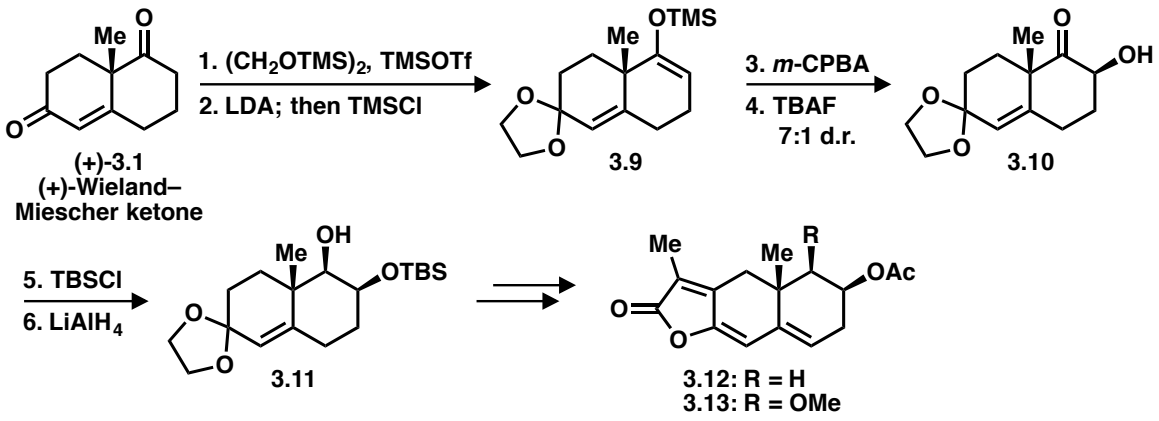

Scheme 3.2 – Previous work at *Meiji Seika Kaisha*.[348]

3.3.2 Formal Allylic Oxidation

Mindful of the requirement to functionalize the allylic position of the enone in the Wieland–Miescher ketone for the purpose of eventually incorporating the quaternary

stereocenter, a number of feasible approaches emerged during a search of the chemical literature (*Scheme 3.4*). Initially, a formal allylic oxidation reaction of enones by way of peroxy-acid oxidation of dienol ethers was particularly appealing. Based on the work of Kirk and Wiles,[360] Heathcock's group reported the oxidation of methoxy diene **3.14** to a mixture of epimeric γ-hydroxy enones (**3.15**).[361] More recent disclosures have performed a similar oxidation with acetoxy dienes instead, often observing a modestly diastereoselective ratio of epimeric γ-hydroxy enones.[362,363] This reactivity has also been observed when Oxone® was substituted for *m*-chloroperbenzoic.[364]

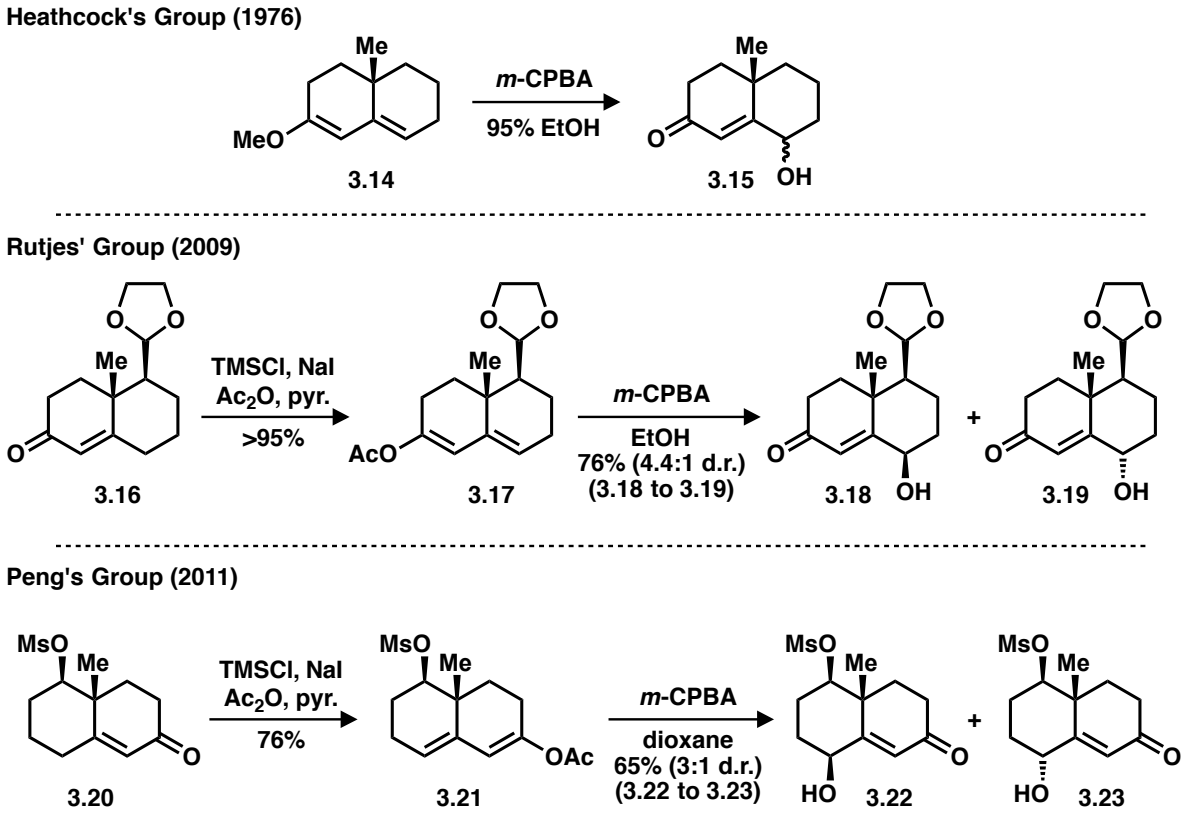

Scheme 3.3 – Formal allylic oxidation with *m*-CPBA.

Notably, the configurations of the alcohols could be inverted through regioselective S_N2 Mitsunobu reactions,[363,364] which provides a potential opportunity for preparing nitrile analogues,[365,366] given that nitriles have been established as effective structures for stereoselective alkylation.[263]

3.3.3 Work by Danishefsky's Group (1996)

Further inspiration for the second-generation synthesis came from work reported by Danishefsky's group, which arose during their studies towards the total synthesis of baccatin III and taxol, with the (+)-Wieland–Miescher ketone as their starting material of choice (*Scheme 3.4*).[367] This approach is complementary to the formal allylic oxidation option described in Section 3.3.2, in that it provides an alternative strategy for oxidizing the Wieland–Miescher scaffold, while encouragingly providing a practical option for installing the ester moiety. The key step of this approach is a hydroboration–oxidation sequence, followed by equilibration of the *cis*-/*trans*-scaffold with sodium methoxide (**3.25** to **3.26**). Notably, the success of the hydroboration–oxidation sequence was highly dependent on the ability to isomerize the alkene to the more stable β,γ-isomer during the ketalization process (**3.24** to **3.25**), as well as isomerize the *cis*-decalone scaffold to the corresponding *trans*-isomer (**3.26**).

One of the key advantages in the Danishefsky group's approach is found in the avoidance of a dissolving metal reduction reaction, which obviates the need to condense significant quantities of ammonia. Although dissolving metal reduction reactions with lithium metal and ammonia are feasible – even on commercial production scales[368] – they nevertheless pose significant challenges and their avoidance is often advantageous.

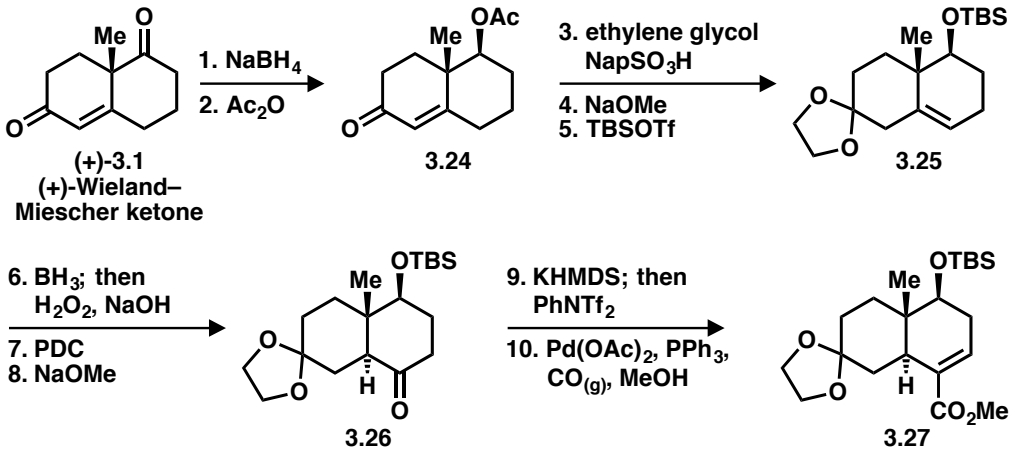

Scheme 3.4 – The Danishefsky group's approach for synthesizing a taxol intermediate.[367]

3.4 Second-Generation Approach

3.4.1 Incorporation of 1,2-*syn*-Diol

The second-generation sequence for the synthesis of nagilactone B, started with 2-methyl-1,3-cyclohexanedione (**3.28**), which was converted to the (–)-Wieland–Miescher ketone using the one-pot procedure reported by Luo's research group (*Scheme 3.5*).[250,252] Although the sequence was rather efficient overall, specific details regarding the combination of the diamine catalyst and trifluoromethanesulfonic acid was oddly lacking from the publication; the paper itself represents the pair as a complex. Initial attempts to prepare a stable salt were largely unsuccessful,[369] but a freshly-prepared concentrated solution of the diamine and trifluoromethanesulfonic acid (1:1 molar ratio) in a minimal amount of dichloromethane was conveniently used without any detrimental effects on the yield or enantiomeric ratio. Interestingly, the proposed transition states for this catalyst (e.g., **TS-3.1**)[252] mirror those described by Lam and Houk[370] for related cinchona-primary-amine-catalyzed intramolecular aldol reactions, in which the arrangement of atoms around the forming C–C bond in the lowest-energy transition structures closely resemble the lowest-energy conformations of cyclooctane.[371]

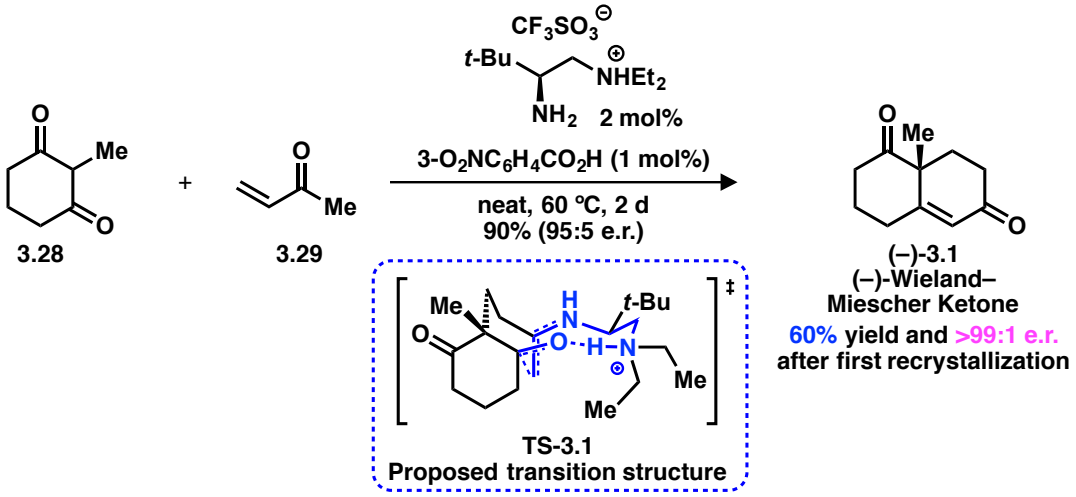

Scheme 3.5 – One-pot procedure for the synthesis of (–)-Wieland–Miescher ketone.[250,252]

While simultaneously working on the first-generation synthesis, an attempt was made to pursue the second-generation sequence by preparing the key *syn*-1,2-diol intermediate

described by the group at *Meija Seika Kaisha* (*Scheme 3.2*, p. 129).[348] In that spirit, the enone moiety of the (–)-Wieland–Miescher ketone was chemoselectively protected at –78 °C in the presence of 1,2-bis(trimethylsiloxy)ethane and 0.02 equivalents of trimethylsilyl trifluoromethanesulfonate to provide ketone **3.30**, using a procedure reported by Hwu and Wetzel,[372] that is modelled on work by Noyori's group (*Scheme 3.6*).[373] Care must be taken to ensure that the temperature remains low for the duration of the reaction, as increasing it to even –65 °C can negatively impact the chemoselectivity and lead to the formation of significantly more product arising from protection of the unconjugated ketone next to the axial methyl group.[372] Deprotonation of ketone **3.30**, followed by treatment with trimethylsilyl chloride provided access to silyl enol ether ***ent*-3.9** that was envisaged to undergo a stereoselective Rubottom oxidation reaction.

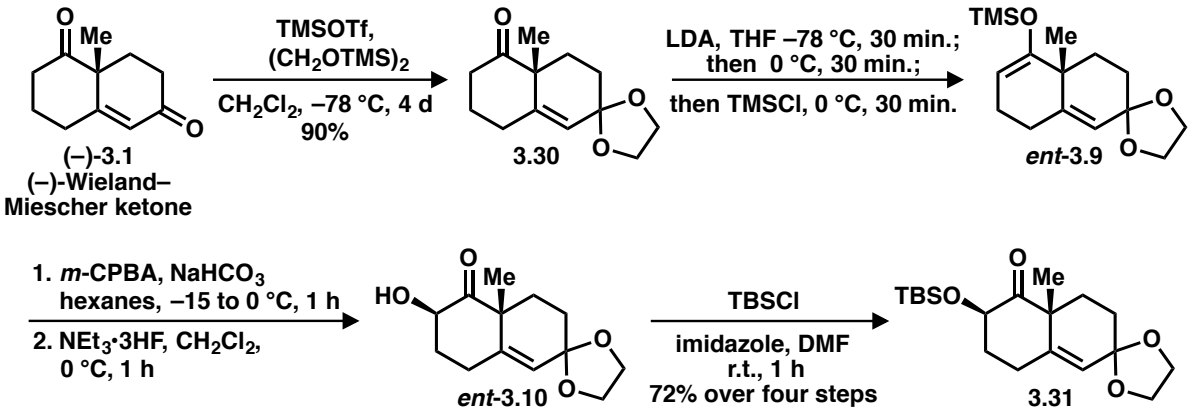

Scheme 3.6 – Rubottom oxidation to prepare α-hydroxy ketone.

Since the group at *Meija Seika Kaisha* did not include specific reaction details in their publication, initial attempts to perform the oxidation were based on the conditions reported by Rubottom's group.[374] By thin-layer chromatographic analysis, oxidations of ***ent*-3.9** with *m*-chloroperbenzoic acid showed a substantial quantity of dissimilar products, which were attributed to be various intermediates and products arising from the instability of the trimethylsilyl ether under the reaction conditions. It was hoped that treatment with a source of fluoride would effectively deprotect the silyl group and cause the various intermediates to converge to α-hydroxy ketone ***ent*-3.10**. Initial attempts with a solution of tetrabutylammonium fluoride in tetrahydrofuran, as reported by the group at *Meija Seika Kaisha*,[348] were highly unsuccessful and the reaction mixture darkened immediately after

addition of the fluoride source, resulting in the recovery of ketal-deprotected material alongside many side products. The challenge was overcome by using triethylamine trihydrofluoride instead, which led to the anticipated convergence of intermediates to furnish (*R*)-configured α-hydroxy ketone ***ent*-3.10** as the major product. The now-established procedure was found to be very robust overall and could efficiently provide multi-gram quantities of material with relative ease. This was particularly promising as (*R*)-configured α-hydroxy ketone ***ent*-3.10** could now be accessed quickly, without recourse to a tedious oxidation–reduction sequence. A related attempt to directly oxidize ketone **3.30** with Davis' oxaziridine was unsuccessful, with no α-hydroxy ketone observed.[375] Finally, following the oxidation sequence, the hydroxy group was protected as the corresponding *tert*-butyldimethylsilyl ether to furnish **3.31** in 72% overall yield over four steps.

Given the presence of the axial methyl group in ***ent*-3.9**, the stereoselectivity of the Rubottom oxidation seemed counterintuitive at first glance, despite it having been described for epoxidation reactions on related systems.[376-378] To further appreciate the observed stereoselectivity, transition structures corresponding to the approach of the peroxy acid from both faces of the bicyclic scaffold were modelled (*Figure 3.4*). Quantum chemical computations were performed with *Gaussian 09*. To identify the lowest energy conformers for the trimethysilyl enol ether, Monte Carlo conformational searches were performed with Macromodel 9.9[299] and the corresponding conformers were then optimized at the B3LYP[300-303]/6-31G(d) level of theory. Transition state searches were performed in the presence of perbenzoic acid at the same level, and the single-point energies of the optimized transition states were evaluated at the B3LYP-D3(BJ),[305-309] ωB97X-D,[379] and M06-2X[310] and levels with the polarized, triple-ζ valence quality def2-TZVPP basis set of Weigend and Ahlrichs.[311] Thermal corrections evaluated from unscaled vibrational frequencies at the B3LYP/6-31G(d) level on optimized geometries were added to the single point electronic energies to obtain the free energies.

An analysis of the lowest energy conformations for the bicyclic trimethylsilyl enol ether reveals that both ring A and B are in a half-chair conformation (*Figure 3.4*). This imparts a slight curvature to the overall scaffold; the methyl group lies on the β face that has a convex

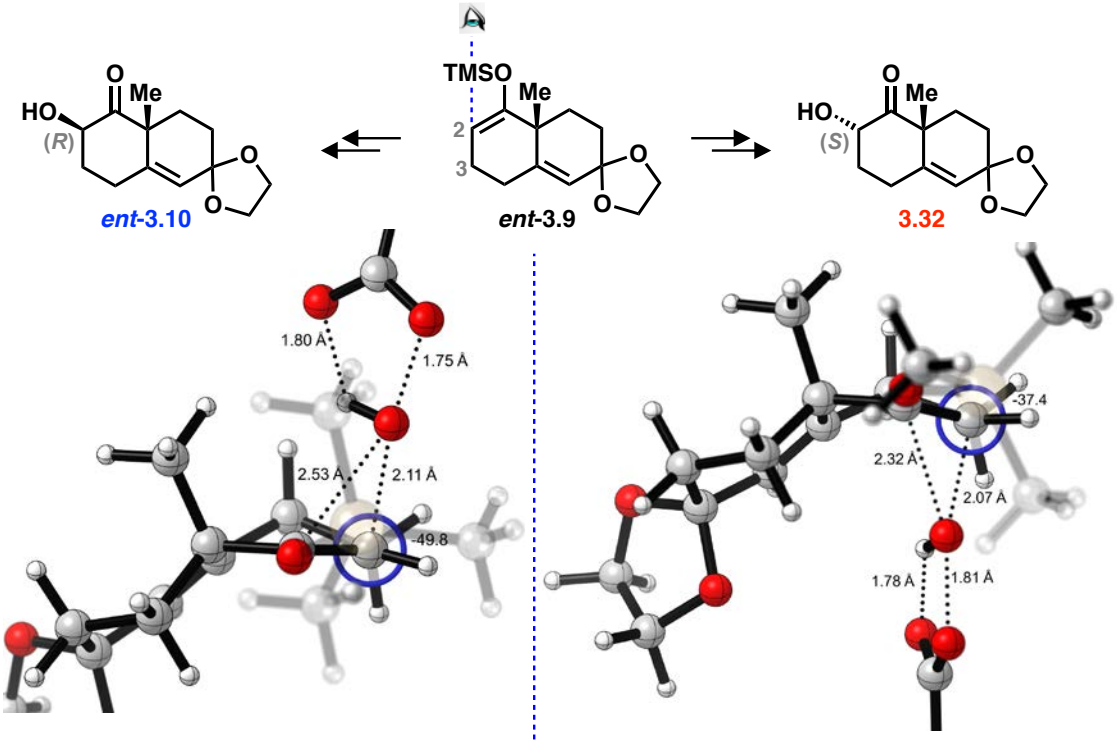

TS-3.2
Chair-like transition structure
Leads to (*R*)-Configuration
$\Delta G^{\ddagger}$ = +17.2 (+26.6, +30.5) kcal/mol
$\Delta\Delta G^{\ddagger}$ = 0.0 (0.0, 0.0) kcal/mol

TS-3.3
Twist-boat-like transition structure
Leads to (*S*)-Configuration
$\Delta G^{\ddagger}$ = +18.4 (+28.1, +33.2) kcal/mol
$\Delta\Delta G^{\ddagger}$ = +1.2 (+1.5, +2.7) kcal/mol

B3LYP-D3(BJ)/def2-TZVPP//B3LYP/6-31G(d) geometries, frequencies, and energies are shown. The corresponding values for the ωB97X-D/def2-TZVPP//B3LYP/6-31G(d) and M06-2X/def2-TZVPP//B3LYP/6-31G(d) levels are provided sequentially in parentheses.

Figure 3.4 – Transition structures for Rubottom oxidation.

topology. In both cases the peroxy acid approaches the silyl enol ether along an axial trajectory, with the plane of the peroxy acid slightly skewed from the plane of the C=C axis of the trimethylsilyl enol ether.[380] As a consequence of the axial trajectory over the C2 position, ring A increasingly adopts a chair-like geometry in the lowest-energy transition structure (**TS-3.2**), while becoming more twist-boat-like in the next-highest transition structure (**TS-3.3**). As a consequence of the topology of the scaffold and asynchronicity of the transition structures, the favourable approach over C2 in **TS-3.2** effectively relieves steric interactions between the axial methyl group and the peroxy acid. The asynchronicity is consistent with studies on related systems.[381] Consequently, the steric influence of the methyl group is largely nullified in **TS-3.2** (*Figure 3.4*) and the oxidation takes place with the desired stereochemical outcome

to furnish the (*R*)-configured hydroxy group in ***ent*-3.10** as a consequence of another influence: torsional strain.

The minimization of torsional strain appears to be one of the major factors contributing to the observed preference for approach of the peroxy acids from the same face as the axial methyl group. In **TS-3.2**, the hydrogen atom at C2 is effectively staggered with respect to the methylene hydrogen atoms at C3. However, in the case of **TS-3.3**, the same hydrogen atom at C2 is nearly eclipsed with the equatorial hydrogen atom at C3, and this unfavourable interaction is further pronounced as the transition structure becomes more product-like. Moreover, transfer of the oxygen atom from the peroxy acid occurs through an orientation that is eclipsed with the axial hydrogen atom at C3 in **TS-3.3**, while this interaction is alleviated in **TS-3.2**. With a route for preparing the C2 hydroxy group firmly established, the second-generation route became more attractive and its exploration continued.

3.4.2 Functionalizing Ring A Through Dienol Ether (Acetonide)

At this point, the detrimental influence of the acetonide protective group on the alkylation reaction (*Scheme 2.32*, p. 109) had not been wholly established and an attempt was made to incorporate it for the purposes of confirming the presence of the *syn*-1,2-diol moiety and exploring the reactivity of this scaffold (*Scheme 3.7*). Reduction of the C1 ketone was accomplished with lithium aluminum hydride and was initially performed on the *tert*-butyldimethylsilyl-protected molecule to substantiate the work performed at *Meija Seika*

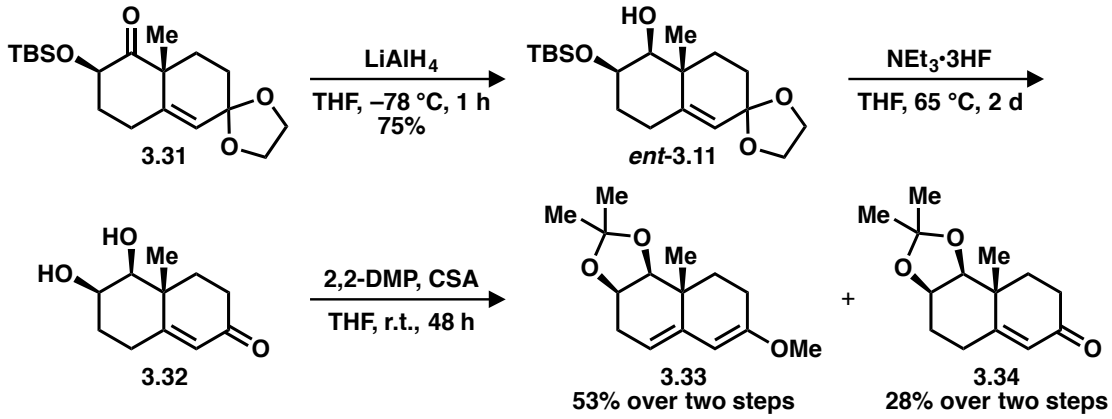

Scheme 3.7 – Synthesis of acetonide-protected *syn*-1,2-diol.

Kaisha.[348] Following reduction of ketone **3.31**, the *tert*-butyldimethylsilyl group was deprotected with triethylamine trihydrofluoride to furnish *syn*-1,2-diol **3.32**. Although the reaction required heating at 65 °C for two days, it was ultimately successful and even resulted in concomitant deprotection of the ketal moiety to restore the enone. Interestingly, attempts to protect diol **3.32** as an acetonide resulted in serendipitous formation of methyl dienol ether **3.33** as the major product. While the result was initially unexpected, in retrospect, the formation of similar products has been well-documented to occur in the presence of catalytic amounts of acid and an appropriate dehydrating reagent.[364,382,383] Nevertheless, this reactivity appeared to be quite beneficial, given the opportunity it provided for directly functionalizing ring A through this, or a similar intermediate.

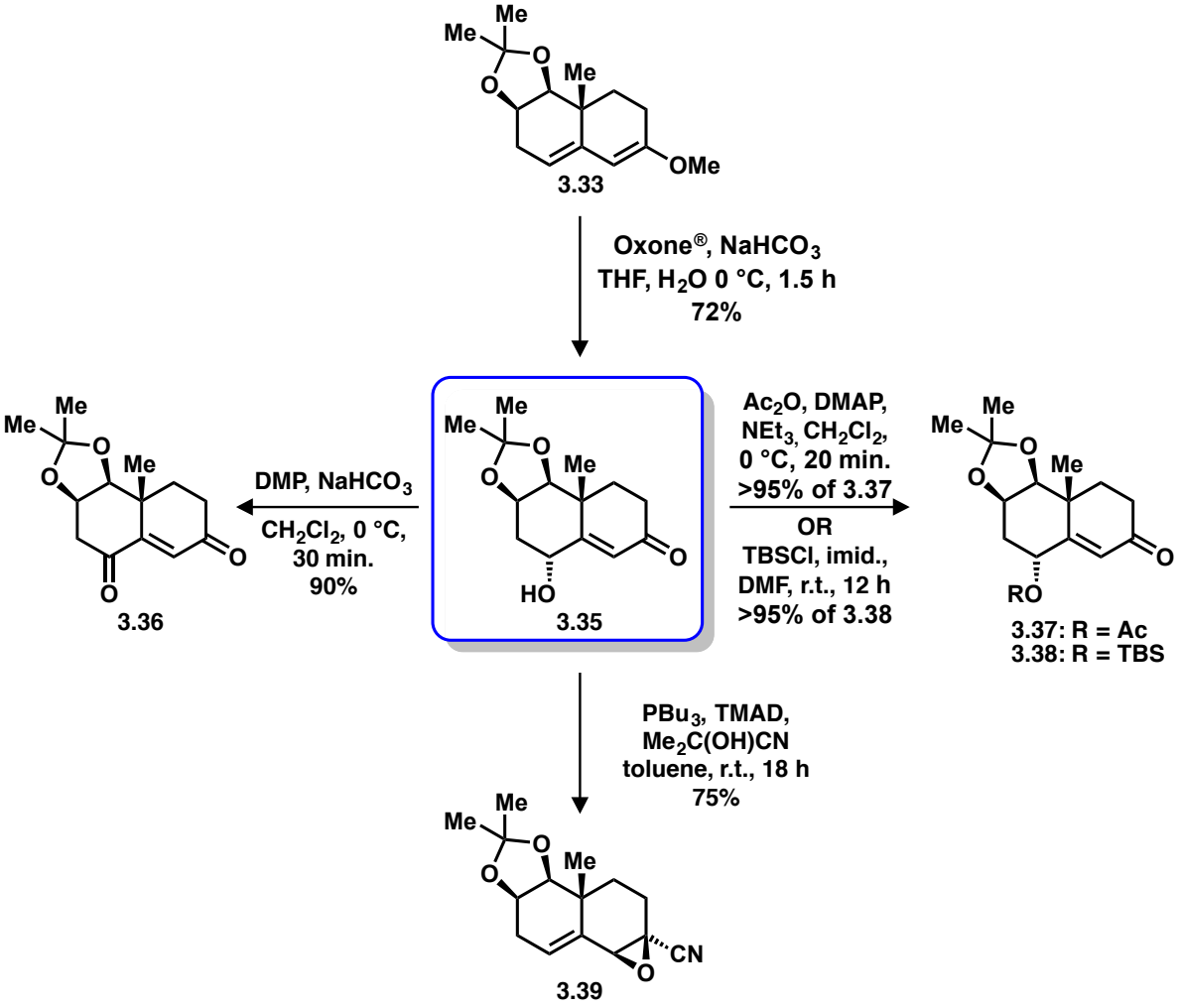

Scheme 3.8 – Oxidation of methoxy dienol ether and subsequent reactivity of alcohol.

To this end, Oxone® was found to be very effective,[364] affording (*R*)-configured γ-hydroxy enone **3.35** in 72% yield (*Scheme 3.8*). The hydroxy group could be oxidized with Dess–Martin periodinane (**3.36**) or protected, as either the corresponding acyl ester (**3.37**) or *tert*-butyldimethylsilyl ether (**3.38**) derivative. While attempts to directly install a nitrile group with *N*-(*p*-toluenesulfonyl)imidazole and sodium cyanide led to multiple unidentified products,[365] the use of acetone cyanohydrin under Mitsunobu conditions led directly to **3.39**.

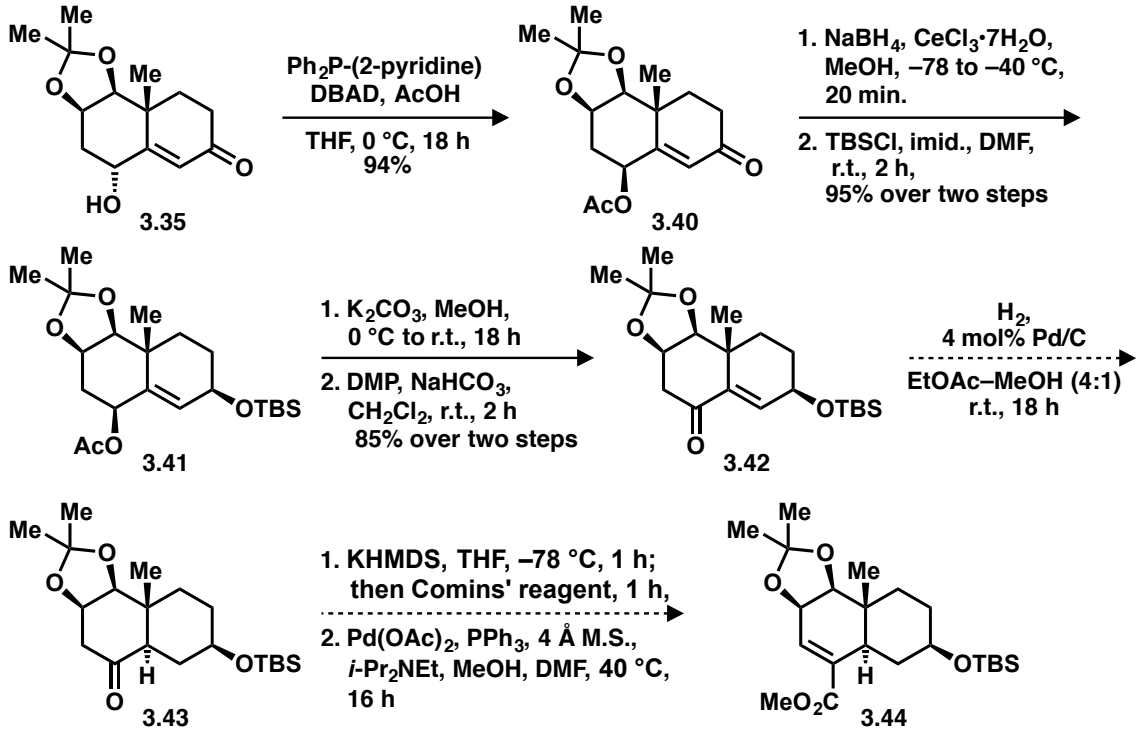

Scheme 3.9 – Ketal approach to functionalize ring A.

Although the Mitsunobu approach to install a nitrile at C4 was not particularly successful overall, it was nevertheless possible to use oxygen-based nucleophiles, such as acetic acid (**3.35** to **3.40**, *Scheme 3.9*). The ketone could then be reduced under Luche's conditions[282] and the alcohol subsequently protected with *tert*-butyldimethylsilyl chloride to afford orthogonally-protected acetonide **3.41**.[285] Hydrolysis of the acyl ester and oxidation with Dess–Martin periodinane afforded enone **3.42**. Preliminary experiments indicated that it may possible to reduce the enone to the *trans*-fused scaffold under hydrogenation conditions, and that that the corresponding methyl ester is accessible through a two-step sequence: conversion of the ketone to an enol triflate,[384] followed by a palladium-catalyzed

carbonylation reaction.[367,385-387] Comins' reagent was preferred over *N*-phenyl-bis(trifluoromethanesulfonimide), as a consequence of the low conversion (<30%) observed when using the latter reagent.

Unfortunately, attempts to reduce enone **3.44** with typical hydrogenation conditions or magnesium in methanol were not particularly encouraging and led to many different products, including those that appeared to stem from elimination of the acetonide moiety.[388] Furthermore, at this point the challenges of stereoselectively methylating ester enolates in the presence of the acetonide protective group became apparent as a consequence of the first-generation synthesis (*Scheme 2.32*, p. 109). For this reason work with the acetonide protective group was ultimately set aside and a more flexible option was used instead. This work is described in Section 3.4.3.

3.4.3 Functionalizing Ring A Through Dienol Ether (Silyl)

For the purpose of providing additional flexibility to the bicyclic scaffold in order to overcome the challenges associated with stereoselective alkylation, a disilyl-protected *syn*-1,2-diol moiety was selected as the intermediate of choice. Following reduction of ketone **3.31** with sodium borohydride, the resultant hydroxy group was protected as the corresponding triethylsilyl ether to yield enone **3.45** (*Scheme 3.10*). The initially used reduction with lithium aluminum hydride (*Scheme 3.7*, p. 136) was substituted in favour of using sodium borohydride, as the latter was found to be more robust and higher yielding when working with larger quantities of material. Protection of the C1 hydroxy group with triethylsilyl trifluoromethanesulfonate led to concomitant deprotection of the enone as well (~50% by thin-layer chromatographic analysis). Taking advantage of this observation, *p*-toluenesulfonic acid monohydrate was added directly to the reaction mixture after the C1 hydroxy group was protected in order to converge all of the material to enone **3.45**, the key synthetic intermediate.

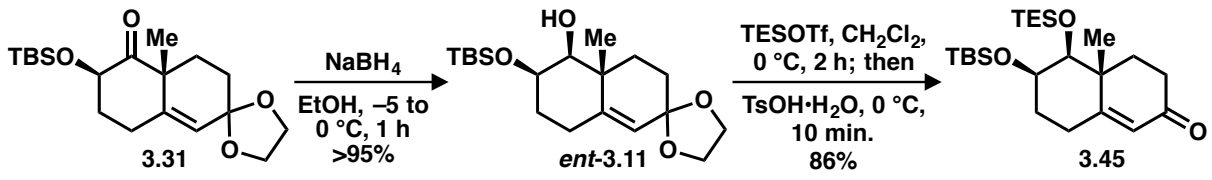

Scheme 3.10 – Preparing the silyl-protected *syn*-1,2-diol.

Given the successful oxidation of ring A using a methoxy dienol ether (*Scheme 3.8*, p. 137), initial efforts with silyl-protected diol **3.45** focused on a similar sequence. Attempts to prepare methoxy dienol ether **3.46** (*Table 3.1*) used trimethyl orthoformate or 2,2,-dimethoxypropane in the presence of catalytic quantities of *p*-toluenesulfonic acid monohydrate,[389] collidinium *p*-toluenesulfonate, or pyridinium *p*-toluenesulfonate.[390] Notably, the major difficulties in this reaction stemmed from performing it on increasingly larger quantities of material. Initial efforts with *p*-toluenesulfonic acid monohydrate (entries 1–2, *Table 3.1*) were promising when larger quantities of trimethyl orthoformate were used (entry 1, *Table 3.1*), but suffered from lower yields overall. Although the use of collidinium *p*-toluenesulfonate and 2,2-dimethoxypropane led to very low conversions (entries 3–4, *Table 3.1*), the related pyridinium *p*-toluenesulfonate catalyst was significantly more efficient, particularly at higher temperatures (entry 6, *Table 3.1*).

Table 3.1 – Synthesis of methoxy dienol ether.

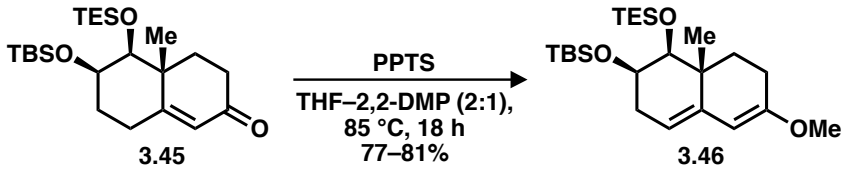

Entry	Acid / Salt	Reagent	Solvent*	Temperature	Time	Result
1	TsOH•H_2O (0.06 eq.)	$HC(OMe)_3$ (17 eq.)	DMF–MeOH (5:1)	r.t.	18 h	40%†
2	TsOH•H_2O (0.06 eq.)	$HC(OMe)_3$ (3 eq.)	DMF–MeOH (5:1)	r.t.	18 h	SM : Prod = 5 : 1
3	CPTS (0.1 eq.)	2,2-DMP (3 eq.)	THF	r.t.	20 h	SM : Prod > 20 : 1
4	CPTS (0.1 eq.)	–	2,2-DMP	85 °C	20 h	SM : Prod = 3 : 1
5	PPTS (0.1 eq)	2,2-DMP (3 eq.)	THF	r.t.	20 h	SM : Prod = 1 : 2
6	PPTS (0.1 eq)	–	THF–2,2-DMP (2:1)	85 °C	18 h	77–81%†

* Concentration is 0.2 M; † Yield after chromatography.

In contrast to the reactivity observed when using the acetonide protective group, oxidation of methoxy dienol ether **3.46** (*Scheme 3.11*) with either Oxone® or *meta*-chloroperbenzoic acid alone was very slow. Interestingly, the addition of *meta*-chloroperbenzoic acid to a mixture of the enone and Oxone® led to a ~1:1 mixture of epimeric γ-hydroxy enones in 73% yield (*Scheme 3.11*), although the reaction was rather inconsistent on larger scales. While the hydroxy groups could be directly converted to the corresponding

acyl esters (**3.47**), an attempt to invert the (*R*)-configured hydroxy group under Mitsunobu conditions* led to recovered starting material.[391,392]

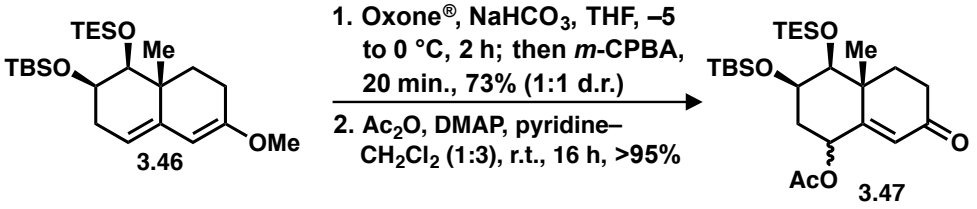

Scheme 3.11 – Oxidation of methoxy dienol ether with Oxone®/*m*-CPBA.

The sequence for oxidizing enone **3.45** via a methoxy dienol ether moiety (**3.46**) was promising, but it was apparent that the ensuing protection–deprotection sequences with the ketone/enone at C7 and the group at C4 would lead to a rather lengthy synthetic route (i.e., *Scheme 3.9*, p. 138). Fortunately, simultaneous experimental success with a hydroboration–oxidation strategy[367] led to a shorter synthetic sequence, which was ultimately favoured over of the methoxy dienol ether approach. The hydroboration–oxidation strategy is described below in Section 3.4.4.

3.4.4 Hydroboration–Oxidation Strategy for Oxidizing Ring A

In order to pursue a hydroboration–oxidation strategy it was crucial to ensure the alkene moiety was in the β,γ-position rather than the α,β-position (*Scheme 3.4*, p. 131). An initial approach involved attempted isomerization of the alkene in unsaturated ketal **3.48** to the β,γ-position in the presence of an appropriate acid catalyst, as had been previously achieved on comparable structures.[393-395] α,β-Unsaturated ketal **3.48** was prepared directly from alcohol **ent-3.11** in the presence of triethylsilyl chloride (*Scheme 3.12*), using conditions that did not result in coinciding ketal deprotection, as had previously been observed (*Scheme 3.10*, p. 139).

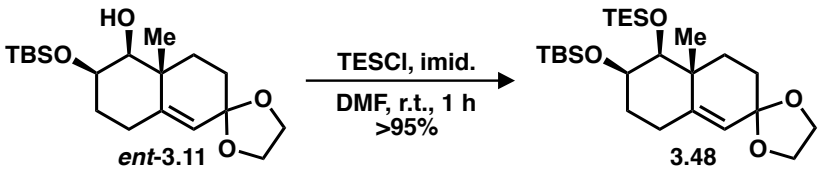

Scheme 3.12 –Protection of secondary hydroxy group with triethylsilyl chloride.

* Diphenyl 2-pyridylphosphine, di-*tert*-butyl azodicarboxylate, and acetic acid.[391]

Table 3.2 – Attempted isomerization of unsaturated ketal.

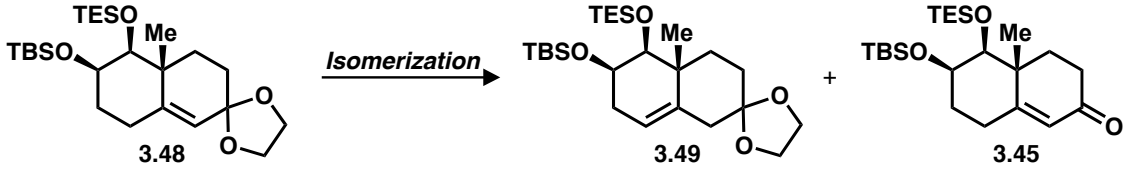

Entry	Acid / Salt	Additive	Ethylene Glycol	[Toluene]	Temp.	Time	Ratio 3.48 : 3.49 : 3.45
1	CPTS (0.2 eq.)	–	–	0.2 M	80 °C	16 h	1 : 0 : 2
2	PPTS (0.2 eq.)	–	–	0.2 M	80 °C	16 h	9 : 1 : 40
3	PPTS (0.05 eq.)	$HC(OMe)_3$ (2 eq.)	2 eq.	0.1 M	80 °C	16 h	1 : 0 : 0
4	$TsOH•H_2O$ (0.05 eq.)	$HC(OMe)_3$ (2 eq.)	2 eq.	0.1 M	80 °C	16 h	1 : 0 : 0
5	$TsOH•H_2O$ (0.05 eq.)	$HC(OMe)_3$ (0.2 eq.)	1 eq.	0.1 M	80 °C	16 h	1 : 0 : 0
6	$TsOH•H_2O$ (0.10 eq.)	$HC(OMe)_3$ (0.2 eq.)	1.2 eq.	0.1 M	80 °C	16 h	0 : 1 : 9

* Ratio determined by ^1H NMR.

Unfortunately, attempts to isomerize the unsaturated ketal in the presence of catalytic quantities of *p*-toluenesulfonic acid monohydrate, collidinium *p*-toluenesulfonate, or pyridinium *p*-toluenesulfonate, were largely unrewarding (*Table 3.2*). In most of the cases, the starting material (**3.48**) was recovered or the ketal was largely deprotected to furnish the corresponding enone (**3.45**). The sensitive nature of the reaction was particularly noteworthy, as even minor variations in the reaction condition could lead to significantly larger quantities of deprotected material (entries 5–6, *Table 3.2*).

To address this challenge, the ketalization–isomerization was performed directly on enone **3.45**.[393,394,396,397] An initial effort culminated in the desired β,γ-unsaturated ketal (**3.49**) being produced in 35% yield, when performed in the presence of the bis-silyl-protected diol.* While this result was promising, it also highlighted the potential shortcomings of performing the ketalization on this intermediate (as well as the sensitivity of the triethylsilyl protective group). A cursory glance at the structure of enone **3.45** (*Scheme 3.13*) revealed the possibility for an acid-catalyzed retro-aldol reaction to occur instead.[398] In particular, this is likely one of the reasons previously-disclosed attempts to implement this isomerization included an acetyl protective group on the C1 hydroxy group.[367,396,399] For example, Danishefsky's group

* Initial ketalization conditions: $TsOH•H_2O$ (0.1 eq.), ethylene glycol (3 eq.), trimethyl orthoformate (3 eq.), toluene (0.1 M), 80 °C, 2 h.

specifically performed the ketalization–isomerization reaction in the presence of a C1 acetyl-protected secondary alcohol, before converting it to the corresponding *tert*-butyldimethylsilyl ether two steps later (*Scheme 3.4*, p. 131).[367] Fortunately, when the molar equivalents of *p*-toluenesulfonic acid and trimethyl orthoformate used in the reaction mixture were halved, the ketalization–isomerization reaction could be consistently performed on multigram scale, affording β,γ-unsaturated ketal **3.49** in 62% yield, in addition to recovered starting material (*Scheme 3.13*). Notably, this yield is on par with that reported by Danishefsky's group who used a similar derivative that has an acetyl-protected alcohol instead.[367] While the yield may likely be improved further, it was certainly acceptable for exploratory work focused on functionalizing ring A at C4.

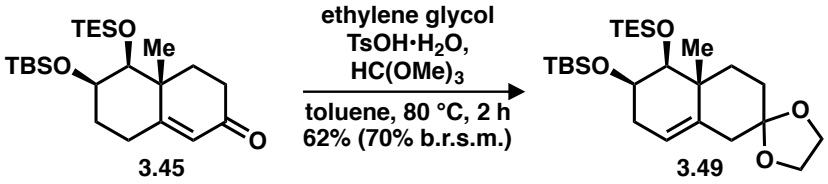

Scheme 3.13 – Ketal protection with concomitant isomerization of alkene.

To that end, β,γ-unsaturated ketal **3.49** (*Scheme 3.14*) was treated with a solution of borane in tetrahydrofuran, followed by hydrogen peroxide and sodium hydroxide. As a consequence of the geometry adopted by the bicyclic scaffold, borane approaches the alkene from a trajectory that is *syn* to the C10 axial methyl group as shown in **TS-3.4**, which leads to the higher-energy *cis*-fused ring junction. This trajectory is more favourable than the alternative one, since steric interactions are minimized on the convex face of the scaffold; the methyl group is effectively pseudo-equatorial with respect to the half-chair conformation of ring A, so its influence on the facial selectivity is greatly diminished. Oxidation of the alcohol with Dess–Martin periodinane afforded a mixture of ketones (i.e., **3.50** and **3.51**), which could be treated with sodium methoxide to effect base-mediated equilibration to the more thermodynamically stable *trans*-fused isomer (**3.51**) in excellent yield over three steps.[367,399] The *cis*-fused isomer (**3.50**) may be separated from *trans*-fused decalone **3.51** by column chromatography, before being resubjected to the isomerization conditions. In contrast to related systems, only partial isomerization of *cis*-isomer **3.50** took place, likely as a

consequence of the unfavourable 1,3-diaxial interactions that arise between the C2 *tert*-butyldimethyl silyl ether and the axial methyl group at C10 in the *trans*-fused system.

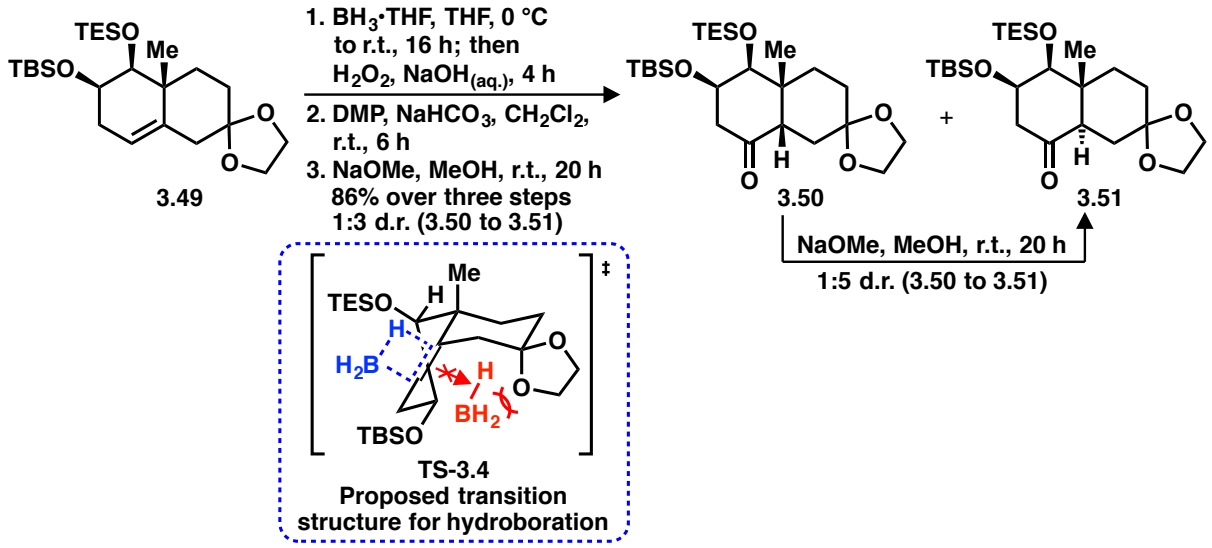

Scheme 3.14 – Hydroboration–reduction sequence to functionalize ring A.

3.4.5 Alkylation to Establish the Quaternary Stereocenter

En route to establishing the quaternary stereocenter, ketone **3.51** was converted to the corresponding vinyl triflate in the presence of *N*-phenyl-bis(trifluoromethanesulfonimide) and potassium bis(trimethylsilyl)amide (*Scheme 3.15*). To ensure that the conversion to the vinyl triflate is efficient, it was found that potassium bis(trimethylsilyl)amide should be added directly to a solution of ketone **3.51** and *N*-phenyl-bis(trifluoromethanesulfonimide),[367] rather than adding the triflating reagent to a solution containing the preformed enolate of **3.51**.[400] A palladium-catalyzed carbonylation reaction in the presence of methanol was used to convert the vinyl triflate to α,β-unsaturated ester **3.52**.[387] While initial efforts to effect the carbonylation were made with palladium(II) acetate in the presence of triphenylphosphine (*Scheme 3.9*, p. 138),* the reaction was significantly more robust and the conversion much higher when tetrakis(triphenylphosphine)palladium(0) was used instead. Reduction of α,β-unsaturated ester **3.52** with magnesium in methanol exclusively furnished (*S*)-configured

* Initial conditions: $Pd(OAc)_2$ (0.12 eq.), PPh_3 (0.24 eq.), $CO_{(g)}$, 4 Å M.S. (0.2 g/mmol), *i*-Pr_2NEt (2.7 eq.), MeOH–DMF (1:2.5, 0.2 M), 40 °C, 14 h, 38% conversion.

methyl ester **3.53**.[197,198] Alkylation at the α-position of the methyl ester proceeded as expected to establish the quaternary stereocenter in **3.54**, with the C4 methyl group incorporated stereoselectively on the α-face of the bicyclic scaffold, opposite to the C10 axial methyl group and silyl-protected *syn*-1,2-diol moiety.

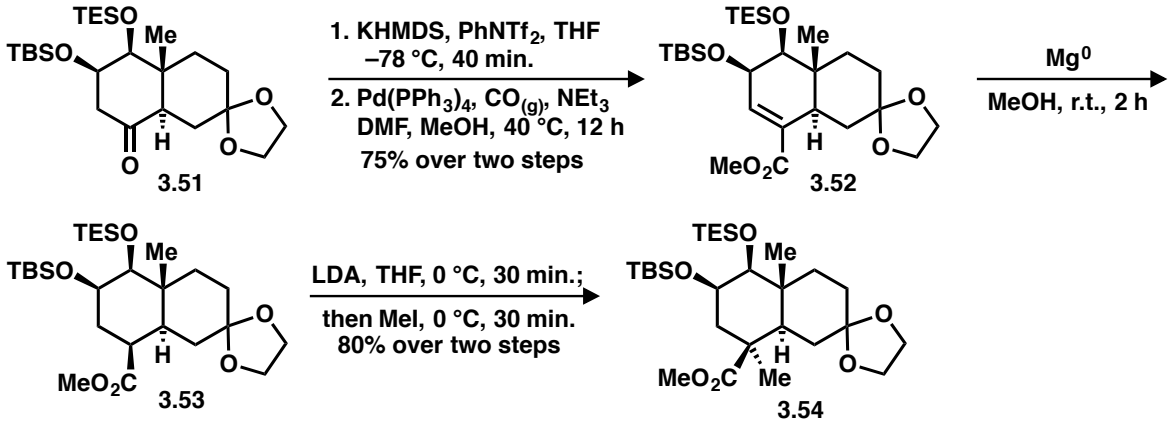

Scheme 3.15 – Methylation to establish quaternary stereocenter.

Transition structures for the alkylation reaction with the analogous bis-trimethylsilyl-protected diols (**3.55** and **3.56**, *Figure 3.5*) were modelled using quantum chemical computations with *Gaussian 09* for comparative purposes against the analogous reaction with the acetonide-protected *syn*-1,2-diol (*Figure 2.12*, p. 112). To identify the lowest energy conformers Monte Carlo conformational searches were performed with Macromodel 9.9[299] and the corresponding conformers were then optimized at the B3LYP[300-303]/6-31+G(d,p) level of theory in conjunction with the IEF-PCM implicit solvation model[304] to account for the solvation effects of tetrahydrofuran, the solvent used experimentally. Transition state searches were performed in the presence of methyl chloride at the same level, and the single-point energies of the optimized transition states were evaluated at the B3LYP-D3(BJ)[305-309] and M06-2X[310] levels with the polarized, triple-ζ valence quality def2-TZVPP basis set of Weigend and Ahlrichs[311] within the IEF-PCM model for tetrahydrofuran. Thermal corrections evaluated from unscaled vibrational frequencies at the B3LYP/6-31+G(d,p) level on optimized geometries were added to the single point electronic energies to obtain the free energies. The free energy corrections were calculated using Truhlar's quasiharmonic approximation.[312,313]

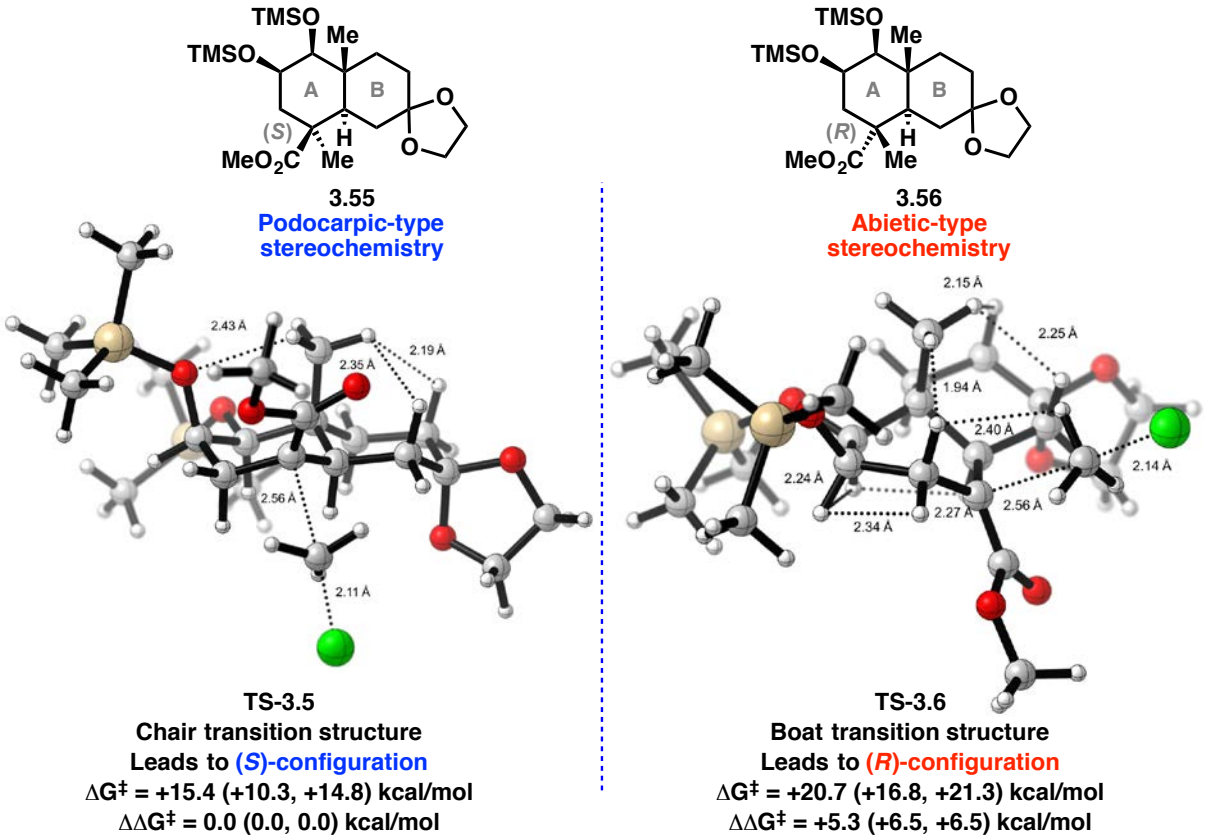

B3LYP/6-31+G(d,p)-IEF-PCM(tetrahydrofuran) geometries, frequencies, and energies are shown. The corresponding values for the B3LYP-D3(BJ)/def2-TZVPP-IEF-PCM(tetrahydrofuran)//B3LYP/6-31+G(d,p)-IEF-PCM(tetrahydrofuran) and M06-2X/def2-TZVPP-IEF-PCM(tetrahydrofuran)//B3LYP/6-31+G(d,p)-IEF-PCM(tetrahydrofuran) levels are provided sequentially in parentheses.

Figure 3.5 – Transition structures for alkylation.

An analysis of the lowest energy transition structures leading to each diastereomer (**TS-3.5** and **TS-3.6**, *Figure 3.5*) reveals that ring B is in a chair conformation and the electrophile approaches ring A along an equatorial trajectory. In the lowest energy transition structure (**TS-3.5**), ring A is also found in a chair conformation, with the electrophile approaching from the α-face of the bicyclic scaffold. This conformation significantly minimizes steric interactions between the incoming electrophile and the C10 axial methyl group, while likewise alleviating 1,3-diaxial interactions within the bicyclic scaffold. The chair conformer is not accessible when the acetonide is used as a protective group as a consequence of the limitations the additional fused five-membered ring imposes on the degrees of torsional freedom within the scaffold. Conversely, the lowest energy transition structure that leads to alkylation on the β-face (**TS-3.6**) reveals that ring A is in a boat

conformation. This conformation is unfavourable compared with the chair conformer as a consequence of diaxial interactions between the C10 axial methyl group and the axial proton of the C3 methylene group, as well as the increased number of eclipsed bonds/atoms within the scaffold.

With the quaternary stereocenter and *syn*-1,2-diol moiety established, it was now possible to tackle the challenge of functionalizing ring B for the purpose of incorporating the γ-lactone and α-pyrone moieties. The advantage of this intermediate was that either functional group could in principle be installed first, which provided some flexibility to the synthetic sequence. Given previous challenges associated with preparing the γ-lactone, the incorporation of that group was addressed first to determine its feasibility. The synthetic strategy used to prepare the γ-lactone is described in Section 3.4.6.

3.4.6 Incorporating the γ-Lactone

The strategy for incorporating the γ-lactone followed the initial retrosynthetic analysis (*Scheme 3.1*, p. 128), in which an appropriate leaving group was envisaged to be displaced directly by the methyl ester (or alternatively with a carboxylic acid); potential candidates for leaving groups included halides[344] and various sulfonate esters (mesylate, tosylate, triflate, imidazylate, etc.).[345-347]

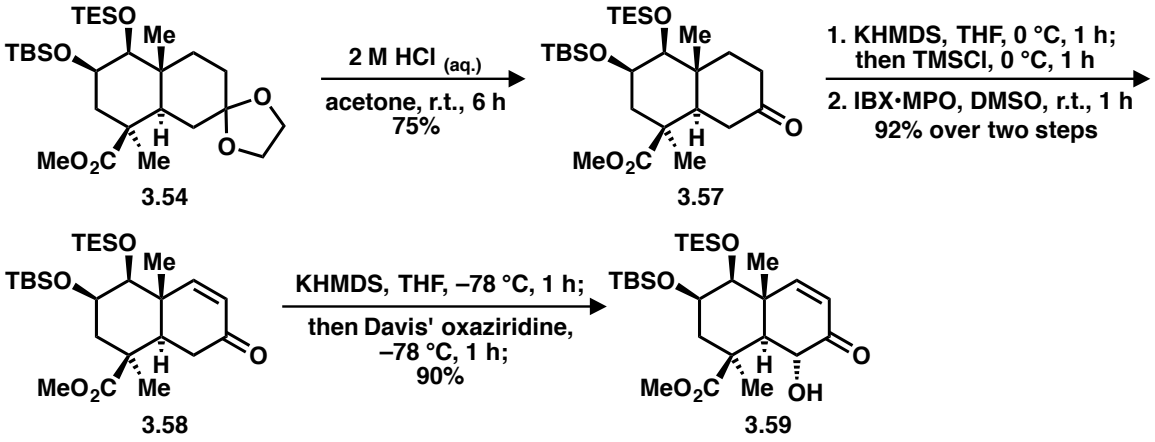

Scheme 3.16 – Oxidation of ring B to prepare γ-lactone precursor.

To this end, the ketal was removed under transketalization conditions with aqueous hydrochloric acid in acetone to afford the corresponding ketone (**3.54** to **3.57**, *Scheme 3.16*).

Although pyridinium *p*-toluenesulfonate was ineffective for the deprotection of ketal **3.54**, catalytic quantities of *p*-toluenesulfonic acid monohydrate in acetone could be used, but those conditions required careful monitoring to ensure that side-products did not begin to form as a consequence of the quick rate of reaction. Regardless of the method used for the deprotection, ketone **3.57** could selectively be deprotonated at the less sterically hindered C8 position, and the resulting enolate trapped as the corresponding trimethylsilyl enol ether analogue. This trimethylsilyl enol ether was effectively oxidized to enone **3.58** in the presence of *o*-iodoxybenzoic acid and 4-methoxypyridine *N*-oxide at ambient temperature. While one can envision elaborating ketone **3.57** to nagilactone B by way of different synthetic sequences, the present strategy was selected for the purpose of immediately incorporating the γ-lactone; the presence of the enone also ensures that further deprotonation occurs at C6, while also activating the C9 position for conjugate addition reactions after the lactonization reaction. Accordingly, enone **3.58** was deprotonated at C6 with potassium bis(trimethylsilyl)amide and Davis' oxaziridine was used to effect hydroxylation at –78 °C to yield alcohol **3.59** in 90% yield.

At this point, it was envisaged that the secondary hydroxy group in **3.59** could be converted to a suitable leaving group and subsequently displaced by the methyl ester or analogous carboxylic acid, with concomitant cleavage of the methyl moiety for the former. Initial attempts to demethylate the hindered methyl ester led largely to silyl deprotection (LiBr[199]) or elimination products (LiOH, KOH), and typically required higher temperatures (50–160 °C), so the strategy of displacing a leaving group with the methyl ester was pursued instead. Preparation of a tosylate or imidazylate ester was unsuccessful and the starting material (**3.59**) was quantitatively recovered. Fortunately, mesylation proceeded smoothly at 0 °C in the presence of 4-dimethylaminopyridine and a mixture of dichloromethane–pyridine to provide **3.61** (*Scheme 3.17*). Triflation was also attempted to prepare **3.62**, and although the reaction was initially capricious, consistent yields were eventually realized with trifluoromethanesulfonic anhydride and pyridine in dichloromethane at ~0 °C, even when carried out on >1 g of the secondary alcohol. Preliminary attempts to improve the conversion often led to multiple side products, but led to the discovery that stronger bases (i.e., sodium bis(trimethylsilyl)amide) and alternative sources of triflate (i.e., Comins' reagent) at –78 °C

could feasibly be used as well. Nevertheless, it was clear that great care had to be taken with respect to the molar equivalents of base and triflating reagent, to avoid the formation of significant quantities of undesirable products. Practically speaking, it was more difficult to follow the progression of the mesylation reaction by thin-layer chromatography as a consequence of the very similar retardation factor values of the alcohol and mesylate, but the overall yield and conversion to **3.61** was significantly higher than the analogous reaction to prepare triflate **3.62**. Regardless, both triflation and mesylation provided access to the corresponding sulfonate esters, which allowed the lactonization reaction to be studied.

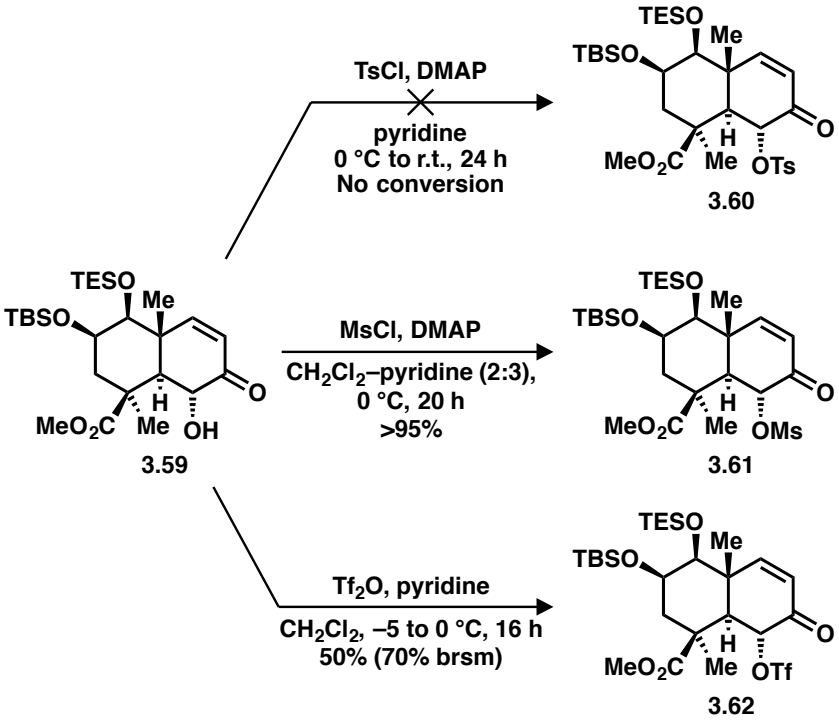

Scheme 3.17 – Sulfonylation of secondary hydroxy group.

Initial efforts to form the lactone were performed on mesylate **3.61** (entries 1–12, *Table 3.3*). The use of sodium hydroxide or potassium carbonate did not result in any conversion to lactone **3.63** between room temperature and 65 °C (entries 1–3, *Table 3.3*). To address this, it was envisaged that the methyl ester itself could displace the mesylate, followed by deprotection of the methyl group with an appropriate nucleophile. Sodium iodide was initially selected as the nucleophilic source with *N*,*N*-dimethylformamide as the solvent; no conversion was observed at or below 100 °C (entries 4–6, *Table 3.3*), but upon heating the reaction to 140

°C, minor quantities of lactone **3.63** and an undesirable elimination product were observed (entry 7, *Table 3.3*). Changing the counterion to lithium (entry 8, *Table 3.3*) or swapping the iodide for chloride (entry 9, *Table 3.3*) did not result in significant differences. Increasing the length of the reaction time was detrimental to the yield of lactone **3.63**, as significant quantities of elimination products were observed (entry 10, *Table 3.3*).

Table 3.3 – Optimization of lactonization reaction.

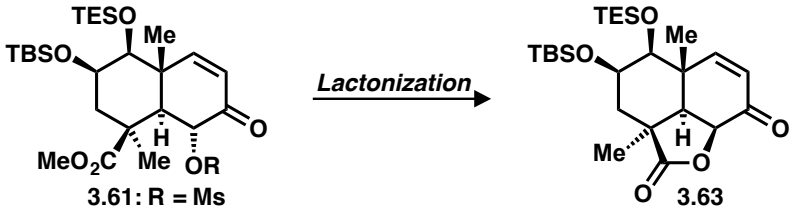

Entry	R	Conditions†	Solvent‡	Temp.	Time	Ratio SM : Lactone : Elim.	Notes*
1	Ms	$NaOH_{(aq.)}$	THF	r.t.	24 h	1 : 0 : 0	No conv.
2	Ms	K_2CO_3 (10 eq.)	THF	r.t.	24 h	1 : 0 : 0	No conv.
3	Ms	K_2CO_3 (10 eq.)	THF	65 °C	24 h	1 : 0 : 0	No conv.
4	Ms	NaI (5 eq.)	DMF	r.t.	24 h	1 : 0 : 0	No conv.
5	Ms	NaI (5 eq.)	DMF	40 °C	24 h	1 : 0 : 0	No conv.
6	Ms	NaI (5 eq.)	DMF	100 °C	12 h	1 : 0 : 0	No conv.
7	Ms	NaI (5 eq.)	DMF	140 °C	6 h	5 : 1.5 : 1	Low conv.
8	Ms	LiI (5 eq.)	DMF	140 °C	6 h	7 : 2 : 1	Low conv.
9	Ms	LiCl (5 eq.)	DMF	140 °C	6 h	4 : 1.5 : 1	Low conv.
10	Ms	LiCl (5 eq.)	DMF	140 °C	24 h	0 : 1 : ≥4	Lots of elim.
11	Ms	LiI (7 eq.), pyr. (2 eq.)	DMF	140 °C	16 h	9 : 2 : 1	Low conv.
12	Ms	LiI (7 eq.), 2,6-lut. (2 eq.)	DMF	140 °C	16 h	9 : 2 : 1	Low conv.
13	Tf	LiCl (5 eq.)	DMF	r.t.	16 h	0 : 1 : 8	Lots of elim.
14	Tf	LiCl (5 eq.), $NaHCO_3$ (5 eq.)	DMF	r.t.	16 h	0 : 1 : 2	Lots of elim.
15	Tf	NaI (5 eq.), $NaHCO_3$ (5 eq.)	DMF	r.t.	16 h	0 : 1 : 3	Lots of elim.
16	Tf	LiI (8 eq.), pyr. (2 eq.)	DMF	r.t.	24 h	0 : 5 : 1	More lactone
17	Tf	LiI (8 eq.), 2,6-lut. (2 eq.)	DMF	r.t.	18 h	0 : 5 : 1	More lactone

* Ratio determined by ^{1}H NMR; † pyr. = pyridine, 2,6-lut. = 2,6-lutidine; ‡ Concentration is 0.02 M

At the same time, triflate **3.62** was explored as a potential candidate for the lactonization reaction (entries 13–17, *Table 3.3*). A preliminary attempt with lithium chloride resulted in complete disappearance of the starting material at ambient temperature, albeit significant quantities of elimination products and only minor amounts of lactone **3.63** were

observed (entry 13, *Table 3.3*).* Encouragingly, when solid sodium bicarbonate was added, the conversion remained high and the ratio of lactone to elimination products became more favourable (entry 14, *Table 3.3*). Although changing the counterion was not advantageous (entry 15, *Table 3.3*), using soluble bases (i.e., pyridine or 2,6-lutidine) led to a significantly more favourable ratio of lactone **3.63** to elimination products (entries 16–17, *Table 3.3*). These bases were also tried in the presence of the mesylate, but they did not lead to a more ideal reaction profile for that leaving group (entries 11–12, *Table 3.3*).

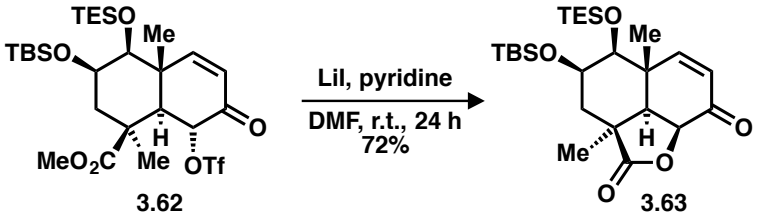

Scheme 3.18 – Lactonization via triflate.

Overall, it was clear that despite the difficulties in preparing the triflate itself (**3.62**), the subsequent lactonization was far more efficient than the corresponding reaction with the mesylate (*Scheme 3.18*). Although it was certainly possible to continue exploring further improvements to the triflation–lactonization sequence, the lactonization strategy was effectively validated and could be carried out on sufficient quantities of material that it was possible to continue exploring this route.

3.4.7 Functionalization of the Enone

To continue the synthesis, a number of different options were available: 1) directly functionalize the enone at C8 using a Morita–Baylis–Hillman reaction (**3.63** to **3.64**, *Scheme 3.19*), followed eventually by a conjugate addition reaction, or 2) a Mukaiyama–Michael reaction with a silyl ketene acetal to prepare a silyl enol ether (**3.63** to **3.65**, *Scheme 3.19*) that could undergo a subsequent aldol reaction. Of course, it was also anticipated that the enone itself could be reduced if necessary and the aldol performed directly on the corresponding

* For a control experiment, when triflate **3.62** (*Scheme 3.17*) was stirred in *N*,*N*-dimethylformamide at ambient temperature without any other additives, the starting material was completely consumed, but none of the desired lactone was observed.

ketone. Initial attempts to functionalize enone **3.63** using a Morita–Baylis–Hillman reaction[202,203] with isobutyraldehyde in the presence of 1,4-diazabicyclo[2.2.2]octane[401,402] (with or without lithium perchlorate[403]), 1,8-diazabicycloundec-7-ene,[404] or 4-dimethylaminopyridine[405,406] were unsuccessful and the enone was recovered. An attempt was also made with dimethylphenylphosphine in a mixture of methanol and chloroform,[201] but alcohol **3.64** was not observed. Despite using freshly redistilled isobutyraldehyde, the propensity of this aldehyde to be oxidized[407] prompted a shift in efforts, and formaldehyde was used instead for comparison. Unfortunately, the results with formaldehyde were similar and none of the desired product was observed in the presence of 1,4-diazabicyclo[2.2.2]octane, 1,8-diazabicycloundec-7-ene, 4-dimethylaminopyridine, or dimethylphenylphosphine.

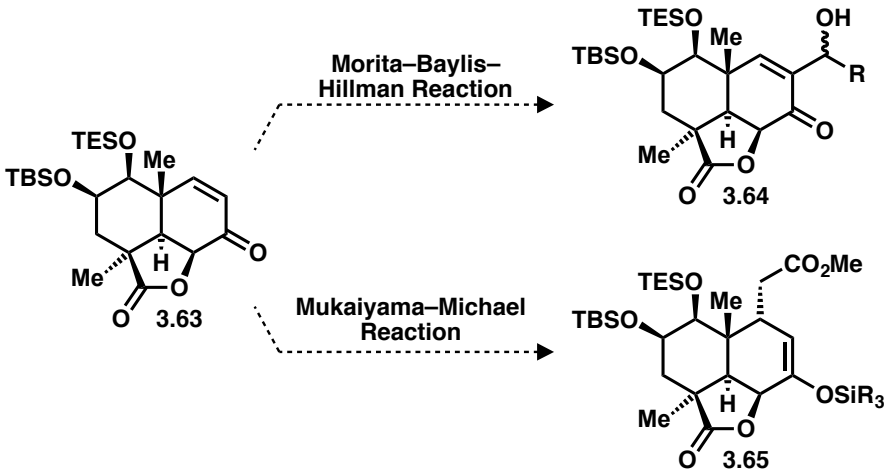

Scheme 3.19 – Options for functionalizing the enone to prepare ring C.

Fortunately, the alternative option – Mukaiyama–Michael conjugate addition reaction with a silyl ketene acetal – was successful and *tert*-butyldimethylsilyl enol ether **3.66** (*Scheme 3.20*) was efficiently prepared in the presence of a catalytic amount of lithium perchlorate using the method described by Reetz and Fox,[341] who built on work previously reported by Grieco's group.[340] This reaction was particularly appealing in that only 0.05 molar equivalents of lithium perchlorate was sufficient for catalyzing the mild and selective conjugate addition reaction of 1-(*tert*-butyldimethylsilyloxy)-1-methoxyethene to enone **3.63**. Furthermore, the product (**3.66**) is a silyl enol ether, which could in principle participate in a subsequent aldol reaction, without the need to regio- and chemoselectively deprotonate the analogous ketone.

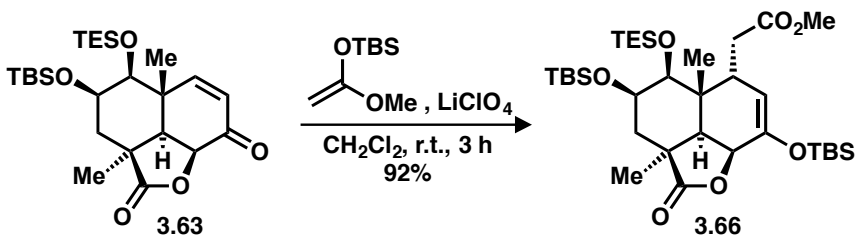

Scheme 3.20 – Mukaiyama–Michael conjugate addition reaction.

Disappointingly, attempts to bring about the Mukaiyama aldol addition with silyl enol ether **3.66** in the presence of titanium tetrachloride or boron trifluoride were rather ineffective and led to silyl-deprotected material (**3.66** to **3.67**, *Scheme 3.21*). Notably, silyl deprotection occurred exclusively from the *syn*-1,2-diol moiety and the *tert*-butyldimethylsilyl enol ether moiety remained intact. This was a noteworthy observation as it provided another option for eventual silyl deprotection towards the end of the synthesis. As an alternative, the *tert*-butyldimethylsilyl enol ether could be selectively converted to the corresponding ketone with triethylamine trihydrofluoride, without concomitant deprotection of the *syn*-1,2-diol moiety (**3.66** to **3.68**). Interestingly, an attempt to hydrolyze the silyl enol ether with aqueous hydrochloric acid in acetone, resulted in removal of the silyl protective groups from the *syn*-1,2-diol moiety and re-protection as the corresponding acetonide (**3.66** to **3.69**); consequently, it appears that this product almost certainly accounts for some of the side-products observed during hydrolysis of the ketal moiety (*Scheme 3.16*, p. 147). Notably, acetonide **3.69** was actually rather intriguing as it provided another opportunity to try the Mukaiyama aldol reaction, without the possibility for silyl deprotection of the *syn*-1,2-diol moiety to occur. Unfortunately, the first attempt at a Mukaiyama aldol reaction with titanium(IV) chloride, and isobutyraldehyde, resulted in effective hydrolysis of the silyl enol ether, which resulted in the observation of ketone **3.70** as the major product.

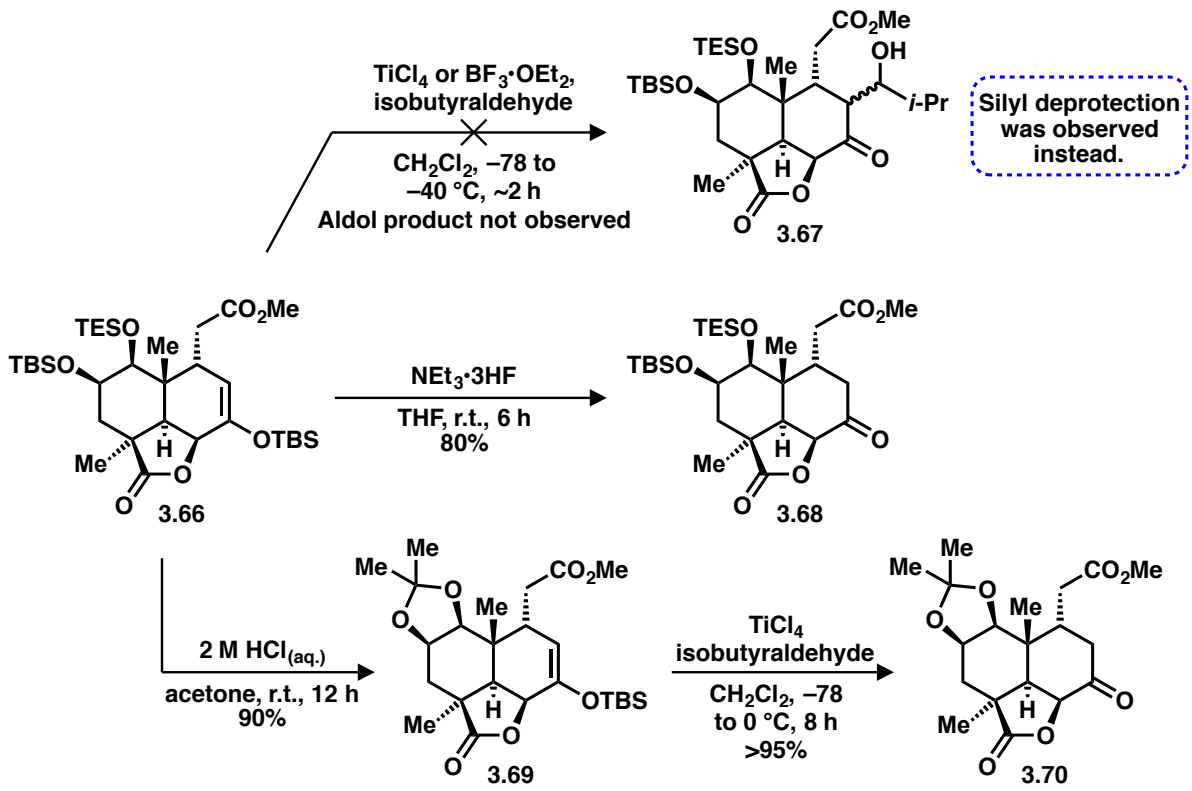

Scheme 3.21 – Reactivity of *tert*-butyldimethylsilyl enol ether.

Although initial attempts to incorporate the isobutyryl moiety directly on **3.68** (*Scheme 3.21*) with *N*-isobutyrylimidazole[408,409] were not particularly promising, it should be noted that another possible synthetic sequence could be pursued by acylating **3.71** instead, which may itself be accessed through reduction of enone **3.63** (*Scheme 3.22*). At this point, it became apparent that it was necessary to prepare more material in order to continue the synthesis and the current state of the route was re-evaluated.

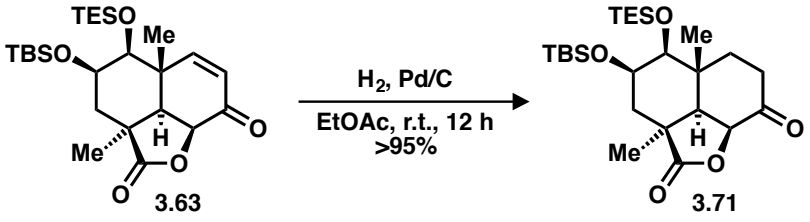

Scheme 3.22 – Hydrogenation of enone.

3.4.8 Summary of Current Route

A summary of the current route is provided in *Scheme 3.23*. Key steps for the synthesis include a stereoselective Rubottom oxidation and ensuing reduction of an α-hydroxy ketone to establish the *syn*-1,2-diol moiety, a ketalization–isomerization reaction, a hydroboration–oxidation sequence, stereoselective alkylation to set the quaternary stereocenter, and lactonization to form the ring D lactone by displacing a triflate leaving group with a methyl ester, along with concomitant methyl deprotection.

The overall yield for the 21-step synthetic sequence from (–)-Wieland–Miescher ketone ((–)-**3.1**) to *tert*-butyldimethylsilyl enol ether **3.66** is approximately 5–6 %, with 12 silica-based purifications, although a few of those are effectively filtrations and additional optimizations could further reduce that number. To this point in the synthesis, all of the stereocenters have been established, save for the alcohol at C7, which one could envision arising by reduction of the ketone functional group at that position. Notably, if the most advanced intermediate from the first-generation synthesis (**2.169**, *Scheme 2.40*, p. 120) was compared against the analogous intermediate from the second-generation route (**3.57**, *Scheme 3.23*), there is a nearly five-fold increase in the yield for the latter sequence (3% compared to 14%). Furthermore, the requirement to use excessive quantities of chromium or liquid ammonia has been completely eliminated. Comparatively speaking, the second-generation sequence is significantly more robust and efficient in that many steps can also be carried out without recourse to time-consuming chromatographic purifications; filtration was often sufficient for obtaining material that could be used in subsequent steps without negatively impacting the yields of those reactions.

For the purpose of preparing nagilactone B, the second generation synthetic approach has a number of advantages, but it is clear that certain sequences could be improved as well, including: 1) the protection–deprotection–re-protection-deprotection sequence with the enone moiety,[*] 2) the yield of the ketalization–isomerization reaction (i.e., **3.45** to **3.49**), and 3) the low yield of the triflation reaction. Furthermore, the presence of silyl protective groups on the *syn*-1,2-diol moiety appeared to limit the initial possibility of pursuing a Mukaiyama-aldol

[*] Compare the enone/ketal moiety in the following: (–)-**3.1**, ***ent*-3.9**, **3.45**, and **3.49**.

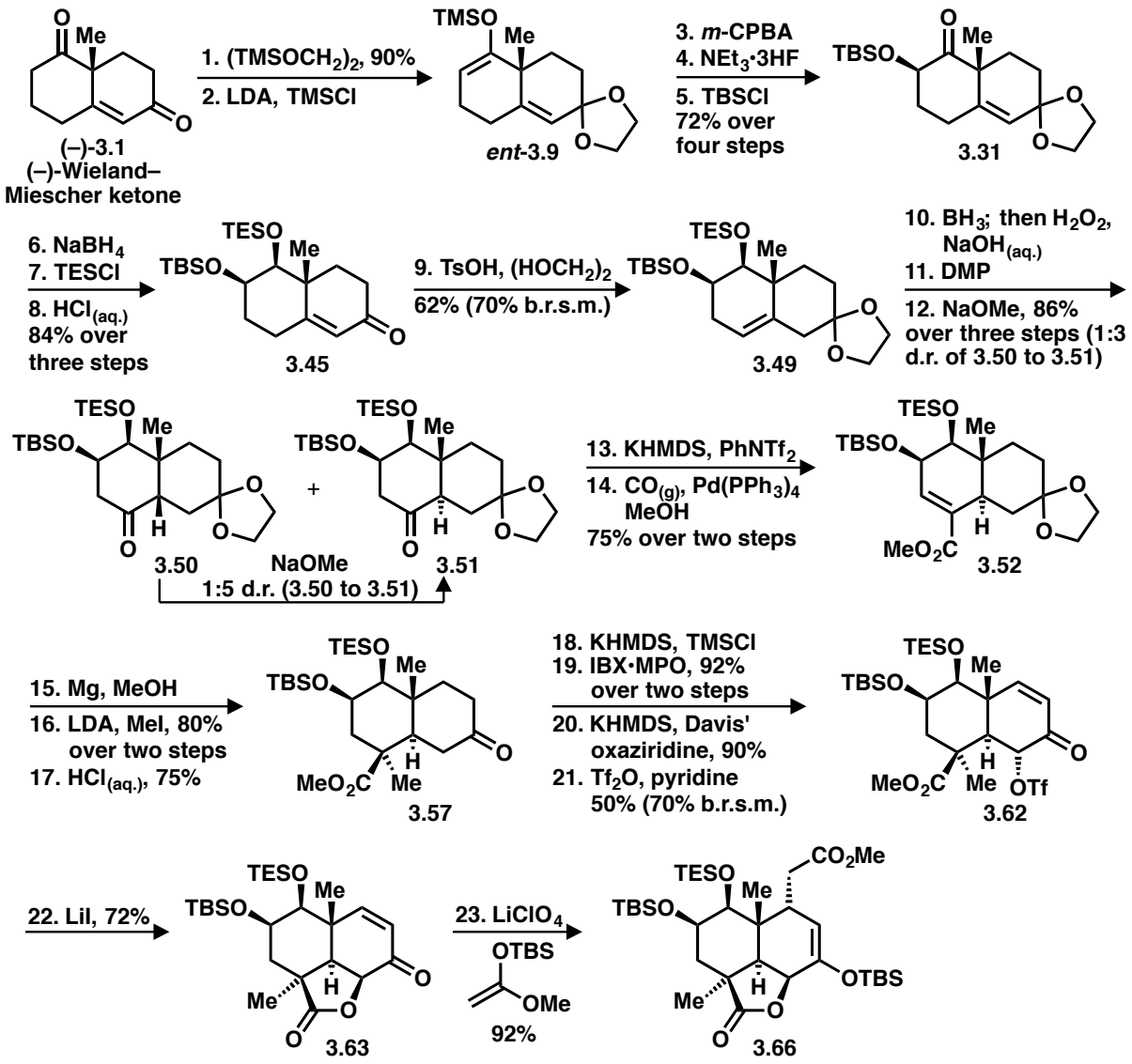

Overall to 3.57: 17 steps, 8 purifications with silica (many are effectively filtrations), ~14% overall yield.
Overall to 3.66: 23 steps, 12 purifications with silica (some are effectively filtrations), ~5–6% overall yield

Reagents and Conditions: 1. TMSOTf, $(TMSOCH_2)_2$, CH_2Cl_2, –78 °C, 4 d, 90%; **2.** LDA,THF –78 to 0 °C, 1 h; then TMSCl, 0 °C to r.t., 45 min.; **3.** *m*-CPBA, $NaHCO_3$, hexanes, –15 to 0 °C, 1 h; **4.** NEt_3•3HF, CH_2Cl_2, 0 °C, 1 h; 5. TBSCl, imidazole, DMF, r.t., 1 h, 72% over four steps; **6.** $NaBH_4$, EtOH, –5 to 0 °C, 1 h; **7.** TESCl, imidazole, DMF, r.t., 1 h; **8.** $HCl_{(aq.)}$, acetone, r.t., 10 min., 84% over three steps; **9.** TsOH•H_2O, $(HOCH_2)_2$, $(MeO)_3CH$, toluene, 80 °C, 2 h, 62% (70% b.r.s.m.); **10.** BH_3•THF, THF, 0 °C to r.t., 16 h; then $H_2O_{2(aq.)}$, $NaOH_{(aq.)}$, 4 h; **11.** DMP, $NaHCO_3$, CH_2Cl_2, r.t., 6 h; **12.** NaOMe, MeOH, r.t., 20 h, 1:3 d.r. (**6** to **7**), 86% over three steps; 13. KHMDS, $PhNTf_2$, THF, –78 °C, 40 min.; **14.** CO, $Pd(PPh_3)_4$, NEt_3, DMF, MeOH, 40 °C, 12 h, 75% over two steps; **15.** Mg, MeOH, r.t., 2 h; **16.** LDA, THF, 0 °C, 30 min.; then MeI, 0 °C, 30 min., 80% over two steps; **17.** 2 M $HCl_{(aq)}$, acetone, r.t., 6 h, 75%; **18.** KHMDS, THF, 0 °C, 1 h; then TMSCl, 0 °C, 1 h; **19.** IBX•MPO, DMSO, r.t., 1 h, 92% over two steps; 20. KHMDS, THF, –78 °C, 1 h; then Davis' oxaziridine, –78 °C, 1 h, 90%; **21.** Tf_2O, pyridine, CH_2Cl_2, –5 to 0 °C, 16 h, 50% (70% brsm); **22.** LiI, pyridine, DMF, rt, 24 h, 72%; **23.** $LiClO_4$, 1-(*tert*-butyldimethylsilyloxy)-1-methoxyethene, CH_2Cl_2, r.t., 3 h, 92%.

Scheme 3.23 – Second-generation sequence for preparing the core of nagilactone B.

strategy from **3.66**, although that may be addressed by using a different protective group or substituting C8 before incorporating the lactone moiety (i.e., formally incorporate an acyl group on ketone **3.57** or enone **3.58**). The former option is particularly appealing since it could also improve the overall yield of the synthetic sequence by minimizing side products stemming from silyl deprotection, while more readily allowing the C1 or C2 hydroxy group to be selectively deprotected. This would provide another opportunity to prepare ring A analogues as well, although one could also imagine using the ketone as a functional handle, rather than installing the *syn*-1,2-diol moiety right away, depending on the analogues of interest. Future work that may be pursued to complete the second-generation synthetic sequence is described in Section 3.5.

3.5 Future Work, Conclusions, and Perspective

Future efforts towards the synthesis of nagilactone B should focus on preparing the α-pyrone moiety. As intended, the second-generation strategy provides multiple options for pursuing that goal, while alleviating the drawbacks associated with the first-generation sequence (*Scheme 2.40*, p. 120). Although it may be possible to install the α-pyrone (δ-lactone) moiety in nagilactone B using one of the intermediates from the Mukaiyama–Michael conjugate addition reaction (i.e., **3.66** or **3.68**, *Scheme 3.21*, p. 154), the initially-encountered difficulties provide an indication that it may be better to install the isobutyryl group before performing the conjugate addition. It would be appropriate to focus on incorporating the isobutyryl group at one of two different stages: before or after the γ-lactone has been established (*Scheme 3.24*). Armed with the knowledge that deprotonation of ketone **3.72** can occur exclusively at C8 (e.g., see **3.57** to **3.58**, *Scheme 3.16*, p. 147), it may be feasible to

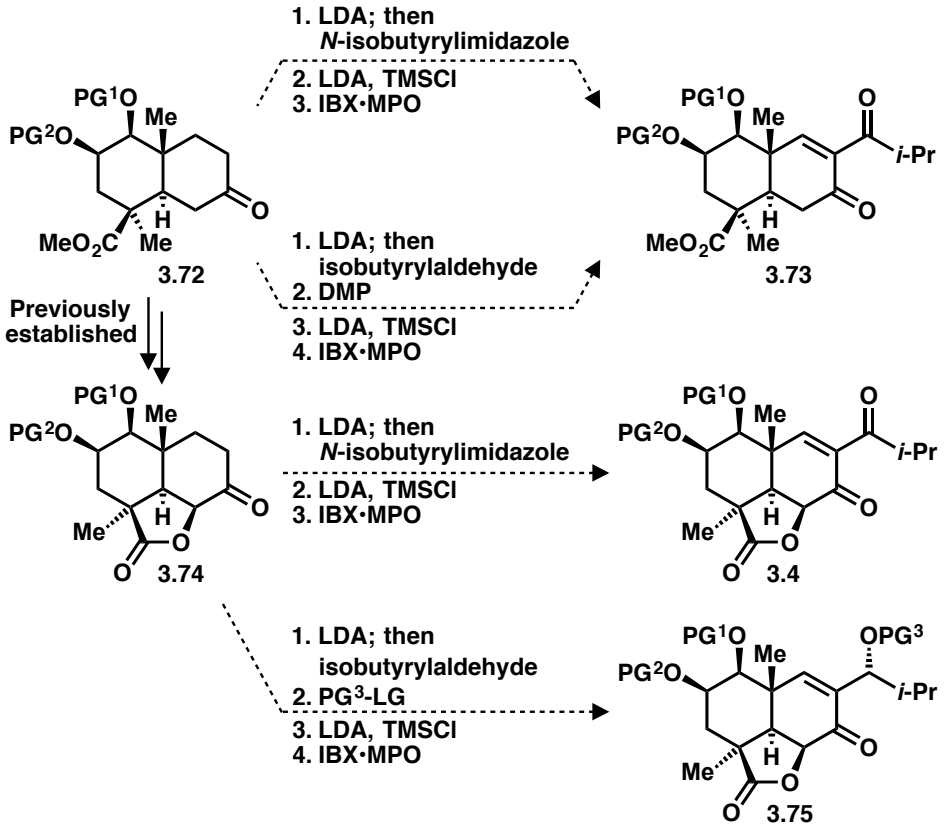

Scheme 3.24 – Incorporation of isobutyryl group.

acylate before establishing the γ-lactone (i.e., **3.72** to **3.73**, *Scheme 3.24*). Alternatively, a similar synthetic sequence to what was described for the second-generation approach could be used if the lactone is incorporated into the scaffold first (i.e., **3.74** to **3.4**). For either of these options, if the isobutyryl group causes difficulties for subsequent reactions, a complementary sequence, in which a protected aldehyde or alcohol (with or without the isopropyl group) is used in its place, should be feasible (i.e., **3.74** to **3.75**).

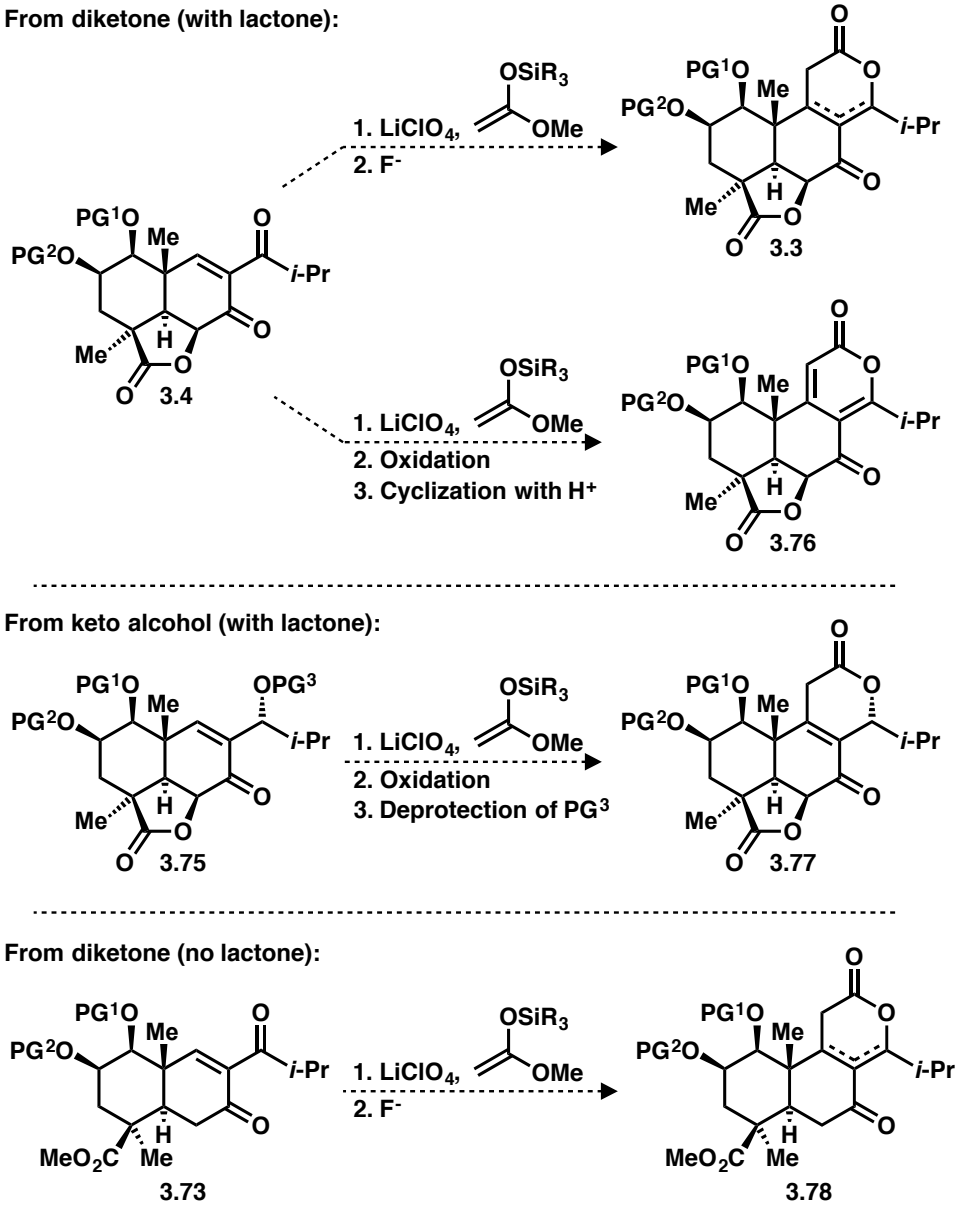

Scheme 3.25 – Options for establishing the δ-lactone.

The α-pyrone (δ-lactone) could then be established using one of a number of different synthetic approaches (*Scheme 3.25*). A Mukaiyama–Michael conjugate addition reaction, followed by deprotection of the silyl enol ether would afford a transient enolate that could potentially lactonize directly (i.e., **3.4** to **3.3**, *Scheme 3.25*). If lactonization does not immediately take place, the ester could also be activated to promote cyclization and the resultant lactone oxidized using a selenium-oxidation sequence, similar to what was previously described by Hayashi's group (*Scheme 2.8*, p. 72). Alternatively, if the intermediate silyl enol ether can readily be oxidized, cyclization would lead directly to the desired α-pyrone (i.e., **3.4** to **3.76**, *Scheme 3.25*). Another option involves using a protected alcohol instead, which could be deprotected to promote the desired lactonization reaction (i.e., **3.75** to **3.77**, *Scheme 3.25*). In each of these examples, it may also be necessary to reduce the ketone at C7 if its presence has a negative influence on the desired reactivity. Lastly, a complementary option in which the lactone is installed towards the end of the synthesis is also feasible (i.e., **3.73** to **3.78**, *Scheme 3.25*), and could be envisaged to take place through similar sequences as those described for the analogous γ-lactone-containing scaffold.

One of the main benefits of the second-generation approach is the flexibility of incorporating functional groups at different stages of the synthesis. Furthermore, the presence of the C7 ketone towards the end of the synthetic route provides an opportunity to prepare diverse analogues of this family of natural products. For the purpose of preparing ring A analogues using this sequence, one can also imagine taking different approaches: 1) differentially protecting alcohols at C1 and C2 and later manipulating them to prepare derivatives, or 2) diversifying from a common intermediate that contains a single hydroxy group, similar to the intermediate described by Danishefsky's group (**3.27**, *Scheme 3.4*, p. 131).

Overall, a robust sequence for preparing the ABD-ring core of nagilactone B has been established starting with the (–)-Wieland-Miescher ketone. Six of the seven stereocenters in nagilactone B have been set, including two quaternary stereocenters, with the remaining stereocenter expected to be readily accessible by reduction of the ketone at C7. Future work will focus on synthesizing the α-pyrone moiety, which is envisaged to be accessible from at

least one of the numerous intermediates that have been prepared during the pursuit of the second-generation sequence.

Chapter 4:

Experimental Section

4.1 General Experimental Details

All non-aqueous reactions were performed in oven- (120 °C) or flame-dried glassware under a positive pressure of argon, with exclusion of moisture from reagents and glassware, using standard techniques for manipulating air-sensitive compounds, unless otherwise stated. Anhydrous tetrahydrofuran, diethyl ether, toluene, and dichloromethane were obtained by passing these solvents through columns of activated alumina, while all other solvents were used as received from chemical suppliers, unless stated otherwise. Reagents were purchased and used without further purification, unless otherwise stated. Yields refer to chromatographically and spectroscopically (^{1}H NMR) homogeneous material, unless otherwise stated.

Reactions were monitored by thin-layer chromatography (TLC) carried out on 0.20 mm EMD Millipore Silica Gel 60 Å F254 silica plates on aluminum support that were visualized using a compact UV lamp (254 nm) and developed using an aqueous solution of cerium ammonium molybdate, basic aqueous potassium permanganate, iodine vapour, or an ethanolic solution of *p*-anisaldehyde.

Flash chromatography was performed using SiliaFlash P60 40-63 μm (230-400 mesh) silica gel and all column dimensions are reported as height × diameter in centimeters. Note that the when solvent ratios are described, they refer to volumetric ratios. NMR spectra were recorded on Bruker AV-300, ARX-400, or AV-400 instruments, calibrated using residual undeuterated solvent as an internal reference (chloroform, δ = 7.26 ppm; CHD_2OD = 3.31 ppm), and reported in parts per million relative to trimethylsilane (δ = 0.00 ppm) as follows: chemical shift (multiplicity, coupling constant (Hz), integration). The following abbreviations were used to explain multiplicities: s = singlet, d = doublet, t = triplet, q = quartet, m = multiplet, br = broad, dd = doublet of doublets, dt = doublet of triplets, ddt = doublet of doublet of triplets, and variations thereof. High-resolution mass spectra (HRMS) were recorded at the Centre Régional de Spectrométrie de Masse de l'Université de Montréal on an Agilent LC-MSD TOF mass spectrometer by electrospray ionization time of flight reflectron experiments, unless noted otherwie. IR spectra were recorded on a Perkin Elmer Spectrum One spectrometer and are reported in reciprocal centimeters (cm^{-1}). Melting points were

recorded on a Büchi Melting Point B-540 apparatus and are uncorrected. Specific rotation measurements were determined on a Perkin-Elmer 343 Polarimeter using the D-line of the sodium lamp (=589.3 nm) and are reported in units of $deg \cdot cm^3 \cdot g^{-1} \cdot dm^{-1}$.

Details regarding the synthetic procedures, computational studies, and X-ray crystallographic analyses that were described in Chapters 1–3, may be found in Annexes 1–5.

References

(1) Alberts, B.; Johnson, A.; Lewis, J.; Morgan, D.; Raff, M.; Roberts, K.; Walter, P. *Molecular Biology of the Cell*; 6 ed.; Garland Science, 2014.
(2) Ohyama, T. *DNA Conformation and Transcription*; Springer US: Boston, MA, 2005.
(3) Elson, D.; Chargaff, E. *Experientia* **1952**, *8*, 143.
(4) Chargaff, E.; Lipshitz, R.; Green, C. *J. Biol. Chem.* **1952**, *195*, 155.
(5) Bansal, M. *Curr. Sci.* **2003**, *85*, 1556.
(6) Brameld, K. A.; Goddard, W. A., III. *J. Am. Chem. Soc.* **1999**, *121*, 985.
(7) Figure compiled using files downloaded from the RSCB Protein Data Bank (A-DNA: 1QPH, B-DNA: 355D, Z-DNA: 2ACJ) http://www.rcsb.org/ (accessed Jul 2, 2015).
(8) Ghosh, A.; Bansal, M. *Acta Cryst.* **2003**, *D59*, 620.
(9) Ha, S. C.; Lowenhaupt, K.; Rich, A.; Kim, Y.-G.; Kim, K. K. *Nature* **2005**, *437*, 1183.
(10) Pabo, C. O.; Sauer, R. T. *Annu. Rev. Biochem.* **1984**, *53*, 293.
(11) Crick, F. *Nature* **1970**, *227*, 561.
(12) Crick, F. *Symp. Soc. Exp. Biol. XII* **1956**, 139.
(13) Adapted from the OpenStax College, Anatomy & Physiology online textbook (July 30, 2014), which is licensed under a Creative Commons Attribution License 3.0 license http://cnx.org/content/col11496/1.6/ (accessed Jul 2, 2015).
(14) Cramer, P.; Bushnell, D. A.; Fu, J. H.; Gnatt, A. L.; Maier-Davis, B.; Thompson, N. E.; Burgess, R. R.; Edwards, A. M.; David, P. R.; Kornberg, R. D. *Science* **2000**, *288*, 640.
(15) Wei, C.-M.; Gershowitz, A.; Moss, B. *Cell* **1975**, *4*, 379.
(16) Reed, R. *Curr. Opin. Cell Biol.* **2000**, *12*, 340.
(17) Ben-Shem, A.; de Loubresse, N. G.; Melnikov, S.; Jenner, L.; Yusupova, G.; Yusupov, M. *Science* **2011**, *334*, 1524.
(18) Korostelev, A.; Noller, H. F. *Trends Biochem. Sci.* **2007**, *32*, 434.
(19) Korostelev, A.; Trakhanov, S.; Laurberg, M.; Noller, H. F. *Cell* **2006**, *126*, 1065.
(20) Nakamoto, T. *Gene* **2009**, *432*, 1.
(21) Anfinsen, C. B. *Biochem. J.* **1972**, *128*, 737.
(22) Anfinsen, C. B. *Science* **1973**, *181*, 223.
(23) Lee, S.; Tsai, F. *J. Biochem. Mol. Biol.* **2005**, *38*, 259.
(24) Bryngelson, J. D.; Onuchic, J. N.; Socci, N. D.; Wolynes, P. G. *Proteins Struct. Funct. Bioinf.* **1995**, *21*, 167.
(25) Nicholls, A.; Sharp, K. A.; Honig, B. *Proteins Struct. Funct. Bioinf.* **1991**, *11*, 281.
(26) With courtesy to the National Human Genome Research Institute website; the image is in the public domain according to Title 17, Chapter 1, Section 105 of the US Code http://www.genome.gov/ (accessed Jul 2, 2015).
(27) Tazi, J.; Bakkour, N.; Stamm, S. *Biochim. Biophys. Acta* **2009**, *1792*, 14.
(28) Venables, J. P. *Bioessays* **2006**, *28*, 378.
(29) Skotheim, R. I.; Nees, M. *Int. J. Biochem. Cell Biol.* **2007**, *39*, 1432.
(30) Robinson, R. *PLoS biology* **2004**, *2*, 18.
(31) Nowotny, M.; Gaidamakov, S. A.; Crouch, R. J.; Yang, W. *Cell* **2005**, *121*, 1005.
(32) Zamecnik, P. C.; Stephenson, M. L. *Proc. Natl. Acad. Sci. U.S.A.* **1978**, *75*, 280.
(33) Bennett, C. F.; Swayze, E. E. *Annu. Rev. Pharmacol. Toxicol.* **2010**, *50*, 259.

(34) Boyer, D. S.; Cowen, S. J.; Danis, R. P.; Diamond, J. G.; Fish, R. H.; Goldstein, D. A.; Jaffe, G. J.; Lalezari, J. P.; Lieberman, R. M.; Belfort, R.; Muccioli, C.; Palestine, A. G.; Perez, J. E.; Territo, C.; Andreu-Andreu, D.; Deschenes, J. G.; deSmet, M. D.; Fisher, M.; Gastaut, J. A.; Gazzard, B. G.; Lightman, S.; Johnson, M. A.; Klauss, V.; Gumbel, H.; Knospe, V.; Mallolas-Masferrer, J.; Cornish, M. J.; Holland, G. N.; Ransome, S. S.; Tufail, A.; Weisz, J. M.; Crooke, S. T.; Kisner, D. L.; Chandler, J. W.; Frost, K. R.; Hutcherson, S. L.; Whitley, R. J.; Grillone, L. R.; Lanz, R.; Grp, V. S. *Am. J. Ophthalmol.* **2002**, *133*, 475.
(35) Geary, D. R. S.; Henry, S. P.; Grillone, L. R. *Clin. Pharmacokin.* **2002**, *41*, 255.
(36) Mulamba, G. B.; Hu, A.; Azad, R. F.; Anderson, K. P.; Coen, D. M. *Antimicrob. Agents Chemother.* **1998**, *42*, 971.
(37) Crooke, S. T.; Geary, R. S. *Br. J. Clin. Pharmacol.* **2013**, *76*, 269.
(38) Harchaoui, El, K.; Akdim, F.; Stroes, E. S. G.; Trip, M. D.; Kastelein, J. J. P. *Am. J. Cardiovasc. Drugs* **2008**, *8*, 233.
(39) Furtado, J. D.; Wedel, M. K.; Sacks, F. M. *J. Lipid Res.* **2012**, *53*, 784.
(40) Merki, E.; Graham, M. J.; Mullick, A. E.; Miller, E. R.; Crooke, R. M.; Pitas, R. E.; Witztum, J. L.; Tsimikas, S. *Circulation* **2008**, *118*, 743.
(41) *Antisense Drug Technology*; Crooke, S. T., Ed.; CRC Press, 2007.
(42) Lesnik, E. A.; Freier, S. M. *Biochemistry* **1995**, *34*, 10807.
(43) Eckstein, F. *Antisense Nucleic Acid Drug Dev.* **2000**, *10*, 117.
(44) Stein, C. A.; Subasinghe, C.; Shinozuka, K.; Cohen, J. S. *Nucl. Acids Res.* **1988**, *16*, 3209.
(45) Marky, L. A.; Breslauer, K. J. *Biopolymers* **1987**, *26*, 1601.
(46) Doktycz, M. J. *Nucleic Acids: Thermal Stability and Denaturation*; John Wiley & Sons, Ltd: Chichester, UK, 2001.
(47) Summers, J. S.; Shaw, B. *Curr. Med. Chem.* **2001**, *8*, 1147.
(48) Micklefield, J. *Curr. Med. Chem.* **2001**, *8*, 1157.
(49) Herdewijn, P. *Antisense Nucleic Acid Drug Dev.* **2000**, *10*, 297.
(50) Sanghvi, Y. S.; Hoke, G. D.; Freier, S. M.; Zounes, M. C.; Gonzalez, C.; Summins, L.; Sasmor, H.; Cook, P. D. *Nucl. Acids Res.* **1993**, *21*, 3197.
(51) Froehler, B. C.; Wadwani, S.; Terhorst, T. J.; Gerrard, S. R. *Tetrahedron Lett.* **1992**, *33*, 5307.
(52) Shen, L. J.; Siwkowski, A.; Wancewicz, E. V.; Lesnik, E.; Butler, M.; Witchell, D.; Vasquez, G.; Ross, B.; Acevedo, O.; Inamati, G.; Sasmor, H.; Manoharan, M.; Monia, B. P. *Antisense Nucleic Acid Drug Dev.* **2003**, *13*, 129.
(53) Gryaznov, S.; Schultz, R. G. *Tetrahedron Lett.* **1994**, *35*, 2489.
(54) Lin, K.-Y.; Jones, R. J.; Matteucci, M. *J. Am. Chem. Soc.* **1995**, *117*, 3873.
(55) Holmes, S. C.; Gait, M. J. *Nucleos. Nucleot. Nucl.* **2003**, *22*, 1259.
(56) Wilds, C. J.; Maier, M. A.; Manoharan, M.; Egli, M. *Helv. Chim. Acta* **2003**, *86*, 966.
(57) Sazani, P.; Astriab-Fischer, A.; Kole, R. *Antisense Nucleic Acid Drug Dev.* **2003**, *13*, 119.
(58) Summerton, J.; Weller, D. *Antisense Nucleic Acid Drug Dev.* **1997**, *7*, 187.
(59) Heasman, J. *Dev. Biol.* **2002**, *243*, 209.
(60) Summerton, J. *Biochim. Biophys. Acta, Gene Struct. Expression* **1999**, *1489*, 141.
(61) Summerton, J.; Stein, D.; Huang, S. B.; Matthews, P.; Weller, D.; Partridge, M. *Antisense Nucleic Acid Drug Dev.* **1997**, *7*, 63.

(62) Griffey, R. H.; Lesnik, E.; Freier, S.; Sanghvi, Y. S.; Teng, K.; Kawasaki, A.; Guinosso, C.; Wheeler, P.; Mohan, V.; Cook, P. D. In *Carbohydrate Modifications in Antisense Research*; Structural Properties of Modified Nucleosides Incorporated into Oligonucleotides; American Chemical Society: Washington, DC, 2009; Vol. 580, pp. 212–224.
(63) Damha, M. J.; Wilds, C. J.; Noronha, A. *J. Am. Chem. Soc.* **1998**, *120*, 12976.
(64) Dupouy, C.; Iché-Tarrat, N.; Durrieu, M.-P.; Rodriguez, F.; Escudier, J.-M.; Vigroux, A. *Angew. Chem. Int. Ed.* **2006**, *45*, 3623.
(65) Steffans, R.; Leumann, C. *Helv. Chim. Acta* **1997**, *80*, 2426.
(66) Steffens, R.; Leumann, C. J. *J. Am. Chem. Soc.* **1999**, *121*, 3249.
(67) Kaur, H.; Babu, B. R.; Maiti, S. *Chem. Rev.* **2007**, *107*, 4672.
(68) Obika, S.; Imanishi, T.; Kawada, Y.; Baba, T.; Fujisaka, A. *Heterocycles* **2010**, *81*, 1347.
(69) Obika, S.; Nanbu, D.; Hari, Y.; Morio, K.-I.; In, Y.; Ishida, T.; Imanishi, T. *Tetrahedron Lett.* **1997**, *38*, 8735.
(70) Koshkin, A. A.; Singh, S. K.; Nielsen, P.; Rajwanshi, V. K.; Kumar, R.; Meldgaard, M.; Olsen, C. E.; Wengel, J. *Tetrahedron* **1998**, *54*, 3607.
(71) Rajwanshi, V.; Håkansson, A.; Sørensen, M.; Pitsch, S.; Singh, S.; Kumar, R.; Nielsen, P.; Wengel, J. *Angew. Chem. Int. Ed.* **2000**, *39*, 1656.
(72) Kaur, H.; Arora, A.; Wengel, J.; Maiti, S. *Biochemistry* **2006**, *45*, 7347.
(73) Kværnø, L.; Kumar, R.; Dahl, B. M.; Olsen, C. E.; Wengel, J. *J. Org. Chem.* **2000**, *65*, 5167.
(74) Kværnø, L.; Wengel, J. *Chem. Commun.* **2001**, 1419.
(75) McTigue, P. M.; Peterson, R. J.; Kahn, J. D. *Biochemistry* **2004**, *43*, 5388.
(76) Hakansson, A. E.; Wengel, J. *Bioorg. Med. Chem. Lett.* **2001**, *11*, 935.
(77) Seth, P. P.; Allerson, C. R.; Østergaard, M. E.; Swayze, E. E. *Bioorg. Med. Chem. Lett.* **2012**, *22*, 296.
(78) Seth, P. P.; Allerson, C. R.; Siwkowski, A.; Vasquez, G.; Berdeja, A.; Migawa, M. T.; Gaus, H.; Prakash, T. P.; Bhat, B.; Swayze, E. E. *J. Med. Chem.* **2010**, *53*, 8309.
(79) Rubin, J.; Brennan, T.; Sundaralingam, M. *Biochemistry* **1972**, *11*, 3112.
(80) *Eur. J. Biochem.* **1983**, *131*, 9.
(81) Markley, J. L.; Bax, A.; Arata, Y.; Hilbers, C. W.; Kaptein, R.; Sykes, B. D.; Wright, P. E.; Wüthrich, K. *Pure Appl. Chem.* **1998**, *70*, 117.
(82) Pallan, P. S.; Yu, J.; Allerson, C. R.; Swayze, E. E.; Seth, P.; Egli, M. *Biochemistry* **2012**, *51*, 7.
(83) Seth, P. P.; Vasquez, G.; Allerson, C. A.; Berdeja, A.; Gaus, H.; Kinberger, G. A.; Prakash, T. P.; Migawa, M. T.; Bhat, B.; Swayze, E. E. *J. Org. Chem.* **2010**, *75*, 1569.
(84) Pallan, P. S.; Allerson, C. R.; Berdeja, A.; Seth, P. P.; Swayze, E. E.; Prakash, T. P.; Egli, M. *Chem. Commun. (Camb.)* **2012**, *48*, 8195.
(85) Seth, P. P.; Yu, J.; Allerson, C. R.; Berdeja, A.; Swayze, E. E. *Bioorg. Med. Chem. Lett.* **2011**, *21*, 1122.
(86) Seth, P. P.; Allerson, C. A.; Østergaard, M. E.; Swayze, E. E. *Bioorg. Med. Chem. Lett.* **2011**, *21*, 4690.
(87) Hanessian, S.; Schroeder, B. R.; Merner, B. L.; Chen, B.; Swayze, E. E.; Seth, P. P. *J. Org. Chem.* **2013**, *78*, 9051.
(88) Gyi, J. I.; Lane, A. N.; Conn, G. L.; Brown, T. *Nucl. Acids Res.* **1998**, *26*, 3104.

(89) Auffinger, P.; Hashem, Y. *Curr. Opin. Struct. Biol.* **2007**, *17*, 325.
(90) Auffinger, P.; Westhof, E. In *Water Management in the Dsign and Distribution of Quality Foods*; Ross, Y. H.; Leslie, R. B.; Lillford, P. J., Eds.; Technomic Publishing Co., Inc.: Basel, 1999; pp. 165–198.
(91) Pastor, N. *Biophys. J.* **2005**, *88*, 3262.
(92) Hanessian, S.; Wagger, J.; Merner, B. L.; Giacometti, R. D.; Østergaard, M. E.; Swayze, E. E.; Seth, P. P. *J. Org. Chem.* **2013**, *78*, 9064.
(93) Hanessian, S.; Schroeder, B. R.; Giacometti, R. D.; Merner, B. L.; Østergaard, M.; Swayze, E. E.; Seth, P. P. *Angew. Chem. Int. Ed.* **2012**, *51*, 11242.
(94) Caruthers, M. H. *Acc. Chem. Res.* **1991**, *24*, 278.
(95) Wengel, J. *Acc. Chem. Res.* **1999**, *32*, 301.
(96) Håkansson, A. E.; Koshkin, A. A.; Sørensen, M. D.; Wengel, J. *J. Org. Chem.* **2000**, *65*, 5161.
(97) Sørensen, M. D.; Kværnø, L.; Bryld, T.; Håkansson, A. E.; Verbeure, B.; Gaubert, G.; Herdewijn, P.; Wengel, J. *J. Am. Chem. Soc.* **2002**, *124*, 2164.
(98) Niedballa, U.; Vorbrüggen, H. *Angew. Chem. Int. Ed.* **1970**, *9*, 461.
(99) In *Comprehensive Organic Name Reactions and Reagents*; Wang, Z., Ed.; (Vorbrüggen Reaction, Vorbrüggen Glycosidation, Vorbrüggen Coupling); John Wiley & Sons, Inc.: Hoboken, NJ, USA, 2010; pp. 2915–2919.
(100) Niedballa, U.; Vorbrüggen, H. *J. Org. Chem.* **1974**, *39*, 3654.
(101) Vougioukalakis, G. C.; Grubbs, R. H. *Chem. Rev.* **2010**, *110*, 1746.
(102) Samojłowicz, C.; Bieniek, M.; Grela, K. *Chem. Rev.* **2009**, *109*, 3708.
(103) Maity, J. K.; Ghosh, R.; Drew, M. G. B.; Achari, B.; Mandal, S. B. *J. Org. Chem.* **2008**, *73*, 4305.
(104) Hrdlicka, P. J.; Andersen, N. K.; Jepsen, J. S.; Hansen, F. G.; Haselmann, K. F.; Nielsen, C.; Wengel, J. *Bioorg. Med. Chem.* **2005**, *13*, 2597.
(105) Youssefyeh, R. D.; Verheyden, J. P. H.; Moffatt, J. G. *J. Org. Chem.* **1979**, *44*, 1301.
(106) Swain, C. G.; Powell, A. L.; Sheppard, W. A.; Morgan, C. R. *J. Am. Chem. Soc.* **1979**, *101*, 3576.
(107) Hosomi, A.; Endo, M.; Sakurai, H. *Chem. Lett.* **1976**, 941.
(108) Hosomi, A.; Sakurai, H. *Tetrahedron Lett.* **1976**, *17*, 1295.
(109) Fleming, I.; Dunoguès, J.; Smithers, R. In *Organic Reactions*; John Wiley & Sons, Inc.: Hoboken, NJ, USA, 2004; pp. 57–193.
(110) Danishefsky, S. J.; DeNinno, M. P.; Phillips, G. B.; Zelle, R. E.; Lartey, P. A. *Tetrahedron* **1986**, *42*, 2809.
(111) Hassler, M.; Wu, Y. Q.; Mallikarjuna Reddy, N.; Chan, T. H.; Damha, M. J. *Tetrahedron Lett.* **2011**, *52*, 2575.
(112) Romieu, A.; Gasparutto, D.; Cadet, J. *J. Chem. Soc., Perkin Trans. 1* **1999**, 1257.
(113) Zehl, A.; Starke, A.; Cech, D.; Hartsch, T.; Merkl, R.; Fritz, H.-J. *Chem. Commun.* **1996**, 2677.
(114) Christensen, S. M.; Hansen, H. F.; Koch, T. *Org. Process Res. Dev.* **2004**, *8*, 777.
(115) Sen, S. E.; Roach, S. L.; Boggs, J. K.; Ewing, G. J.; Magrath, J. *J. Org. Chem.* **1997**, *62*, 6684.
(116) Bowden, K.; Heilbron, I. M.; Jones, E. R. H.; Weedon, B. C. L. *J. Chem. Soc.* **1946**, 39.
(117) Nahm, S.; Weinreb, S. M. *Tetrahedron Lett.* **1981**, *22*, 3815.

(118) Tojo, G.; Fernández, M. *Oxidation of Primary Alcohols to Carboxylic Acids*; Springer New York: New York, NY, 2007.
(119) Corey, E. J.; Schmidt, G. *Tetrahedron Lett.* **1979**, 399.
(120) Coates, W. M.; Corrigan, J. R. *Chem. Ind.* **1969**, 1594.
(121) Campos, K. R.; Cai, D.; Journet, M.; Kowal, J. J.; Larsen, R. D.; Reider, P. J. *J. Org. Chem.* **2001**, *66*, 3634.
(122) Lindlar, H.; Dubuis, R. *Org. Synth.* **1966**, *46*, 89.
(123) Lindlar, H. *Helv. Chim. Acta* **1952**, *35*, 446.
(124) Braasch, D. A.; Corey, D. R. *Chem. Biol.* **2001**, *8*, 1.
(125) Nauwelaerts, K.; Vastmans, K.; Froeyen, M.; Kempeneers, V.; Rozenski, J.; Rosemeyer, H.; Van Aerschot, A.; Busson, R.; Lacey, J. C.; Efimtseva, E.; Mikhailov, S.; Lescrinier, E.; Herdewijn, P. *Nucl. Acids Res.* **2003**, *31*, 6758.
(126) Østergaard, M. E.; Dwight, T.; Berdeja, A.; Swayze, E. E.; Jung, M. E.; Seth, P. P. *J. Org. Chem.* **2014**, *79*, 8877.
(127) Sekiguchi, M.; Obika, S.; Harada, Y.; Osaki, T.; Somjing, R.; Mitsuoka, Y.; Shibata, N.; Masaki, M.; Imanishi, T. *J. Org. Chem.* **2006**, *71*, 1306.
(128) Shaikh, K. I.; Kumar, S.; Lundhus, L.; Bond, A. D.; Sharma, P. K.; Nielsen, P. *J. Org. Chem.* **2009**, *74*, 1557.
(129) Ravn, J.; Thorup, N.; Nielsen, P. *J. Chem. Soc., Perkin Trans. 1* **2001**, 1855.
(130) Stauffiger, A.; Leumann, C. J. *Eur. J. Org. Chem.* **2009**, *2009*, 1153.
(131) Barrero, A. F.; Del Moral, J.; Herrador, M. M. *Stud. Nat. Prod. Chem.* **2003**, *28*, 453.
(132) Banerjee, A.; Laya, M.; Mora, H.; Cabrera, E. *Curr. Org. Chem.* **2008**, *12*, 1050.
(133) Itô, S.; Kodama, M. *Heterocycles* **1976**, *4*, 595.
(134) Kupchan, S. M.; Baxter, R. L.; Ziegler, M. F.; Smith, P. M.; Bryan, R. F. *Experientia* **1975**, *31*, 137.
(135) Cassady, J. M.; Lightner, T. K.; McCloud, T. G.; Hembree, J. A.; Byrn, S. R.; Chang, C. *J. Org. Chem.* **1984**, *49*, 942.
(136) Hembree, J. A.; Chang, C.-J.; McLaughlin, J. L.; Cassady, J. M.; Watts, D. J.; Wenkert, E.; Fonseca, S. F.; Campello, J. D. P. *Phytochemistry* **1979**, *18*, 1691.
(137) Hayashi, Y.; Sakan, T.; Sakurai, Y.; Tashiro, T. *Gann.* **1975**, *66*, 587.
(138) Hayashi, Y.; Matsumoto, T.; Tashiro, T. *Gann.* **1979**, *70*, 365.
(139) Ichikawa, K.; Ikunaka, M.; Kojima, N.; Nishida, H.; Yoshikawa, N. Terpenoid lactone compounds and their production process. EP 0 933 373 A1, 1999.
(140) Hayashi, Y.; Kim, Y.; Hayashi, Y.; Hayashi, Y.; Chairul. *Biosci., Biotechnol., Biochem.* **1992**, *56*, 1302.
(141) Zhang, M.; Ying, B.-P.; Kubo, I. *J. Nat. Prod.* **1992**, *55*, 1057.
(142) Hosoe, T.; Nozawa, K.; Lumley, T. C.; Currah, R. S.; Fukushima, K.; Takizawa, K.; Miyaji, M.; Kawai, K.-I. *Chem. Pharm. Bull.* **1999**, *47*, 1591.
(143) Barrero, A. F.; Arseniyadis, S.; Quílez del Moral, J. F.; Herrador, M. M.; Valdivia, M.; Jiménez, D. *J. Org. Chem.* **2002**, *67*, 2501.
(144) Hayashi, Y.; Yokoi, J.; Watanabe, Y.; Sakan, T.; Masuda, Y.; Yamamoto, R. *Chem. Lett.* **1972**, *1*, 759.
(145) Barrero, A. F.; Sánchez, J. F.; Elmerabet, J.; Jiménez-González, D.; Macías, F. A.; Simonet, A. M. *Tetrahedron* **1999**, *55*, 7289.
(146) Macías, F. A.; Simonet, A. M.; Pacheco, P. C.; Barrero, A. F.; Cabrera, E.; Jiménez-González, D. *J. Agric. Food Chem.* **2000**, *48*, 3003.

(147) Hayashi, Y.; Takahashi, S.; Ona, H.; Sakan, T. *Tetrahedron Lett.* **1968**, *9*, 2071.
(148) Sato, M.; Kakisawa, H. *J. Chem. Soc., Perkin Trans. 1* **1976**, 2407.
(149) Kakisawa, H.; Sato, M.; Ruo, T.-I.; Hayashi, T. *J. Chem. Soc., Chem. Commun.* **1973**, 802.
(150) Senoh, S.; Sakan, T. In *Biological and Chemical Aspects of Oxygenases*; Block, K.; Hayaishi, O., Eds.; Maruzen: Tokyo, 1966; pp. 93–99.
(151) Senoh, S.; Imamoto, S.; Maeno, Y.; Yamashita, K.; Matsui, M.; Tokuyama, T.; Sakan, T.; Komamine, A.; Hattori, S. *Tetrahedron Lett.* **1964**, *5*, 3437.
(152) Saeki, Y.; Nozaki, M.; Senoh, S. *J. Biol. Chem.* **1980**, *255*, 8465.
(153) Barrero, A. F.; Quílez Del Moral, J. F.; Cuerva, J. M.; Cabrera, E.; Jiménez-González, D. *Tetrahedron Lett.* **2000**, *41*, 5203.
(154) Hayashi, Y.; Yuki, Y.; Matsumoto, T.; Sakan, T. *Tetrahedron Lett.* **1977**, 2953.
(155) Hayashi, Y.; Matsumoto, T. *J. Org. Chem.* **1982**, *47*, 3421.
(156) Brown, K. S., Jr.; Sánchez, W. E., L. *Tetrahedron Lett.* **1974**, 675.
(157) Hayashi, Y.; Matsumoto, T.; Hyono, T.; Sakan, T. *Chem. Lett.* **1977**, 1461.
(158) Itô, S.; Kodama, M.; Sunagawa, M.; Koreeda, M.; Nakanishi, K. *J. Chem. Soc. D* **1971**, 855.
(159) Adinolfi, M.; Mangoni, L.; Barone, G.; Laonigro, G. *Tetrahedron Lett.* **1972**, *13*, 695.
(160) Welch, S. C.; Hagan, C. P.; White, D. H.; Fleming, W. P.; Trotter, J. W. *J. Am. Chem. Soc.* **1977**, *99*, 549.
(161) Hayashi, Y.; Matsumoto, T.; Nishizawa, M.; Togami, M.; Hyono, T.; Nishikawa, N.; Uemura, M.; Sakan, T. *J. Org. Chem.* **1982**, *47*, 3428.
(162) Reuvers, J. T. A.; De Groot, A. *J. Org. Chem.* **1986**, *51*, 4594.
(163) Burke, S. D.; Kort, M. E.; Strickland, S. M. S.; Organ, H. M.; Silks, L. A., III. *Tetrahedron Lett.* **1994**, *35*, 1503.
(164) Barrero, A. F.; Herrador, M. M.; Quílez del Moral, J. F.; Valdivia, M. V. *Org. Lett.* **2002**, *4*, 1379.
(165) Hanessian, S.; Boyer, N.; Reddy, G. J.; Deschênes-Simard, B. *Org. Lett.* **2009**, *11*, 4640.
(166) Sánchez-Larios, E.; Giacometti, R. D.; Hanessian, S. *Eur. J. Org. Chem.* **2014**, 5664.
(167) Addo, E. M.; Chai, H.-B.; Hymete, A.; Yeshak, M. Y.; Slebodnick, C.; Kingston, D. G. I.; Rakotondraibe, L. H. *J. Nat. Prod.* **2015**, *78*, 827.
(168) Cocker, W.; Cross, B. E.; Duff, S. R.; Edward, J. T.; Holley, T. F. *J. Chem. Soc.* **1953**, 2540.
(169) Hardy, D. G.; Rigby, W.; Moody, D. P. *J. Chem. Soc.* **1957**, 2955.
(170) Mangoni, L.; Adinolfi, M.; Laonigro, G.; Caputo, R. *Tetrahedron* **1972**, *28*, 611.
(171) Swaminathan, S.; Narayanan, K. V. *Chem. Rev.* **1971**, *71*, 429.
(172) Ramachandran, S.; Newman, M. S. *Org. Synth.* **1961**, *41*, 38.
(173) Spencer, T. A.; Smith, R. A. J.; Storm, D. L.; Villarica, R. M. *J. Am. Chem. Soc.* **1971**, *93*, 4856.
(174) Spencer, T. A.; Weaver, T. D.; Villarica, R. M.; Friary, R. J.; Posler, J.; Schwartz, M. A. *J. Org. Chem.* **1968**, *33*, 712.
(175) Spencer, T. A.; Friary, R. J.; Schmiegel, W. W.; Simeone, J. F.; Watt, D. S. *J. Org. Chem.* **1968**, *33*, 719.
(176) Wenkert, E.; Afonso, A.; Bredenberg, J. B.-S.; Kaneko, C.; Tahara, A. *J. Am. Chem. Soc.* **1964**, *86*, 2038.

(177) Coates, R. M.; Shaw, J. E. *J. Org. Chem.* **1970**, *35*, 2601.
(178) DeWolfe, R. H.; Young, W. G. *Chem. Rev.* **1956**, *56*, 753.
(179) Haworth, R. D.; Moore, B. P. *J. Chem. Soc.* **1946**, 633.
(180) Wenkert, E.; Tahara, A. *J. Am. Chem. Soc.* **1960**, *82*, 3229.
(181) Meyer, W. L.; Maheshwari, K. K. *Tetrahedron Lett.* **1964**, *5*, 2175.
(182) *Organoselenium Chemistry*; Wirth, T., Ed.; Wiley-VCH Verlag GmbH & Co. KGaA: Weinheim, Germany, 2011.
(183) Barrero, A. F.; Sánchez, J. F.; Altarejos C, J. *Tetrahedron Lett.* **1989**, *30*, 5515.
(184) Rönn, M.; Andersson, P. G.; Bäckvall, J.-E. *Acta Chem. Scand.* **1998**, *52*, 524.
(185) Jonasson, C.; Rönn, M.; Bäckvall, J.-E. *J. Org. Chem.* **2000**, *65*, 2122.
(186) Reuvers, J. T. A.; De Groot, A. *J. Org. Chem.* **1984**, *49*, 1110.
(187) Dorner, J. W.; Cole, R. J.; Springer, J. P.; Cox, R. H.; Cutler, H.; Wicklow, D. T. *Phytochemistry* **1980**, *19*, 1157.
(188) Zoretic, P. A.; Fang, H.; Ribeiro, A. A. *J. Org. Chem.* **1998**, *63*, 4779.
(189) Trotta, A. H. *Org. Lett.* **2015**, *17*, 3358.
(190) Yang, D.; Xu, M. *Org. Lett.* **2001**, *3*, 1785.
(191) Snider, B. B. *Chem. Rev.* **1996**, *96*, 339.
(192) Thompson, R.; Nakamaru-Ogiso, E.; Chen, C.-H.; Pink, M.; Mindiola, D. J. *Organometallics* **2014**, *33*, 429.
(193) Mander, L. N.; Sethi, S. P. *Tetrahedron Lett.* **1983**, *24*, 5425.
(194) Crabtree, S. R.; Chu, W. L. A.; Mander, L. N. *Synlett* **1990**, 169.
(195) Bissember, A. C. *Synlett* **2009**, 681.
(196) Scott, W. J.; Stille, J. K. *J. Am. Chem. Soc.* **1986**, *108*, 3033.
(197) Youn, I. K.; Yon, G. H.; Pak, C. S. *Tetrahedron Lett.* **1986**, *27*, 2409.
(198) Hudlicky, T.; Sinai-Zingde, G.; Natchus, M. G. *Tetrahedron Lett.* **1987**, *28*, 5287.
(199) Ling, T.; Chowdhury, C.; Kramer, B. A.; Vong, B. G.; Palladino, M. A.; Theodorakis, E. A. *J. Org. Chem.* **2001**, *66*, 8843.
(200) Nicolaou, K. C.; Montagnon, T.; Baran, P. S.; Zhong, Y.-L. *J. Am. Chem. Soc.* **2002**, *124*, 2245.
(201) Ito, H.; Takenaka, Y.; Fukunishi, S.; Iguchi, K. *Synthesis* **2005**, *2005*, 3035.
(202) Wei, Y.; Shi, M. *Chem. Rev.* **2013**, *113*, 6659.
(203) Basavaiah, D.; Rao, A. J.; Satyanarayana, T. *Chem. Rev.* **2003**, *103*, 811.
(204) Burgess, E. M.; Penton, H. R., Jr.; Taylor, E. A. *J. Org. Chem.* **1973**, *38*, 26.
(205) Kubo, I.; Sutisna, M.; Tan, K.-S. *Phytochemistry* **1991**, *30*, 455.
(206) National Center for Biotechnology Information. PubChem Substance Database; SID=17505749, https://pubchem.ncbi.nlm.nih.gov/substance/17505749 (accessed July 2, 2015).
(207) National Center for Biotechnology Information. PubChem BioAssay Database; AID=1498, Source=National Clinic Guideline Centre, http://pubchem.ncbi.nlm.nih.gov/assay/assay.cgi?aid=1498 (accessed July 2, 2015).
(208) De Sandre-Giovannoli, A.; Bernard, R.; Cau, P.; Navarro, C.; Amiel, J.; Boccaccio, I.; Lyonnet, S.; Stewart, C. L.; Munnich, A.; Le Merrer, M.; Lévy, N. *Science* **2003**, *300*, 2055.
(209) Scaffidi, P.; Misteli, T. *Nat. Med.* **2005**, *11*, 440.
(210) Misteli, T. personal correspondence, 2015.
(211) Scaffidi, P.; Misteli, T. *Nat. Cell Biol.* **2008**, *10*, 452.

(212) Lopez-Mejia, I. C.; Vautrot, V.; De Toledo, M.; Behm-Ansmant, I.; Bourgeois, C. F.; Navarro, C. L.; Osorio, F. G.; Freije, J. M. P.; Stévenin, J.; De Sandre-Giovannoli, A.; Lopez-Otin, C.; Lévy, N.; Branlant, C.; Tazi, J. *Hum. Mol. Genet.* **2011**, *20*, 4540.
(213) Liu, C.-T. Studies Toward the Synthesis of AB Ring System of Nagilactone B, ProQuest Dissertations and Theses, 1980, pp. 1–144.
(214) *Quaternary Stereocenters: Challenges and Solutions for Organic Synthesis*; Christoffers, J.; Baro, A., Eds.; John Wiley & Sons, 2006.
(215) Fuji, K. *Chem. Rev.* **1993**, *93*, 2037.
(216) Bradshaw, B.; Bonjoch, J. *Synlett* **2011**, *23*, 337.
(217) Aranda, G.; Bertranne-Delahaye, M.; Azerad, R.; Maurs, M.; Cortés, M.; Ramirez, H.; Vernal, G.; Prangé, T. *Synth. Comm.* **1997**, *27*, 45.
(218) Banerjee, A. K.; Cabrera, E. V.; Ng, P. S. P.; Vera, W. J.; Laya, M. S. *J. Chem. Res.-S* **2003**, 327.
(219) Aranda, G.; Cortés, M.; Maurs, M.; Azerad, R. *Tetrahedron-Asymmetry* **2001**, *12*, 2013.
(220) Nicolaou, K. C.; Kubota, S.; Li, W. S. *J. Chem. Soc., Chem. Commun.* **1989**, 512.
(221) Zhao, J.; Zhao, F.; Wang, Y.; Li, H.; Zhang, Q.; Guénard, D.; Ge, Q.; Wei, E.; Jiang, H.; Wu, Y.; Wang, L.; Jiang, H.; Guéritte, F.; Wu, X.; Cheng, C. H. K.; Lee, S.-S.; Zhao, Y. *Helv. Chim. Acta* **2004**, *87*, 1832.
(222) Binot, G.; Quiclet-Sire, B.; Saleh, T.; Zard, S. Z. *Synlett* **2003**, 382.
(223) Trost, B. M.; Gutierrez, A. C.; Ferreira, E. M. *J. Am. Chem. Soc.* **2010**, *132*, 9206.
(224) Csuk, R.; Barthel-Niesen, A.; Ströhl, D.; Kluge, R.; Wagner, C.; Al-Harrasi, A. *Tetrahedron* **2015**, *71*, 2025.
(225) Waters, S. P.; Tian, Y.; Li, Y.-M.; Danishefsky, S. J. *J. Am. Chem. Soc.* **2005**, *127*, 13514.
(226) Wieland, P.; Miescher, K. *Helv. Chim. Acta* **1950**, *33*, 2215.
(227) List, B.; Lerner, R. A.; Barbas, C. F. *J. Am. Chem. Soc.* **2000**, *122*, 2395.
(228) Ahrendt, K. A.; Borths, C. J.; MacMillan, D. W. C. *J. Am. Chem. Soc.* **2000**, *122*, 4243.
(229) Buchschacher, P.; Fürst, A.; Gutzwiller, J. *Org. Synth.* **1985**, *63*, 37.
(230) Gutzwiller, J.; Buchschacher, P.; Fürst, A. *Synthesis* **1977**, 167.
(231) Harada, N.; Sugioka, T.; Uda, H.; Kuriki, T. *Synthesis* **1990**, 53.
(232) Tietze, L. F.; Utecht, J. *Synthesis* **1993**, *1993*, 957.
(233) Kasai, Y.; Shimanuki, K.; Kuwahara, S.; Watanabe, M.; Harada, N. *Chirality* **2006**, *18*, 177.
(234) Hioki, H.; Hashimoto, T.; Kodama, M. *Tetrahedron-Asymmetry* **2000**, *11*, 829.
(235) Bahmanyar, S.; Houk, K. N. *J. Am. Chem. Soc.* **2001**, *123*, 12911.
(236) Clemente, F. R.; Houk, K. N. *Angew. Chem. Int. Ed.* **2004**, *43*, 5766.
(237) Cheong, P. H.-Y.; Legault, C. Y.; Um, J. M.; Çelebi-Ölçüm, N.; Houk, K. N. *Chem. Rev.* **2011**, *111*, 5042.
(238) Clemente, F. R.; Houk, K. N. *J. Am. Chem. Soc.* **2005**, *127*, 11294.
(239) Cheong, P. H.-Y.; Houk, K. N. *Synthesis* **2005**, 1533.
(240) Cheong, P. H.-Y.; Houk, K. N.; Warrier, J. S.; Hanessian, S. *Adv. Synth. Catal.* **2004**, *346*, 1111.
(241) Seebach, D.; Beck, A. K.; Badine, D. M.; Limbach, M.; Eschenmoser, A.; Treasurywala, A. M.; Hobi, R.; Prikoszovich, W.; Linder, B. *Helv. Chim. Acta* **2007**,

90, 425.
(242) Armstrong, A.; Boto, R. A.; Dingwall, P.; Contreras-García, J.; Harvey, M. J.; Mason, N. J.; Rzepa, H. S. *Chem. Sci.* **2014**, *5*, 2057.
(243) 3D structural representations were generated with CYLview: CYLview, 1.0b; Legault, C. Y., Université de Sherbrooke, 2009 (http://www.cylview.org).
(244) Davies, S. G.; Sheppard, R. L.; Smith, A. D.; Thomson, J. E. *Chem. Commun.* **2005**, 3802.
(245) Kanger, T.; Kriis, K.; Laars, M.; Kailas, T.; Müürisepp, A.-M.; Pehk, T.; Lopp, M. *J. Org. Chem.* **2007**, *72*, 5168.
(246) D'Elia, V.; Zwicknagl, H.; Reiser, O. *J. Org. Chem.* **2008**, *73*, 3262.
(247) Guillena, G.; Nájera, C.; Viózquez, S. *Synlett* **2008**, 3031.
(248) Almaşi, D.; Alonso, D. A.; Nájera, C. *Adv. Synth. Catal.* **2008**, *350*, 2467.
(249) Fuentes de Arriba, A. L.; Seisdedos, D. G.; Simón, L.; Alcázar, V.; Raposo, C.; Morán, J. R. *J. Org. Chem.* **2010**, *75*, 8303.
(250) Zhou, P.; Zhang, L.; Luo, S.; Cheng, J.-P. *J. Org. Chem.* **2012**, *77*, 2526.
(251) Bradshaw, B.; Etxebarria-Jardí, G.; Bonjoch, J.; Viózquez, S.; Guillena, G.; Nájera, C. *Org. Synth.* **2011**, *88*, 330.
(252) Xu, C.; Zhang, L.; Zhou, P.; Luo, S.; Cheng, J.-P. *Synthesis* **2013**, *45*, 1939.
(253) Ciceri, P.; Demnitz, F. W. J. *Tetrahedron Lett.* **1997**, *38*, 389.
(254) Crabtree, S. R.; Mander, L. N.; Sethi, S. P. *Org. Synth.* **1992**, *70*, 256.
(255) Pradhan, S. K. *Tetrahedron* **1986**, *42*, 6351.
(256) Caine, D. In *Organic Reactions*; John Wiley & Sons, Inc.: Hoboken, NJ, USA, 1976; Vol. 23, pp. 1–258.
(257) Stork, G.; Darling, S. D. *J. Am. Chem. Soc.* **1964**, *86*, 1761.
(258) Robinson, M. J. T. *Tetrahedron* **1965**, *21*, 2475.
(259) Fukui, K. In *Fortschritte der Chemischen Forschung*; Springer-Verlag: Berlin/Heidelberg, 1970; Vol. 15/1, pp. 1–85.
(260) Evans, D. A. In *Asymmetric Synthesis*; Elsevier, 1984; Vol. 3, pp. 1–110.
(261) Ando, K.; Green, N. S.; Li, Y.; Houk, K. N. *J. Am. Chem. Soc.* **1999**, *121*, 5334.
(262) Kuehne, M. E.; Nelson, J. A. *J. Org. Chem.* **1970**, *35*, 161.
(263) Fleming, F. F.; Zhang, Z. *Tetrahedron* **2005**, *61*, 747.
(264) Welch, S. C.; Hagan, C. P.; Kim, J. H.; Chu, P. S. *J. Org. Chem.* **1977**, *42*, 2879.
(265) Pelletier, S. W.; Chappell, R. L.; Prabhakar, S. *Tetrahedron Lett.* **1966**, *7*, 3489.
(266) Pelletier, S. W.; Chappell, R. L.; Prabhakar, S. *J. Am. Chem. Soc.* **1968**, *90*, 2889.
(267) Ziegler, F. E.; Kloek, J. A. *Tetrahedron Lett.* **1974**, *15*, 315.
(268) House, H. O.; Bare, T. M. *J. Org. Chem.* **1968**, *33*, 943.
(269) Stork, G.; Schulenberg, J. W. *J. Am. Chem. Soc.* **1962**, *84*, 284.
(270) Hutt, O. E.; Mander, L. N. *J. Org. Chem.* **2007**, *72*, 10130.
(271) Spencer, T. A.; Weaver, T. D.; Greco, W. J., Jr. *J. Org. Chem.* **1965**, *30*, 3333.
(272) Matlin, S. A.; Prazeres, M. A.; Bittner, M.; Silva, M. *Phytochemistry* **1984**, *23*, 2863.
(273) Salmond, W. G.; Barta, M. A.; Havens, J. L. *J. Org. Chem.* **1978**, *43*, 2057.
(274) Humphrey, J. M.; Liao, Y.; Ali, A.; Rein, T.; Wong, Y.-L.; Chen, H.-J.; Courtney, A. K.; Martin, S. F. *J. Am. Chem. Soc.* **2002**, *124*, 8584.
(275) Catino, A. J.; Forslund, R. E.; Doyle, M. P. *J. Am. Chem. Soc.* **2004**, *126*, 13622.
(276) Shing, T. K. M.; Yeung, Y.-Y.; Su, P. L. *Org. Lett.* **2006**, *8*, 3149.
(277) Davis, F. A.; Chen, B.-C. *Chem. Rev.* **1992**, *92*, 919.

(278) Bach, R. D.; Andrés, J. L.; Davis, F. A. *J. Org. Chem.* **1992**, *57*, 613.
(279) Shing, T.; Yeung, Y. Y. *Chem. Eur. J.* **2006**, *12*, 8367.
(280) Cumper, C. W. N.; Leton, G. B.; Vogel, A. I. *J. Chem. Soc.* **1965**, 2067.
(281) Trost, B. M.; Dong, G.; Vance, J. A. *Chem. Eur. J.* **2010**, *16*, 6265.
(282) Luche, J. L. *J. Am. Chem. Soc.* **1978**, *100*, 2226.
(283) Gregg, B. T.; Golden, K. C.; Quinn, J. F. *J. Org. Chem.* **2007**, *72*, 5890.
(284) Ward, D. E.; Rhee, C. K.; Zoghaib, W. M. *Tetrahedron Lett.* **1988**, *29*, 517.
(285) Corey, E. J.; Venkateswarlu, A. *J. Am. Chem. Soc.* **1972**, *94*, 6190.
(286) Kim, M.; Gross, R. S.; Sevestre, H.; Dunlap, N. K.; Watt, D. S. *J. Org. Chem.* **1988**, *53*, 93.
(287) Nakazaki, K.; Hayashi, K.; Hosoe, S.; Tashiro, T.; Kuse, M.; Takikawa, H. *Tetrahedron* **2012**, *68*, 9029.
(288) Yu, J.-Q.; Corey, E. J. *J. Am. Chem. Soc.* **2003**, *125*, 3232.
(289) Dalko, M.; Cavezza, A.; Wohlfromm, V. Methods for preparing 7alpha-hydroxy-dehydroepiandrosterone. US 20040133020, July 8, 2004.
(290) Marwah, P.; Lardy, H. A. Process for effecting allylic oxidation using dicarboxylic acid imides and chromium reagents. US 6384251, May 7, 2002.
(291) Recupero, F.; Punta, C. *Chem. Rev.* **2007**, *107*, 3800.
(292) Mehta, G.; Reddy, D. S. *J. Chem. Soc., Perkin Trans. 1* **2001**, 1153.
(293) Tojo, G.; Fernández, M. *Oxidation of Alcohols to Aldehydes and Ketones*; Springer-Verlag: New York, 2006.
(294) Andrews, G. C. *Tetrahedron Lett.* **1980**, *21*, 697.
(295) Diao, T.; Stahl, S. S. *J. Am. Chem. Soc.* **2011**, *133*, 14566.
(296) Volp, K. A.; Harned, A. M. *J. Org. Chem.* **2013**, *78*, 7554.
(297) Harned, A. M. *Chem. Commun.* **2015**, *51*, 2076.
(298) Ando, K. *J. Am. Chem. Soc.* **2005**, *127*, 3964.
(299) *MacroModel, version 9.9, Schrödinger, LLC, New York, NY, 2012.*
(300) Becke, A. D. *J. Chem. Phys.* **1993**, *98*, 5648.
(301) Lee, C.; Yang, W.; Parr, R. G. *Phys. Rev. B* **1988**, *37*, 785.
(302) Vosko, S. H.; Wilk, L.; Nusair, M. *Can. J. Phys.* **1980**, *58*, 1200.
(303) Stephens, P. J.; Devlin, F. J.; Chabalowski, C. F.; Frisch, M. J. *J. Phys. Chem.* **1994**, *98*, 11623.
(304) Tomasi, J.; Mennucci, B.; Cammi, R. *Chem. Rev.* **2005**, *105*, 2999.
(305) Grimme, S.; Antony, J.; Ehrlich, S.; Krieg, H. *J. Chem. Phys.* **2010**, *132*, 154104.
(306) Grimme, S.; Ehrlich, S.; Goerigk, L. *J. Comput. Chem.* **2011**, *32*, 1456.
(307) Johnson, E. R.; Becke, A. D. *J. Chem. Phys.* **2006**, *124*, 174104.
(308) Johnson, E. R.; Becke, A. D. *J. Chem. Phys.* **2005**, *123*, 024101.
(309) Goerigk, L.; Grimme, S. *Phys. Chem. Chem. Phys.* **2011**, *13*, 6670.
(310) Zhao, Y.; Truhlar, D. G. *Theor. Chem. Acc.* **2008**, *120*, 215.
(311) Weigend, F.; Ahlrichs, R. *Phys. Chem. Chem. Phys.* **2005**, *7*, 3297.
(312) Ribeiro, R. F.; Marenich, A. V.; Cramer, C. J.; Truhlar, D. G. *J. Phys. Chem. B* **2011**, *115*, 14556.
(313) Zhao, Y.; Truhlar, D. G. *Phys. Chem. Chem. Phys.* **2008**, *10*, 2813.
(314) Alvarez-Manzaneda, E.; Chahboun, R.; Bentaleb, F.; Alvarez, E.; Escobar, M. A.; Sad-Diki, S.; Cano, M. J.; Messouri, I. *Tetrahedron* **2007**, *63*, 11204.
(315) Coates, R. M.; Kang, H. Y. *J. Org. Chem.* **1987**, *52*, 2065.

(316) Fujimoto, Y.; Tatsuno, T. *Tetrahedron Lett.* **1976**, *17*, 3325.
(317) Lee, H.-J.; Ravn, M. M.; Coates, R. M. *Tetrahedron* **2001**, *57*, 6155.
(318) Krishnamurthy, S.; Brown, H. C. *J. Org. Chem.* **1980**, *45*, 849.
(319) Garegg, P. J.; Samuelsson, B. *J. Chem. Soc., Chem. Commun.* **1979**, 978.
(320) Garegg, P. J.; Samuelsson, B. *J. Chem. Soc., Perkin Trans. 1* **1980**, 2866.
(321) Lindgren, B. O.; Nilsson, T. *Acta Chem. Scand.* **1973**, *27*, 888.
(322) Bal, B. S.; Childers, W. E.; Pinnick, H. W. *Tetrahedron* **1981**, *37*, 2091.
(323) Presser, A.; Hüfner, A. *Monatsh. Chem.* **2004**, *135*, 1015.
(324) Travis, B. R.; Sivakumar, M.; Hollist, G. O.; Borhan, B. *Org. Lett.* **2003**, *5*, 1031.
(325) Sabitha, G.; Syamala, M.; Yadav, J. S. *Org. Lett.* **1999**, *1*, 1701.
(326) Wender, P. A. *Nat. Prod. Rep.* **2014**, *31*, 433.
(327) Seeman, J. I. *Angew. Chem. Int. Ed.* **2012**, *51*, 3012.
(328) Nicolaou, K. C.; Vourloumis, D.; Winssinger, N.; Baran, P. S. *Angew. Chem. Int. Ed.* **2000**, *39*, 44.
(329) Woodward, R. B. *Pure Appl. Chem.* **1968**, *17*, 519.
(330) Woodward, R. B. *Pure Appl. Chem.* **1971**, *25*, 283.
(331) Woodward, R. B. *Pure Appl. Chem.* **1973**, *33*, 145.
(332) Eschenmoser, A.; Wintner, C. *Science* **1977**, *196*, 1410.
(333) Brown, M. K.; May, T. L.; Baxter, C. A.; Hoveyda, A. H. *Angew. Chem. Int. Ed.* **2007**, *46*, 1097.
(334) May, T. L.; Brown, M. K.; Hoveyda, A. H. *Angew. Chem. Int. Ed.* **2008**, *47*, 7358.
(335) Mulzer, J. *Nat. Prod. Rep.* **2014**, *31*, 595.
(336) Dicks, A. P.; Hent, A. *Green Chemistry Metrics*; Springer International Publishing, 2015.
(337) Eissen, M.; Metzger, J. O. *Chem. Eur. J.* **2002**, *8*, 3580.
(338) Hudlicky, T.; Reed, J. W. *The Way of Synthesis*; Wiley-VHC: Weinheim, 2007.
(339) Bommarius, A. S.; Schwarm, M.; Stingl, K.; Kottenhahn, M.; Huthmacher, K.; Drauz, K. *Tetrahedron-Asymmetry* **1995**, *6*, 2851.
(340) Grieco, P. A.; Cooke, R. J.; Henry, K. J.; VanderRoest, J. M. *Tetrahedron Lett.* **1991**, *32*, 4665.
(341) Reetz, M. T.; Fox, D. N. A. *Tetrahedron Lett.* **1993**, *34*, 1119.
(342) Kita, Y.; Segawa, J.; Haruta, J.-I.; Yasuda, H.; Tamura, Y. *J. Chem. Soc., Perkin Trans. 1* **1982**, 1099.
(343) Danishefsky, S. J.; Simoneau, B. *J. Am. Chem. Soc.* **1989**, *111*, 2599.
(344) Toyota, M.; Yokota, M.; Ihara, M. *J. Am. Chem. Soc.* **2001**, *123*, 1856.
(345) Khan, F. A.; Nageswara Rao, C. *Tetrahedron Lett.* **2006**, *47*, 7567.
(346) Béguin, C.; Richards, M. R.; Li, J.-G.; Wang, Y.; Xu, W.; Liu-Chen, L.-Y.; Carlezon, W. A.; Cohen, B. M. *Bioorg. Med. Chem. Lett.* **2006**, *16*, 4679.
(347) Behme, C. *N,N′-Sulfuryldiimidazole, e-EROS Encyclopedia of Reagents for Organic Synthesis*; John Wiley & Sons, Ltd: Chichester, 2001.
(348) Kurihara, K.; Tanabe, K.; Yamamoto, Y.; Shinei, R.; Ajito, K.; Okonogi, T. *Bioorg. Med. Chem. Lett.* **1999**, *9*, 1837.
(349) Morita, M.; Kojima, Y.; Kato, N.; Miwa, K.; Tanaka, I.; Yamane, T.; Ashida, T. *Tetrahedron Lett.* **1983**, *24*, 5631.
(350) Coombes, P. H.; Naidoo, D.; Mulholland, D. A.; Randrianarivelojosia, M. *Phytochemistry* **2005**, *66*, 2734.

(351) Topcu, G.; Eriş, C.; Ulubelen, A. *J. Nat. Prod.* **1997**, *60*, 1045.
(352) Julianti, E.; Jang, K. H.; Lee, S.; Lee, D.; Mar, W.; Oh, K.-B.; Shin, J. *Phytochemistry* **2012**, *80*, 70.
(353) Bremner, P. D.; Simmonds, M.; Blaney, W. M.; Veitch, N. C. *Phytochemistry* **1998**, *47*, 1227.
(354) Nakamura, H.; Vasudevan, S.; Kim, M.; Brock, C. P.; Watt, D. S. *J. Org. Chem.* **1992**, *57*, 2223.
(355) He, H.-P.; Shen, Y.-M.; Zuo, G.-Y.; Yang, X.-S.; Hao, X.-J. *Helv. Chim. Acta* **2003**, *86*, 3187.
(356) Topcu, G.; Eriş, C.; Ulubelen, A.; Krawiec, M.; Watson, W. H. *Tetrahedron* **1995**, *51*, 11793.
(357) Wijeratne, E. M. K.; Bashyal, B. P.; Liu, M. X.; Rocha, D. D.; Gunaherath, G. M. K. B.; U'Ren, J. M.; Gunatilaka, M. K.; Arnold, A. E.; Whitesell, L.; Gunatilaka, A. A. L. *J. Nat. Prod.* **2012**, *75*, 361.
(358) Marco, J. A.; Sanz-Cervera, J. F.; García-Lliso, V.; Batlle, N. *Phytochemistry* **1997**, *45*, 755.
(359) Rubottom, G. M.; Vasquez, M. A.; Pelegrina, D. R. *Tetrahedron Lett.* **1974**, *15*, 4319.
(360) Kirk, D. N.; Wiles, J. M. *J. Chem. Soc. D* **1970**, 1015.
(361) Wege, P. M.; Clark, R. D.; Heathcock, C. H. *J. Org. Chem.* **1976**, *41*, 3144.
(362) Waalboer, D. C. J.; van Kalkeren, H. A.; Schaapman, M. C.; van Delft, F. L.; Rutjes, F. P. J. T. *J. Org. Chem.* **2009**, *74*, 8878.
(363) Lu, Y.-S.; Peng, X.-S. *Org. Lett.* **2011**, *13*, 2940.
(364) Díaz, S.; González, A.; Bradshaw, B.; Cuesta, J.; Bonjoch, J. *J. Org. Chem.* **2005**, *70*, 3749.
(365) Soltani Rad, M. N.; Khalafi-Nezhad, A.; Behrouz, S.; Faghihi, M. A. *Tetrahedron Lett.* **2007**, *48*, 6779.
(366) Tsuji, Y.; Yamada, N.; Tanaka, S. *J. Org. Chem.* **1993**, *58*, 16.
(367) Danishefsky, S. J.; Masters, J. J.; Young, W. B.; Link, J. T.; Snyder, L. B.; Magee, T. V.; Jung, D. K.; Isaacs, R. C. A.; Bornmann, W. G.; Alaimo, C. A.; Coburn, C. A.; Di Grandi, M. J. *J. Am. Chem. Soc.* **1996**, *118*, 2843.
(368) Joshi, D. K.; Sutton, J. W.; Carver, S.; Blanchard, J. P. *Org. Process Res. Dev.* **2005**, *9*, 997.
(369) Nakadai, M.; Saito, S.; Yamamoto, H. *Tetrahedron* **2002**, *58*, 8167.
(370) Lam, Y.-H.; Houk, K. N. *J. Am. Chem. Soc.* **2015**, *137*, 2116.
(371) Wiberg, K. B. *J. Org. Chem.* **2003**, *68*, 9322.
(372) Hwu, J. R.; Wetzel, J. M. *J. Org. Chem.* **1985**, *50*, 3946.
(373) Tsunoda, T.; Suzuki, M.; Noyori, R. *Tetrahedron Lett.* **1980**, *21*, 1357.
(374) Rubottom, G. M.; Gruber, J. M.; Juve, H. D., Jr.; Charleson, D. A. *Org. Synth.* **1986**, *64*, 118.
(375) Ling, T. T.; Rivas, F.; Theodorakls, E. A. *Tetrahedron Lett.* **2002**, *43*, 9019.
(376) Cheong, P. H.-Y.; Yun, H.; Danishefsky, S. J.; Houk, K. N. *Org. Lett.* **2006**, *8*, 1513.
(377) Blay, G.; Cardona, L.; Garcia, B.; Pedro, J. R. *J. Org. Chem.* **1993**, *58*, 7204.
(378) Bargues, V.; Blay, G.; García, B.; García, C. L.; Pedro, J. R. *Tetrahedron* **1995**, *51*, 5609.
(379) Chai, J.-D.; Head-Gordon, M. *Phys. Chem. Chem. Phys.* **2008**, *10*, 6615.
(380) Singleton, D. A.; Merrigan, S. R.; Liu, J.; Houk, K. N. *J. Am. Chem. Soc.* **1997**, *119*,

3385.
(381) Houk, K. N.; Liu, J.; DeMello, N. C. *J. Am. Chem. Soc.* **1997**, *119*, 10147.
(382) Swaminathan, S.; Newman, M. S. *Tetrahedron* **1958**, *2*, 88.
(383) Blazejewski, J.-C.; Guilhem, J.; Le Guyader, F. *J. Chem. Soc., Perkin Trans. 1* **1997**, 1913.
(384) Comins, D. L.; Dehghani, A. *Tetrahedron Lett.* **1992**, *33*, 6299.
(385) Nicolaou, K. C.; Roecker, A. J.; Monenschein, H.; Guntupalli, P.; Follmann, M. *Angew. Chem. Int. Ed.* **2003**, *42*, 3637.
(386) Hagiwara, H.; Hamano, K.; Nozawa, M.; Hoshi, T.; Suzuki, T.; Kido, F. *J. Org. Chem.* **2005**, *70*, 2250.
(387) Cacchi, S.; Morera, E.; Ortar, G. *Tetrahedron Lett.* **1985**, *26*, 1109.
(388) Kang, S.-K.; Kim, S.-G.; Park, D.-C.; Lee, J.-S.; Yoo, W.-J.; Pak, C. S. *J. Chem. Soc., Perkin Trans. 1* **1993**, 9.
(389) Paquette, L. A.; Wang, T.-Z.; Philippo, C. M. G.; Wang, S. *J. Am. Chem. Soc.* **1994**, *116*, 3367.
(390) Ring, S.; Bohlmann, R.; Kuhnke, J.; Zorn, L.; Borden, S.; Prelle, K. C-ring-substituted pregn-4-ene-21,17-carbolactones, and pharmaceutical preparations comprising the same. US 2011130371, 2011.
(391) Kiankarimi, M.; Lowe, R.; McCarthy, J. R.; Whitten, J. P. *Tetrahedron Lett.* **1999**, *40*, 4497.
(392) Harding, W. W.; Schmidt, M.; Tidgewell, K.; Kannan, P.; Holden, K. G.; Gilmour, B.; Navarro, H.; Rothman, R. B.; Prisinzano, T. E. *J. Nat. Prod.* **2006**, *69*, 107.
(393) Nitz, T. J.; Paquette, L. A. *Tetrahedron Lett.* **1984**, *25*, 3047.
(394) Smith, A. B., III; Leenay, T. L. *J. Am. Chem. Soc.* **1989**, *111*, 5761.
(395) Enomoto, M.; Morita, A.; Kuwahara, S. *Angew. Chem. Int. Ed.* **2012**, *51*, 12833.
(396) Ferraz, H. M. C.; Souza, A. J. C.; Tenius, B. S. M.; Bianco, G. G. *Tetrahedron* **2006**, *62*, 9232.
(397) Nishitani, K.; Suzuki, J.; Ishibashi, H.; Saitoh, Y.; Kariya, S.; Yamakawa, K. *Heterocycles* **1994**, *39*, 43.
(398) Los, M.; Mighell, A. D. *Tetrahedron* **1965**, *21*, 2297.
(399) Heathcock, C. H.; Ratcliffe, R. *J. Am. Chem. Soc.* **1971**, *93*, 1746.
(400) Magee, T. V.; Bornmann, W. G.; Isaacs, R. C. A.; Danishefsky, S. J. *J. Org. Chem.* **1992**, *57*, 3274.
(401) Aggarwal, V. K.; Tarver, G. J.; McCague, R. *Chem. Commun.* **1996**, 2713.
(402) Aggarwal, V. K.; Mereu, A.; Tarver, G. J.; McCague, R. *J. Org. Chem.* **1998**, *63*, 7183.
(403) Kawamura, M.; Kobayashi, S. *Tetrahedron Lett.* **1999**, *40*, 1539.
(404) Aggarwal, V. K.; Mereu, A. *Chem. Commun.* **1999**, 2311.
(405) Lee, K. Y.; Gong, J. H.; Kim, J. N. *Bull. Korean Chem. Soc.* **2002**, *23*, 659.
(406) Rezgui, F.; Gaied, El, M. M. *Tetrahedron Lett.* **1998**, *39*, 5965.
(407) Armarego, W. L. F.; Chai, C. L. L. In *Purification of Laboratory Chemicals*; Elsevier, 2009; pp. 88–444.
(408) Tomaszewski, M. J.; Warkentin, J.; Werstiuk, N. H. *Aust. J. Chem.* **1995**, *48*, 291.
(409) Mycock, D. K.; Glossop, P. A.; Lewis, W.; Hayes, C. J. *Tetrahedron Lett.* **2013**, *54*, 55.
(410) Heathcock, C. H.; Badger, R. A.; Patterson, J. W. *J. Am. Chem. Soc.* **1967**, *89*, 4133.

Annex 1:

Experimental Data for Chapter 1

Experimental Procedures for α-L-TriNA 1

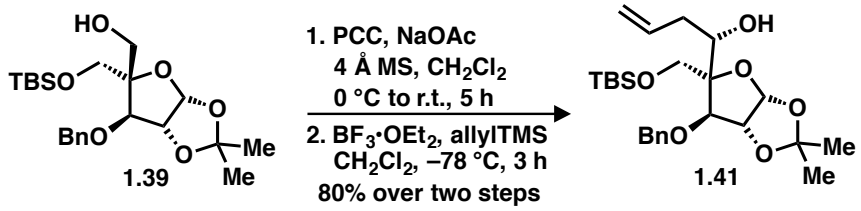

(*S*)-1-((3a*R*,5*R*,6*R*,6a*R*)-6-(Benzyloxy)-5-(((*tert*-butyldimethylsilyl)oxy)methyl)-2,2-dimethyltetrahydrofuro[2,3-*d*][1,3]dioxol-5-yl)but-3-en-1-ol (1.41).

A solution of **1.39** (11.2 g, 25.5 mmol) in anhydrous dichloromethane (80 mL) was added to a stirred, 0 °C mixture of pyridinium chlorochromate (16.2 g, 75.2 mmol), sodium acetate (6.3 g, 76 mmol), and powdered 4 Å molecular sieves (20.0 g) in anhydrous dichloromethane (300 mL). The reaction mixture was allowed to warm to room temperature and stirred for a period of 5 h, at which point diethyl ether and silica gel were added and the resulting mixture was stirred for an additional 20 minutes. The mixture was filtered through a short pad of silica gel and eluted with diethyl ether before the filtrate was concentrated under reduced pressure. The residue (10.9 g, 25.1 mmol) was dissolved in anhydrous dichloromethane (230 mL) and cooled to –78 °C. Boron trifluoride diethyl etherate (6.3 mL, 50 mmol) was added and the solution was stirred for 10 minutes before the dropwise addition of allyltrimethylsilane (7.0 mL, 44 mmol). After 3 h a saturated aqueous solution of sodium bicarbonate (40 mL) was added dropwise. The solution was warmed to room temperature and partitioned with a saturated aqueous solution of sodium bicarbonate (200 mL). The layers were separated and the aqueous portion was extracted with dichloromethane (3 × 150 mL). The combined organic extracts were washed with brine (250 mL), dried over magnesium sulfate, filtered, and concentrated under reduced pressure. The residue was purified by flash column chromatography (22 × 5 cm) on silica gel (2:3 ethyl acetate–hexanes) to afford **1.41** as a colorless oil (9.3 g, 80% yield over two steps): R_f 0.18 (1:9 ethyl acetate–hexanes); $[\alpha]^{20}_D$ –24.0 (*c* = 0.62, chloroform); IR (film, cm^{-1}) ν 3545, 2931, 1382, 1109; ^1H NMR (300 MHz, chloroform-*d*) δ 7.39–7.28 (m, 5H), 6.07 (d, *J* = 4.3 Hz, 1H), 5.93 (ddt, *J* = 17.1, 10.1, 6.9 Hz, 1H), 5.16–5.03 (m, 2H), 4.79–4.72 (m, 2H), 4.62 (d, *J* = 11.4 Hz, 1H), 4.32 (d, *J* = 1.9 Hz,

1H), 3.97 (dt, J = 10.1, 3.1 Hz, 1H), 3.71 (d, J = 10.3 Hz, 1H), 3.64 (d, J = 10.3 Hz, 1H), 2.91 (dd, J = 3.3, 1.6 Hz, 1H), 2.43–2.31 (m, 1H), 2.28–2.17 (m, 1H), 1.56 (s, 3H), 1.38 (s, 3H), 0.88 (s, 9H), 0.05 (s, 3H), 0.04 (s, 3H); ^{13}C NMR (75 MHz, chloroform-*d*) δ 137.1, 136.3, 128.7, 128.3, 127.9, 116.6, 113.7, 105.1, 90.7, 87.5, 87.4, 73.3, 72.0, 65.0, 34.8, 28.0, 27.4, 26.0, 18.4, –5.3, –5.5; HRMS (ESI) calc'd for $C_{25}H_{40}O_6SiNa$ $[M+Na]^+$ *m/z* 487.2486, found 487.2504.

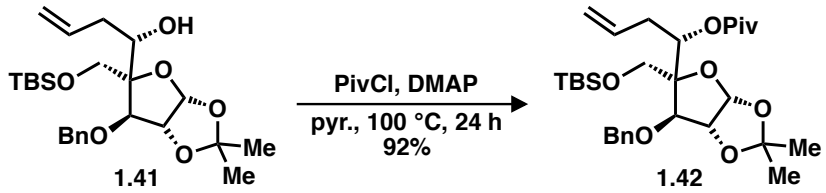

(*S*)-1-((3a*R*,5*R*,6*R*,6a*R*)-6-(Benzyloxy)-5-(((*tert*-butyldimethylsilyl)oxy)methyl)-2,2-dimethyltetrahydrofuro[2,3-*d*][1,3]dioxol-5-yl)but-3-en-1-yl pivalate (1.42).

Pivaloyl chloride (11.0 mL, 84.6 mmol) and 4-(dimethylamino)pyridine (1.03 g, 8.50 mmol) were added to a stirred solution of **1.41** (7.86 g, 16.9 mmol) in pyridine (86 mL) at room temperature. The resulting mixture was heated to 100 °C until all of the starting material had been consumed as indicated by TLC analysis (24 h). The solution was cooled to room temperature and partitioned between ethyl acetate (300 mL) and water (150 mL). The aqueous layer was separated and extracted with ethyl acetate (3 × 150 mL). The combined organic extracts were washed with 0.5 M hydrochloric acid (4 × 150 mL), a saturated aqueous solution of sodium bicarbonate (150 mL), and brine (150 mL), dried over magnesium sulfate, and concentrated under reduced pressure. The residue was purified by flash column chromatography (25 × 4 cm) on silica gel (1:9 ethyl acetate–hexanes) to afford **1.42** as a colorless oil (8.56 g, 92% yield): R_f 0.50 (1:9 ethyl acetate–hexanes); $[\alpha]_D^{20}$ +32.9 (c = 1.98, chloroform); IR (film, cm^{-1}) ν 2956, 2931, 1733, 1115; ^{1}H NMR (400 MHz, chloroform-*d*) δ 7.34–7.23 (m, 5H), 6.00 (d, J = 4.3 Hz, 1H), 5.80–5.72 (m, 1H), 5.34 (dd, J = 8.4, 4.1 Hz, 1H), 5.03–4.93 (m, 2H), 4.74 (dd, J = 4.3, 2.1 Hz, 1H), 4.63 (d, J = 11.7 Hz, 1H), 4.57 (d, J = 11.7 Hz, 1H), 4.26 (d, J = 2.0 Hz, 1H), 3.78 (d, J = 10.3 Hz, 1H), 3.65 (d, J = 10.3 Hz, 1H), 2.47–2.32 (m, 2H), 1.57 (s, 3H), 1.39 (s, 3H), 1.08 (s, 9H), 0.88 (s, 9H), 0.05 (s, 3H), 0.04 (s, 3H); ^{13}C NMR (101 MHz, chloroform-*d*) δ 176.8, 137.6, 134.8, 128.3, 127.7, 127.6, 117.2,

113.8, 104.8, 89.3, 87.5, 86.5, 72.9, 72.1, 65.0, 38.5, 35.1, 28.1, 27.5, 27.4, 26.0, 18.4, –5.3, –5.5; HRMS (ESI) calc'd for $C_{30}H_{48}O_7SiNa$ $[M+Na]^+$ *m/z* 571.3062, found 571.3077.

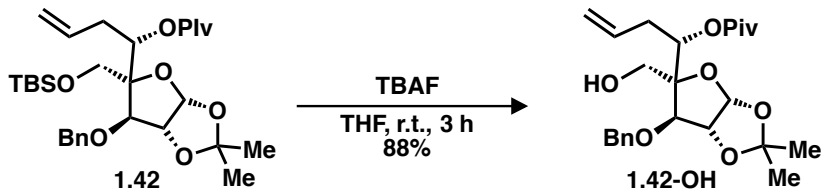

(*S*)-1-((3a*R*,5*R*,6*R*,6a*R*)-6-(Benzyloxy)-5-(hydroxymethyl)-2,2-dimethyltetrahydrofuro-[2,3-*d*][1,3]dioxol-5-yl)but-3-en-1-yl pivalate (142-OH).

Tetrabutylammonium fluoride (1 M in tetrahydrofuran, 31.7 mL, 31.7 mmol) was added to a stirred solution of **1.42** (8.70 g, 15.8 mmol) in tetrahydrofuran (89 mL). The mixture was stirred at room temperature for 3 h before a saturated aqueous solution of sodium bicarbonate (40 mL) was added in one portion. The resulting solution was diluted with ethyl acetate (200 mL) and washed with a saturated aqueous solution of sodium bicarbonate (100 mL). The layers were separated and the aqueous portion was extracted with ethyl acetate (3 × 75 mL). The combined organic extracts were washed with brine (200 mL), dried over magnesium sulfate, and concentrated under reduced pressure. The residue was purified by flash column chromatography (18 × 3 cm) on silica gel (1:4 ethyl acetate–hexanes) to afford **1.42-OH** as a colorless oil (6.05 g, 88% yield): R_f 0.63 (1:2 ethyl acetate–hexanes); $[\alpha]_D^{20}$ +21.9 (*c* = 1.48, chloroform); IR (film, cm^{-1}) ν 3496, 2977, 1731, 1158; ^1H NMR (400 MHz, chloroform-*d*) δ 7.36–7.26 (m, 5H), 5.96 (d, *J* = 4.6 Hz, 1H), 5.74–5.69 (m, 1H), 5.25 (dd, *J* = 9.0, 3.5 Hz, 1H), 5.02–4.94 (m, 2H), 4.79 (dd, *J* = 4.5, 2.8, Hz, 1H), 4.70 (d, *J* = 11.8 Hz, 1H), 4.54 (d, *J* = 11.8 Hz, 1H), 4.26 (d, *J* = 2.7 Hz, 1H), 3.70 (d, *J* = 11.8 Hz, 1H), 3.56 (d, *J* = 11.8 Hz, 1H), 2.51–2.42 (m, 1H), 2.36–2.26 (m, 1H), 2.20 (br s, 1H), 1.56 (s, 3H), 1.37 (s, 3H), 1.13 (s, 9H); ^{13}C NMR (101 MHz, chloroform-*d*) δ 177.1, 137.4, 134.3, 128.4, 127.8, 127.6, 117.5, 114.0, 104.7, 89.5, 86.9, 85.0, 72.7, 71.7, 62.6, 38.6, 35.1, 27.9, 27.5, 27.4; HRMS (ESI) calc'd for $C_{24}H_{34}O_7Na$ $[M+Na]^+$ *m/z* 457.2197, found 457.2198.

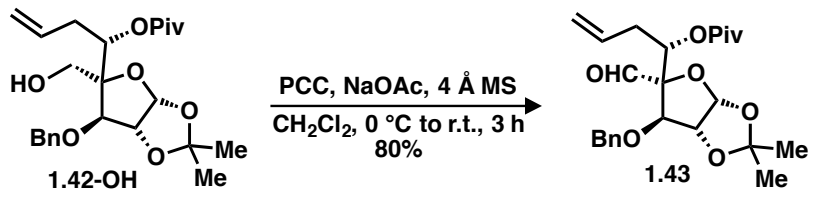

(*S*)-1-((3a*R*,5*R*,6*R*,6a*R*)-6-(Benzyloxy)-5-formyl-2,2-dimethyltetrahydrofuro[2,3-*d*][1,3]-dioxol-5-yl)but-3-en-1-yl pivalate (1.43).

A solution **1.42-OH** (4.9 g, 11 mmol) in anhydrous dichloromethane (70 mL) was added to a stirred, 0 °C mixture of pyridinium chlorochromate (7.3 g, 33 mmol), sodium acetate (2.8 g, 34 mmol), and powdered 4 Å molecular sieves (9.0 g) in anhydrous dichloromethane (220 mL). The resulting mixture was allowed to warm to room temperature over a period of 3 h. Diethyl ether and silica gel were added to the reaction mixture, which was stirred for an additional 20 minutes. The resulting mixture was filtered through a short pad of silica gel, eluted with diethyl ether, and the filtrate was concentrated under reduced pressure. The residue was purified by flash column chromatography (15 × 3 cm) on silica gel (1:7 ethyl acetate–hexanes) to afford **1.43** as a colorless oil (3.90 g, 80% yield): R_f 0.38 (1:9 ethyl acetate–hexanes); $[\alpha]_D^{20}$ –31.1 (*c* = 0.98, chloroform); IR (film, cm^{-1}) ν 2979, 1733, 1160, 1073; ^1H NMR (400 MHz, chloroform-*d*) δ 9.68 (s, 1H), 7.38–7.28 (m, 5H), 6.03 (d, *J* = 3.9 Hz, 1H), 5.62–5.51 (m, 2H), 4.98 (s, 1H), 4.96–4.92 (m, 1H), 4.69 (d, *J* = 11.5 Hz, 1H), 4.62 (d, *J* = 4.0 Hz, 1H), 4.52 (d, *J* = 11.5 Hz, 1H), 4.27 (s, 1H), 2.30–2.12 (m, 2H), 1.40 (s, 3H), 1.27 (s, 3H), 1.17 (s, 9H); ^{13}C NMR (101 MHz, chloroform-*d*) δ 202.2, 177.2, 136.6, 133.1, 128.7, 128.3, 127.9, 118.1, 112.0, 105.5, 94.0, 84.0, 82.8, 73.4, 72.4, 39.0, 34.5, 27.3, 25.9, 25.7; HRMS (ESI) calc'd for $C_{24}H_{32}O_7Na$ $[M+Na]^+$ *m/z* 455.2040, found 455.2039.

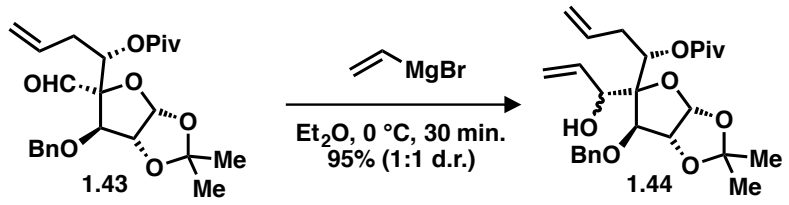

(1*S*)-1-((3a*R*,5*R*,6*R*,6a*R*)-6-(Benzyloxy)-5-(1-hydroxyallyl)-2,2-dimethyltetrahydrofuro-[2,3-*d*][1,3]dioxol-5-yl)but-3-en-1-yl pivalate (1.44).

Vinylmagnesium bromide (1 M in tetrahydrofuran, 11.9 mL, 11.9 mmol) was added dropwise to a stirred 0 °C solution of **1.43** (2.58 g, 5.97 mmol) in anhydrous diethyl ether (50 mL). After the addition, the reaction was stirred 0 °C for 30 minutes, at which point a saturated aqueous solution of ammonium chloride (5 mL) was added. The mixture was diluted with ethyl acetate (100 mL) and an additional portion of saturated aqueous ammonium chloride (100 mL). The layers were separated and the aqueous portion was extracted with ethyl acetate (3 × 50 mL). The combined organic extracts were washed with a saturated aqueous solution of sodium bicarbonate (100 mL), brine (100 mL), dried over magnesium sulfate, filtered, and concentrated under reduced pressure. The residue was purified by flash column chromatography (22 × 2 cm) on silica gel (1:9 ethyl acetate–hexanes) to afford **1.44** as a colorless oil (2.61 g, 95% yield, dr = 1:1 [determined by ^{1}H NMR]): R_f 0.50 (1:4 ethyl acetate–hexanes); $[\alpha]_D^{20}$ +44.6 (*c* = 1.18, chloroform); IR (f film, cm^{-1}) ν 2979, 1732, 1152; ^{1}H NMR (400 MHz, chloroform-*d*) δ 7.37–7.24 (m, 10H), 6.02 (d, *J* = 4.6 Hz, 1H), 6.00–5.90 (m, 2H), 5.83–5.66 (m, 3H), 5.51–5.38 (m, 2H), 5.31–5.19 (m, 5H), 5.06–4.92 (m, 4H), 4.80–4.74 (m, 2H), 4.66 (d, *J* = 11.8 Hz, 1H), 4.60 (d, *J* = 11.8 Hz, 1H), 4.51 (d, *J* = 11.8 Hz, 1H), 4.47 (d, *J* = 11.8 Hz, 1H), 4.34–4.28 (m, 3H), 4.11 (d, *J* = 2.5 Hz, 1H), 2.71–2.62 (m, 1H), 2.52–2.35 (m, 3H), 1.61 (s, 3H), 1.54 (s, 3H), 1.38 (s, 3H), 1.37 (s, 3H), 1.11 (s, 9H), 1.07 (s, 9H); ^{13}C NMR (101 MHz, chloroform-*d*) δ 176.8, 176.4, 137.4, 137.2, 135.4, 134.9, 134.2, 133.3, 128.5, 128.3, 128.1, 128.0, 127.7, 127.6, 118.9, 117.7, 117.2, 116.9, 114.5, 114.4, 104.8, 104.6, 93.3, 90.4, 87.4, 87.3, 85.7, 83.2, 74.7, 72.7, 72.4, 72.0, 71.7, 71.4, 38.6, 38.5, 35.1, 34.8, 28.1, 27.9, 27.8, 27.6, 27.5, 27.4; HRMS (ESI) calc'd for $C_{26}H_{36}O_7Na$ $[M+Na]^+$ *m/z* 483.2353, found 483.2351.

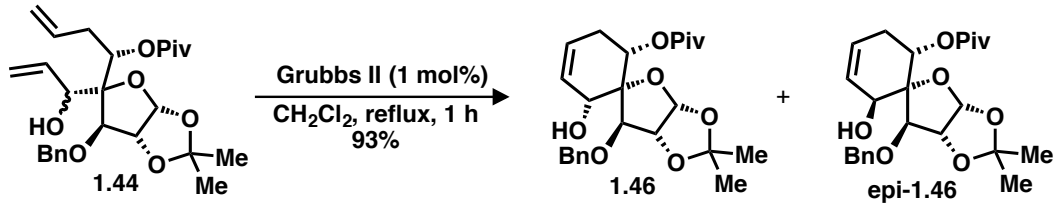

(1*R*,2*R*,3a'*R*,6*S*,6'*R*,6a'*R*)-6'-(Benzyloxy)-2-hydroxy-2',2'-dimethyl-3a',6a'-dihydro-6'*H*-spiro[cyclohexane-1,5'-furo[2,3-*d*][1,3]dioxol]-3-en-6-yl pivalate (1.46) and (1*R*,2*S*,3a'*R*,6*S*,6'*R*,6a'*R*)-6'-(Benzyloxy)-2-hydroxy-2',2'-dimethyl-3a',6a'-dihydro-6'*H*-spiro[cyclohexane-1,5'-furo[2,3-*d*][1,3]dioxol]-3-en-6-yl pivalate (epi-1.46).

Grubbs' second generation catalyst (0.048 g, 0.056 mmol) was added to a stirred solution of **13** (2.60 g, 5.65 mmol) in anhydrous dichloromethane (60 mL). The solution was heated to reflux and stirred for 1 h then cooled to room temperature and concentrated under reduced pressure. The residue was purified by flash column chromatography (10 × 3 cm) on silica gel (1:6 ethyl acetate–hexanes) to afford **1.46** (1.12 g, 46% yield) and **epi-1.46** (1.16 g, 47% yield) as a separable mixture of colorless oils:

Compound **1.46**: R_f 0.37 (1:4 ethyl acetate–hexanes); $[\alpha]_D^{20}$ +12.5 (*c* = 1.23, chloroform); IR (film, cm^{-1}) ν 3500, 2977, 1732, 1150; ^{1}H NMR (400 MHz, chloroform-*d*) δ 7.36–7.23 (m, 5H), 6.07 (d, *J* = 4.8 Hz, 1H), 5.67–5.56 (m, 2H), 5.13 (dd, *J* = 9.9, 5.9 Hz, 1H), 4.90 (dd, *J* = 4.7, 3.7 Hz, 1H), 4.75 (d, *J* = 11.9 Hz, 1H), 4.58 (d, *J* = 11.9 Hz, 1H), 4.41 (d, *J* = 3.5 Hz, 1H), 4.17 (d, *J* = 7.0 Hz, 1H), 2.56 (d, *J* = 10.7 Hz, 1H), 2.44–2.39 (m, 1H), 2.27–2.17 (m, 1H), 1.62 (s, 3H), 1.42 (s, 3H), 1.16 (s, 9H); ^{13}C NMR (101 MHz, chloroform-*d*) δ 176.5, 137.4, 128.8, 128.2, 127.5, 127.1, 125.4, 114.7, 105.0, 86.8, 86.7, 84.7, 72.4, 70.5, 68.5, 38.2, 28.2, 28.1, 27.4, 27.2; HRMS (ESI) calc'd for $C_{24}H_{32}O_7Na$ $[M+Na]^+$ *m/z* 455.2040, found 455.2050.

Compound **epi-1.46**: R_f 0.29 (1:4 ethyl acetate–hexanes); $[\alpha]_D^{20}$ +81.4 (*c* = 0.83, chloroform); IR (film, cm^{-1}) ν 3500, 2975, 1732, 1151; ^{1}H NMR (400 MHz, chloroform-*d*) δ 7.30–7.17 (m, 5H), 6.01 (d, *J* = 4.4 Hz, 1H), 5.78–5.69 (m, 2H), 5.37 (dd, *J* = 8.7, 5.9 Hz, 1H), 4.75 (dd, *J* = 4.3, 2.3 Hz, 1H), 4.63 (s, 2H), 4.32 (d, *J* = 2.1 Hz, 1H), 4.07 (s, 1H), 3.01 (br s, 1H), 2.51–2.43 (m, 1H), 2.25–2.18 (m, 1H), 1.53 (s, 3H), 1.39 (s, 3H), 1.09 (s, 9H); ^{13}C NMR (101 MHz, chloroform-*d*) δ 177.3, 137.6, 128.0, 127.8, 127.3, 127.2, 126.3, 114.0, 104.7, 87.7, 87.6, 86.7,

72.6, 72.5, 69.0, 38.2, 28.6, 28.0, 27.6, 27.1; HRMS (ESI) calc'd for $C_{24}H_{32}O_7Na$ $[M+Na]^+$ *m/z* 455.2040, found 455.2048.

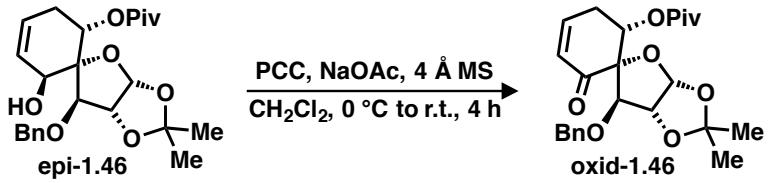

(1*R*,3a'*R*,6*S*,6'*R*,6a'*R*)-6'-(Benzyloxy)-2',2'-dimethyl-2-oxo-3a',6a'-dihydro-6'*H*-spiro-[cyclohexane-1,5'-furo[2,3-*d*][1,3]dioxol]-3-en-6-yl pivalate (oxid-1.46).

A solution of **epi-1.46** (1.15 g, 2.60 mmol) in dichloromethane (30 mL) was added to a stirred, 0 °C mixture of pyridinium chlorochromate (1.55 g, 7.20 mmol), sodium acetate (0.60 g, 7.3 mmol), and powdered 4 Å molecular sieves (1.9 g) in dichloromethane (63 mL). After 4 h, diethyl ether and silica gel were added to the reaction mixture, which was stirred for an additional 30 minutes. The mixture was filtered through a short pad of silica gel and eluted with diethyl ether. The filtrate was concentrated under reduced pressure to afford a light brown residue (1.15 g), which was used in the next step without further purification. A portion of the residue was purified by flash column chromatography (18 × 1 cm) on silica gel (1:5 ethyl acetate–hexanes) to afford **oxid-1.46** as a colorless oil: R_f 0.53 (1:4 ethyl acetate–hexanes); $[\alpha]^{20}_D$ +71.6 (*c* = 0.85, chloroform); IR (film, cm^{-1}) ν 2975, 1738, 1694, 1277, 1143; ^1H NMR (400 MHz, chloroform-*d*) δ 7.34–7.20 (m, 5H), 6.93–6.89 (m, 1H), 6.14 (dd, 10.1, 1.3 Hz, 1H), 6.08 (d, *J* = 4.6 Hz, 1H), 5.29 (dd, *J* = 8.6, 5.2 Hz, 1H), 4.98 (d, *J* = 2.2 Hz, 1H), 4.88 (dd, 4.3, 3.2 Hz, 1H), 4.67 (d, *J* = 11.7 Hz, 1H), 4.55 (d, *J* = 11.7 Hz, 1H), 2.78–2.74 (m, 1H), 2.65–2.62 (m, 1H), 1.53 (s, 3H), 1.43 (s, 3H), 1.15 (s, 9H); ^{13}C NMR (101 MHz, chloroform-*d*) δ 191.4, 176.5, 148.0, 137.2, 128.2, 127.6, 127.2, 114.7, 106.0, 87.6, 87.1, 83.2, 72.7, 70.9, 38.3, 28.6, 28.0, 27.4, 27.1; HRMS (ESI) calc'd for $C_{24}H_{30}O_7Na$ $[M+Na]^+$ *m/z* 453.1884, found 453.1898.

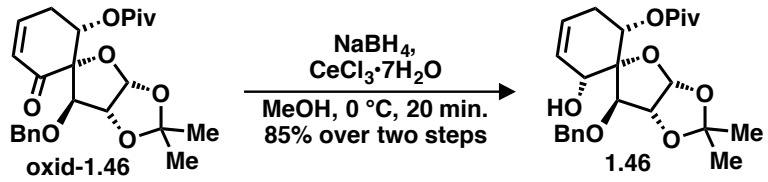

(1*R*,2*R*,3a'*R*,6*S*,6'*R*,6a'*R*)-6'-(Benzyloxy)-2-hydroxy-2',2'-dimethyl-3a',6a'-dihydro-6'*H*-spiro[cyclohexane-1,5'-furo[2,3-*d*][1,3]dioxol]-3-en-6-yl pivalate (1.46).

Cerium(III) chloride heptahydrate (1.8 g, 4.8 mmol) was added at 0 °C to a stirred solution of crude **oxid-1.46** (1.15 g, 2.41 mmol) in methanol (55 mL). The resulting solution was stirred for 10 minutes before sodium borohydride (0.18 g, 4.8 mmol) was added in portionwise fashion. Upon complete consumption of the starting material by TLC analysis (~10 minutes), acetone (3 mL) was added and the mixture was concentrated under reduced pressure. The residue was dissolved in ethyl acetate (100 mL), washed sequentially with water (50 mL), 0.5 M hydrochloric acid (50 mL), and brine (50 mL), dried over magnesium sulfate, filtered, and concentrated under reduced pressure. The residue was purified by flash column chromatography (15 × 2.5 cm) on silica gel (1:5 ethyl acetate–hexanes) to afford **1.46** as a colorless oil (0.982 g, 85% yield over two steps): R_f 0.37 (1:4 ethyl acetate–hexanes); $[\alpha]_D^{20}$ +12.5 (*c* = 1.23, chloroform); IR (film, cm^{-1}) ν 3500, 2977, 1732, 1150; ^1H NMR (400 MHz, chloroform-*d*) δ 7.36–7.23 (m, 5H), 6.07 (d, *J* = 4.8 Hz, 1H), 5.67–5.56 (m, 2H), 5.13 (dd, *J* = 9.9, 5.9 Hz, 1H), 4.90 (dd, *J* = 4.7, 3.7 Hz, 1H), 4.75 (d, *J* = 11.9 Hz, 1H), 4.58 (d, *J* = 11.9 Hz, 1H), 4.41 (d, *J* = 3.5 Hz, 1H), 4.17 (d, *J* = 7.0 Hz, 1H), 2.56 (d, *J* = 10.7 Hz, 1H), 2.44–2.39 (m, 1H), 2.27–2.17 (m, 1H), 1.62 (s, 3H), 1.42 (s, 3H), 1.16 (s, 9H); ^{13}C NMR (101 MHz, chloroform-*d*) δ 176.5, 137.4, 128.8, 128.2, 127.5, 127.1, 125.4, 114.7, 105.0, 86.8, 86.7, 84.7, 72.4, 70.5, 68.5, 38.2, 28.2, 28.1, 27.4, 27.2; HRMS (ESI) calc'd for $C_{24}H_{32}O_7Na$ $[M+Na]^+$ *m/z* 455.2040, found 455.2050.

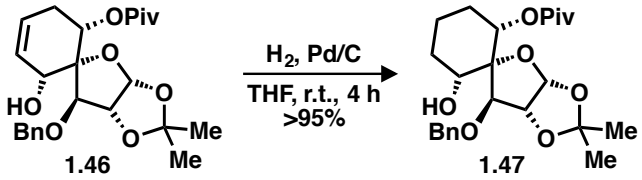

(1*R*,2*R*,3a'*R*,6*S*,6'*R*,6a'*R*)-6'-(Benzyloxy)-2-hydroxy-2',2'-dimethyldihydro-6'*H*-spiro-[cyclohexane-1,5'-furo[2,3-*d*][1,3]dioxol]-6-yl pivalate (1.47).

Palladium on carbon (0.10 g, 10% w/w) was added to a stirred solution of **1.46** (1.97 g, 4.55 mmol) in tetrahydrofuran (50 mL) at room temperature. The suspension was purged with hydrogen gas and maintained under an atmosphere of hydrogen gas (via a hydrogen filled balloon) for 4 h. The reaction mixture was diluted with ethyl acetate, filtered through a pad of Celite® 545, and concentrated under reduced pressure. The residue was purified by flash column chromatography (19 × 2 cm) on silica gel (1:4 ethyl acetate–hexanes) to give **1.47** as a colorless foam (1.90 g, 96% yield): R_f 0.33 (1:4 ethyl acetate–hexanes); $[\alpha]_D^{20}$ +18.6 (*c* = 0.29, chloroform); IR (film, cm^{-1}) ν 3512, 2941, 1731, 1159, 1089, 1035; ^1H NMR (400 MHz, chloroform-*d*) δ 7.37–7.18 (m, 5H), 6.03 (d, *J* = 4.8 Hz, 1H), 4.85–4.78 (m, 2H), 4.72 (d, *J* = 12.0 Hz, 1H), 4.56 (d, *J* = 12.0 Hz, 1H), 4.48 (d, *J* = 3.4 Hz, 1H), 3.38 (dd, *J* = 11.5, 4.8 Hz, 1H), 2.16 (br s, 1H), 1.91–1.82 (m, 1H), 1.80–1.73 (m, 1H), 1.71–1.62 (m, 1H), 1.59 (s, 3H), 1.57–1.41 (m, 2H), 1.39 (s, 3H), 1.33–1.20 (m, 1H), 1.14 (s, 9H); ^{13}C NMR (101 MHz, chloroform-*d*) δ 176.67, 137.69, 128.27, 127.55, 127.15, 114.12, 104.54, 90.19, 87.13, 83.85, 72.86, 72.39, 70.04, 38.38, 30.99, 28.21, 27.93, 27.26, 25.58, 19.62; HRMS (ESI) calc'd for $C_{24}H_{34}O_7Na$ $[M+Na]^+$ *m/z* 457.2197, found 457.2210.

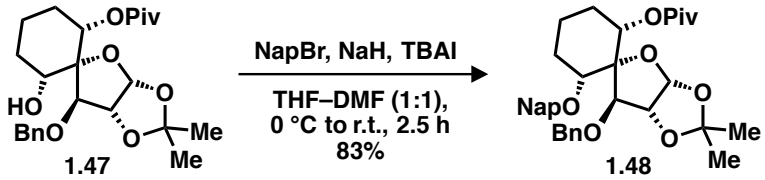

(1*R*,2*R*,3a'*R*,6*S*,6'*R*,6a'*R*)-6'-(Benzyloxy)-2',2'-dimethyl-2-(naphthalen-2-ylmethoxy)-dihydro-6'*H*-spiro[cyclohexane-1,5'-furo[2,3-*d*][1,3]dioxol]-6-yl pivalate (1.48).

Sodium hydride, as a 60% (w/w) dispersion in mineral oil, (0.148 g, 6.18 mmol), 2-(bromomethyl)naphthalene (1.37 g, 6.18 mmol), and tetrabutylammonium iodide (0.761 g, 2.06 mmol) were added at 0 °C to a stirred solution of **1.47** (1.79 g, 4.12 mmol) in

tetrahydrofuran (25 mL) and *N*,*N*-dimethylformamide (25 mL). After 2.5 h, the reaction was cooled to 0 °C, methanol (5 mL) was added, and the mixture was partitioned between dichloromethane (200 mL) and water (100 mL). The layers were separated and the aqueous portion extracted with dichloromethane (3 × 50 mL). The combined extracts were washed with a saturated aqueous solution of sodium bicarbonate (4 × 100 mL) and brine (100 mL), then dried over magnesium sulfate, filtered, and concentrated under reduced pressure. The residue was purified by flash column chromatography (25 × 2 cm) on silica gel (1:9 ethyl acetate–hexanes) to afford **1.48** as a colorless oil (1.96 g, 83% yield): R_f 0.61 (1:4 ethyl acetate–hexanes); $[\alpha]_D^{20}$ –24.6 (*c* = 1.80, chloroform); IR (film, cm^{-1}) ν 2968, 1729, 1148, 1027; ^1H NMR (300 MHz, chloroform-*d*) δ 7.83–7.74 (m, 3H), 7.64 (s, 1H), 7.51–7.42 (m, 2H), 7.35–7.21 (m, 4H), 7.20–7.12 (m, 2H), 6.09 (d, *J* = 4.8 Hz, 1H), 4.86–4.70 (m, 2H), 4.67–4.59 (m, 2H), 4.43 (d, *J* = 3.2 Hz, 1H), 4.27–4.21 (m, 2H), 3.23 (dd, *J* = 11.5, 4.5 Hz, 1H), 2.04–1.93 (m, 1H), 1.79–1.58 (m, 5H), 1.51 (s, 3H), 1.40 (s, 3H), 1.17 (s, 9H); ^{13}C NMR (75 MHz, chloroform-*d*) δ 176.9, 137.8, 135.4, 133.2, 133.0, 128.3, 128.01, 127.96, 127.8, 127.7, 127.6, 127.2, 126.6, 126.2, 126.0, 114.8, 104.8, 88.3, 88.1, 82.7, 76.7, 73.8, 71.93, 71.87, 38.5, 28.4, 28.0, 27.4, 26.2, 25.8, 19.9; HRMS (ESI) calc'd for $C_{35}H_{42}O_7Na$ $[M+Na]^+$ *m/z* 597.2823, found 597.2834.

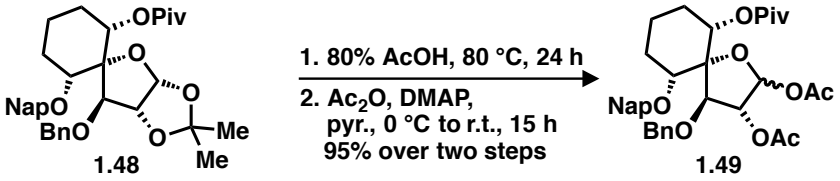

(3*R*,4*R*,5*R*,6*R*,10*S*)-4-(Benzyloxy)-6-(naphthalen-2-ylmethoxy)-10-(pivaloyloxy)-1-oxa-spiro[4.5]decane-2,3-diyl diacetate (1.49).

A stirred solution of **1.48** (1.96 g, 3.42 mmol) in 80% (v/v) aqueous acetic acid (20 mL) was heated to 80 °C for 24 h. The solution was cooled to room temperature and concentrated under reduced pressure. The residue was dissolved in toluene and concentrated under reduced pressure (5 × 50 mL) to remove residual acetic acid. The resulting oil was placed under high vacuum for 3 h, dissolved in pyridine (20 mL), and cooled to 0 °C. Acetic anhydride (3.35 mL, 35.1 mmol) and 4-(dimethylamino)pyridine (0.043 g, 0.35 mmol) were added to this

cooled solution, before it was warmed to room temperature and stirred for 8 h. The resulting solution was partitioned between ethyl acetate (100 mL) and water (100 mL). The layers were separated and the aqueous portion was extracted with ethyl acetate (2 × 50 mL). The combined organic extracts were washed with 0.5 M hydrochloric acid (5 × 100 mL), a saturated aqueous solution of sodium bicarbonate (100 mL), and brine (100 mL), dried over magnesium sulfate, filtered, and concentrated under reduced pressure. The residue was purified by flash column chromatography (20 × 2 cm) on silica gel (1:4 ethyl acetate–hexanes) to afford **1.49** as an amorphous solid (2.01 g, 95% yield over two steps, dr = 9:1): R_f 0.71 (3:7 ethyl acetate–hexanes); $[\alpha]_D^{20}$ +12.6 (*c* = 1.36, chloroform); IR (film, cm^{-1}) ν 2956, 1752, 1728, 1220; ^{1}H NMR (400 MHz, chloroform-*d*) δ 7.91–7.76 (m, 4H), 7.59–7.48 (m, 2H), 7.43 (d, *J* = 8.2 Hz, 1H), 7.30–7.16 (m, 5H), 6.37 (d, *J* = 4.9 Hz, 1H), 5.57 (dd, *J* =8.5, 5.1 Hz, 1H), 4.87–4.77 (m, 2H), 4.72 (d, *J* = 11.9 Hz, 1H), 4.53 (d, *J* = 12.3 Hz, 1H), 4.38 (d, *J* = 12.2 Hz, 1H), 4.26 (d, *J* = 11.8 Hz, 1H), 3.06 (dd, *J* = 11.5, 4.2 Hz, 1H), 2.12 (s, 3H), 1.98 (d, *J* = 12.2 Hz, 1H), 1.83–1.56 (m, 8H), 1.26 (s, 9H); ^{13}C NMR (101 MHz, chloroform-*d*, major diastereomer) δ 177.2, 170.3, 170.2, 138.0, 136.1, 133.3, 133.0, 128.5, 128.1, 127.90, 127.87, 127.85, 127.80, 126.4, 126.3, 126.05, 125.95, 91.8, 85.5, 77.7, 77.0, 73.2, 72.3, 71.4, 38.8, 27.34, 27.30, 25.8, 25.6, 21.2, 20.8, 19.7; HRMS (ESI) calc'd for $C_{36}H_{42}O_9Na$ $[M+Na]^+$ *m/z* 641.2721, found 641.2732.

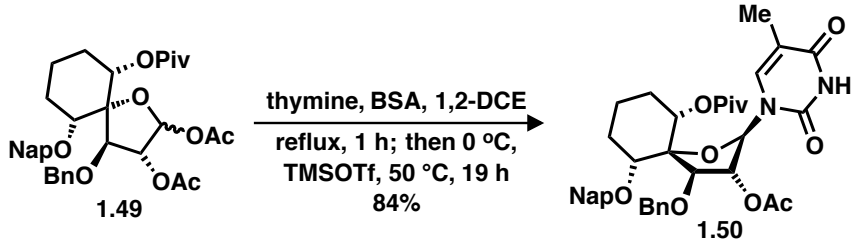

(2*R*,3*R*,4*R*,5*R*,6*S*,10*R*)-3-Acetoxy-4-(benzyloxy)-2-(5-methyl-2,4-dioxo-3,4-dihydropyrimidin-1(2*H*)-yl)-10-(naphthalen-2-ylmethoxy)-1-oxaspiro[4.5]decan-6-yl pivalate (1.50).

N,*O*-Bis(trimethylsilyl)acetamide (4.52 mL, 31.5 mmol) was added to a stirred solution of thymine (0.795 g, 6.30 mmol) in anhydrous 1,2-dichloroethane (30 mL). The resulting mixture was heated to 80 °C for 1 h and then cooled to 0 °C, upon which a solution of **1.49** (1.95 g,

3.15 mmol) in anhydrous 1,2-dichloroethane (10 mL), and trimethylsilyl trifluoromethylsulfonate (1.14 mL, 6.30 mmol) were added. The solution was heated to 50 °C for 18 h, cooled to 0 °C, and a saturated aqueous solution of sodium bicarbonate (2 mL) was added. The mixture was partitioned between ethyl acetate (100 mL) and a saturated aqueous solution of sodium bicarbonate (50 mL). The layers were separated and the aqueous portion was extracted with ethyl acetate (3 × 50 mL). The combined organic extracts were washed with brine (100 mL), dried over magnesium sulfate, filtered, and concentrated under reduced pressure. The residue was purified by flash column chromatography (18 × 3 cm) on silica gel (1:2 ethyl acetate–hexanes) to afford **1.50** as a colorless foam (2.02 g, 84% yield): R_f 0.50 (1:1 ethyl acetate–hexanes); $[\alpha]_D^{20}$ +9.19 (*c* = 2.22, chloroform); IR (film, cm^{-1}) ν 3187, 2957, 1748, 1694, 1226, 1141; ^{1}H NMR (400 MHz, chloroform-*d*) δ 8.83 (br s, 1H), 7.85 (td, *J* = 7.5, 2.2 Hz, 3H), 7.76 (s, 1H), 7.68 (d, *J* = 1.2 Hz, 1H), 7.50–7.42 (m, 3H), 7.27–7.24 (m, 3H), 7.05–7.01 (m, 2H), 6.20 (d, *J* = 8.0 Hz, 1H), 5.48 (t, *J* = 8.1 Hz, 1H), 4.83 (dd, *J* = 12.1, 4.6 Hz, 1H), 4.82 (d, *J* = 12.4 Hz, 1H), 4.69 (d, *J* = 8.4 Hz, 1H), 4.37 (d, *J* = 12.3 Hz, 1H), 4.27 (d, *J* = 12.0 Hz, 1H), 4.15 (d, *J* = 12.0 Hz, 1H), 3.05 (dd, *J* = 11.5, 4.6 Hz, 1H), 2.04 (s, 3H), 2.01–1.92 (m, 4H), 1.83–1.69 (m, 2H), 1.69–1.51 (m, 2H), 1.27–1.22 (m, 10H); ^{13}C NMR (101 MHz, chloroform-*d*) δ 177.0, 170.7, 163.7, 150.8, 137.5, 135.4, 134.8, 133.4, 133.1, 128.4, 128.1, 128.0, 127.9, 127.8, 126.7, 126.5, 126.2, 125.9, 111.3, 85.1, 83.2, 79.5, 78.8, 78.7, 73.7, 72.4, 71.2, 38.7, 27.5, 26.3, 25.5, 20.9, 19.6, 12.6; HRMS (ESI) calc'd for $C_{39}H_{45}N_2O_9$ $[M+H]^+$ *m/z* 685.3120, found 685.3127.

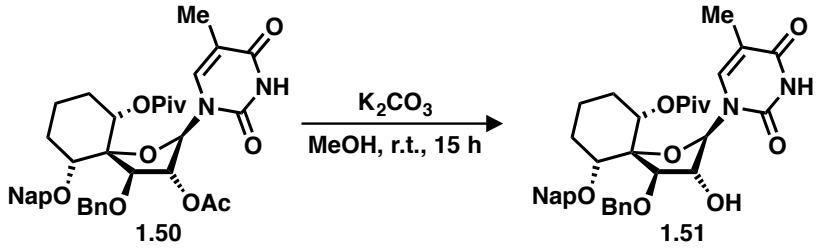

(2*R*,3*R*,4*R*,5*R*,6*S*,10*R*)-4-(Benzyloxy)-3-hydroxy-2-(5-methyl-2,4-dioxo-3,4-dihydropyrimidin-1(2*H*)-yl)-10-(naphthalen-2-ylmethoxy)-1-oxaspiro[4.5]decan-6-yl pivalate (1.51).

Potassium carbonate (0.050 g, 0.36 mmol) was added to a stirred solution of **1.50** (2.48 g, 3.60 mmol) in methanol (25 mL). The resulting solution was kept at room temperature for 12 h before it was concentrated under reduced pressure. The residue was dissolved in ethyl acetate (100 mL) and partitioned with water (75 mL). The layers were separated and the aqueous portion was extracted with ethyl acetate (3 × 75 mL). The combined organic extracts were washed with brine (100 mL), dried over magnesium sulfate, filtered, and concentrated under reduced pressure to afford a residue (2.20 g) that was used in the next step without further purification. A portion of the residue was purified by flash column chromatography (18 × 1 cm) on silica gel with (2:3 ethyl acetate–hexanes) to afford **1.51** as a colorless foam: R_f 0.50 (1:1 ethyl acetate–hexanes); $[\alpha]_D^{20}$ −11.3 (*c* = 1.26, chloroform); IR (film, cm^{-1}) ν 3419, 2956, 1694, 1144, 753; ^{1}H NMR (400 MHz, chloroform-*d*) δ 9.33 (br s, 1H), 7.85–7.80 (m, 3H), 7.72 (s, 1H), 7.62 (d, *J* = 0.8 Hz, 1H), 7.49–7.40 (m, 3H), 7.29–7.21 (m, 3H), 7.18–7.16 (m, 2H), 5.94 (d, *J* = 7.0 Hz, 1H), 4.83 (dd, *J* = 12.1, 4.7 Hz, 1H), 4.69–4.54 (m, 3H), 4.39–4.27 (m, 3H), 4.16 (br s, 1H), 3.07 (dd, *J* = 11.3, 4.4 Hz, 1H), 2.06–1.93 (m, 1H), 1.90–1.82 (m, 4H), 1.81–1.71 (m, 1H), 1.68–1.50 (m, 2H), 1.32–1.19 (m, 1H), 1.12 (s, 9H); ^{13}C NMR (101 MHz, chloroform-*d*) δ 176.8, 163.9, 151.7, 138.1, 135.4, 135.3, 133.3, 133.1, 128.38, 128.36, 128.13, 128.09, 127.8, 126.6, 126.3, 126.1, 126.0, 110.6, 88.7, 87.0, 82.4, 81.8, 78.5, 72.7, 72.2, 71.6, 38.6, 27.4, 26.7, 25.9, 19.6, 12.7; HRMS (ESI) calc'd for $C_{37}H_{43}N_2O_8$ $[M+H]^+$ *m/z* 643.3014, found 643.3020.

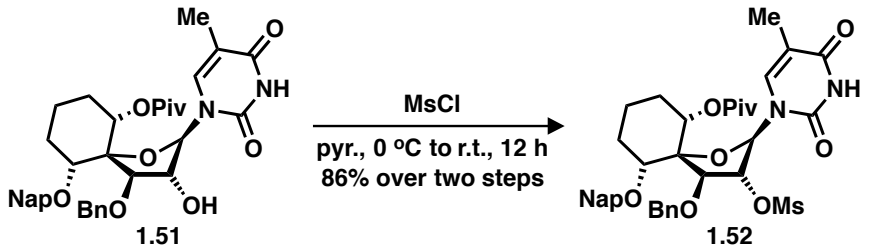

(2*R*,3*R*,4*R*,5*R*,6*S*,10*R*)-4-(Benzyloxy)-2-(5-methyl-2,4-dioxo-3,4-dihydropyrimidin-1(2*H*)-yl)-3-((methylsulfonyl)oxy)-10-(naphthalen-2-ylmethoxy)-1-oxaspiro[4.5]decan-6-yl pivalate (1.52).

Methanesulfonyl chloride (1.4 mL, 14 mmol) was added to a stirred solution of crude **1.51** (2.2 g, 3.2 mmol) in pyridine (61 mL). The resulting solution was kept at room temperature for 16 h and partitioned between dichloromethane (150 mL) and water (100 mL). The layers were separated and the aqueous portion was extracted with dichloromethane (3 × 75 mL). The combined organic extracts were washed sequentially with 0.5 M hydrochloric acid (3 × 150 mL), a saturated aqueous solution of sodium bicarbonate (150 mL), and brine (150 mL), dried over magnesium sulfate, filtered, and concentrated under reduced pressure. The residue was purified by flash column chromatography (15 × 4 cm) on silica gel (2:1 ethyl acetate–hexanes) to afford **1.52** as a colorless foam (2.25 g, 86% yield over two steps): R_f 0.58 (1:1 ethyl acetate–hexanes); $[\alpha]_D^{20}$ +17.7 (*c* = 0.82, chloroform); IR (film, cm^{-1}) ν 2936, 1694, 1180, 1140; ^1H NMR (400 MHz, chloroform-*d*) δ 10.14 (br s, 1H), 7.93–7.79 (m, 3H), 7.75 (s, 1H), 7.64 (d, *J* = 1.2 Hz, 1H), 7.54–7.39 (m, 3H), 7.26 (s, 3H), 7.10 (s, 2H), 6.41 (d, *J* = 7.9 Hz, 1H), 5.24 (t, *J* = 7.8 Hz, 1H), 4.85 (dd, *J* = 11.4, 3.1 Hz, 1H), 4.76–4.68 (m, 2H), 4.44 (d, *J* = 11.6 Hz, 1H), 4.33 (d, *J* = 12.2 Hz, 1H), 4.21 (d, *J* = 11.5 Hz, 1H), 3.03 (dd, *J* = 10.8, 2.9 Hz, 1H), 2.98 (s, 3H), 2.03–1.84 (m, 4H), 1.84–1.52 (m, 4H), 1.25 (s, 10H); ^{13}C NMR (101 MHz, chloroform-*d*) δ 176.6, 163.8, 151.1, 136.9, 135.0, 134.0, 133.1, 132.9, 128.3, 128.2, 128.1, 127.92, 127.86, 127.6, 126.5, 126.3, 126.0, 125.7, 111.8, 84.7, 82.6, 82.0, 78.7, 78.2, 73.4, 72.1, 70.9, 38.5, 38.4, 27.3, 25.9, 25.2, 19.2, 12.4; HRMS (ESI) calc'd for $C_{38}H_{44}N_2O_{10}SNa$ $[M+Na]^+$ *m/z* 743.2609, found 743.2617.

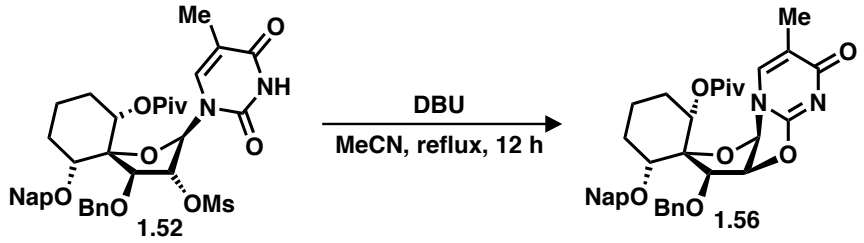

(1*R*,2*R*,3'*R*,3a'*S*,6*S*,9a'*R*)-3'-(Benzyloxy)-7'-methyl-2-(naphthalen-2-ylmethoxy)-6'-oxo-3a',9a'-dihydro-3'*H*,6'*H*-spiro[cyclohexane-1,2'-furo[2',3':4,5]oxazolo[3,2-*a*]pyrimidin]-6-yl pivalate (1.56).

1,8-Diazabicyclo[5.4.0]undec-7-ene (4.7 mL, 31 mmol) was added to a stirred solution of **1.52** (2.25 g, 3.12 mmol) in acetonitrile (69 mL). The resulting solution was heated to reflux for 12 h, cooled to room temperature, and partitioned between 0.5 M hydrochloric acid (100 mL) and ethyl acetate (150 mL). The layers were separated and the aqueous portion was extracted with ethyl acetate (3 × 100 mL). The combined organic extracts were washed with brine (150 mL), dried over magnesium sulfate, filtered, and concentrated under reduced pressure to afford crude **1.56** (2.0 g) as a pale brown foam. The crude residue was used in the next step of the synthetic sequence without further purification: R_f 0.02 (1:1 ethyl acetate–hexanes); $[\alpha]_D^{20}$ −86.9 (*c* = 1.38, chloroform); IR (film, cm^{-1}) ν 2954, 1720, 1644, 1559, 1481; ^1H NMR (400 MHz, chloroform-*d*) δ 7.84–7.75 (m, 3H), 7.62 (s, 1H), 7.50–7.39 (m, 2H), 7.33–7.23 (m, 2H), 7.22–7.08 (m, 5H), 6.11 (d, *J* = 5.2 Hz, 1H), 5.32 (t, *J* = 5.2 Hz, 1H), 4.79 (dd, *J* = 11.5, 4.8 Hz, 1H), 4.71 (d, *J* = 11.5 Hz, 1H), 4.55 (d, *J* = 11.2 Hz, 1H), 4.34 (d, *J* = 11.5 Hz, 1H), 4.13 (d, *J* = 11.2 Hz, 1H), 4.06 (d, *J* = 6.0 Hz, 1H), 3.02 (dd, *J* = 11.3, 3.5 Hz, 1H), 1.97–1.87 (m, 4H), 1.71–1.66 (m, 2H), 1.53–1.46 (m, 2H), 1.23–1.07 (m, 1H), 0.71 (s, 9H); ^{13}C NMR (101 MHz, chloroform-*d*) δ 176.6, 172.2, 159.7, 136.3, 134.4, 133.0, 132.9, 131.3, 129.0, 128.6, 128.2, 128.0, 127.8, 127.6, 127.0, 126.4, 126.3, 125.7, 118.5, 91.7, 91.0, 82.2, 80.82, 80.81, 74.3, 71.1, 69.2, 38.0, 27.7, 26.2, 24.8, 19.0, 13.7; HRMS (ESI) calc'd for $C_{37}H_{41}O_7N_2$ $[M+H]^+$ *m/z* 625.2908, found 625.2917.

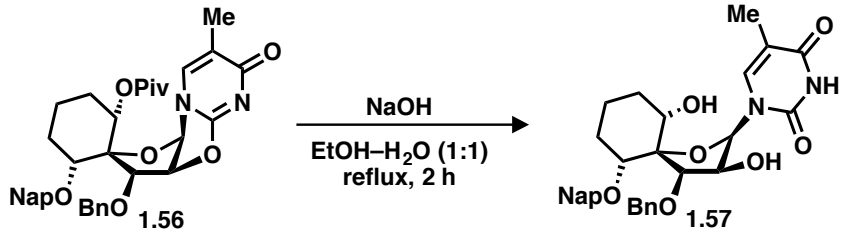

1-((2*R*,3*S*,4*R*,5*S*,6*S*,10*R*)-4-(benzyloxy)-3,6-dihydroxy-10-(naphthalen-2-ylmethoxy)-1-oxaspiro[4.5]decan-2-yl)-5-methylpyrimidine-2,4(1*H*,3*H*)-dione (1.57).

Sodium hydroxide (1.3 g, 32 mmol) was added to a stirred solution of crude 2,2′-anhydronucleoside **1.56** (2.0 g, 3.1 mmol) in 1:1 (v/v) ethanol/water (80 mL). The resulting mixture was heated to reflux for 2 h, cooled to room temperature, and partitioned between ethyl acetate (300 mL) and water (150 mL). The layers were separated and the aqueous portion was extracted with ethyl acetate (4 × 100 mL). The combined organic extracts were washed with 0.5 M hydrochloric acid (100 mL) and brine (100 mL), dried over magnesium sulfate, filtered, and concentrated under reduced pressure to afford a crude residue that was used without further purification in the next step. A portion of the residue was purified by flash column chromatography (18 × 1 cm) on silica gel (3:2 ethyl acetate–hexanes) to afford **1.57** as a colorless foam: R_f 0.20 (1:1 ethyl acetate–hexanes); $[\alpha]_D^{20}$ +10.4 (*c* = 0.74, chloroform); IR (film, cm^{-1}) ν 3270, 2941, 1711, 1697, 1661, 1070; ^{1}H NMR (400 MHz, methanol–d_4) δ 7.85 (d, *J* = 1.2, 1H), 7.84–7.75 (m, 3H), 7.65 (s, 1H), 7.47–7.39 (m, 2H), 7.29 (dd, *J* = 8.4, 1.6 Hz, 1H), 7.25–7.11 (m, 5H), 5.99 (d, *J* = 2.9 Hz, 1H), 4.62 (d, *J* = 11.8 Hz, 1H), 4.57 (d, *J* = 5.0 Hz, 1H), 4.52 (d, *J* = 11.8 Hz, 1H), 4.28 (dd, *J* = 4.9, 3.0 Hz, 1H), 4.17 (d, *J* = 11.8 Hz, 1H), 4.04 (d, *J* = 11.7 Hz, 1H), 3.63 (dd, *J* = 11.9, 4.8 Hz, 1H), 3.14 (dd, *J* = 11.6, 4.6 Hz, 1H), 1.99 (dd, *J* = 12.4, 3.4 Hz, 1H), 1.84 (s, 3H), 1.82–1.75 (m, 1H), 1.73–1.65 (m, 1H), 1.55 (m, 2H), 1.23–1.10 (m, 1H); ^{13}C NMR (101 MHz, methanol–d_4) δ 166.4, 152.1, 139.9, 138.9, 136.8, 134.6, 134.4, 129.4, 129.2, 129.1, 129.0, 128.9, 128.7, 127.7, 127.23, 127.18, 127.1, 109.3, 88.6, 87.2, 79.7, 78.7, 72.9, 72.4, 70.0, 69.2, 30.8, 27.0, 20.7, 12.6; HRMS (ESI) calc'd for $C_{32}H_{35}O_7N_2$ $[M+H]^+$ *m/z* 559.2439, found 559.2450.

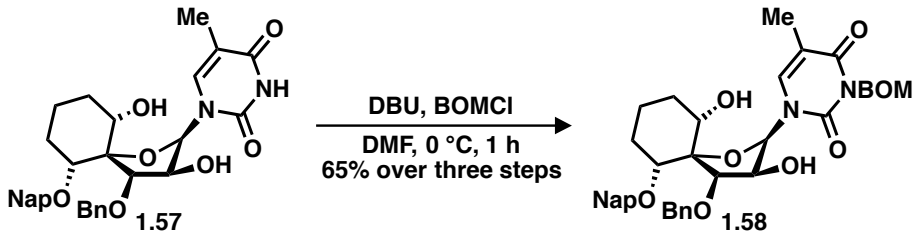

1-((2*R*,3*S*,4*R*,5*S*,6*S*,10*R*)-4-(Benzyloxy)-3,6-dihydroxy-10-(naphthalen-2-ylmethoxy)-1-oxaspiro[4.5]decan-2-yl)-3-((benzyloxy)methyl)-5-methylpyrimidine-2,4(1*H*,3*H*)-dione (1.58).

A 60% technical grade solution of benzyl chloromethyl ether (0.74 mL, 3.2 mmol) and 1,8-diazabicyclo[5.4.0]undec-7-ene (0.52 mL, 3.5 mmol) were added to a stirred 0 °C solution of crude **1.57** (1.62 g, 2.91 mmol) in *N*,*N*-dimethylformamide (53 mL). After 1 h the reaction mixture was partitioned between ethyl acetate (200 mL) and water (100 mL). The layers were separated and the aqueous portion was extracted with ethyl acetate (3 × 75 mL). The combined organic extracts were washed with a saturated aqueous solution of sodium bicarbonate (3 × 100 mL) and brine (100 mL), dried over magnesium sulfate, filtered, and concentrated under reduced pressure. The residue was purified by flash column chromatography (17 × 3.5 cm) on silica gel (2:3 ethyl acetate–hexanes) to afford **1.58** as a colorless foam (1.32 g, 65% yield over three steps): R_f 0.55 (1:1 ethyl acetate–hexanes); $[\alpha]_D^{20}$ +14.2 (*c* = 0.24, chloroform); IR (film, cm^{-1}) ν 3322, 1704, 1664, 1067; ^1H NMR (400 MHz, chloroform-*d*) δ 7.89–7.81 (m, 3H), 7.73 (s, 1H), 7.66 (s, 1H), 7.54–7.46 (m, 2H), 7.41–7.26 (m, 9H), 7.20–7.13 (m, 2H), 6.11 (d, *J* = 2.6 Hz, 1H), 5.52–5.41 (m, 2H), 4.71–4.64 (m, 3H), 4.64–4.53 (m, 2H), 4.40–4.35 (m, 1H), 4.29 (d, *J* = 11.9 Hz, 1H), 4.11 (d, *J* = 11.6 Hz, 1H), 3.68 (dd, *J* = 11.8, 4.5 Hz, 1H), 3.13 (dd, *J* = 11.6, 4.5 Hz, 1H), 2.01–1.96 (m, 1H), 1.92 (s, 3H), 1.84–1.48 (m, 4H), 1.23–1.08 (m, 1H); ^{13}C NMR (101 MHz, chloroform-*d*) δ 164.0, 150.9, 138.0, 137.3, 137.1, 135.3, 133.2, 133.1, 128.6, 128.44, 128.35, 128.2, 128.1, 128.0, 127.9, 127.8, 127.7, 126.8, 126.4, 126.2, 126.0, 108.0, 87.2, 86.6, 78.6, 78.1, 72.4, 72.1, 71.5, 70.4, 69.7, 68.5, 29.7, 25.9, 19.8, 13.5; HRMS (ESI) calc'd for $C_{40}H_{43}O_8N_2$ $[M+H]^+$ *m/z* 679.3018, found 679.3014.

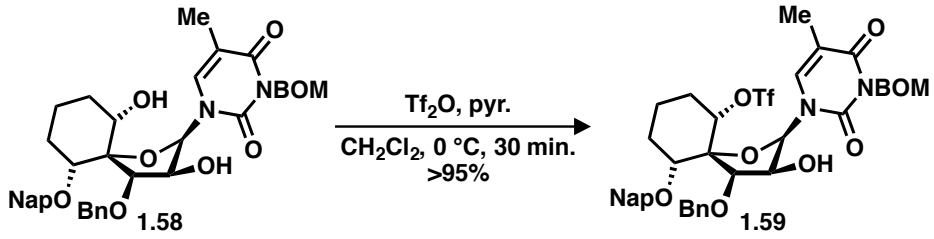

(2*R*,3*S*,4*R*,5*S*,6*S*,10*R*)-4-(Benzyloxy)-2-(3-((benzyloxy)methyl)-5-methyl-2,4-dioxo-3,4-dihydropyrimidin-1(2*H*)-yl)-3-hydroxy-10-(naphthalen-2-ylmethoxy)-1-oxaspiro[4.5]decan-6-yl trifluoromethanesulfonate (1.59).

Pyridine (0.37 mL, 4.5 mmol) was added dropwise to a stirred 0 °C solution of trifluoromethanesulfonic anhydride (0.57 mL, 3.4 mmol) in anhydrous dichloromethane (16 mL). After 10 minutes, a solution of **1.58** (1.54 g, 2.27 mmol) in dichloromethane (16 mL) was added. The mixture was kept at 0 °C for an additional 30 minutes and then partitioned between dichloromethane (75 mL) and water (75 mL). The layers were separated and the aqueous portion was extracted with dichloromethane (3 × 50 mL). The combined organic extracts were washed with 0.5 M hydrochloric acid (75 mL), a saturated aqueous solution of sodium bicarbonate (75 mL), and brine (75 mL), then dried over magnesium sulfate, filtered, and concentrated under reduced pressure to afford a crude residue that was used in the next step without further purification. A portion the residue was purified by flash column chromatography (14 × 1 cm) on silica gel (1:3 ethyl acetate–hexanes) to afford **1.59** as a colorless foam: R_f 0.50 (3:7 ethyl acetate–hexanes); $[\alpha]_D^{20}$ +13.8 (*c* = 0.34, chloroform); IR (film, cm^{-1}) ν 2946, 1709, 1666, 1650, 1210; ^{1}H NMR (400 MHz, chloroform-*d*) δ 7.93–7.81 (m, 3H), 7.76 (s, 1H), 7.65 (s, 1H), 7.57–7.47 (m, 2H), 7.45–7.26 (m, 9H), 7.20–7.16 (m, 2H), 6.40 (d, *J* = 3.3 Hz, 1H), 5.55–5.43 (m, 3H), 4.78 (d, *J* = 12.0 Hz, 1H), 4.73 (d, *J* = 5.5 Hz, 1H), 4.69 (s, 2H), 4.59 (d, *J* = 11.9 Hz, 1H), 4.16 (d, *J* = 12.0 Hz, 1H), 4.12 (d, *J* = 11.9 Hz, 1H), 3.58 (dd, *J* = 12.0, 4.5 Hz, 1H), 2.75 (dd, *J* = 11.4, 4.4 Hz, 1H), 2.60 (br s, 1H), 1.98 (s, 3H), 1.94–1.71 (m, 3H), 1.69–1.47 (s, 2H) 1.19–1.05 (m, 1H); ^{13}C NMR (101 MHz, chloroform-*d*) δ 163.4, 150.8, 137.9, 136.0, 135.2, 135.0, 133.3, 133.1, 129.0, 128.90, 128.86, 128.7, 128.4, 128.0, 127.88, 127.86, 127.8, 126.63, 126.61, 126.4, 125.6, 109.9, 88.3, 83.6, 82.9, 79.6, 77.5, 74.9, 72.1, 71.3, 70.5, 70.3, 28.3, 25.7, 19.8, 13.3; HRMS (ESI) calc'd for $C_{41}H_{41}O_{10}N_2SF_3Na$ $[M+Na]^+$ *m/z* 833.2326, found 833.2347.

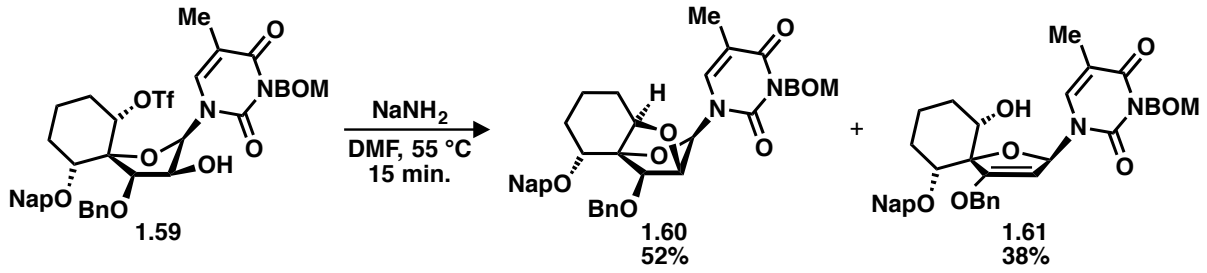

1-((2*S*,3*R*,4a*R*,5*R*,8a*R*,9*R*)-9-(Benzyloxy)-5-(naphthalen-2-ylmethoxy)hexahydro-5*H*-2,4a-methanobenzo[*b*][1,4]dioxin-3-yl)-3-((benzyloxy)methyl)-5-methylpyrimidine-2,4(1*H*,3*H*)-dione (1.60) and 1-((2*R*,5*S*,6*S*,10*R*)-4-(benzyloxy)-6-hydroxy-10-(naphthalen-2-ylmethoxy)-1-oxaspiro[4.5]dec-3-en-2-yl)-3-((benzyloxy)methyl)-5-methylpyrimidine-2,4(1*H*,3*H*)-dione (1.61).

A solution of **1.59** (1.54 g, 1.82 mmol) in anhydrous *N*,*N*-dimethylformamide (24 mL) was added to a stirred suspension of sodium amide (0.17 g, 4.5 mmol) in *N*,*N*-dimethylformamide (300 mL) at 55 °C. After 15 minutes the reaction mixture was cooled to 0 °C and methanol (1 mL) was added in one portion. The resulting solution was partitioned between ethyl acetate (500 mL) and a saturated aqueous solution of sodium bicarbonate (250 mL). The layers were separated and the aqueous portion extracted with ethyl acetate (3 × 200 mL). The combined organic extracts were washed with a saturated aqueous solution of sodium bicarbonate (3 × 200 mL) and brine (200 mL), dried over magnesium sulfate, filtered, and concentrated under reduced pressure. The residue was purified by flash column chromatography (16 × 2 cm) on silica gel (3:7 ethyl acetate–hexanes) to afford **1.60** (0.62 g, 52% yield over two steps; yield is ~55% if triflate **1.59** is purified first) and **1.61** (0.45 g, 38% yield over two steps) as a separable mixture of colorless oils:

Tricyclic nucleoside **1.60**: R_f 0.44 (3:7 ethyl acetate–hexanes); $[\alpha]_D^{20}$ +17.3 (*c* = 0.22, chloroform); IR (film, cm^{-1}) ν 2926, 1706, 1663, 1068 cm^{-1}; ^1H NMR (chloroform-*d*) δ 7.88–7.79 (m, 4H), 7.57 (d, *J* = 1.0 Hz, 1H), 7.54–7.46 (m, 3H), 7.42–7.24 (m, 10 H), 5.76 (d, *J* = 1.1 Hz, 1H), 5.52 (d, *J* = 9.7 Hz, 1H), 5.47 (d, *J* = 9.7 Hz, 1H), 4.90 (s, 1H), 4.89–4.81 (m, 2H), 4.74 (d, *J* = 11.9 Hz, 1H), 4.71 (s, 2H), 4.53 (d, *J* = 11.9 Hz, 1H), 4.26 (dd, *J* = 10.4, 7.4 Hz, 1H), 4.19 (s, 1H), 4.09 (s, 1H), 2.12–1.96 (m, 2H), 1.94–1.88 (m, 1H), 1.87 (s, 3H), 1.84–1.60 (m, 2H), 1.60–1.46 (m, 2H); ^{13}C NMR (101 MHz, chloroform-*d*) δ 163.7, 151.1, 138.1, 137.0, 136.3, 134.2, 133.4, 133.1, 128.7, 128.4, 128.25, 128.18, 127.88, 127.86, 127.8,

127.6, 126.3, 126.1, 126.0, 125.6, 109.2, 89.1, 87.9, 82.4, 81.5, 76.7, 75.1, 72.4, 72.30, 72.28, 70.4, 29.6, 27.9, 17.0, 13.6; HRMS (ESI) calc'd for $C_{40}H_{41}O_7N_2$ $[M+H]^+$ *m/z* 661.2908, found 661.2930.

Benzyl enol ether **1.61**: R_f 0.08 (1:2 ethyl acetate–hexanes); $[\alpha]_D^{20}$ +38.4 (*c* = 1.0, chloroform); IR (film, cm^{-1}) ν 2941, 2865, 1706, 1661, 1247, 1075, 1019, 775; ^1H NMR (400 MHz, chloroform-*d*) δ δ 7.84–7.75 (m, 3H), 7.69 (s, 2H), 7.50–7.44 (m, 2H), 7.43–7.36 (m, 3H), 7.34–7.28 (m, 6H), 7.28–7.24 (m, 2H), 7.11 (d, *J* = 1.2 Hz, 1H), 5.52 (s, 2H), 4.94 (d, *J* = 11.7 Hz, 1H), 4.87 (d, *J* = 11.8 Hz, 1H), 4.76–4.67 (m, 4H), 4.58 (d, *J* = 12.4 Hz, 1H), 3.75 (m, 1H), 3.43 (dd, *J* = 11.5, 4.4 Hz, 1H), 1.97–1.90 (m, 1H), 1.87 (s, 3H), 1.84–1.57 (m, 4H), 1.55–1.48 (m, 1H), 1.23–1.09 (m, 1H); ^{13}C NMR (75 MHz, chloroform-*d*) δ 163.9, 159.3, 151.9, 138.3, 136.3, 136.0, 135.4, 133.3, 133.1, 128.7, 128.6, 128.4, 128.2, 128.0, 127.9, 127.8, 127.7, 126.3, 126.2, 126.0, 125.8, 109.9, 93.8, 91.5, 89.0, 77.7, 72.9, 72.3, 71.8, 70.7, 70.3, 30.2, 26.4, 19.9, 13.3; HRMS (ESI) calc'd for $C_{40}H_{40}O_7N_2Na$ $[M+Na]^+$ m/z 683.2728, found 683.2734.

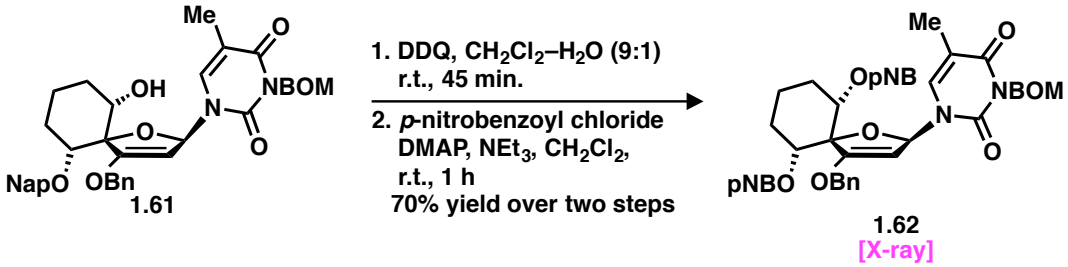

(2*R*,5*s*,6*R*,10*S*)-4-(Benzyloxy)-2-(3-((benzyloxy)methyl)-5-methyl-2,4-dioxo-3,4-dihydro-pyrimidin-1(2*H*)-yl)-1-oxaspiro[4.5]dec-3-ene-6,10-diyl bis(4-nitrobenzoate) (1.62).
2,3-Dichloro-5,6-dicyano-1,4-benzoquinone (0.032 g, 0.14 mmol) was added to a stirred solution of **1.61** (0.046 g, 0.070 mmol) in dichloromethane (2.5 mL) and water (0.28 mL). After 45 minutes the mixture was concentrated under reduced pressure and the residue dissolved in ethyl acetate (5 mL). The solution was washed with a saturated aqueous solution of sodium bicarbonate (5 mL), 10% (w/v) sodium hydrogen sulfite (5 mL), and brine (5 mL), dried through a phase separator cartridge, and concentrated under reduced pressure. The residue was purified by flash column chromatography (15 × 1 cm) on silica gel (3:1 ethyl

acetate–hexanes) to afford the intermediate alcohol, which was immediately converted to the *p*-nitrobenzoate ester: Triethylamine (28 μL, 0.20 mmol), *p*-nitrobenzoyl chloride (0.033 g, 0.17 mmol) and 4-(dimethylamino)pyridine (0.004 g, 0.034 mmol) were added to a stirred solution of the intermediate alcohol (0.035 g, 0.067 mmol) in dichloromethane (1.2 mL). After 1 h, the reaction mixture was partitioned between dichloromethane (5 mL) and water (5 mL), the layers were separated, and the aqueous portion extracted with dichloromethane (2 × 5 mL). The combined organic extracts were washed with 1 M hydrochloric acid (5 mL), a saturated aqueous solution of sodium bicarbonate (5 mL), and brine (5 mL), dried through a phase separator cartridge, and concentrated under reduced pressure. The residue was purified by flash column chromatography (15 × 1) on silica gel (1:4 ethyl acetate–hexanes) to afford **1.62** as a colorless solid (0.040 g, 70% yield over two steps): R_f 0.35 (1:3 ethyl acetate–hexanes); $[\alpha]_D^{20}$ –6.0 (*c* = 0.2, chloroform); IR (film, cm^{-1}) ν 2949, 1729, 1716, 1662, 1527, 1267, 1100, 1015, 873; ^{1}H NMR (400 MHz, chloroform-*d*) δ 8.32 (d, *J* = 8.9 Hz, 2H), 8.25 (d, *J* = 8.8 Hz, 2H), 8.17 (d, *J* = 8.9 Hz, 2H), 8.04 (d, *J* = 8.8 Hz, 2H), 7.41 (d, *J* = 7.0 Hz, 2H), 7.33 (t, *J* = 7.4 Hz, 2H), 7.30–7.23 (m, 1H), 7.21–7.15 (m, 3H), 7.11–7.05 (m, 4H), 5.53 (s, 2H), 5.41 (dd, *J* = 12.0, 4.6 Hz, 1H), 5.31 (dd, *J* = 11.6, 5.1 Hz, 1H), 4.90 (d, *J* = 12.1 Hz, 1H), 4.79 (d, *J* = 12.1 Hz, 1H), 4.75 (s, 2H), 4.65 (s, 1H), 2.12–1.85 (m, 4H), 1.68–1.52 (m, 2H), 1.51 (s, 3H); ^{13}C NMR (101 MHz, chloroform-*d*) δ 164.7, 164.1, 164.0, 158.0, 152.3, 151.6, 151.5, 138.7, 136.1, 135.7, 135.5, 134.9, 131.6, 131.4, 129.4, 129.3, 129.2, 128.6, 128.52, 128.48, 124.6, 110.8, 95.0, 89.7, 89.3, 74.9, 74.2, 73.8, 73.2, 71.4, 27.3, 27.2, 20.3, 14.3; HRMS (ESI) calc'd for $C_{43}H_{38}O_{13}N_4Na$ $[M+Na]^+$ m/z 841.2328, found 841.2319. Recrystallization from methanol–benzene afforded crystals that were suitable for X-ray crystallographic analysis.

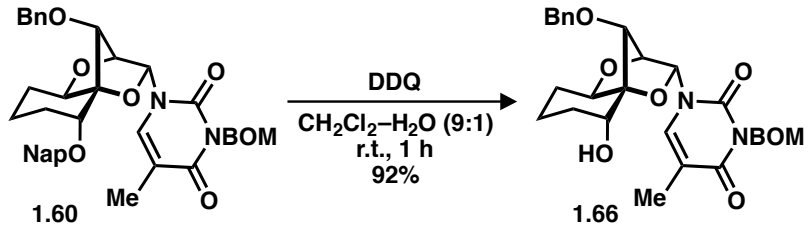

1-((2*S*,3*R*,4a*R*,5*R*,8a*R*,9*R*)-9-(Benzyloxy)-5-hydroxyhexahydro-5*H*-2,4a-methanobenzo-[*b*][1,4]dioxin-3-yl)-3-((benzyloxy)methyl)-5-methylpyrimidine-2,4(1*H*,3*H*)-dione (1.66). 2,3-Dichloro-5,6-dicyano-1,4-benzoquinone (0.43 g, 1.9 mmol) was added to a stirred solution of **1.60** (0.62 g, 0.94 mmol) in dichloromethane (30.6 mL) and water (3.4 mL). After 1 h, the reaction mixture was concentrated under reduced pressure and dissolved in ethyl acetate (50 mL). The solution was washed with a saturated aqueous solution of sodium bicarbonate (50 mL), 10% (w/v) sodium hydrogen sulfite (50 mL), and brine (50 mL), dried over magnesium sulfate, filtered, and concentrated under reduced pressure. The residue was purified by flash column chromatography (18 × 2 cm) on silica gel (1:1 ethyl acetate–hexanes) to afford **1.66** as a colorless foam (0.45 g, 92% yield): R_f 0.19 (1:2 ethyl acetate–hexanes); $[\alpha]^{20}_D$ +2.5 (*c* = 0.12, chloroform); IR (film, cm^{-1}) ν 3444, 2926, 1709, 1666, 1109; ^{1}H NMR (400 MHz, chloroform-*d*) δ 7.50 (d, *J* = 1.0 Hz, 1H), 7.41–7.24 (m, 10H), 5.79 (d, *J* = 0.9 Hz, 1H), 5.50 (d, *J* = 9.7 Hz, 1H), 5.45 (d, *J* = 9.7 Hz, 1H), 4.81 (s, 1H), 4.73 (d, *J* = 11.9 Hz, 1H), 4.69 (s, 2H), 4.53 (d, *J* = 11.9 Hz, 1H), 4.41–4.39 (m, *J* = 2.3 Hz, 1H), 4.21 (dd, *J* = 7.2, 3.6 Hz, 1H), 4.05 (s, 1H), 2.30 (br s, 1H), 2.09–2.00 (m, 1H), 1.98 (s, 3H), 1.94–1.82 (m, 3H), 1.80–1.66 (m, 1H), 1.56–1.47 (m, 1H); ^{13}C NMR (101 MHz, chloroform-*d*) δ 163.5, 151.2, 138.0, 136.9, 133.9, 128.8, 128.4, 128.2, 127.9, 127.8, 127.5, 109.5, 88.7, 87.6, 82.0, 81.4, 72.5, 72.3, 70.5, 67.8, 29.44, 29.42, 16.6, 13.6; HRMS (ESI) calc'd for $C_{29}H_{33}O_7N_2$ $[M+H]^+$ *m/z* 521.2282, found 521.2297.

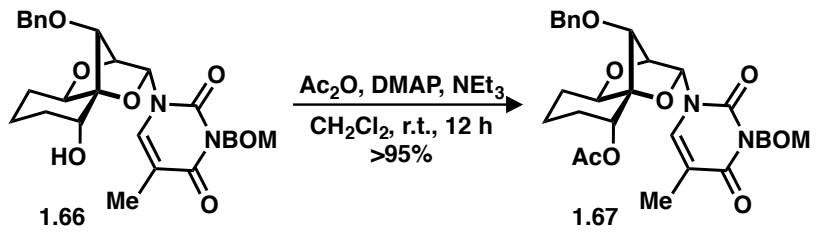

(2*S*,3*R*,4a*S*,5*R*,8a*R*,9*R*)-9-(Benzyloxy)-3-(3-((benzyloxy)methyl)-5-methyl-2,4-dioxo-3,4-dihydropyrimidin-1(2*H*)-yl)hexahydro-5*H*-2,4a-methanobenzo[*b*][1,4]dioxin-5-yl acetate (1.67).

Triethylamine (0.36 mL, 2.6 mmol), acetic anhydride (0.69 mL, 6.9 mmol) and 4-(dimethylamino)pyridine (0.05 g, 0.4 mmol) were added to a stirred solution of **1.66** (0.451 g, 0.87 mmol) in dichloromethane (14 mL). After 12 h, the reaction mixture was partitioned between dichloromethane (20 mL) and water (25 mL), the layers were separated, and the aqueous portion extracted with dichloromethane (2 × 50 mL). The combined organic extracts were washed with 1 M hydrochloric acid (50 mL), a saturated aqueous solution of sodium bicarbonate (50 mL), and brine (50 mL), dried over magnesium sulfate, filtered, and concentrated under reduced pressure. The residue was purified by flash column chromatography (15 × 2 cm) on silica gel (1:2 ethyl acetate–hexanes) to afford **1.67** as a colorless solid (0.47 g, >95% yield): R_f 0.55 (1:1 ethyl acetate–hexanes); $[\alpha]_D^{20}$ +32.9 (*c* = 0.14, chloroform); IR (film, cm^{-1}) ν 2926, 1740, 1707, 1666, 1071; ^1H NMR (400 MHz, chloroform-*d*) δ 7.46–7.23 (m, 11H), 5.68 (d, *J* = 0.8 Hz, 1H) 5.67–5.64 (m, 1H), 5.49 (d, *J* = 9.8 Hz, 1H), 5.45 (d, *J* = 9.7 Hz, 1H), 4.89 (s, 1H), 4.74 (d, *J* = 11.8 Hz, 1H), 4.69 (s, 2H), 4.54 (d, *J* = 11.8 Hz, 1H), 4.14–4.08 (m, 2H), 2.12 (s, 3H), 2.11–2.00 (m, 1H), 1.98 (s, 3H), 1.94–1.84 (m, 3H), 1.66–1.53 (m, 2H); ^{13}C NMR (101 MHz, chloroform-*d*) δ 169.7, 163.6, 151.0, 138.0, 136.7, 133.7, 128.8, 128.4, 128.3, 127.9, 127.8, 127.6, 109.1, 87.8, 86.3, 82.1, 81.3, 76.9, 72.5, 72.3, 70.4, 69.5, 29.3, 28.1, 21.2, 17.2, 13.9; HRMS (ESI) calc'd for $C_{31}H_{35}O_8N_2$ $[M+H]^+$ *m/z* 563.2388, found 563.2400.

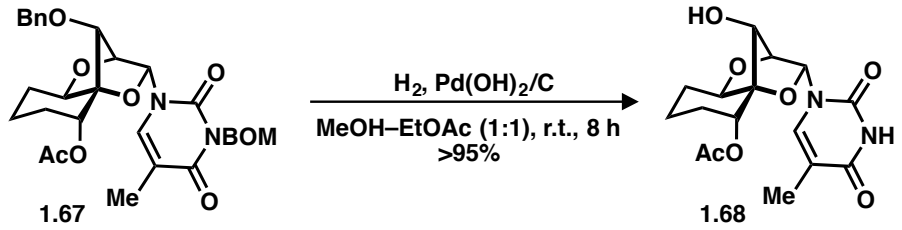

(2*S*,3*R*,4a*S*,5*R*,8a*R*,9*R*)-9-Hydroxy-3-(5-methyl-2,4-dioxo-3,4-dihydropyrimidin-1(2*H*)-yl)hexahydro-5*H*-2,4a-methanobenzo[*b*][1,4]dioxin-5-yl acetate (1.68).

Palladium hydroxide on carbon (0.01 g, 20% (w/w)) was added to a stirred solution of **1.67** (0.166 g, 0.295 mmol) in 1:1 methanol–ethyl acetate (20 mL). The suspension was purged with hydrogen gas and maintained under an atmosphere of hydrogen gas with a hydrogen-filled balloon. After 8 h, the reaction mixture was diluted with ethyl acetate (10 mL), filtered through a pad of Celite® 545, and concentrated under reduced pressure. The residue was purified by flash column chromatography (16 × 1 cm) on silica gel (9:1 ethyl acetate–hexanes) to afford **1.68** as a colorless foam (0.104 g, >95% yield): R_f 0.47 (9:1 ethyl acetate–hexanes); $[\alpha]_D^{20}$ +109 (*c* = 0.31, methanol); IR (film, cm^{-1}) ν 3410, 2935, 1701, 1269, 1057; ^1H NMR (400 MHz, methanol-d_4) δ 7.58 (d, *J* = 0.7 Hz, 1H), 5.73 (d, *J* = 0.7 Hz, 1H), 5.61 (s, 1H), 4.55 (s, 1H), 4.37 (s, 1H), 4.17 (dd, *J* = 10.5, 7.5 Hz, 1H), 2.17–2.07 (m, 4H), 1.98–1.89 (m, 4H), 1.88–1.80 (m, 2H), 1.71–1.51 (m, 2H); ^{13}C NMR (methanol-d_4) δ 171.6, 166.4, 152.0, 137.0, 110.1, 88.3, 87.5, 82.3, 81.4, 76.9, 71.2, 30.2, 28.9, 21.0, 18.3, 12.8; HRMS (ESI) calc'd for $C_{16}H_{21}O_7N_2$ $[M+H]^+$ *m/z* 353.1343, found 353.1345.

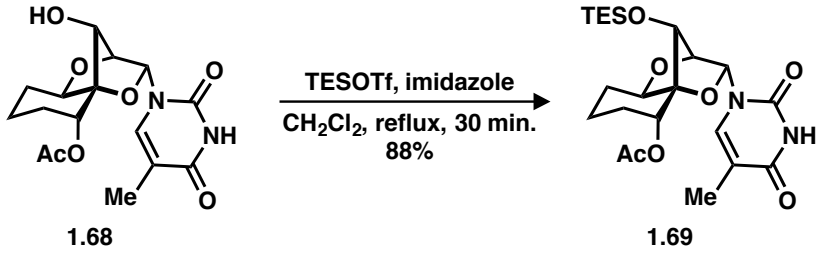

(2*S*,3*R*,4a*S*,5*R*,8a*R*,9*R*)-3-(5-Methyl-2,4-dioxo-3,4-dihydropyrimidin-1(2*H*)-yl)-9-((triethylsilyl)oxy)hexahydro-5*H*-2,4a-methanobenzo[*b*][1,4]dioxin-5-yl acetate (1.69).

Imidazole (0.106 g, 1.56 mmol) and triethylsilyl trifluoromethanesulfonate (0.142 mL, 0.780 mmol) were added to a stirred solution of **1.68** (0.090 g, 0.26 mmol) in dichloromethane (12 mL). The resulting solution was heated to reflux for 30 minutes, cooled to room temperature,

and partitioned between dichloromethane (50 mL) and water (50 mL). The layers were separated and the aqueous portion was extracted with dichloromethane (2 × 50 mL). The combined organic extracts were washed with 0.5 M hydrochloric acid (50 mL), a saturated aqueous solution of sodium bicarbonate (50 mL), and brine (50 mL), dried over magnesium sulfate, filtered, and concentrated under reduced pressure. The residue was purified by flash column chromatography (14 × 1 cm) on silica gel (1:1 ethyl acetate–hexanes) to afford thymidine **1.69** as a colorless oil (0.121 g, 88% yield): R_f 0.40 (1:1 ethyl acetate–hexanes); $[\alpha]_D^{20}$ +56.5 (*c* = 0.57, chloroform); IR (film, cm^{-1}) ν 3207, 2955, 1694, 1463, 1233, 1066; ^1H NMR (400 MHz, chloroform-*d*) δ 9.68 (br s, 1H), 7.42 (d, *J* = 1.1 Hz, 1H), 5.73 (d, *J* = 1.2 Hz, 1H), 5.58 (t, *J* = 2.5 Hz, 1H), 4.52 (s, 1H), 4.27 (s, 1H), 4.11 (dd, *J* = 10.6, 7.3 Hz, 1H), 2.09 (s, 3H), 2.08–1.99 (m, 1H), 1.93 (s, 3H), 1.93 (d, *J* = 1.0 Hz, 3H), 1.91–1.80 (m, 3H), 1.67–1.48 (m, 2H), 0.96 (t, *J* = 7.9 Hz, 9H), 0.65 (q, *J* = 7.8 Hz, 6H); ^{13}C NMR (101 MHz, chloroform-*d*) δ 169.7, 164.3, 150.5, 135.1, 109.6, 86.9, 86.3, 81.2, 80.0, 76.6, 69.7, 29.2, 28.0, 21.1, 17.2, 13.0, 6.7, 4.6; HRMS (ESI) calc'd for $C_{22}H_{35}O_7N_2Si$ $[M+H]^+$ *m/z* 467.2208, found 467.2216.

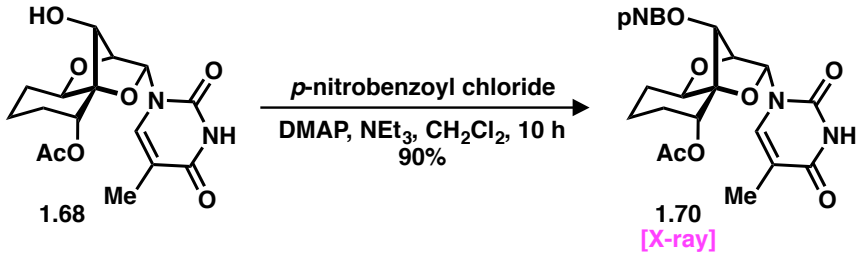

(2*S*,3*R*,4a*S*,5*R*,8a*R*,9*R*)-5-Acetoxy-3-(5-methyl-2,4-dioxo-3,4-dihydropyrimidin-1(2*H*)-yl)hexahydro-5*H*-2,4a-methanobenzo[*b*][1,4]dioxin-9-yl 4-nitrobenzoate (1.70).

Triethylamine (52 μL, 0.56 mmol), *p*-nitrobenzoyl chloride (0.061 g, 0.31 mmol) and 4-(dimethylamino)pyridine (0.008 g, 0.6 mmol) were added to a solution of **1.68** (0.044 g, 0.12 mmol) in dichloromethane (2 mL). After 10 h, the reaction mixture was partitioned between dichloromethane (5 mL) and water (5 mL), the layers were separated, and the aqueous layer was extracted with dichloromethane (2 × 5 mL). The combined organic extracts were washed with 1 M hydrochloric acid (5 mL), a saturated aqueous solution of sodium bicarbonate (5 mL), and brine (5 mL), dried through a phase separator cartridge, and concentrated under

reduced pressure. The residue was purified by flash column chromatography (14 × 1 cm) on silica gel (3:1 ethyl acetate–hexanes) to afford **1.70** as a colorless solid (0.057 g, 90% yield): R_f 0.22 (2:1 ethyl acetate–hexanes); m.p. 213–214 °C (ethyl acetate–hexanes); $[\alpha]_D^{20}$ +42.3 (*c* = 1.0, chloroform); IR (KBr disc, cm^{-1}) ν 3310, 3104, 2958, 1735, 1711, 1684, 1607, 1527, 1346, 1267, 1232, 1105, 1073, 1022; ^{1}H NMR (300 MHz, chloroform-*d*) δ 8.78 (s, 1H), 8.36 (d, *J* = 8.9 Hz, 2H), 8.21 (d, *J* = 8.9 Hz, 2H), 7.45 (d, *J* = 1.1 Hz, 1H), 5.86 (d, *J* = 1.2 Hz, 1H), 5.79–5.77 (m, 1H), 5.51 (s, 1H), 5.07 (s, 1H), 4.26 (dd, *J* = 10.4, 7.3 Hz, 1H), 2.15 (s, 3H), 2.14–2.05 (m, 1H), 1.98 (s, 3H), 1.97–1.58 (m, 4H), 1.57–1.43 (m, 1H); ^{13}C NMR (75 MHz, chloroform-*d*) δ 169.4, 163.7, 163.5, 151.3, 150.1, 134.7, 133.9, 131.1, 124.2, 110.1, 87.0, 86.5, 80.7, 78.7, 76.4, 68.4, 29.6, 28.5, 21.1, 17.0, 13.2; HRMS (ESI) calc'd for $C_{23}H_{24}O_{10}N_3$ $[M+H]^+$ m/z 502.1456, found 502.1455. Recrystallization from ethyl acetate–hexanes afforded crystals that were suitable for X-ray crystallography.

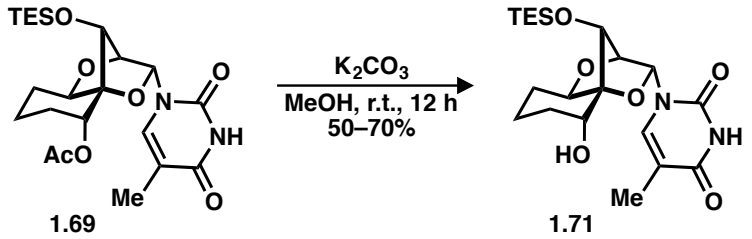

1-((2*S*,3*R*,4a*R*,5*R*,8a*R*,9*R*)-5-hydroxy-9-((triethylsilyl)oxy)hexahydro-5*H*-2,4a-methano-benzo[*b*][1,4]dioxin-3-yl)-5-methylpyrimidine-2,4(1*H*,3*H*)-dione (1.71).

Potassium carbonate (3 mg, 0.03 mmol) was added to a stirred solution of **1.69** (118 mg, 0.253 mmol) in methanol (3 mL). After 12 h, water (0.5 mL) was added and the resulting mixture was partitioned between ethyl acetate (25 mL) and water (25 mL). The layers were separated and the aqueous portion was extracted with ethyl acetate (3 × 25 mL). The combined organic extracts were washed with brine, dried over magnesium sulfate, filtered, and concentrated under reduced pressure. The residue was purified by flash column chromatography (17 × 1 cm) on silica gel (2:1 ethyl acetate–hexanes) to afford alcohol **1.71** as a colorless oil (75 mg, 70% yield): R_f 0.17 (1:1 ethyl acetate–hexanes); $[\alpha]_D^{20}$ +38.5 (*c* = 0.33, chloroform); IR (film, cm^{-1}) ν 3444, 3204, 2955, 1694, 1273, 1064; ^{1}H NMR (400 MHz, chloroform-*d*) δ 9.49 (br s, 1H), 7.54 (s, 1H), 5.88 (s, 1H), 4.44 (s, 1H), 4.36 (s, 1H), 4.26–4.16 (m, 2H), 2.70 (br s, 1H),

2.10–1.97 (m, 1H), 1.93 (s, 3H), 1.90–1.64 (m, 4H), 1.52–1.43 (m, 1H), 0.96 (t, J = 7.9 Hz, 9H), 0.65 (q, J = 7.9 Hz, 6H); ^{13}C NMR (101 MHz, chloroform-*d*) δ 164.2, 150.7, 135.5, 110.0, 88.8, 86.5, 81.4, 80.1, 76.5, 67.8, 29.4, 16.6, 12.8, 6.7, 4.7; HRMS (ESI) calc'd for $C_{20}H_{33}O_6N_2Si$ $[M+H]^+$ *m/z* 425.2112, found 425.2102.

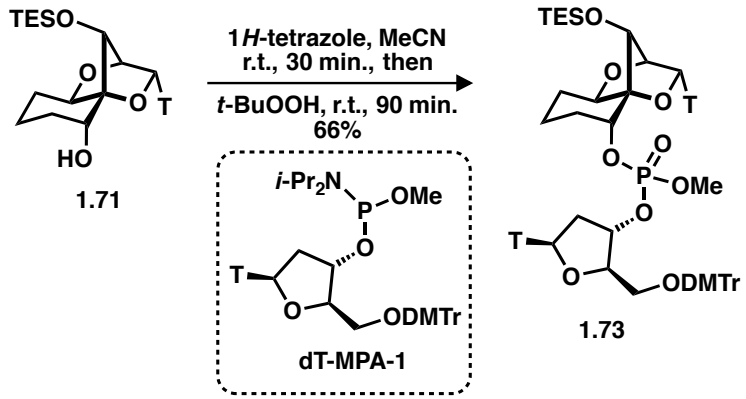

(2*R*,3*S*,5*R*)-2-((Bis(4-methoxyphenyl)(phenyl)methoxy)methyl)-5-(5-methyl-2,4-dioxo-3,4-dihydropyrimidin-1(2*H*)-yl)tetrahydrofuran-3-yl methyl ((2*S*,3*R*,4a*R*,5*R*,8a*R*,9*R*)-3-(5-methyl-2,4-dioxo-3,4-dihydropyrimidin-1(2*H*)-yl)-9-((triethylsilyl)oxy)hexahydro-5*H*-2,4a-methanobenzo[*b*][1,4]dioxin-5-yl) phosphate (1.73).

1*H*-Tetrazole (0.19 g, 2.6 mmol) was added to a stirred solution of **1.71** (0.11 g, 0.26 mmol) and dT-Methyl phosphoramidite (**dT-MPA-1**) (0.55 g, 0.78 mmol) in anhydrous acetonitrile (4.3 mL). After 30 minutes, an acetonitrile solution of *tert*-butyl hydroperoxide (0.71 mL, 2.2 M) was added and stirring was continued at room temperature for an additional 90 minutes. The reaction was then diluted with ethyl acetate (30 mL) and the resulting mixture was washed with water and brine, dried over sodium sulfate, and concentrated under reduced pressure. The residue was purified by reverse phase column chromatography on a Biotage KP-C18-HS 12M column with a gradient of 40–60% acetonitrile/water. Fractions containing dimer **1.73** were then combined and concentrated under reduced pressure to remove most of the acetonitrile. The resulting white suspension was diluted with ethyl acetate (100 mL), washed with water and brine, concentrated under reduced pressure to provide dimer **1.73** (0.18 g, 66%) as a mixture of diastereomers at phosphorus: ^{31}P NMR (121 MHz, chloroform-*d*) δ –1.14, –1.52; HRMS (QTOF) calc'd for $C_{52}H_{64}N_4O_{15}PSi$ $[M–H]^–$ *m/z* 1043.3875, found 1043.3971.

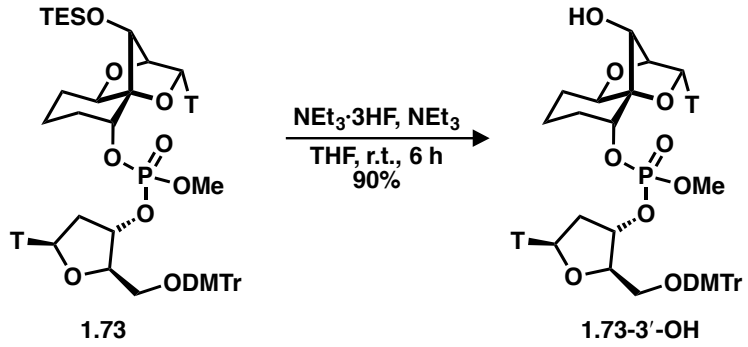

(2*R*,3*S*,5*R*)-2-((Bis(4-methoxyphenyl)(phenyl)methoxy)methyl)-5-(5-methyl-2,4-dioxo-3,4-dihydropyrimidin-1(2*H*)-yl)tetrahydrofuran-3-yl ((2*S*,3*R*,4a*S*,5*R*,8a*R*,9*R*)-9-hydroxy-3-(5-methyl-2,4-dioxo-3,4-dihydropyrimidin-1(2*H*)-yl)hexahydro-5*H*-2,4a-methanobenzo[*b*][1,4]dioxin-5-yl) methyl phosphate (1.73-3′-OH).

Triethylamine trihydrofluoride (0.08 mL, 0.5 mmol) was added to a stirred solution of dimer **1.73** (1.75 g, 0.170 mmol) and triethylamine (0.03 mL, 0.2 mmol) in tetrahydrofuran (1 mL). After 6 h, the reaction mixture was concentrated under reduced pressure and the residue was purified by flash column chromatography (7 × 2 cm) on silica gel (5–10% methanol–dichloromethane) to afford alcohol **1.73-3′-OH** as a mixture of diastereomers at phosphorus (0.13 g, 90% yield): ^{31}P NMR (121 MHz, chloroform-*d*) δ –2.26, –3.50; HRMS (QTOF) calc'd for $C_{46}H_{50}N_4O_{15}P$ $[M–H]^-$ *m/z* 929.3010, found 929.3099.

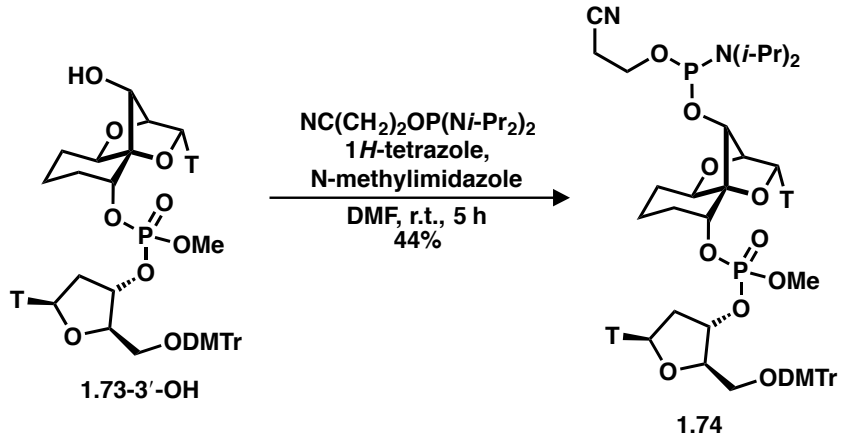

(2*S*,3*R*,4a*S*,5*R*,8a*R*,9*R*)-5-(((((2*R*,3*S*,5*R*)-2-((Bis(4-methoxyphenyl)(phenyl)methoxy)-methyl)-5-(5-methyl-2,4-dioxo-3,4-dihydropyrimidin-1(2*H*)-yl)tetrahydrofuran-3-yl)oxy)(methoxy)phosphoryl)oxy)-3-(5-methyl-2,4-dioxo-3,4-dihydropyrimidin-1(2*H*)-

yl)hexahydro-5*H*-2,4a-methanobenzo[*b*][1,4]dioxin-9-yl (2-cyanoethyl) diisopropylphosphoramidite (1.74).

2-Cyanoethyl *N*,*N*,*N*′,*N*′-tetraisopropylphosphorodiamidite (0.08 mL) was added to a stirred *N*,*N*-dimethylformamide (0.7 mL) solution of **1.73-3′-OH** (0.125 g, 0.134 mmol), *N*-methylimidazole (5 μL, 0.07 mmol), and 1*H*-tetrazole (8.7 mg, 0.12 mmol). After 5 h, the reaction mixture was diluted with ethyl acetate (15 mL) and the resulting solution was washed with brine, dried over sodium sulfate, and concentrated under reduced pressure. The residue was purified by flash column chromatography (7 × 2 cm) on silica gel (20–60% acetone/dichloromethane) to afford **1.74** as a mixture of diastereomers at phosphorus (0.066 g, 44% yield): ^{31}P NMR (121 MHz, chloroform-*d*) δ 150.08, 149.98, 149.69, 149.38, –1.32, –1.41, –1.62, –1.78; HRMS (QTOF) calc'd for $C_{55}H_{69}N_6O_{16}P_2$ $[M–H]^-$ *m/z* 1129.4089, found 1129.4159.

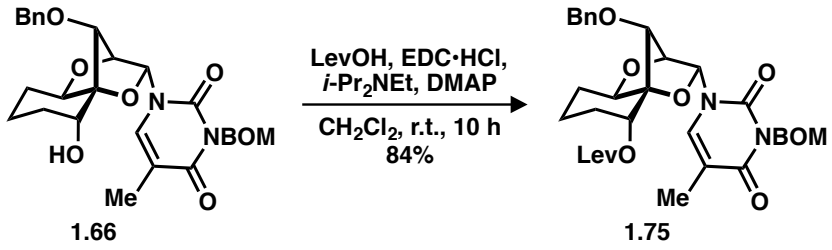

1.66 1.75

(2*S*,3*R*,4a*S*,5*R*,8a*R*,9*R*)-9-(Benzyloxy)-3-(3-((benzyloxy)methyl)-5-methyl-2,4-dioxo-3,4-dihydropyrimidin-1(2*H*)-yl)hexahydro-5*H*-2,4a-methanobenzo[*b*][1,4]dioxin-5-yl 4-oxopentanoate (1.75).

Levulinic acid (0.11 mL, 1.1 mmol), *N*-(3-dimethyl-aminopropyl)-*N*′-ethylcarbodiimide hydrochloride (0.16 g, 0.84 mmol), 4-(dimethylamino)pyridine (0.05 g, 0.4 mmol), and *N*,*N*-diisopropylethylamine (0.29 mL, 1.7 mmol) were added to a stirred solution of **1.66** (0.29 g, 0.56 mmol) in dichloromethane (26.5 mL). After 10 h, the reaction mixture was partitioned between dichloromethane (40 mL) and 1 M hydrochloric acid (25 mL). The layers were separated, and the organic portion was further washed with 1 M hydrochloric acid (50 mL × 2), a saturated aqueous solution of sodium bicarbonate (25 mL), and brine (50 mL), dried over magnesium sulfate, filtered, and concentrated under reduced pressure. The residue was purified by flash column chromatography (12 × 2 cm) on silica gel (1:1 ethyl acetate–hexanes)

to afford **1.75** as a colorless solid (0.29 g, 84% yield): R_f 0.53 (3:1 ethyl acetate–hexanes); $[\alpha]_D^{20}$ +85.2 (*c* = 0.4, chloroform); IR (solid, cm^{-1}) ν 2955, 1728, 1707, 1647, 1072; ^{1}H NMR (400 MHz, chloroform-*d*) δ 7.61 (d, *J* = 1.2 Hz, 1H), 7.41–7.29 (m, 9H), 7.29–7.26 (m, 1H), 5.67 (d, *J* = 1.3 Hz, 1H), 5.65 (t, *J* = 2.8 Hz, 1H), 5.50 (d, *J* = 9.7 Hz, 1H), 5.45 (d, *J* = 9.7 Hz, 1H), 4.93 (d, *J* = 1.1 Hz, 1H), 4.74 (d, *J* = 11.9 Hz, 1H), 4.69 (s, 2H), 4.53 (d, *J* = 11.9 Hz, 1H), 4.15–4.07 (m, 2H), 2.82–2.75 (m, 2H), 2.66–2.61 (m, 2H), 2.19 (s, 3H), 2.14–2.02 (m, 1H), 2.00 (d, *J* = 1.1 Hz, 3H), 1.98–1.82 (m, 3H), 1.66–1.56 (m, 2H); ^{13}C NMR (75 MHz, chloroform-*d*) δ 206.3, 171.6, 163.7, 151.1, 138.1, 136.7, 134.2, 128.8, 128.44, 128.36, 127.9, 127.8, 127.7, 109.3, 88.0, 86.4, 82.0, 81.2, 76.9, 72.5, 72.3, 70.4, 69.7, 38.0, 30.0, 29.3, 28.2, 28.1, 17.3, 13.6; HRMS (ESI) calc'd for $C_{34}H_{39}O_9N_2$ $[M+H]^+$ *m/z* 619.2650, found 619.2650.

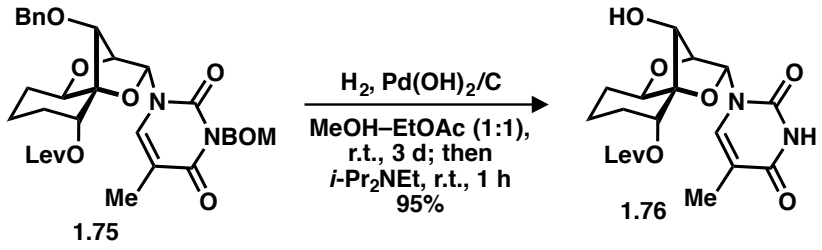

(2*S*,3*R*,4a*S*,5*R*,8a*R*,9*R*)-9-Hydroxy-3-(5-methyl-2,4-dioxo-3,4-dihydropyrimidin-1(2*H*)-yl)hexahydro-5*H*-2,4a-methanobenzo[*b*][1,4]dioxin-5-yl 4-oxopentanoate (1.76).

Palladium hydroxide on carbon (0.066 g, 20% (w/w)) was added to a stirred solution of **1.75** (0.29 g, 0.47 mmol) in 1:1 methanol–ethyl acetate (31 mL). The suspension was purged with hydrogen gas and maintained under an atmosphere of hydrogen gas with a hydrogen-filled balloon. After 3 d, *N*,*N*-diisopropylethylamine (0.10 mL, 0.61 mmol) was added and the mixture stirred for an additional 1 h. The reaction mixture was filtered through a pad of Celite® 545 (1 × 2 cm, h × d), and concentrated under reduced pressure. The residue was purified by flash column chromatography (16 × 1 cm) on silica gel (9:1 ethyl acetate–hexanes) to afford **1.76** as a colorless foam (0.104 g, >95% yield): R_f 0.14 (1:20 methanol–dichloromethane); $[\alpha]_D^{20}$ +229.0 (*c* = 0.2, methanol); IR (solid, cm^{-1}) ν 3208, 2941, 1700, 1646, 1629, 1051; ^{1}H NMR (400 MHz, chloroform-*d*) δ 9.59 (s, 1H), 7.64 (d, *J* = 0.9 Hz, 1H), 5.68 (s, 2H), 4.77 (s, 1H), 4.40 (s, 1H), 4.13 (dd, *J* = 10.2 Hz, 7.8, 1H), 2.84–2.73 (m, 2H), 2.68–2.60 (m, 2H), 2.19 (s, 3H), 2.06–1.76 (m, 8H), 1.69 – 1.54 (m, 2H); ^{13}C NMR (101

MHz, chloroform-*d*) δ 206.7, 171.8, 164.5, 150.7, 135.8, 110.0, 87.2, 86.6, 81.1, 80.3, 76.1, 70.0, 38.0, 30.0, 29.5, 28.2, 28.0, 17.4, 12.9; HRMS (ESI) calc'd for $C_{19}H_{25}O_8N_2$ $[M+H]^+$ *m/z* 409.1605, found 409.1623.

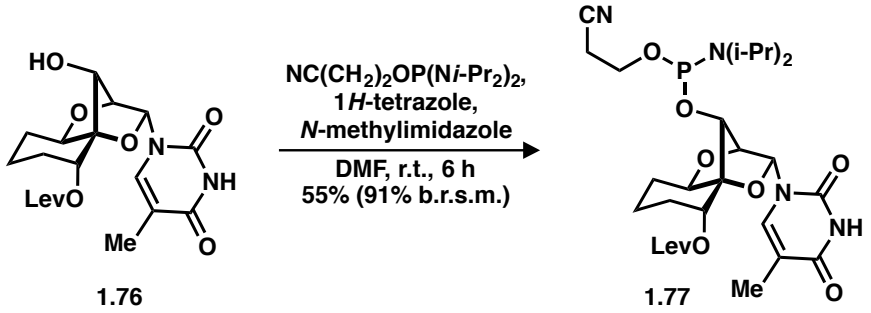

(2*S*,3*R*,4a*S*,5*R*,8a*R*,9*R*)-9-(((2-cyanoethoxy)(diisopropylamino)phosphanyl)oxy)-3-(5-methyl-2,4-dioxo-3,4-dihydropyrimidin-1(2*H*)-yl)hexahydro-5*H*-2,4a-methanobenzo-[*b*][1,4]dioxin-5-yl 4-oxopentanoate (1.77).

2-Cyanoethyl *N*,*N*,*N*′,*N*′-tetraisopropylphosphorodiamidite (0.17 mL, 0.57 mmol) was added to a stirred solution of **1.76** (0.154 g, 0.38 mmol), *N*-methylimidazole (8 μL, 0.1 mmol), and 1*H*-tetrazole (22 mg, 0.30 mmol) in *N*,*N*-dimethylformamide (1.9 mL). After 6 h, the reaction mixture was diluted with ethyl acetate (10 mL) and the resulting solution was washed with brine, dried over sodium sulfate, and concentrated under reduced pressure. The residue was purified by flash column chromatography (2.5 X 8 cm) on silica gel (95% ethyl acetate–hexanes) to afford unreacted alcohol **1.76** (55 mg, 36%) and phosphoramidite **1.77** (127 mg, 55% yield): ^{31}P NMR (121 MHz, chloroform-*d*) δ 150.05, 149.69; LRMS (ESI) calc'd for $C_{28}H_{42}N_4O_9P$ $[M+H]^+$ *m/z* 609.3, found 609.2.

Details for the Synthesis of Oligonucleotides Containing α-L-TriNA 1

Oligonucleotide syntheses: ONs were synthesized on an ABI 394 DNA/RNA Synthesizer. ONs were made on a 2 μmol scale using UnyLinker™ support. Standard conditions were used for incorporation of DNA amidites, *i.e.* 3% dichloroacetic acid (DCA) in dichloromethane for deblocking; 1 M 4,5-dicyanoimidazole, 0.1 M *N*-methylimidazole in acetonitrile, 0.1 M DNA amidite in acetonitrile, 2 × 4 min. coupling times for coupling; Cap A: acetic acid in tetrahydrofuran, Cap B: 10% *N*-methylimidazole in tetrahydrofuran/pyridine for capping and 10% *tert*-butyl hydroperoxide in acetonitrile for oxidation (10 min). Incorporation of the α-L-LNA building block was similar to DNA cycles except for prolonged coupling time (2 × 6 min). **A4**, **A7**, **A9**, and **A12** were synthesized on 1 μmol scale. Incorporation of DNA amidites were carried out using identical conditions as those described above. To incorporate phosphoramidite **1.77** and dimer **1.74**, they were dissolved in dichloromethane and dfurther diluted to 0.08 M, before they were mixed with 0.5 M 5-(ethylthio)tetrazole in acetonitrile (0.6 mL) prior to contact with the solid support. The synthesis column was removed from the synthesizer and the coupling was carried out manually by passing the solution through the column using syringes. Coupling time was extended to 30 min. resulting in >95% coupling efficiency for phosphoramidite **1.77**. Deprotection of the 5′-levulinyl protecting groups in **A7**, **A9** and **A12** were performed manually by passing a solution of 0.5 M hydrazine in pyridine–acetic acid 1:1 (v/v) through the synthesis column using syringes over 10 min. The synthesis column was then placed back on the synthesizer to complete the remainder of the synthesis. After synthesis, the final DMT was cleaved, cyanoethyl protecting groups were removed using triethylamine–acetonitrile 1:1 (v/v) and remaining protecting groups were removed using conc. aq. ammonia at 55 °C for 8 h. ONs were purified using IE-HPLC using a linear gradient of buffer A and B. Buffer A: 50 mM $NaHCO_3$ in acetonitrile–water 3:7 (v/v), Buffer B: 1.5 M NaBr, 50 mM $NaHCO_3$ in acetonitrile–water 3:7 (v/v). Purified ONs were desalted using C18 reverse phase cartridges.

Analytical data for oligonucleotides

Entry	Sequence (5′ to 3′)[a]	Modification	Mass (calc.)	Mass (exp.)	UV Purity
A1	d(GCGTTTTTTGCT)	DNA	3633.4	3632.9	-
A2	d(GCGTT**T**TTTGCT)	α-L-LNA (**1.11**)	3661.4	3660.6	98.7
A3	d(GCGTT**T**TTTGCT)	α-L-TriNA 1 (**1.27**)	3701.5	3700.5	98.9
A4	d(GCGTT**T**TTTGCT)	α-L-TriNA 2 (**1.28**)	3701.5	3700.9	-
A5	d(CCAGTGATATGC)	DNA	3645.5	3645.2	-
A6	d(CCAG**T**GATATGC)	α-L-LNA (**1.11**)	3673.5	3672.6	95.9
A7	d(CCAG**T**GATATGC)	α-L-TriNA 1 (**1.27**)	3713.5	3712.7	98.0
A8	d(CCAGTGA**T**ATGC)	α-L-LNA	3673.5	3672.6	95.0
A9	d(CCAGTGA**T**ATGC)	α-L-TriNA 1 (**1.27**)	3713.5	3712.7	98.1
A10	d(CCAGTGA**T**ATGC)	α-L-TriNA 2 (**1.28**)	3713.5	3712.9	-
A11	d(CCAGTGATA**T**GC)	α-L-LNA	3673.5	3672.6	92.7
A12	d(CCAGTGATA**T**GC)	α-L-TriNA 1 (**1.27**)	3713.5	3712.7	99.3

[a]Boldface and underlined letters indicate site of modified nucleotide, base code: T = thymine, U = uracil, C = cytosine, A = adenine and G = guanine. DNA oligonucleotides **A1** and **A5** were purchased by commercial vendors and used as supplied.

***T*m Measurements.** For the T_m experiments, oligonucleotides were prepared at a concentration of 8 μM in a buffer of 100 mM NaCl, 10 mM phosphate, 0.1 mM EDTA at pH 7. The concentration of oligonucleotides was determined at 85 °C. The final oligonucleotide concentration was 4 μM with mixing of equal volumes of test oligonucleotide and complementary RNA strand. Oligonucleotides were hybridized with the complementary RNA strand by heating duplex to 90 °C for 5 min and allowed to cool to room temperature. Using the spectrophotometer, T_m measurements were taken by heating duplex solution at a rate of 0.5 °C/min in cuvette starting at 15 °C and heating to 85 °C. T_m values were determined using van't Hoff calculations (A_{260} *vs* temperature curve) using non self-complementary sequences where the minimum absorbance which relates to the duplex and the maximum absorbance which relates to the non-duplex single strand are manually integrated into the program.

Experimental Procedures for TriNA 1

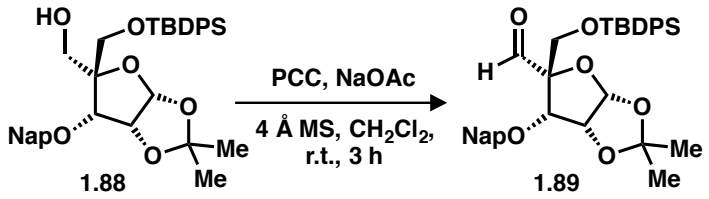

(3a*R*,5*R*,6*S*,6a*R*)-5-(((*tert*-butyldiphenylsilyl)oxy)methyl)-2,2-dimethyl-6-(naphthalen-2-ylmethoxy)tetrahydrofuro[2,3-*d*][1,3]dioxole-5-carbaldehyde (1.89).

Pyridinium chlorochromate (17.8 g, 82.7 mmol) was added to a stirred, room-temperature mixture of alcohol **1.88** (16.5 g, 27.6 mmol), sodium acetate (6.9 g, 84 mmol), and powdered 4 Å molecular sieves (13.8 g) in anhydrous dichloromethane (170 mL). The reaction mixture was stirred at room temperature for a period of 3 h, at which point diethyl ether and silica gel were added and the resulting mixture was stirred for an additional 20 minutes. The mixture was filtered through a short pad of silica gel and eluted with dichloromethane before the filtrate was concentrated under reduced pressure to afford a clear oil (16.5 g, crude) that often crystallized upon standing, and which was used directly in the next step without purification. A portion of the residue was purified by flash column chromatography on silica gel (1:9 ethyl acetate–hexane) to afford **2** as a white solid: R_f 0.32 (1:9 ethyl acetate–hexanes); $[\alpha]^{20}_D$ +5.4 (*c* = 0.25, chloroform); IR (thin film, cm^{-1}) ν 3051, 2931, 2857, 1730, 1427, 1383, 1215, 1112, 1021; ^{1}H NMR (400 MHz, chloroform-*d*) δ 9.95 (s, 1H), 7.87–7.77 (m, 4H), 7.62–7.55 (m, 4H), 7.53–7.47 (m, 3H), 7.44–7.38 (m, 2H), 7.37–7.31 (m, 4H), 5.87 (d, *J* = 3.3 Hz, 1H), 4.92 (d, *J* = 12.3 Hz, 1H), 4.81 (d, *J* = 12.3 Hz, 1H), 4.70–4.65 (m, 1H), 4.59 (d, *J* = 4.4 Hz, 1H), 3.91 (d, *J* = 11.4 Hz, 1H), 3.82 (d, *J* = 11.4 Hz, 1H), 1.66 (s, 3H), 1.39 (s, 3H), 0.93 (s, 9H); ^{13}C NMR (101 MHz, chloroform-*d*) δ 200.40, 135.69, 135.61, 134.57, 133.35, 133.29, 132.92, 132.66, 129.99, 129.93, 128.62, 128.05, 127.91, 127.88, 127.11, 126.39, 126.29, 125.78, 114.33, 105.03, 90.79, 79.14, 78.75, 73.09, 63.20, 26.80, 26.29, 19.30; HRMS (ESI) calc'd for $C_{36}H_{40}NaO_6Si$ $[M+Na]^+$ *m/z* 619.2486, found 619.2501.

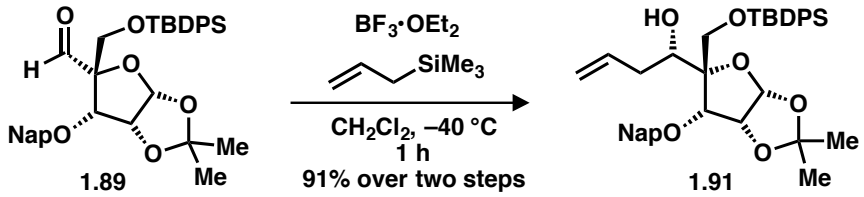

(*S*)-1-((3a*R*,5*S*,6*S*,6a*R*)-5-(((*tert*-butyldiphenylsilyl)oxy)methyl)-2,2-dimethyl-6-(naphthalen-2-ylmethoxy)tetrahydrofuro[2,3-*d*][1,3]dioxol-5-yl)but-3-en-1-ol (1.91).

Boron trifluoride diethyl etherate (6.9 mL, 55 mmol) was added to a stirred, –40 °C solution of crude aldehyde **1.89** (16.5 g, 27.6 mmol) in anhydrous dichloromethane (680 mL). The solution was stirred for 10 minutes before allyltrimethylsilane (7.0 mL, 44 mmol) was added dropwise. After 1 h the reaction mixture was poured into a saturated aqueous solution of sodium bicarbonate (300 mL) and warmed to room temperature. The layers were separated and the aqueous portion was extracted with dichloromethane (3 × 150 mL). The combined organic extracts were washed with brine (250 mL), dried over magnesium sulfate, filtered, and concentrated under reduced pressure. The residue was purified by flash column chromatography on silica gel (1:5 ethyl acetate–hexanes) to afford **1.91** as a white solid (16.1 g, 91% yield over two steps): R_f 0.31 (1:9 ethyl acetate–hexanes); $[\alpha]^{20}_D$ +9.9 (*c* = 0.15, chloroform); IR (thin film, cm^{-1}) ν 3543, 3071, 2933, 2857, 1641, 1471, 1428, 1382, 1373, 1214, 1166, 1112, 1026; ^{1}H NMR (400 MHz, chloroform-*d*) δ = 7.88–7.79 (m, 1H), 7.63–7.58 (m, 1H), 7.57–7.47 (m, 1H), 7.43–7.37 (m, 1H), 7.37–7.28 (m, 1H), 5.92–5.79 (m, 1H), 5.09–4.97 (m, 1H), 4.77 (dd, *J* = 5.1, 3.9 Hz, 1H), 4.72 (s, 1H), 4.69 (d, *J* = 5.2 Hz, 1H), 4.47 (dt, *J* = 10.9, 2.1 Hz, 1H), 3.97 (d, *J* = 11.2 Hz, 1H), 3.81 (d, *J* = 11.2 Hz, 1H), 3.36 (t, *J* = 2.2 Hz, 1H), 2.53 (dd, *J* = 14.4, 6.6 Hz, 1H), 1.97–1.85 (m, 1H), 1.65 (s, 3H), 1.40 (s, 3H), 0.91 (s, 9H); ^{13}C NMR (chloroform-*d*, 101 MHz) δ 136.53, 135.70, 135.61, 134.41, 133.41, 133.34, 133.25, 133.11, 129.87, 129.79, 128.87, 128.10, 127.89, 127.87, 127.81, 127.42, 126.49, 126.43, 125.82, 116.37, 113.89, 104.82, 88.34, 79.30, 78.23, 73.20, 72.68, 62.59, 34.77, 27.20, 26.85, 26.66, 19.27; HRMS (ESI) calc'd for $C_{39}H_{46}NaO_6Si$ $[M+Na]^+$ *m/z* 661.2956, found 661.2971.

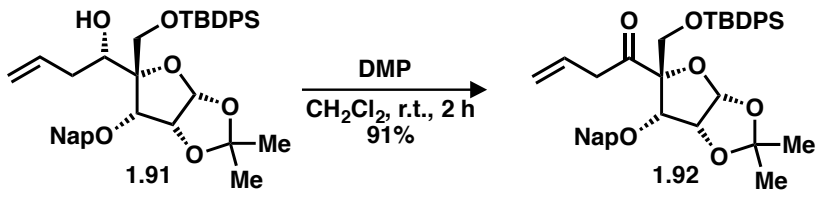

1-((3a*R*,5*R*,6*S*,6a*R*)-5-(((*tert*-Butyldiphenylsilyl)oxy)methyl)-2,2-dimethyl-6-(naphthalen-2-ylmethoxy)tetrahydrofuro[2,3-*d*][1,3]dioxol-5-yl)but-3-en-1-one (1.92).

Dess–Martin periodinane (10.0 g, 24.2 mmol) was added to a stirred, room-temperature solution of alcohol **1.91** (10.8 g, 16.9 mmol) in anhydrous dichloromethane (150 mL). The reaction mixture was stirred at room temperature for a period of 2 h, at which point it was filtered through a short pad of Celite® 545 and eluted with dichloromethane. The filtrate was concentrated under reduced pressure and purified by flash column chromatography on silica gel (1:9 to 1:6 ethyl acetate–hexane) to afford **1.92** as a colourless oil (9.7 g, 91%): R_f 0.43 (1:5 ethyl acetate–hexanes); $[\alpha]^{20}_D$ +52.0 (*c* = 1.0, chloroform); IR (KBr disc, cm^{-1}) ν 3072, 2932, 2858, 1718, 1428, 1382, 1217, 1113, 1027; ^{1}H NMR (400 MHz, chloroform-*d*) δ = 7.86–7.78 (m, 3H), 7.71 (s, 1H), 7.62–7.58 (m, 2H), 7.57–7.53 (m, 2H), 7.51–7.45 (m, 2H), 7.43–7.36 (m, 5H), 7.33–7.27 (m, 2H), 6.09 (d, *J* = 4.3 Hz, 1H), 6.00–5.87 (m, 1H), 5.13 (ddd, *J* = 10.3, 2.9, 1.2 Hz, 1H), 5.05 (ddd, *J* = 17.2, 3.1, 1.5 Hz, 1H), 4.90 (d, *J* = 11.9 Hz, 1H), 4.86 (dd, *J* = 5.6, 4.3 Hz, 1H), 4.63 (d, *J* = 11.9 Hz, 1H), 4.23 (d, *J* = 5.6 Hz, 1H), 3.92 (d, *J* = 10.8 Hz, 1H), 3.72–3.56 (m, 2H), 3.71 (d, *J* = 10.8 Hz, 1H), 1.62 (s, 3H), 1.44 (s, 3H), 0.99 (s, 9H); ^{13}C NMR (75 MHz, chloroform-*d*) δ 207.53, 135.64, 135.63, 135.03, 133.34, 133.17, 132.60, 132.57, 130.84, 130.10, 130.02, 128.23, 128.07, 127.98, 127.82, 126.68, 126.20, 126.04, 125.93, 118.55, 115.04, 107.06, 96.56, 81.27, 80.26, 73.66, 67.89, 45.07, 27.74, 26.93, 26.80, 19.25; HRMS (ESI) calc'd for $C_{39}H_{44}NaO_6Si$ $[M+Na]^+$ *m/z* 659.2799, found 659.2814.

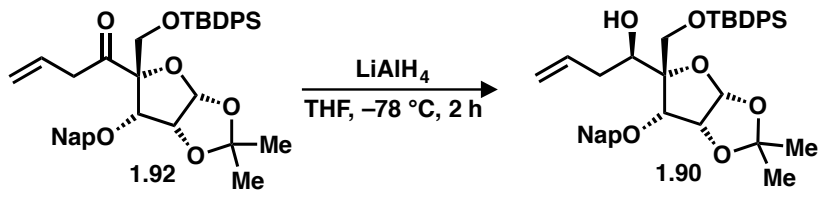

(*R*)-1-((3a*R*,5*S*,6*S*,6a*R*)-5-(((*tert*-Butyldiphenylsilyl)oxy)methyl)-2,2-dimethyl-6-(naphthalen-2-ylmethoxy)tetrahydrofuro[2,3-*d*][1,3]dioxol-5-yl)but-3-en-1-ol (1.90).

Lithium aluminum hydride (1.69 g, 44.6 mmol) was added portionwise to a stirred, –78 °C solution of ketone **1.92** (15.8 g, 24.8 mmol) in anhydrous tetrahydrofuran (500 mL). The reaction mixture was stirred at –78 °C for a period of 2 h, at which point water (1.69 mL), a 15% (w/v) aqueous solution of sodium hydroxide (1.69 mL), and water (5.07 mL) were sequentially added to the mixture, dropwise at –78 °C. The mixture was allowed to warm to room temperature and stirred for 15 min. Anhydrous magnesium sulfate was added and the mixture stirred for an additional 15 min, before the mixture was filtered and the solid washed with dichloromethane (3 × 25 mL). The filtrate was concentrated under reduced pressure to afford a clear oil (15.0 g, crude), which was used directly in the next step without purification. A portion of the residue was purified by flash column chromatography on silica gel (1:8 ethyl acetate–hexane) to afford **1.90** (88% yield for purified material) as a clear oil: R_f 0.31 (1:5 ethyl acetate–hexanes); $[\alpha]^{20}_D$ +22.8 (*c* = 0.5, chloroform); IR (KBr disc, cm^{-1}) ν 3545, 3071, 2931, 2857, 1641, 1428, 1384, 1216, 1113, 1021; ^{1}H NMR (300 MHz, chloroform-*d*) δ = 7.90–7.76 (m, 4H), 7.62–7.55 (m, 2H), 7.55–7.45 (m, 5H), 7.41–7.28 (m, 6H), 5.96–5.81 (m, 2H), 5.05–4.95 (m, 3H), 4.78 (dd, *J* = 5.3, 3.9 Hz, 1H), 4.64 (d, *J* = 11.9 Hz, 1H), 4.51 (d, *J* = 5.4 Hz, 1H), 4.18 (dd, *J* = 10.1, 2.3 Hz, 1H), 3.76 (d, *J* = 10.7 Hz, 1H), 3.53 (d, *J* = 10.7 Hz, 1H), 3.01 (br s, 1H), 2.34 (dd, *J* = 13.0, 6.3 Hz, 1H), 2.13–1.99 (m, 1H), 1.68 (s, 3H), 1.40 (s, 3H), 0.92 (s, 9H); ^{13}C NMR (75 MHz, chloroform-*d*) δ 136.53, 135.66, 135.64, 134.93, 133.35, 133.28, 133.01, 132.87, 129.97, 129.90, 128.54, 128.06, 127.90, 126.97, 126.41, 126.27, 125.80, 116.25, 114.50, 104.86, 90.28, 79.87, 78.25, 72.93, 71.17, 64.64, 36.04, 27.11, 26.94, 26.87, 19.25; HRMS (ESI) calc'd for $C_{39}H_{46}NaO_6Si$ $[M+Na]^+$ *m/z* 661.2956, found 661.2963.

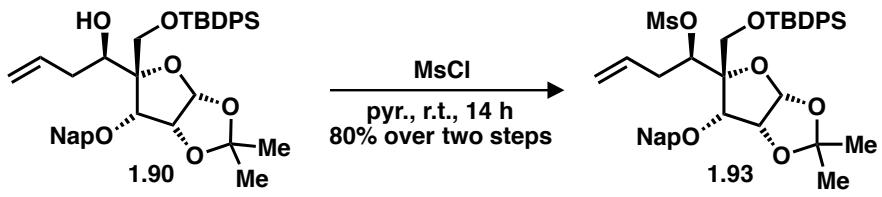

(*R*)-1-((3a*R*,5*R*,6*S*,6a*R*)-5-(((*tert*-Butyldiphenylsilyl)oxy)methyl)-2,2-dimethyl-6-(naphthalen-2-ylmethoxy)tetrahydrofuro[2,3-*d*][1,3]dioxol-5-yl)but-3-en-1-yl methanesulfonate (1.93).

Methanesulfonyl chloride (2.76 mL, 28.2 mmol) was added to a stirred mixture of 4-(dimethylamino)pyridine (0.30 g, 2.5 mmol) and crude **1.90** (15.0 g, 23.5 mmol) in pyridine (208 mL). The resulting solution was stirred at room temperature for 14 h before it was partitioned between dichloromethane (300 mL) and water (300 mL). The layers were separated and the aqueous portion was extracted with dichloromethane (3 × 100 mL). The combined organic extracts were washed sequentially with aqueous 1 M hydrochloric acid (3 × 200 mL), a saturated aqueous solution of sodium bicarbonate (200 mL), and brine (200 mL), dried over magnesium sulfate, filtered, and concentrated under reduced pressure. The residue was purified by flash column chromatography (23 × 7 cm) on silica gel (1:9 to 1:6 ethyl acetate–hexanes) to afford **1.93** as a colorless oil (15.1 g, 80% yield over two steps): R_f 0.23 (1:4 ethyl acetate–hexanes); $[\alpha]^{20}_D$ +2.4 (*c* = 1.0, chloroform); IR (KBr disc, cm^{-1}) ν 3071, 2933, 2858, 1644, 1472, 1428, 1384, 1358, 1334, 1174, 1113, 1020; ^{1}H NMR (300 MHz, chloroform-*d*) δ = 7.88–7.78 (m, 4H), 7.61–7.30 (m, 13H), 5.94 (d, *J* = 4.2 Hz, 1H), 5.85–5.69 (m, 1H), 5.23 (dd, *J* = 10.0, 1.8 Hz, 1H), 5.09–4.92 (m, 3H), 4.89 (dd, *J* = 5.4, 4.3 Hz, 1H), 4.60 (d, *J* = 11.7 Hz, 1H), 4.34 (d, *J* = 5.5 Hz, 1H), 3.85 (d, *J* = 10.9 Hz, 1H), 3.65 (d, *J* = 10.9 Hz, 1H), 3.08 (s, 3H), 2.77–2.65 (m, 1H), 2.13–1.98 (m, 1H), 1.67 (s, 3H), 1.42 (s, 3H), 0.98 (s, 9H); ^{13}C NMR (75 MHz, chloroform-*d*) δ 135.69, 135.68, 134.56, 133.57, 133.31, 133.28, 132.61, 132.60, 130.17, 130.10, 128.55, 128.06, 128.00, 127.90, 127.24, 126.48, 126.35, 126.00, 118.42, 114.88, 105.52, 89.30, 85.88, 81.02, 77.82, 73.23, 64.06, 39.37, 36.35, 27.27, 26.96, 26.80, 19.20; HRMS (ESI) calc'd for $C_{40}H_{48}NaO_8SSi$ $[M+Na]^+$ *m/z* 739.2731, found 739.2728.

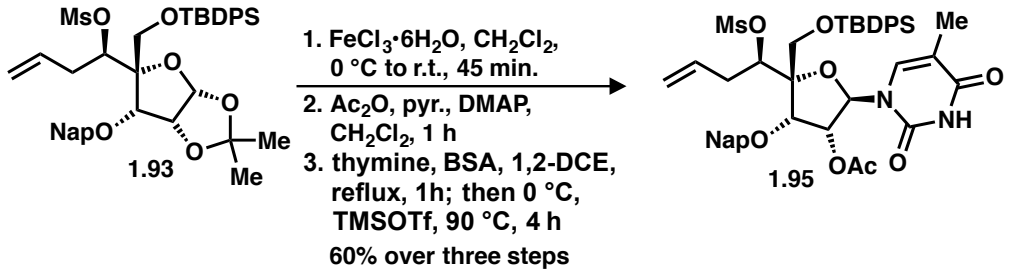

(2*R*,3*R*,4*S*,5*R*)-5-(((*tert*-Butyldiphenylsilyl)oxy)methyl)-2-(5-methyl-2,4-dioxo-3,4-dihydropyrimidin-1(2*H*)-yl)-5-((*R*)-1-((methylsulfonyl)oxy)but-3-en-1-yl)-4-(naphthalen-2-ylmethoxy)tetrahydrofuran-3-yl acetate (1.95).

Iron(III) chloride hexahydrate (1.3 g, 3.7 mmol) was added in one portion to a stirred, 0 °C solution of **1.93** (6.7 g, 9.3 mmol) in anhydrous dichloromethane (130 mL). The mixture was warmed to room temperature over 45 min. before it was poured into water (100 mL). The layers were separated and the aqueous portion was extracted with dichloromethane (3 × 40 mL). The combined organic extracts were washed sequentially with a saturated aqueous solution of sodium bicarbonate (100 mL) and brine (100 mL), dried over magnesium sulfate, filtered, and concentrated under reduced pressure. The resulting oil was placed under high vacuum for 2 h, before it was dissolved in dichloromethane (120 mL). Acetic anhydride (5.3 mL, 56 mmol) and 4-(dimethylamino)pyridine (0.17 g, 1.4 mmol) were added and the mixture was stirred at room temperature for 1 h before it was poured into aqueous 1 M hydrochloric acid (100 mL). The layers were separated and the aqueous portion was extracted with dichloromethane (3 × 50 mL). The combined organic extracts were washed sequentially a saturated aqueous solution of sodium bicarbonate (100 mL) and brine (100 mL), dried over magnesium sulfate, filtered, and concentrated under reduced pressure to afford crude diacetate **1.94**. The crude oil of **1.94** was placed under high vacuum for 12 h. *N*,*O*-Bis(trimethylsilyl)acetamide (9.6 mL, 67 mmol) was added to a stirred solution of thymine (2.1 g, 17 mmol) in anhydrous 1,2-dichloroethane (98 mL). The resulting mixture was heated to 80 °C for 1 h and then cooled to 0 °C, upon which a solution of the crude oil in anhydrous 1,2-dichloroethane (21 mL), and trimethylsilyl trifluoromethylsulfonate (3.0 mL, 17 mmol) were added. The solution was heated to 90 °C for 4 h, then cooled to 0 °C before a saturated aqueous solution of sodium bicarbonate (10 mL) was added. The mixture was further partitioned between dichloromethane (200 mL) and a saturated aqueous solution of sodium

bicarbonate (100 mL). The layers were separated and the aqueous portion was extracted with dichloromethane (3 × 75 mL). The combined organic extracts were washed with brine (150 mL), dried over magnesium sulfate, filtered, and concentrated under reduced pressure. The residue was purified by flash column chromatography (18 × 5.5 cm) on silica gel (2:3 to 1:1 ethyl acetate–hexanes) to afford **1.95** as an oil (4.6 g, 60% yield over three steps) that often crystallized upon standing: R_f 0.24 (1:1 ethyl acetate–hexanes); m.p. 140–142 °C (ethyl acetate–hexanes); $[\alpha]_D^{20}$ –17.4 (*c* = 1.0, chloroform); IR (film, cm^{-1}) ν 3053, 2931, 2858, 1750, 1715, 1696, 1471, 1428, 1361, 1226, 1173, 1105; ^1H NMR (400 MHz, chloroform-*d*) δ = 8.50 (s, 1H), 7.88–7.82 (m, 3H), 7.75 (s, 1H), 7.67–7.60 (m, 4H), 7.55–7.49 (m, 2H), 7.49–7.30 (m, 8H), 6.34 (d, *J* = 6.8 Hz, 1H), 5.69–5.56 (m, 2H), 5.13 (dd, *J* = 9.3, 2.1 Hz, 1H), 4.97 (d, *J* = 10.2 Hz, 1H), 4.91–4.82 (m, 2H), 4.56 (d, *J* = 11.3 Hz, 1H), 4.46 (d, *J* = 5.5 Hz, 1H), 3.98 (d, *J* = 11.4 Hz, 1H), 3.86 (d, *J* = 11.4 Hz, 1H), 2.93 (s, 3H), 2.38 (dd, *J* = 14.3, 4.0 Hz, 1H), 2.15–2.06 (m, 4H), 1.55 (s, 1H), 1.12 (s, 2H); ^{13}C NMR (75 MHz, chloroform-*d*) δ 170.28, 163.44, 150.37, 135.76, 135.61, 135.50, 133.94, 133.31, 133.29, 133.17, 132.49, 132.02, 130.53, 130.39, 128.67, 128.25, 128.20, 128.11, 127.90, 127.26, 126.62, 126.53, 125.92, 118.74, 112.02, 88.05, 85.98, 83.27, 77.98, 75.13, 74.36, 64.03, 39.13, 35.65, 27.21, 20.86, 19.49, 12.04; HRMS (ESI) calc'd for $C_{44}H_{50}N_2NaO_{10}SSi$ $[M+Na]^+$ *m/z* 849.2848, found 849.2873.

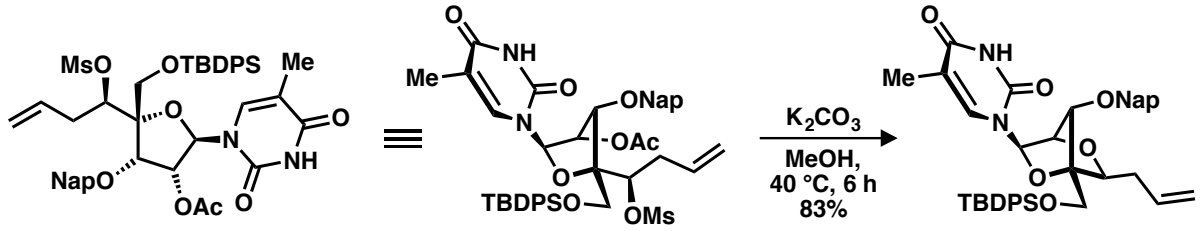

1-((1*S*,3*R*,4*R*,6*S*,7*S*)-6-Allyl-1-(((*tert*-butyldiphenylsilyl)oxy)methyl)-7-(naphthalen-2-ylmethoxy)-2,5-dioxabicyclo[2.2.1]heptan-3-yl)-5-methylpyrimidine-2,4(1*H*,3*H*)-dione (1.97).

Potassium carbonate (2.2 g, 16 mmol) was added to a stirred solution of **1.95** (5.5 g, 6.3 mmol) in methanol (570 mL). The mixture was warmed to 40 °C and stirred at that temperature for 6 h, at which point the mixture was concentrated to near dryness under

reduced pressure. The solids were dissolved in chloroform (75 mL) and partitioned with aqueous 0.5 M hydrochloric acid (50 mL). The layers were separated and the aqueous portion was extracted with chloroform (3 × 50 mL). The combined organic extracts were washed with a saturated aqueous solution of sodium bicarbonate (200 mL), dried over magnesium sulfate, filtered, and concentrated under reduced pressure. The residue was purified by flash column chromatography (13 × 4 cm) on silica gel (2:1 ethyl acetate–hexanes) to afford alcohol **1.97** as a colorless oil (3.6 g, 83% yield) that often crystallized upon standing: R_f 0.23 (1:2 ethyl acetate–hexanes); $[\alpha]^{20}_D$ +2.5 (*c* = 1.0, chloroform); IR (KBr disc, cm^{-1}) ν 3070, 2929, 2856, 1694, 1463, 1428, 1384, 1267, 1105, 1069, 1050; ^{1}H NMR (400 MHz, chloroform-*d*) δ 8.51 (s, 1H), 7.88–7.62 (m, 8H), 7.54–7.28 (m, 10H), 5.80 – 5.68 (m, 1H), 5.65 (s, 1H), 5.05–4.95 (m, 2H), 4.83 (d, *J* = 11.3 Hz, 1H), 4.72 (s, 1H), 4.66 (d, *J* = 11.3 Hz, 1H), 4.09–3.98 (m, 4H), 2.71–2.59 (m, 1H), 2.28–2.17 (m, 1H), 1.58 (s, 3H), 1.09 (s, 9H); ^{13}C NMR (75 MHz, chloroform-*d*) δ 163.63, 149.72, 135.70, 135.47, 134.46, 134.23, 134.11, 133.25, 133.22, 132.91, 132.45, 130.23, 130.18, 128.57, 128.11, 128.07, 127.97, 127.87, 127.03, 126.58, 126.43, 125.86, 117.51, 110.44, 89.71, 87.29, 84.14, 77.03, 72.67, 59.38, 35.44, 27.06, 19.56, 12.26; HRMS (ESI) calc'd for $C_{41}H_{44}N_2NaO_6Si$ $[M+Na]^+$ *m/z* 711.2861, found 711.2874.

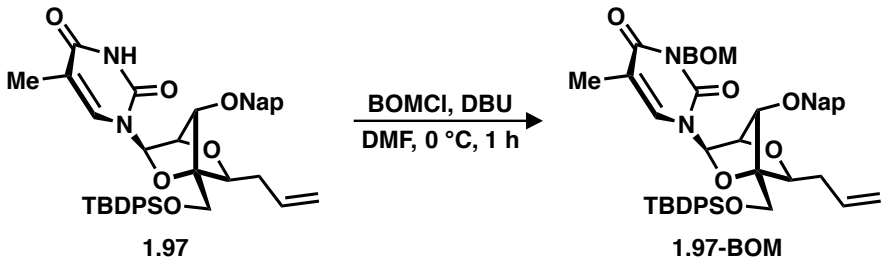

1.97 1.97-BOM

1-((1*S*,3*R*,4*R*,6*S*,7*S*)-6-Allyl-1-(((*tert*-butyldiphenylsilyl)oxy)methyl)-7-(naphthalen-2-ylmethoxy)-2,5-dioxabicyclo[2.2.1]heptan-3-yl)-3-((benzyloxy)methyl)-5-methylpyrimidine-2,4(1*H*,3*H*)-dione (1.97-BOM).

1,8-diazabicyclo[5.4.0]undec-7-ene (1.1 mL, 7.3 mmol) and a 60% technical grade solution of benzyl chloromethyl ether (2.6 mL, 11 mmol) were sequentially added to a stirred 0 °C solution of **1.97** (4.2 g, 6.1 mmol) in *N*,*N*-dimethylformamide (110 mL). After 1 h the reaction mixture was partitioned between diethyl ether (300 mL) and water (100 mL). The layers were separated and the aqueous portion was extracted with ethyl acetate (3 × 75 mL). The combined

organic extracts were washed with a saturated aqueous solution of sodium bicarbonate (3 × 100 mL) and brine (100 mL), dried over magnesium sulfate, filtered, and concentrated under reduced pressure to afford an oil, which was used directly in the next step without purification. A portion of the residue was purified by flash column chromatography on silica gel (1:6 ethyl acetate–hexanes) to afford benzyloxymethylated nucleoside **1.97-BOM** as a colorless oil: R_f 0.46 (1:2 ethyl acetate–hexanes); $[\alpha]^{20}_D$ +11.58 (*c* = 1.0, chloroform); IR (KBr disc, cm^{-1}) ν 3071, 2930, 2857, 1709, 1664, 1461, 1428, 1282, 1112, 1056, 1027; ^{1}H NMR (400 MHz, chloroform-*d*) δ 7.86–7.64 (m, 8H), 7.52 – 7.27 (m, 15H), 5.81–5.68 (m, 1H), 5.64 (s, 1H), 5.48 (d, *J* = 9.5 Hz, 1H), 5.42 (d, *J* = 9.5 Hz, 1H), 5.03–4.95 (m, 2H), 4.82 (d, *J* = 11.3 Hz, 1H), 4.73–4.63 (m, 4H), 4.09–4.00 (m, 4H), 2.73–2.57 (m, 1H), 2.33–2.20 (m, 1H), 1.60 (d, *J* = 0.9 Hz, 3H), 1.11 (s, 9H); ^{13}C NMR (75 MHz, chloroform-*d*) δ 163.46, 150.52, 138.12, 135.71, 135.48, 134.35, 134.16, 133.25, 133.20, 132.95, 132.48, 130.23, 130.18, 128.53, 128.44, 128.10, 128.06, 127.96, 127.87, 127.85, 127.82, 126.91, 126.52, 126.37, 125.81, 117.47, 109.85, 89.66, 87.64, 84.11, 77.01, 72.71, 72.44, 70.44, 59.47, 35.50, 27.08, 19.58, 12.97; HRMS (APCI) calc'd for $C_{49}H_{53}N_2O_7Si$ $[M+H]^+$ *m/z* 809.3616, found 809.3634.

1.97-BOM 1.98

1-((1*S*,3*R*,4*R*,6*S*,7*S*)-6-Allyl-1-(hydroxymethyl)-7-(naphthalen-2-ylmethoxy)-2,5-dioxabicyclo[2.2.1]heptan-3-yl)-3-((benzyloxy)methyl)-5-methylpyrimidine-2,4(1*H*,3*H*)-dione (1.98).

Tetrabutylammonium fluoride (1 M in tetrahydrofuran, 9.1 mL, 9.1 mmol) was added to a stirred solution of crude **1.97-BOM** (4.9 g, theor. 6.1 mmol) in tetrahydrofuran (174 mL). The mixture was stirred at room temperature for 9 h before the volatiles were removed under reduced pressure. The residue was reconstituted in ethyl acetate (100 mL) and partitioned with aqueous 1 M hydrochloric acid (75 mL). The layers were separated and the aqueous portion was extracted with ethyl acetate (3 × 50 mL). The combined organic extracts were washed

with a saturated aqueous solution of sodium bicarbonate (75 mL) and brine (75 mL), dried over magnesium sulfate, and concentrated under reduced pressure. The residue was purified by flash column chromatography on silica gel (2:3 to 2:1 ethyl acetate–hexanes) to afford primary alcohol **1.98** as a colorless oil (2.89 g, 83% yield over two steps): R_f 0.11 (1:2 ethyl acetate–hexanes); $[\alpha]_D^{20}$ +21.7 (*c* = 0.5, chloroform); IR (KBr disc, cm^{-1}) ν 3460, 3067, 2924, 1707, 1663, 1462, 1279, 1058; ^{1}H NMR (400 MHz, chloroform-*d*) δ 7.86–7.73 (m, 4H), 7.51–7.41 (m, 3H), 7.39–7.24 (m, 6H), 5.90–5.77 (m, 1H), 5.61 (s, 1H), 5.46 (d, *J* = 9.6 Hz, 1H), 5.41 (d, *J* = 9.6 Hz, 1H), 5.17–5.09 (m, 2H), 4.82 (d, *J* = 11.5 Hz, 1H), 4.72–4.62 (m, 4H), 4.06 (dd, *J* = 8.7, 5.3 Hz, 1H), 4.02 (s, 2H), 3.91 (s, 1H), 2.76–2.66 (m, 1H), 2.40–2.32 (m, 1H), 1.81 (d, *J* = 0.9 Hz, 3H), 1.80–1.74 (br s, 1H); ^{13}C NMR (75 MHz, chloroform-*d*) δ 163.33, 150.51, 138.08, 134.34, 134.26, 133.32, 133.24, 133.22, 128.63, 128.45, 127.95, 127.89, 127.85, 127.83, 127.06, 126.63, 126.49, 125.74, 117.62, 109.88, 88.86, 87.55, 84.10, 77.30, 76.88, 72.73, 72.47, 70.50, 58.15, 35.34, 13.48; HRMS (APCI) calc'd for $C_{33}H_{35}N_2O_7$ $[M+H]^+$ *m/z* 571.2439, found 571.2431.

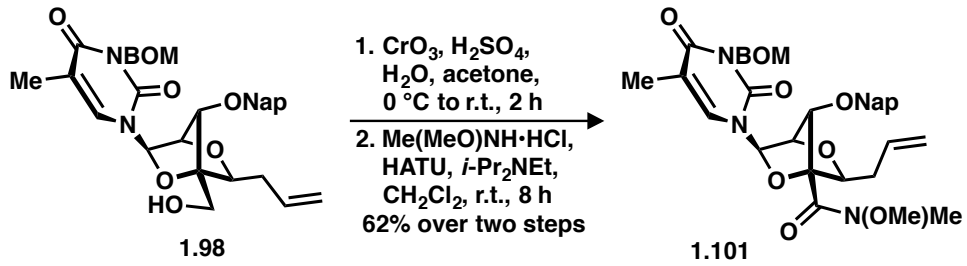

(1*S*,3*R*,4*R*,6*S*,7*S*)-6-Allyl-3-(3-((benzyloxy)methyl)-5-methyl-2,4-dioxo-3,4-dihydropyrimidin-1(2*H*)-yl)-*N*-methoxy-*N*-methyl-7-(naphthalen-2-ylmethoxy)-2,5-dioxabicyclo[2.2.1]heptane-1-carboxamide (1.101).

A portion (1.4 mL) of a premade solution of chromium trioxide (3.0 g, 30 mmol) and sulphuric acid (2 mL) in water (10 mL) and was added dropwise to a stirred, 0 °C solution of **1.98** (0.500 g, 0.876 mmol) in acetone (87 mL). The reaction was warmed to room temperature and stirred until near complete consumption of the starting material by TLC analysis (~2 h). The mixture was filtered through Celite® 545 and the volatiles removed under reduced pressure. The residue was dissolved in dichloromethane (50 mL) and partitioned with aqueous 1 M hydrochloric acid (40 mL). The layers were separated and the aqueous portion

was extracted with dichloromethane (3 × 30 mL). The combined organic extracts were washed with brine (30 mL), dried over magnesium sulfate, filtered, and concentrated under reduced pressure to afford the crude carboxylic acid, which was used directly in the next step without purification. *N*,*O*-dimethylmethylamine hydrochloride (0.27 g, 2.6 mmol), *O*-(7-azabenzotriazol-1-yl)-*N,N,N′,N′*-tetramethyluronium hexafluorophosphate (0.39 g, 0.96 mmol), and *N*,*N*,-diisopropylethylamine (0.76 mL, 4.4 mmol) were added sequentially to a solution of crude carboxylic acid (0.512 g, theor. 0.876 mmol) in dichloromethane (13 mL). The mixture was stirred at room temperature for 8 h, before aqueous 1 M hydrochloric acid (10 mL) was added to the flask. The layers were separated and the aqueous portion was extracted with dichloromethane (3 × 7 mL). The combined organic extracts were washed with a saturated aqueous solution of sodium bicarbonate (10 mL) and brine (10 mL), dried over magnesium sulfate, and concentrated under reduced pressure. The residue was purified by flash column chromatography on silica gel (1:2 ethyl acetate–hexanes) to afford **1.101** as a colorless oil (0.35 g, 62% yield over two steps): R_f 0.15 (2:3 ethyl acetate–hexanes); $[\alpha]_D^{20}$ – 57.8 (*c* = 1.0, chloroform); IR (KBr disc, cm^{-1}) ν 3433, 3058, 2936, 1711, 1666, 1461, 1384, 1278, 1062; ^{1}H NMR (300 MHz, chloroform-*d*) δ 7.85–7.73 (m, 4H), 7.53–7.41 (m, 3H), 7.39–7.21 (m, 5H), 6.96 (d, *J* = 1.1 Hz, 1H), 5.95–5.76 (m, 1H), 5.70 (s, 1H), 5.41 (d, *J* = 9.6 Hz, 1H), 5.35 (d, *J* = 9.6 Hz, 1H), 5.16–5.10 (m, 1H), 5.08 (s, 1H), 5.02 (d, *J* = 11.8 Hz, 1H), 4.91 (d, *J* = 11.7 Hz, 1H), 4.65 (s, 2H), 4.45 (dd, *J* = 9.1, 4.7 Hz, 1H), 4.38 (s, 1H), 4.11 (s, 1H), 3.78 (s, 3H), 3.29 (s, 3H), 2.85–2.72 (m, 1H), 2.45–2.33 (m, 1H), 1.75 (d, *J* = 1.0 Hz, 3H); ^{13}C NMR (75 MHz, chloroform-*d*) δ 163.09, 150.39, 138.09, 134.82, 134.24, 133.24, 133.16, 132.42, 128.43, 128.39, 128.08, 127.94, 127.82, 127.78, 127.76, 127.75, 127.06, 126.41, 126.26, 126.01, 117.24, 110.21, 87.67, 87.55, 83.22, 79.54, 77.21, 73.22, 72.38, 70.48, 62.11, 35.19, 13.29; HRMS (ESI) calc'd for $C_{35}H_{38}N_3O_8$ $[M+H]^+$ *m/z* 628.2653, found 628.2662.

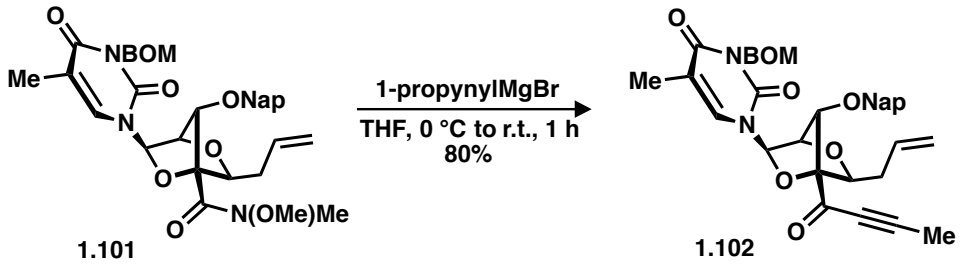

1.101 1.102

1-((1*S*,3*R*,4*R*,6*S*,7*S*)-6-Allyl-1-(but-2-ynoyl)-7-(naphthalen-2-ylmethoxy)-2,5-dioxabicyclo[2.2.1]heptan-3-yl)-3-((benzyloxy)methyl)-5-methylpyrimidine-2,4(1*H*,3*H*)-dione (1.102).

A 0.5 M solution of 1-propynylmagnesium bromide (9.1 mL, 4.5 mmol) in tetrahydrofuran was added dropwise to a stirred, 0 °C solution of Weinreb amide **1.101** (0.95 g, 1.5 mmol) in tetrahydrofuran (55 mL). The reaction was warmed to room temperature and stirred until near complete consumption of the starting material by TLC analysis (~1 h). The reaction mixture was poured into a 0 °C, aqueous solution of 1 M hydrochloric acid (100 mL), warmed to room temperature, and subsequently diluted with ethyl acetate (75 mL). The layers were separated and the aqueous portion was extracted with ethyl acetate (2 × 75 mL). The combined organic extracts were washed with a saturated aqueous solution of sodium bicarbonate (75 mL), dried over magnesium sulfate, and concentrated under reduced pressure. The residue was purified by flash column chromatography on silica gel (1:3 to 1:2 ethyl acetate–hexanes) to afford **1.102** as a colorless oil (0.74 g, 80% yield): R_f 0.34 (2:3 ethyl acetate–hexanes); $[\alpha]_D^{20}$ +53.0 (*c* = 1.0, chloroform); IR (KBr disc, cm^{-1}) ν 3058, 3030, 2925, 2238, 2205, 1709, 1666, 1461, 1365, 1277, 1065; ^{1}H NMR (400 MHz, chloroform-*d*) δ 7.87–7.70 (m, 4H), 7.52–7.25 (m, 9H), 5.94–5.81 (m, 1H), 5.61 (s, 1H), 5.45 (d, *J* = 9.6 Hz, 1H), 5.40 (d, *J* = 9.6 Hz, 1H), 5.19–5.09 (m, 2H), 4.82 (d, *J* = 11.7 Hz, 1H), 4.75 (d, *J* = 11.7 Hz, 1H), 4.69 (s, 3H), 4.24 (dd, *J* = 10.1, 3.6 Hz, 1H), 4.02 (s, 1H), 2.90–2.81 (m, 1H), 2.71–2.62 (m, 1H), 2.00 (s, 3H), 1.79 (d, *J* = 1.0 Hz, 3H); ^{13}C NMR (75 MHz, chloroform-*d*) δ 179.09, 163.11, 150.34, 138.02, 134.34, 133.85, 133.25, 133.21, 132.93, 128.62, 128.45, 127.95, 127.87, 127.81, 127.23, 126.61, 126.51, 125.84, 117.52, 109.97, 95.59, 89.34, 88.05, 85.07, 79.72, 79.56, 78.03, 73.12, 72.49, 70.50, 35.52, 13.54, 4.48; HRMS (ESI) calc'd for $C_{36}H_{35}N_2O_7$ $[M+H]^+$ *m/z* 607.2432, found 607.2439.

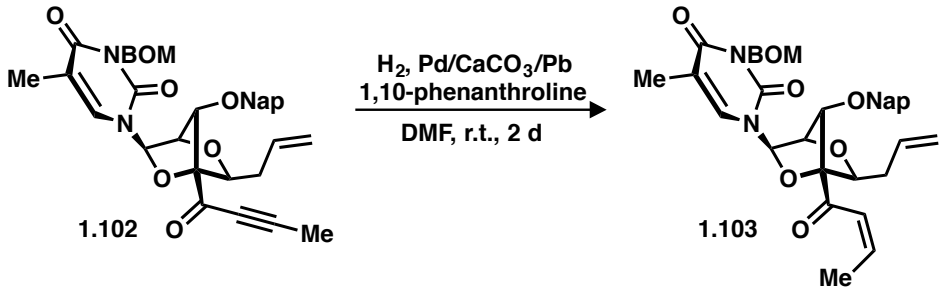

1-((1*S*,3*R*,4*R*,6*S*,7*S*)-6-Allyl-1-((*Z*)-but-2-enoyl)-7-(naphthalen-2-ylmethoxy)-2,5-dioxabicyclo[2.2.1]heptan-3-yl)-3-((benzyloxy)methyl)-5-methylpyrimidine-2,4(1*H*,3*H*)-dione (1.103).

1,10-Phenanthroline (0.17 g, 0.95 mmol) and 5% (w/w) palladium on calcium carbonate poisoned with lead (0.13 g, 0.061 mmol) were added sequentially to a stirred solution of **1.102** (0.46 g, 0.76 mmol) in *N,N*-dimethylformamide (8 mL). The suspension was purged with hydrogen gas and maintained under an atmosphere of hydrogen gas with a hydrogen-filled balloon. After 2 d, the reaction mixture was filtered through a pad of Celite® 545, the filter cake was washed with dichloromethane, and the filtrate was concentrated under reduced pressure. The residue was reconstituted in diethyl ether (20 mL) and partitioned with aqueous 1 M hydrochloric acid (20 mL). The layers were separated and the aqueous portion was extracted with diethyl ether (3 × 15 mL). The combined organic extracts were washed with a saturated aqueous solution of sodium bicarbonate (15 mL) and brine (15 mL), dried over magnesium sulfate, and concentrated under reduced pressure to afford the crude alkene, which was used directly in the next step without purification. A portion of the residue was purified by flash column chromatography on silica gel (1:5 to 1:3 ethyl acetate–hexane) to afford **1.103** as a colorless oil: R_f 0.27 (1:3 ethyl acetate–hexanes); $[\alpha]_D^{20}$ +13.3 (*c* = 1.0, chloroform); IR (KBr disc, cm^{-1}) ν 3060, 2926, 1708, 1666, 1625, 1461, 1278, 1061; ^{1}H NMR (400 MHz, chloroform-*d*) δ 7.85–7.75 (m, 4H), 7.50–7.45 (m, 3H), 7.38–7.15 (m, 6H), 6.97 (d, *J* = 1.2 Hz, 1H), 6.65 (dd, *J* = 15.4, 1.7 Hz, 1H), 5.86–5.74 (m, 1H), 5.61 (s, 1H), 5.44 (d, *J* = 9.6 Hz, 1H), 5.38 (d, *J* = 9.6 Hz, 1H), 5.15–5.07 (m, 2H), 4.92–4.83 (m, 2H), 4.71–4.66 (m, 3H), 4.24 (dd, *J* = 9.7, 4.1 Hz, 1H), 3.96 (s, 1H), 2.88–2.77 (m, 1H), 2.38–2.29 (m, 1H), 1.97 (dd, *J* = 7.0, 1.6 Hz, 3H), 1.76 (d, *J* = 1.1 Hz, 3H); ^{13}C NMR (75 MHz, chloroform-*d*) δ 191.19, 163.10, 150.37, 147.09, 138.02, 134.21, 133.94, 133.22, 133.20, 132.65, 128.56, 128.42, 127.94, 127.84, 127.79, 127.48, 127.13, 126.54, 126.42, 125.84, 117.76, 110.27, 89.53, 87.30,

85.35, 78.91, 78.20, 73.11, 72.45, 70.50, 35.58, 18.86, 13.35; HRMS (APCI) calc'd for $C_{36}H_{37}N_2O_7$ $[M+H]^+$ *m/z* 609.2595, found 609.2594.

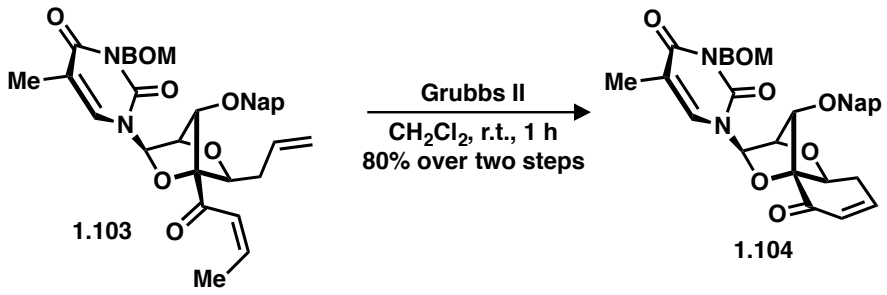

3-((Benzyloxy)methyl)-5-methyl-1-((2*R*,3*R*,4a*S*,8a*S*,9*S*)-9-(naphthalen-2-ylmethoxy)-5-oxo-3,5,8,8a-tetrahydro-2*H*-2,4a-methanobenzo[*b*][1,4]dioxin-3-yl)pyrimidine-2,4(1*H*,3*H*)-dione (1.104).

Grubbs' second generation catalyst (0.021 g, 0.024 mmol) was added to a stirred solution of the crude alkene **1.103** (0.46 g, theor. 0.76 mmol) in anhydrous dichloromethane (100 mL). The solution was stirred at room temperature for 1 h before the volatiles were removed under reduced pressure. The residue was purified by flash column chromatography on silica gel (1:2 to 2:3 ethyl acetate–hexanes) to afford **1.104** (0.34 g, 80% yield over two steps) as a colorless oil: R_f 0.24 (2:3 ethyl acetate–hexanes); $[\alpha]_D^{20}$ +103.2 (*c* = 1.0, chloroform); IR (KBr disc, cm^{-1}) ν 2924, 1707, 1683, 1664, 1461, 1277, 1070; ^{1}H NMR (400 MHz, chloroform-*d*) δ 7.85–7.72 (m, 3H), 7.63 (s, 1H), 7.53–7.44 (m, 3H), 7.40–7.22 (m, 6H), 6.91 (ddd, *J* = 10.2, 5.5, 2.6 Hz, 1H), 6.25 (dd, *J* = 10.3, 1.8 Hz, 1H), 5.60 (s, 1H), 5.45 (d, *J* = 9.6 Hz, 1H), 5.40 (d, *J* = 9.6 Hz, 1H), 4.74–4.54 (m, 6H), 4.06 (s, 1H), 3.07 (ddt, *J* = 19.2, 7.9, 2.8 Hz, 1H), 2.94–2.82 (m, 1H), 1.89 (d, *J* = 0.9 Hz, 3H); ^{13}C NMR (75 MHz, chloroform-*d*) δ 191.78, 163.18, 150.42, 149.32, 138.03, 133.49, 133.19, 133.11, 132.95, 129.38, 128.64, 128.39, 127.90, 127.83, 127.80, 127.73, 126.96, 126.61, 126.54, 125.42, 110.40, 88.00, 84.97, 82.18, 81.05, 78.95, 73.57, 72.45, 70.48, 32.83, 13.48; HRMS (ESI) calc'd for $C_{33}H_{31}N_2O_7$ $[M+H]^+$ *m/z* 567.2126, found 567.2107.

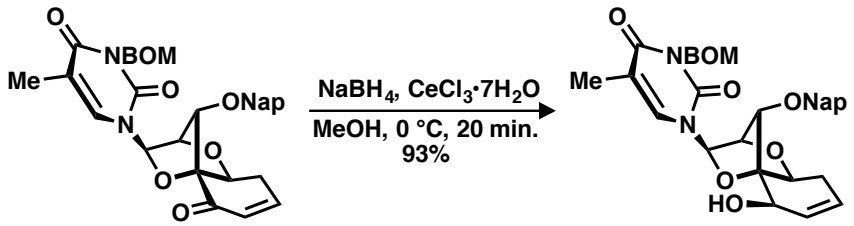

1.104 1.105

3-((Benzyloxy)methyl)-1-((2*R*,3*R*,4a*S*,5*R*,8a*S*,9*S*)-5-hydroxy-9-(naphthalen-2-ylmethoxy)-3,5,8,8a-tetrahydro-2*H*-2,4a-methanobenzo[*b*][1,4]dioxin-3-yl)-5-methylpyrimidine-2,4(1*H*,3*H*)-dione (1.105).

Cerium(III) chloride heptahydrate (0.30 g, 0.79 mmol) was added at 0 °C to a stirred solution of enone **1.104** (0.30 g, 0.53 mmol) in methanol (12 mL). The resulting solution was stirred for 10 min. before sodium borohydride (0.060 g, 1.6 mmol) was added in portionwise fashion. Upon complete consumption of the starting material by TLC analysis (~20 min.), acetone (3 mL) was added and the mixture was concentrated under reduced pressure. The residue was dissolved in dichloromethane (20 mL), washed sequentially with 1 M hydrochloric acid (10 mL), a saturated aqueous solution of sodium bicarbonate (15 mL), and brine (50 mL); then dried over magnesium sulfate, filtered, and concentrated under reduced pressure. The residue was purified by flash column chromatography on silica gel (1:1 ethyl acetate–hexanes) to afford **1.105** as a colorless oil (0.28 g, 93% yield): R_f 0.23 (1:1 ethyl acetate–hexanes); $[\alpha]_D^{20}$ +24.0 (*c* = 1.0, chloroform); IR (KBr disc, cm^{-1}) ν 3451, 3029, 2919, 1706, 1662, 1636, 1463, 1274, 1067, 1027; ^{1}H NMR (400 MHz, chloroform-*d*) δ 7.84–7.72 (m, 3H), 7.69 (s, 1H), 7.50–7.44 (m, 2H), 7.40–7.22 (m, 7H), 5.78–5.65 (m, 2H), 5.61 (s, 1H), 5.47 (d, *J* = 9.6 Hz, 1H), 5.42 (d, *J* = 9.6 Hz, 1H), 4.85–4.67 (m, 5H), 4.58 (s, 1H), 4.24 (t, *J* = 8.2 Hz, 1H), 4.04 (s, 1H), 2.75–2.52 (m, 2H), 1.98 (br s, 1H), 1.82 (d, *J* = 1.0 Hz, 3H); ^{13}C NMR (75 MHz, chloroform-*d*) δ 163.33, 150.55, 138.11, 134.50, 133.24, 133.14, 133.10, 128.57, 128.44, 127.93, 127.88, 127.83, 127.79, 127.69, 126.84, 126.82, 126.56, 126.39, 125.53, 109.91, 87.35, 87.32, 79.40, 78.12, 77.25, 73.05, 72.48, 70.53, 67.41, 32.27, 13.50; HRMS (ESI) calc'd for $C_{33}H_{32}N_2NaO_7$ $[M+Na]^+$ *m/z* 591.2102, found 591.2115.

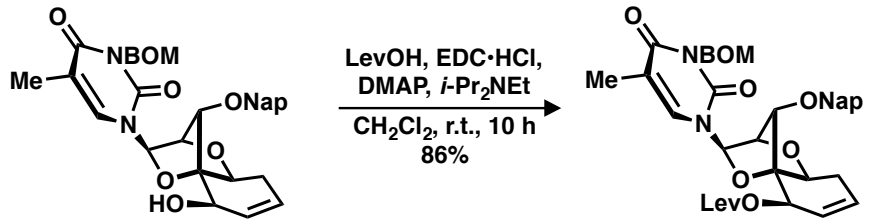

1.105 **1.106**

(2*R*,3*R*,4a*R*,5*R*,8a*S*,9*S*)-3-(3-((Benzyloxy)methyl)-5-methyl-2,4-dioxo-3,4-dihydropyrimidin-1(2*H*)-yl)-9-(naphthalen-2-ylmethoxy)-3,5,8,8a-tetrahydro-2*H*-2,4a-methanobenzo[*b*][1,4]dioxin-5-yl 4-oxopentanoate (1.106).

Levulinic acid (0.096 mL, 0.95 mmol), *N*-(3-dimethyl-aminopropyl)-*N*′-ethylcarbodiimide hydrochloride (0.14 g, 0.71 mmol), 4-(dimethylamino)pyridine (0.029 g, 0.24 mmol), and *N*,*N*-diisopropylethylamine (0.25 mL, 1.4 mmol) were added sequentially to a stirred solution of **1.105** (0.27 g, 0.47 mmol) in dichloromethane (23 mL). After 10 h, the reaction mixture was diluted with dichloromethane (40 mL) and washed with 1 M hydrochloric acid (25 mL × 3), a saturated aqueous solution of sodium bicarbonate (25 mL), and brine (25 mL); then dried over magnesium sulfate, filtered, and concentrated under reduced pressure. The residue was purified by flash column chromatography on silica gel (1:2 ethyl acetate–hexanes) to afford **1.106** as a colorless oil (0.27 g, 86% yield): R_f 0.38 (1:40 methanol–dichloromethane); $[\alpha]_D^{20}$ +31.2 (*c* = 0.5, chloroform); IR (KBr disc, cm^{-1}) ν 2918, 2850, 1740, 1708, 1663, 1636, 1462, 1384, 1273, 1148, 1060; ^{1}H NMR (400 MHz, chloroform-*d*) δ 7.84–7.69 (m, 4H), 7.50–7.43 (m, 2H), 7.42–7.23 (m, 7H), 6.01–5.95 (br s, 1H), 5.88–5.81 (m, 1H), 5.68–5.61 (m, 1H), 5.57 (s, 1H), 5.46 (d, *J* = 9.6 Hz, 1H), 5.40 (d, *J* = 9.6 Hz, 1H), 4.78 (s, 2H), 4.70 (s, 2H), 4.62 (s, 1H), 4.30 (t, *J* = 8.3 Hz, 1H), 4.02 (s, 1H), 2.91–2.69 (m, 3H), 2.68–2.49 (m, 3H), 2.16 (s, 3H), 1.82 (s, 3H); ^{13}C NMR (75 MHz, chloroform-*d*) δ 206.33, 172.42, 163.39, 150.54, 138.10, 134.62, 133.37, 133.23, 133.14, 129.42, 128.45, 128.39, 127.91, 127.84, 126.73, 126.48, 126.31, 125.68, 123.09, 109.75, 87.60, 85.34, 79.74, 78.36, 78.00, 73.19, 72.45, 70.49, 69.71, 38.00, 31.84, 29.84, 28.28, 13.32; HRMS (ESI) calc'd for $C_{38}H_{38}N_2NaO_9$ $[M+Na]^+$ *m/z* 689.2470, found 689.2467.

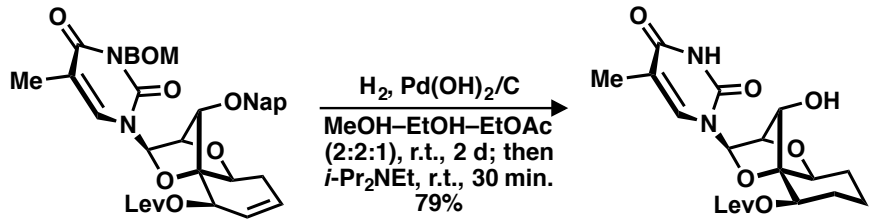

1.106 **1.107**

(2*R*,3*R*,4a*R*,5*R*,8a*S*,9*S*)-9-Hydroxy-3-(5-methyl-2,4-dioxo-3,4-dihydropyrimidin-1(2*H*)-yl)hexahydro-2*H*-2,4a-methanobenzo[*b*][1,4]dioxin-5-yl 4-oxopentanoate (1.107).

20% (w/w) Palladium hydroxide on carbon (0.057 g, 0.081 mmol) was added to a stirred solution of **1.106** (0.27 g, 0.40 mmol) in 2:2:1 methanol–ethanol–ethyl acetate (8 mL). The suspension was purged with hydrogen gas and maintained under an atmosphere of hydrogen gas with a hydrogen-filled balloon. After 2 d, *N*,*N*-diisopropylethylamine (0.14 mL, 0.81 mmol) was added and the mixture stirred for an additional 30 min. The reaction mixture was filtered through a pad of Celite® 545, the filter cake washed with methanol, and the filtrate concentrated under reduced pressure. The residue was purified by flash column chromatography on silica gel (1:22 methanol–dichloromethane) to afford **1.107** as a colorless solid (0.13 g, 79% yield): R_f 0.14 (1:20 methanol–dichloromethane); $[\alpha]_D^{20}$ +25.7 (*c* = 0.75, chloroform); IR (KBr disc, cm^{-1}) ν 3426, 2948, 1738, 1465, 1384, 1272, 1154, 1053; ^{1}H NMR (400 MHz, chloroform-*d*) δ 9.11 (br s, 1H), 7.44 (s, 1H), 5.55 (s, 1H), 5.32–5.22 (m, 1H), 4.56 (s, 1H), 4.29 (d, *J* = 4.6 Hz, 1H), 4.03 (dd, *J* = 10.9, 7.2 Hz, 1H), 3.05 (br s, 1H), 2.93–2.73 (m, 2H), 2.64 (t, *J* = 6.1 Hz, 2H), 2.21 (s, 3H), 2.09–1.98 (m, 2H), 1.95–1.75 (m, 6H), 1.45–1.32 (m, 1H); ^{13}C NMR (75 MHz, chloroform-*d*) δ 206.77, 172.09, 164.00, 150.00, 134.82, 110.40, 86.74, 86.30, 83.21, 80.85, 71.67, 71.62, 38.05, 29.93, 29.43, 28.35, 27.68, 19.99, 12.66; HRMS (ESI) calc'd for $C_{19}H_{25}N_2O_8$ $[M+H]^+$ *m/z* 409.1605, found 409.1614.

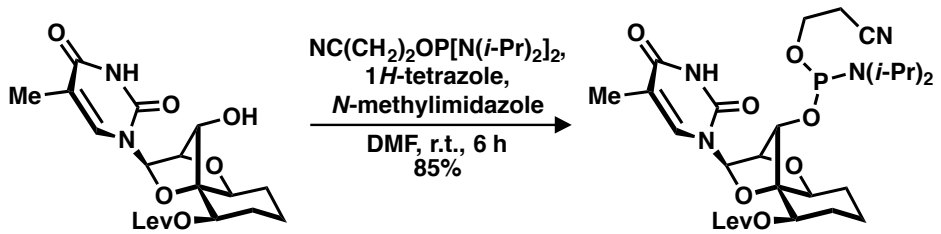

1.107 1.108

(2*R*,3*R*,4a*R*,5*R*,8a*S*,9*S*)-9-(((2-Cyanoethoxy)(diisopropylamino)phosphanyl)oxy)-3-(5-methyl-2,4-dioxo-3,4-dihydropyrimidin-1(2*H*)-yl)hexahydro-5*H*-2,4a-methanobenzo[*b*][1,4]dioxin-5-yl 4-oxopentanoate (1.108).

2-Cyanoethyl *N*,*N*,*N*′,*N*′-tetraisopropylphosphorodiamidite (0.14 mL, 0.48 mmol) was added to a stirred solution of **1.107** (0.12 g, 0.32 mmol), *N*-methylimidazole (5 μL, 0.08 mmol), and 1*H*-tetrazole (18 mg, 0.25 mmol) in *N*,*N*-dimethylformamide (1.6 mL). The mixture was stirred at ambient temperature for 6 h, before it was diluted with ethyl acetate and washed with brine, dried over sodium sulfate, and concentrated under reduced pressure. The residue was purified by flash column chromatography on silica gel (80 to 95% ethyl acetate–hexanes) to afford phosphoramidite **1.108** (153 mg, 85% yield): ^{31}P NMR (121 MHz, chloroform-*d*) δ 148.96 (overlapped signals); HRMS (QTOF) calc'd for $C_{28}H_{40}N_4O_9P$ $[M-H]^-$ *m/z* 607.2538, found 607.2569.

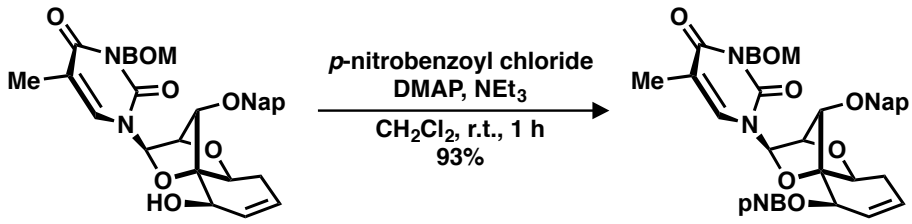

1.105 1.109 [X-ray]

(2*R*,3*R*,4a*R*,5*R*,8a*S*,9*S*)-3-(3-((Benzyloxy)methyl)-5-methyl-2,4-dioxo-3,4-dihydropyrimidin-1(2*H*)-yl)-9-(naphthalen-2-ylmethoxy)-3,5,8,8a-tetrahydro-2*H*-2,4a-methanobenzo[*b*][1,4]dioxin-5-yl 4-nitrobenzoate (1.109).

p-Nitrobenzoyl chloride (10 mg, 0.053 mmol), 4-(dimethylamino)pyridine (0.5 mg, 0.004 mmol), and *N*,*N*,-diisopropylethylamine (9 μL, 0.053 mmol) were added sequentially to a solution of **1.105** (10 mg, 0.12 mmol) in dichloromethane (440 μL). After 2 h, the reaction

mixture was partitioned between dichloromethane (1 mL) and water (1 mL), the layers were separated, and the aqueous layer was extracted with dichloromethane (3 × 1 mL). The combined organic extracts were washed with 1 M hydrochloric acid (1 mL), a saturated aqueous solution of sodium bicarbonate (1 mL), and brine (1 mL), dried through a phase separator cartridge, and concentrated under reduced pressure. The residue was purified by flash column chromatography on silica gel (1:3 ethyl acetate–hexanes) to afford **1.109** as a colorless solid (11 mg, 93% yield): R_f 0.20 (1:3 ethyl acetate–hexanes); $[\alpha]_D^{20}$ +30.5 (*c* = 0.5, chloroform); IR (solid, cm^{-1}) ν 2923, 1585, 1511, 1383, 1257, 1033, 1015; ^1H NMR (400 MHz, chloroform-*d*) δ 7.94–7.88 (m, 2H), 7.86–7.78 (m, 3H), 7.77–7.66 (m, 3H), 7.56–7.47 (m, 2H) 7.41–7.23 (m, 6H), 6.98 (d, *J* = 1.1 Hz, 1H), 6.27–6.22 (m, 1H), 5.99–5.92 (m, 1H), 5.79–5.72 (m, 1H), 5.62 (s, 1H), 5.48 (d, *J* = 9.6 Hz, 1H), 5.43 (d, *J* = 9.5 Hz, 1H), 4.90 (d, *J* = 12.2 Hz, 1H), 4.81 (s, 1H), 4.72 (s, 2H), 4.63 (d, *J* = 12.0 Hz, 1H), 4.41 (t, *J* = 8.2 Hz, 1H), 3.95 (s, 1H), 2.88–2.66 (m, 2H), 1.31 (d, *J* = 0.9 Hz, 3H); ^{13}C NMR (75 MHz, chloroform-*d*) δ 164.18, 163.04, 150.90, 150.44, 137.99, 134.48, 133.80, 133.23, 133.14, 132.42, 130.57, 130.25, 128.63, 128.49, 127.92, 127.90, 127.83, 127.38, 126.98, 126.90, 126.04, 123.86, 122.22, 109.87, 87.62, 85.37, 79.69, 77.75, 72.69, 72.55, 70.96, 70.50, 32.27, 13.03; HRMS (ESI) calc'd for $C_{40}H_{35}N_3NaO_{10}$ $[M+Na]^+$ *m/z* 740.2215, found 740.2211. Recrystallization from ethyl acetate–petroleum ether (b.p. range: 65–110 °C) afforded crystals that were suitable for X-ray crystallographic analysis.

Annex 2:

Experimental Data for Chapter 2

Experimental Procedures

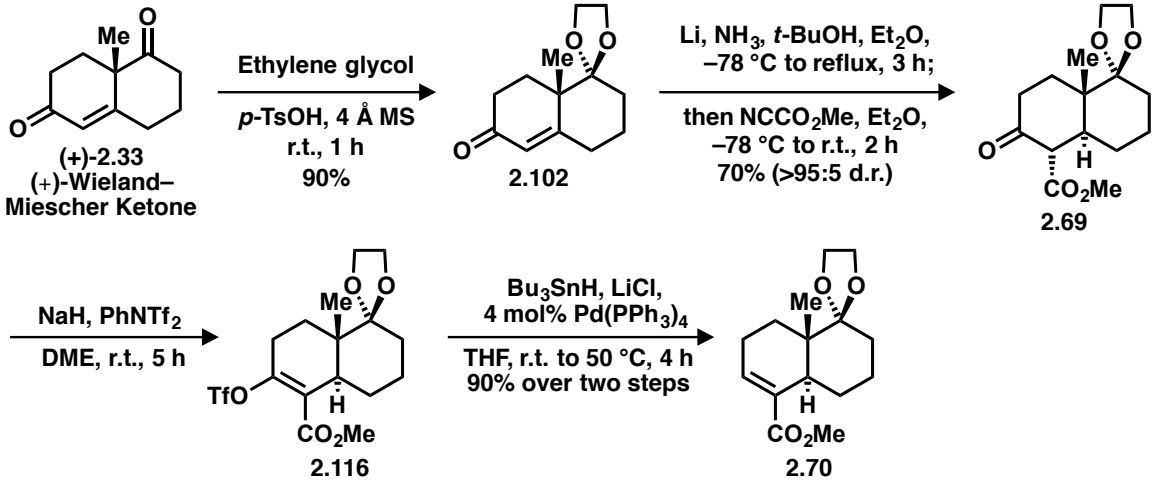

Methyl (4a*R*,8a*S*)-8a-methyl-3,4,4a,7,8,8a-hexahydro-2*H*-spiro[naphthalene-1,2'-[1,3]dioxolane]-5-carboxylate (2.70).

α,β-Unsaturated ester **2.70** was synthesized from (+)-Wieland–Miescher ketone using previously-described procedures and all data was in accordance that described in the literature. The unsaturated ketone was selectively protected using the procedure of Ciceri and Demnitz,[253] while the reductive carbomethoxylation, triflation, and ensuing reduction were realized through procedures described by the groups of Danishefsky[225] and Hanessian.[165] The only notable modification was for the reductive alkylation, in which the volume of liquid ammonia used was halved (i.e., the concentration of the reaction was increased) and one equivalent of *tert*-butyl alcohol was used.

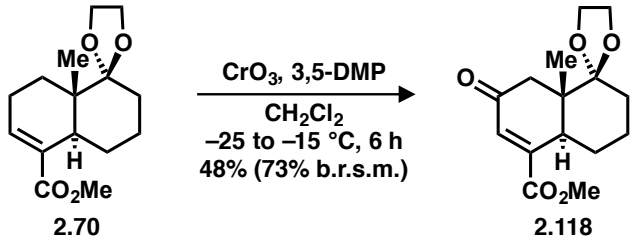

Methyl (4a*R*,8a*S*)-8a-methyl-7-oxo-3,4,4a,7,8,8a-hexahydro-2*H*-spiro[naphthalene-1,2'-[1,3]dioxolane]-5-carboxylate (2.118).

Anhydrous chromium trioxide (45.0 g, 450 mmol) was suspended in vigorously stirred dichloromethane (400 mL) and the resultant mixture was cooled to –25 °C. 3,5-Dimethylpyrazole (43.4 g, 451 mmol) was added in one portion and the mixture was stirred at –25 °C for 20 min. before a solution of α,β-unsaturated ester **2.70** (10.9 g, 40.9 mmol) in anhydrous dichloromethane (25 mL) was slowly added to the mixture. The mixture was vigorously stirred between –20 °C and –15 °C for 6 h, at which pointed it was diluted with diethyl ether (1 L), poured into a 2 M aqueous solution of sodium hydroxide (200 mL), and vigorously stirred for an additional 30 min. as it warmed to ambient temperature. The phases were separated and the organic phase was successively washed with 2 M aqueous hydrochloric acid (2 × 75 mL), 2 M aqueous sodium hydroxide (3 × 200 mL), and brine (200 mL), before it was dried over sodium sulfate, filtered, and concentrated under reduced pressure. The residue was purified by flash column chromatography (13.5 × 7.5 cm) on silica gel (1:3 to 1:1 diethyl ether–hexanes) to afford recovered α,β-unsaturated ester **2.70** (3.7 g) and desired enone **2.118** as a colourless oil (5.5 g, 48%; 73% b.r.s.m.): R_f 0.26 (1:1 diethyl ether–hexanes); $[\alpha]^{20}_D$ –16.4 (*c* = 1.0, chloroform); IR (film, cm^{-1}) ν 2955, 2888, 1724, 1680, 1439, 1235, 1181, 1075, 1024, 950, 868, 752; ^{1}H NMR (400 MHz, chloroform-*d*) δ 6.30 (dd, *J* = 3.3, 1.2 Hz, 1H), 4.02 – 3.85 (m, 4H), 3.80 (s, 3H), 3.13 (dt, *J* = 12.9, 3.3 Hz, 1H), 2.60 (dd, *J* = 16.0, 1.0 Hz, 1H), 2.39 (d, *J* = 15.9 Hz, 1H), 2.07 – 1.98 (m, 1H), 1.80 – 1.58 (m, 4H), 1.36 – 1.24 (m, 1H), 1.06 (d, *J* = 1.2 Hz, 3H); ^{13}C NMR (75 MHz, chloroform-*d*) δ 200.1, 167.8, 151.7, 130.2, 111.2, 65.5, 65.3, 52.4, 45.7, 44.8, 41.8, 29.4, 22.6, 22.1, 14.9; HRMS (ESI) calc'd for $C_{15}H_{21}O_5$ $[M+H]^+$ *m/z* 281.1384, found 281.1387.

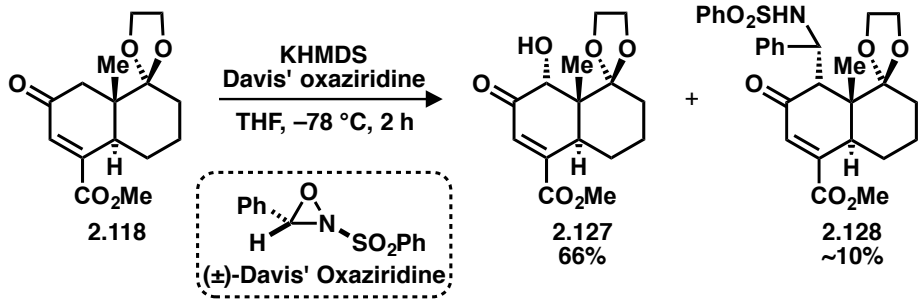

Methyl (4a*R*,8*R*,8a*R*)-8-hydroxy-8a-methyl-7-oxo-3,4,4a,7,8,8a-hexahydro-2*H*-spiro[naphthalene-1,2'-[1,3]dioxolane]-5-carboxylate (2.127) and methyl (4a*R*,8*R*,8a*R*)-

8a-methyl-7-oxo-8-((*R*)-phenyl(phenylsulfonamido)methyl)-3,4,4a,7,8,8a-hexahydro-2*H*-spiro[naphthalene-1,2'-[1,3]dioxolane]-5-carboxylate (2.128).

A 0.5 M solution of potassium bis(trimethylsilyl)amide in toluene (24.0 mL, 12.0 mmol) was added slowly to a –78 °C solution of ketone **2.118** (2.80 g, 10.0 mmol) in anhydrous tetrahydrofuran (120 mL) and the solution was stirred at that temperature for 45 min. A solution of 3-phenyl-2-(phenylsulfonyl)-1,2-oxaziridine (4.2 g, 16 mmol) in tetrahydrofuran (23 mL) was added and the resultant mixture was stirred at –78 °C for 1 h. A saturated aqueous solution of ammonium chloride (20 mL) was added and the mixture was allowed to warm to ambient temperature. The mixture was diluted with diethyl ether (80 mL) and an additional amount of a saturated aqueous solution of ammonium chloride (80 mL). The phases were separated and the aqueous portion was extracted with diethyl ether (3 × 75 mL). The combined organic extracts were washed with a 1:1 (v/v) mixture of 10% (w/v) aqueous sodium thiosulfate and a saturated aqueous solution of sodium bicarbonate (100 mL), 2 M aqueous sodium hydroxide (2 × 100 mL), and brine (75 mL), dried over sodium sulfate, filtered, and concentrated under reduced pressure. The residue was purified by flash column chromatography (14 × 4.5 cm) on silica gel (1:1 diethyl ether–hexanes) to afford **2.127** (1.96 g, 66%), which was difficult to separate from the sulfonamide side product (**2.128**) with traditional silica-based column chromatography.

Sulfonamide **2.128**: R_f 0.15 (1:1 diethyl ether–hexanes); ^{1}H NMR (400 MHz, chloroform-*d*) δ 7.43 – 7.37 (m, 2H), 7.31 – 7.21 (m, 1H), 7.15 – 7.07 (m, 2H), 7.00 – 6.93 (m, 3H), 6.92 – 6.84 (m, 2H), 5.96 (dd, *J* = 3.0, 0.8 Hz, 1H), 5.80 (d, *J* = 9.4 Hz, 1H), 5.74 (dd, *J* = 9.4, 2.5 Hz, 1H), 4.53 – 4.45 (m, 1H), 4.20 – 4.07 (m, 3H), 3.54 (s, 3H), 3.06 (d, *J* = 2.4 Hz, 1H), 2.96 (dt, *J* = 12.6, 3.3 Hz, 1H), 1.80 – 1.63 (m, 5H), 1.27 – 1.11 (m, 1H), 1.04 (s, 3H); ^{13}C NMR (75 MHz, chloroform-*d*) δ 202.2, 166.7, 150.8, 141.2, 137.2, 131.8, 131.7, 128.5, 128.4, 127.6, 127.5, 126.7, 112.3, 64.7, 63.8, 59.4, 55.6, 52.0, 45.4, 38.2, 29.5, 22.4, 22.2, 19.7; HRMS (ESI) calc'd for $C_{28}H_{31}N_1O_7S_1Na$ $[M+Na]^+$ *m/z* 548.1713, found 548.1725.

α-Hydroxy ketone **2.127**: R_f 0.11 (1:1 diethyl ether–hexanes); ^{1}H NMR (400 MHz, chloroform-*d*) δ 6.40 (dd, *J* = 3.2, 1.4 Hz, 1H), 4.73 (s, 1H), 4.16 – 4.07 (m, 3H), 4.04 – 3.94 (m, 2H), 3.80 (s, 3H), 3.40 (dt, *J* = 12.8, 3.2 Hz, 1H), 2.23 – 2.10 (m, 1H), 1.80 – 1.62 (m,

4H), 1.43 – 1.29 (m, 1H), 0.94 (s, 3H); ^{13}C NMR (75 MHz, chloroform-*d*) δ 195.6, 167.4, 150.6, 129.3, 113.9, 76.0, 65.2, 64.2, 52.5, 45.9, 37.4, 29.6, 22.5, 21.6, 14.2; HRMS (ESI) calc'd for $C_{15}H_{21}O_6$ $[M+H]^+$ *m/z* 297.1333, found 297.1339.

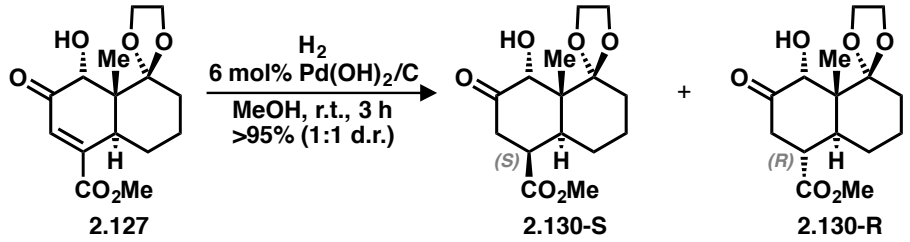

Methyl (4a*S*,5*S*,8*R*,8a*R*)-8-hydroxy-8a-methyl-7-oxooctahydro-2*H*-spiro[naphthalene-1,2'-[1,3]dioxolane]-5-carboxylate (2.130-S) and methyl (4a*S*,5*R*,8*R*,8a*R*)-8-hydroxy-8a-methyl-7-oxooctahydro-2*H*-spiro[naphthalene-1,2'-[1,3]dioxolane]-5-carboxylate (2.130-R).

Palladium hydroxide on carbon (0.064 g, 0.091 mmol, 20% w/w) was added to a stirred solution of enone **2.127** (0.730 g, 2.46 mmol) in methanol (40 mL) at ambient temperature. The suspension was purged with hydrogen gas and maintained under an atmosphere of hydrogen gas (using a hydrogen-filled balloon) for 3 h. The reaction mixture was filtered through a pad of Celite® 545, the filter cake was washed with diethyl ether, and the filtrate was concentrated under reduced pressure to afford a crude oil containing (*S*)-configured methyl ester **2.130-S** and (*R*)-configured methyl ester **2.130-R** in a ~1:1 diastereomeric ratio. The crude oil was purified by flash column chromatography (14 × 2.5 cm) on silica gel (1:50 to 1:30 acetone–dichloromethane) to give **2.130-R** (0.34 g, 46%) and **2.130-S** (0.38 g, 52%):

(*R*)-configured methyl ester **2.130-R**: R_f 0.49 (1:20 acetone–dichloromethane); ^{1}H NMR (400 MHz, chloroform-*d*) δ 5.18 (s, 1H), 4.16 – 3.93 (m, 5H), 3.72 (s, 3H), 3.32 (t, *J* = 13.1 Hz, 1H), 2.82 (td, *J* = 12.0, 3.7 Hz, 1H), 2.58 (ddd, *J* = 12.8, 11.6, 4.9 Hz, 1H), 2.28 (ddd, *J* = 13.4, 4.9, 1.0 Hz, 1H), 1.77 – 1.46 (m, 5H), 1.34 – 1.17 (m, 1H), 0.85 (s, 3H); ^{13}C NMR (75 MHz, chloroform-*d*) δ 207.4, 174.2, 114.6, 78.8, 64.9, 64.0, 52.2, 45.8, 45.7, 38.9, 36.1, 29.8, 24.6, 22.0, 13.5; HRMS (ESI) calc'd for $C_{15}H_{23}O_6$ $[M+H]^+$ *m/z* 299.1489, found 299.1499.

(*S*)-configured methyl ester **2.130-S**: R_f 0.35 (1:1 diethyl ether–hexanes); ^{1}H NMR (400 MHz, chloroform-*d*) δ 5.44 (s, 1H), 4.14 – 3.94 (m, 5H), 3.65 (s, 3H), 3.27 (dd, *J* = 13.8, 8.1 Hz,

1H), 3.08 (ddd, J = 8.1, 6.6, 1.4 Hz, 1H), 2.91 (ddd, J = 12.3, 6.6, 3.6 Hz, 1H), 2.51 (dt, J = 13.8, 1.2 Hz, 1H), 1.88 – 1.47 (m, 6H), 0.88 (s, 3H); ^{13}C NMR (75 MHz, chloroform-*d*) δ 207.2, 174.3, 115.0, 78.9, 64.7, 64.0, 51.9, 46.5, 45.0, 37.2, 36.1, 29.8, 25.4, 22.4, 14.1; HRMS (ESI) calc'd for $C_{15}H_{23}O_6$ $[M+H]^+$ *m/z* 299.1489, found 299.1497.

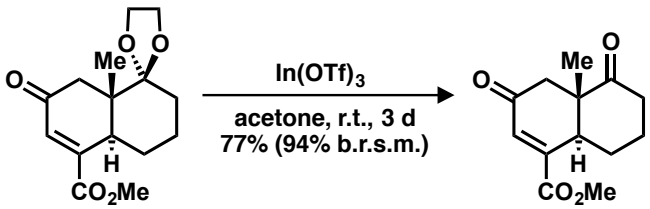

2.118 2.136

Methyl (4a*S*,8a*R*)-4a-methyl-3,5-dioxo-3,4,4a,5,6,7,8,8a-octahydronaphthalene-1-carboxylate (2.136).

Indium(III) trifluoromethanesulfonate (0.15 g, 0.27 mmol) was added to a vigorously stirred solution of ketal **2.118** (0.48 g, 1.7 mmol) in acetone (17 mL) at ambient temperature. The reaction mixture was vigorously stirred at ambient temperature for 3 d, at which point the volatiles were evaporated under reduced pressure. The residue was reconstituted in diethyl ether and successively washed with a saturated aqueous solution of ammonium chloride, a 1:1 (v/v) mixture of 10% (w/v) aqueous sodium thiosulfate and a saturated aqueous solution of sodium bicarbonate, and brine before it was dried over magnesium sulfate, filtered, and concentrated under reduced pressure. The residue was purified by flash column chromatography (15 × 2.5 cm) on silica gel (2:3 diethyl ether–hexanes) to afford recovered starting material (**2.118**, 0.090 g) and diketone **2.136** (0.31 g, 77%; 94% b.r.s.m.). The conversion often varied between 60–80%, but the starting material could be recovered in excellent yield regardless. Data for diketone **2.136**: R_f 0.26 (1:1 diethyl ether–hexanes); ^{1}H NMR (400 MHz, chloroform-*d*) δ 6.40 (dd, J = 3.2, 1.1 Hz, 1H), 3.82 (s, 3H), 2.92 (dt, J = 12.2, 3.2 Hz, 1H), 2.73 – 2.61 (m, 2H), 2.53 (dd, J = 16.8, 0.6 Hz, 1H), 2.39 – 2.29 (m, 2H), 2.23 – 2.11 (m, 1H), 1.88 – 1.65 (m, 2H), 1.19 (d, J = 0.6 Hz, 3H); ^{13}C NMR (75 MHz, chloroform-*d*) δ 211.1, 198.4, 167.2, 149.0, 131.4, 52.7, 50.5, 46.4, 44.8, 36.3, 25.4, 22.2, 17.0; HRMS (ESI) calc'd for $C_{13}H_{17}O_4$ $[M+H]^+$ *m/z* 237.1121, found 237.1121.

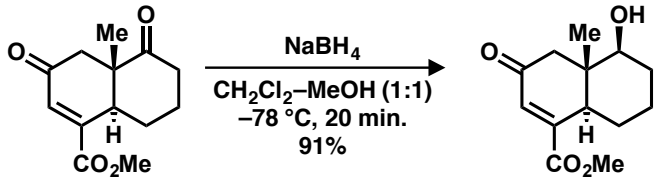

2.136 2.137

Methyl (4a*S*,5*S*,8a*R*)-5-hydroxy-4a-methyl-3-oxo-3,4,4a,5,6,7,8,8a-octahydronaphthalene-1-carboxylate (2.137).

Sodium borohydride (0.099 g, 2.6 mmol) was added portionwise to a –78 °C solution of diketone **2.136** (0.31 g, 1.3 mmol) in 1:1 (v/v) methanol–dichloromethane (60 mL), and the mixture was vigorously stirred at –78 °C for 20 minutes. Acetone (1.9 mL) was added and the cooling bath was removed to allow the mixture to warm to ambient temperature. The mixture was diluted with dichloromethane and partitioned with 2 M aqueous sodium hydroxide, at which point the phases were separated. (*Note:* on larger quantities of material, it was more convenient to evaporate some of the methanol, before partitioning the organic phase). The organic phase was washed with a saturated aqueous solution of sodium bicarbonate and brine, before it was dried over sodium sulfate, filtered, and concentrated under reduced pressure. The crude residue could be used directly in the next step, but was purified by flash column chromatography (14 × 2 cm) on silica gel (1:2 to 1:1 ethyl acetate–hexanes) to afford alcohol **2.137** (0.285 g, 91%): R_f 0.25 (1:1 ethyl acetate–hexanes); ^{1}H NMR (400 MHz, chloroform-*d*) δ 6.32 (dd, *J* = 3.2, 1.1 Hz, 1H), 3.80 (s, 3H), 3.58 – 3.47 (m, 1H), 2.83 (d, *J* = 16.1 Hz, 1H), 2.58 (dt, *J* = 12.6, 3.2 Hz, 1H), 2.18 (dd, *J* = 16.1, 1.3 Hz, 1H), 2.05 – 1.96 (m, 1H), 1.90 – 1.76 (m, 2H), 1.63 – 1.41 (m, 3H), 1.34 – 1.20 (m, 1H), 0.92 (d, *J* = 1.1 Hz, 3H); ^{13}C NMR (75 MHz, chloroform-*d*) δ 199.0, 167.7, 151.3, 130.7, 77.1, 52.5, 50.1, 43.9, 42.7, 29.8, 23.9, 22.2, 10.9; HRMS (ESI) calc'd for $C_{13}H_{19}O_4$ $[M+H]^+$ *m/z* 239.1278, found 239.1283.

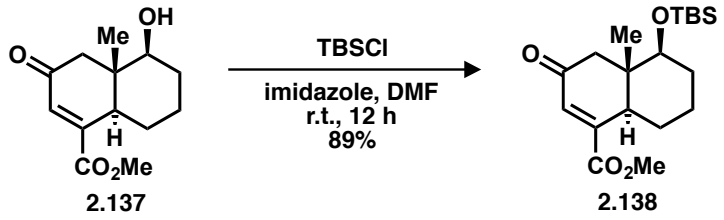

Methyl (4a*S*,5*S*,8a*R*)-5-((*tert*-butyldimethylsilyl)oxy)-4a-methyl-3-oxo-3,4,4a,5,6,7,8,8a-octahydronaphthalene-1-carboxylate (2.138).

tert-Butyldimethylsilyl chloride (0.47 g, 3.1 mmol) was added to a stirred solution of secondary alcohol **2.137** (0.491 g, 2.06 mmol) and imidazole (0.35 g, 5.2 mmol) in *N*,*N*-dimethylformamide (0.7 mL). The mixture was stirred at ambient temperature for 12 h, before it was diluted with diethyl ether (4 mL) and partitioned with a 10% (w/v) aqueous solution of lithium chloride (4 mL). The phases were separated and the ethereal phase was sequentially washed with 10% (w/v) aqueous solution of lithium chloride (2 × 4 mL) and brine, before it was dried over magnesium sulfate, filtered, and concentrated under reduced pressure. The residue was purified by flash column chromatography (12 × 2.5 cm) on silica gel (1:8 ethyl acetate–hexanes) to afford enone **2.138** (0.65 g, 89%) as a colorless oil, which sometimes crystallized upon standing: R_f 0.21 (1:8 ethyl acetate–hexanes); R_f 0.24 (1:3 diethyl ether–hexanes); $[\alpha]^{20}_D$ +8.7 (*c* = 2.0, chloroform); IR (film, cm^{-1}) ν 2951, 2857, 1727, 1683, 1472, 1233, 1105, 980, 836, 774; ^{1}H NMR (400 MHz, chloroform-*d*) δ 6.29 (dd, *J* = 3.2, 1.2 Hz, 1H), 3.79 (s, 3H), 3.47 (dd, *J* = 10.7, 4.6 Hz, 1H), 2.73 (d, *J* = 16.0 Hz, 1H), 2.56 (dt, *J* = 12.6, 3.2 Hz, 1H), 2.05 (dd, *J* = 16.1, 1.3 Hz, 1H), 1.96 (dq, *J* = 13.0, 3.3 Hz, 1H), 1.84 – 1.77 (m, 1H), 1.70 – 1.63 (m, 1H), 1.59 – 1.36 (m, 2H), 1.25 (qd, *J* = 12.7, 3.8 Hz, 1H), 0.89 (s, 3H), 0.87 (s, 9H), 0.04 (s, 6H); ^{13}C NMR (101 MHz, chloroform-*d*) δ 199.4, 167.8, 151.5, 130.6, 77.7, 52.4, 50.6, 44.0, 43.1, 30.2, 25.9, 23.9, 22.3, 18.1, 11.2, –3.8, –4.7; HRMS (ESI) calc'd for $C_{19}H_{32}O_4SiNa$ $[M+Na]^+$ *m/z* 375.1962, found 375.1962.

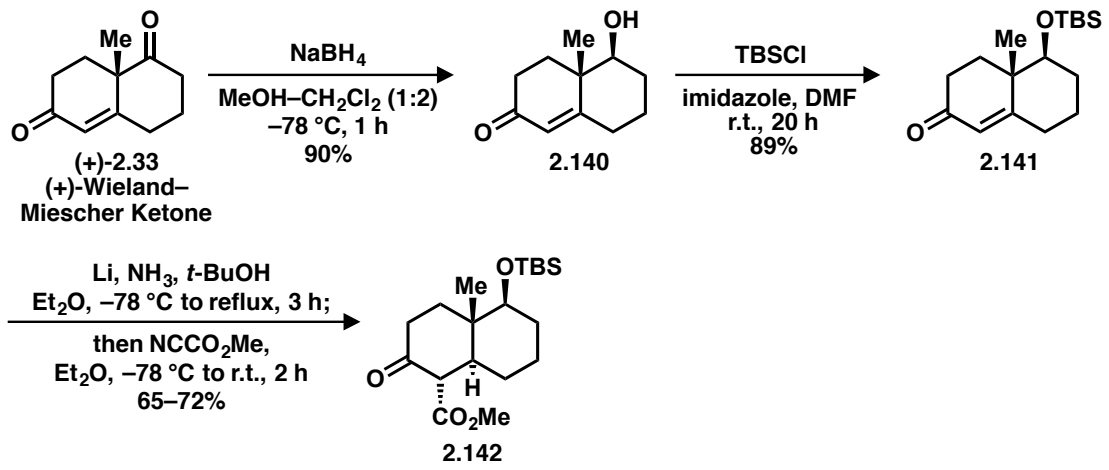

Methyl (1*S*,4a*S*,5*S*,8a*S*)-5-((*tert*-butyldimethylsilyl)oxy)-4a-methyl-2-oxodecahydronaphthalene-1-carboxylate (2.142).

β-Ketoester **2.142** was synthesized from (+)-Wieland–Miescher ketone using previously-described procedures; all data was in accordance that described in the literature. The reduction of **(+)-2.33** to **2.140** on large scale was described by Heathcock's group in ethanol, [410] but the procedure reported by Ward's group was found to be more convenient. [284] For the latter procedure, it was scaled up to ~20 g with the following modifications: more than five-fold increase in the concentration of diketone **(+)-2.33** in methanol–dichloromethane (1:2, v/v) to 0.14 M with a corresponding higher proportion of dichloromethane to methanol, 1.3 equivalents of sodium borohydride were used for the reduction, and 13 equivalents of acetone were used to quench the reaction. Protection of alcohol **2.140** was successfully realized through a procedure reported by Watt's group [354] that is based on the method reported by Corey's group. [285] Although the reductive carbomethoxylation of **2.141** to furnish **2.142** was previously reported by Takikawa's group, [287] the procedure and conditions used by Danishefky's group[225] on the analogous ketal were used to perform the reaction, with the following modifications: the volume of liquid ammonia used was halved and one equivalent of *tert*-butyl alcohol was used.

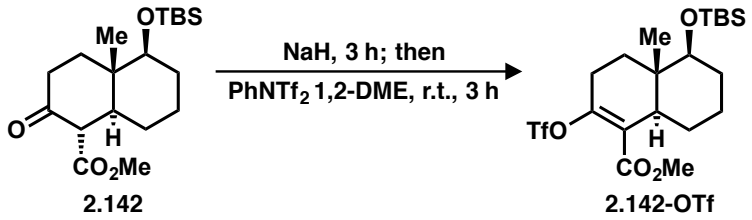

2.142 2.142-OTf

Methyl (4a*S*,5*S*,8a*R*)-5-((*tert*-butyldimethylsilyl)oxy)-4a-methyl-2-(((trifluoromethyl)sulfon-yl)oxy)-3,4,4a,5,6,7,8,8a-octahydronaphthalene-1-carboxylate (2.142-OTf).

Sodium hydride (2.40 g, 60.6 mmol, 60% w/w dispersion in mineral oil), was added portionwise to a vigorously stirred solution of β-ketoester **2.142** (17.2 g, 48.5 mmol) in anhydrous 1,2-dimethoxyethane (110 mL) at ambient temperature. The reaction mixture was stirred at ambient temperature for 3 h, before *N*-phenyl-bis(trifluoromethanesulfonimide) (20.8 g, 58.2 mmol) was added in one portion. The resultant mixture was stirred at ambient temperature for 3 h before it was poured into a saturated aqueous solution of ammonium chloride (250 mL) and diluted with diethyl ether (300 mL). The phases were separated and the aqueous portion was extracted with diethyl ether (3 × 100 mL). The combined organic extracts were washed with brine (100 mL), dried over sodium sulfate, filtered, and concentrated under reduced pressure to afford a crude oil (23.6 g) that was used in the next step without further purification. A portion of the residue was purified by flash column chromatography (15 × 1.5 cm) on silica gel (1:22 diethyl ether–hexanes) to afford **2.142-OTf** as a colourless oil: R_f 0. 61 (1:10 diethyl ether–hexanes); $[\alpha]^{20}_D$ –4.3 (*c* = 2.0, chloroform); IR (film, cm^{-1}) ν 2960, 2865, 1738, 1423, 1251, 1208, 1142, 1089, 933, 774; ^{1}H NMR (400 MHz, chloroform-*d*) δ 3.79 (s, 3H), 3.27 (dd, *J* = 10.6, 5.2 Hz, 1H), 2.58 – 2.43 (m, 1H), 2.38 – 2.26 (m, 2H), 2.08 (dd, *J* = 13.0, 6.3 Hz, 1H), 1.83 – 1.73 (m, 1H), 1.69 – 1.52 (m, 2H), 1.49 – 1.39 (m, 1H), 1.39 – 1.21 (m, 3H), 0.88 (s, 12H), 0.03 (s, 3H), 0.02 (s, 3H); ^{13}C NMR (101 MHz, chloroform-*d*) δ 165.6, 147.2, 127.4, 118.38 (d, $^2J_{C-F}$ = 319.7 Hz), 77.6, 52.2, 43.7, 38.3, 33.1, 30.5, 26.0, 25.0, 24.1, 23.1, 18.2, 10.3, –3.8, –4.8; HRMS (ESI) calc'd for $C_{20}H_{33}F_3O_6SSiNa$ $[M+Na]^+$ *m/z* 509.1611, found 509.1613.

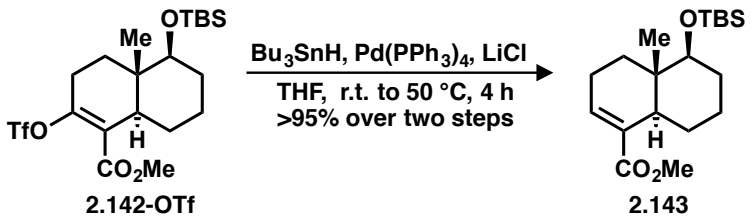

Methyl (4a*S*,5*S*,8a*R*)-5-((*tert*-butyldimethylsilyl)oxy)-4a-methyl-3,4,4a,5,6,7,8,8a-octahydronaphthalene-1-carboxylate (2.143).

Anhydrous lithium chloride (6.20 g, 145 mmol; flame-dried under reduced pressure) and tetrakis(triphenylphosphine)palladium (2.2 g, 1.9 mmol) were added to a vigorously stirred solution of crude enol triflate **2.142-OTf** (23.6 g, ≈48.5 mmol) in anhydrous tetrahydrofuran (167 mL) at ambient temperature. The reaction mixture was stirred at ambient temperature for 10 min., before a solution of tributyltin hydride (37.8 mL, 141 mmol) in tetrahydrofuran (21 mL) was slowly added over 50 min. The mixture was heated to 50 °C and vigorously stirred at this temperature for 4 h. The mixture was then cooled to ambient temperature and the volatiles removed under reduced pressure. The resultant residue was dissolved in diethyl ether (500 mL) and washed successively with a 10% (w/v) aqueous solution of potassium fluoride (3 × 100 mL) and brine, before being dried over sodium sulfate, filtered, and concentrated under reduced pressure. The residue was purified by flash column chromatography (21 × 9 cm) on silica gel (1:25 diethyl ether–hexanes) to afford **2.143** as a colourless oil (15.7 g, >95% over two steps), which sometimes crystallized upon standing: R_f 0.27 (0.1:1:4 diethyl ether–dichloromethane–hexanes); $[\alpha]^{20}_D$ −68.1 (*c* = 2.0, chloroform); IR (film, cm^{-1}) ν 2949, 2855, 1715, 1360, 1253, 1234, 1088, 831, 772; ^{1}H NMR (400 MHz, chloroform-*d*) δ 6.56 (q, *J* = 3.0 Hz, 1H), 3.69 (s, 3H), 3.28 (dd, *J* = 10.1, 5.7 Hz, 1H), 2.21 – 2.13 (m, 2H), 2.13 – 2.03 (m, 1H), 2.01 – 1.87 (m, 2H), 1.78 – 1.68 (m, 1H), 1.67 – 1.59 (m, 2H), 1.44 – 1.28 (m, 1H), 1.15 – 1.00 (m, 2H), 0.87 (s, 9H), 0.78 (s, 3H), 0.02 (s, 3H), 0.02 (s, 3H); ^{13}C NMR (101 MHz, chloroform-*d*) δ 169.0, 137.3, 133.6, 78.2, 51.4, 42.8, 38.6, 32.4, 30.9, 26.0, 24.3, 23.2, 22.5, 18.2, 10.6, –3.8, –4.7; HRMS (ESI) calc'd for $C_{19}H_{34}O_3SiNa$ $[M+Na]^+$ *m/z* 361.2169, found 361.2170.

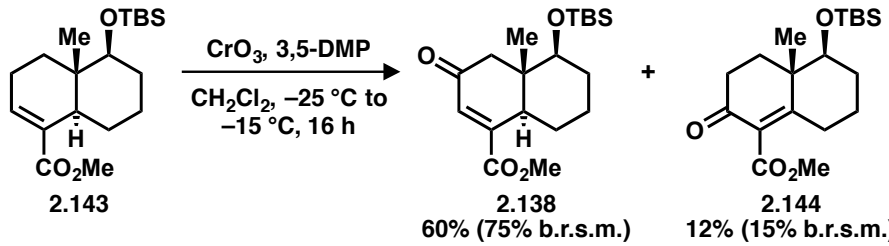

Methyl (4a*S*,5*S*,8a*R*)-5-((*tert*-butyldimethylsilyl)oxy)-4a-methyl-3-oxo-3,4,4a,5,6,7,8,8a-octahydronaphthalene-1-carboxylate (2.138) and methyl (4a*S*,5*S*)-5-((*tert*-butyldimethylsilyl)oxy)-4a-methyl-2-oxo-2,3,4,4a,5,6,7,8-octahydronaphthalene-1-carboxylate (2.144).

Anhydrous chromium trioxide (26.0 g, 260 mmol) was suspended in vigorously stirred dichloromethane (217 mL) and the resultant mixture was cooled to –25 °C. 3,5-Dimethylpyrazole (25.0 g, 260 mmol) was added in one portion and the mixture was stirred at –25 °C for 20 min. before a solution of α,β-unsaturated ester **2.143** (7.34 g, 21.7 mmol) in anhydrous dichloromethane (11 mL) was slowly added to the mixture. The mixture was vigorously stirred between –20 °C and –15 °C for 16 h. A 5 M aqueous solution of sodium hydroxide (104 mL) was added and the reaction mixture was warmed to 0 °C and stirred at that temperature for 1 h, before it was warmed to ambient temperature and stirred for an additional hour. The phases were separated and the organic phase was washed with 1 M aqueous hydrochloric acid (75 mL) and brine (75 mL), dried over sodium sulfate, filtered, and concentrated under reduced pressure. The residue was purified by flash column chromatography (18 × 7.5 cm) on silica gel (1:12 to 1:8 diethyl ether–hexanes) to afford undesired enone **2.144** as a colourless crystalline solid (0.95 g, 12%; 15% b.r.s.m.; experimental data reported above) and desired γ-keto-α,β-unsaturated ester **2.138** as a colourless oil (4.60 g, 60%; 75% b.r.s.m.), which sometimes crystallized upon standing.

γ-Keto-α,β-unsaturated ester **2.138**: R_f 0.24 (1:3 diethyl ether–hexanes); $[\alpha]^{20}_D$ +8.7 (*c* = 2.0, chloroform); IR (film, cm^{-1}) ν 2951, 2857, 1727, 1683, 1472, 1233, 1105, 980, 836, 774; ^1H NMR (400 MHz, chloroform-*d*) δ 6.29 (dd, *J* = 3.2, 1.2 Hz, 1H), 3.79 (s, 3H), 3.47 (dd, *J* = 10.7, 4.6 Hz, 1H), 2.73 (d, *J* = 16.0 Hz, 1H), 2.56 (dt, *J* = 12.6, 3.2 Hz, 1H), 2.05 (dd, *J* = 16.1, 1.3 Hz, 1H), 1.96 (dq, *J* = 13.0, 3.3 Hz, 1H), 1.84 – 1.77 (m, 1H), 1.70 – 1.63 (m, 1H), 1.59 – 1.36 (m, 2H), 1.25 (qd, *J* = 12.7, 3.8 Hz, 1H), 0.89 (s, 3H), 0.87 (s, 9H), 0.04 (s, 6H); ^{13}C NMR (101 MHz, chloroform-*d*) δ 199.4, 167.8, 151.5, 130.6, 77.7, 52.4, 50.6, 44.0, 43.1,

30.2, 25.9, 23.9, 22.3, 18.1, 11.2, –3.8, –4.7; HRMS (ESI) calc'd for $C_{19}H_{32}O_4SiNa$ $[M+Na]^+$ *m/z* 375.1962, found 375.1962.

Enone **2.144:** R_f 0.15 (1:3 diethyl ether–hexanes); ^{1}H NMR (400 MHz, chloroform-*d*) δ 3.80 (s, 3H), 3.43 (dd, *J* = 11.0, 4.9 Hz, 1H), 2.52 – 2.39 (m, 2H), 2.34 – 2.21 (m, 2H), 2.10 (dt, *J* = 13.7, 4.5 Hz, 1H), 1.85 (dd, *J* = 10.6, 6.9 Hz, 1H), 1.81 – 1.59 (m, 3H), 1.49 – 1.32 (m, 1H), 1.20 (s, 3H), 0.89 (s, 9H), 0.06 (s, 3H), 0.04 (s, 3H); ^{13}C NMR (75 MHz, chloroform-*d*) δ 195.4, 167.8, 165.5, 132.1, 78.6, 52.4, 42.2, 33.8, 33.6, 30.5, 29.2, 25.9, 22.6, 18.2, 16.0, –3.8, –4.8; HRMS (ESI) calc'd for $C_{19}H_{32}O_4SiNa$ $[M+Na]^+$ *m/z* 375.1962, found 375.1966. Recrystallization from diethyl ether–hexanes afforded crystals that were suitable for X-ray crystallographic analysis.

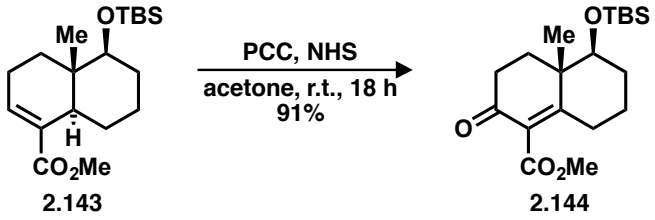

Methyl (4a*S*,5*S*)-5-((*tert*-butyldimethylsilyl)oxy)-4a-methyl-2-oxo-2,3,4,4a,5,6,7,8-octahydronaphthalene-1-carboxylate (2.144).

Pyridinium chlorochromate (0.052 g, 0.24 mmol) was added to a vigorously stirred solution of α,β-unsaturated ester **2.143** (0.039 g, 0.115 mmol) and *N*-hydroxy succinimide (0.046 g, 0.40 mmol) in acetone (1.0 mL) at ambient temperature. The reaction mixture was vigorously stirred at ambient temperature for 18 h, at which point the volatiles were evaporated under reduced pressure. The residue was reconstituted in diethyl ether and filtered through a short pad of silica gel (Pasteur pipette, 1 cm height of silica gel). The ethereal filtrate was washed with a saturated aqueous solution of sodium bicarbonate and brine, before it was dried over magnesium sulfate, filtered, and concentrated under reduced pressure. The residue was purified by flash column chromatography (14 × 1.75 cm) on silica gel (1:3 diethyl ether–hexanes) to afford enone **2.144** as a crystalline solid (0.037 g, 91%). Experimental data for enone **2.144** is reported within the preceding procedure.

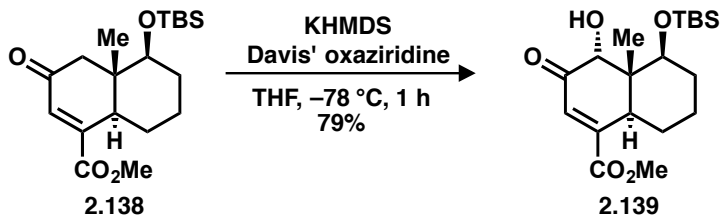

2.138 2.139

Methyl (4*R*,4a*R*,5*S*,8a*R*)-5-((*tert*-butyldimethylsilyl)oxy)-4-hydroxy-4a-methyl-3-oxo-3,4,4a,5,6,7,8,8a-octahydronaphthalene-1-carboxylate (2.139).

A 0.5 M solution of potassium bis(trimethylsilyl)amide in toluene (31.3 mL, 15.7 mmol) was added slowly to a –78 °C solution of ketone **2.138** (4.60 g, 13.0 mmol) in tetrahydrofuran (260 mL) and the solution was stirred at that temperature for 1 h. A solution of 3-phenyl-2-(phenylsulfonyl)-1,2-oxaziridine (6.82 g, 26.1 mmol) in tetrahydrofuran (37 mL) was added and the resultant mixture was stirred at –78 °C for 1 h. A saturated aqueous solution of ammonium chloride (20 mL) was added and the mixture was allowed to warm to ambient temperature, at which point 80% of the volatiles were removed under reduced pressure. The residue was diluted with diethyl ether (100 mL) and an additional amount of a saturated aqueous solution of ammonium chloride (100 mL). The phases were separated and the aqueous portion was extracted with diethyl ether (3 × 75 mL). The combined organic extracts were washed with a 1:1 (v/v) mixture of 10% (w/v) aqueous sodium thiosulfate and a saturated aqueous solution of sodium bicarbonate (100 mL), 1 M aqueous sodium hydroxide (100 mL), and brine (75 mL), dried over sodium sulfate, filtered, and concentrated under reduced pressure. The residue was purified by flash column chromatography (15 × 7.5 cm) on silica gel (1:7 to 1:2 diethyl ether–hexanes) to afford **2.139** as an oil (3.80 g, 79%), which readily foamed under reduced pressure (i.e., be careful when evaporating solvents!): R_f 0.25 (1:2 diethyl ether–hexanes); $[\alpha]^{20}_D$ +63.5 (*c* = 1.0, chloroform); IR (film, cm^{-1}) ν 3488, 2951, 2856, 1728, 1678, 1471, 1246, 1093, 835, 775; ^{1}H NMR (400 MHz, chloroform-*d*) δ 6.28 – 6.27 (m, 1H), 4.02 (dd, *J* = 11.0, 4.7 Hz, 1H), 3.85 (d, *J* = 3.6 Hz, 1H), 3.79 (s, 3H), 2.87 (dt, *J* = 12.7, 3.3 Hz, 1H), 2.54 – 2.41 (m, 1H), 1.96 (dd, *J* = 12.7, 3.5 Hz, 1H), 1.81 – 1.68 (m, 2H), 1.61 – 1.36 (m, 2H), 1.27 (qd, *J* = 12.8, 3.6 Hz, 1H), 0.87 (s, 9H), 0.80 (s, 3H), 0.07 (s, 3H), 0.06 (s, 3H); ^{13}C NMR (75 MHz, chloroform-*d*) δ 199.0, 167.6, 152.6, 128.0, 74.1, 70.2, 52.4, 45.5, 37.9, 29.8, 26.0, 23.8, 21.9, 18.1, 10.1, –4.0, –4.8; HRMS (ESI) calc'd for $C_{19}H_{32}O_5SiNa$ $[M+Na]^+$ *m/z* 391.1911, found 391.1905.

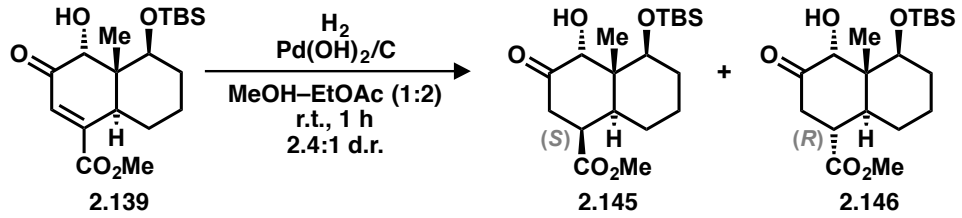

Methyl (1*S*,4*R*,4a*R*,5*S*,8a*S*)-5-((*tert*-butyldimethylsilyl)oxy)-4-hydroxy-4a-methyl-3-oxodecahydronaphthalene-1-carboxylate (2.145) and methyl (1*R*,4*R*,4a*R*,5*S*,8a*S*)-5-((*tert*-butyldimethylsilyl)oxy)-4-hydroxy-4a-methyl-3-oxodecahydronaphthalene-1-carboxylate (2.146).

Palladium hydroxide on carbon (0.28 g, 0.40 mmol, 20% w/w) was added to a stirred solution of enone **2.139** (3.70 g, 10.0 mmol) in 1:2 (v/v) methanol–ethyl acetate (50 mL) at ambient temperature. The suspension was purged with hydrogen gas and maintained under an atmosphere of hydrogen gas (using a hydrogen-filled balloon) for 1 h. The reaction mixture was filtered through a pad of Celite® 545, the filter cake was washed with ethyl acetate, and the filtrate was concentrated under reduced pressure to afford a crude oil (3.65 g) containing (*S*)-configured methyl ester **2.145** and (*R*)-configured methyl ester **2.146** in a 2.4:1 diastereomeric ratio. The crude oil was used directly in the next step without further purification. A portion of the residue was purified by flash column chromatography (15 × 1.5 cm) on silica gel (1:2 to 2:1 diethyl ether–hexanes) to give **2.146** as a colourless oil and **2.145** as a colourless crystalline solid:

(*R*)-configured methyl ester **2.146**: R_f 0.39 (1:1 diethyl ether–hexanes); $[\alpha]^{20}_D$ +6.8 (*c* = 1.0, chloroform); IR (film, cm^{-1}) ν 3507, 2950, 2857, 1739, 1719, 1437, 1251, 1105, 837, 776; ^1H NMR (400 MHz, chloroform-*d*) δ 3.96 (dd, *J* = 11.3, 4.4 Hz, 1H), 3.77 (d, *J* = 4.0 Hz, 1H), 3.69 (s, 3H), 3.16 (dd, *J* = 13.8, 12.8 Hz, 1H), 2.60 (ddd, *J* = 12.8, 11.7, 4.6 Hz, 1H), 2.34 – 2.22 (m, 3H), 1.75 – 1.61 (m, 2H), 1.53 – 1.07 (m, 4H), 0.87 (s, 9H), 0.71 (s, 3H), 0.05 (s, 4H), 0.05 (s, 3H); ^{13}C NMR (75 MHz, chloroform-*d*) δ 210.1, 174.5, 76.9, 70.5, 52.1, 45.9, 45.7, 39.4, 37.4, 30.0, 26.0, 24.7, 23.3, 18.2, 9.2, –3.9, –4.7; HRMS (ESI) calc'd for $C_{19}H_{35}O_5Si$ $[M+H]^+$ *m/z* 371.2248, found 371.2250.

(*S*)-configured methyl ester **2.145**: R_f 0.18 (1:1 diethyl ether–hexanes); $[\alpha]^{20}_D$ +39.4 (*c* = 2.0, chloroform); IR (film, cm^{-1}) ν 3482, 2946, 2856, 1734, 1709, 1447, 1249, 1100, 832, 773; ^1H

NMR (400 MHz, chloroform-*d*) δ 3.92 (dd, *J* = 11.2, 4.3 Hz, 1H), 3.73 (d, *J* = 3.6 Hz, 1H), 3.64 (s, 3H), 3.07 – 2.95 (m, 2H), 2.62 – 2.53 (m, 1H), 2.35 – 2.28 (m, 1H), 2.24 (d, *J* = 4.1 Hz, 1H), 1.81 – 1.69 (m, 1H), 1.69 – 1.59 (m, 3H), 1.46 – 1.22 (m, 2H), 0.86 (s, 9H), 0.70 (s, 3H), 0.05 (s, 3H), 0.04 (s, 3H); ^{13}C NMR (75 MHz, chloroform-*d*) δ 209.7, 174.2, 76.9, 71.1, 51.8, 46.3, 45.6, 38.1, 37.8, 30.1, 25.99, 25.95, 23.9, 18.2, 9.4, –3.8, –4.6; HRMS (ESI) calc'd for $C_{19}H_{35}O_5Si$ $[M+H]^+$ *m/z* 371.2248, found 371.2254. Recrystallization from diethyl ether–hexanes afforded crystals that were suitable for X-ray crystallographic analysis.

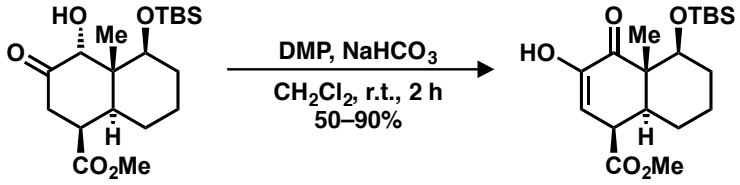

2.145 2.147

Methyl (1*R*,4a*S*,5*S*,8a*S*)-5-((*tert*-butyldimethylsilyl)oxy)-3-hydroxy-4a-methyl-4-oxo-1,4,4a,5,6,7,8,8a-octahydronaphthalene-1-carboxylate (2.147).

Dess-Martin periodinane (0.20 g, 0.49 mmol) was added to a stirred solution of α-hydroxy ketone **2.145** (0.090 g, 0.23 mmol) and solid sodium bicarbonate (0.24 g, 2.9 mmol) in anhydrous dichloromethane (3.2 mL) at ambient temperature. The reaction mixture was stirred at ambient temperature for 2 h, at which point it was diluted with diethyl ether and a 1:1 (v/v) mixture of 10% (w/v) aqueous sodium dithionite and a saturated aqueous solution of sodium bicarbonate (100 mL). The biphasic mixture was vigorously stirred until the phases were clear and colourless (approximately 10 min.). The phases were separated and the organic phase was dried over sodium sulfate, filtered, and concentrated under reduced pressure to afford crude **2.147** as a colourless oil (0.081 g, 90%): R_f 0.54 and 0.21 (1:1 ethyl acetate–hexanes, diketone and tautomer on TLC); ^{1}H NMR (400 MHz, chloroform-*d*) δ 6.21 (s, 1H), 5.96 (d, *J* = 5.9 Hz, 1H), 3.76 – 3.70 (m, 1H), 3.69 (s, 3H), 3.32 (t, *J* = 6.0 Hz, 1H), 2.16 (ddd, *J* = 12.7, 6.2, 3.2 Hz, 1H), 1.85 – 1.67 (m, 3H), 1.62 (dp, *J* = 12.4, 3.0, 2.4 Hz, 1H), 1.42 (dddd, *J* = 14.5, 12.7, 9.8, 3.3 Hz, 1H), 1.34 – 1.17 (m, 1H), 1.14 (s, 3H), 0.88 (s, 9H), 0.13 (s, 3H), 0.05 (s, 3H); ^{13}C NMR (101 MHz, chloroform-*d*) δ 199.4, 172.3, 145.1, 111.3, 72.1, 52.1, 49.7, 43.5, 43.1, 32.5, 26.5, 26.2, 24.1, 18.3, 11.0, –3.9, –4.5; HRMS (ESI) calc'd for $C_{19}H_{33}O_5Si$ $[M+H]^+$ *m/z* 369.2092, found 369.2096.

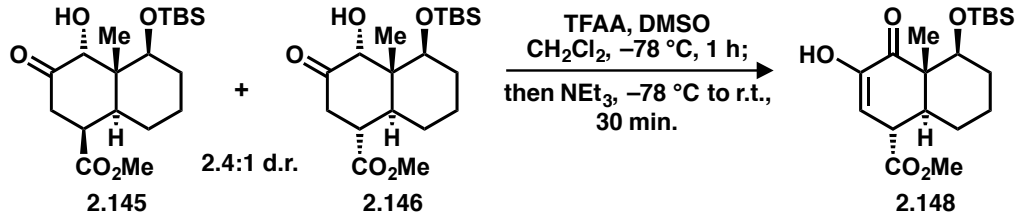

Methyl (1*S*,4a*S*,5*S*,8a*S*)-5-((*tert*-butyldimethylsilyl)oxy)-3-hydroxy-4a-methyl-4-oxo-1,4,4a,5,6,7,8,8a-octahydronaphthalene-1-carboxylate (2.148).

Trifluoroacetic anhydride (2.74 mL, 19.7 mmol) was added slowly to a –78 °C solution of dimethyl sulfoxide (2.80 mL, 39.4 mmol) in dichloromethane (45 mL). The solution was stirred at –78 °C for 15 min. before a solution of crude α-hydroxy ketones **2.145** and **2.146** (3.65 g, 9.85 mmol, dr = 2.4:1) in dichloromethane (19 mL) was added slowly. The solution was stirred at –78 °C for 1 h, at which point triethylamine (9.16 mL, 65.7 mmol) was added slowly. The resultant solution was stirred at –78 °C for 10 min., then allowed to warm to ambient temperature and stirred for an additional 30 min. The mixture was poured into a saturated aqueous solution of ammonium chloride (40 mL) was added and the phases were separated. The aqueous portion was extracted with dichloromethane (3 × 40 mL). The combined organic extracts were washed with brine (75 mL), dried over sodium sulfate, filtered, and concentrated under reduced pressure to afford **2.148** as a crude oil (3.63 g) that was used in the next step without further purification: R_f 0.67 and 0.15 (1:1 diethyl ether–hexanes, diketone and tautomer on TLC); ^{1}H NMR (300 MHz, chloroform-*d*) δ 6.05 (s, 1H), 5.74 (d, *J* = 2.5 Hz, 1H), 3.84 (dd, *J* = 10.9, 4.9 Hz, 1H), 3.73 (s, 3H), 3.29 (dd, *J* = 10.4, 2.6 Hz, 1H), 2.11 (td, *J* = 10.8, 3.9 Hz, 1H), 1.82 – 1.60 (m, 2H), 1.51 – 1.22 (m, 4H), 1.16 (s, 3H), 0.88 (s, 9H), 0.16 (s, 3H), 0.08 (s, 3H); ^{13}C NMR (75 MHz, chloroform-*d*) δ 199.3, 173.5, 145.4, 110.5, 71.4, 52.5, 48.9, 45.1, 43.9, 32.1, 26.2, 25.2, 23.3, 18.3, 9.8, –3.9, –4.5; HRMS (ESI) calc'd for $C_{19}H_{33}O_5Si$ $[M+H]^+$ *m/z* 369.2092, found 369.2089.

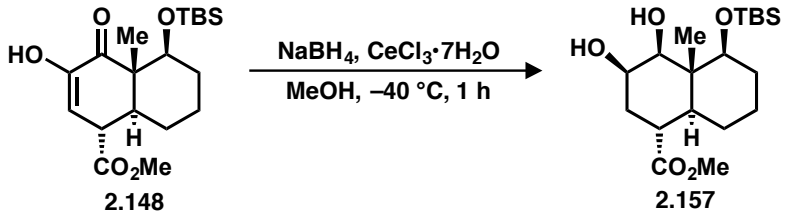

Methyl (1*R*,3*R*,4*S*,4a*R*,5*S*,8a*S*)-5-((*tert*-butyldimethylsilyl)oxy)-3,4-dihydroxy-4a-methyldecahydronaphthalene-1-carboxylate (2.157).

Cerium(III) chloride heptahydrate (7.34 g, 19.7 mmol) was added at –40 °C to a stirred solution of crude diketone **2.148** (3.63 g, 9.85 mmol) in methanol (225 mL). The resultant mixture was stirred at –40 °C for 15 min. before sodium borohydride (1.49 g, 39.4 mmol) was added in one portion. Upon complete consumption of the starting material by TLC analysis (*ca*. 1 h), a saturated aqueous solution of ammonium chloride (25 mL) was added and the mixture was allowed to warm to ambient temperature before the volatiles were removed under reduced pressure. The residue was dissolved in chloroform (100 mL) and partitioned with an additional volume of a saturated aqueous solution of ammonium chloride (50 mL). The phases were separated and the aqueous portion was extracted with chloroform (3 × 75 mL). The combined organic extracts were washed with brine (75 mL), dried over sodium sulfate, filtered, and concentrated under reduced pressure to afford diol **2.157** as a crude oil (3.67 g) that was used in the next step without further purification: R_f 0.34 (1:1 diethyl ether–hexanes); ^{1}H NMR (400 MHz, chloroform-*d*) δ 4.48 (s, 1H), 4.03 (q, *J* = 3.3 Hz, 1H), 3.65 (s, 3H), 3.65 – 3.59 (m, 1H), 3.52 (d, *J* = 3.5 Hz, 1H), 2.76 – 2.66 (m, 2H), 2.08 (dt, *J* = 14.2, 3.2 Hz, 1H), 1.80 – 1.66 (m, 2H), 1.59 (dd, *J* = 9.3, 6.0 Hz, 2H), 1.33 – 1.18 (m, 4H), 1.12 (d, *J* = 1.0 Hz, 3H), 0.91 (d, *J* = 1.0 Hz, 9H), 0.14 (s, 3H), 0.12 (s, 3H); ^{13}C NMR (101 MHz, chloroform-*d*) δ 176.6, 83.5, 79.6, 68.6, 51.6, 45.0, 42.9, 39.3, 33.8, 29.9, 26.0, 23.9, 23.7, 18.1, 8.2, –3.0, –4.5; HRMS (ESI) calc'd for $C_{19}H_{37}O_5Si$ $[M+H]^+$ *m/z* 373.2405, found 373.2408.

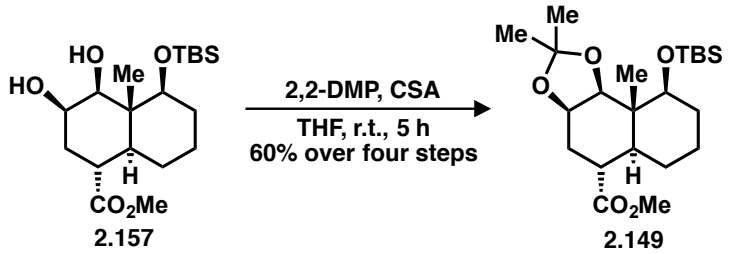

Methyl (3a*R*,5*R*,5a*S*,9*S*,9a*R*,9b*S*)-9-((*tert*-butyldimethylsilyl)oxy)-2,2,9a-trimethyldecahydronaphtho[1,2-*d*][1,3]dioxole-5-carboxylate (2.149).

Camphorsulfonic acid (0.686 g, 2.96 mmol) and 2,2-dimethoxypropane (4.84 mL, 39.4 mmol) were added sequentially to a stirred solution of crude diol **2.157** (3.67 g, 9.85 mmol) in tetrahydrofuran (98 mL) and the resultant solution was stirred at ambient temperature for 5 h. The volatiles were removed under reduced pressure and the residue was dissolved in diethyl ether (75 mL) and partitioned with a saturated aqueous solution of sodium bicarbonate (50 mL). The phases were separated and the aqueous portion was extracted with diethyl ether (3 × 75 mL). The combined organic extracts were washed with brine (75 mL), dried over sodium sulfate, filtered, and concentrated under reduced pressure. The residue was purified by flash column chromatography (12 × 5.5 cm) on silica gel (1:10 to 1:9 diethyl ether–hexanes) to afford acetonide **2.149** as a clear and colourless oil (2.50 g, 60% over four steps): R_f 0.55 (1:1 diethyl ether–hexanes); $[\alpha]^{20}_D$ +2.4 (*c* = 2.0, chloroform); IR (film, cm^{-1}) ν 2985, 2932, 2856, 1735, 1462, 1435, 1367, 1250, 1097, 836, 772; ^{1}H NMR (400 MHz, chloroform-*d*) δ 4.30 (dt, *J* = 8.4, 6.6 Hz, 1H), 3.87 (d, *J* = 6.9 Hz, 1H), 3.66 (s, 3H), 3.31 (dd, *J* = 11.1, 4.4 Hz, 1H), 2.44 (ddd, *J* = 10.5, 7.9, 5.3 Hz, 1H), 2.02 – 1.85 (m, 2H), 1.68 – 1.61 (m, 1H), 1.57 – 1.50 (m, 1H), 1.48 – 1.31 (m, 6H), 1.27 (s, 3H), 1.20 (qd, *J* = 13.1, 3.5 Hz, 2H), 0.92 (s, 3H), 0.88 (s, 9H), 0.05 (s, 3H), 0.02 (s, 3H); ^{13}C NMR (75 MHz, chloroform-*d*) δ 177.0, 107.9, 82.6, 81.2, 72.7, 51.8, 43.0, 41.7, 40.5, 30.9, 29.1, 27.2, 26.5, 26.0, 25.4, 23.6, 18.1, 9.2, –3.6, –5.0; HRMS (ESI) calc'd for $C_{22}H_{40}O_5SiNa$ $[M+Na]^+$ *m/z* 435.2537, found 435.2542.

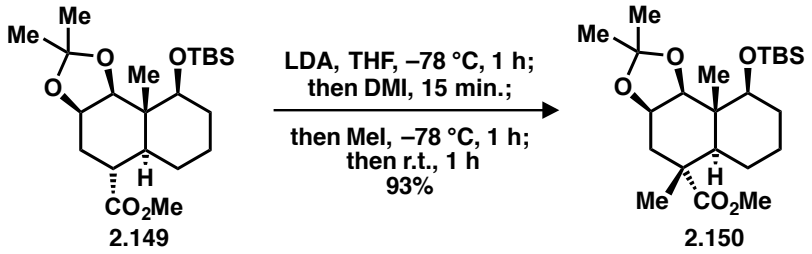

Methyl (3a*R*,5*R*,5a*R*,9*S*,9a*R*,9b*S*)-9-((*tert*-butyldimethylsilyl)oxy)-2,2,5,9a-tetramethyldecahydronaphtho[1,2-*d*][1,3]dioxole-5-carboxylate (2.150).

A 2.3 M solution of *n*-butyllithium in hexanes (0.79 mL, 1.8 mmol) was added slowly to a –78 °C solution of *N*,*N*-diisopropylamine (0.38 mL, 2.7 mmol) in tetrahydrofuran (4.3 mL). The solution was stirred at –78 °C for 30 min. before a solution of methyl ester **2.149** (0.125 g, 0.30 mmol) in tetrahydrofuran (0.9 mL) was added slowly. The solution was stirred at –78 °C for 1 h, at which point 1,3-dimethyl-2-imidazolidinone (0.085 mL, 0.79 mmol) was added dropwise and the mixture was stirred at –78 °C for 15 min. [*Note*: A few solid droplets appeared upon the addition of 1,3-dimethyl-2-imidazolidinone, which is perhaps unsurprising given the freezing temperature of 1,3-dimethyl-2-imidazolidinone. Since the overall conversion to the intended product was quite high, 1,3-dimethyl-2-imidazolidinone may not be necessary. It was not, for example, used in another procedure where benzyl chloromethyl ether was the electrophile.] Methyl iodide (0.15 mL, 2.5 mmol) was added dropwise to the solution, which was stirred at –78 °C for 1 h, then allowed to warm to ambient temperature and stirred for an additional 1 h. Diethyl ether (4 mL) and a saturated aqueous solution of ammonium chloride (6 mL) were added to the mixture and the phases were separated. The aqueous portion was extracted with diethyl ether (3 × 6 mL) and the combined organic extracts were washed with 1:1 (v/v) mixture of 10% (w/v) aqueous sodium dithionite and a saturated aqueous solution of sodium bicarbonate (5 mL), followed by water (3 × 5 mL), and brine (5 mL). The organic portion was then dried over sodium sulfate, filtered, and concentrated under reduced pressure. The residue was purified by flash column chromatography (10 × 1.5 cm) on silica gel (1:3 diethyl ether–hexanes) to afford **2.150** (0.12 g, 93%): R_f 0.35 (1:3 diethyl ether–hexanes); ^{1}H NMR (400 MHz, chloroform-*d*) δ 4.29 (ddd, *J* = 12.5, 7.2, 5.3 Hz, 1H), 3.91 (d, *J* = 7.2 Hz, 1H), 3.65 (s, 3H), 3.30 (dd, *J* = 11.3, 4.2 Hz, 1H), 2.07 (dd, *J* = 13.7, 5.1 Hz, 1H), 1.74 – 1.50 (m, 4H), 1.49 – 1.32 (m, 6H), 1.28 (s, 3H), 1.26 – 1.19 (m, 1H), 1.18 (s, 3H), 1.00

(s, 3H), 0.89 (s, 9H), 0.05 (s, 3H), 0.03 (s, 3H); ^{13}C NMR (101 MHz, chloroform-*d*) δ 178.6, 107.8, 82.5, 82.1, 73.0, 52.3, 44.9, 44.3, 41.7, 37.8, 31.0, 27.9, 26.0, 25.4, 23.9, 23.5, 22.2, 18.1, 10.3, –3.4, –4.9; HRMS (ESI) calc'd for $C_{23}H_{42}O_5SiNa$ $[M+Na]^+$ *m/z* 449.2694, found 449.2700.

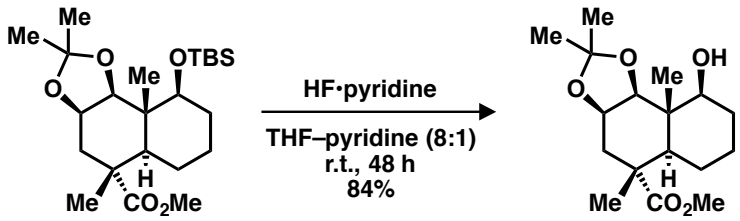

2.150 2.151

Methyl (3a*R*,5*R*,5a*R*,9*S*,9a*S*,9b*S*)-9-hydroxy-2,2,5,9a-tetramethyldecahydronaphtho[1,2-*d*][1,3]dioxole-5-carboxylate (2.151).

A 70% hydrogen fluoride–pyridine (0.073 mL, 2.25 mmol) was added in one portion to a stirred solution of *tert*-butyldimethylsilyl ether **2.150** (0.12 g, 0.225 mmol) in 8:1 (v/v) tetrahydrofuran–pyridine (0.71 mL : 0.09 mL) at ambient temperature in a polypropylene round-bottom flask. The mixture was stirred at ambient temperature for 16 h before a supplementary quantity of 70% hydrogen fluoride–pyridine (0.14 mL, 4.28 mmol) was added and the reaction was allowed to stir for an additional 32 h. A saturated aqueous solution of sodium bicarbonate (4 mL) was slowly added (lots of effervescence!) and the mixture was further diluted with ethyl acetate (4 mL). The phases were separated and the aqueous portion was extracted with ethyl acetate (3 × 4 mL). The combined organic extracts were washed with brine (5 mL), dried over sodium sulfate, filtered, and concentrated under reduced pressure. The residue was purified by flash column chromatography (10 × 1.5 cm) on silica gel (1:1 diethyl ether–hexanes) to afford secondary alcohol **2.151** (0.059 g, 84%): R_f 0.24 (1:1 diethyl ether–hexanes); ^{1}H NMR (400 MHz, chloroform-*d*) δ 4.50 – 4.38 (m, 1H), 3.91 (d, *J* = 8.2 Hz, 1H), 3.67 (s, 3H), 3.39 (dd, *J* = 11.0, 4.2 Hz, 1H), 2.84 (s, 1H), 2.35 (dd, *J* = 14.1, 6.9 Hz, 1H), 1.81 – 1.72 (m, 1H), 1.72 – 1.58 (m, 3H), 1.47 (d, *J* = 6.8 Hz, 4H), 1.45 – 1.22 (m, 6H), 1.21 (s, 3H), 0.97 (s, 3H); ^{13}C NMR (75 MHz, chloroform-*d*) δ 178.6, 108.4, 84.0, 82.0, 72.1, 52.4, 43.6, 42.7, 42.3, 37.5, 28.4, 26.4, 24.3, 23.8, 23.4, 22.9, 9.2; HRMS (ESI) calc'd for $C_{17}H_{28}O_5Na$ $[M+Na]^+$ *m/z* 335.1829, found 335.1827.

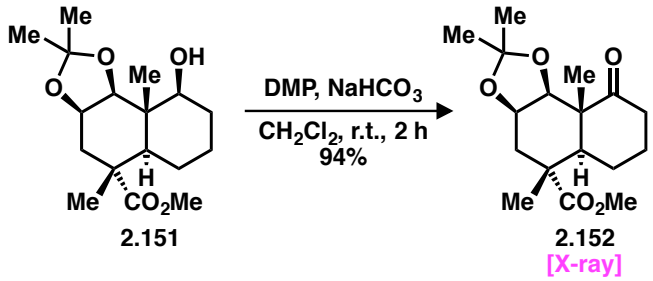

Methyl (3a*R*,5*R*,5a*R*,9a*R*,9b*S*)-2,2,5,9a-tetramethyl-9-oxodecahydronaphtho[1,2-*d*][1,3]dioxole-5-carboxylate (2.152).

Dess-Martin periodinane (0.036 g, 0.086 mmol) was added to a stirred solution of secondary alcohol **2.151** (0.015 g, 0.048 mmol) and solid sodium bicarbonate (0.040 g, 0.48 mmol) in anhydrous dichloromethane (1 mL) at ambient temperature. The reaction mixture was stirred at ambient temperature for 2 h, at which point it was diluted with diethyl ether (3 mL) and a 1:1 (v/v) mixture of 10% (w/v) aqueous sodium dithionite and a saturated aqueous solution of sodium bicarbonate (3 mL). The biphasic mixture was vigorously stirred until the phases were clear and colourless (approximately 10 min.). The phases were separated and the aqueous portion was extracted with diethyl ether (3 × 3 mL). The combined organic extracts were washed with brine, dried over sodium sulfate, filtered, and concentrated under reduced pressure. The residue was purified by flash column chromatography (10 × 1.5 cm) on silica gel (1:1 diethyl ether–hexanes) to afford ketone **2.152** (0.014 g, 94%): R_f 0.49 (1:20 acetone–dichloromethane); ^{1}H NMR (400 MHz, chloroform-*d*) δ 4.62 (d, *J* = 7.8 Hz, 1H), 4.30 (ddd, *J* = 12.0, 7.8, 5.8 Hz, 1H), 3.67 (s, 3H), 2.57 (td, *J* = 14.1, 6.2 Hz, 1H), 2.34 – 2.22 (m, 2H), 2.10 – 2.00 (m, 1H), 1.94 (dd, *J* = 12.0, 3.6 Hz, 1H), 1.92 – 1.82 (m, 1H), 1.82 – 1.74 (m, 1H), 1.58 (dd, *J* = 14.0, 12.0 Hz, 1H), 1.50 (ddt, *J* = 11.2, 5.9, 3.2 Hz, 0H), 1.46 (s, 3H), 1.40 (s, 3H), 1.30 (s, 3H), 1.24 (s, 3H); ^{13}C NMR (75 MHz, chloroform-*d*) δ 212.1, 177.8, 108.2, 74.7, 71.9, 52.9, 52.5, 44.9, 43.5, 37.8, 37.7, 27.1, 25.4, 24.8, 23.5, 22.6, 15.3; HRMS (ESI) calc'd for $C_{17}H_{26}O_5Na$ $[M+Na]^+$ *m/z* 333.1672, found 333.1669. Recrystallization from diethyl ether–hexanes afforded crystals that were suitable for X-ray crystallographic analysis.

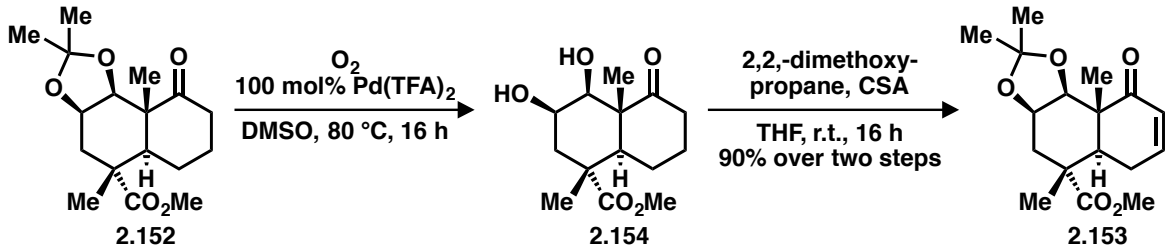

Methyl (3a*R*,5*R*,5a*R*,9a*R*,9b*S*)-2,2,5,9a-tetramethyl-9-oxodecahydronaphtho[1,2-*d*][1,3]dioxole-5-carboxylate (2.153).

Palladium(II) trifluoroacetate (0.044 g, 0.13 mmol) was added to a stirred solution of ketone **2.152** (0.041 g, 0.13 mmol) and sodium carbonate (~0.001 g, ~0.01 mmol) in dimethyl sulfoxide (0.64 mL) at ambient temperature. The suspension was purged with oxygen gas and fitted with an oxygen-filled balloon. The mixture was heated to 80 °C and stirred under an atmosphere of oxygen gas for 16 h. The reaction mixture was cooled to ambient temperature and diluted with diethyl ether (5 mL) and water (3 mL). The phases were separated and the organic phase was washed with water (3 × 3 mL) and brine (3 mL). The organic phase was then dried over sodium sulfate, filtered through a short plug of silica gel (Pasteur pipette, 1 cm height of silica gel), and concentrated under reduced pressure. The crude residue, which contained a mixture of *syn*-1,2-diol **2.154** and acetonide **2.153**, was immediately dissolved in tetrahydrofuran (1.2 mL) and used in the next step. Camphorsulfonic acid (0.010 g, 0.042 mmol) and 2,2-dimethoxypropane (0.073 mL, 0.60 mmol) were added sequentially to the stirred mixture of **2.154** and **2.153** and the resultant solution was stirred at ambient temperature for 16 h. The mixture was diluted with diethyl ether (4 mL) and a saturated aqueous solution of sodium bicarbonate (4 mL). The phases were separated and the aqueous portion was extracted with diethyl ether (3 × 4 mL). The combined organic extracts were washed with brine (5 mL), dried over sodium sulfate, filtered, and concentrated under reduced pressure. The residue was purified by flash column chromatography (10 × 1 cm) on silica gel (1:1 to 2:1 diethyl ether–hexanes) to afford acetonide **2.153** (0.033 g, 90% over two steps): R_f 0.25 (1:1 diethyl ether–hexanes); ^{1}H NMR (400 MHz, chloroform-*d*) δ 6.93 (ddd, *J* = 10.0, 5.4, 2.3 Hz, 1H), 5.99 (dd, *J* = 10.1, 2.8 Hz, 1H), 4.43 (d, *J* = 7.2 Hz, 1H), 4.26 (ddd, *J* = 12.2, 7.2, 5.2 Hz, 1H), 3.69 (s, 3H), 2.60 – 2.38 (m, 3H), 2.27 (dd, *J* = 13.9, 5.2 Hz, 1H), 1.60 (dd, *J* = 13.9, 11.9 Hz, 1H), 1.50 (s, 3H), 1.41 (s, 3H), 1.34 (s, 3H), 1.20 (s, 3H); ^{13}C NMR (101

MHz, chloroform-*d*) δ 202.9, 177.6, 148.4, 127.7, 108.6, 75.6, 72.4, 52.6, 49.6, 39.5, 37.1, 27.5, 25.6, 25.2, 23.2, 14.5; HRMS (ESI) calc'd for $C_{17}H_{24}O_5Na$ $[M+Na]^+$ *m/z* 331.1516, found 331.1519.

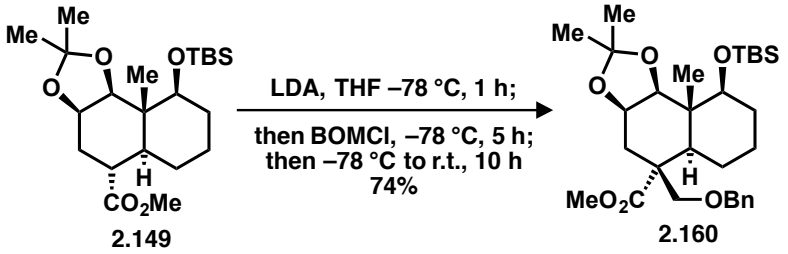

Methyl (3a*R*,5*R*,5a*R*,9*S*,9a*R*,9b*S*)-5-((benzyloxy)methyl)-9-((*tert*-butyldimethylsilyl)oxy)-2,2,9a-trimethyldecahydronaphtho[1,2-*d*][1,3]dioxole-5-carboxylate (2.160).

A 2.3 M solution of *n*-butyllithium in hexanes (1.52 mL, 3.49 mmol) was added slowly to a –78 °C solution of *N*,*N*-diisopropylamine (0.733 mL, 5.23 mmol) in tetrahydrofuran (8.3 mL). The solution was stirred at –78 °C for 30 min. before a solution of methyl ester **2.149** (0.24 g, 0.58 mmol) in tetrahydrofuran (1.6 mL) was added slowly. The solution was stirred at –78 °C for 1 h, at which point benzyl chloromethyl ether (0.69 mL, 3.5 mmol, 70%) was added slowly and the resultant solution was stirred for an additional 5 h at –78 °C. The reaction mixture was continuously stirred for 10 h during which time the temperature of the contents of the flask was allowed to slowly increase to ambient temperature (i.e., the acetone–dry-ice bath was not removed, but the temperature was allowed to equilibrate with that of the surroundings over 10 h). Diethyl ether (15 mL) and a saturated aqueous solution of ammonium chloride (15 mL) were added. The phases were separated and the aqueous portion was extracted with diethyl ether (3 × 15 mL). The combined organic extracts were washed with a saturated aqueous solution of sodium bicarbonate (15 mL) and brine (15 mL), dried over sodium sulfate, filtered, and concentrated under reduced pressure. The residue was purified by flash column chromatography (16 × 2.5 cm) on silica gel (1:8 to 1:6 diethyl ether–hexanes) to afford **2.160** as a clear and colourless oil (0.23 g, 74%), which often crystallized upon standing: R_f 0.39 (1:2 diethyl ether–hexanes); $[\alpha]^{20}_D$ +38.6 (*c* = 1.0, chloroform); IR (film, cm^{-1}) ν 2931, 2856, 1730, 1638, 1454, 1366, 1248, 1211, 1095, 836, 772; ^1H NMR (400 MHz, chloroform-*d*) δ 7.36 – 7.26 (m, 5H), 4.51 (d, *J* = 12.3 Hz, 1H), 4.44 (d, *J* = 12.4 Hz, 1H), 4.39 (ddd, *J* = 12.5, 7.2, 5.1

Hz, 1H), 3.86 (dd, *J* = 11.7, 7.9 Hz, 2H), 3.68 (s, 3H), 3.44 (d, *J* = 8.5 Hz, 1H), 3.25 (dd, *J* = 11.3, 4.2 Hz, 1H), 2.38 (dd, *J* = 13.8, 5.3 Hz, 1H), 1.88 – 1.79 (m, 1H), 1.68 (dt, *J* = 12.8, 3.1 Hz, 1H), 1.64 – 1.49 (m, 2H), 1.48 – 1.31 (m, 5H), 1.29 (s, 3H), 1.27 – 1.05 (m, 2H), 0.94 (s, 3H), 0.88 (s, 9H), 0.04 (s, 3H), 0.02 (s, 3H); ^{13}C NMR (101 MHz, chloroform-*d*) δ 176.6, 138.5, 128.4, 127.6, 127.5, 107.7, 82.3, 82.0, 74.0, 73.4, 73.3, 52.2, 49.3, 44.3, 42.6, 33.0, 30.9, 27.8, 26.0, 25.3, 24.0, 22.6, 18.1, 10.8, –3.5, –4.9; HRMS (ESI) calc'd for $C_{30}H_{48}O_6SiNa$ $[M+Na]^+$ *m/z* 555.3112, found 555.3111.

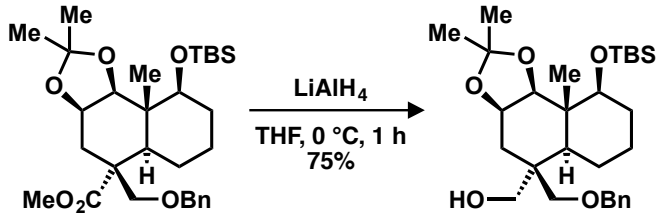

2.160 2.161

((3a*R*,5*S*,5a*S*,9*S*,9a*R*,9b*S*)-5-((Benzyloxy)methyl)-9-((*tert*-butyldimethylsilyl)oxy)-2,2,9a-trimethyldecahydronaphtho[1,2-*d*][1,3]dioxol-5-yl)methanol (2.161).

Lithium aluminum hydride (0.049 g, 1.3 mmol) was added portionwise to a stirred, 0 °C solution of ester **2.160** (0.20 g, 0.39 mmol) in anhydrous tetrahydrofuran (3.8 mL). The reaction mixture was stirred at 0 °C for 1 h, at which point water (0.049 mL), a 5 M aqueous solution of sodium hydroxide (0.037 mL), and water (0.148 mL) were sequentially added to the mixture, dropwise at 0 °C. The mixture was allowed to warm to ambient temperature and stirred for 15 min. Anhydrous magnesium sulfate was added and the mixture stirred for an additional 15 min, before the mixture was filtered through Celite® 545 and the solid washed with diethyl ether (3 × 2 mL). The filtrate was concentrated under reduced pressure and the resultant residue was purified by flash column chromatography (15 × 2.5 cm) on silica gel (1:2 to 1:1 diethyl ether–hexanes) to afford **2.161** as a clear and colourless oil (0.15 g, 75%), which often foamed under reduced pressure: R_f 0.22 (1:1 diethyl ether–hexanes); $[\alpha]^{20}_D$ +16.3 (*c* = 2.0, chloroform); IR (film, cm^{-1}) ν 3444, 2930, 2856, 1454, 1366, 1251, 1210, 1097, 1047, 966, 836, 771, 697; ^{1}H NMR (400 MHz, chloroform-*d*) δ 7.38 – 7.27 (m, 5H), 4.49 (d, *J* = 11.9 Hz, 1H), 4.42 (d, *J* = 11.9 Hz, 1H), 4.16 (ddd, *J* = 12.7, 7.4, 5.5 Hz, 1H), 3.82 (d, *J* = 7.3 Hz, 1H), 3.68 (dd, *J* = 10.9, 4.1 Hz, 1H), 3.59 (d, *J* = 9.0 Hz, 1H), 3.40 (d, *J* = 9.1 Hz, 1H),

3.35 (dd, *J* = 10.9, 7.8 Hz, 1H), 3.24 (dd, *J* = 11.3, 4.2 Hz, 1H), 2.54 (dd, *J* = 7.8, 4.1 Hz, 1H), 2.08 (dd, *J* = 13.6, 5.4 Hz, 1H), 1.69 (dt, *J* = 13.7, 3.4 Hz, 2H), 1.55 (d, *J* = 20.1 Hz, 2H), 1.42 (s, 3H), 1.40 – 1.33 (m, 1H), 1.28 (s, 4H), 1.27 – 1.08 (m, 2H), 0.96 (s, 3H), 0.89 (s, 10H), 0.88 – 0.79 (m, 1H), 0.04 (s, 3H), 0.02 (s, 3H); ^{13}C NMR (75 MHz, chloroform-*d*) δ 137.9, 128.6, 127.9, 127.7, 107.6, 82.6, 82.0, 76.3, 73.7, 73.0, 69.3, 44.2, 42.6, 41.1, 31.5, 31.0, 27.8, 26.0, 25.2, 24.4, 23.1, 18.1, 10.7, –3.4, –4.9; HRMS (ESI) calc'd for $C_{29}H_{48}O_5SiNa$ $[M+Na]^+$ *m/z* 527.3163, found 527.3143.

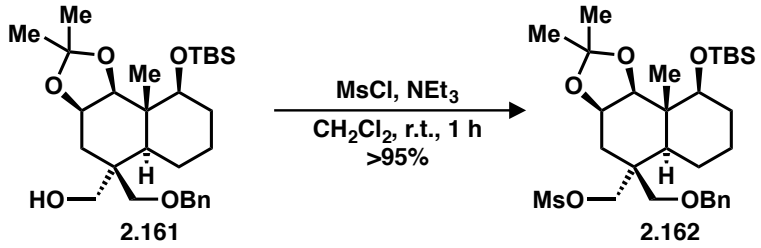

2.161 2.162

((3a*R*,5*R*,5a*S*,9*S*,9a*R*,9b*S*)-5-((Benzyloxy)methyl)-9-((*tert*-butyldimethylsilyl)oxy)-2,2,9a-trimethyldecahydronaphtho[1,2-*d*][1,3]dioxol-5-yl)methyl methanesulfonate (2.162).

Triethylamine (0.014 mL, 0.10 mmol) and methanesulfonyl chloride (0.014 g, 0.10 mmol) were added sequentially to a stirred solution of alcohol **2.161** (0.025 g, 0.050 mmol) in dichloromethane (0.45 mL) at ambient temperature and the resultant solution was stirred at that temperature for 1 h. The reaction mixture was diluted with dichloromethane (6 mL) and washed with a saturated aqueous solution of ammonium chloride (2 mL), water (2 mL), and brine (2 mL), before being dried over sodium sulfate, filtered, and concentrated under reduced pressure. The resultant residue was purified by flash column chromatography (14 × 1.5 cm) on silica gel (1:2 to 1:1 diethyl ether–hexanes) to afford **2.162** (0.032 g, >95%): R_f 0.24 (1:1 diethyl ether–hexanes); ^{1}H NMR (400 MHz, chloroform-*d*) δ 7.38 – 7.24 (m, 5H), 4.51 – 4.37 (m, 2H), 4.24 – 4.09 (m, 3H), 3.85 (d, *J* = 7.3 Hz, 1H), 3.46 (d, *J* = 9.2 Hz, 1H), 3.34 (d, *J* = 9.2 Hz, 1H), 3.26 (dd, *J* = 11.3, 4.2 Hz, 1H), 2.94 (s, 3H), 1.87 (dd, *J* = 14.1, 5.5 Hz, 1H), 1.70 (dq, *J* = 11.5, 4.0, 3.4 Hz, 2H), 1.65 – 1.51 (m, 2H), 1.41 (s, 3H), 1.40 – 1.30 (m, 1H), 1.28 (s, 3H), 1.27 – 1.10 (m, 3H), 0.96 (s, 3H), 0.89 (s, 10H), 0.05 (s, 3H), 0.02 (s, 3H); ^{13}C NMR (75 MHz, chloroform-*d*) δ 138.1, 128.5, 127.8, 127.6, 107.8, 82.4, 81.8, 74.6, 73.5, 72.8, 44.2,

41.6, 40.7, 37.1, 33.3, 30.9, 27.7, 26.0, 25.2, 24.2, 22.7, 18.1, 10.8, –3.4, –4.9; HRMS (ESI) calc'd for $C_{30}H_{50}O_7SiSNa$ $[M+Na]^+$ *m/z* 605.2939, found 605.2935.

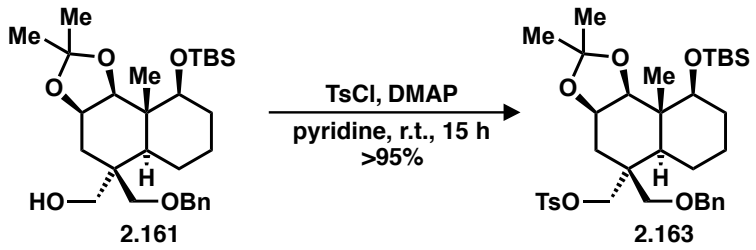

((3a*R*,5*R*,5a*S*,9*S*,9a*R*,9b*S*)-5-((Benzyloxy)methyl)-9-((*tert*-butyldimethylsilyl)oxy)-2,2,9a-trimethyldecahydronaphtho[1,2-*d*][1,3]dioxol-5-yl)methyl 4-methylbenzenesulfonate (2.163).

Para-toluenesulfonyl chloride (0.28 g, 0.15 mmol) and 4-(dimethylamino)pyridine (0.030 g, 0.025 mmol) were added sequentially to a stirred solution of alcohol **2.161** (0.025 g, 0.050 mmol) in pyridine (0.45 mL) at ambient temperature and the resultant solution was stirred at that temperature for 15 h. The solution was then cooled to 0 °C and 3-(dimethylamino)-1-propylamine (0.038 mL, 0.28 mmol) was added. The resultant solution was stirred at 0 °C for 30 min. before 1 M aqueous hydrochloric acid (2 mL) and diethyl ether (6 mL) were added. The phases were separated and the organic phase was washed sequentially with a saturated aqueous solution of sodium bicarbonate (2 × 2 mL) and brine (2 mL), before being dried over sodium sulfate, filtered through a short plug of silica gel (Pasteur pipette, 1 cm height of silica gel), and concentrated under reduced pressure. Residual amounts of pyridine were removed by co-evaporation with toluene under reduced pressure to afford **2.163** (0.028 g, >95%): R_f 0.51 (1:1 diethyl ether–hexanes); ^{1}H NMR (400 MHz, chloroform-*d*) δ 7.79 – 7.73 (m, 2H), 7.34 – 7.27 (m, 5H), 7.21 – 7.15 (m, 2H), 4.34 (s, 2H), 4.13 (ddd, *J* = 12.8, 7.4, 5.6 Hz, 1H), 3.98 (d, *J* = 9.2 Hz, 1H), 3.91 (d, *J* = 9.3 Hz, 1H), 3.78 (d, *J* = 7.4 Hz, 1H), 3.35 (d, *J* = 9.2 Hz, 1H), 3.27 (d, *J* = 9.2 Hz, 1H), 3.20 (dd, *J* = 11.3, 4.2 Hz, 1H), 2.42 (s, 3H), 1.73 (dd, *J* = 14.1, 5.6 Hz, 1H), 1.68 – 1.59 (m, 1H), 1.59 – 1.48 (m, 3H), 1.38 (s, 3H), 1.38 – 1.27 (m, 1H), 1.26 (s, 3H), 1.23 – 1.03 (m, 3H), 0.91 (s, 3H), 0.88 (s, 9H), 0.05 (s, 3H), 0.02 (s, 3H); ^{13}C NMR (75 MHz, chloroform-*d*) δ 144.9, 138.3, 132.9, 130.0, 128.4, 128.0, 127.6, 127.3, 107.6, 82.5, 81.8, 75.1, 73.3, 72.9, 72.8, 44.2, 41.4, 40.7, 33.4, 31.0, 27.6, 26.0, 25.1, 24.1, 22.5, 21.8, 18.1,

10.8, –3.5, –4.9; HRMS (ESI) calc'd for $C_{36}H_{54}O_7SiSNa$ $[M+Na]^+$ *m/z* 681.3252, found 681.3255.

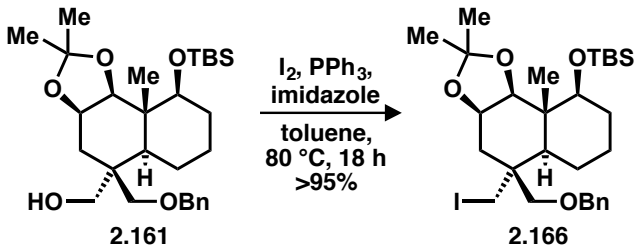

2.161 2.166

(((3a*R*,5*R*,5a*R*,9*S*,9a*R*,9b*S*)-5-((Benzyloxy)methyl)-5-(iodomethyl)-2,2,9a-trimethyldeca-hydronaphtho[1,2-*d*][1,3]dioxol-9-yl)oxy)(*tert*-butyl)dimethylsilane (2.166).

Triphenylphosphine (0.051 g, 0.19 mmol), imidazole (0.026 g, 0.039 mmol), and iodine (0.054 g, 0.21 mmol) were added sequentially to a stirred solution of alcohol **2.161** (0.075 g, 0.15 mmol) in toluene (1.4 mL) at ambient temperature. The resultant solution was heated to 80 °C and stirred at that temperature for 18 h. The mixture was cooled to ambient temperature, filtered, and the volatiles were removed under reduced pressure. The residue was dissolved in diethyl ether (10 mL) and partitioned with a 1:1 (v/v) mixture of 10% (w/v) aqueous sodium dithionite and a saturated aqueous solution of sodium bicarbonate (5 mL). The phases were separated and diethyl ether phase was washed with water (5 mL) and brine (5 mL), dried over sodium sulfate, filtered, and concentrated under reduced pressure. The residue was purified by filtration through a short plug of silica gel (Pasteur pipette, 1 cm height of silica gel) and washed with (1:20 diethyl ether–hexanes) to afford **2.166** as a clear and colourless oil (0.090 g, >95%), which sometimes foamed under reduced pressure: R_f 0.45 (1:10 diethyl ether–hexanes); $[\alpha]^{20}_D$ +20.5 (*c* = 1.0, chloroform); IR (film, cm^{-1}) ν 2932, 2855, 1454, 1366, 1254, 1209, 1100, 1063, 963, 836, 772; ^{1}H NMR (400 MHz, chloroform-*d*) δ 7.38 – 7.27 (m, 5H), 4.49 – 4.40 (m, 2H), 4.23 (ddd, *J* = 12.6, 7.4, 5.5 Hz, 1H), 3.83 (d, *J* = 7.4 Hz, 1H), 3.57 (d, *J* = 9.7 Hz, 1H), 3.44 (d, *J* = 9.5 Hz, 1H), 3.32 – 3.17 (m, 3H), 1.93 (dd, *J* = 14.0, 5.5 Hz, 1H), 1.83 (dd, *J* = 13.6, 3.4 Hz, 1H), 1.76 – 1.65 (m, 1H), 1.56 – 1.43 (m, 2H), 1.42 (s, 3H), 1.40 – 1.24 (m, 2H), 1.29 (s, 3H), 1.23 – 0.99 (m, 2H), 0.96 (s, 3H), 0.89 (s, 10H), 0.05 (s, 3H), 0.03 (s, 3H); ^{13}C NMR (101 MHz, chloroform-*d*) δ 138.6, 128.4, 127.62, 127.59, 107.7, 82.7, 82.0,

75.0, 73.5, 72.5, 45.2, 44.9, 39.8, 34.6, 31.0, 27.6, 26.0, 25.1, 24.3, 23.1, 19.7, 18.2, 10.5, –3.4, –4.9; HRMS (ESI) calc'd for $C_{29}H_{47}O_4SiINa$ $[M+Na]^+$ *m/z* 637.2180, found 637.2187.

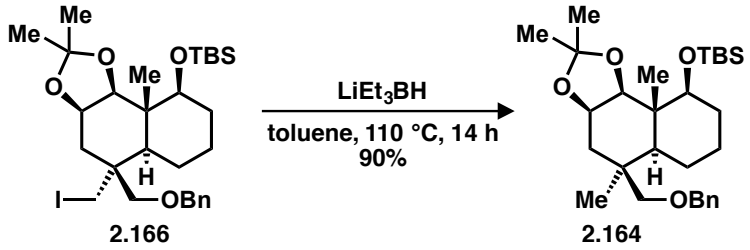

2.166 2.164

(((3a*R*,5*S*,5a*S*,9*S*,9a*R*,9b*S*)-5-((Benzyloxy)methyl)-2,2,5,9a-tetramethyldecahydro-naphtho[1,2-*d*][1,3]dioxol-9-yl)oxy)(*tert*-butyl)dimethylsilane (2.164).

A 0.97 M solution of lithium triethylborohydride (0.74 mL, 0.72 mmol) in tetrahydrofuran was added slowly to a vigorously stirred solution of alkyl iodide **2.166** (0.097 g, 0.17 mmol) in toluene (0.80 mL) at ambient temperature. The reaction mixture was heated to 110 °C and vigorously stirred at this temperature for 14 h. The mixture was cooled to ambient temperature before a 1 M aqueous solution of sodium hydroxide (1 mL) was added slowly to the mixture. The mixture was partitioned with diethyl ether (2 mL) and the phases were separated. The aqueous portion was extracted with diethyl ether (3 × 2 mL) and the combined organic extracts were washed with brine (4 mL), dried over sodium sulfate, filtered, and concentrated under reduced pressure. The residue was purified by flash column chromatography (13 × 1.5 cm) on silica gel (1:10 diethyl ether–hexanes) to afford **2.164** (0.073 g, 90%): R_f 0.44 (1:4 diethyl ether–hexanes); $[\alpha]^{20}_D$ +22.8 (*c* = 2.0, chloroform); IR (film, cm^{-1}) ν 2949, 2855, 1471, 1454, 1377, 1366, 1251, 1098, 1056, 836; ^1H NMR (400 MHz, chloroform-*d*) δ 7.37 – 7.23 (m, 5H), 4.47 (s, 2H), 4.16 (dt, *J* = 12.5, 6.3 Hz, 1H), 3.86 (d, *J* = 7.2 Hz, 1H), 3.31 (d, *J* = 8.7 Hz, 1H), 3.26 – 3.18 (m, 2H), 1.74 – 1.63 (m, 3H), 1.63 – 1.48 (m, 2H), 1.43 (s, 3H), 1.37 (td, *J* = 12.8, 12.3, 3.7 Hz, 1H), 1.30 (s, 3H), 1.28 – 1.08 (m, 2H), 1.04 (s, 3H), 0.97 (s, 3H), 0.90 (s, 9H), 0.94 – 0.82 (m, 1H), 0.06 (s, 3H), 0.03 (s, 3H); ^{13}C NMR (101 MHz, chloroform-*d*) δ 139.0, 128.3, 127.39, 127.36, 107.6, 83.2, 82.3, 77.5, 73.6, 73.4, 47.3, 44.2, 36.9, 36.8, 31.0, 28.0, 26.0, 25.8, 25.5, 24.6, 22.0, 18.2, 10.8, –3.4, –4.9; HRMS (ESI) calc'd for $C_{29}H_{48}O_4SiNa$ $[M+Na]^+$ *m/z* 511.3214, found 511.3224.

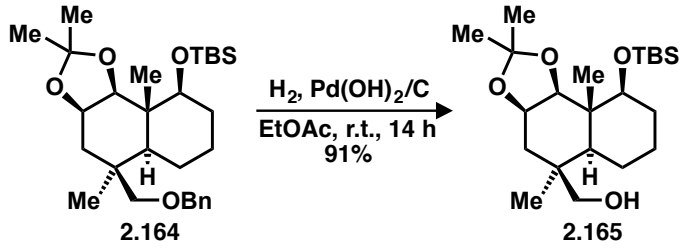

((3a*R*,5*S*,5a*S*,9*S*,9a*R*,9b*S*)-9-((*tert*-butyldimethylsilyl)oxy)-2,2,5,9a-tetramethyldeca-hydronaphtho[1,2-*d*][1,3]dioxol-5-yl)methanol (2.165).

Palladium hydroxide on carbon (0.005 g, 0.007 mmol, 20% w/w) was added to a stirred solution of benzyl ether **2.164** (0.067 g, 0.14 mmol) in ethyl acetate (1.4 mL). The suspension was purged with hydrogen gas and maintained under an atmosphere of hydrogen gas (using a hydrogen-filled balloon) for 14 h. The reaction mixture was diluted with ethyl acetate, filtered through a pad of Celite® 545, and the filter cake was subsequently washed with ethyl acetate before the filtrate was concentrated under reduced pressure. The residue was purified by flash column chromatography on silica gel (1:1 diethyl ether–hexanes) to afford primary alcohol **2.165** as a white solid (0.050 g, 91% yield): R_f 0.32 (2:1 diethyl ether–hexanes); $[\alpha]^{20}_D$ +30.3 (*c* = 2.0, chloroform); IR (film, cm^{-1}) ν 3354, 2931, 2856, 1472, 1368, 1251, 1211, 1164, 1100, 1078, 967, 836, 771; ^{1}H NMR (400 MHz, chloroform-*d*) δ 4.15 (dt, *J* = 12.4, 6.4 Hz, 1H), 3.87 (d, *J* = 7.1 Hz, 1H), 3.51 (d, *J* = 10.7 Hz, 1H), 3.41 (d, *J* = 10.8 Hz, 1H), 3.22 (dd, *J* = 11.3, 4.2 Hz, 1H), 1.77 – 1.68 (m, 1H), 1.64 – 1.48 (m, 4H), 1.45 – 1.33 (m, 5H), 1.29 (s, 3H), 1.27 – 1.05 (m, 2H), 1.00 (s, 3H), 0.99 (s, 3H), 0.92 (d, *J* = 3.0 Hz, 1H), 0.88 (s, 9H), 0.04 (s, 3H), 0.02 (s, 3H); ^{13}C NMR (101 MHz, chloroform-*d*) δ 107.8, 83.1, 82.2, 73.6, 69.9, 47.2, 44.2, 37.3, 36.3, 31.0, 28.0, 26.0, 25.5, 24.8, 24.6, 21.9, 18.1, 10.9, –3.4, –4.9; HRMS (ESI) calc'd for $C_{22}H_{42}O_4SiNa$ $[M+Na]^+$ *m/z* 421.2745, found 421.2726.

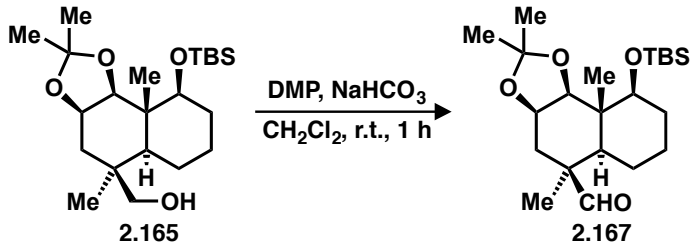

(3a*R*,5*S*,5a*R*,9*S*,9a*R*,9b*S*)-9-((*tert*-butyldimethylsilyl)oxy)-2,2,5,9a-tetramethyldeca-hydronaphtho[1,2-*d*][1,3]dioxole-5-carbaldehyde (2.167).

Dess-Martin periodinane (0.042 g, 0.10 mmol) was added to a stirred solution of primary alcohol **2.165** (0.020 g, 0.050 mmol) and solid sodium bicarbonate (0.042 g, 0.50 mmol) in anhydrous dichloromethane (1.0 mL) at ambient temperature. The reaction mixture was stirred at ambient temperature for 2 h, at which point it was diluted with dichloromethane and a 1:1 (v/v) mixture of 10% (w/v) aqueous sodium dithionite and a saturated aqueous solution of sodium bicarbonate (2 mL). The biphasic mixture was vigorously stirred until the phases were clear and colourless (approximately 10 min.). The phases were separated and the aqueous portion was extracted with dichloromethane (3 × 2 mL). The combined organic extracts were washed with brine, dried over sodium sulfate, filtered, and concentrated under reduced pressure to afford crude aldehyde **2.167** as a colourless oil (0.020 g): R_f 0.32 (1:4 diethyl ether–hexanes); ^{1}H NMR (400 MHz, chloroform-*d*) δ 9.60 (s, 1H), 4.22 (ddd, *J* = 12.4, 7.1, 5.2 Hz, 1H), 3.92 (d, *J* = 7.1 Hz, 1H), 3.27 (dd, *J* = 11.3, 4.2 Hz, 1H), 2.09 (t, *J* = 12.9 Hz, 1H), 1.74 (dq, *J* = 12.9, 3.2 Hz, 1H), 1.63 – 1.51 (m, 2H), 1.45 (s, 3H), 1.53 – 1.33 (m, 2H), 1.31 (s, 3H), 1.29 – 1.15 (m, 2H), 1.12 (s, 3H), 1.02 (s, 4H), 0.89 (s, 10H), 0.06 (s, 3H), 0.03 (s, 3H); ^{13}C NMR (101 MHz, chloroform-*d*) δ 205.2, 108.3, 82.7, 81.6, 72.9, 48.5, 47.8, 43.8, 32.8, 30.9, 27.9, 26.0, 25.4, 24.6, 23.2, 22.7, 18.1, 10.7, –3.4, –4.9; HRMS (ESI) calc'd for $C_{22}H_{40}O_4SiNa$ $[M+Na]^+$ *m/z* 419.2588, found 419.2585.

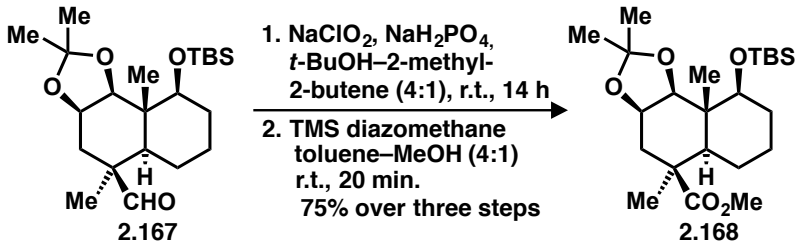

Methyl (3a*R*,5*S*,5a*R*,9*S*,9a*R*,9b*S*)-9-((*tert*-butyldimethylsilyl)oxy)-2,2,5,9a-tetramethyldecahydronaphtho[1,2-*d*][1,3]dioxole-5-carboxylate (2.168).

To a solution of crude aldehyde **2.167** (0.020 g, 0.050 mmol) in 4:1 (v/v) *tert*-butanol–2-methyl-2-butene (1.12 mL : 0.28 mL) at ambient temperature, was added a freshly prepared solution of sodium dihydrogen phosphate (0.051 g, 0.43 mmol) in water (0.27 mL), followed by a solution of sodium chlorite (0.024 g, 0.21 mmol) in water (0.13 mL). The biphasic mixture was stirred vigorously at ambient temperature for 14 h. The mixture was diluted with water (1 mL) and ethyl acetate (1.5 mL) and the phases were separated. The aqueous portion

was extracted with ethyl acetate (4 × 1.5 mL). The combined organic extracts were washed with brine, dried over sodium sulfate, filtered, and concentrated under reduced pressure to afford the crude carboxylic as a colourless oil (0.021 g) that was converted directly to the corresponding methyl ester, without any further purification. A 2 M solution of (trimethylsilyl)diazomethane in hexanes (0.028 mL, 0.056 mmol) was added dropwise to a solution of the crude carboxylic acid (0.021 g, 0.050 mmol) in 4:1 (v/v) toluene–methanol (1.27 mL : 0.32 mL) at ambient temperature, until the yellow colour of (trimethylsilyl)diazomethane persisted in the mixture. The mixture was allowed to stir at ambient for an additional 10 min., before it was diluted with water (1 mL) and diethyl ether (1.5 mL). The phases were separated and the aqueous portion was extracted with diethyl ether (3 × 1.5 mL). The combined organic extracts were washed with brine, dried over sodium sulfate, filtered, and concentrated under reduced pressure. The residue was purified by flash column chromatography (15 × 1.5 cm) on silica gel (1:11 ethyl acetate–hexanes) to afford methyl ester **2.168** (0.016 g, 75% over three steps) as a white solid: R_f 0.40 (1:3 diethyl ether–hexanes); $[\alpha]^{20}_D$ +16.5 (*c* = 1.0, chloroform); IR (film, cm^{-1}) ν 2929, 2855, 1727, 1471, 1366, 1234, 1203, 1155, 1103, 1058, 967, 836, 772; ^{1}H NMR (400 MHz, chloroform-*d*) δ 4.14 (ddd, *J* = 12.6, 7.3, 5.3 Hz, 1H), 3.85 (d, *J* = 7.3 Hz, 1H), 3.65 (s, 3H), 3.20 (dd, *J* = 11.2, 4.3 Hz, 1H), 2.40 (dd, *J* = 12.9 Hz, 1H), 1.74 – 1.65 (m, 1H), 1.63 – 1.48 (m, 3H), 1.44 (s, 3H), 1.44 – 1.34 (m, 1H), 1.30 (s, 3H), 1.22 (s, 3H), 1.20 – 1.03 (m, 2H), 1.02 (s, 3H), 0.89 (s, 9H), 0.87 – 0.82 (m, 1H), 0.05 (s, 3H), 0.02 (s, 3H); ^{13}C NMR (101 MHz, chloroform-*d*) δ 176.5, 107.9, 82.9, 82.1, 72.9, 51.6, 48.0, 45.2, 44.1, 35.8, 30.8, 27.6, 26.4, 26.0, 25.1, 24.2, 23.5, 18.2, 9.8, –3.5, –4.9; HRMS (ESI) calc'd for $C_{23}H_{42}O_5SiNa$ $[M+Na]^+$ *m/z* 449.2694, found 449.2676.

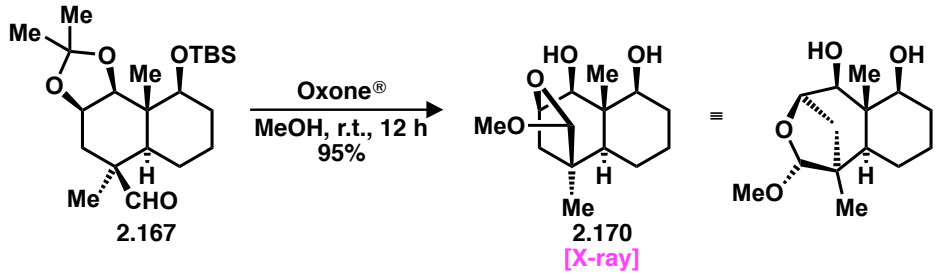

(1*S*,2*R*,4*R*,5*S*,5a*S*,6*S*,9a*R*)-2-Methoxy-1,5a-dimethyldecahydro-1,4-methanobenzo[*d*]oxepine-5,6-diol (2.170).

Oxone® (0.010 g, 0.033 mmol) was added to a solution of aldehyde **2.167** (0.013 g, 0.033 mmol) in methanol (0.33 mL) at ambient temperature. The mixture was stirred at ambient temperature for 12 h before it was diluted with 1 M aqueous hydrochloric acid (1.5 mL) and ethyl acetate 1.5 mL). The phases were separated and the aqueous portion was extracted with ethyl acetate (3 × 1.5 mL). The combined organic extracts were washed with brine, dried over sodium sulfate, filtered, and concentrated under reduced pressure. The residue was purified by flash column chromatography (Pasteur pipette, 9 cm × 0.5 cm) on silica gel (1:1 to 2:1 ethyl acetate–hexanes) to afford **2.170** as a white crystalline solid (0.008 g, 95%): R_f 0.28 (2:1 ethyl acetate–hexanes); $[\alpha]^{20}_D$ –66.9 (*c* = 0.35, chloroform); IR (film, cm^{-1}) ν 3368, 2924, 2854, 1727, 1464, 1414, 1176, 1129, 1091, 971, 774; ^{1}H NMR (400 MHz, chloroform-*d*) δ 4.56 (s, 1H), 4.32 (d, *J* = 6.7 Hz, 1H), 3.53 – 3.42 (m, 2H), 3.35 (s, 3H), 2.72 (d, *J* = 5.6 Hz, 1H), 2.42 (d, *J* = 2.6 Hz, 1H), 2.08 (dd, *J* = 11.3, 6.7 Hz, 1H), 1.85 – 1.77 (m, 1H), 1.61 (ddd, *J* = 10.5, 5.0, 2.6 Hz, 1H), 1.56 (s, 1H), 1.54 – 1.41 (m, 1H), 1.41 – 1.25 (m, 3H), 1.23 (s, 3H), 1.05 (dd, *J* = 12.6, 2.8 Hz, 1H), 0.98 (s, 3H); ^{13}C NMR (101 MHz, chloroform-*d*) δ 105.4, 82.3, 81.9, 80.7, 55.3, 51.2, 46.4, 45.1, 43.5, 29.3, 24.3, 20.7, 18.7, 7.6; HRMS (ESI) calc'd for $C_{14}H_{24}O_4Na$ $[M+Na]^+$ *m/z* 279.1567, found 279.1556. Recrystallization from diethyl ether–pentane afforded crystals that were suitable for X-ray crystallographic analysis.

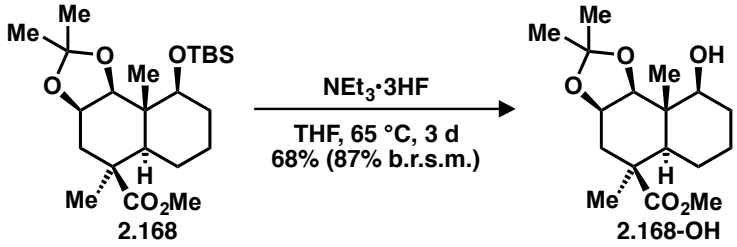

Methyl (3a*R*,5*S*,5a*R*,9*S*,9a*S*,9b*S*)-9-hydroxy-2,2,5,9a-tetramethyldecahydronaphtho[1,2-*d*][1,3]dioxole-5-carboxylate (2.168-OH).

Triethylamine trihydrofluoride (0.37 mL, 1.97 mmol) was added to a solution of *tert*-butyldimethylsilyl ether **2.168** (0.56 g, 1.3 mmol) in tetrahydrofuran (6.5 mL) at ambient temperature. The mixture was heated to 65 °C and stirred at that temperature for 24 h, before it was cooled to ambient temperature and an additional quantity of triethylamine trihydrofluoride (0.37 mL, 1.97 mmol) was added. The mixture was again heated to 65 °C and stirred at that temperature for 24 h, before it was cooled to ambient temperature and a final additional amount of triethylamine trihydrofluoride (0.37 mL, 1.97 mmol) was added. The mixture was again heated to 65 °C and stirred at that temperature for 24 h, before it was cooled to ambient temperature, slowly neutralized with a saturated aqueous solution of sodium bicarbonate (8 mL), and diluted with ethyl acetate (8 mL). The phases were separated and the aqueous portion was extracted with ethyl acetate (3 × 8 mL). The combined organic extracts were washed with brine, dried over sodium sulfate, filtered, and concentrated under reduced pressure. The residue was purified by flash column chromatography (12 × 3.5 cm) on silica gel (1:1 diethyl ether–hexanes) to afford *tert*-butyldimethylsilyl ether starting material ## (0.118 g, 21%) in addition to secondary alcohol **2.168-OH** (0.280 g, 68%; 87% b.r.s.m.), of which the latter was isolated as a clear and colourless oil: R_f 0.21 (1:1 diethyl ether–hexanes); $[\alpha]^{20}_D$ –18.2 (*c* = 1.0, chloroform); IR (film, cm^{-1}) ν 3552, 2937, 2868, 1727, 1452, 1382, 1209, 1162, 1066, 1034, 983, 874; ^{1}H NMR (400 MHz, chloroform-*d*) δ 4.32 (ddd, *J* = 11.0, 8.2, 6.9 Hz, 1H), 3.86 (d, *J* = 8.2 Hz, 1H), 3.66 (s, 3H), 3.32 (dd, *J* = 11.2, 4.2 Hz, 1H), 2.87 (s, 1H), 2.51 (dd, *J* = 13.5, 11.0 Hz, 1H), 1.83 (dd, *J* = 13.5, 6.9 Hz, 1H), 1.72 (ddd, *J* = 11.3, 5.8, 2.6 Hz, 1H), 1.67 – 1.59 (m, 1H), 1.51 (s, 4H), 1.35 (s, 3H), 1.34 – 1.23 (m, 1H), 1.23 – 1.21 (m, 3H), 1.21 – 1.05 (m, 2H), 1.03 (s, 3H), 0.84 (dd, *J* = 12.4, 3.5 Hz, 1H); ^{13}C NMR (101 MHz, chloroform-*d*) δ 176.4, 108.6, 84.2, 81.8, 72.1, 51.8, 48.3, 44.7, 42.3, 35.7, 28.3,

27.3, 26.3, 24.3, 24.0, 23.3, 8.9; HRMS (ESI) calc'd for $C_{17}H_{28}O_5Na$ $[M+Na]^+$ *m/z* 335.1829, found 335.1830.

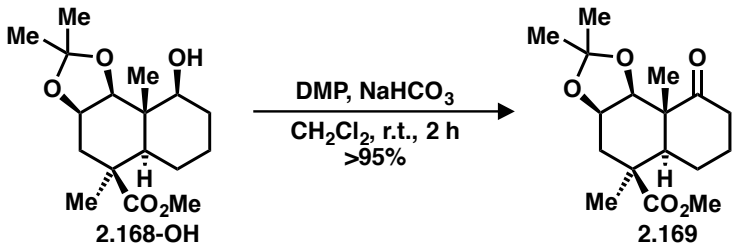

Methyl (3a*R*,5*S*,5a*R*,9a*R*,9b*S*)-2,2,5,9a-tetramethyl-9-oxodecahydronaphtho[1,2-*d*][1,3]dioxole-5-carboxylate (2.169).

Dess-Martin periodinane (0.074 g, 0.18 mmol) was added to a stirred solution of secondary alcohol **2.168-OH** (0.031 g, 0.099 mmol) and solid sodium bicarbonate (0.083 g, 0.99 mmol) in anhydrous dichloromethane (2.0 mL) at ambient temperature. The reaction mixture was stirred at ambient temperature for 2 h, at which point it was diluted with dichloromethane (2 mL) and a 1:1 (v/v) mixture of 10% (w/v) aqueous sodium dithionite and a saturated aqueous solution of sodium bicarbonate (4 mL). The biphasic mixture was vigorously stirred until the phases were clear and colourless (approximately 15 min.). The phases were separated and the aqueous portion was extracted with dichloromethane (3 × 4 mL). The combined organic extracts were washed with brine, dried over sodium sulfate, filtered, and concentrated under reduced pressure. The residue was purified by filtration through a short plug of silica gel (Pasteur pipette, 1 cm height of silica gel) and washed with (1:1 diethyl ether–hexanes) to afford ketone **2.169** as a white crystalline solid: R_f 0.18 (1:1 diethyl ether–hexanes); $[\alpha]^{20}_D$ +22.8 (*c* = 2.0, chloroform); IR (film, cm^{-1}) ν 2984, 2938, 1724, 1710, 1454, 1432, 1379, 1231, 1206, 1154, 1048, 995, 873; ^1H NMR (400 MHz, chloroform-*d*) δ 4.56 (d, *J* = 7.8 Hz, 1H), 4.22 (ddd, *J* = 11.5, 7.8, 5.8 Hz, 1H), 3.71 (s, 3H), 2.60 (td, *J* = 14.0, 6.3 Hz, 1H), 2.40 (dd, *J* = 13.6, 11.6 Hz, 1H), 2.24 (ddt, *J* = 13.7, 4.1, 1.8 Hz, 1H), 2.03 (ddq, *J* = 12.7, 6.1, 2.9 Hz, 1H), 1.87 – 1.78 (m, 1H), 1.74 (dd, *J* = 13.6, 5.8 Hz, 1H), 1.63 (qd, *J* = 13.1, 3.7 Hz, 1H), 1.48 (s, 3H), 1.49 – 1.35 (m, 1H), 1.41 (s, 3H), 1.27 (s, 3H), 1.24 (s, 3H), 1.19 (dd, *J* = 12.6, 3.6 Hz, 1H); ^{13}C NMR (101 MHz, chloroform-*d*) δ 212.3, 176.1, 108.3, 75.1, 71.8, 52.9, 52.0,

49.7, 45.3, 37.4, 36.0, 26.8, 26.6, 25.9, 24.7, 23.3, 15.2; HRMS (ESI) calc'd for $C_{17}H_{26}O_5Na$ $[M+Na]^+$ *m/z* 333.1672, found 333.1678.

Annex 3:

Experimental Data for Chapter 3

Experimental Procedures for Second-Generation Synthesis

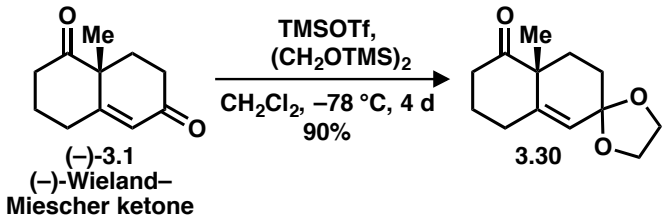

(*R*)-4a-Methyl-4,4a,7,8-tetrahydro-3*H*-spiro[naphthalene-2,2'-[1,3]dioxolan]-5(6*H*)-one (3.30).

Trimethylsilyl trifluoromethanesulfonate (0.22 mL, 1.2 mmol) was added dropwise to a vigorously stirred –78 °C solution of (*R*)-configured Wieland-Miescher ketone (–)-3.1 (11.0 g, 61.7 mmol) and 1,2-bis(trimethylsiloxy)ethane (21.2 mL, 86.4 mmol) in dichloromethane (41 mL). The reaction mixture was stirred at –78 °C for 4 d in total, with an additional quantity of trimethylsilyl trifluoromethanesulfonate (0.22 mL, 1.2 mmol) added after 24, 48, and 60 h (total quantity of trimethylsilyl trifluoromethanesulfonate used in the reaction = 0.88 mL, 4.9 mmol). After 4 d, pyridine (1.1 mL) was added and the reaction was warmed to ~10 °C and diluted with a saturated aqueous solution of sodium bicarbonate (40 mL). The phases were separated and the aqueous portion was extracted with dichloromethane (3 × 40 mL). The combined organic extracts were dried over 1:1 (w/w) sodium sulfate–sodium carbonate, filtered, and concentrated under reduced pressure. The residue was purified by flash column chromatography (15 × 7.5 cm) on silica gel (1:8 to 1:3 ethyl acetate–hexanes, with a slow and gradual increase in the ratio of ethyl acetate to hexanes) to afford mono-protected ketal **3.30** (12.4 g, 90%) as a clear and colorless oil, which often solidified upon standing: R_f 0.20 (1:4 ethyl acetate–hexanes); $[\alpha]^{20}_D$ –116.5 (*c* = 1.0, chloroform); IR (film, cm^{-1}) ν 2948, 2872, 1709, 1660, 1444, 1360, 1213, 1147, 1095, 1003, 886; ^{1}H NMR (400 MHz, chloroform-*d*) δ 5.40 (s, 1H), 4.03 – 3.83 (m, 4H), 2.63 (ddd, *J* = 15.2, 13.4, 6.3 Hz, 1H), 2.54 (dddd, *J* = 18.2, 13.2, 4.8, 0.8 Hz, 1H), 2.42 – 2.32 (m, 1H), 2.30 – 2.22 (m, 1H), 2.11 (ddd, *J* = 13.5, 11.5, 4.6 Hz, 1H), 2.06 – 1.96 (m, 1H), 1.84 – 1.59 (m, 4H), 1.30 (s, 3H); ^{13}C NMR (101 MHz, chloroform-*d*) δ 212.7, 146.8, 123.6, 105.6, 64.8, 64.5, 50.4, 38.0, 31.0, 30.0, 28.8, 24.5, 24.0; HRMS (ESI) calc'd for $C_{13}H_{18}O_3Na$ $[M+Na]^+$ *m/z* 245.1148, found 245.1154.

(4a*R*,6*R*)-6-Hydroxy-4a-methyl-4,4a,7,8-tetrahydro-3*H*-spiro[naphthalene-2,2'-[1,3]dioxolan]-5(6*H*)-one (*ent*-3.10) and (4a*R*,6*R*)-6-((*tert*-butyldimethylsilyl)oxy)-4a-methyl-4,4a,7,8-tetrahydro-3*H*-spiro[naphthalene-2,2'-[1,3]dioxolan]-5(6*H*)-one (3.31).

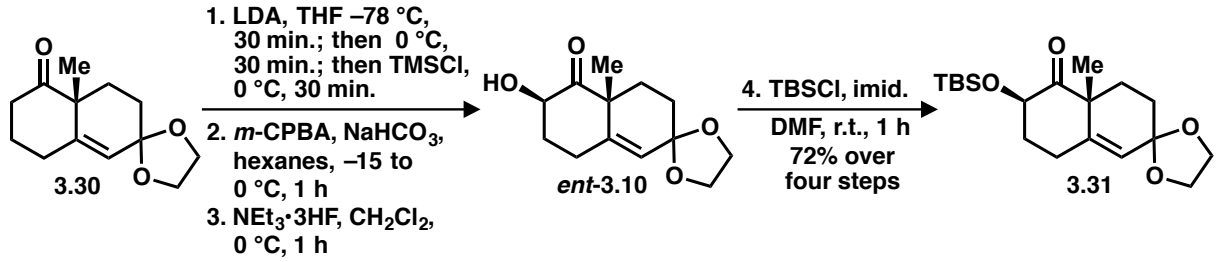

A 2.3 M solution of *n*-butyllithium in hexanes (40.0 mL, 92.0 mmol) was added slowly to a –78 °C solution of *N*,*N*-diisopropylamine (16.1 mL, 115 mmol) in tetrahydrofuran (160 mL). The solution was stirred at –78 °C for 15 min. before a solution of ketone **3.30** (12.4 g, 55.8 mmol) in tetrahydrofuran (22 mL) was added slowly. The solution was stirred at –78 °C for 30 min. before it was allowed to warm to 0 °C and stirred for 30 min. Trimethylsilyl chloride (16.1 mL, 127 mmol) was added in dropwise fashion at 0 °C and the resultant solution was stirred at 0 °C for 30 min. Triethylamine (18.0 mL, 129 mmol) was added and the solution was allowed to slowly warm to ambient temperature, at which point the volatiles were removed under reduced pressure. The residue was reconstituted in hexanes (100 mL) and the solids were removed by filtration through a sintered-glass funnel. The organic filtrate was diluted with a saturated aqueous solution of sodium bicarbonate (50 mL) and the phases were separated. The aqueous portion was extracted with hexanes (4 × 50 mL). The combined organic extracts were washed with brine (50 mL), dried over sodium sulfate, filtered through a short plug of silica gel (sintered-glass funnel, 2 cm height of silica gel), and concentrated under reduced pressure to afford a crude oil that was used directly in the next step without further purification. Solid *meta*-chloroperoxybenzoic acid (15.4 g, 66.8 mmol, 75%) was added in one portion to a vigorously stirred –15 °C mixture of sodium bicarbonate (8.60 g, 227 mmol) and crude trimethylsilyl enol ether in hexanes (290 mL). The mixture was vigorously stirred between –15 and 0 °C for 1 h, before the mixture was filtered through sodium sulfate (sintered-glass funnel, 2 cm height of sodium sulfate) and concentrated under reduced pressure. The residue was immediately dissolved in dichloromethane (220 mL) and the resultant solution cooled to 0 °C. Triethylamine trihydrofluoride (4.60 mL, 24.5 mmol) was

added and the solution was stirred at 0 °C for 1 h. The solution was diluted with a saturated aqueous solution of sodium bicarbonate (100 mL) and the phases were separated. The aqueous portion was extracted with dichloromethane (3 × 75 mL), and the combined organic extracts were washed with brine (100 mL), dried over sodium sulfate, filtered, and concentrated under reduced pressure. The crude residue was vacuum-dried for 1 h and used directly in the next step, but the intermediate material could also be purified by flash column chromatography (14 × 2 cm) on silica gel (1:1 ethyl acetate–hexanes) to afford of alcohol ***ent*-3.10**: R_f 0.17 (1:1 ethyl acetate–hexanes); ^{1}H NMR (400 MHz, chloroform-*d*) δ 5.53 – 5.45 (m, 2H), 4.23 (dd, *J* = 11.6, 8.1 Hz, 1H), 4.02 – 3.83 (m, 4H), 3.41 (s, 0H), 2.67 – 2.51 (m, 1H), 2.51 – 2.41 (m, 1H), 2.40 – 2.28 (m, 1H), 1.89 – 1.73 (m, 4H), 1.62 (*app.* tdd, *J* = 12.8, 10.7, 6.6 Hz, 1H), 1.29 (s, 3H); ^{13}C NMR (101 MHz, chloroform-*d*) δ 215.7, 142.7, 125.2, 105.4, 72.1, 64.9, 64.5, 47.3, 30.6, 29.6, 26.6, 26.0, 21.3; HRMS (ESI) calc'd for $C_{13}H_{19}O_4$ $[M+H]^+$ *m/z* 239.1278, found 239.1284.

After it had been vacuum-dried for 1 h, the crude residue of ***ent*-3.10** was dissolved in *N*,*N*-dimethylformamide (27 mL), along with imidazole (8.34 g, 123 mmol). *tert*-Butyldimethylsilyl chloride (9.20 g, 61.3 mmol) was added in one portion and the resultant solution was stirred at ambient temperature for 1 h. The solution was diluted with diethyl ether (100 mL) and partitioned with a 10% (w/v) aqueous solution of lithium chloride (75 mL). The aqueous portion was extracted with diethyl ether (3 × 100 mL), and the combined organic extracts were washed with 1 M aqueous hydrochloric acid (2 × 75 mL), a saturated aqueous solution of sodium bicarbonate (75 mL), and brine (75 mL), before they were dried over sodium sulfate, filtered, and concentrated under reduced pressure. The residue was purified by flash column chromatography (16 × 7.5 cm) on silica gel (1:9 ethyl acetate–hexanes) to afford silyl-protected α-hydroxy ketone **3.31** (14.2 g, 72% over four steps) as a clear and colorless oil: R_f 0.36 (1:4 ethyl acetate–hexanes); $[\alpha]^{20}_D$ –126.4 (*c* = 1.0, chloroform); IR (film, cm^{-1}) ν 2952, 2932, 2857, 1733, 1717, 1471, 1464, 1360, 1254, 1139, 1089, 995, 837, 779; ^{1}H NMR (400 MHz, chloroform-*d*) δ 5.41 (s, 1H), 4.17 (dd, *J* = 6.8, 6.0 Hz, 1H), 4.06 – 3.84 (m, 4H), 2.81 – 2.65 (m, 1H), 2.24 (ddd, *J* = 14.6, 6.8, 4.7 Hz, 1H), 2.00 – 1.70 (m, 6H), 1.36 (s, 3H), 0.88 (s, 9H), 0.08 (s, 3H), 0.04 (s, 3H); ^{13}C NMR (101 MHz, chloroform-*d*) δ 212.1, 145.7,

123.6, 105.7, 74.3, 64.8, 64.5, 49.0, 30.6, 30.3, 29.7, 26.3, 25.9, 22.8, 18.4, –4.7, –5.3; HRMS (ESI) calc'd for $C_{19}H_{33}O_4Si$ $[M+H]^+$ *m/z* 353.2143, found 353.2150.

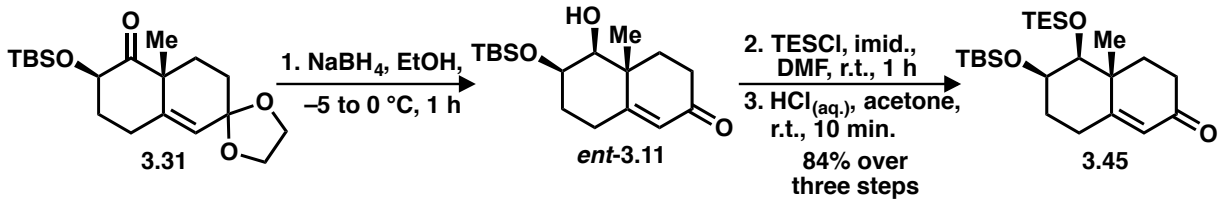

(4a*R*,5*S*,6*R*)-6-((*tert*-Butyldimethylsilyl)oxy)-5-hydroxy-4a-methyl-4,4a,5,6,7,8-hexahydronaphthalen-2(3*H*)-one (*ent*-3.11) and (4a*R*,5*S*,6*R*)-6-((*tert*-butyldimethylsilyl)oxy)-4a-methyl-5-((triethylsilyl)oxy)-4,4a,5,6,7,8-hexahydronaphthalen-2(3*H*)-one (3.45).

Sodium borohydride (0.804 g, 21.3 mmol) was added portionwise to a –5 °C solution of ketone **3.31** (15.0 g, 42.5 mmol) in anhydrous ethanol (106 mL). The mixture was vigorously stirred between –5 and 0 °C for 1 h, before a saturated aqueous solution of ammonium chloride (10 mL) was added and the contents of the round-bottom flask were evaporated to near dryness under reduced pressure. The residue was dissolved in chloroform and partitioned with water. The phases were separated and the aqueous portion was extracted with chloroform (3 × 100 mL). The combined organic extracts were washed with brine (100 mL), dried over sodium sulfate, filtered, and concentrated under reduced pressure to afford a crude oil that was used in the next step without further purification. The intermediate material could also be purified by flash column chromatography (13 × 1.5 cm) on silica gel (1:6 ethyl acetate–hexanes) to afford alcohol ***ent*-3.11**: R_f 0.17 (1:6 ethyl acetate–hexanes); ^{1}H NMR (400 MHz, chloroform-*d*) δ 5.34 (s, 1H), 4.11 – 3.83 (m, 5H), 3.18 (dd, *J* = 11.1, 3.5 Hz, 1H), 2.54 – 2.42 (m, 1H), 2.13 (d, *J* = 11.1 Hz, 1H), 1.84 (dtd, *J* = 11.4, 5.8, 2.3 Hz, 3H), 1.79 – 1.64 (m, 3H), 1.60 – 1.46 (m, 1H), 1.16 (s, 3H), 0.91 (s, 9H), 0.10 (s, 3H), 0.08 (s, 3H); ^{13}C NMR (101 MHz, chloroform-*d*) δ 149.0, 122.3, 106.2, 78.7, 71.6, 64.7, 64.4, 40.8, 34.2, 32.2, 29.4, 26.2, 25.9, 18.6, 18.1, –4.4, –5.0; HRMS (ESI) calc'd for $C_{19}H_{35}O_4Si$ $[M+H]^+$ *m/z* 355.2299, found 355.2288.

Triethylsilyl chloride (7.8 mL, 46.5 mmol) was added to a stirred solution of crude secondary alcohol ***ent*-3.11** and imidazole (6.34 g, 93.1 mmol) in *N*,*N*-dimethylformamide (21 mL). The mixture was stirred at ambient temperature for 1 h, before it was diluted with diethyl ether (100 mL) and partitioned with a 10% (w/v) aqueous solution of lithium chloride (75 mL). The aqueous portion was extracted with diethyl ether (3 × 100 mL), and the combined organic extracts were washed with a saturated aqueous solution of sodium bicarbonate (75 mL), dried over sodium sulfate, filtered, and concentrated under reduced pressure. The residue was immediately dissolved in acetone (140 mL) and an aqueous 2 M solution of hydrochloric acid was added (6.3 mL). The solution was stirred at ambient temperature until the starting material had been completely consumed (~10 min.), at which point a saturated aqueous solution of sodium bicarbonate (150 mL) was added along with diethyl ether (100 mL). The phases were separated and the aqueous portion was extracted with diethyl ether (3 × 100 mL). The combined organic extracts were washed with brine (100 mL), dried over sodium sulfate, filtered, and concentrated under reduced pressure. The residue was purified by flash column chromatography (15 × 7.5 cm) on silica gel (1:15 ethyl acetate–hexanes) to afford enone **3.45** (15.2 g, 84% over three steps) as a clear and colorless oil, which often crystallized upon standing: R_f 0.15 (1:15 ethyl acetate–hexanes); $[\alpha]^{20}_D$ –88.2 (*c* = 2.0, chloroform); IR (film, cm^{-1}) ν 2951, 2872, 1676, 1463, 1382, 1251, 1118, 1086, 1064, 997, 834; ^{1}H NMR (400 MHz, chloroform-*d*) δ 5.78 (s, 1H), 3.99 (dd, *J* = 5.2, 2.9 Hz, 1H), 3.26 (d, *J* = 2.8 Hz, 1H), 2.81 (tdd, *J* = 14.2, 5.2, 2.0 Hz, 1H), 2.49 (dd, *J* = 14.9, 5.1 Hz, 1H), 2.45 (dd, *J* = 14.8, 5.2 Hz, 1H), 2.37 – 2.28 (m, 1H), 2.10 – 1.99 (m, 2H), 1.89 – 1.79 (m, 1H), 1.65 (td, *J* = 14.9, 14.5, 5.2 Hz, 1H), 1.53 (tdd, *J* = 13.9, 4.2, 2.2 Hz, 1H), 1.33 (s, 3H), 0.98 (t, *J* = 7.9 Hz, 9H), 0.91 (s, 9H), 0.64 (qd, *J* = 7.9, 3.6 Hz, 6H), 0.11 (s, 3H), 0.08 (s, 3H); ^{13}C NMR (101 MHz, chloroform-*d*) δ 199.8, 169.8, 125.2, 80.4, 72.1, 42.4, 35.9, 33.6, 31.5, 27.3, 26.0, 18.2, 17.6, 7.2, 5.4, –4.5; HRMS (ESI) calc'd for $C_{23}H_{44}O_3Si_2Na$ $[M+Na]^+$ *m/z* 447.2721, found 447.2723.

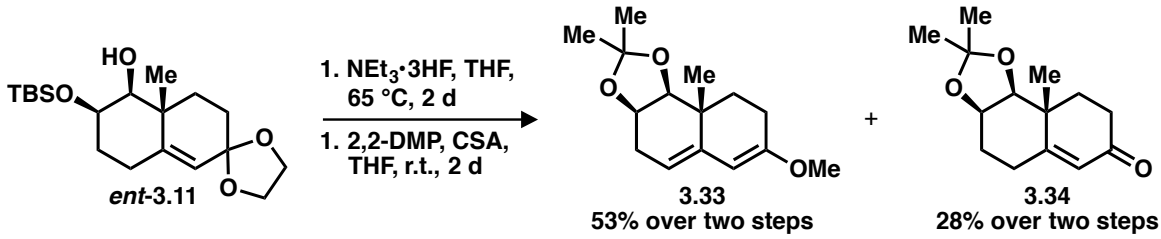

(3a*R*,9a*R*,9b*S*)-7-methoxy-2,2,9a-trimethyl-3a,4,8,9,9a,9b-hexahydronaphtho[1,2-*d*][1,3]dioxole (3.33) and (3a*R*,9a*R*,9b*S*)-2,2,9a-trimethyl-4,5,8,9,9a,9b-hexahydronaphtho[1,2-*d*][1,3]dioxol-7(3a*H*)-one (3.34).

Triethylamine trihydrofluoride (1.56 mL, 8.26 mmol) was added to a solution of *tert*-butyldimethylsilyl ether ***ent*-3.11** (2.93 g, 8.26 mmol) in tetrahydrofuran (28 mL) at ambient temperature. The mixture was heated to 65 °C and stirred at that temperature for 2 d, at which point it was cooled to ambient temperature, slowly neutralized with a saturated aqueous solution of sodium bicarbonate, and diluted with ethyl acetate. The phases were separated and the aqueous portion was thrice extracted with ethyl acetate. The combined organic extracts were washed with brine, dried over sodium sulfate, filtered, and concentrated under reduced pressure to afford crude diol (1.38 g was recovered) that was immediately used in the next step. Camphorsulfonic acid (0.16 g, 0.70 mmol) and 2,2-dimethoxypropane (1.73 mL, 14.1 mmol) were added sequentially to a stirred solution of crude diol in tetrahydrofuran (70 mL) and the resultant solution was stirred at ambient temperature for 2 d. The mixture was diluted with diethyl ether and partitioned with a saturated aqueous solution of sodium bicarbonate. The phases were separated and the aqueous portion was thrice extracted with diethyl ether. The combined organic extracts were washed with brine, dried over magnesium sulfate, filtered, and concentrated under reduced pressure. The residue was purified by flash column chromatography (14 × 3.5 cm) on silica gel (1:10 to 1:2 ethyl acetate–hexanes) to afford methyl dienol ether **3.33** (1.1 g, 53% over two steps) and acetonide **3.34** (28% over two steps).

Methyl dienol ether **3.33:** R_f 0.48 (1:6 ethyl acetate–hexanes); ^{1}H NMR (400 MHz, chloroform-*d*) δ 5.30 – 5.20 (m, 2H), 4.43 (dd, *J* = 15.4, 8.2 Hz, 1H), 3.80 (d, *J* = 8.1 Hz, 1H), 3.58 (s, 3H), 2.74 (ddd, *J* = 16.0, 8.9, 7.1 Hz, 1H), 2.44 – 2.28 (m, 2H), 2.06 (ddd, *J* = 16.8, 5.4, 2.2 Hz, 1H), 1.91 (ddd, *J* = 12.8, 5.2, 2.2 Hz, 1H), 1.52 (s, 4H), 1.37 (s, 3H), 0.97 (s, 3H); ^{13}C NMR (101 MHz, chloroform-*d*) δ 157.8, 141.0, 114.3, 108.3, 97.7, 83.6, 73.6, 54.5, 37.2,

35.3, 28.7, 26.5, 24.9, 24.8, 16.9; HRMS (ESI) calc'd for $C_{15}H_{22}O_3Na$ $[M+Na]^+$ *m/z* 273.1461, found 273.1470.

Acetonide **3.34:** R_f 0.07 (1:6 ethyl acetate–hexanes); ^{1}H NMR (400 MHz, chloroform-*d*) δ 5.86 (s, 1H), 4.44 (dd, *J* = 15.1, 7.6 Hz, 1H), 3.89 (d, *J* = 7.5 Hz, 1H), 2.72 – 2.46 (m, 2H), 2.46 – 2.24 (m, 2H), 2.21 – 1.96 (m, 2H), 1.88 (td, *J* = 13.2, 5.0 Hz, 1H), 1.53 (s, 3H), 1.39 (s, 3H), 1.29 (s, 3H), 1.28 – 1.19 (m, 1H); ^{13}C NMR (101 MHz, chloroform-*d*) δ 198.7, 168.0, 126.1, 109.0, 81.2, 73.4, 39.4, 37.0, 33.7, 27.3, 26.1, 25.5, 24.8, 21.5; HRMS (ESI) calc'd for $C_{14}H_{21}O_3$ $[M+H]^+$ *m/z* 237.1485, found 237.1492.

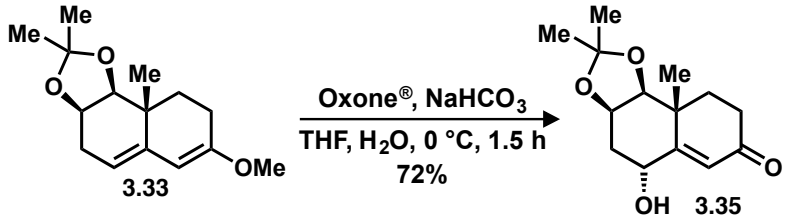

(3a*R*,5*R*,9a*R*,9b*S*)-5-hydroxy-2,2,9a-trimethyl-4,5,8,9,9a,9b-hexahydronaphtho[1,2-*d*][1,3]dioxol-7(3a*H*)-one (3.35).

A solution of Oxone® (0.33 g, 1.1 mmol) in water (1.5 mL) was added slowly (~1 min.) to a mixture of methyl dienol ether **3.33** (0.18 g, 0.72 mmol) and sodium bicarbonate (0.082 g, 2.2 mmol) in tetrahydrofuran (5 mL) at 0 °C. The mixture was vigorously stirred at 0 °C for 1.5 h, before it was diluted with diethyl ether and further partitioned with a saturated aqueous solution of sodium bicarbonate. The phases were separated and the aqueous portion was thrice extracted with diethyl ether. The combined organic extracts were washed with brine, dried over magnesium sulfate, filtered, and concentrated under reduced pressure. The residue was purified by flash column chromatography (12 × 1.5 cm) on silica gel (3:2 ethyl acetate–hexanes) to afford alcohol **3.35** (0.13 g, 72%): R_f 0.25 (2:1 ethyl acetate–hexanes); ^{1}H NMR (400 MHz, chloroform-*d*) δ 6.08 (d, *J* = 1.3 Hz, 1H), 4.66 (ddd, *J* = 7.2, 3.9, 3.3 Hz, 1H), 4.57 (ddd, *J* = 6.8, 6.7, 4.8 Hz, 1H), 4.07 (d, *J* = 6.7 Hz, 1H), 2.53 – 2.43 (m, 2H), 2.35 (dt, *J* = 14.4, 4.7 Hz, 1H), 2.13 (ddd, *J* = 14.6, 8.0, 6.9 Hz, 1H), 2.07 – 1.91 (m, 3H), 1.54 (s, 3H), 1.38 (s, 3H), 1.29 (s, 3H); ^{13}C NMR (101 MHz, chloroform-*d*) δ 199.2, 169.1, 124.0, 109.0, 80.3,

72.3, 66.4, 39.3, 36.5, 34.9, 33.8, 26.1, 25.0, 22.9; HRMS (ESI) calc'd for $C_{14}H_{20}O_4Na$ $[M+Na]^+$ *m/z* 275.1254, found 275.1266.

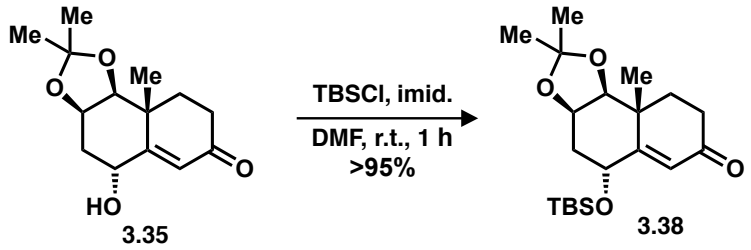

(3a*R*,5*R*,9a*R*,9b*S*)-5-((*tert*-butyldimethylsilyl)oxy)-2,2,9a-trimethyl-4,5,8,9,9a,9b-hexahydronaphtho[1,2-*d*][1,3]dioxol-7(3a*H*)-one (3.38)

tert-Butyldimethylsilyl chloride (0.029 g, 0.190 mmol) was added in one portion to a solution of alcohol **3.35** (0.040 g, 0.159 mmol) and imidazole (0.026 g, 0.380 mmol) in *N*,*N*-dimethylformamide (0.2 mL). The resultant solution was stirred at ambient temperature for 12 h. The solution was diluted with diethyl ether and partitioned with a 10% (w/v) aqueous solution of lithium chloride. The phases were separated and the aqueous portion was thrice extracted with diethyl ether. The combined organic extracts were washed with brine, dried over sodium sulfate, filtered, and concentrated under reduced pressure. The residue was purified by flash column chromatography (11 × 1.5 cm) on silica gel (1:5 to 1:4 ethyl acetate–hexanes) to afford enone **3.38** (0.057 g, >95%): R_f 0.56 (1:1 ethyl acetate–hexanes); ^{1}H NMR (400 MHz, chloroform-*d*) δ 6.07 (d, *J* = 1.5 Hz, 1H), 4.64 (ddd, *J* = 9.6, 5.2, 1.5 Hz, 1H), 4.46 (td, *J* = 6.5, 3.0 Hz, 1H), 4.04 (d, *J* = 6.4 Hz, 1H), 2.49 – 2.37 (m, 2H), 2.32 (ddd, *J* = 14.5, 5.3, 3.0 Hz, 1H), 2.02 – 1.83 (m, 3H), 1.52 (s, 3H), 1.35 (s, 3H), 1.26 (s, 3H), 0.88 (s, 9H), 0.07 (s, 3H), 0.05 (s, 3H); ^{13}C NMR (101 MHz, chloroform-*d*) δ 199.0, 169.8, 122.7, 108.7, 80.3, 72.9, 66.2, 39.5, 37.7, 36.0, 33.8, 26.2, 25.9, 25.1, 23.6, 18.3, –4.7, –4.8; HRMS (ESI) calc'd for $C_{20}H_{35}O_4Si$ $[M+H]^+$ *m/z* 367.2299, found 367.2299.

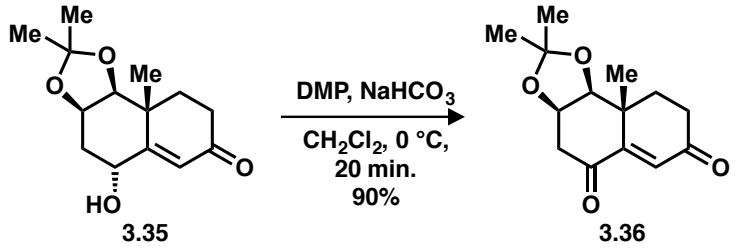

(3a*R*,9a*R*,9b*S*)-2,2,9a-Trimethyl-3a,4,8,9,9a,9b-hexahydronaphtho[1,2-*d*][1,3]dioxole-5,7-dione (3.36).

Dess-Martin periodinane (0.11 g, 0.27 mmol) was added to a stirred solution of alcohol **3.35** (0.045 g, 0.18 mmol) and solid sodium bicarbonate (0.15 g, 0.27 mmol) in anhydrous dichloromethane (1.2 mL) at ambient temperature. The reaction mixture was stirred at ambient temperature for 30 min., at which point it was diluted with diethyl ether and a 1:1 (v/v) mixture of 10% (w/v) aqueous sodium dithionite and a saturated aqueous solution of sodium bicarbonate. The biphasic mixture was vigorously stirred until the phases were clear and colourless (~10 min.). The phases were separated and the aqueous portion was thrice extracted with diethyl ether. The combined organic extracts were washed with brine, dried over sodium sulfate, filtered, and concentrated under reduced pressure. The residue was purified by flash column chromatography (11 × 1.5 cm) on silica gel (1:2 ethyl acetate–hexanes) to afford diketone **3.36** (0.040 g, 90%): R_f 0.6 (1:3 ethyl acetate–hexanes); ^{1}H NMR (400 MHz, chloroform-*d*) δ 6.57 (s, 1H), 4.58 (q, *J* = 8.1 Hz, 1H), 4.00 (d, *J* = 7.8 Hz, 1H), 3.18 (dd, *J* = 16.5, 8.2 Hz, 1H), 2.95 (dd, *J* = 16.5, 8.2 Hz, 1H), 2.61 – 2.43 (m, 2H), 2.21 (ddd, *J* = 13.6, 4.9, 3.6 Hz, 1H), 1.98 (td, *J* = 13.4, 5.6 Hz, 1H), 1.55 (s, 3H), 1.40 (s, 3H), 1.38 (s, 3H); ^{13}C NMR (101 MHz, chloroform-*d*) δ 199.2, 196.8, 152.1, 129.5, 109.8, 80.2, 71.1, 42.9, 38.8, 36.5, 33.9, 26.0, 24.5, 20.0; HRMS (ESI) calc'd for $C_{14}H_{19}O_4$ $[M+H]^+$ *m/z* 251.1278, found 251.1277.

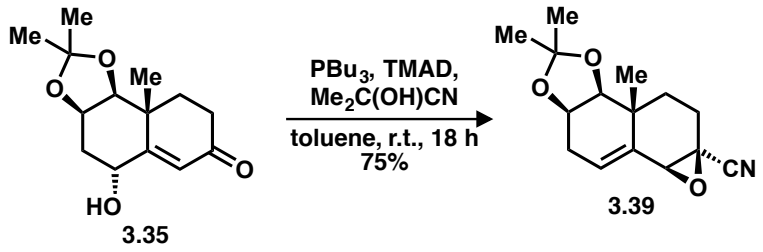

(3a*S*,3b*R*,5a*S*,6a*S*,8a*R*)-2,2,3b-Trimethyl-3a,4,5,6a,8,8a-hexahydrooxireno[2',3':5,6]naphtho[1,2-*d*][1,3]dioxole-5a(3b*H*)-carbonitrile (3.39).

Tributylphosphine (0.029 mL, 0.12) and *N*,*N*,*N*′,*N*′-tetramethylazodicarboxamide (0.021 g, 0.12 mmol), mmol) were added consecutively to a solution of alcohol **3.35** (0.020 g, 0.079 mmol) and acetone cyanohydrin (0.011 mL, 0.12 mmol) in anhydrous toluene (0.3 mL) at ambient temperature. The mixture was stirred at ambient temperature for 18 h, at which point it was diluted with diethyl ether and a saturated aqueous solution of sodium bicarbonate. The phases were separated and the aqueous portion was thrice extracted with diethyl ether. The combined organic extracts were washed with brine, dried over sodium sulfate, filtered, and concentrated under reduced pressure. The residue was purified by flash column chromatography (12 × 1.5 cm) on silica gel (1:6 ethyl acetate–hexanes) to afford **3.39** (0.016 g, 77%): R_f 0.75 (3:1 ethyl acetate–hexanes); ^{1}H NMR (400 MHz, chloroform-*d*) δ 6.09 (dd, *J* = 7.1, 2.4 Hz, 1H), 4.36 (td, *J* = 8.3, 6.3 Hz, 1H), 3.80 (s, 1H), 3.70 (d, *J* = 8.0 Hz, 1H), 2.85 (ddd, *J* = 17.3, 8.6, 7.1 Hz, 1H), 2.41 – 2.29 (m, 2H), 2.23 – 2.11 (m, 1H), 1.65 – 1.57 (m, 1H), 1.53 (dd, *J* = 13.2, 4.6 Hz, 1H), 1.48 (s, 3H), 1.34 (s, 3H), 0.93 (s, 3H); ^{13}C NMR (75 MHz, chloroform-*d*) δ 135.4, 132.4, 118.3, 108.8, 82.4, 72.0, 58.5, 49.0, 35.8, 29.3, 29.0, 26.3, 24.6, 23.3, 17.6; HRMS (ESI) calc'd for $C_{15}H_{19}NO_3Na$ $[M+Na]^+$ *m/z* 284.1257, found 284.1260.

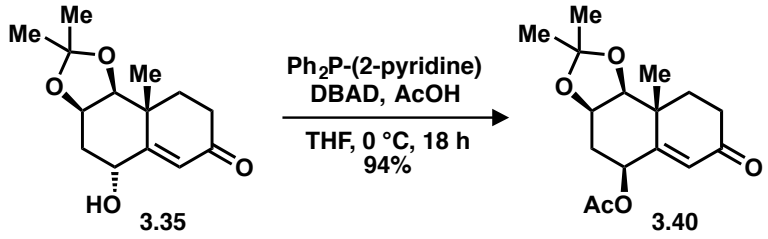

(3a*R*,5*S*,9a*R*,9b*S*)-2,2,9a-Trimethyl-7-oxo-3a,4,5,7,8,9,9a,9b-octahydronaphtho[1,2-*d*][1,3]dioxol-5-yl acetate (3.40).

Di-*tert*-butylazodicarboxylate (0.096 g, 0.42 mmol) was added to a solution of alcohol 3.35 (0.080g, 0.317 mmol), diphenyl-2-pyridinylphosphine (0.10 g, 0.38 mmol) and acetic acid (0.022 mL, 0.38 mmol) in tetrahydrofuran (2 mL) at 0 °C. The mixture was stirred at 0 °C for 18 h, before it was diluted with diethyl ether and an aqueous 2 M solution of hydrochloric acid. The phases were separated and the aqueous portion was thrice extracted with diethyl ether. The combined organic extracts were washed with brine, dried over magnesium sulfate, filtered, and concentrated under reduced pressure. The residue was purified by flash column chromatography (13 × 1.5 cm) on silica gel (1:3 to 1:2 ethyl acetate–hexanes) to afford **3.40** (0.088 g, 94%): R_f 0.42 (2:1 ethyl acetate–hexanes); ^{1}H NMR (400 MHz, chloroform-*d*) δ 5.91 (d, *J* = 1.5 Hz, 1H), 5.54 (ddd, *J* = 13.7, 5.1, 2.2 Hz, 1H), 4.55 (dtd, *J* = 9.2, 7.8, 1.4 Hz, 1H), 3.86 (d, *J* = 7.8 Hz, 1H), 2.67 – 2.40 (m, 3H), 2.21 – 2.07 (m, 5H), 1.88 (td, *J* = 13.7, 5.2 Hz, 1H), 1.52 (s, 3H), 1.38 (s, 6H); ^{13}C NMR (75 MHz, chloroform-*d*) δ 198.5, 170.3, 163.7, 125.9, 109.7, 79.9, 71.5, 67.1, 39.8, 37.0, 33.5, 30.8, 25.8, 24.6, 21.9, 21.1; HRMS (ESI) calc'd for $C_{16}H_{22}O_5Na$ $[M+Na]^+$ *m/z* 284.1359, found 284.1356.

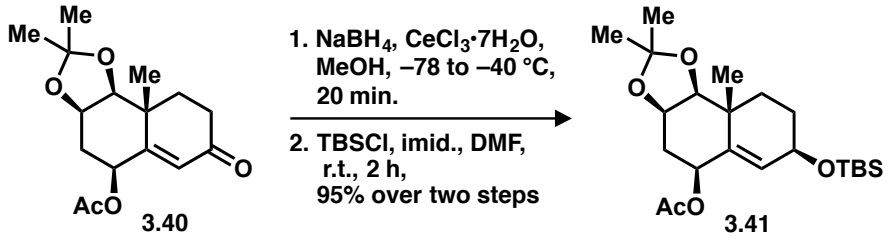

(3a*R*,5*S*,7*R*,9a*R*,9b*S*)-7-((*tert*-butyldimethylsilyl)oxy)-2,2,9a-trimethyl-3a,4,5,7,8,9,9a,9b-octahydronaphtho[1,2-*d*][1,3]dioxol-5-yl acetate (3.41).

Cerium(III) chloride heptahydrate (0.12 g, 0.33 mmol) was added at –40 °C to a stirred solution of enone **3.40** (0.081 g, 0.27 mmol) in 20:1 methanol–dichloromethane (1.8 mL : 0.1

mL). The resulting solution was stirred for 10 min. before sodium borohydride (0.013 g, 0.33 mmol) was added in in one portion. Upon complete consumption of the starting material by TLC analysis (~20 min.), a small quantity of a saturated aqueous solution of ammonium chloride was added, the mixture was allowed to warm to ambient temperature, and the volatiles were removed under reduced pressure. The residue was dissolved in ethyl acetate and washed sequentially with water (twice) and brine, before it was dried over sodium sulfate, filtered, and concentrated under reduced pressure. The crude material was dried under vacuum for 1 h before it was used directly in the next step. *tert*-Butyldimethylsilyl chloride (0.049 g, 0.32 mmol) was added in one portion to a solution of the crude alcohol and imidazole (0.044 g, 0.65 mmol) in *N*,*N*-dimethylformamide (0.3 mL). The resultant solution was stirred at ambient temperature for 2 h. The solution was diluted with diethyl ether and partitioned with a 10% (w/v) aqueous solution of lithium chloride. The phases were separated and the aqueous portion was thrice extracted with diethyl ether. The combined organic extracts were washed with a 10% (w/v) aqueous solution of lithium chloride (twice) and brine, before they were dried over sodium sulfate, filtered, and concentrated under reduced pressure. The residue was purified by flash column chromatography (13 × 2.5 cm) on silica gel (1:8 ethyl acetate–hexanes) to afford enone **3.41** (0.105 g, 95%): R_f 0.69 (1:1 ethyl acetate–hexanes); ^{1}H NMR (400 MHz, chloroform-*d*) δ 5.72 (s, 1H), 5.45 – 5.35 (m, 1H), 4.28 – 4.17 (m, 2H), 3.74 (d, J = 7.7 Hz, 1H), 2.40 (dt, J = 13.5, 6.9 Hz, 1H), 2.06 (s, 3H), 2.05 – 1.94 (m, 1H), 1.90 – 1.79 (m, 2H), 1.71 – 1.55 (m, 1H), 1.50 (s, 3H), 1.48 – 1.38 (m, 1H), 1.33 (s, 3H), 1.25 (s, 3H), 0.88 (s, 9H), 0.06 (s, 6H); ^{13}C NMR (101 MHz, chloroform-*d*) δ 170.9, 139.3, 134.4, 108.9, 82.0, 71.6, 69.1, 68.1, 38.1, 36.9, 31.6, 28.6, 26.4, 26.0, 24.6, 22.8, 21.5, 18.4, –4.2, –4.3; HRMS (ESI) calc'd for $C_{22}H_{38}O_5SiNa$ $[M+Na]^+$ *m/z* 433.2381, found 433.2379.

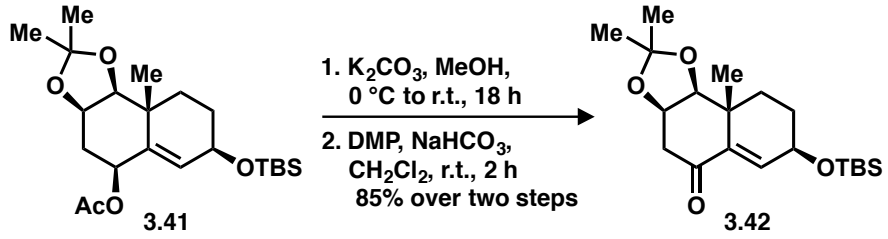

(3a*R*,7*R*,9a*R*,9b*S*)-7-((*tert*-Butyldimethylsilyl)oxy)-2,2,9a-trimethyl-3a,7,8,9,9a,9b-hexahydronaphtho[1,2-*d*][1,3]dioxol-5(4*H*)-one (3.42).

Potassium carbonate (0.043 g, 0.31 mmol) was added to a solution of acetonide **3.41** (0.090 g, 0.21 mmol) in methanol at 0 °C. The mixture was stirred at 0 °C for 1 h, before the ice–water cooling bath was remove and the mixture was allowed to warm to ambient temperature and stirred for an additional 17 h. A small quantity of a saturated aqueous solution of ammonium chloride was added and the volatiles were removed under reduced pressure. The residue was dissolved in diethyl ether and washed sequentially with saturated aqueous solution of ammonium chloride and brine, before it was dried over sodium sulfate, filtered, and concentrated under reduced pressure. The crude material was dried under vacuum for 1 h before it was used directly in the next step. Dess-Martin periodinane (0.13 g, 0.31 mmol) was added to a stirred solution of the crude alcohol intermediate and solid sodium bicarbonate (0.17 g, 2.1 mmol) in anhydrous dichloromethane (1.4 mL) at ambient temperature. The reaction mixture was stirred at ambient temperature for 2 h, at which point it was diluted with dichloromethane and a 1:1 (v/v) mixture of 10% (w/v) aqueous sodium dithionite and a saturated aqueous solution of sodium bicarbonate. The biphasic mixture was vigorously stirred until the phases were clear and colourless (~10 min.). The phases were separated and the aqueous portion was thrice extracted with dichloromethane. The combined organic extracts were washed with brine, dried over sodium sulfate, filtered, and concentrated under reduced pressure. The residue was purified by flash column chromatography (14 × 2 cm) on silica gel (1:9 ethyl acetate–hexanes) to afford ketone **3.42** (0.065 g, 85% over two steps): R_f 0.47 (1:3 ethyl acetate–hexanes); ^{1}H NMR (400 MHz, chloroform-*d*) δ 6.77 (s, 1H), 4.47 (q, *J* = 8.1 Hz, 1H), 4.37 – 4.26 (m, 1H), 3.87 (d, *J* = 8.0 Hz, 1H), 3.02 (dd, *J* = 16.7, 8.1 Hz, 1H), 2.86 (dd, *J* = 16.7, 8.4 Hz, 1H), 1.99 – 1.83 (m, 2H), 1.75 – 1.60 (m, 1H), 1.60 – 1.47 (m, 4H), 1.36 (s, 3H), 1.25 (s, 3H), 0.89 (s, 9H), 0.09 (s, 3H), 0.08 (s, 3H); ^{13}C NMR (101 MHz, chloroform-*d*) δ 196.3, 141.7, 137.7, 109.3, 81.9, 71.4, 68.3, 42.8, 37.9, 36.2, 28.3, 26.1, 26.0, 24.5, 21.9,

18.3, –4.45, –4.52; HRMS (ESI) calc'd for $C_{20}H_{34}O_4SiNa$ $[M+Na]^+$ *m/z* 389.2119, found 389.2115.

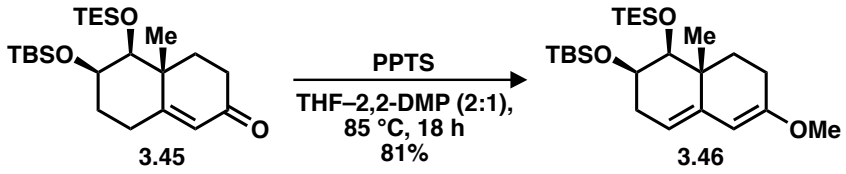

***tert*-Butyl(((1*S*,2*R*,8a*R*)-6-methoxy-8a-methyl-1-((triethylsilyl)oxy)-1,2,3,7,8,8a-hexahydronaphthalen-2-yl)oxy)dimethylsilane (3.46).**

Pyridinium *para*-toluenesulfonate (0.028 g, 0.11 mmol) was added to a solution of enone **3.45** (0.36 g, 0.85 mmol) in 2:1 tetrahydrofuran–2,2,-dimethoxypropane at ambient temperature. The mixture was heated to 85 °C and stirred at that temperature for 18 h, before it was cooled to ambient temperature and the solids were removed by filtration through a short pad of Celite® 545 (sintered-glass funnel, 1 cm height of Celite® 545). The volatiles removed under reduced pressure and the crude residue was purified by flash column chromatography (11 × 2.5 cm) on silica gel (1:20 diethyl ether/hexanes) to afford methyl dienol ether **3.46** (0.30 g, 81%): R_f 0.34 (1:20 ethyl acetate–hexanes); ^{1}H NMR (400 MHz, chloroform-*d*) δ 5.20 (s, 1H), 5.11 – 5.05 (m, 1H), 4.07 – 3.99 (m, 1H), 3.58 (s, 3H), 3.42 (d, *J* = 2.5 Hz, 1H), 2.46 – 2.18 (m, 3H), 2.07 (dd, *J* = 17.5, 6.1 Hz, 1H), 1.88 (dd, *J* = 12.0, 5.9 Hz, 1H), 1.32 – 1.23 (m, 1H), 1.20 (s, 3H), 0.98 (t, *J* = 7.9 Hz, 9H), 0.88 (d, *J* = 0.7 Hz, 9H), 0.64 (qd, *J* = 7.8, 2.5 Hz, 6H), 0.08 (s, 3H), 0.06 (s, 3H); ^{13}C NMR (101 MHz, chloroform-*d*) δ 156.0, 139.9, 114.3, 98.4, 78.3, 71.8, 54.5, 38.0, 35.2, 34.3, 26.1, 25.0, 18.3, 17.3, 7.3, 5.5, –4.4, –4.5; HRMS (ESI) calc'd for $C_{24}H_{47}O_3Si_2$ $[M+H]^+$ *m/z* 439.3058, found 439.3078.

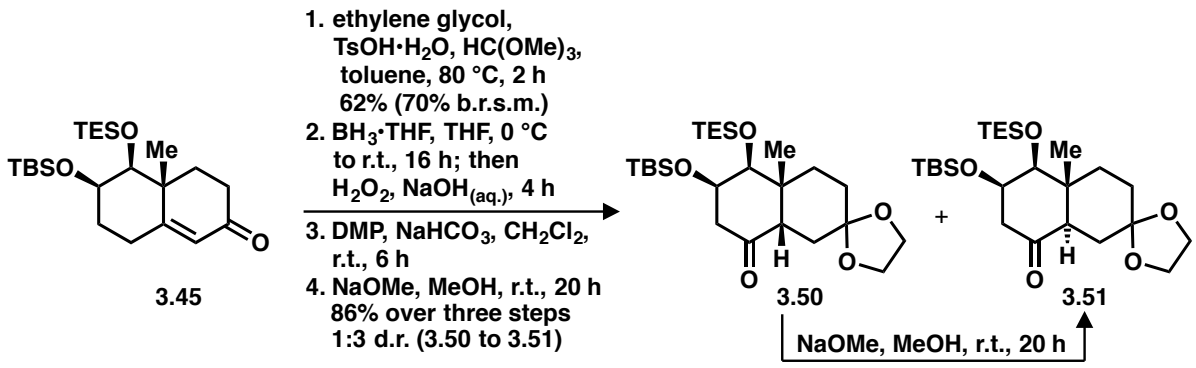

(4a*R*,5*S*,6*R*,8a*R*)-6-((*tert*-Butyldimethylsilyl)oxy)-4a-methyl-5-((triethylsilyl)oxy)octahydro-8*H*-spiro[naphthalene-2,2'-[1,3]dioxolan]-8-one (3.51) and (4a*R*,5*S*,6*R*,8a*S*)-6-((*tert*-butyldimethylsilyl)oxy)-4a-methyl-5-((triethylsilyl)oxy)octahydro-8*H*-spiro-[naphthalene-2,2'-[1,3]dioxolan]-8-one (3.50).

Ethylene glycol (2.56 mL, 46.0 mmol), trimethyl orthoformate (2.51 mL, 23.0 mmol), and *para*-toluenesulfonic acid monohydrate (0.159 g, 0.836 mmol) were added sequentially to a stirred solution of enone **3.45** (7.10 g, 16.7 mmol) in toluene (167 mL) at ambient temperature. The mixture was heated to 80 °C and vigorously stirred for 2 h, before it was allowed to slowly cool to ambient temperature. The mixture was diluted with a saturated aqueous solution of sodium bicarbonate (150 mL) and partitioned with diethyl ether (100 mL). The phases were separated and the aqueous portion was extracted with diethyl ether (3 × 100 mL). The combined organic extracts were washed with brine (100 mL), dried over magnesium sulfate, filtered, and concentrated under reduced pressure. The residue was purified by flash column chromatography (15 × 5.5 cm) on silica gel (1:20 ethyl acetate–hexanes) to afford enone starting material **3.45** (0.74 g) in addition to β,γ-unsaturated ketal **3.49** (4.90 g, 62%; 70% b.r.s.m.). A 1 M solution of borane in tetrahydrofuran (12.5 mL, 12.5 mmol) was added dropwise to a solution of β,γ-unsaturated ketal **3.49** (4.90 g, 10.4 mmol) in tetrahydrofuran (35 mL) at 0 °C. The solution was stirred for 16 h, during which time the temperature of the contents of the flask was allowed to slowly increase to ambient temperature (i.e., the ice–water bath was not removed, but the temperature was allowed to equilibrate with that of the surroundings over 16 h). A mixture containing a 3 M aqueous solution of sodium hydroxide (3.35 mL, 10.0 mmol) and 30% hydrogen peroxide (3.36 mL, 32.9 mmol) was slowly added to the flask and the resulting mixture was stirred at ambient temperature for 4 h. The reaction

mixture was partitioned between diethyl ether (75 mL) and water (40 mL), and the phases were separated. The aqueous portion was extracted with diethyl ether (4 × 40 mL) and the combined organic extracts were washed with brine (2 × 40 mL), dried over magnesium sulfate, filtered, and concentrated under reduced pressure. The crude residue was vacuum-dried for 1 h, before it was used in the next step. Dess-Martin periodinane (6.49 g, 15.7 mmol) was added to a stirred solution of the crude secondary alcohol and solid sodium bicarbonate (8.78 g, 104 mmol) in anhydrous dichloromethane (70 mL) at ambient temperature. The reaction mixture was stirred at ambient temperature for 6 h, at which point it was diluted with dichloromethane (20 mL) and a 1:1 (v/v) mixture of 10% (w/v) aqueous sodium dithionite and a saturated aqueous solution of sodium bicarbonate (100 mL). The biphasic mixture was vigorously stirred until the phases were clear and colourless (approximately 15 min.). The phases were separated and the aqueous portion was extracted with dichloromethane (3 × 75 mL). The combined organic extracts were washed with brine (50 mL), dried over sodium sulfate, filtered, and concentrated under reduced pressure. The residue was dissolved in 1:3 (v/v) diethyl ether–hexanes and purified by filtration through a short plug of Celite® 545 (sintered-glass funnel, 2 cm height of Celite® 545) before it was vacuum-dried for 1 h and subsequently used in the next step. Sodium methoxide (2.26 g, 41.8 mmol) was added to a solution of the crude ketone in anhydrous methanol (26 mL) at ambient temperature, and resultant mixture was vigorously stirred for 20 h. The contents of the round-bottom flask were evaporated to near dryness under reduced pressure, before the residue was dissolved in diethyl ether (100 mL) and partitioned with water (100 mL). The phases were separated and the aqueous portion was extracted with diethyl ether (3 × 80 mL). The combined organic extracts were washed with brine (75 mL), dried over magnesium sulfate, filtered, and concentrated under reduced pressure. The residue was purified by flash column chromatography (17 × 5.5 cm) on silica gel (1:15 to 1:8 ethyl acetate–hexanes, with a slow and gradual increase in the ratio of ethyl acetate to hexanes) to afford *cis*-fused ketone **3.50** (1.08 g, 21%) as a clear and colorless oil that often solidified upon standing and *trans*-fused ketone **3.51** (3.27 g, 65%) as a clear and colorless oil:

Cis-fused ketone **3.50**: R_f 0.42 (1:4 ethyl acetate–hexanes); $[\alpha]^{20}_D$ –3.5 (*c* = 2.0, chloroform); IR (film, cm^{-1}) ν 2953, 2877, 1710, 1470, 1363, 1253, 1163, 1132, 1088, 867, 777; ^1H NMR

(400 MHz, chloroform-*d*) δ 4.29 (ddd, *J* = 10.9, 5.3, 2.1 Hz, 1H), 4.05 – 3.94 (m, 2H), 3.92 – 3.81 (m, 2H), 3.66 (s, 1H), 2.68 (dd, *J* = 15.9, 10.9 Hz, 1H), 2.55 (dt, *J* = 14.2, 2.6 Hz, 1H), 2.47 (dd, *J* = 16.0, 5.2 Hz, 1H), 2.31 – 2.25 (m, 1H), 1.85 (td, *J* = 12.7, 4.1 Hz, 1H), 1.72 – 1.62 (m, 1H), 1.61 – 1.54 (m, 1H), 1.46 (dd, *J* = 14.1, 6.3 Hz, 1H), 1.35 – 1.27 (m, 1H), 1.19 (s, 3H), 0.96 (t, *J* = 7.9 Hz, 9H), 0.90 (s, 9H), 0.72 – 0.65 (m, 6H), 0.08 (s, 3H), 0.07 (s, 3H); ^{13}C NMR (101 MHz, chloroform-*d*) δ 209.1, 108.1, 78.9, 68.4, 64.4, 63.6, 49.5, 44.5, 38.9, 31.6, 31.4, 27.9, 26.3, 23.4, 18.6, 7.2, 5.4, –4.4, –4.5; HRMS (ESI) calc'd for $C_{25}H_{49}O_5Si_2$ $[M+H]^+$ *m/z* 485.3113, found 485.3125. The recovered *cis*-fused ketone may be epimerized to the *trans*-fused epimer using the previously described conditions, however the ratio of *trans*-fused to *cis*-fused ketone when starting from the purified *cis*-isomer is ~5:1.

Trans-fused ketone **3.51**: R_f 0.37 (1:4 ethyl acetate–hexanes); ^{1}H NMR (400 MHz, chloroform-*d*) δ 4.29 (dd, *J* = 6.4, 3.0 Hz, 1H), 3.99 – 3.86 (m, 4H), 3.74 (d, *J* = 3.0 Hz, 1H), 2.61 (ddd, *J* = 13.8, 3.9, 1.3 Hz, 1H), 2.50 (dd, *J* = 11.5, 4.2 Hz, 1H), 2.38 (dd, *J* = 13.9, 2.8 Hz, 1H), 1.80 – 1.55 (m, 5H), 1.46 – 1.35 (m, 1H), 1.02 – 0.96 (m, 12H), 0.85 (s, 9H), 0.66 (qd, *J* = 7.9, 4.4 Hz, 6H), 0.05 (s, 3H), 0.05 (s, 3H); ^{13}C NMR (101 MHz, chloroform-*d*) δ 208.3, 109.2, 79.6, 75.5, 64.5, 64.3, 53.3, 48.8, 43.5, 36.3, 30.3, 29.6, 25.8, 18.1, 12.8, 7.2, 5.4, –4.6, –4.7; HRMS (ESI) calc'd for $C_{25}H_{49}O_5Si_2$ $[M+H]^+$ *m/z* 485.3113, found 485.3119.

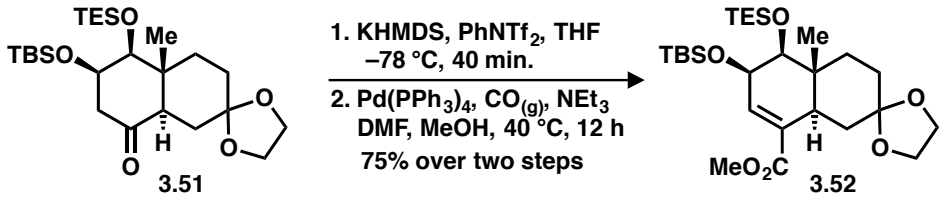

Methyl (4a*R*,5*S*,6*R*,8a*R*)-6-((*tert*-butyldimethylsilyl)oxy)-4a-methyl-5-((triethylsilyl)oxy)-3,4,4a,5,6,8a-hexahydro-1*H*-spiro[naphthalene-2,2'-[1,3]dioxolane]-8-carboxylate (3.52). Solid *N*-phenyl-bis(trifluoromethanesulfonimide) (2.67 g, 7.47 mmol) was added to a solution of ketone **3.51** (3.15 g, 6.50 mmol) in tetrahydrofuran (81 mL) at ambient temperature. The resultant solution was cooled to –78 °C before a 1 M solution of potassium bis(trimethylsilyl)amide in tetrahydrofuran (7.80 mL, 7.80 mmol) was steadily at the same temperature. The mixture was stirred at –78 °C for 40 min. before a saturated aqueous solution

of ammonium chloride (20 mL) was added and 80% of the volatiles were removed under reduced pressure. The residue was diluted with diethyl ether (100 mL) and an additional quantity of ammonium chloride (50 mL). The phases were separated and the aqueous portion was extracted with diethyl ether (3 × 60 mL), before the combined organic extracts were washed sequentially with a saturated aqueous solution of copper(II) sulfate (2 × 50 mL) and brine (50 mL), then dried over magnesium sulfate, filtered, and concentrated under reduced pressure. The crude vinyl triflate was vacuum-dried for 3 h, before it was used in the next step. Triethylamine (1.67 mL, 12.0 mmol) and methanol (12.1 mL, 300 mmol) were added sequentially to a solution of crude vinyl triflate in *N*,*N*-dimethylformamide (20 mL) at ambient temperature. The mixture was vigorously stirred as the reaction vessel was purged with carbon monoxide gas, which was bubbled through the solution for ~3 min. Tetrakis(triphenylphosphine)palladium (0.55 g, 0.48 mmol) was added to the reaction vessel, and the vigorously-stirred mixture was placed under an atmosphere of carbon monoxide gas (using a carbon-monoxide-filled balloon), heated to 40 °C, and stirred at that temperature for 12 h. The reaction mixture was cooled to ambient temperature and diluted with diethyl ether (100 mL) and a 10% (w/v) aqueous solution of lithium chloride (60 mL). The phases were separated and the aqueous portion was extracted with diethyl ether (3 × 50 mL), before the combined ethereal extracts were washed with brine (60 mL), dried over magnesium sulfate, and concentrated under reduced pressure. The residue was reconstituted in 1:10 (v/v) ethyl acetate–hexanes and purified by filtration through a short plug of silica gel (sintered-glass funnel, 3 × 7 cm (h × w) of silica gel), to afford α,β-unsaturated methyl ester **3.52** (2.58 g, 75% over two steps): R_f 0.20 (1:10 ethyl acetate–hexanes); ^{1}H NMR (400 MHz, chloroform-*d*) δ 6.48 (dd, *J* = 4.9, 3.0 Hz, 1H), 4.15 (td, *J* = 5.0, 1.8 Hz, 1H), 4.03 – 3.91 (m, 4H), 3.71 (s, 3H), 3.39 (d, *J* = 5.0 Hz, 1H), 2.46 (dq, *J* = 13.2, 2.6 Hz, 1H), 2.25 (dt, *J* = 12.9, 2.7 Hz, 1H), 1.88 – 1.75 (m, 2H), 1.68 – 1.59 (m, 1H), 1.44 (t, *J* = 13.1 Hz, 1H), 1.31 – 1.20 (m, 1H), 0.96 (t, *J* = 8.0 Hz, 9H), 0.95 (s, 3H), 0.88 (s, 9H), 0.62 (qd, *J* = 7.8, 2.7 Hz, 6H), 0.10 (s, 3H), 0.09 (s, 3H); ^{13}C NMR (101 MHz, chloroform-*d*) δ 168.2, 136.5, 133.9, 109.3, 78.2, 67.7, 64.4, 64.3, 51.8, 42.5, 37.8, 33.4, 31.9, 30.7, 25.9, 18.3, 11.1, 7.2, 5.4, –3.5, –4.7; HRMS (ESI) calc'd for $C_{27}H_{50}O_6Si_2Na$ $[M+Na]^+$ *m/z* 549.3038, found 549.3015.

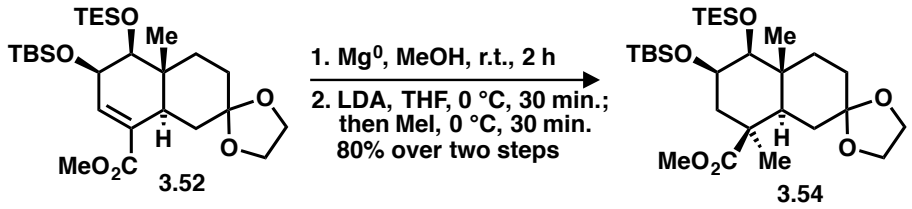

Methyl (4a*R*,5*S*,6*R*,8*S*,8a*R*)-6-((*tert*-butyldimethylsilyl)oxy)-4a,8-dimethyl-5-((triethylsilyl)oxy)octahydro-1*H*-spiro[naphthalene-2,2'-[1,3]dioxolane]-8-carboxylate (3.54).

Magnesium turnings (0.714 g, 29.4 mmol) were added to a stirred solution of α,β-unsaturated methyl ester **3.52** (2.58 g, 4.90 mmol) in anhydrous methanol (73 mL) at ambient temperature. The mixture was sonicated for 2 min., before a few small crystals of iodine were added to the flask and the mixture was again subjected to sonication until bubbles began to form on the surface of the magnesium turnings (~2 min.). The reaction mixture was removed from the sonication bath and stirred vigorously at ambient temperature until the α,β-unsaturated methyl ester starting material had been completely reduced (~2 h). If the conversion was incomplete, an additional two equivalents of magnesium turnings were added with a small crystal of iodine, followed by sonication and vigorous stirring, as described above. The reaction mixture was cooled to 0 °C and 1 M aqueous hydrochloric acid was slowly added until the mixture became clear, at which point the pH was adjusted to ~8–9 with a 1 M aqueous solution of sodium hydroxide and the mixture was diluted with diethyl ether. The phases were separated and the aqueous portion was thrice extracted with diethyl ether, before the combined organic extracts were washed with brine, dried over magnesium sulfate, filtered, and concentrated under reduced pressure. The crude methyl ester was vacuum-dried for 3 h, before it was used in the next step. A 2.4 M solution of *n*-butyllithium in hexanes (11.1 mL, 26.7 mmol) was added slowly to a 0 °C solution of *N*,*N*-diisopropylamine (4.48 mL, 32.0 mmol) in tetrahydrofuran (55 mL). The solution was stirred at 0 °C for 30 min. before a solution of crude methyl ester in tetrahydrofuran (13.0 mL) was added slowly. The solution was stirred at 0 °C for 30 min., at which point methyl iodide (1.83 mL, 29.3 mmol) was added in dropwise fashion to the solution. The solution was stirred 0 °C for 30 min. before a saturated aqueous solution of ammonium chloride was added to the mixture and it was allowed to warm to ambient temperature. Diethyl ether was added and the phases were separated. The aqueous

portion was thrice extracted with diethyl ether and the combined organic extracts were washed thrice with a saturated aqueous solution of copper(II) sulfate and once with brine, before the ethereal portion was dried over magnesium sulfate, filtered, and concentrated under reduced pressure. The residue was reconstituted in 1:10 (v/v) ethyl acetate–hexanes and purified by filtration through a short plug of silica gel (sintered-glass funnel, 3 × 4.5 cm (h × w) of silica gel), to afford **3.54** (2.14 g, 80% over two steps): R_f 0.26 (1:8 ethyl acetate–hexanes); ^{1}H NMR (400 MHz, chloroform-*d*) δ 4.00 – 3.91 (m, 4H), 3.91 – 3.86 (m, 1H), 3.58 (s, 3H), 3.12 (d, *J* = 2.9 Hz, 1H), 2.58 (dd, *J* = 14.4, 3.5 Hz, 1H), 2.45 (t, *J* = 13.4 Hz, 1H), 1.84 – 1.67 (m, 3H), 1.64 – 1.54 (m, 1H), 1.38 (td, *J* = 14.3, 13.7, 2.6 Hz, 2H), 1.16 (s, 3H), 1.14 – 1.06 (m, 4H), 0.95 (t, *J* = 7.9 Hz, 9H), 0.86 (s, 9H), 0.62 (qd, *J* = 7.7, 4.2 Hz, 6H), 0.07 (s, 3H), 0.05 (s, 3H); ^{13}C NMR (101 MHz, chloroform-*d*) δ 176.5, 109.9, 81.8, 72.7, 64.3, 64.2, 51.3, 50.0, 44.2, 41.7, 39.5, 38.6, 32.6, 30.5, 29.8, 26.0, 18.4, 13.5, 7.3, 5.5, –4.0, –4.5; HRMS (ESI) calc'd for $C_{28}H_{54}O_6Si_2Na$ $[M+Na]^+$ *m/z* 565.3351, found 565.3354.

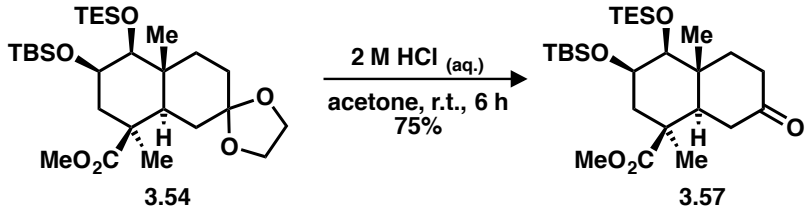

3.54 3.57

Methyl (1*S*,3*R*,4*S*,4a*R*,8a*R*)-3-((*tert*-butyldimethylsilyl)oxy)-1,4a-dimethyl-7-oxo-4-((triethylsilyl)oxy)decahydronaphthalene-1-carboxylate (3.57).

An aqueous 2 M solution of hydrochloric acid (0.838 mL, 1.68 mmol) was added to a solution of ketal **3.54** (1.82 g, 3.35 mmol) in acetone (17 mL). The solution was stirred at ambient temperature for 6 h, at which point a saturated aqueous solution of sodium bicarbonate was added, followed by diethyl ether. The phases were separated and the aqueous phase was thrice extracted with diethyl ether. The combined ethereal extracts were washed with brine, dried over magnesium sulfate, filtered, and concentrated under reduced pressure. The residue was purified by flash column chromatography (14 × 2.5 cm) on silica gel (1:10 ethyl acetate–hexanes) to afford ketone **3.57** (1.26 g, 75%): R_f 0.21 (1:8 ethyl acetate–hexanes); ^{1}H NMR (400 MHz, chloroform-*d*) δ 3.93 (dd, *J* = 5.8, 2.9 Hz, 1H), 3.61 (s, 3H), 3.42 (t, *J* = 14.5 Hz, 1H), 3.12 (d, *J* = 2.8 Hz, 1H), 2.61 (dd, *J* = 14.5, 3.6 Hz, 1H), 2.53 (td, *J* = 14.8, 6.7 Hz, 1H),

2.44 (dt, *J* = 14.9, 2.8 Hz, 1H), 2.26 (ddt, *J* = 15.2, 4.6, 2.2 Hz, 1H), 2.05 (ddd, *J* = 12.9, 6.6, 2.2 Hz, 1H), 1.43 (dd, *J* = 14.0, 3.3 Hz, 1H), 1.37 (dd, *J* = 14.5, 2.6 Hz, 1H), 1.32 (s, 3H), 1.27 – 1.17 (m, 1H), 1.16 (s, 3H), 0.96 (t, *J* = 7.9 Hz, 9H), 0.88 (s, 9H), 0.62 (qd, *J* = 7.9, 4.1 Hz, 6H), 0.08 (s, 3H), 0.07 (s, 3H); ^{13}C NMR (101 MHz, chloroform-*d*) δ 212.5, 176.0, 81.5, 72.6, 52.9, 51.5, 44.2, 41.8, 40.8, 40.1, 39.7, 37.4, 29.5, 26.0, 18.4, 13.7, 7.2, 5.4, –4.0, –4.5; HRMS (ESI) calc'd for $C_{26}H_{50}O_5Si_2Na$ $[M+Na]^+$ *m/z* 521.3089, found 521.3093.

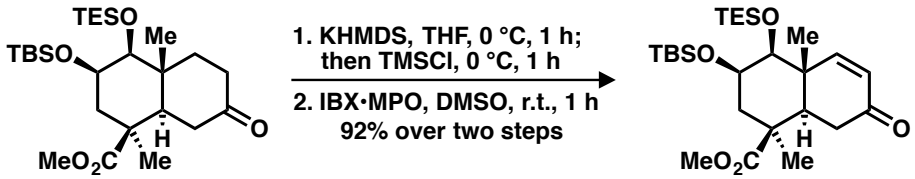

3.57 3.58

Methyl (1*S*,3*R*,4*S*,4a*R*,8a*R*)-3-((*tert*-butyldimethylsilyl)oxy)-1,4a-dimethyl-7-oxo-4-((triethylsilyl)oxy)-1,2,3,4,4a,7,8,8a-octahydronaphthalene-1-carboxylate (3.58).

A 1 M solution of potassium bis(trimethylsilyl)amide in tetrahydrofuran (5.37 mL, 5.37 mmol) was added slowly to a solution of ketone **3.57** (1.34 g, 2.69 mmol) in tetrahydrofuran (13.4 mL) at 0 °C and the solution was stirred at that temperature for 1 h. Trimethylsilyl chloride (0.750 mL, 5.91 mmol) was added in dropwise fashion to the reaction mixture, which was stirred at 0 °C for 1 h. The reaction mixture was diluted with a saturated aqueous solution of ammonium chloride and diethyl ether, before it was allowed to warm to ambient temperature. The phases were separated and the aqueous portion was thrice extracted with diethyl ether. The combined organic extracts were washed with brine, dried over magnesium sulfate, filtered, and concentrated under reduced pressure. The residue was vacuum-dried for 3 h, before it was used in the next step. A freshly prepared solution of 2-iodoxybenzoic acid (2.25 g, 8.05 mmol) and 4-methoxypyridine *N*-oxide hydrate (1.01 g) in dimethyl sulfoxide (14.6 mL) was added in one portion to a solution of crude silyl enol ether in a minimal amount of dichloromethane (3 mL). The reaction mixture was vigorously stirred at ambient temperature for 1 h, before the mixture was diluted with a saturated aqueous solution of sodium bicarbonate, followed by diethyl ether. The phases were separated and the aqueous phase was thrice extracted with diethyl ether. The combined ethereal extracts were washed with brine, dried over magnesium sulfate, filtered, and concentrated under reduced pressure.

The residue was purified by flash column chromatography (14 × 2.5 cm) on silica gel (1:12 ethyl acetate–hexanes) to afford enone **3.58** (1.23 g, 92% over two steps): R_f 0.24 (1:8 ethyl acetate–hexanes); ^{1}H NMR (400 MHz, chloroform-*d*) δ 7.02 (d, *J* = 10.2 Hz, 1H), 5.80 (dd, *J* = 10.1, 0.9 Hz, 1H), 3.99 (dd, *J* = 5.8, 2.8 Hz, 1H), 3.63 (s, 3H), 3.34 (dd, *J* = 17.4, 14.4 Hz, 1H), 3.28 (d, *J* = 2.9 Hz, 1H), 2.66 (dd, *J* = 14.6, 3.4 Hz, 1H), 2.58 (dd, *J* = 17.4, 2.8 Hz, 1H), 1.80 (dd, *J* = 14.4, 3.1 Hz, 1H), 1.40 (dd, *J* = 14.6, 2.8 Hz, 1H), 1.27 (s, 3H), 1.21 (s, 3H), 0.98 (t, *J* = 7.9 Hz, 9H), 0.87 (s, 9H), 0.67 (qd, *J* = 7.9, 2.4 Hz, 6H), 0.10 (s, 3H), 0.08 (s, 3H); ^{13}C NMR (101 MHz, chloroform-*d*) δ 201.1, 175.9, 158.7, 125.0, 76.6, 72.6, 51.6, 50.0, 43.9, 43.3, 41.5, 36.9, 29.2, 26.0, 18.3, 15.4, 7.2, 5.4, –4.0, –4.5; HRMS (ESI) calc'd for $C_{26}H_{49}O_5Si_2$ $[M+H]^+$ *m/z* 497.3113, found 497.3119.

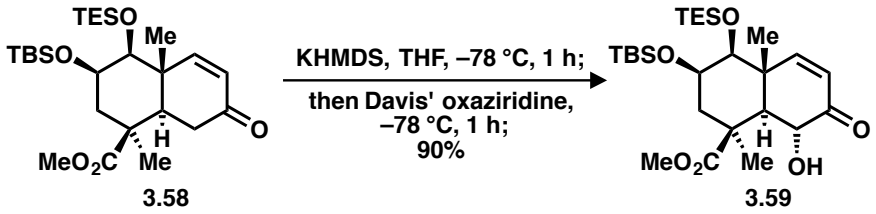

Methyl (1*S*,3*R*,4*S*,4a*R*,8*R*,8a*R*)-3-((*tert*-butyldimethylsilyl)oxy)-8-hydroxy-1,4a-dimethyl-7-oxo-4-((triethylsilyl)oxy)-1,2,3,4,4a,7,8,8a-octahydronaphthalene-1-carboxylate (3.59). A 1.0 M solution of potassium bis(trimethylsilyl)amide in tetrahydrofuran (3.10 mL, 3.09 mmol) was added slowly to a –78 °C solution of enone **3.58** (1.18 g, 2.37 mmol) in tetrahydrofuran (34 mL) and the solution was stirred at that temperature for 1 h. A solution of 3-phenyl-2-(phenylsulfonyl)-1,2-oxaziridine (1.01 g, 3.86 mmol) in tetrahydrofuran (5 mL) was added and the resultant mixture was stirred at –78 °C for 1 h. A saturated aqueous solution of ammonium chloride (1 mL) was added, before the mixture was diluted diethyl ether and allowed to warm to ambient temperature. The mixture was further diluted with 1 M aqueous hydrochloric acid and the phases were separated. The ethereal portion was washed with 1 M aqueous hydrochloric acid (twice), a freshly-prepared saturated aqueous solution of sodium bisulfite (thrice), a saturated aqueous solution of sodium bicarbonate, and brine, before it was dried over magnesium sulfate, filtered, and concentrated under reduced pressure. The residue was reconstituted in *n*-pentane and the solids were removed by filtration through a sintered-glass funnel. The residue was then purified by flash column chromatography (16 × 3

cm) on silica gel (1:12 ethyl acetate–hexanes) to afford α-hydroxy ketone **3.59** (1.01 g, 90%): R_f 0.24 (1:8 ethyl acetate–hexanes); ^{1}H NMR (400 MHz, chloroform-*d*) δ 7.12 (d, *J* = 10.1 Hz, 1H), 5.94 (d, *J* = 10.1 Hz, 1H), 5.24 (dd, *J* = 12.7, 2.1 Hz, 1H), 3.96 (dd, *J* = 5.5, 2.6 Hz, 1H), 3.70 (s, 3H), 3.64 (d, *J* = 2.1 Hz, 1H), 3.28 (d, *J* = 3.0 Hz, 1H), 2.62 (dd, *J* = 15.0, 3.3 Hz, 1H), 1.76 (d, *J* = 12.7 Hz, 1H), 1.50 – 1.41 (m, 4H), 1.37 (s, 3H), 0.99 (t, *J* = 7.9 Hz, 9H), 0.89 (s, 9H), 0.67 (qd, *J* = 7.8, 2.6 Hz, 6H), 0.11 (s, 3H), 0.09 (s, 3H); ^{13}C NMR (75 MHz, chloroform-*d*) δ 202.0, 176.3, 160.0, 121.5, 76.1, 73.8, 72.5, 55.5, 51.8, 45.3, 45.0, 42.4, 32.6, 26.0, 18.3, 16.0, 7.2, 5.4, –4.0, –4.5; HRMS (ESI) calc'd for $C_{26}H_{48}O_6Si_2Na$ $[M+Na]^+$ *m/z* 535.2882, found 535.2889.

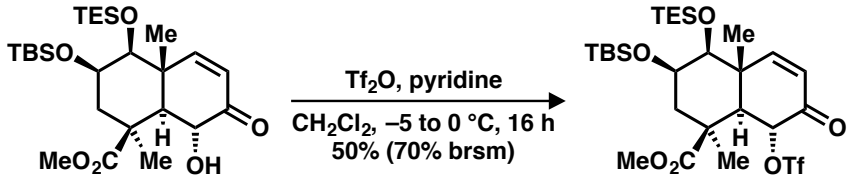

Methyl (1*S*,3*R*,4*S*,4a*R*,8*R*,8a*R*)-3-((*tert*-butyldimethylsilyl)oxy)-1,4a-dimethyl-7-oxo-4-((triethylsilyl)oxy)-8-(((trifluoromethyl)sulfonyl)oxy)-1,2,3,4,4a,7,8,8a-octahydro-naphthalene-1-carboxylate (3.62).

Pyridine (0.89 mL, 11 mmol) was added to a –5 °C solution of α-hydroxy ketone **3.59** (1.13 g, 2.20 mmol) in dichloromethane (44 mL). Trifluoromethanesulfonic anhydride (0.93 mL, 5.5 mmol) was added to the vigorously stirred solution in dropwise fashion at the same temperature, and the resultant solution was allowed to stand at –5 to 0 °C for 16 h. The mixture was diluted with a saturated aqueous solution of sodium bicarbonate and diethyl ether. The phases were separated and the aqueous phase was thrice extracted with diethyl ether. The combined ethereal extracts were washed with a saturated aqueous solution of copper(II) sulfate and brine, before they were dried over magnesium sulfate, filtered, and concentrated under reduced pressure. The residue was purified by flash column chromatography (14 × 2 cm) on silica gel (1:20 then 1:8 ethyl acetate–hexanes) to afford enone **3.62** (0.712 g, 50%; 70% b.r.s.m.): R_f 0.44 (1:8 ethyl acetate–hexanes); ^{1}H NMR (400 MHz, chloroform-*d*) δ 7.13 (d, *J* = 10.1 Hz, 1H), 6.36 (d, *J* = 13.0 Hz, 1H), 5.95 (d, *J* = 10.1 Hz, 1H), 3.96 (dd, *J* = 5.6, 2.8 Hz, 1H), 3.71 (s, 3H), 3.30 (d, *J* = 2.8 Hz, 1H), 2.64 (dd, *J* = 15.0, 3.4 Hz, 1H), 2.22 (d, *J* =

13.0 Hz, 1H), 1.51 (dd, *J* = 15.0, 2.8 Hz, 1H), 1.43 (s, 3H), 1.36 (s, 3H), 0.99 (t, *J* = 7.9 Hz, 9H), 0.88 (s, 9H), 0.67 (qd, *J* = 7.8, 2.9 Hz, 6H), 0.11 (s, 3H), 0.09 (s, 3H); ^{13}C NMR (101 MHz, chloroform-*d*) δ 191.7, 174.9, 159.1, 122.1, 87.3, 75.7, 72.1, 53.9, 52.1, 46.5, 45.0, 41.7, 31.5, 25.9, 18.3, 16.2, 7.2, 5.3, –4.1, –4.5; HRMS (APCI) calc'd for $C_{27}H_{47}O_8F_3Si_2S$ $[M+H]^+$ *m/z* 645.2555, found 645.2525.

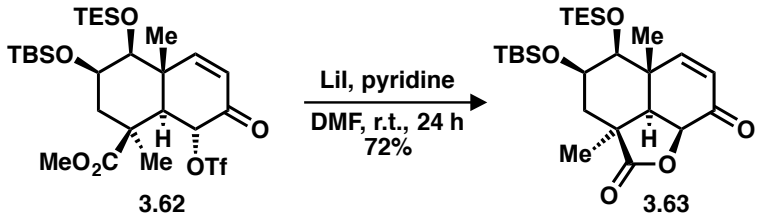

(2a*S*,2a^1*R*,4*R*,5*S*,5a*R*,8a*S*)-4-((*tert*-Butyldimethylsilyl)oxy)-2a,5a-dimethyl-5-((triethylsilyl)oxy)-2a^1,3,4,5,5a,8a-hexahydro-2*H*-naphtho[1,8-*bc*]furan-2,8(2a*H*)-dione (3.63).

Pyridine (0.19 mL, 2.3 mmol) and lithium iodide (1.24 g, 9.30 mmol) were added sequentially to a solution of triflate **3.62** (0.750 g, 1.16 mmol) in *N*,*N*-dimethylformamide (38 mL). The mixture was stirred at ambient temperature for 24 h, before it was diluted with a 10% (w/v) aqueous solution of lithium chloride and diethyl ether. The phases were separated and the ethereal portion was washed with a 10% (w/v) aqueous solution of lithium chloride (thrice), 1:1 (v/v) mixture of 10% (w/v) aqueous sodium thiosulfate and a saturated aqueous solution of sodium bicarbonate (once), a saturated aqueous solution of copper(II) sulfate, and brine, before it was dried over magnesium sulfate, filtered, and concentrated under reduced pressure. The residue was purified by flash column chromatography (14 × 2.5 cm) on silica gel (1:10 to 1:4 ethyl acetate–hexanes, with a slow and gradual increase in the ratio of ethyl acetate to hexanes) to afford γ-lactone **3.63** (0.404 g, 72%) as a colourless solid: R_f 0.09 (1:6 ethyl acetate–hexanes); ^{1}H NMR (400 MHz, chloroform-*d*) δ 7.34 (d, *J* = 9.9 Hz, 1H), 6.01 (dd, *J* = 9.8, 0.7 Hz, 1H), 4.71 (dd, *J* = 5.8, 0.8 Hz, 1H), 3.93 (ddd, *J* = 7.0, 4.9, 4.8 Hz, 1H), 3.76 (d, *J* = 4.9 Hz, 1H), 2.46 (dd, *J* = 15.0, 7.1 Hz, 1H), 2.27 (d, *J* = 5.8 Hz, 1H), 1.70 (dd, *J* = 15.0, 4.8 Hz, 1H), 1.33 (s, 3H), 1.22 (s, 3H), 0.99 (t, *J* = 7.9 Hz, 9H), 0.90 (s, 9H), 0.68 (qd, *J* = 7.9, 3.0 Hz, 6H), 0.13 (s, 3H), 0.09 (s, 3H); ^{13}C NMR (101 MHz, chloroform-*d*) δ 191.9, 179.1, 160.0,

127.2, 75.2, 73.3, 69.7, 49.4, 41.4, 40.9, 36.6, 26.1, 24.2, 18.3, 7.2, 5.5, –4.0, –4.3; HRMS (ESI) calc'd for $C_{25}H_{44}O_5Si_2Na$ $[M+Na]^+$ *m/z* 503.2620, found 503.2625.

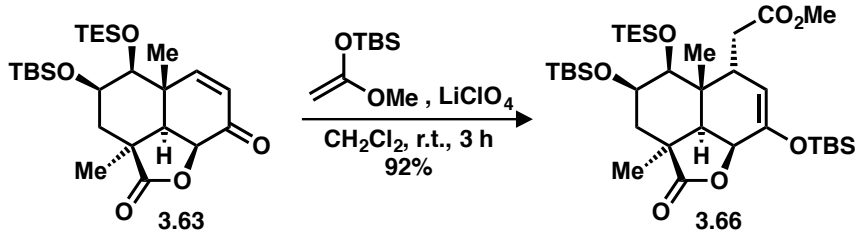

Methyl 2-((2a*S*,2a^1*R*,4*R*,5*S*,5a*R*,6*R*,8a*S*)-4,8-bis((*tert*-butyldimethylsilyl)oxy)-2a,5a-dimethyl-2-oxo-5-((triethylsilyl)oxy)-2a,2a^1,3,4,5,5a,6,8a-octahydro-2*H*-naphtho[1,8-*bc*]furan-6-yl)acetate (3.66).

Lithium perchlorate (0.6 mg, 0.005 mmol) was added to a solution of enone **3.63** (0.050 g, 0.10 mmol) and 1-(*tert*-butyldimethylsilyloxy)-1-methoxyethene (0.025 mL, 0.11 mmol) in dichloromethane (2 mL) at ambient temperature. The mixture was stirred at ambient temperature for 3 h, before it was diluted with a saturated aqueous solution of sodium bicarbonate and additional dichloromethane. The phases were separated and the aqueous phase was thrice extracted with dichloromethane. The combined organic extracts were washed with brine, dried over sodium sulfate, filtered, and concentrated under reduced pressure. The residue was purified by flash column chromatography (12 × 1.5 cm) on silica gel (1:10 ethyl acetate–hexanes) to afford silyl enol ether **3.66** (0.064 g, 92%) as a colourless solid: R_f 0.61 (1:3 ethyl acetate–hexanes); ^{1}H NMR (400 MHz, chloroform-*d*) δ 5.20 (d, *J* = 6.0 Hz, 1H), 4.64 (d, *J* = 5.1 Hz, 1H), 3.80 (ddd, *J* = 7.4, 4.5, 4.4 Hz, 1H), 3.71 (d, *J* = 4.7 Hz, 1H), 3.69 (s, 3H), 2.64 – 2.54 (m, 2H), 2.43 (dd, *J* = 14.7, 7.3 Hz, 1H), 2.12 – 2.02 (m, 1H), 1.91 (d, *J* = 5.1 Hz, 1H), 1.56 (dd, *J* = 14.8, 4.4 Hz, 1H), 1.29 (s, 3H), 1.19 (s, 3H), 0.96 (t, *J* = 8.0 Hz, 9H), 0.93 (s, 9H), 0.90 (s, 9H), 0.69 – 0.56 (m, 6H), 0.19 (s, 3H), 0.17 (s, 3H), 0.16 (s, 3H), 0.08 (s, 3H); ^{13}C NMR (101 MHz, chloroform-*d*) δ 180.6, 172.7, 146.6, 112.2, 74.9, 72.0, 70.1, 51.9, 45.1, 41.7, 40.4, 40.0, 35.9, 35.8, 26.3, 25.8, 25.0, 19.4, 18.4, 18.2, 7.2, 5.6, –3.7, –4.06, –4.09, –4.4; HRMS (ESI) calc'd for $C_{34}H_{64}O_7Si_3Na$ $[M+Na]^+$ *m/z* 691.3852, found 691.3853.

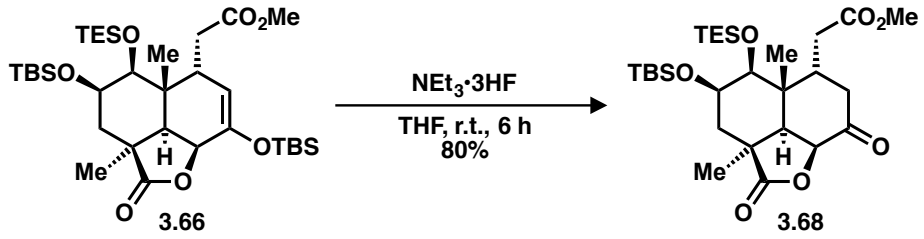

Methyl 2-((2a*S*,2a[1]*R*,4*R*,5*S*,5a*R*,6*S*,8a*S*)-4-((*tert*-butyldimethylsilyl)oxy)-2a,5a-dimethyl-2,8-dioxo-5-((triethylsilyl)oxy)decahydro-2*H*-naphtho[1,8-*bc*]furan-6-yl)acetate (3.68).

Triethylamine trihydrofluoride (0.014 mL, 0.075 mmol) was added to a solution of *tert*-butyldimethylsilyl enol ether **3.66** (0.050 g, 0.075 mmol) in tetrahydrofuran (1.5 mL) at ambient temperature. The mixture stirred at ambient temperature for 6 h, at which point it was slowly neutralized with a saturated aqueous solution of sodium bicarbonate, and diluted with diethyl ether. The phases were separated and the aqueous portion was thrice extracted with diethyl ether. The combined organic extracts were washed with brine, dried over magnesium sulfate, filtered, and concentrated under reduced pressure. The residue was purified by flash column chromatography (14 × 1.5 cm) on silica gel (2:3 ethyl acetate–hexanes) to afford ketone **3.68** (0.033 g, 80%): R_f 0.20 (1:2 ethyl acetate–hexanes); ^{1}H NMR (400 MHz, chloroform-*d*) δ 4.64 (d, *J* = 6.1 Hz, 1H), 3.97 (dd, *J* = 7.1, 3.5 Hz, 1H), 3.71 (s, 3H), 3.51 (d, *J* = 3.4 Hz, 1H), 2.89 (dd, *J* = 17.0, 9.1 Hz, 1H), 2.63 (dd, *J* = 14.6, 3.0 Hz, 1H), 2.51 (ddd, *J* = 15.3, 10.1, 5.6 Hz, 2H), 2.38 (d, *J* = 6.1 Hz, 1H), 2.32 (dd, *J* = 14.6, 11.9 Hz, 1H), 2.07 (dd, *J* = 17.0, 4.4 Hz, 1H), 1.60 (dd, *J* = 15.4, 4.4 Hz, 1H), 1.28 (s, 3H), 1.11 (s, 3H), 0.96 (t, *J* = 7.9 Hz, 9H), 0.86 (s, 9H), 0.73 – 0.57 (m, 6H), 0.21 (s, 3H), 0.07 (s, 3H); ^{13}C NMR (101 MHz, chloroform-*d*) δ 204.8, 177.8, 172.4, 75.8, 73.3, 71.0, 52.1, 47.3, 41.5, 40.2, 40.0, 39.7, 37.7, 36.3, 26.5, 26.1, 18.7, 18.2, 7.2, 5.8, –3.2, –4.7; HRMS (ESI) calc'd for $C_{28}H_{50}O_7Si_2Na$ $[M+Na]^+$ *m/z* 577.2987, found 577.2970.

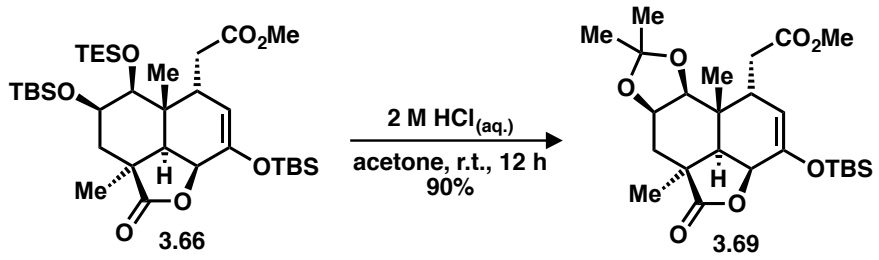

Methyl 2-((1*R*,3a*S*,3a^1*R*,5a*S*,6a*R*,9a*S*,9b*R*)-3-((*tert*-butyldimethylsilyl)oxy)-5a,8,8,9b-tetramethyl-5-oxo-3a,3a^1,5,5a,6,6a,9a,9b-octahydro-1*H*-furo[4',3',2':4,5]naphtho[1,2-*d*][1,3]dioxol-1-yl)acetate (3.69).

An aqueous 2 M solution of hydrochloric acid (0.007 mL, 0.015 mmol) was added to a solution of silyl enol ether **3.66** (0.020 g, 0.030 mmol) in acetone (0.15 mL). The solution was stirred at ambient temperature for 12 h, at which point a saturated aqueous solution of sodium bicarbonate was added, followed by ethyl acetate. The phases were separated and the aqueous phase was thrice extracted with ethyl acetate. The combined organic extracts were washed with brine, dried over sodium sulfate, filtered, and concentrated under reduced pressure. The residue was purified by flash column chromatography (12 × 1.5 cm) on silica gel (1:2 ethyl acetate–hexanes) to afford acetonide **3.69** (0.13 g, 90%): R_f 0.13 (1:3 ethyl acetate–hexanes); ^{1}H NMR (400 MHz, chloroform-*d*) δ 5.19 (d, *J* = 6.3 Hz, 1H), 4.70 (d, *J* = 6.0 Hz, 1H), 4.36 (ddd, *J* = 10.1, 8.3, 8.3 Hz, 1H), 3.91 (d, *J* = 8.3 Hz, 1H), 3.68 (s, 3H), 2.76 (ddd, *J* = 9.1, 6.2, 6.2 Hz, 1H), 2.60 (dd, *J* = 14.6, 6.1 Hz, 1H), 2.22 – 2.06 (m, 3H), 1.84 (d, *J* = 6.0 Hz, 1H), 1.46 (s, 3H), 1.37 (s, 3H), 1.32 (s, 3H), 1.04 (s, 3H), 0.94 (s, 9H), 0.19 (s, 3H), 0.17 (s, 3H); ^{13}C NMR (101 MHz, chloroform-*d*) δ 181.6, 172.5, 146.6, 111.3, 108.9, 75.9, 74.1, 71.8, 51.9, 45.6, 41.6, 41.2, 37.1, 36.3, 34.5, 26.3, 25.8, 25.3, 24.1, 18.9, 18.2, –4.1, –4.4; HRMS (ESI) calc'd for $C_{25}H_{40}O_7SiNa$ $[M+Na]^+$ *m/z* 503.2436, found 503.2455.

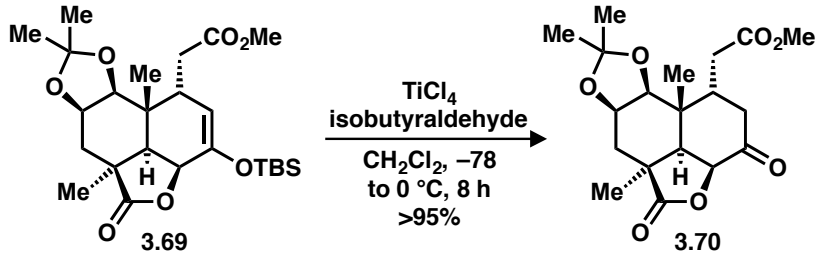

Methyl 2-((1*S*,3a*S*,3a^1*R*,5a*S*,6a*R*,9a*S*,9b*R*)-5a,8,8,9b-tetramethyl-3,5-dioxodecahydro-1*H*-furo[4',3',2':4,5]naphtho[1,2-*d*][1,3]dioxol-1-yl)acetate (3.70).

A 1 M solution of titanium tetrachloride in dichloromethane (0.046 mL, 0.046 mmol) was added to a solution of freshly distilled isobutyraldehyde (42 μL, 0.046 mmol) in dichloromethane (0.15 mL) at –78 °C and the solution was stirred at –78 °C for 15 min. A solution of silyl enol ether **3.69** (0.011 g, 0.023 mmol) in dichloromethane (0.10 mL) was added dropwise and the solution was stirred at –78 °C for 10 min., before it was warmed to 0 °C and stirred at that temperature for an additional 7.5 h. The mixture was diluted with a saturated aqueous solution of ammonium chloride and additional dichloromethane. The phases were separated and the aqueous phase was thrice extracted with dichloromethane. The combined organic extracts were washed with brine, dried over sodium sulfate, filtered, and concentrated under reduced pressure. The residue was purified by flash column chromatography (Pasteur pipette, 9 cm × 0.5 cm) on silica gel (1:1 ethyl acetate–hexanes) to afford ketone **3.70** (0.008 g, ≥95%): R_f 0.10 (1:1 ethyl acetate–hexanes); ^{1}H NMR (400 MHz, chloroform-*d*) δ 4.82 (d, *J* = 8.0 Hz, 1H), 4.42 (ddd, *J* = 10.3, 8.0, 8.0 Hz, 1H), 3.98 (d, *J* = 8.3 Hz, 1H), 3.70 (d, *J* = 0.8 Hz, 3H), 2.85 – 2.72 (m, 2H), 2.57 (ddd, *J* = 14.1, 9.2, 5.5 Hz, 1H), 2.50 – 2.35 (m, 2H), 2.33 – 2.19 (m, 2H), 2.05 (dd, *J* = 14.6, 10.5 Hz, 1H), 1.46 (s, 3H), 1.40 (s, 3H), 1.34 (s, 3H), 0.94 (s, 3H); ^{13}C NMR (75 MHz, chloroform-*d*) δ 204.1, 180.0, 172.3, 109.2, 76.9, 75.9, 71.7, 52.2, 48.2, 41.5, 41.4, 40.0, 38.5, 37.0, 34.3, 26.3, 26.2, 24.1, 19.1; HRMS (ESI) calc'd for $C_{19}H_{26}O_7Na$ $[M+Na]^+$ *m/z* 389.1571, found 389.1581.

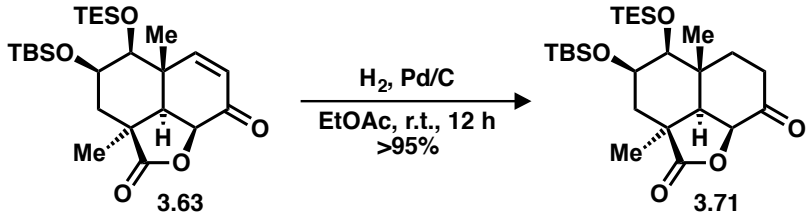

(2a*S*,2a^1*R*,4*R*,5*S*,5a*R*,8a*S*)-4-((*tert*-Butyldimethylsilyl)oxy)-2a,5a-dimethyl-5-((triethylsilyl)oxy)octahydro-2*H*-naphtho[1,8-*bc*]furan-2,8(2a*H*)-dione (3.71).

Palladium on carbon (0.004 g, 0.004 mmol, 10% w/w) was added to a stirred solution of enone **3.63** (0.050 g, 0.10 mmol) in ethyl acetate (2.6 mL). The suspension was purged with hydrogen gas and maintained under an atmosphere of hydrogen gas (using a hydrogen-filled balloon) for 12 h. The reaction mixture was diluted with ethyl acetate, filtered through a short plug of silica gel (Pasteur pipette, 1 cm height of silica gel), and concentrated under reduced pressure to afford ketone **3.71** as a white solid (0.049 g, >95% yield): R_f 0.23 (1:2 ethyl acetate–hexanes); ^{1}H NMR (400 MHz, chloroform-*d*) δ 4.68 (d, *J* = 5.9 Hz, 1H), 3.96 – 3.89 (m, 1H), 3.31 (d, *J* = 3.2 Hz, 1H), 2.62 – 2.42 (m, 3H), 2.31 (d, *J* = 5.9 Hz, 1H), 1.94 (ddd, *J* = 14.4, 10.0, 4.5 Hz, 1H), 1.74 – 1.64 (m, 2H), 1.26 (s, 3H), 1.00 (s, 3H), 0.96 (t, *J* = 7.9 Hz, 9H), 0.85 (s, 9H), 0.70 – 0.52 (m, 6H), 0.10 (s, 3H), 0.03 (s, 3H); ^{13}C NMR (101 MHz, chloroform-*d*) δ 206.3, 178.0, 77.3, 75.7, 70.8, 52.6, 40.2, 38.8, 37.2, 35.6, 34.1, 26.2, 25.8, 18.1, 16.3, 7.2, 5.3, –4.56, –4.60; HRMS (ESI) calc'd for $C_{25}H_{46}O_5Si_2Na$ $[M+Na]^+$ *m/z* 505.2782, found 505.2776.

Annex 4:

Computational Details

Alkylation of Acetonide-Protected Diol: TS-2.7–2.9

Quantum chemical computations were performed with *Gaussian 09*. To identify the lowest energy conformers for the bicyclic enolate, Monte Carlo conformational searches were performed with Macromodel 9.9[299] and the corresponding conformers were then optimized at the B3LYP[300-303]/6-31+G(d,p) level in conjunction with the IEF-PCM implicit solvation model[304] to account for the influence of tetrahydrofuran, the solvent used experimentally. Transition state searches were performed in the presence of methyl chloride at the same level, and additional single-point energies of the optimized transition states were evaluated at the B3LYP-D3(BJ)[305-309] and M06-2X[310] levels with the polarized, triple-ζ valence quality def2-TZVPP basis set of Weigend and Ahlrichs[311] within the IEF-PCM model for tetrahydrofuran. Thermal corrections evaluated from unscaled vibrational frequencies at the B3LYP/6-31+G(d,p) level on optimized geometries were added to the single point electronic energies to obtain the free energies. The free energy corrections were calculated using Truhlar's quasiharmonic approximation.[312,313] Cartesian coordinates and energies (in hartrees) are provided below.

TS-2.7 $C_{20}H_{36}ClO_5Si$ (1-)

C,–1.83514600,1.45853100,0.05288800
C,–0.93186000,–0.90436300,–0.56024600
C,0.34283700,–0.42658300,0.23501100
C,0.70276100,0.97922400,–0.31786200
C,–0.48949800,1.98380600,–0.44513500
C,0.16576300,–0.39510300,1.76900300
C,1.48460400,–1.43293200,–0.13237900
C,–1.31731300,–2.35303800,–0.18417900
C,–0.17462800,–3.33243600,–0.47768900
C,1.12938000,–2.88862400,0.19784100
O,1.64857900,1.67489600,0.51038500
O,–0.07352900,3.13047100,0.32176800
C,1.34433900,3.06836300,0.47027000
C,1.72660800,3.68925700,1.80582700
C,2.04444600,3.74742700,–0.71573400
O,2.70272200,–1.08714900,0.53747300
C,5.28340200,–0.15604400,1.19523300
C,4.25321600,–0.02165600,–1.73149400
C,4.92755400,–2.74147000,–0.46497700
C,–2.10278600,0.08955300,–0.54104300

C,–3.03665800,–0.05331500,–1.59139600
O,–3.14278200,–1.01259100,–2.39463500
O,–3.96646700,0.99870400,–1.68947900
C,–4.98227500,0.84867900,–2.67914500
Si,4.24446500,–1.01071800,–0.12128200
H,–0.59531100,2.27819600,–1.49860100
H,–1.81608700,1.45625300,1.15103700
H,1.14399500,0.83452300,–1.31527100
H,–2.61958500,2.16047700,–0.23745300
H,–0.59570100,–0.97752300,–1.61266400
H,–0.45211000,0.44089300,2.09761400
H,–0.29616400,–1.31314700,2.13968100
H,1.14127500,–0.29148000,2.24772700
H,–2.20356200,–2.62849500,–0.76158500
H,–1.59404400,–2.41262100,0.87507800
H,–0.43923800,–4.34611500,–0.15108000
H,–0.01968600,–3.38631500,–1.56530400
H,2.80686900,3.61670100,1.96158500
H,1.44283000,4.74544800,1.82568800
H,1.21330200,3.16466500,2.61549300
H,1.77733800,4.80793600,–0.75477200
H,3.13066400,3.66338800,–0.61251500
H,1.75050900,3.28344500,–1.66178900
H,1.63407100,–1.35530200,–1.22070100
H,1.04695900,–2.99202900,1.28703100
H,1.96387600,–3.52811500,–0.11341200
H,5.27800300,0.06582700,–2.11307800
H,3.65258500,–0.50099200,–2.51305200
H,3.86141100,0.98847300,–1.57253300
H,4.34329100,–3.26347200,–1.23174300
H,5.96280300,–2.67888100,–0.82316000
H,4.92171800,–3.35767200,0.44151700
H,–5.60584900,–0.03077900,–2.48654300
H,–5.59307600,1.75233800,–2.61562200
H,–4.55746700,0.76028000,–3.68430100
H,6.32714500,–0.06223500,0.87261700
H,4.89676900,0.84806100,1.40102400
H,5.26961600,–0.72245500,2.13340000
C,–3.88495300,–0.60926200,1.16579400
Cl,–5.32401900,–1.06303100,2.67307900
H,–4.29508800,0.32792500,0.82684200
H,–4.03476600,–1.47735500,0.54518700
H,–3.00841100,–0.58298100,1.79163100

Electronic energy = –1909.874459
Sum of electronic and zero-point energies = –1909.340088

Sum of electronic and thermal energies = –1909.307404
Sum of electronic and thermal enthalpies = –1909.306460
Sum of electronic and thermal free energies = –1909.403688
Free energy with quasiharmonic correction = –1909.397544
Frequencies = –434.5946, 23.9216, 32.0012, 39.6616, 41.4784
SCF(B3LYP-D3(BJ)/def2-TZVPP) = –1910.447054
SCF (M06-2X/def2-TZVPP) = –1909.930212

TS-2.8 $C_{20}H_{36}ClO_5Si$ (1-)

C,1.84581100,0.95555100,1.19248300
C,0.93822100,–0.95244500,–0.13245700
C,–0.46502200,–0.27423800,–0.41434200
C,–0.74206100,0.75617800,0.73686800
C,0.44853100,1.57498500,1.29060200
C,–0.48833400,0.40674400,–1.79173000
C,–1.55817900,–1.38561100,–0.33123400
C,1.20034000,–2.15440800,–1.06199300
C,0.08720600,–3.20428500,–0.96096900
C,–1.28552700,–2.58374400,–1.24638100
O,–1.67433400,1.79228500,0.35671100
O,0.35738000,2.80534800,0.55225900
C,–1.03196300,3.08139300,0.41358500
C,–1.25510000,3.84022300,–0.88880700
C,–1.57165100,3.86131400,1.62100700
O,–2.85295500,–0.84327900,–0.63206000
C,–5.55510200,–0.03338400,–0.66200500
C,–4.08358300,–0.52274000,2.02492300
C,–4.78825900,–2.90348400,0.21053700
C,2.05171800,0.07861400,–0.01733100
C,2.85564200,0.48320100,–1.10136000
O,2.98874400,–0.04312800,–2.23236700
O,3.65999800,1.60662600,–0.80306600
C,4.57249600,2.01001600,–1.82061500
Si,–4.27329600,–1.08317900,0.23041700
H,0.24157100,1.79980400,2.34876700
H,2.57970500,1.76250200,1.25255600
H,–1.19325000,0.20170600,1.56926700
H,1.96547600,0.35712400,2.11378400
H,0.83814600,–1.38927900,0.88181700
H,0.27343700,1.18704400,–1.84396800
H,–0.28114400,–0.30695600,–2.59247400
H,–1.46651900,0.85448700,–1.97272800
H,2.16105100,–2.60625200,–0.79230400
H,1.30957100,–1.81566000,–2.09485600

H,0.27657900,–4.03066100,–1.65769000
H,0.08378700,–3.64328800,0.04835100
H,–2.32497400,4.00494700,–1.04750800
H,–0.75796400,4.81398300,–0.84393700
H,–0.85322000,3.27448600,–1.73043600
H,–1.09784100,4.84647900,1.67807600
H,–2.65274400,3.99879800,1.52178200
H,–1.38029900,3.32430800,2.55371200
H,–1.55195700,–1.75495100,0.70854000
H,–1.34427700,–2.25828100,–2.29230900
H,–2.08361100,–3.32165900,–1.10195100
H,–5.04346700,–0.59952200,2.55043600
H,–3.35928600,–1.13696000,2.57235200
H,–3.74963200,0.51923000,2.07041800
H,–4.03919800,–3.54147100,0.69398800
H,–5.73431100,–3.03825400,0.74976000
H,–4.93035900,–3.26635900,–0.81379700
H,5.31009100,1.22954800,–2.03700100
H,4.05473100,2.26518400,–2.75104900
H,5.08108200,2.89440000,–1.42875600
H,–6.53939400,–0.13283900,–0.18906300
H,–5.27509000,1.02547900,–0.64403900
H,–5.65102000,–0.34008400,–1.70965600
C,4.01582000,–1.24658200,0.93799500
Cl,5.54626400,–2.34060700,1.91119300
H,4.33472200,–0.24954000,1.19516900
H,3.16994300,–1.65726800,1.46560900
H,4.19263100,–1.58201400,–0.07144000

Electronic energy = –1909.872402
Sum of electronic and zero-point energies = –1909.338270
Sum of electronic and thermal energies = –1909.305716
Sum of electronic and thermal enthalpies = –1909.304772
Sum of electronic and thermal free energies = –1909.401505
Free energy with quasiharmonic correction = –1909.395465
Frequencies = –428.1099, 24.5535, 31.8708, 37.0232, 41.0951, 44.7556
SCF(B3LYP-D3(BJ)/def2-TZVPP) = –1910.445642
SCF(M06-2X/def2-TZVPP) = –1909.929203

TS-2.9 $C_{20}H_{36}ClO_5Si$ (1-)
C,1.84789500,1.39174900,–0.26078800
C,0.94268600,–1.02577000,–0.13056300
C,–0.44653400,–0.38586500,–0.55329700
C,–0.61355300,0.92773000,0.27300100
C,0.69366100,1.61446500,0.70694800
C,–0.50026900,–0.11820200,–2.06898300

C,–1.59462400,–1.35225900,–0.12607200
C,1.08130400,–2.47480600,–0.64110100
C,–0.08981000,–3.36305600,–0.20660100
C,–1.43199600,–2.77682500,–0.65743900
O,–1.28154000,1.97086300,–0.45419500
O,0.33249200,3.00862900,0.78929100
C,–0.94879100,3.21149200,0.16274000
C,–0.83118600,4.27383200,–0.92451400
C,–1.97478800,3.58894000,1.23710000
O,–2.85572200,–0.80347800,–0.53070100
C,–4.12055500,–0.31129700,2.08043800
C,–5.05934000,–2.61010700,0.26651800
C,–5.44266600,0.31054600,–0.66319400
C,2.11746300,–0.09540200,–0.46527200
C,3.18750300,–0.45179400,–1.31200200
O,3.57321100,–1.57234700,–1.72485700
O,3.95943600,0.67722600,–1.67839100
C,5.12843600,0.41200500,–2.44950400
Si,–4.32367800,–0.86777600,0.28579100
H,0.97521400,1.29484300,1.71702100
H,1.59378900,1.90361500,–1.20333200
H,–1.20074400,0.69873700,1.17388000
H,2.73072300,1.91705400,0.12418400
H,0.87384400,–1.11862600,0.97216600
H,–1.47309100,0.28652100,–2.35228800
H,0.26916800,0.59404300,–2.37224100
H,–0.33446600,–1.04028000,–2.63207000
H,2.02303100,–2.89089500,–0.27657400
H,1.16473800,–2.48293200,–1.73229700
H,0.03579100,–4.37467500,–0.61238900
H,–0.08960900,–3.46590300,0.88914500
H,–0.08216900,3.96929100,–1.65944800
H,–1.79299100,4.40865800,–1.42877300
H,–0.53153000,5.23007000,–0.48563900
H,–2.95576900,3.75993000,0.78292000
H,–2.06416100,2.79175000,1.98038900
H,–1.66173200,4.50341800,1.75035300
H,–1.56452600,–1.40935300,0.97424300
H,–1.49977800,–2.77236000,–1.75243600
H,–2.26558900,–3.38777500,–0.29279100
H,–6.06950900,–2.59975800,0.69485300
H,–5.13215000,–2.99842700,–0.75582100
H,–4.45827400,–3.31376000,0.85362700
H,–5.55864600,–0.01402900,–1.70352200
H,–6.44014100,0.35239300,–0.20978700
H,–5.02737200,1.32408000,–0.67023400

H,5.83415700,–0.22934300,–1.91068200
H,4.88351900,–0.06737000,–3.40306000
H,5.58775600,1.38614400,–2.63547000
H,–3.44385300,–0.96701200,2.64041100
H,–3.72932500,0.71010300,2.14012600
H,–5.09138500,–0.32929400,2.59080200
C,3.67191700,–0.55190600,1.51050800
Cl,4.86820200,–0.91043900,3.22259300
H,4.26670500,0.22508900,1.05686800
H,2.76575800,–0.25993200,2.01526800
H,3.71112900,–1.53566200,1.07074600

Electronic energy = –1909.870901
Sum of electronic and zero-point energies = –1909.337330
Sum of electronic and thermal energies = –1909.304348
Sum of electronic and thermal enthalpies = –1909.303403
Sum of electronic and thermal free energies = –1909.402103
Free energy with quasiharmonic correction = –1909.395153
Frequencies = –435.0492, 20.6100, 25.9138, 31.5006, 41.1190
SCF(B3LYP-D3(BJ)/def2-TZVPP) = –1910.443008
SCF(M06-2X/def2-TZVPP) = –1909.92646

Rubottom Oxidation of Silyl Enol Ether: TS-3.2 & TS-3.3

Quantum chemical computations were performed with *Gaussian 09*. To identify the lowest energy conformers for the trimethysilyl enol ether, Monte Carlo conformational searches were performed with Macromodel 9.9[299] and the corresponding conformers were then optimized at the B3LYP[300-303]/6-31G(d) level of theory. Transition state searches were performed in the presence of perbenzoic acid at the same level, and the single-point energies of the optimized transition states were evaluated at the B3LYP-D3(BJ),[305-309] ωB97X-D,[379] and M06-2X[310] and levels with the polarized, triple-ζ valence quality def2-TZVPP basis set of Weigend and Ahlrichs.[311] Thermal corrections evaluated from unscaled vibrational frequencies at the B3LYP/6-31G(d) level on optimized geometries were added to the single point electronic energies to obtain the free energies. Cartesian coordinates and energies (in hartrees) are provided below.

TS-3.2 $C_{23}H_{32}O_6Si$ (0)

C,–0.81336800,–0.26410700,2.56807000

C,–1.15302300,–1.48828500,1.69913300
C,–2.14637800,–1.08864100,0.63664000
C,–1.68939000,0.00458600,–0.33230800
C,–0.90221700,1.07822800,0.42366100
C,–0.47347000,0.93880800,1.72928700
C,–0.76472900,–0.59915900,–1.42949900
C,–2.92859000,0.68138200,–0.98679600
C,–3.37349600,–1.62206800,0.59029100
C,–4.46127200,–1.21464300,–0.36691200
C,–3.93203400,–0.34977200,–1.50759100
O,–0.68658700,2.18065700,–0.29786200
O,–5.11617400,–2.36140700,–0.92879000
O,–5.46552700,–0.51694700,0.39815500
C,–0.36992100,4.85102600,–1.08139700
C,1.94445300,2.81889700,–1.40615200
C,1.12591000,3.80065200,1.42570800
C,–6.38520500,–2.50019700,–0.29908300
C,–6.73453400,–1.05625700,0.04300900
Si,0.53083200,3.39210700,–0.31062300
H,–0.22874200,–1.87257600,1.24545200
H,–1.55951000,–2.29307200,2.32029400
H,0.02813600,–0.48651800,3.23437700
H,–1.67166900,–0.02412800,3.21377800
H,–1.31762400,–1.29698300,–2.06438500
H,–0.35995300,0.19932600,–2.05954500
H,0.07354500,–1.12896100,–0.97511500
H,–0.08432500,1.80857300,2.24353300
H,–3.65719000,–2.39170500,1.30619600
H,–3.47310300,–1.01009900,–2.25124300
H,–4.77836200,0.14686400,–1.99508300
H,–3.43044900,1.31205800,–0.24274800
H,–2.59888800,1.33982600,–1.79539400
H,–1.23973000,5.14352000,–0.48213900
H,0.29135600,5.72279600,–1.15872300
H,–0.72524300,4.61101200,–2.08992600
H,2.67294000,3.62452900,–1.55871000
H,2.46631600,1.97260200,–0.94492400
H,1.58166200,2.51457100,–2.39464200
H,1.75145100,2.99382000,1.82253400
H,1.72425100,4.72055100,1.40590900
H,0.29175400,3.97050400,2.11635200
H,–7.40788400,–0.94450000,0.89762300
H,–7.16282800,–0.53412500,–0.82601400
H,–6.31656400,–3.11946400,0.60787000
H,–7.07021200,–2.97547500,–1.00706800
C,3.28434500,–0.93662700,0.30561700

O,2.31123000,–1.69689200,0.16738400
O,3.19434900,0.29288000,0.73874800
O,1.45252400,0.60453900,1.01996000
C,4.67723900,–1.37871300,–0.03486800
C,4.85997200,–2.66276500,–0.56389400
C,5.78303400,–0.54018500,0.15804100
C,6.13829300,–3.10358900,–0.90008300
C,7.06040200,–0.98521900,–0.17837700
C,7.23978000,–2.26558900,–0.70810200
H,1.28427700,–0.33530700,0.73799700
H,3.98978900,–3.29528200,–0.70356700
H,5.63163700,0.45214200,0.56923800
H,6.27648100,–4.09979100,–1.31188600
H,7.91691300,–0.33352800,–0.02772600
H,8.23680600,–2.60990000,–0.97072000

Electronic energy = –1636.501056
Sum of electronic and zero-point energies = –1635.985610
Sum of electronic and thermal energies = –1635.954206
Sum of electronic and thermal enthalpies = –1635.953262
Sum of electronic and thermal free energies = –1636.050290
Free energy with quasiharmonic correction = –1636.041571
Frequencies = –403.0399, 16.7842, 19.5651, 24.2106, 30.7524
SCF(B3LYP-D3(BJ)/def2-TZVPP) = –1637.209066
SCF(ωB97XD/def2-TZVPP) = –1636.61439
SCF(M06-2X/def2-TZVPP) = –1636.453497

TS-3.3 $C_{23}H_{32}O_6Si$ (0)

C,–1.63735700,0.12179400,2.98065600
C,–0.83504400,1.42316900,2.71743400
C,–0.72220600,1.84456600,1.25996600
C,–1.83237600,1.43597700,0.29503100
C,–2.22962400,–0.01962500,0.54662100
C,–2.12208800,–0.59450600,1.75347300
C,–3.10538900,2.29225900,0.56259800
C,–1.35956200,1.59924700,–1.17100400
C,0.32665000,2.57437300,0.86162600
C,0.55377500,3.09126100,–0.53351800
C,–0.68871800,2.95293700,–1.40883200
O,–2.93340500,–0.54683700,–0.46299300
O,0.94417100,4.47444500,–0.50537900
O,1.66938100,2.37243000,–1.08652400
C,–4.24440800,–1.84770000,–2.56015500
C,–4.97552800,–2.48319100,0.37514400
C,–2.23309100,–3.41147800,–0.77825600

C,2.33911100,4.54540000,–0.78362100
C,2.55523400,3.32204600,–1.66752900
Si,–3.56952600,–2.09684000,–0.82521300
H,–1.28609300,2.23823300,3.29874900
H,0.17984000,1.29583900,3.10346700
H,–2.52784700,0.34446500,3.58883400
H,–1.04207900,–0.57229700,3.58486300
H,–2.89059300,3.35408100,0.41205300
H,–3.91294200,1.99896000,–0.11608600
H,–3.46351500,2.16922400,1.59097700
H,–2.56732100,–1.57085200,1.91549300
H,1.11660600,2.81723400,1.56966600
H,–1.36567500,3.78395100,–1.17950800
H,–0.39231800,3.05860700,–2.45828500
H,–0.64208100,0.80218300,–1.39331300
H,–2.21093900,1.46864500,–1.84519500
H,–3.44535800,–1.55915200,–3.25208600
H,–4.69867900,–2.77084200,–2.94019100
H,–5.00942300,–1.06333900,–2.58502800
H,–4.62025700,–2.75911700,1.37434100
H,–5.65513100,–1.62969700,0.48273800
H,–5.56578200,–3.32730900,–0.00343400
H,–1.82471800,–3.55200200,0.22666200
H,–2.63833700,–4.37123800,–1.12466200
H,–1.38991700,–3.13671700,–1.41954900
H,3.56833500,2.91206900,–1.63311100
H,2.28550200,3.53513300,–2.71331200
H,2.93445900,4.48118400,0.13939400
H,2.54313500,5.50039600,–1.27676800
C,1.90006100,–1.42449700,0.54019400
O,1.70211600,–0.64028000,1.50929600
O,0.94580000,–1.85820800,–0.22806500
O,–0.56786800,–1.12868300,0.53336800
C,3.28476000,–1.91306300,0.21856600
C,4.36145800,–1.46563600,0.99373800
C,3.51241600,–2.80585200,–0.83614600
C,5.65424100,–1.90678400,0.71639900
C,4.80639700,–3.24580200,–1.11199100
C,5.87860400,–2.79745000,–0.33666400
H,0.10295400,–0.64163800,1.11198000
H,4.16240900,–0.77460100,1.80605400
H,2.66959100,–3.14514400,–1.42894600
H,6.48757100,–1.55744200,1.32077700
H,4.97948500,–3.93895300,–1.93123400
H,6.88704100,–3.14171400,–0.55236800

Electronic energy = –1636.495686
Sum of electronic and zero-point energies = –1635.980903
Sum of electronic and thermal energies = –1635.949141
Sum of electronic and thermal enthalpies = –1635.948196
Sum of electronic and thermal free energies = –1636.046852
Free energy with quasiharmonic correction = –1636.037365
Frequencies = –408.3601, 11.7080, 22.2694, 27.3312, 27.8264
SCF(B3LYP-D3(BJ)/def2-TZVPP) = –1637.205213
SCF(ωB97XD/def2-TZVPP) = –1636.610046
SCF(M06-2X/def2-TZVPP) = –1636.44733

Alkylation of Acetonide-Protected Diol: TS-3.5 & TS-3.6

Quantum chemical computations were performed with *Gaussian 09*. To identify the lowest energy conformers for the bicyclic enolate, Monte Carlo conformational searches were performed with Macromodel 9.9[299] and the corresponding conformers were then optimized at the B3LYP[300-303]/6-31+G(d,p) level in conjunction with the IEF-PCM implicit solvation model[304] to account for the influence of tetrahydrofuran, the solvent used experimentally. Transition state searches were performed in the presence of methyl chloride at the same level, and additional single-point energies of the optimized transition states were evaluated at the B3LYP-D3(BJ)[305-309] and M06-2X[310] levels with the polarized, triple-ζ valence quality def2-TZVPP basis set of Weigend and Ahlrichs[311] within the IEF-PCM model for tetrahydrofuran. Thermal corrections evaluated from unscaled vibrational frequencies at the B3LYP/6-31+G(d,p) level on optimized geometries were added to the single point electronic energies to obtain the free energies. The free energy corrections were calculated using Truhlar's quasiharmonic approximation.[312,313] Cartesian coordinates and energies (in hartrees) are provided below.

TS-3.5 $C_{22}H_{42}ClO_6Si_2$ (1-)

C,–0.27994000,1.34807200,1.03612300
C,1.31208200,–0.16075400,–0.16783300
C,0.14660100,–1.08249000,–0.69992400
C,–1.01738500,–0.96486600,0.32851600
C,–1.48954700,0.47433600,0.62725400
C,–0.30494400,–0.69000900,–2.11959800
C,0.64772800,–2.55193200,–0.69157000
C,2.61393000,–0.36948200,–0.96594700

C,3.06765200,–1.83074900,–0.96267600
C,1.96542900,–2.76385500,–1.45305100
C,0.86849100,1.27729600,0.05410100
C,1.12879000,2.32211300,–0.85381700
O,1.88567100,2.33828800,–1.85578000
O,0.48371600,3.53206800,–0.50725000
C,0.74715200,4.64562900,–1.35534900
O,4.24242200,–1.95932700,–1.79991100
O,3.48620700,–2.25666200,0.34678200
C,4.90376900,–2.08389800,0.41376900
C,5.33462500,–2.43637100,–1.00521300
O,–2.12729100,–1.79179600,–0.04607100
O,–2.18629400,1.02999100,–0.48998300
C,–3.30052300,3.52955600,0.62217500
C,–5.05591600,1.05132200,0.17968100
C,–3.81769300,2.49949000,–2.25724200
C,–4.37792300,–3.49063400,–0.11626100
C,–3.52248600,–2.12050100,2.53633100
C,–1.80630900,–4.36982100,1.36291700
Si,–2.92210400,–2.90861200,0.92572200
Si,–3.55098500,2.00086000,–0.46165300
H,–2.17918300,0.40764500,1.48392800
H,–0.62284900,2.37324000,1.18546900
H,–0.60542200,–1.32481600,1.28632800
H,0.04182000,0.97482600,2.02669300
H,1.52695000,–0.56347200,0.83980300
H,–0.56441600,0.36703300,–2.16934000
H,0.48125200,–0.88545500,–2.85459800
H,–1.18702200,–1.27092000,–2.40689800
H,3.41324700,0.24612400,–0.54179400
H,2.49832500,–0.04524700,–2.00152900
H,0.79720600,–2.87207800,0.34784800
H,1.82941800,–2.57434000,–2.52329200
H,2.30826600,–3.79979100,–1.34887700
H,0.43652000,4.45027800,–2.38728800
H,0.16235500,5.47425700,–0.94762200
H,1.80891000,4.91515900,–1.35912800
H,–0.12247800,–3.20686700,–1.11281800
H,5.45380900,–3.52110300,–1.13112500
H,6.24997700,–1.93075500,–1.32488500
H,5.29540500,–2.75730800,1.17933800
H,5.16287300,–1.04800300,0.67101600
H,–4.18503400,4.17706900,0.57602600
H,–3.14222900,3.25934300,1.67287300
H,–2.43336200,4.10927000,0.28922300
H,–4.92398300,0.73256500,1.21973800

H,–5.94801900,1.68902300,0.14177400
H,–5.25158900,0.15995700,–0.42659200
H,–4.68860800,3.15903200,–2.35291900
H,–2.94374300,3.03184800,–2.64820500
H,–3.98834700,1.62027200,–2.88841400
H,–5.04023600,–2.65506600,–0.36735900
H,–4.03366200,–3.94286200,–1.05318300
H,–4.96839500,–4.24040300,0.42373700
H,–4.03816800,–2.86835900,3.15136800
H,–2.68970600,–1.72492300,3.12935600
H,–4.22294800,–1.30041200,2.34672700
H,–2.36222400,–5.09511000,1.97011600
H,–1.44940000,–4.88422900,0.46412300
H,–0.93069500,–4.05595800,1.94210500
C,2.67171900,2.18711800,1.63197600
Cl,4.06493000,2.82707600,3.08261500
H,1.90766900,2.93171900,1.78664400
H,2.49081700,1.19302300,2.00842000
H,3.28907200,2.28612300,0.75331300

Electronic energy = –2354.498903
Sum of electronic and zero-point energies = –2353.886241
Sum of electronic and thermal energies = –2353.846317
Sum of electronic and thermal enthalpies = –2353.845373
Sum of electronic and thermal free energies = –2353.958941
Free energy with quasiharmonic correction = –2353.950562
Frequencies = –423.8580, 26.6971, 30.5298, 35.8242, 36.5242
SCF(B3LYP-D3(BJ)/def2-TZVPP) = –2355.18446
SCF(M06-2X/def2-TZVPP) = –2354.576683

TS-3.6 $C_{22}H_{42}ClO_6Si_2$ (1-)

C,2.32810100,2.87493700,–0.53938900
Cl,3.31749100,4.44300500,–1.60389000
H,1.64627200,3.47976400,0.03496900
H,3.18974500,2.46903400,–0.03513000
H,1.93998400,2.33781200,–1.38865000
C,–0.38116700,1.56350800,0.18174300
C,1.38096000,–0.34693500,0.15145700
C,0.28513200,–1.08279800,–0.69203700
C,–1.02332100,–0.94660600,0.12720300
C,–1.53323300,0.52735500,0.27683400
C,0.09552600,–0.56997800,–2.13867100
C,0.71287300,–2.57378000,–0.75733900
C,2.76284000,–0.45831200,–0.52924100

C,3.19057600,–1.92469000,–0.68662800
C,2.11484600,–2.77387500,–1.36211400
C,0.96668300,1.04738000,0.63469500
C,1.52647800,1.45635000,1.86360800
O,2.48970600,0.92843300,2.47231300
O,0.94704300,2.61488200,2.41575300
C,1.54499400,3.10102900,3.61607800
O,4.41964900,–1.98698100,–1.45128400
O,3.50788300,–2.51387300,0.58214700
C,4.90424400,–2.30042900,0.79928000
C,5.47640900,–2.46427500,–0.60682600
O,–2.04469600,–1.79987500,–0.38530800
O,–2.54311400,0.80864100,–0.69599700
C,–2.98393100,3.59578200,–1.53362200
C,–4.17717300,2.48301100,1.08779700
C,–5.14124300,1.40085100,–1.65757800
C,–4.19812300,–3.57060600,–0.78811800
C,–4.08882700,–1.78594600,1.74858600
C,–2.10854600,–4.10888800,1.43814400
Si,–3.07689300,–2.78253000,0.50225500
Si,–3.66696800,2.05457700,–0.68146600
H,–1.99245900,0.59550400,1.27313000
H,–0.35747800,1.89442000,–0.86551100
H,–0.76080200,–1.26974800,1.14704000
H,–0.65524700,2.44648000,0.76421800
H,1.48492300,–0.95841000,1.06202700
H,–0.19223800,0.47946100,–2.18700800
H,1.00495200,–0.68835700,–2.73334300
H,–0.69591200,–1.14885400,–2.62664300
H,3.51079100,0.06255500,0.07460000
H,2.76403800,0.00702000,–1.52075100
H,0.69770500,–2.99474100,0.25592600
H,2.11292100,–2.50962800,–2.42480300
H,2.41576800,–3.82555000,–1.29621100
H,2.59364600,3.37698000,3.46219300
H,0.96967400,3.98670800,3.89620200
H,1.49574800,2.35938500,4.42005200
H,–0.01454800,–3.14331400,–1.34521000
H,5.69171200,–3.51639600,–0.83514800
H,6.37395500,–1.86462500,–0.78436200
H,5.25758000,–3.04856000,1.51200400
H,5.09025800,–1.29657700,1.20254200
H,–3.75409200,4.37448900,–1.59863000
H,–2.12895200,4.01100800,–0.98969400
H,–2.65343500,3.36401400,–2.55268300
H,–3.33597200,2.86679700,1.67612100

H,–4.95112800,3.26018900,1.07347500
H,–4.58713900,1.61264400,1.61232900
H,–5.91525400,2.17071700,–1.76199800
H,–4.83546000,1.09230500,–2.66379300
H,–5.58959000,0.53291600,–1.16138200
H,–4.75653500,–2.80639300,–1.33999600
H,–3.61509600,–4.15098600,–1.51211500
H,–4.92174400,–4.24691500,–0.31769400
H,–4.75612800,–2.44909500,2.31302800
H,–3.44465800,–1.27260800,2.47192000
H,–4.70618900,–1.03076500,1.25049200
H,–2.79665300,–4.74856200,2.00463100
H,–1.54063400,–4.74709700,0.75222000
H,–1.40199300,–3.67108500,2.15255800

Electronic energy = –2354.490146
Sum of electronic and zero-point energies = –2353.877431
Sum of electronic and thermal energies = –2353.837083
Sum of electronic and thermal enthalpies = –2353.836139
Sum of electronic and thermal free energies = –2353.952820
Free energy with quasiharmonic correction = –2353.94214
Frequencies = –438.5552, 15.5259, 17.3091, 25.0731, 29.9727
434.5946, 23.9216, 32.0012, 39.6616, 41.4784
SCF(B3LYP-D3(BJ)/def2-TZVPP) = –2355.173759
SCF(M06-2X/def2-TZVPP) = –2354.5660

Annex 5:

X-ray Crystallographic Data

Benzyl enol ether 1.62

Université de Montréal

CRYSTAL AND MOLECULAR STRUCTURE OF

C43 H38 N4 O13 COMPOUND (bent79)

Equipe Hanessian

Département de chimie, Université de Montréal,

C.P. 6128, Succ. Centre-Ville, Montréal, Québec, H3C 3J7 (Canada)

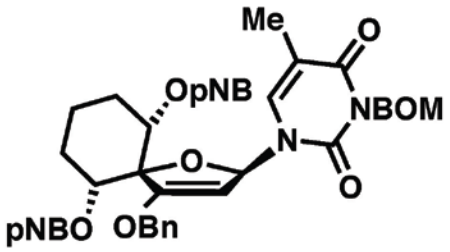

1.62
[X-ray]

Structure solved and refined in the laboratory of X-ray diffraction Université de Montréal by Benoît Deschênes Simard.

Table 1. Crystal data and structure refinement for C43 H38 N4 O13.

Identification code	bent79
Empirical formula	C43 H38 N4 O13
Formula weight	818.77
Temperature	100K
Wavelength	1.54178 Å
Crystal system	Monoclinic
Space group	P21
Unit cell dimensions	a = 12.7095(6) Å α = 90° b = 7.6449(3) Å β = 90.002(2)° c = 19.7593(9) Å γ = 90°
Volume	1919.87(15)Å^3
Z	2
Density (calculated)	1.416 g/cm^3
Absorption coefficient	0.889 mm^{-1}
F(000)	856
Crystal size	0.10 x 0.02 x 0.01 mm
Theta range for data collection	2.24 to 61.64°
Index ranges	$-13 \le h \le 14$, $-8 \le k \le 8$, $-22 \le \ell \le 22$
Reflections collected	34453
Independent reflections	5816 [R_{int} = 0.052]
Absorption correction	Semi-empirical from equivalents
Max. and min. transmission	0.9911 and 0.7990
Refinement method	Full-matrix least-squares on F^2
Data / restraints / parameters	5816 / 2 / 543
Goodness-of-fit on F^2	0.888
Final R indices [I>2sigma(I)]	R_1 = 0.0364, wR_2 = 0.0781
R indices (all data)	R_1 = 0.0554, wR_2 = 0.0824
Absolute structure parameter	0.00(17)
Extinction coefficient	0.00229(17)
Largest diff. peak and hole	0.202 and -0.254 e/Å^3

Table 2. Atomic coordinates (x 10^4) and equivalent isotropic displacement parameters ($Å^2$ x 10^3) for C43 H38 N4 O13.

U_{eq} is defined as one third of the trace of the orthogonalized Uij tensor.

	x	y	z	U_{eq}
O(1)	4283(1)	9219(3)	7541(1)	37(1)
O(2)	4634(1)	5250(2)	8458(1)	38(1)
O(3)	5232(1)	9368(2)	8866(1)	38(1)
O(4)	2627(1)	6547(3)	7463(1)	40(1)
O(5)	5121(2)	8493(3)	9953(1)	43(1)
O(6)	1070(2)	5669(3)	7903(1)	60(1)
O(7)	5063(2)	10616(3)	6015(1)	44(1)
O(8)	8419(2)	12268(3)	6514(1)	45(1)
O(9)	6191(2)	14301(3)	6077(1)	46(1)
O(10)	1166(2)	-1269(4)	5651(2)	96(1)
O(11)	2831(2)	-1362(3)	5813(1)	57(1)
O(12)	9854(2)	12779(3)	10417(1)	57(1)
O(13)	10220(2)	12437(3)	9349(1)	58(1)
N(1)	5881(2)	9286(3)	6906(1)	35(1)
N(2)	6731(2)	11470(3)	6271(1)	36(1)
N(3)	1975(2)	-661(4)	5889(1)	52(1)
N(4)	9652(2)	12242(4)	9845(2)	46(1)
C(1)	4923(2)	8281(4)	7055(2)	37(1)
C(2)	5147(2)	6556(4)	7387(2)	36(1)
C(3)	4659(2)	6474(4)	7966(2)	33(1)
C(4)	3976(2)	8077(4)	8089(1)	34(1)
C(5)	4118(2)	8952(4)	8765(2)	37(1)
C(6)	3480(2)	10644(4)	8818(2)	43(1)
C(7)	2308(2)	10259(4)	8714(2)	43(1)
C(8)	2121(2)	9284(4)	8057(2)	41(1)
C(9)	2791(2)	7630(4)	8051(2)	36(1)
C(10)	5830(2)	10458(4)	6376(2)	35(1)
C(11)	7680(2)	11287(4)	6631(2)	37(1)
C(12)	7691(2)	9923(4)	7135(2)	38(1)
C(13)	6799(2)	9026(4)	7268(1)	36(1)
C(14)	8721(2)	9551(4)	7485(2)	47(1)
C(15)	6660(2)	12816(4)	5757(2)	42(1)
C(16)	5994(2)	15686(4)	5600(2)	47(1)
C(17)	6926(2)	16887(4)	5478(2)	43(1)
C(18)	7885(3)	16599(5)	5794(2)	53(1)
C(19)	8732(3)	17703(5)	5649(2)	62(1)
C(20)	8615(3)	19088(5)	5206(2)	58(1)
C(21)	7648(3)	19390(5)	4904(2)	55(1)
C(22)	6817(3)	18282(4)	5038(2)	50(1)
C(23)	5415(2)	3870(4)	8383(2)	41(1)
C(24)	6529(2)	4540(4)	8443(2)	38(1)
C(25)	7238(2)	4329(4)	7917(2)	41(1)
C(26)	8277(2)	4884(4)	7991(2)	46(1)
C(27)	8597(2)	5630(4)	8584(2)	46(1)
C(28)	7899(2)	5850(4)	9120(2)	45(1)
C(29)	6869(2)	5295(4)	9045(2)	41(1)
C(30)	1764(2)	5474(4)	7489(2)	44(1)
C(31)	1823(2)	3993(4)	7011(2)	41(1)
C(32)	905(2)	3199(4)	6797(2)	48(1)

C(33)	940(2)	1700(4)	6414(2)	48(1)
C(34)	1906(2)	995(4)	6267(2)	41(1)
C(35)	2834(2)	1763(4)	6464(2)	41(1)
C(36)	2790(2)	3291(4)	6834(2)	41(1)
C(37)	5601(2)	9157(4)	9497(2)	34(1)
C(38)	6693(2)	9889(4)	9571(2)	35(1)
C(39)	7233(2)	10545(4)	9021(2)	38(1)
C(40)	8230(2)	11283(4)	9109(2)	41(1)
C(41)	8631(2)	11349(4)	9746(2)	35(1)
C(42)	8129(2)	10674(4)	10307(2)	39(1)
C(43)	7140(2)	9928(4)	10208(2)	38(1)

Table 3. Hydrogen coordinates (x 10^4) and isotropic displacement parameters ($Å^2$ x 10^3) for C43 H38 N4 O13.

	x	y	z	U_{eq}
H(1)	4514	8090	6629	44
H(2)	5579	5661	7203	43
H(5)	3885	8131	9129	44
H(6A)	3724	11485	8471	52
H(6B)	3589	11178	9269	52
H(7A)	2045	9549	9097	52
H(7B)	1911	11373	8707	52
H(8A)	2311	10037	7668	50
H(8B)	1368	8972	8016	50
H(9)	2606	6926	8461	43
H(13)	6803	8187	7623	43
H(14A)	9199	8957	7171	70
H(14B)	8596	8800	7879	70
H(14C)	9040	10654	7634	70
H(15A)	7368	13114	5584	51
H(15B)	6220	12413	5374	51
H(16A)	5396	16396	5766	57
H(16B)	5781	15161	5163	57
H(18)	7965	15662	6106	63
H(19)	9395	17499	5857	74
H(20)	9196	19829	5108	70
H(21)	7557	20356	4608	66
H(22)	6159	18479	4823	60
H(23A)	5324	3310	7934	49
H(23B)	5293	2968	8733	49
H(25)	7016	3805	7505	50
H(26)	8761	4743	7629	55
H(27)	9306	6003	8632	55
H(28)	8126	6372	9531	54
H(29)	6387	5433	9409	49
H(32)	244	3693	6916	58
H(33)	312	1167	6254	57
H(35)	3491	1253	6348	49
H(36)	3421	3861	6967	49
H(39)	6927	10495	8583	46
H(40)	8615	11726	8734	49
H(42)	8444	10715	10742	46
H(43)	6770	9443	10581	45

Table 4. Anisotropic parameters ($Å^2$ x 10^3) for C43 H38 N4 O13.

The anisotropic displacement factor exponent takes the form:

$$-2\pi^2 [h^2 a^{*2} U_{11} + ... + 2 h k a^* b^* U_{12}]$$

	U11	U22	U33	U23	U13	U12
O(1)	30(1)	37(1)	45(1)	-1(1)	2(1)	-1(1)
O(2)	28(1)	35(1)	51(1)	0(1)	1(1)	0(1)
O(3)	25(1)	40(1)	49(1)	-2(1)	-4(1)	-5(1)
O(4)	29(1)	42(1)	49(1)	-5(1)	-1(1)	-5(1)
O(5)	35(1)	46(1)	47(1)	3(1)	2(1)	-6(1)
O(6)	40(1)	67(2)	73(2)	-26(1)	15(1)	-14(1)
O(7)	29(1)	50(1)	54(1)	5(1)	-5(1)	0(1)
O(8)	37(1)	44(1)	55(1)	0(1)	1(1)	-8(1)
O(9)	45(1)	43(1)	49(1)	0(1)	4(1)	4(1)
O(10)	46(2)	85(2)	157(3)	-62(2)	-6(2)	-11(2)
O(11)	43(2)	53(2)	76(2)	-13(1)	1(1)	5(1)
O(12)	45(1)	68(2)	60(2)	-5(1)	-10(1)	-9(1)
O(13)	38(1)	68(2)	67(2)	-7(1)	9(1)	-9(1)
N(1)	25(1)	38(1)	41(1)	2(1)	-2(1)	-4(1)
N(2)	28(1)	36(1)	42(1)	4(1)	-2(1)	-3(1)
N(3)	44(2)	44(2)	67(2)	-8(2)	-1(1)	-7(2)
N(4)	34(2)	48(2)	55(2)	-3(2)	-7(1)	3(1)
C(1)	29(2)	36(2)	46(2)	-7(2)	2(1)	-2(1)
C(2)	28(2)	35(2)	43(2)	-4(2)	-4(1)	-3(1)
C(3)	26(2)	36(2)	37(2)	1(2)	-3(1)	-3(1)
C(4)	27(2)	34(2)	40(2)	2(2)	0(1)	-1(1)
C(5)	22(2)	41(2)	47(2)	-4(2)	-1(1)	-5(1)
C(6)	34(2)	40(2)	57(2)	-8(2)	0(1)	-2(1)
C(7)	30(2)	39(2)	60(2)	-6(2)	4(1)	2(1)
C(8)	24(2)	45(2)	56(2)	2(2)	1(1)	0(2)
C(9)	26(2)	39(2)	44(2)	-7(2)	-2(1)	-7(1)
C(10)	31(2)	35(2)	39(2)	-3(2)	1(1)	0(1)
C(11)	32(2)	34(2)	45(2)	-5(2)	2(1)	-1(1)
C(12)	32(2)	39(2)	42(2)	-4(2)	-1(1)	1(1)
C(13)	29(2)	36(2)	43(2)	1(2)	-4(1)	-4(1)
C(14)	33(2)	52(2)	56(2)	2(2)	-7(1)	-5(2)
C(15)	40(2)	41(2)	46(2)	2(2)	1(2)	3(2)
C(16)	42(2)	42(2)	58(2)	2(2)	-2(2)	6(2)
C(17)	45(2)	39(2)	46(2)	-5(2)	1(2)	-3(2)
C(18)	50(2)	50(2)	58(2)	-2(2)	-4(2)	-11(2)
C(19)	52(2)	63(3)	70(3)	-10(2)	-3(2)	-14(2)
C(20)	72(3)	48(2)	54(2)	-10(2)	12(2)	-20(2)
C(21)	72(3)	40(2)	54(2)	-2(2)	15(2)	-3(2)
C(22)	60(2)	41(2)	49(2)	-6(2)	4(2)	2(2)
C(23)	34(2)	32(2)	56(2)	-4(2)	3(1)	3(1)
C(24)	33(2)	30(2)	51(2)	3(2)	-1(2)	2(1)
C(25)	40(2)	40(2)	45(2)	-3(2)	2(1)	4(2)
C(26)	33(2)	48(2)	56(2)	-1(2)	4(2)	5(2)
C(27)	32(2)	41(2)	64(2)	5(2)	1(2)	-2(2)
C(28)	39(2)	42(2)	54(2)	-6(2)	-4(2)	0(2)
C(29)	34(2)	35(2)	52(2)	-2(2)	2(2)	3(1)
C(30)	36(2)	46(2)	49(2)	-8(2)	-3(2)	-8(2)
C(31)	35(2)	44(2)	43(2)	-7(2)	-2(1)	-3(2)
C(32)	32(2)	52(2)	61(2)	-17(2)	1(2)	-7(2)

C(33)	33(2)	50(2)	60(2)	-11(2)	-1(2)	-7(2)
C(34)	40(2)	36(2)	45(2)	-7(2)	-2(1)	-3(1)
C(35)	33(2)	42(2)	48(2)	1(2)	-6(1)	-2(2)
C(36)	29(2)	45(2)	48(2)	-3(2)	-2(1)	-5(1)
C(37)	33(2)	30(2)	39(2)	-3(1)	-4(1)	3(1)
C(38)	30(2)	31(2)	44(2)	-2(1)	-5(1)	1(1)
C(39)	38(2)	37(2)	41(2)	-2(2)	-6(1)	-2(2)
C(40)	32(2)	38(2)	53(2)	3(2)	1(2)	-3(1)
C(41)	22(2)	31(2)	52(2)	-4(2)	-7(1)	3(1)
C(42)	32(2)	38(2)	45(2)	-3(2)	-6(1)	5(1)
C(43)	33(2)	34(2)	45(2)	0(1)	0(1)	1(1)

Table 5. Bond lengths [Å] and angles [°] for C43 H38 N4 O13

		C(21)-C(22)	1.379(4)
O(1)-C(4)	1.444(3)	C(23)-C(24)	1.511(4)
O(1)-C(1)	1.447(3)	C(24)-C(25)	1.385(4)
O(2)-C(3)	1.351(3)	C(24)-C(29)	1.389(4)
O(2)-C(23)	1.456(3)	C(25)-C(26)	1.394(4)
O(3)-C(37)	1.342(3)	C(26)-C(27)	1.366(4)
O(3)-C(5)	1.464(3)	C(27)-C(28)	1.391(4)
O(4)-C(30)	1.371(3)	C(28)-C(29)	1.385(4)
O(4)-C(9)	1.442(3)	C(30)-C(31)	1.476(4)
O(5)-C(37)	1.200(3)	C(31)-C(32)	1.382(4)
O(6)-C(30)	1.212(3)	C(31)-C(36)	1.385(4)
O(7)-C(10)	1.214(3)	C(32)-C(33)	1.375(4)
O(8)-C(11)	1.223(3)	C(33)-C(34)	1.373(4)
O(9)-C(15)	1.429(3)		
O(9)-C(16)	1.440(3)	C(34)-C(35)	1.373(4)
O(10)-N(3)	1.223(3)	C(35)-C(36)	1.379(4)
O(11)-N(3)	1.222(3)	C(37)-C(38)	1.504(4)
O(12)-N(4)	1.231(3)	C(38)-C(43)	1.379(4)
O(13)-N(4)	1.225(3)	C(38)-C(39)	1.380(4)
N(1)-C(10)	1.381(4)	C(39)-C(40)	1.397(4)
N(1)-C(13)	1.383(3)	C(40)-C(41)	1.359(4)
N(1)-C(1)	1.469(3)	C(41)-C(42)	1.379(4)
N(2)-C(10)	1.397(3)	C(42)-C(43)	1.395(4)
N(2)-C(11)	1.407(3)		
N(2)-C(15)	1.449(4)	C(4)-O(1)-C(1)	110.5(2)
N(3)-C(34)	1.472(4)	C(3)-O(2)-C(23)	114.3(2)
N(4)-C(41)	1.480(4)	C(37)-O(3)-C(5)	116.0(2)
C(1)-C(2)	1.500(4)	C(30)-O(4)-C(9)	115.4(2)
C(2)-C(3)	1.303(4)	C(15)-O(9)-C(16)	111.6(2)
C(3)-C(4)	1.521(4)	C(10)-N(1)-C(13)	121.7(2)
C(4)-C(5)	1.505(4)	C(10)-N(1)-C(1)	116.9(2)
C(4)-C(9)	1.547(4)	C(13)-N(1)-C(1)	121.4(2)
C(5)-C(6)	1.530(4)	C(10)-N(2)-C(11)	125.0(2)
C(6)-C(7)	1.532(4)	C(10)-N(2)-C(15)	116.5(2)
C(7)-C(8)	1.515(4)	C(11)-N(2)-C(15)	118.5(2)
C(8)-C(9)	1.525(4)	O(11)-N(3)-O(10)	122.3(3)
C(11)-C(12)	1.441(4)	O(11)-N(3)-C(34)	119.5(3)
C(12)-C(13)	1.351(4)	O(10)-N(3)-C(34)	118.2(3)
C(12)-C(14)	1.509(4)	O(13)-N(4)-O(12)	124.9(3)
C(16)-C(17)	1.518(4)	O(13)-N(4)-C(41)	117.8(3)
C(17)-C(22)	1.384(4)	O(12)-N(4)-C(41)	117.2(3)
C(17)-C(18)	1.387(4)	O(1)-C(1)-N(1)	109.9(2)
C(18)-C(19)	1.397(4)	O(1)-C(1)-C(2)	104.6(2)
C(19)-C(20)	1.382(5)	N(1)-C(1)-C(2)	112.9(2)
C(20)-C(21)	1.386(5)	C(3)-C(2)-C(1)	109.6(3)

C(2)-C(3)-O(2)	132.6(3)	O(2)-C(23)-C(24)	112.7(2)
C(2)-C(3)-C(4)	111.9(3)	C(25)-C(24)-C(29)	119.2(3)
O(2)-C(3)-C(4)	115.5(2)	C(25)-C(24)-C(23)	120.7(3)
O(1)-C(4)-C(5)	111.4(2)	C(29)-C(24)-C(23)	120.0(3)
O(1)-C(4)-C(3)	102.3(2)	C(24)-C(25)-C(26)	120.2(3)
C(5)-C(4)-C(3)	115.6(2)	C(27)-C(26)-C(25)	119.9(3)
O(1)-C(4)-C(9)	111.1(2)	C(26)-C(27)-C(28)	121.0(3)
C(5)-C(4)-C(9)	104.9(2)	C(29)-C(28)-C(27)	118.9(3)
C(3)-C(4)-C(9)	111.7(2)	C(28)-C(29)-C(24)	120.9(3)
O(3)-C(5)-C(4)	109.4(2)	O(6)-C(30)-O(4)	122.3(3)
O(3)-C(5)-C(6)	108.6(2)	O(6)-C(30)-C(31)	124.3(3)
C(4)-C(5)-C(6)	111.9(2)	O(4)-C(30)-C(31)	113.2(3)
C(5)-C(6)-C(7)	110.1(2)	C(32)-C(31)-C(36)	120.1(3)
C(8)-C(7)-C(6)	111.2(2)	C(32)-C(31)-C(30)	119.3(3)
C(7)-C(8)-C(9)	109.1(2)	C(36)-C(31)-C(30)	120.3(3)
O(4)-C(9)-C(8)	113.7(2)	C(33)-C(32)-C(31)	120.5(3)
O(4)-C(9)-C(4)	107.8(2)	C(34)-C(33)-C(32)	118.2(3)
C(8)-C(9)-C(4)	111.1(2)	C(33)-C(34)-C(35)	122.7(3)
O(7)-C(10)-N(1)	123.3(3)	C(33)-C(34)-N(3)	119.9(3)
O(7)-C(10)-N(2)	121.1(3)	C(35)-C(34)-N(3)	117.4(3)
N(1)-C(10)-N(2)	115.6(2)	C(34)-C(35)-C(36)	118.6(3)
O(8)-C(11)-N(2)	120.1(3)	C(35)-C(36)-C(31)	119.9(3)
O(8)-C(11)-C(12)	124.5(3)	O(5)-C(37)-O(3)	124.7(3)
N(2)-C(11)-C(12)	115.4(3)	O(5)-C(37)-C(38)	123.6(3)
C(13)-C(12)-C(11)	119.6(3)	O(3)-C(37)-C(38)	111.7(2)
C(13)-C(12)-C(14)	122.9(3)	C(43)-C(38)-C(39)	120.4(3)
C(11)-C(12)-C(14)	117.5(3)	C(43)-C(38)-C(37)	118.5(3)
C(12)-C(13)-N(1)	122.3(3)	C(39)-C(38)-C(37)	121.1(3)
O(9)-C(15)-N(2)	106.3(2)	C(38)-C(39)-C(40)	120.0(3)
O(9)-C(16)-C(17)	114.4(2)	C(41)-C(40)-C(39)	118.0(3)
C(22)-C(17)-C(18)	119.6(3)	C(40)-C(41)-C(42)	123.8(3)
C(22)-C(17)-C(16)	119.2(3)	C(40)-C(41)-N(4)	117.9(3)
C(18)-C(17)-C(16)	121.2(3)	C(42)-C(41)-N(4)	118.2(3)
C(17)-C(18)-C(19)	119.3(3)	C(41)-C(42)-C(43)	117.2(3)
C(20)-C(19)-C(18)	120.7(3)	C(38)-C(43)-C(42)	120.5(3)
C(19)-C(20)-C(21)	119.7(3)		
C(22)-C(21)-C(20)	119.7(3)		
C(21)-C(22)-C(17)	121.1(3)		

Table 6. Torsion angles [°] for C43 H38 N4 O13.

		C(2)-C(3)-C(4)-C(5)	-130.2(3)
C(4)-O(1)-C(1)-N(1)	-130.3(2)	O(2)-C(3)-C(4)-C(5)	50.8(3)
C(4)-O(1)-C(1)-C(2)	-8.9(3)	C(2)-C(3)-C(4)-C(9)	110.0(3)
C(10)-N(1)-C(1)-O(1)	-90.2(3)	O(2)-C(3)-C(4)-C(9)	-69.0(3)
C(13)-N(1)-C(1)-O(1)	91.9(3)	C(37)-O(3)-C(5)-C(4)	-141.9(2)
C(10)-N(1)-C(1)-C(2)	153.5(2)	C(37)-O(3)-C(5)-C(6)	95.6(3)
C(13)-N(1)-C(1)-C(2)	-24.5(4)	O(1)-C(4)-C(5)-O(3)	-62.1(3)
O(1)-C(1)-C(2)-C(3)	3.0(3)	C(3)-C(4)-C(5)-O(3)	54.2(3)
N(1)-C(1)-C(2)-C(3)	122.4(3)	C(9)-C(4)-C(5)-O(3)	177.6(2)
C(1)-C(2)-C(3)-O(2)	-177.4(3)	O(1)-C(4)-C(5)-C(6)	58.4(3)
C(1)-C(2)-C(3)-C(4)	3.8(3)	C(3)-C(4)-C(5)-C(6)	174.6(2)
C(23)-O(2)-C(3)-C(2)	10.6(4)	C(9)-C(4)-C(5)-C(6)	-61.9(3)
C(23)-O(2)-C(3)-C(4)	-170.6(2)	O(3)-C(5)-C(6)-C(7)	179.9(2)
C(1)-O(1)-C(4)-C(5)	134.7(2)	C(4)-C(5)-C(6)-C(7)	59.0(3)
C(1)-O(1)-C(4)-C(3)	10.6(3)	C(5)-C(6)-C(7)-C(8)	-53.9(3)
C(1)-O(1)-C(4)-C(9)	-108.7(2)	C(6)-C(7)-C(8)-C(9)	55.3(3)
C(2)-C(3)-C(4)-O(1)	-8.9(3)	C(30)-O(4)-C(9)-C(8)	-81.4(3)
O(2)-C(3)-C(4)-O(1)	172.1(2)	C(30)-O(4)-C(9)-C(4)	154.9(2)

C(7)-C(8)-C(9)-O(4)	176.6(2)	C(25)-C(26)-C(27)-C(28)	-0.1(5)
C(7)-C(8)-C(9)-C(4)	-61.5(3)	C(26)-C(27)-C(28)-C(29)	0.2(5)
O(1)-C(4)-C(9)-O(4)	68.3(3)	C(27)-C(28)-C(29)-C(24)	-0.4(4)
C(5)-C(4)-C(9)-O(4)	-171.2(2)	C(25)-C(24)-C(29)-C(28)	0.6(4)
C(3)-C(4)-C(9)-O(4)	-45.3(3)	C(23)-C(24)-C(29)-C(28)	177.3(3)
O(1)-C(4)-C(9)-C(8)	-57.0(3)	C(9)-O(4)-C(30)-O(6)	14.8(4)
C(5)-C(4)-C(9)-C(8)	63.6(3)	C(9)-O(4)-C(30)-C(31)	-159.9(2)
C(3)-C(4)-C(9)-C(8)	-170.5(2)	O(6)-C(30)-C(31)-C(32)	29.0(5)
C(13)-N(1)-C(10)-O(7)	174.0(3)	O(4)-C(30)-C(31)-C(32)	-156.4(3)
C(1)-N(1)-C(10)-O(7)	-4.0(4)	O(6)-C(30)-C(31)-C(36)	-144.3(3)
C(13)-N(1)-C(10)-N(2)	-5.7(4)	O(4)-C(30)-C(31)-C(36)	30.3(4)
C(1)-N(1)-C(10)-N(2)	176.3(2)	C(36)-C(31)-C(32)-C(33)	0.6(5)
C(11)-N(2)-C(10)-O(7)	-175.1(3)	C(30)-C(31)-C(32)-C(33)	-172.7(3)
C(15)-N(2)-C(10)-O(7)	5.7(4)	C(31)-C(32)-C(33)-C(34)	1.8(5)
C(11)-N(2)-C(10)-N(1)	4.6(4)	C(32)-C(33)-C(34)-C(35)	-2.7(5)
C(15)-N(2)-C(10)-N(1)	-174.6(2)	C(32)-C(33)-C(34)-N(3)	176.7(3)
C(10)-N(2)-C(11)-O(8)	-178.2(3)	O(11)-N(3)-C(34)-C(33)	-173.4(3)
C(15)-N(2)-C(11)-O(8)	1.0(4)	O(10)-N(3)-C(34)-C(33)	7.8(4)
C(10)-N(2)-C(11)-C(12)	0.7(4)	O(11)-N(3)-C(34)-C(35)	6.0(4)
C(15)-N(2)-C(11)-C(12)	179.9(2)	O(10)-N(3)-C(34)-C(35)	-172.8(3)
O(8)-C(11)-C(12)-C(13)	173.6(3)	C(33)-C(34)-C(35)-C(36)	1.0(5)
N(2)-C(11)-C(12)-C(13)	-5.2(4)	N(3)-C(34)-C(35)-C(36)	-178.4(3)
		C(34)-C(35)-C(36)-C(31)	1.5(4)
O(8)-C(11)-C(12)-C(14)	-7.2(4)		
N(2)-C(11)-C(12)-C(14)	174.0(2)	C(32)-C(31)-C(36)-C(35)	-2.3(5)
C(11)-C(12)-C(13)-N(1)	4.3(4)	C(30)-C(31)-C(36)-C(35)	170.9(3)
C(14)-C(12)-C(13)-N(1)	-174.8(3)	C(5)-O(3)-C(37)-O(5)	8.1(4)
C(10)-N(1)-C(13)-C(12)	1.4(4)	C(5)-O(3)-C(37)-C(38)	-170.8(2)
C(1)-N(1)-C(13)-C(12)	179.3(3)	O(5)-C(37)-C(38)-C(43)	-5.2(4)
C(16)-O(9)-C(15)-N(2)	-175.0(2)	O(3)-C(37)-C(38)-C(43)	173.6(3)
C(10)-N(2)-C(15)-O(9)	83.8(3)	O(5)-C(37)-C(38)-C(39)	176.2(3)
C(11)-N(2)-C(15)-O(9)	-95.4(3)	O(3)-C(37)-C(38)-C(39)	-5.0(4)
C(15)-O(9)-C(16)-C(17)	-85.5(3)	C(43)-C(38)-C(39)-C(40)	-1.2(4)
O(9)-C(16)-C(17)-C(22)	-178.9(3)	C(37)-C(38)-C(39)-C(40)	177.4(3)
O(9)-C(16)-C(17)-C(18)	1.9(4)	C(38)-C(39)-C(40)-C(41)	-0.9(4)
C(22)-C(17)-C(18)-C(19)	-1.4(5)	C(39)-C(40)-C(41)-C(42)	2.4(4)
C(16)-C(17)-C(18)-C(19)	177.8(3)	C(39)-C(40)-C(41)-N(4)	-175.8(3)
C(17)-C(18)-C(19)-C(20)	1.2(5)	O(13)-N(4)-C(41)-C(40)	-20.1(4)
C(18)-C(19)-C(20)-C(21)	0.3(5)	O(12)-N(4)-C(41)-C(40)	157.9(3)
C(19)-C(20)-C(21)-C(22)	-1.5(5)	O(13)-N(4)-C(41)-C(42)	161.6(3)
C(20)-C(21)-C(22)-C(17)	1.3(5)	O(12)-N(4)-C(41)-C(42)	-20.4(4)
C(18)-C(17)-C(22)-C(21)	0.2(5)	C(40)-C(41)-C(42)-C(43)	-1.8(4)
C(16)-C(17)-C(22)-C(21)	-179.0(3)	N(4)-C(41)-C(42)-C(43)	176.4(3)
C(3)-O(2)-C(23)-C(24)	64.8(3)	C(39)-C(38)-C(43)-C(42)	1.8(4)
O(2)-C(23)-C(24)-C(25)	-121.0(3)	C(37)-C(38)-C(43)-C(42)	-176.8(3)
O(2)-C(23)-C(24)-C(29)	62.4(4)	C(41)-C(42)-C(43)-C(38)	-0.3(4)
C(29)-C(24)-C(25)-C(26)	-0.5(4)		
C(23)-C(24)-C(25)-C(26)	-177.2(3)		
C(24)-C(25)-C(26)-C(27)	0.3(4)		

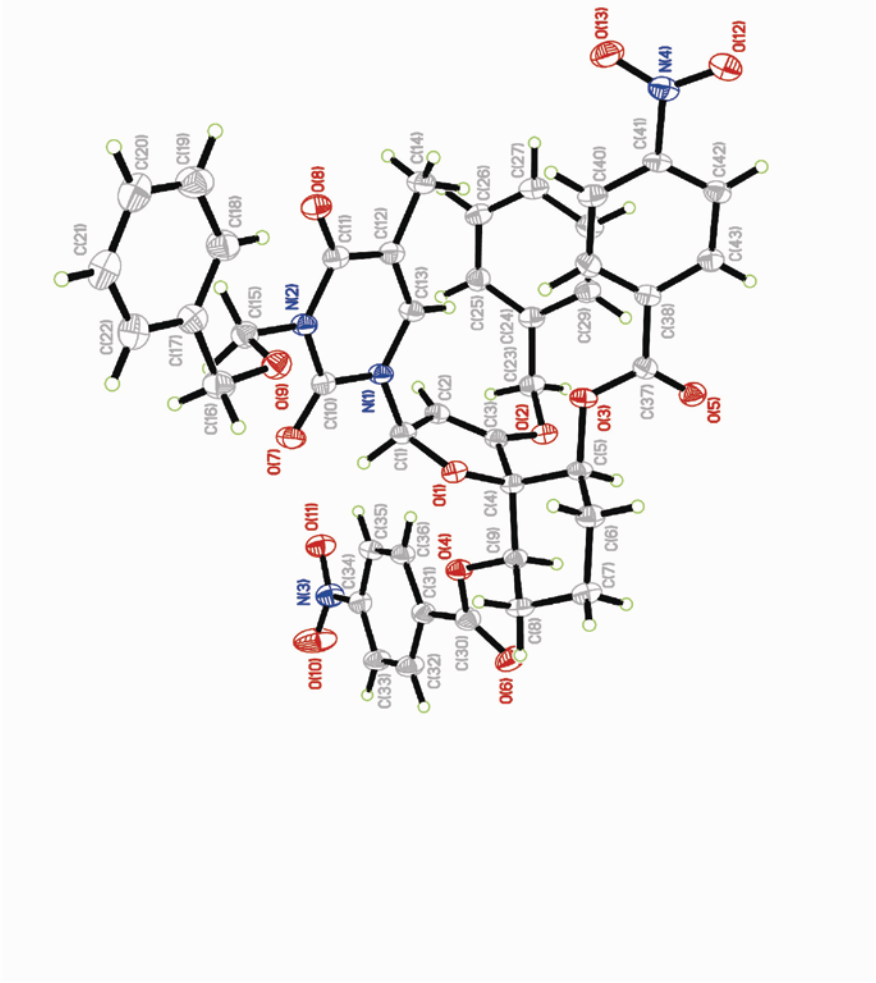

ORTEP view of the C43 H38 N4 O13 compound with the numbering scheme adopted. Ellipsoids drawn at 30% probability level. Hydrogen atoms are represented by sphere of arbitrary size.

REFERENCES

Flack, H.D. (1983). Acta Cryst. A39, 876-881.

Flack, H.D. and Schwarzenbach, D. (1988). Acta Cryst. A44, 499-506.

SAINT (2006) Release 7.34A; Integration Software for Single Crystal Data.
Bruker AXS Inc., Madison, WI 53719-1173.

Sheldrick, G.M. (1996). SADABS, Bruker Area Detector Absorption Corrections.
Bruker AXS Inc., Madison, WI 53719-1173.

Sheldrick, G.M. (2008). Acta Cryst. A64, 112-122.

SHELXTL (2001) version 6.12; Bruker Analytical X-ray Systems Inc.,
Madison, WI 53719-1173.

APEX2 (2009) ; Bruker Molecular Analysis Research Tool.
Bruker AXS Inc., Madison, WI 53719-1173.

Spek, A.L. (2008). PLATON, A Multipurpose Crystallographic Tool,
Utrecht University, Utrecht, The Netherlands.

Maris, T. (2004). UdMX, University of Montréal, Montréal, QC, Canada.

XPREP (2008) Version 2008/2; X-ray data Preparation and Reciprocal space
Exploration Program. Bruker AXS Inc., Madison, WI 53719-1173.

α-L-TriNA 1 nucleoside 1.70

Université de Montréal

CRYSTAL AND MOLECULAR STRUCTURE OF

2(C23 H32 N3 O10) • C4 H8 O2 COMPOUND (bent84)

Equipe Hanessian

Département de chimie, Université de Montréal,

C.P. 6128, Succ. Centre-Ville, Montréal, Québec, H3C 3J7 (Canada)

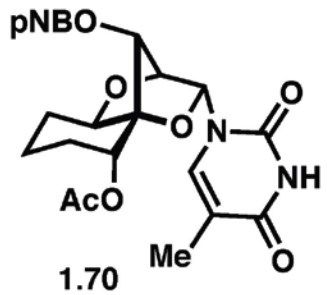

1.70
[X-ray]

As Ethyl Acetate Solvate

Structure solved and refined in the laboratory of X-ray diffraction Université de Montréal by Benoît Deschênes Simard.

Table 1. Crystal data and structure refinement for C50 H54 N6 O22.

Identification code	bent84
Empirical formula with solvent	2(C23 H32 N3 O10) • C4 H8 O2
Empirical formula	2(C23 H32 N3 O10)
Formula weight	1090.99
Temperature	100K
Wavelength	1.54178 Å
Crystal system	Monoclinic
Space group	P21
Unit cell dimensions	a = 14.9960(2) Å α = 90° b = 8.7021(1) Å β = 99.394(1)° c = 19.7522(2) Å γ = 90°
Volume	2543.03(5)Å^3
Z	2
Density (calculated)	1.425 g/cm^3
Absorption coefficient	0.964 mm^{-1}
F(000)	1144
Crystal size	0.10 x 0.05 x 0.04 mm
Theta range for data collection	2.27 to 70.96°
Index ranges	$-18 \le h \le 18$, $-10 \le k \le 10$, $-24 \le \ell \le 24$
Reflections collected	67609
Independent reflections	9524 [R_{int} = 0.032]
Absorption correction	Semi-empirical from equivalents
Max. and min. transmission	0.9622 and 0.8720
Refinement method	Full-matrix least-squares on F^2
Data / restraints / parameters	9524 / 68 / 762
Goodness-of-fit on F^2	0.962
Final R indices [I>2sigma(I)]	R_1 = 0.0332, wR_2 = 0.0871
R indices (all data)	R_1 = 0.0401, wR_2 = 0.0896
Absolute structure parameter	0.09(10)
Largest diff. peak and hole	0.306 and -0.450 e/Å^3

Table 2. Atomic coordinates (x 10^4) and equivalent isotropic displacement parameters ($Å^2$ x 10^3) for C50 H54 N6 O22.

U_{eq} is defined as one third of the trace of the orthogonalized Uij tensor.

	Occ.	x	y	z	U_{eq}
O(11)	1	4212(1)	11478(1)	5937(1)	22(1)
O(12)	1	4167(1)	8307(1)	5606(1)	23(1)
O(13)	1	2354(1)	8793(2)	5702(1)	27(1)
O(14)	1	4279(1)	11645(2)	7284(1)	29(1)
O(15)	1	4727(1)	9904(2)	4087(1)	30(1)
O(16)	1	7671(1)	9085(2)	5000(1)	39(1)
O(17)	1	1302(1)	10546(2)	5878(1)	39(1)
O(18)	1	-539(1)	2939(2)	6077(1)	57(1)
O(19)	1	-1691(1)	4421(2)	5779(1)	51(1)
O(110)	1	3724(1)	13993(2)	6963(1)	38(1)
N(11)	1	5204(1)	10621(2)	5196(1)	21(1)
N(12)	1	6215(1)	9639(2)	4542(1)	26(1)
N(13)	1	-874(1)	4178(3)	5897(1)	39(1)
C(11)	1	4255(1)	10942(2)	5259(1)	22(1)
C(12)	1	3671(1)	9485(2)	5201(1)	22(1)
C(13)	1	2969(1)	10007(2)	5632(1)	25(1)
C(14)	1	3707(1)	10320(2)	6252(1)	22(1)
C(15)	1	3462(1)	10945(2)	6916(1)	26(1)
C(16)	1	3180(1)	9667(2)	7365(1)	31(1)
C(17)	1	3872(1)	8351(2)	7470(1)	31(1)
C(18)	1	3966(1)	7628(2)	6782(1)	27(1)
C(19)	1	4265(1)	8839(2)	6314(1)	23(1)
C(110)	1	5340(1)	10060(2)	4570(1)	23(1)
C(111)	1	6948(1)	9678(2)	5075(1)	28(1)
C(112)	1	6770(1)	10440(2)	5691(1)	27(1)
C(113)	1	5915(1)	10869(2)	5724(1)	25(1)
C(114)	1	7541(1)	10714(3)	6258(1)	41(1)
C(115)	1	1513(1)	9235(2)	5794(1)	28(1)
C(116)	1	896(1)	7883(2)	5784(1)	27(1)
C(117)	1	1220(1)	6381(2)	5801(1)	29(1)
C(118)	1	642(1)	5154(3)	5835(1)	31(1)
C(119)	1	-262(1)	5473(3)	5835(1)	33(1)
C(120)	1	-614(1)	6959(3)	5782(1)	36(1)
C(121)	1	-24(1)	8168(3)	5764(1)	32(1)
C(122)	1	4336(2)	13205(2)	7233(1)	31(1)
C(123)	1	5253(2)	13756(3)	7524(1)	45(1)
O(21)	1	802(1)	7353(1)	9060(1)	24(1)
O(22)	1	844(1)	4196(1)	9394(1)	23(1)
O(23)	1	2668(1)	4678(2)	9315(1)	29(1)
O(24)	1	789(1)	7508(2)	7703(1)	26(1)
O(25)	1	294(1)	5883(2)	10929(1)	31(1)
O(26)	1	-2655(1)	5026(2)	10043(1)	43(1)
O(210)	1	1282(1)	9868(2)	8064(1)	33(1)
N(21)	1	-194(1)	6517(2)	9808(1)	23(1)
N(22)	1	-1196(1)	5565(2)	10481(1)	27(1)
C(21)	1	758(1)	6830(2)	9741(1)	24(1)
C(22)	1	1340(1)	5359(2)	9804(1)	23(1)
C(23)	1	2049(1)	5885(2)	9383(1)	25(1)
C(24)	1	1325(1)	6200(2)	8755(1)	22(1)

C(25)	1	1592(1)	6827(2)	8099(1)	24(1)
C(26)	1	1901(1)	5548(2)	7667(1)	28(1)
C(27)	1	1215(1)	4223(2)	7546(1)	29(1)
C(28)	1	1091(1)	3504(2)	8228(1)	26(1)
C(29)	1	763(1)	4722(2)	8684(1)	22(1)
C(210)	1	-322(1)	5991(2)	10444(1)	25(1)
C(211)	1	-1933(1)	5589(2)	9957(1)	31(1)
C(212)	1	-1754(1)	6319(2)	9326(1)	32(1)
C(213)	1	-900(1)	6723(2)	9285(1)	27(1)
C(214)	1	-2537(2)	6553(3)	8763(1)	47(1)
O(27)	0.87	3705(2)	6416(3)	9110(1)	37(1)
O(28)	0.87	5558(1)	-1271(3)	9027(1)	57(1)
O(29)	0.87	6693(1)	269(3)	9203(1)	62(1)
N(23)	0.87	5886(2)	-4(3)	9134(1)	40(1)
C(215)	0.87	3502(2)	5096(4)	9195(1)	29(1)
C(216)	0.87	4107(2)	3731(3)	9204(1)	30(1)
C(217)	0.87	3773(2)	2240(3)	9134(1)	30(1)
C(218)	0.87	4350(2)	1003(3)	9116(1)	34(1)
C(219)	0.87	5266(2)	1307(3)	9183(1)	35(1)
C(220)	0.87	5626(2)	2783(4)	9284(1)	37(1)
C(221)	0.87	5038(2)	4003(3)	9287(1)	34(1)
O(37)	0.13	3727(15)	6570(20)	9282(3)	37(1)
O(38)	0.13	5881(12)	-653(15)	9103(6)	57(1)
O(39)	0.13	6879(7)	1156(18)	9062(5)	62(1)
N(33)	0.13	6120(8)	710(17)	9106(5)	40(1)
C(315)	0.13	3478(14)	5250(20)	9281(1)	29(1)
C(316)	0.13	4165(12)	4030(20)	9234(4)	30(1)
C(317)	0.13	3917(13)	2520(20)	9231(4)	30(1)
C(318)	0.13	4548(10)	1380(20)	9186(5)	34(1)
C(319)	0.13	5414(9)	1876(16)	9154(5)	35(1)
C(320)	0.13	5660(10)	3433(18)	9166(5)	37(1)
C(321)	0.13	5039(11)	4580(20)	9204(5)	34(1)
C(222)	1	703(1)	9048(2)	7760(1)	29(1)
C(223)	1	-203(2)	9581(3)	7409(1)	42(1)
O(31)	0.87	8729(1)	5775(3)	7304(1)	69(1)
O(32)	0.87	7586(1)	4142(3)	7399(1)	55(1)
C(31)	0.87	7907(2)	5419(4)	7169(2)	56(1)
C(32)	0.87	7157(2)	6341(4)	6754(2)	59(1)
C(33)	0.87	8270(2)	3172(4)	7829(2)	50(1)
C(34)	0.87	7731(2)	2002(5)	8174(2)	71(1)
O(41)	0.13	7712(8)	7271(14)	6559(6)	69(1)
O(42)	0.13	7382(7)	5227(13)	7256(7)	55(1)
C(41)	0.13	7304(9)	6585(15)	6954(7)	56(1)
C(42)	0.13	6467(10)	7400(20)	7093(10)	59(1)
C(43)	0.13	8323(9)	4696(19)	7518(9)	50(1)
C(44)	0.13	8249(18)	3440(30)	8048(12)	71(1)

Table 3. Hydrogen coordinates ($\times 10^4$) and isotropic displacement parameters ($Å^2 \times 10^3$) for C50 H54 N6 O22.

	Occ.	x	y	z	U_{eq}
H(12A)	1	6325	9307	4143	32
H(11)	1	3990	11719	4910	26
H(12B)	1	3417	9174	4721	27
H(13)	1	2652	10968	5449	29
H(15)	1	2970	11728	6815	31
H(16A)	1	2586	9254	7149	37
H(16B)	1	3110	10098	7818	37
H(17A)	1	4466	8753	7694	37
H(17B)	1	3674	7562	7775	37
H(18A)	1	4417	6787	6854	32
H(18B)	1	3380	7187	6567	32
H(19)	1	4914	9098	6479	27
H(113)	1	5796	11363	6129	30
H(11A)	1	7327	11281	6629	61
H(11B)	1	8008	11314	6084	61
H(11C)	1	7795	9726	6433	61
H(117)	1	1841	6198	5790	35
H(118)	1	858	4126	5857	37
H(120)	1	-1243	7134	5758	43
H(121)	1	-243	9194	5738	38
H(12C)	1	5584	14013	7151	67
H(12D)	1	5577	12948	7810	67
H(12E)	1	5205	14672	7805	67
H(22A)	1	-1298	5241	10884	32
H(21)	1	1027	7611	10086	29
H(22B)	1	1585	5042	10285	28
H(23)	1	2363	6845	9570	30
H(25)	1	2078	7618	8209	28
H(26A)	1	2489	5145	7900	33
H(26B)	1	1991	5974	7218	33
H(27A)	1	627	4616	7307	35
H(27B)	1	1432	3434	7251	35
H(28A)	1	644	2659	8147	31
H(28B)	1	1672	3070	8459	31
H(29)	1	117	4976	8506	27
H(213)	1	-780	7174	8871	33
H(21A)	1	-2338	7136	8389	71
H(21B)	1	-3013	7124	8939	71
H(21C)	1	-2772	5552	8589	71
H(21D)	0.87	3141	2067	9098	36
H(21E)	0.87	4126	-18	9060	40
H(220)	0.87	6261	2945	9349	44
H(221)	0.87	5265	5022	9345	41
H(31A)	0.13	3310	2257	9259	36
H(31B)	0.13	4394	317	9177	40
H(32D)	0.13	6270	3701	9148	44
H(32E)	0.13	5186	5643	9210	41
H(22C)	1	-537	10027	7748	62
H(22D)	1	-542	8707	7184	62
H(22E)	1	-125	10359	7065	62
H(32A)	0.87	6595	5747	6696	88
H(32B)	0.87	7315	6571	6302	88

H(32C)	0.87	7075	7304	6993	88
H(33A)	0.87	8656	3804	8177	60
H(33B)	0.87	8660	2646	7542	60
H(34A)	0.87	8146	1258	8431	107
H(34B)	0.87	7307	1462	7824	107
H(34C)	0.87	7394	2534	8490	107
H(42A)	0.13	6585	7870	7551	88
H(42B)	0.13	5969	6668	7071	88
H(42C)	0.13	6303	8209	6748	88
H(43A)	0.13	8695	5560	7733	60
H(43B)	0.13	8607	4283	7137	60
H(44A)	0.13	8309	3896	8507	107
H(44B)	0.13	8731	2679	8040	107
H(44C)	0.13	7660	2928	7938	107

Table 4. Anisotropic parameters ($Å^2$ x 10^3) for C50 H54 N6 O22.

The anisotropic displacement factor exponent takes the form:

$$-2\,\pi^2\,[\,h^2\,a^{*2}\,U_{11} + \ldots + 2\,h\,k\,a^*\,b^*\,U_{12}\,]$$

	U11	U22	U33	U23	U13	U12
O(11)	32(1)	16(1)	23(1)	-1(1)	15(1)	-3(1)
O(12)	30(1)	16(1)	26(1)	-2(1)	12(1)	0(1)
O(13)	25(1)	24(1)	35(1)	0(1)	15(1)	-2(1)
O(14)	42(1)	21(1)	26(1)	-2(1)	15(1)	-6(1)
O(15)	32(1)	34(1)	24(1)	-5(1)	10(1)	-2(1)
O(16)	29(1)	36(1)	55(1)	0(1)	18(1)	3(1)
O(17)	35(1)	35(1)	53(1)	-3(1)	22(1)	5(1)
O(18)	43(1)	47(1)	82(1)	7(1)	16(1)	-14(1)
O(19)	28(1)	71(1)	52(1)	6(1)	2(1)	-17(1)
O(110)	56(1)	22(1)	44(1)	2(1)	27(1)	2(1)
N(11)	26(1)	17(1)	24(1)	-2(1)	13(1)	-3(1)
N(12)	30(1)	22(1)	31(1)	-4(1)	17(1)	-1(1)
N(13)	31(1)	57(1)	32(1)	1(1)	7(1)	-13(1)
C(11)	26(1)	20(1)	23(1)	0(1)	11(1)	0(1)
C(12)	25(1)	19(1)	25(1)	-1(1)	10(1)	-2(1)
C(13)	25(1)	21(1)	31(1)	2(1)	14(1)	0(1)
C(14)	28(1)	17(1)	26(1)	-1(1)	14(1)	0(1)
C(15)	34(1)	20(1)	27(1)	-1(1)	18(1)	-1(1)
C(16)	40(1)	28(1)	29(1)	1(1)	19(1)	-5(1)
C(17)	43(1)	25(1)	28(1)	5(1)	15(1)	-6(1)
C(18)	34(1)	18(1)	31(1)	4(1)	12(1)	-2(1)
C(19)	28(1)	17(1)	25(1)	0(1)	12(1)	1(1)
C(110)	31(1)	17(1)	26(1)	-1(1)	14(1)	-3(1)
C(111)	28(1)	18(1)	39(1)	2(1)	14(1)	-5(1)
C(112)	27(1)	23(1)	32(1)	4(1)	9(1)	-5(1)
C(113)	31(1)	20(1)	25(1)	0(1)	11(1)	-7(1)
C(114)	33(1)	45(1)	44(1)	-1(1)	6(1)	-10(1)
C(115)	26(1)	35(1)	26(1)	1(1)	13(1)	1(1)
C(116)	26(1)	39(1)	19(1)	1(1)	9(1)	-2(1)
C(117)	25(1)	37(1)	28(1)	-4(1)	13(1)	-3(1)
C(118)	31(1)	37(1)	27(1)	-4(1)	10(1)	-6(1)
C(119)	31(1)	44(1)	24(1)	-1(1)	8(1)	-12(1)
C(120)	25(1)	58(1)	27(1)	5(1)	7(1)	-2(1)
C(121)	28(1)	43(1)	26(1)	4(1)	8(1)	1(1)

C(122)	52(1)	24(1)	22(1)	-1(1)	22(1)	-7(1)
C(123)	68(2)	36(1)	29(1)	1(1)	6(1)	-21(1)
O(21)	37(1)	15(1)	24(1)	0(1)	17(1)	1(1)
O(22)	31(1)	15(1)	27(1)	2(1)	14(1)	-1(1)
O(23)	25(1)	29(1)	36(1)	1(1)	14(1)	1(1)
O(24)	37(1)	18(1)	26(1)	0(1)	11(1)	3(1)
O(25)	36(1)	32(1)	27(1)	4(1)	15(1)	2(1)
O(26)	31(1)	44(1)	58(1)	-1(1)	20(1)	-2(1)
O(210)	47(1)	18(1)	38(1)	-2(1)	25(1)	-1(1)
N(21)	30(1)	17(1)	26(1)	0(1)	14(1)	1(1)
N(22)	33(1)	21(1)	31(1)	4(1)	19(1)	1(1)
C(21)	32(1)	19(1)	24(1)	0(1)	15(1)	-2(1)
C(22)	29(1)	20(1)	24(1)	1(1)	12(1)	-2(1)
C(23)	28(1)	22(1)	28(1)	-1(1)	13(1)	-1(1)
C(24)	28(1)	17(1)	25(1)	0(1)	14(1)	0(1)
C(25)	30(1)	19(1)	24(1)	1(1)	13(1)	-2(1)
C(26)	37(1)	23(1)	27(1)	-1(1)	17(1)	2(1)
C(27)	42(1)	19(1)	28(1)	-4(1)	13(1)	2(1)
C(28)	34(1)	16(1)	30(1)	-3(1)	13(1)	-1(1)
C(29)	28(1)	17(1)	24(1)	1(1)	10(1)	-1(1)
C(210)	33(1)	16(1)	28(1)	1(1)	17(1)	3(1)
C(211)	33(1)	22(1)	42(1)	-4(1)	17(1)	7(1)
C(212)	33(1)	31(1)	34(1)	-3(1)	14(1)	9(1)
C(213)	36(1)	22(1)	27(1)	1(1)	12(1)	8(1)
C(214)	33(1)	67(2)	43(1)	-2(1)	10(1)	16(1)
O(27)	37(1)	46(1)	32(1)	-3(1)	16(1)	-12(1)
O(28)	40(1)	56(1)	78(1)	0(1)	17(1)	12(1)
O(29)	26(1)	81(2)	76(2)	-16(1)	1(1)	14(1)
N(23)	28(1)	64(1)	29(1)	-3(1)	6(1)	11(1)
C(215)	27(1)	41(1)	20(1)	-1(1)	11(1)	-6(1)
C(216)	26(1)	46(2)	20(1)	0(1)	11(1)	-1(1)
C(217)	22(1)	43(2)	26(1)	1(1)	7(1)	1(1)
C(218)	29(1)	46(2)	26(1)	3(1)	6(1)	5(1)
C(219)	29(1)	57(1)	21(1)	4(1)	8(1)	9(1)
C(220)	23(1)	66(1)	23(1)	3(1)	6(1)	1(1)
C(221)	28(1)	53(1)	22(1)	0(1)	10(1)	-5(1)
O(37)	37(1)	46(1)	32(1)	-3(1)	16(1)	-12(1)
O(38)	40(1)	56(1)	78(1)	0(1)	17(1)	12(1)
O(39)	26(1)	81(2)	76(2)	-16(1)	1(1)	14(1)
N(33)	28(1)	64(1)	29(1)	-3(1)	6(1)	11(1)
C(315)	27(1)	41(1)	20(1)	-1(1)	11(1)	-6(1)
C(316)	26(1)	46(2)	20(1)	0(1)	11(1)	-1(1)
C(317)	22(1)	43(2)	26(1)	1(1)	7(1)	1(1)
C(318)	29(1)	46(2)	26(1)	3(1)	6(1)	5(1)
C(319)	29(1)	57(1)	21(1)	4(1)	8(1)	9(1)
C(320)	23(1)	66(1)	23(1)	3(1)	6(1)	1(1)
C(321)	28(1)	53(1)	22(1)	0(1)	10(1)	-5(1)
C(222)	46(1)	20(1)	26(1)	3(1)	22(1)	5(1)
C(223)	57(1)	33(1)	36(1)	2(1)	12(1)	15(1)
O(31)	56(1)	87(2)	70(1)	-20(1)	25(1)	-37(1)
O(32)	45(1)	61(1)	60(1)	-9(1)	13(1)	-8(1)
C(31)	62(2)	61(2)	48(2)	-14(2)	16(2)	-18(2)
C(32)	57(2)	64(2)	54(2)	6(2)	6(2)	-16(2)
C(33)	38(1)	59(2)	50(2)	-12(2)	-1(2)	12(2)
C(34)	61(2)	91(3)	60(2)	14(2)	7(2)	12(2)
O(41)	56(1)	87(2)	70(1)	-20(1)	25(1)	-37(1)
O(42)	45(1)	61(1)	60(1)	-9(1)	13(1)	-8(1)
C(41)	62(2)	61(2)	48(2)	-14(2)	16(2)	-18(2)
C(42)	57(2)	64(2)	54(2)	6(2)	6(2)	-16(2)
C(43)	38(1)	59(2)	50(2)	-12(2)	-1(2)	12(2)
C(44)	61(2)	91(3)	60(2)	14(2)	7(2)	12(2)

Table 5. Bond lengths [Å] and angles [°] for C50 H54 N6 O22

O(11)-C(11)	1.429(2)	N(22)-C(211)	1.387(3)
O(11)-C(14)	1.460(2)	C(21)-C(22)	1.542(3)
O(12)-C(12)	1.432(2)	C(22)-C(23)	1.524(2)
O(12)-C(19)	1.457(2)	C(23)-C(24)	1.535(3)
O(13)-C(115)	1.359(2)	C(24)-C(25)	1.517(2)
O(13)-C(13)	1.424(2)	C(24)-C(29)	1.532(2)
O(14)-C(122)	1.365(2)	C(25)-C(26)	1.521(3)
O(14)-C(15)	1.453(2)	C(26)-C(27)	1.538(3)
O(15)-C(110)	1.220(2)	C(27)-C(28)	1.524(3)
O(16)-C(111)	1.231(2)	C(28)-C(29)	1.523(2)
O(17)-C(115)	1.202(3)	C(211)-C(212)	1.461(3)
O(18)-N(13)	1.218(3)	C(212)-C(213)	1.344(3)
O(19)-N(13)	1.227(2)	C(212)-C(214)	1.493(3)
O(110)-C(122)	1.199(3)	O(27)-C(215)	1.206(3)
N(11)-C(110)	1.374(2)	O(28)-N(23)	1.212(3)
N(11)-C(113)	1.383(2)	O(29)-N(23)	1.219(3)
N(11)-C(11)	1.475(2)	N(23)-C(219)	1.484(3)
N(12)-C(110)	1.372(2)	C(215)-C(216)	1.493(4)
N(12)-C(111)	1.392(2)	C(216)-C(217)	1.390(4)
N(13)-C(119)	1.472(3)	C(216)-C(221)	1.399(3)
C(11)-C(12)	1.534(2)	C(217)-C(218)	1.386(3)
C(12)-C(13)	1.527(2)	C(218)-C(219)	1.384(3)
C(13)-C(14)	1.536(3)	C(219)-C(220)	1.394(4)
C(14)-C(15)	1.519(2)	C(220)-C(221)	1.380(4)
C(14)-C(19)	1.531(2)	O(37)-C(315)	1.201(17)
C(15)-C(16)	1.525(3)	O(38)-N(33)	1.239(15)
C(16)-C(17)	1.537(3)	O(39)-N(33)	1.219(14)
C(17)-C(18)	1.525(3)	N(33)-C(319)	1.480(14)
C(18)-C(19)	1.518(2)	C(315)-C(316)	1.495(16)
C(111)-C(112)	1.449(3)	C(316)-C(317)	1.362(16)
C(112)-C(113)	1.346(3)	C(316)-C(321)	1.405(16)
C(112)-C(114)	1.492(3)	C(317)-C(318)	1.389(16)
C(115)-C(116)	1.496(3)	C(318)-C(319)	1.381(15)
C(116)-C(117)	1.393(3)	C(319)-C(320)	1.403(16)
C(116)-C(121)	1.394(3)	C(320)-C(321)	1.376(16)
C(117)-C(118)	1.383(3)	C(222)-C(223)	1.495(3)
C(118)-C(119)	1.383(3)	O(31)-C(31)	1.257(3)
C(119)-C(120)	1.394(3)	O(32)-C(31)	1.321(4)
C(120)-C(121)	1.379(3)	O(32)-C(33)	1.485(4)
C(122)-C(123)	1.481(3)	C(31)-C(32)	1.510(5)
O(21)-C(21)	1.431(2)	C(33)-C(34)	1.529(5)
O(21)-C(24)	1.462(2)	O(41)-C(41)	1.223(8)
O(22)-C(22)	1.427(2)	O(42)-C(41)	1.321(9)
O(22)-C(29)	1.461(2)	O(42)-C(43)	1.494(9)
O(23)-C(315)	1.33(2)	C(41)-C(42)	1.507(10)
O(23)-C(215)	1.360(4)	C(43)-C(44)	1.533(11)
O(23)-C(23)	1.422(2)		
O(24)-C(222)	1.353(2)	C(11)-O(11)-C(14)	106.29(13)
O(24)-C(25)	1.450(2)	C(12)-O(12)-C(19)	105.71(13)
O(25)-C(210)	1.221(2)	C(115)-O(13)-C(13)	115.66(15)
O(26)-C(211)	1.227(2)	C(122)-O(14)-C(15)	116.00(16)
O(210)-C(222)	1.206(2)	C(110)-N(11)-C(113)	121.66(16)
N(21)-C(213)	1.364(2)	C(110)-N(11)-C(11)	115.49(15)
N(21)-C(210)	1.379(2)	C(113)-N(11)-C(11)	122.85(15)
N(21)-C(21)	1.482(2)	C(110)-N(12)-C(111)	127.25(16)
N(22)-C(210)	1.375(2)	O(18)-N(13)-O(19)	124.0(2)
		O(18)-N(13)-C(119)	117.97(18)

O(19)-N(13)-C(119)	118.0(2)	O(21)-C(21)-C(22)	103.22(13)
O(11)-C(11)-N(11)	109.44(14)	N(21)-C(21)-C(22)	112.36(15)
O(11)-C(11)-C(12)	103.12(14)	O(22)-C(22)-C(23)	104.40(14)
N(11)-C(11)-C(12)	112.59(14)	O(22)-C(22)-C(21)	107.93(15)
O(12)-C(12)-C(13)	104.12(14)	C(23)-C(22)-C(21)	98.17(14)
O(12)-C(12)-C(11)	108.18(14)	O(23)-C(23)-C(22)	110.77(15)
C(13)-C(12)-C(11)	98.63(14)	O(23)-C(23)-C(24)	116.27(15)
O(13)-C(13)-C(12)	110.51(15)	C(22)-C(23)-C(24)	91.70(14)
O(13)-C(13)-C(14)	116.62(15)	O(21)-C(24)-C(25)	109.82(14)
C(12)-C(13)-C(14)	91.39(14)	O(21)-C(24)-C(29)	106.86(14)
O(11)-C(14)-C(15)	109.70(14)	C(25)-C(24)-C(29)	116.23(15)
O(11)-C(14)-C(19)	107.47(14)	O(21)-C(24)-C(23)	98.41(13)
C(15)-C(14)-C(19)	116.03(16)	C(25)-C(24)-C(23)	120.23(15)
O(11)-C(14)-C(13)	97.96(14)	C(29)-C(24)-C(23)	103.24(15)
C(15)-C(14)-C(13)	120.50(16)	O(24)-C(25)-C(24)	107.25(14)
C(19)-C(14)-C(13)	103.16(15)	O(24)-C(25)-C(26)	107.31(15)
O(14)-C(15)-C(14)	106.21(14)	C(24)-C(25)-C(26)	111.32(15)
O(14)-C(15)-C(16)	107.81(15)	C(25)-C(26)-C(27)	112.22(16)
C(14)-C(15)-C(16)	111.77(15)	C(28)-C(27)-C(26)	110.26(16)
C(15)-C(16)-C(17)	112.09(16)	C(29)-C(28)-C(27)	109.57(15)
C(18)-C(17)-C(16)	110.23(16)	O(22)-C(29)-C(28)	111.43(15)
C(19)-C(18)-C(17)	109.64(15)	O(22)-C(29)-C(24)	102.58(14)
O(12)-C(19)-C(18)	111.73(14)	C(28)-C(29)-C(24)	114.38(15)
O(12)-C(19)-C(14)	102.87(14)	O(25)-C(210)-N(22)	122.82(17)
C(18)-C(19)-C(14)	114.91(15)	O(25)-C(210)-N(21)	122.73(18)
O(15)-C(110)-N(12)	122.84(17)	N(22)-C(210)-N(21)	114.43(17)
O(15)-C(110)-N(11)	122.63(17)	O(26)-C(211)-N(22)	120.32(19)
N(12)-C(110)-N(11)	114.49(16)	O(26)-C(211)-C(212)	125.5(2)
O(16)-C(111)-N(12)	120.04(18)	N(22)-C(211)-C(212)	114.18(18)
O(16)-C(111)-C(112)	125.47(19)	C(213)-C(212)-C(211)	118.30(19)
N(12)-C(111)-C(112)	114.49(17)	C(213)-C(212)-C(214)	124.1(2)
C(113)-C(112)-C(111)	118.40(18)	C(211)-C(212)-C(214)	117.64(19)
C(113)-C(112)-C(114)	123.15(19)	C(212)-C(213)-N(21)	123.26(18)
C(111)-C(112)-C(114)	118.45(18)	O(28)-N(23)-O(29)	124.3(3)
C(112)-C(113)-N(11)	122.89(18)	O(28)-N(23)-C(219)	118.1(2)
O(17)-C(115)-O(13)	123.92(19)	O(29)-N(23)-C(219)	117.6(3)
O(17)-C(115)-C(116)	124.89(18)	O(27)-C(215)-O(23)	122.6(3)
O(13)-C(115)-C(116)	111.18(17)	O(27)-C(215)-C(216)	126.4(3)
C(117)-C(116)-C(121)	120.45(19)	O(23)-C(215)-C(216)	111.0(2)
C(117)-C(116)-C(115)	121.70(17)	C(217)-C(216)-C(221)	120.5(3)
C(121)-C(116)-C(115)	117.85(19)	C(217)-C(216)-C(215)	122.2(2)
C(118)-C(117)-C(116)	120.44(18)	C(221)-C(216)-C(215)	117.3(3)
C(119)-C(118)-C(117)	117.8(2)	C(218)-C(217)-C(216)	120.7(2)
C(118)-C(119)-C(120)	123.0(2)	C(219)-C(218)-C(217)	117.6(3)
C(118)-C(119)-N(13)	118.1(2)	C(218)-C(219)-C(220)	123.0(2)
C(120)-C(119)-N(13)	118.88(19)	C(218)-C(219)-N(23)	117.9(3)
C(121)-C(120)-C(119)	118.23(19)	C(220)-C(219)-N(23)	119.1(2)
C(120)-C(121)-C(116)	119.9(2)	C(221)-C(220)-C(219)	118.5(2)
O(110)-C(122)-O(14)	123.3(2)	C(220)-C(221)-C(216)	119.6(3)
O(110)-C(122)-C(123)	125.6(2)	O(39)-N(33)-O(38)	125.3(14)
O(14)-C(122)-C(123)	111.05(19)	O(39)-N(33)-C(319)	118.1(13)
C(21)-O(21)-C(24)	106.18(13)	O(38)-N(33)-C(319)	116.6(13)
C(22)-O(22)-C(29)	106.04(13)	O(37)-C(315)-O(23)	130.2(18)
C(315)-O(23)-C(215)	9.5(6)	O(37)-C(315)-C(316)	117.4(19)
C(315)-O(23)-C(23)	110.1(8)	O(23)-C(315)-C(316)	112.4(15)
C(215)-O(23)-C(23)	116.87(18)	C(317)-C(316)-C(321)	125.7(15)
C(222)-O(24)-C(25)	116.23(15)	C(317)-C(316)-C(315)	119.7(15)
C(213)-N(21)-C(210)	121.86(16)	C(321)-C(316)-C(315)	114.6(15)
C(213)-N(21)-C(21)	123.17(15)	C(316)-C(317)-C(318)	120.3(16)
C(210)-N(21)-C(21)	114.96(15)	C(319)-C(318)-C(317)	115.6(15)
C(210)-N(22)-C(211)	127.28(17)	C(318)-C(319)-C(320)	123.3(12)
O(21)-C(21)-N(21)	109.58(14)	C(318)-C(319)-N(33)	118.3(13)

C(320)-C(319)-N(33)	118.3(12)	O(32)-C(31)-C(32)	110.7(3)
C(321)-C(320)-C(319)	121.6(14)	O(32)-C(33)-C(34)	105.5(2)
C(320)-C(321)-C(316)	113.5(15)	C(41)-O(42)-C(43)	116.2(1)
O(210)-C(222)-O(24)	123.83(19)	O(41)-C(41)-O(42)	135.1(12)
O(210)-C(222)-C(223)	124.99(19)	O(41)-C(41)-C(42)	113.8(1)
O(24)-C(222)-C(223)	111.17(18)	O(42)-C(41)-C(42)	110.9(1)
C(31)-O(32)-C(33)	114.8(2)	O(42)-C(43)-C(44)	106.7(11)
O(31)-C(31)-O(32)	122.3(3)		
O(31)-C(31)-C(32)	127.0(3)		

Table 6. Torsion angles [°] for C50 H54 N6 O22.

		C(13)-C(14)-C(19)-O(12)	30.29(17)
C(14)-O(11)-C(11)-N(11)	-115.31(15)	O(11)-C(14)-C(19)-C(18)	165.78(14)
C(14)-O(11)-C(11)-C(12)	4.73(17)	C(15)-C(14)-C(19)-C(18)	42.6(2)
C(110)-N(11)-C(11)-O(11)	178.56(14)	C(13)-C(14)-C(19)-C(18)	-91.36(18)
C(113)-N(11)-C(11)-O(11)	-1.7(2)	C(111)-N(12)-C(110)-O(15)	-175.59(18)
C(110)-N(11)-C(11)-C(12)	64.5(2)	C(111)-N(12)-C(110)-N(11)	2.1(3)
C(113)-N(11)-C(11)-C(12)	-115.78(18)	C(113)-N(11)-C(110)-O(15)	-176.35(17)
C(19)-O(12)-C(12)-C(13)	-39.17(16)	C(11)-N(11)-C(110)-O(15)	3.4(3)
C(19)-O(12)-C(12)-C(11)	65.04(16)	C(113)-N(11)-C(110)-N(12)	5.9(2)
O(11)-C(11)-C(12)-O(12)	-73.56(16)	C(11)-N(11)-C(110)-N(12)	-174.35(14)
N(11)-C(11)-C(12)-O(12)	44.29(19)	C(110)-N(12)-C(111)-O(16)	170.87(18)
O(11)-C(11)-C(12)-C(13)	34.47(17)	C(110)-N(12)-C(111)-C(112)	-8.7(3)
N(11)-C(11)-C(12)-C(13)	152.33(15)		
C(115)-O(13)-C(13)-C(12)	-152.20(16)	O(16)-C(111)-C(112)-C(113)	-172.1(2)
C(115)-O(13)-C(13)-C(14)	105.30(18)	N(12)-C(111)-C(112)-C(113)	7.4(3)
O(12)-C(12)-C(13)-O(13)	-64.88(18)	O(16)-C(111)-C(112)-C(114)	7.9(3)
C(11)-C(12)-C(13)-O(13)	-176.20(15)	N(12)-C(111)-C(112)-C(114)	-172.5(2)
O(12)-C(12)-C(13)-C(14)	54.30(15)	C(111)-C(112)-C(113)-N(11)	-0.4(3)
C(11)-C(12)-C(13)-C(14)	-57.02(15)	C(114)-C(112)-C(113)-N(11)	179.57(18)
C(11)-O(11)-C(14)-C(15)	-168.40(15)	C(110)-N(11)-C(113)-C(112)	-6.9(3)
C(11)-O(11)-C(14)-C(19)	64.63(17)	C(11)-N(11)-C(113)-C(112)	173.40(17)
C(11)-O(11)-C(14)-C(13)	-41.93(16)	C(13)-O(13)-C(115)-O(17)	-6.9(3)
O(13)-C(13)-C(14)-O(11)	174.25(14)	C(13)-O(13)-C(115)-C(116)	173.75(15)
C(12)-C(13)-C(14)-O(11)	60.41(14)	O(17)-C(115)-C(116)-C(117)	-168.9(2)
O(13)-C(13)-C(14)-C(15)	-67.2(2)	O(13)-C(115)-C(116)-C(117)	10.5(3)
C(12)-C(13)-C(14)-C(15)	178.93(16)	O(17)-C(115)-C(116)-C(121)	10.5(3)
O(13)-C(13)-C(14)-C(19)	64.13(18)	O(13)-C(115)-C(116)-C(121)	-170.1(2)
C(12)-C(13)-C(14)-C(19)	-49.71(15)	C(121)-C(116)-C(117)-C(118)	-3.4(3)
C(122)-O(14)-C(15)-C(14)	99.46(17)	C(115)-C(116)-C(117)-C(118)	176.0(2)
C(122)-O(14)-C(15)-C(16)	-140.60(16)	C(116)-C(117)-C(118)-C(119)	1.4(3)
O(11)-C(14)-C(15)-O(14)	-46.38(19)	C(117)-C(118)-C(119)-C(120)	2.0(3)
C(19)-C(14)-C(15)-O(14)	75.61(19)	C(117)-C(118)-C(119)-N(13)	-177.7(2)
C(13)-C(14)-C(15)-O(14)	-158.82(15)	O(18)-N(13)-C(119)-C(118)	14.0(3)
O(11)-C(14)-C(15)-C(16)	-163.71(15)	O(19)-N(13)-C(119)-C(118)	-167.70(19)
C(19)-C(14)-C(15)-C(16)	-41.7(2)	O(18)-N(13)-C(119)-C(120)	-165.8(2)
C(13)-C(14)-C(15)-C(16)	83.9(2)	O(19)-N(13)-C(119)-C(120)	12.6(3)
O(14)-C(15)-C(16)-C(17)	-65.49(19)	C(118)-C(119)-C(120)-C(121)	-3.4(3)
C(14)-C(15)-C(16)-C(17)	50.9(2)	N(13)-C(119)-C(120)-C(121)	176.30(18)
C(15)-C(16)-C(17)-C(18)	-60.9(2)	C(119)-C(120)-C(121)-C(116)	1.3(3)
C(16)-C(17)-C(18)-C(19)	59.0(2)	C(117)-C(116)-C(121)-C(120)	2.0(3)
C(12)-O(12)-C(19)-C(18)	128.76(15)	C(115)-C(116)-C(121)-C(120)	-177.4(2)
C(12)-O(12)-C(19)-C(14)	4.96(16)	C(15)-O(14)-C(122)-O(110)	7.4(3)
C(17)-C(18)-C(19)-O(12)	-166.89(15)	C(15)-O(14)-C(122)-C(123)	-170.19(15)
C(17)-C(18)-C(19)-C(14)	-50.2(2)	C(24)-O(21)-C(21)-N(21)	-116.75(15)
O(11)-C(14)-C(19)-O(12)	-72.57(16)	C(24)-O(21)-C(21)-C(22)	3.14(17)
C(15)-C(14)-C(19)-O(12)	164.26(15)	C(213)-N(21)-C(21)-O(21)	-0.3(2)

```
C(210)-N(21)-C(21)-O(21) 179.54(14)
C(213)-N(21)-C(21)-C(22) -114.43(19)
C(210)-N(21)-C(21)-C(22)  65.4(2)
C(29)-O(22)-C(22)-C(23)  -38.30(17)
C(29)-O(22)-C(22)-C(21)  65.43(16)
O(21)-C(21)-C(22)-O(22)  -72.50(16)
N(21)-C(21)-C(22)-O(22)  45.46(18)
O(21)-C(21)-C(22)-C(23)  35.59(17)
N(21)-C(21)-C(22)-C(23)  153.55(14)
C(315)-O(23)-C(23)-C(22) -148.19(17)
C(215)-O(23)-C(23)-C(22) -155.53(16)
C(315)-O(23)-C(23)-C(24) 108.95(19)
C(215)-O(23)-C(23)-C(24) 101.61(19)
O(22)-C(22)-C(23)-O(23)  -65.32(18)
C(21)-C(22)-C(23)-O(23) -176.29(14)
O(22)-C(22)-C(23)-C(24)  53.68(15)
C(21)-C(22)-C(23)-C(24)  -57.29(15)
C(21)-O(21)-C(24)-C(25) -166.95(15)
C(21)-O(21)-C(24)-C(29)  66.17(17)
C(21)-O(21)-C(24)-C(23)  -40.49(16)
O(23)-C(23)-C(24)-O(21)  174.34(14)
C(22)-C(23)-C(24)-O(21)  60.13(14)
O(23)-C(23)-C(24)-C(25)  -66.8(2)
C(22)-C(23)-C(24)-C(25)  179.00(16)
O(23)-C(23)-C(24)-C(29)  64.72(18)
C(22)-C(23)-C(24)-C(29)  -49.50(15)
C(222)-O(24)-C(25)-C(24) 97.53(18)
C(222)-O(24)-C(25)-C(26) -142.77(16)
O(21)-C(24)-C(25)-O(24)  -47.12(19)
C(29)-C(24)-C(25)-O(24)  74.29(18)
C(23)-C(24)-C(25)-O(24) -160.07(15)
O(21)-C(24)-C(25)-C(26) -164.22(15)
C(29)-C(24)-C(25)-C(26)  -42.8(2)
C(23)-C(24)-C(25)-C(26)  82.8(2)
O(24)-C(25)-C(26)-C(27)  -65.65(19)
C(24)-C(25)-C(26)-C(27)  51.4(2)
C(25)-C(26)-C(27)-C(28)  -61.1(2)
C(26)-C(27)-C(28)-C(29)  58.9(2)
C(22)-O(22)-C(29)-C(28)  127.12(16)
C(22)-O(22)-C(29)-C(24)  4.31(17)
C(27)-C(28)-C(29)-O(22) -166.13(15)
C(27)-C(28)-C(29)-C(24)  -50.4(2)
O(21)-C(24)-C(29)-O(22)  -72.70(16)
C(25)-C(24)-C(29)-O(22)  164.32(14)
C(23)-C(24)-C(29)-O(22)  30.49(16)
O(21)-C(24)-C(29)-C(28)  166.50(14)
C(25)-C(24)-C(29)-C(28)  43.5(2)
C(23)-C(24)-C(29)-C(28)  -90.31(18)
C(211)-N(22)-C(210)-O(25) -177.43(18)
C(211)-N(22)-C(210)-N(21)  1.1(3)
C(213)-N(21)-C(210)-O(25) -175.74(17)
C(21)-N(21)-C(210)-O(25)  4.4(3)
C(213)-N(21)-C(210)-N(22)  5.8(2)
C(21)-N(21)-C(210)-N(22) -174.07(15)
C(210)-N(22)-C(211)-O(26) 172.35(18)
C(210)-N(22)-C(211)-C(212) -7.5(3)
O(26)-C(211)-C(212)-C(213) -172.4(2)
N(22)-C(211)-C(212)-C(213) 7.5(3)
O(26)-C(211)-C(212)-C(214) 6.9(3)
N(22)-C(211)-C(212)-C(214) -173.3(2)
C(211)-C(212)-C(213)-N(21) -1.6(3)
C(214)-C(212)-C(213)-N(21) 179.2(2)
C(210)-N(21)-C(213)-C(212) -5.6(3)
C(21)-N(21)-C(213)-C(212) 174.25(18)
C(315)-O(23)-C(215)-O(27) -50(4)
C(23)-O(23)-C(215)-O(27)  -4.1(3)
C(315)-O(23)-C(215)-C(216) 128(4)
C(23)-O(23)-C(215)-C(216) 174.37(16)
O(27)-C(215)-C(216)-C(217) -163.7(2)
O(23)-C(215)-C(216)-C(217) 18.0(3)
O(27)-C(215)-C(216)-C(221) 16.4(4)
O(23)-C(215)-C(216)-C(221) -162.0(2)
C(221)-C(216)-C(217)-C(218) -2.7(4)
C(215)-C(216)-C(217)-C(218) 177.3(2)
C(216)-C(217)-C(218)-C(219) 1.2(4)
C(217)-C(218)-C(219)-C(220) 1.7(4)
C(217)-C(218)-C(219)-N(23) -177.3(2)
O(28)-N(23)-C(219)-C(218)  1.1(3)
O(29)-N(23)-C(219)-C(218) -179.0(2)
O(28)-N(23)-C(219)-C(220) -178.0(2)
O(29)-N(23)-C(219)-C(220)  1.9(3)
C(218)-C(219)-C(220)-C(221) -2.9(4)
N(23)-C(219)-C(220)-C(221) 176.1(2)
C(219)-C(220)-C(221)-C(216) 1.3(3)
C(217)-C(216)-C(221)-C(220) 1.4(4)
C(215)-C(216)-C(221)-C(220) -178.6(2)
C(215)-O(23)-C(315)-O(37)  134(4)
C(23)-O(23)-C(315)-O(37)  -2.10(13)
C(215)-O(23)-C(315)-C(316) -45(4)
C(23)-O(23)-C(315)-C(316) 177.9(4)
O(37)-C(315)-C(316)-C(317) 180.0(6)
O(23)-C(315)-C(316)-C(317) 0.0(8)
O(37)-C(315)-C(316)-C(321) 0.7(8)
O(23)-C(315)-C(316)-C(321) -179.4(5)
C(321)-C(316)-C(317)-C(318) -0.9(13)
C(315)-C(316)-C(317)-C(318) 179.8(6)
C(316)-C(317)-C(318)-C(319) 0.7(12)
C(317)-C(318)-C(319)-C(320) 0.1(12)
C(317)-C(318)-C(319)-N(33) 179.9(7)
O(39)-N(33)-C(319)-C(318) 178.3(8)
O(38)-N(33)-C(319)-C(318) -0.5(11)
O(39)-N(33)-C(319)-C(320) -2(11)
O(38)-N(33)-C(319)-C(320) 179.3(8)
C(318)-C(319)-C(320)-C(321) -0.8(12)
N(33)-C(319)-C(320)-C(321) 179.5(7)
C(319)-C(320)-C(321)-C(316) 0.5(11)
C(317)-C(316)-C(321)-C(320) 0.3(12)
C(315)-C(316)-C(321)-C(320) 179.6(6)
C(25)-O(24)-C(222)-O(210)  6.8(3)
C(25)-O(24)-C(222)-C(223) -172.05(15)
C(33)-O(32)-C(31)-O(31)  0.2(4)
C(33)-O(32)-C(31)-C(32) -178.5(2)
C(31)-O(32)-C(33)-C(34)  166.6(3)
C(43)-O(42)-C(41)-O(41)  40(3)
C(43)-O(42)-C(41)-C(42) -145.8(15)
C(41)-O(42)-C(43)-C(44)  160.7(17)
```

Table 7. Bond lengths [Å] and angles [°] related to the hydrogen bonding for C50 H54 N6 O22.

D-H	..A	d(D-H)	d(H..A)	d(D..A)	<DHA
N(12)-H(12A)	O(110)#1	0.88	2.19	3.041(2)	162.4
N(22)-H(22A)	O(210)#2	0.88	2.1	2.959(2)	165.4

Symmetry transformations used to generate equivalent atoms:

#1 -x+1,y-1/2,-z+1 #2 -x,y-1/2,-z+2

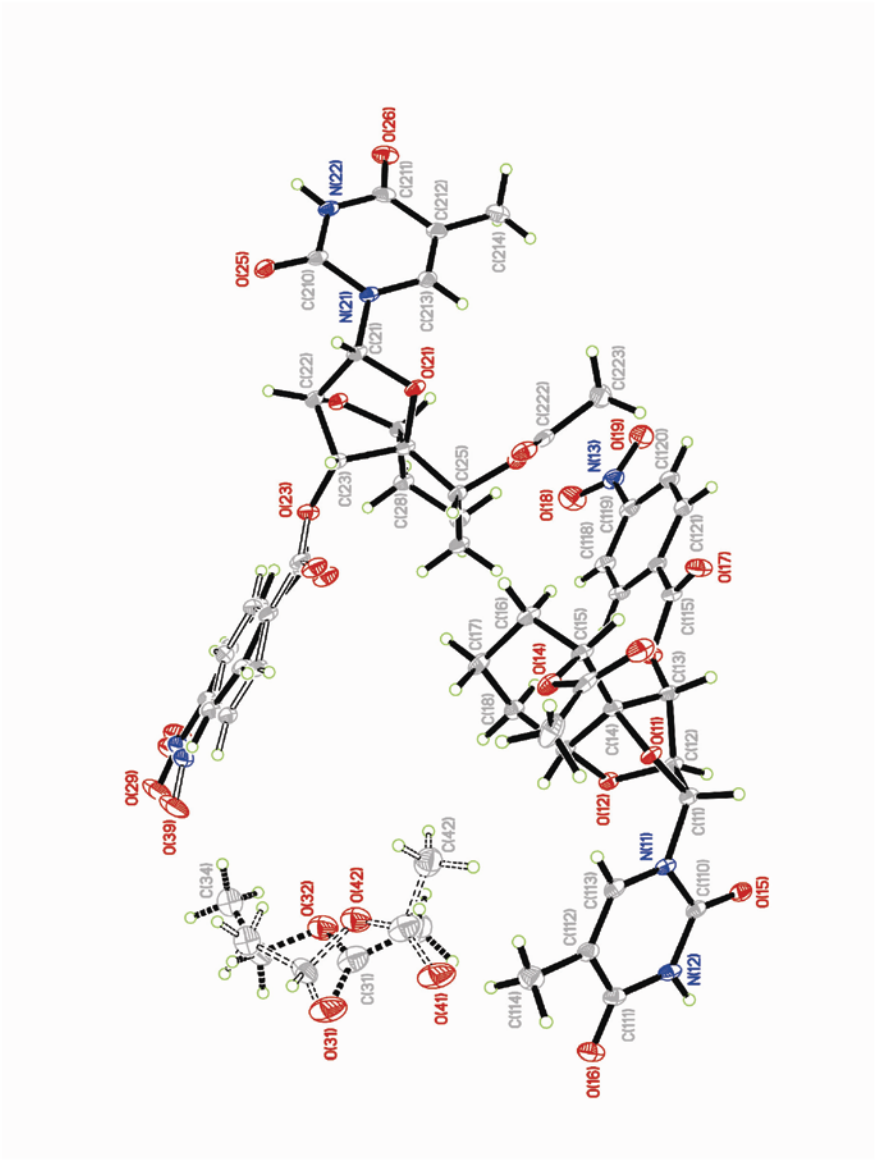

ORTEP view of the C50 H54 N6 O22 compound with the numbering scheme adopted. Ellipsoids drawn at 30% probability level. Hydrogen atoms are represented by sphere of arbitrary size.

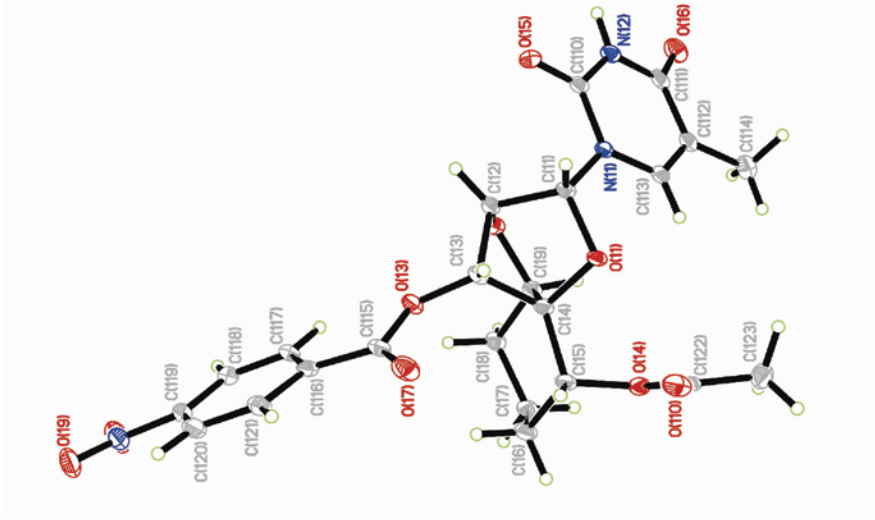

ORTEP view of molecule #1 (C23 H32 N3 O10) in the C50 H54 N6 O22 crystal structure with the numbering scheme adopted. Ellipsoids drawn at 30% probability level. Hydrogen atoms are represented by sphere of arbitrary size.

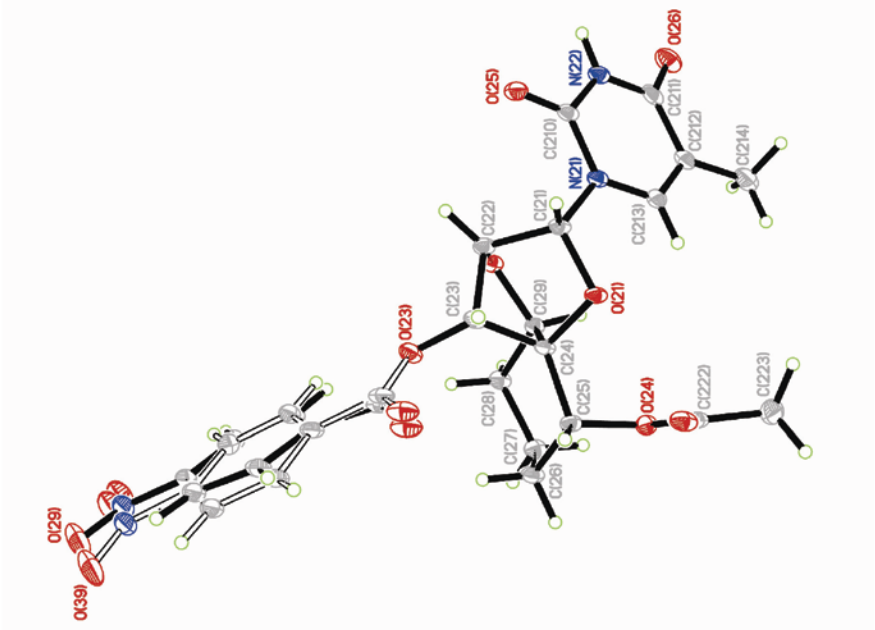

ORTEP view of molecule #2(C23 H32 N3 O10) in the C50 H54 N6 O22 crystal structure with the numbering scheme adopted. Ellipsoids drawn at 30% probability level. Hydrogen atoms are represented by sphere of arbitrary size.

REFERENCES

Flack, H.D. (1983). Acta Cryst. A39, 876-881.

Flack, H.D. and Schwarzenbach, D. (1988). Acta Cryst. A44, 499-506.

SAINT (2006) Release 7.34A; Integration Software for Single Crystal Data.
Bruker AXS Inc., Madison, WI 53719-1173.

Sheldrick, G.M. (1996). SADABS, Bruker Area Detector Absorption Corrections.
Bruker AXS Inc., Madison, WI 53719-1173.

Sheldrick, G.M. (2008). Acta Cryst. A64, 112-122.

SHELXTL (2001) version 6.12; Bruker Analytical X-ray Systems Inc.,
Madison, WI 53719-1173.

APEX2 (2009) ; Bruker Molecular Analysis Research Tool.
Bruker AXS Inc., Madison, WI 53719-1173.

Spek, A.L. (2008). PLATON, A Multipurpose Crystallographic Tool,
Utrecht University, Utrecht, The Netherlands.

Maris, T. (2004). UdMX, University of Montréal, Montréal, QC, Canada.

XPREP (2008) Version 2008/2; X-ray data Preparation and Reciprocal space

Exploration Program. Bruker AXS Inc., Madison, WI 53719-1173.

TriNA 1 nucleoside 1.109

Université de Montréal

oleole

CRYSTAL AND MOLECULAR STRUCTURE OF

C40 H35 N3 O10 COMPOUND (BEN102)

Equipe Hanessian

Département de chimie, Université de Montréal,

C.P. 6128, Succ. Centre-Ville, Montréal, Québec, H3C 3J7 (Canada)

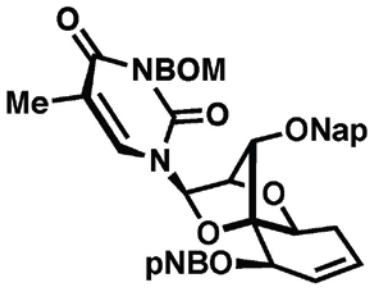

1.109
[X-ray]

Structure solved and refined in the laboratory of X-ray diffraction at the Université de Montréal by Benoît Deschênes Simard.

Table 1. Crystal data and structure refinement for C40 H35 N3 O10.

Identification code	BEN102
Empirical formula	$C_{40}H_{35}N_3O_{10}$
Formula weight	717.71
Temperature/K	100.15
Crystal system	monoclinic
Space group	$P2_1$
a/Å	14.2003(3)
b/Å	7.6452(2)
c/Å	17.2049(4)
α/°	90
β/°	113.4900(10)
γ/°	90
Volume/Å^3	1713.05(7)
Z	2
ρ_{calc}g/cm^3	1.391
μ/mm^{-1}	0.838
F(000)	752.0
Crystal size/mm^3	0.11 × 0.04 × 0.02
Radiation	CuKα (λ = 1.54178)
2Θ range for data collection/°	5.6 to 141.364
Index ranges	-17 ≤ h ≤ 15, -9 ≤ k ≤ 9, -20 ≤ l ≤ 21
Reflections collected	10927
Independent reflections	6032 [R_{int} = 0.0289, R_{sigma} = 0.0611]
Data/restraints/parameters	6032/342/541
Goodness-of-fit on F^2	0.978
Final R indexes [I>=2σ (I)]	R_1 = 0.0555, wR_2 = 0.1380
Final R indexes [all data]	R_1 = 0.0693, wR_2 = 0.1435
Largest diff. peak/hole / e Å^{-3}	0.50/-0.29
Flack parameter	0.15(14)

Table 2. Fractional atomic coordinates ($\times 10^4$) and equivalent isotropic displacement parameters ($Å^2 \times 10^3$) for C40 H35 N3 O10.

U_{eq} is defined as one third of the trace of the orthogonalized Uij tensor.

Atom	x	y	z	U(eq)
O1	8066(3)	-960(18)	9556(2)	27.6(8)
O2	9726(3)	1020(18)	10569(2)	30.0(8)
O3	8069(3)	3456(18)	10265(2)	28.0(8)
O4	6206(3)	512(18)	9688(2)	30.5(8)
O5	5216(3)	-1434(18)	9986(3)	42.3(10)
O6	1059(4)	2684(19)	6899(3)	72.6(16)
O7	2089(3)	4155(18)	6522(3)	49.7(11)
N1	8201(3)	65(18)	8295(2)	27.3(9)
N3	1919(4)	3014(19)	6953(3)	43.3(12)
C1	8747(4)	-220(19)	9216(3)	26.6(11)
C2	9074(4)	1501(18)	9717(3)	27.7(11)
C3	8057(4)	2017(18)	9756(3)	24.5(10)
C4	8006(4)	283(18)	10180(3)	26.3(10)
C5	7103(4)	-159(19)	10381(3)	29.5(11)
C6	7209(4)	621(19)	11221(3)	34.8(12)
C7	8082(5)	1169(19)	11808(3)	37.9(13)
C8	9088(4)	1194(19)	11717(3)	33.3(12)
C9	9048(4)	220(18)	10928(3)	29.5(11)
C26	5301(4)	-247(19)	9554(3)	30.8(12)
C27	4437(4)	527(19)	8838(3)	29.7(11)
C28	3445(4)	86(19)	8727(3)	32.4(12)
C29	2609(4)	868(19)	8097(3)	35.3(12)
C30	2807(5)	2100(19)	7582(3)	36.9(13)
C31	3764(4)	2516(19)	7653(3)	36.7(13)
C32	4587(4)	1750(19)	8291(3)	30.9(11)
O8A	9775(4)	276(19)	8238(4)	35.2(13)
O9A	6915(5)	1220(20)	5827(3)	46.2(17)
O10A	9023(5)	-1239(19)	6218(4)	42.9(14)
N2A	8331(4)	498(19)	6993(3)	30.1(12)
C10A	8839(5)	276(19)	7874(4)	31.1(15)
C11A	7276(6)	800(20)	6573(4)	32.4(18)
C12A	6660(5)	470(20)	7068(4)	29.1(17)
C13A	7146(5)	70(30)	7882(6)	28.1(13)
C14A	5521(6)	590(20)	6612(4)	34.9(19)
C15A	8178(6)	5120(20)	9900(4)	27.7(11)
C16A	7334(5)	5400(20)	9038(4)	31.7(11)
C17A	7536(5)	5240(20)	8316(4)	39.4(13)
C18A	6747(5)	5450(20)	7507(4)	46.0(14)
C19A	6940(7)	5240(20)	6780(4)	64(2)
C20A	6130(7)	5340(20)	5985(4)	62(2)
C21A	5138(8)	5740(20)	5909(5)	63(2)
C22A	4937(6)	5970(20)	6627(4)	61.7(19)
C23A	5749(5)	5820(20)	7431(4)	45.0(15)
C24A	5554(5)	6060(20)	8161(4)	46.5(16)
C25A	6337(5)	5810(20)	8961(4)	38.4(14)
C33A	8962(5)	480(20)	6487(4)	40.1(16)
C34A	8126(5)	-1790(20)	5504(4)	46.6(19)
C35A	8277(3)	-3479(18)	5140(3)	38.9(17)
C36A	7443(3)	-4152(19)	4460(3)	50(2)
C37A	7540(4)	-5714(19)	4086(3)	52(2)
C38A	8471(4)	-6604(18)	4391(3)	54(2)
C39A	9305(3)	-5931(19)	5071(4)	53.3(19)
C40A	9208(3)	-4368(19)	5446(3)	45.5(19)
O8B	9678(14)	860(40)	8184(18)	35.2(13)

O9B	6650(30)	1530(60)	5863(15)	46.2(17)
O10B	8633(17)	330(30)	5865(12)	42.9(14)
N2B	8171(16)	1140(30)	6996(11)	30.1(12)
C10B	8743(16)	700(40)	7845(13)	31.1(15)
C11B	7093(17)	1130(60)	6615(16)	32.4(18)
C12B	6580(16)	700(70)	7178(18)	29.1(17)
C13B	7135(15)	100(110)	7950(20)	28.1(13)
C14B	5430(20)	660(80)	6810(30)	34.9(19)
C15B	8143(19)	5121(5)	9883(13)	27.7(11)
C16B	7295(15)	5343.9(2)	9020(12)	31.7(11)
C17B	7522(16)	5336(8)	8302(14)	39.4(13)
C18B	6742(15)	5542(9)	7493(13)	46.0(14)
C19B	6980(20)	5533(16)	6778(15)	64(2)
C20B	6190(30)	5740(18)	5977(14)	62(2)
C21B	5170(30)	5956(16)	5884(15)	63(2)
C22B	4936(18)	5966(15)	6596(16)	61.7(19)
C23B	5725(14)	5758(10)	7401(14)	45.0(15)
C24B	5500(17)	5765(14)	8122(16)	46.5(16)
C25B	6278(17)	5560(11)	8929(16)	38.4(14)
C33B	8720(20)	1640(40)	6462(15)	40.1(16)
C34B	9160(30)	-1250(40)	6210(20)	46.6(19)
C35B	8853(16)	-2820(30)	5660(12)	38.9(17)
C36B	7826(15)	-3110(40)	5143(16)	50(2)
C37B	7537(16)	-4600(40)	4640(16)	52(2)
C38B	8280(20)	-5800(30)	4653(16)	54(2)
C39B	9300(20)	-5520(40)	5170(20)	53.3(19)
C40B	9592(14)	-4030(40)	5673(18)	45.5(19)

Table 3. Hydrogen atom coordinates ($\times 10^4$) and isotropic displacement parameters ($Å^2 \times 10^3$) for C40 H35 N3 O10.

U_{eq} is defined as one third of the trace of the orthogonalized Uij tensor.

Atom	x	y	z	U(eq)
H1	9355	-998	9336	32
H2	9371	2395	9455	33
H3	7495	2115	9177	29
H5	7046	-1459	10406	35
H6	6607	720	11332	42
H7	8073	1578	12326	45
H8A	9621	654	12225	40
H8B	9291	2424	11688	40
H9	9254	-1027	11077	35
H28	3338	-762	9087	39
H29	1926	578	8019	42
H31	3865	3317	7271	44
H32	5265	2055	8362	37
H13A	6749	-231	8195	34
H14A	5193	182	6984	52
H14B	5295	-138	6102	52
H14C	5327	1810	6452	52
H15A	8850	5153	9851	33
H15B	8167	6083	10281	33
H17A	8213	4978	8368	47
H19A	7620	5036	6825	77
H20A	6254	5135	5489	74
H21A	4599	5846	5364	76
H22A	4261	6230	6578	74

H24A	4887	6389	8111	56
H25A	6195	5920	9453	46
H33A	8649	1257	5988	48
H33B	9660	926	6833	48
H34A	7939	-877	5060	56
H34B	7546	-1912	5682	56
H36A	6807	-3544	4251	59
H37A	6970	-6174	3621	62
H38A	8537	-7672	4135	65
H39A	9941	-6539	5280	64
H40A	9778	-3908	5911	55
H13B	6787	-321	8283	34
H14D	5194	136	7222	52
H14E	5180	-37	6290	52
H14F	5165	1856	6683	52
H15C	8814	5189	9835	33
H15D	8112	6086	10256	33
H17B	8212	5190	8363	47
H19B	7668	5387	6837	77
H20B	6346	5735	5489	74
H21B	4644	6096	5335	76
H22B	4246	6112	6535	74
H24B	4810	5911	8062	56
H25B	6117	5566	9414	46
H33C	8435	2747	6165	48
H33D	9456	1833	6825	48
H34C	9078	-1507	6739	56
H34D	9905	-1048	6359	56
H36B	7320	-2286	5135	59
H37B	6835	-4793	4287	62
H38B	8080	-6821	4309	65
H39B	9809	-6341	5178	64
H40B	10294	-3834	6026	55

Table 4. Anisotropic displacement parameters ($Å^2$ x 10^3) for C40 H35 N3 O10.

The anisotropic displacement factor exponent takes the form:

$$-2\pi^2[h^2a^{*2}U_{11} + \ldots + 2hka^*b^*U_{12}]$$

Atom	U_{11}	U_{22}	U_{33}	U_{23}	U_{13}	U_{12}
O1	38(2)	15.1(15)	30.5(19)	-3.1(14)	14.5(17)	-0.3(14)
O2	32.4(19)	25.8(17)	27.8(17)	-1.0(14)	7.9(16)	-1.5(15)
O3	39(2)	15.4(15)	29.0(18)	0.2(14)	13.2(17)	-1.2(14)
O4	34.0(18)	22.6(16)	33.8(18)	3.7(15)	12.2(16)	1.1(15)
O5	48(2)	32.2(19)	48(2)	13.7(18)	20(2)	-2.8(18)
O6	34(3)	73(3)	90(4)	30(3)	3(3)	0(2)
O7	62(3)	46(2)	40(2)	12(2)	19(2)	15(2)
N1	37(2)	21(2)	26(2)	-2.1(17)	14(2)	0.2(17)
N3	39(3)	43(3)	41(3)	6(2)	8(2)	0(2)
C1	35(3)	21(2)	24(2)	-1.0(19)	11(2)	0.6(19)
C2	35(3)	18(2)	28(3)	0.5(19)	12(2)	-2(2)
C3	33(3)	13(2)	24(2)	0.1(18)	8(2)	-4.1(19)
C4	39(3)	13(2)	24(2)	-2.8(19)	10(2)	-1(2)
C5	39(3)	18(2)	29(3)	2(2)	11(2)	1(2)
C6	44(3)	28(3)	36(3)	2(2)	20(3)	-1(2)
C7	55(4)	27(3)	33(3)	-2(2)	19(3)	-5(2)
C8	39(3)	29(3)	26(3)	-1(2)	8(2)	-3(2)
C9	39(3)	19(2)	31(3)	7(2)	15(2)	0(2)
C26	41(3)	19(2)	37(3)	-3(2)	19(3)	-2(2)
C27	37(3)	20(2)	31(3)	-3(2)	12(2)	-2(2)

C28	42(3)	18(2)	39(3)	0(2)	17(3)	-5(2)
C29	35(3)	31(3)	37(3)	-4(2)	11(2)	-7(2)
C30	41(3)	27(3)	37(3)	-2(2)	9(3)	0(2)
C31	47(3)	26(3)	37(3)	5(2)	17(3)	5(2)
C32	34(3)	26(2)	34(3)	-3(2)	15(2)	-2(2)
O8A	38(2)	30(3)	36(2)	4(3)	13(2)	1(2)
O9A	53(4)	55(4)	28(2)	5(2)	14(2)	4(3)
O10A	46(3)	52(3)	33(3)	-7(2)	18(2)	-2(2)
N2A	35(3)	28(3)	25(2)	-1(2)	10(2)	-4(3)
C10A	40(3)	23(4)	31(3)	4(3)	15(3)	3(3)
C11A	51(4)	21(4)	29(3)	-3(3)	20(3)	0(3)
C12A	38(3)	23(4)	28(3)	-13(3)	14(2)	2(3)
C13A	41(3)	18(2)	26(3)	-3(3)	15(2)	1(2)
C14A	44(4)	40(3)	24(4)	-5(4)	16(3)	1(3)
C15A	38(3)	13(2)	31(3)	-0.5(19)	12(2)	-4.8(19)
C16A	39(3)	13(2)	37(3)	2(2)	8(2)	-7(2)
C17A	47(3)	22(3)	43(3)	5(2)	12(3)	-4(2)
C18A	61(4)	27(3)	44(3)	7(3)	14(3)	-6(3)
C19A	94(6)	36(4)	57(4)	7(4)	23(4)	-9(4)
C20A	81(5)	47(5)	42(4)	5(4)	8(4)	-10(5)
C21A	79(5)	47(4)	43(4)	13(3)	2(4)	-6(4)
C22A	78(5)	29(3)	59(4)	5(3)	7(4)	-7(3)
C23A	60(4)	15(2)	45(3)	7(2)	6(3)	-8(2)
C24A	39(3)	23(3)	68(4)	-5(3)	11(3)	-3(3)
C25A	48(3)	17(3)	44(3)	2(3)	11(3)	-1(2)
C33A	39(4)	49(4)	32(3)	1(4)	15(3)	-11(4)
C34A	43(4)	53(5)	36(4)	-4(3)	8(4)	-1(4)
C35A	49(5)	41(4)	29(3)	2(3)	18(4)	-2(3)
C36A	44(4)	55(5)	45(4)	10(4)	13(4)	-3(4)
C37A	60(5)	39(4)	46(5)	-5(3)	10(4)	-14(4)
C38A	78(6)	37(4)	51(5)	-3(4)	28(4)	-5(4)
C39A	67(5)	47(5)	47(4)	1(4)	23(4)	12(4)
C40A	37(4)	63(5)	31(4)	3(4)	7(4)	1(4)
O8B	38(2)	30(3)	36(2)	4(3)	13(2)	1(2)
O9B	53(4)	55(4)	28(2)	5(2)	14(2)	4(3)
O10B	46(3)	52(3)	33(3)	-7(2)	18(2)	-2(2)
N2B	35(3)	28(3)	25(2)	-1(2)	10(2)	-4(3)
C10B	40(3)	23(4)	31(3)	4(3)	15(3)	3(3)
C11B	51(4)	21(4)	29(3)	-3(3)	20(3)	0(3)
C12B	38(3)	23(4)	28(3)	-13(3)	14(2)	2(3)
C13B	41(3)	18(2)	26(3)	-3(3)	15(2)	1(2)
C14B	44(4)	40(3)	24(4)	-5(4)	16(3)	1(3)
C15B	38(3)	13(2)	31(3)	-0.5(19)	12(2)	-4.8(19)
C16B	39(3)	13(2)	37(3)	2(2)	8(2)	-7(2)
C17B	47(3)	22(3)	43(3)	5(2)	12(3)	-4(2)
C18B	61(4)	27(3)	44(3)	7(3)	14(3)	-6(3)
C19B	94(6)	36(4)	57(4)	7(4)	23(4)	-9(4)
C20B	81(5)	47(5)	42(4)	5(4)	8(4)	-10(5)
C21B	79(5)	47(4)	43(4)	13(3)	2(4)	-6(4)
C22B	78(5)	29(3)	59(4)	5(3)	7(4)	-7(3)
C23B	60(4)	15(2)	45(3)	7(2)	6(3)	-8(2)
C24B	39(3)	23(3)	68(4)	-5(3)	11(3)	-3(3)
C25B	48(3)	17(3)	44(3)	2(3)	11(3)	-1(2)
C33B	39(4)	49(4)	32(3)	1(4)	15(3)	-11(4)
C34B	43(4)	53(5)	36(4)	-4(3)	8(4)	-1(4)
C35B	49(5)	41(4)	29(3)	2(3)	18(4)	-2(3)
C36B	44(4)	55(5)	45(4)	10(4)	13(4)	-3(4)
C37B	60(5)	39(4)	46(5)	-5(3)	10(4)	-14(4)
C38B	78(6)	37(4)	51(5)	-3(4)	28(4)	-5(4)
C39B	67(5)	47(5)	47(4)	1(4)	23(4)	12(4)
C40B	37(4)	63(5)	31(4)	3(4)	7(4)	1(4)

Table 5. Bond lengths [Å] for C40 H35 N3 O10.

Atom	Atom	Length/Å	Atom	Atom	Length/Å
O1	C1	1.432(6)	C16A	C25A	1.403(5)
O1	C4	1.461(5)	C17A	C18A	1.405(4)
O2	C2	1.436(6)	C18A	C19A	1.393(4)
O2	C9	1.468(6)	C18A	C23A	1.400(4)
O3	C3	1.403(5)	C19A	C20A	1.395(5)
O3	C15A	1.456(5)	C20A	C21A	1.395(5)
O3	C15B	1.455(8)	C21A	C22A	1.386(5)
O4	C5	1.448(6)	C22A	C23A	1.409(4)
O4	C26	1.344(6)	C23A	C24A	1.401(4)
O5	C26	1.209(6)	C24A	C25A	1.395(5)
O6	N3	1.213(6)	C34A	C35A	1.487(8)
O7	N3	1.229(6)	C35A	C36A	1.3900
N1	C1	1.476(6)	C35A	C40A	1.3900
N1	C10A	1.377(7)	C36A	C37A	1.3900
N1	C13A	1.378(8)	C37A	C38A	1.3900
N1	C10B	1.378(19)	C38A	C39A	1.3900
N1	C13B	1.39(2)	C39A	C40A	1.3900
N3	C30	1.469(7)	O8B	C10B	1.22(2)
C1	C2	1.540(6)	O9B	C11B	1.23(2)
C2	C3	1.525(7)	O10B	C33B	1.40(2)
C3	C4	1.529(6)	O10B	C34B	1.42(2)
C4	C5	1.494(7)	N2B	C10B	1.400(19)
C4	C9	1.526(7)	N2B	C11B	1.40(2)
C5	C6	1.515(7)	N2B	C33B	1.476(19)
C6	C7	1.317(7)	C11B	C12B	1.46(2)
C7	C8	1.499(8)	C12B	C13B	1.33(2)
C8	C9	1.530(7)	C12B	C14B	1.50(3)
C26	C27	1.473(7)	C15B	C16B	1.503(10)
C27	C28	1.385(7)	C16B	C17B	1.395(5)
C27	C32	1.402(7)	C16B	C25B	1.398(5)
C28	C29	1.385(7)	C17B	C18B	1.401(5)
C29	C30	1.397(7)	C18B	C19B	1.398(5)
C30	C31	1.353(8)	C18B	C23B	1.399(5)
C31	C32	1.375(7)	C19B	C20B	1.396(5)
O8A	C10A	1.223(7)	C20B	C21B	1.396(5)
O9A	C11A	1.221(7)	C21B	C22B	1.394(5)
O10A	C33A	1.410(9)	C22B	C23B	1.400(5)
O10A	C34A	1.436(9)	C23B	C24B	1.399(5)
N2A	C10A	1.406(7)	C24B	C25B	1.397(5)
N2A	C11A	1.399(8)	C34B	C35B	1.483(19)
N2A	C33A	1.478(8)	C35B	C36B	1.3900
C11A	C12A	1.466(8)	C35B	C40B	1.3900
C12A	C13A	1.327(8)	C36B	C37B	1.3900
C12A	C14A	1.493(8)	C37B	C38B	1.3900
C15A	C16A	1.504(7)	C38B	C39B	1.3900
C16A	C17A	1.389(4)	C39B	C40B	1.3900

Table 6. Bond angles [Å] for C40 H35 N3 O10.

Atom	Atom	Atom	Angle/°	Atom	Atom	Atom	Angle/°
C1	O1	C4	106.8(3)	C17A	C16A	C25A	119.7(5)
C2	O2	C9	105.8(3)	C25A	C16A	C15A	120.2(4)
C3	O3	C15A	113.1(4)	C16A	C17A	C18A	120.5(5)
C3	O3	C15B	112.8(11)	C19A	C18A	C17A	120.7(4)
C26	O4	C5	117.2(4)	C19A	C18A	C23A	119.6(4)
C10A	N1	C1	114.1(4)	C23A	C18A	C17A	119.6(4)
C10A	N1	C13A	122.5(5)	C18A	C19A	C20A	119.6(6)
C13A	N1	C1	123.4(5)	C21A	C20A	C19A	120.7(6)
C10B	N1	C1	118.8(10)	C22A	C21A	C20A	120.3(6)
C10B	N1	C13B	120.7(15)	C21A	C22A	C23A	119.0(6)
C13B	N1	C1	118.6(14)	C18A	C23A	C22A	120.7(4)
O6	N3	O7	122.3(5)	C18A	C23A	C24A	119.8(4)
O6	N3	C30	119.9(5)	C24A	C23A	C22A	119.5(5)
O7	N3	C30	117.7(5)	C25A	C24A	C23A	120.1(5)
O1	C1	N1	110.2(4)	C24A	C25A	C16A	120.1(5)
O1	C1	C2	102.2(4)	O10A	C33A	N2A	109.4(5)
N1	C1	C2	112.8(4)	O10A	C34A	C35A	112.7(6)
O2	C2	C1	106.3(3)	C36A	C35A	C34A	117.3(4)
O2	C2	C3	105.0(4)	C36A	C35A	C40A	120.0
C3	C2	C1	99.5(4)	C40A	C35A	C34A	122.7(4)
O3	C3	C2	117.0(4)	C35A	C36A	C37A	120.0
O3	C3	C4	111.9(4)	C38A	C37A	C36A	120.0
C2	C3	C4	91.2(4)	C37A	C38A	C39A	120.0
O1	C4	C3	100.7(3)	C40A	C39A	C38A	120.0
O1	C4	C5	109.2(4)	C39A	C40A	C35A	120.0
O1	C4	C9	106.1(4)	C33B	O10B	C34B	115(2)
C5	C4	C3	121.0(4)	C10B	N2B	C11B	123.9(15)
C5	C4	C9	115.6(4)	C10B	N2B	C33B	118.8(16)
C9	C4	C3	102.5(4)	C11B	N2B	C33B	117.3(15)
O4	C5	C4	106.5(4)	N1	C10B	N2B	116.6(14)
O4	C5	C6	111.5(4)	O8B	C10B	N1	120.7(19)
C4	C5	C6	111.3(4)	O8B	C10B	N2B	122.7(19)
C7	C6	C5	124.2(5)	O9B	C11B	N2B	120(2)
C6	C7	C8	124.7(5)	O9B	C11B	C12B	125(2)
C7	C8	C9	112.8(4)	N2B	C11B	C12B	115.3(15)
O2	C9	C4	102.2(3)	C11B	C12B	C14B	118(2)
O2	C9	C8	111.8(4)	C13B	C12B	C11B	119.2(18)
C4	C9	C8	114.4(4)	C13B	C12B	C14B	122(3)
O4	C26	C27	113.1(4)	C12B	C13B	N1	123.2(18)
O5	C26	O4	122.8(5)	O3	C15B	C16B	111.8(9)
O5	C26	C27	124.2(5)	C17B	C16B	C15B	119.8(8)
C28	C27	C26	118.7(4)	C17B	C16B	C25B	119.5(11)
C28	C27	C32	119.2(5)	C25B	C16B	C15B	120.6(9)
C32	C27	C26	122.0(5)	C16B	C17B	C18B	120.7(9)
C29	C28	C27	120.7(5)	C19B	C18B	C17B	120.2(7)
C28	C29	C30	117.5(5)	C19B	C18B	C23B	120.0(6)
C29	C30	N3	117.2(5)	C23B	C18B	C17B	119.8(7)
C31	C30	N3	119.4(5)	C20B	C19B	C18B	119.3(8)
C31	C30	C29	123.3(5)	C21B	C20B	C19B	120.8(10)
C30	C31	C32	118.4(5)	C22B	C21B	C20B	120.1(10)
C31	C32	C27	120.8(5)	C21B	C22B	C23B	119.3(8)
C33A	O10A	C34A	113.9(6)	C18B	C23B	C22B	120.5(7)
C10A	N2A	C33A	117.7(5)	C24B	C23B	C18B	119.4(9)
C11A	N2A	C10A	124.1(5)	C24B	C23B	C22B	120.1(8)
C11A	N2A	C33A	118.2(5)	C25B	C24B	C23B	120.8(13)
N1	C10A	N2A	114.8(5)	C24B	C25B	C16B	119.8(13)
O8A	C10A	N1	122.7(6)	O10B	C33B	N2B	110.8(15)

O8A	C10A	N2A	122.5(6)	O10B	C34B	C35B	117(2)
O9A	C11A	N2A	120.0(6)	C36B	C35B	C34B	120.3(11)
O9A	C11A	C12A	124.0(6)	C36B	C35B	C40B	120.0
N2A	C11A	C12A	115.9(5)	C40B	C35B	C34B	119.7(11)
C11A	C12A	C14A	117.2(5)	C37B	C36B	C35B	120.0
C13A	C12A	C11A	118.2(6)	C36B	C37B	C38B	120.0
C13A	C12A	C14A	124.6(6)	C39B	C38B	C37B	120.0
C12A	C13A	N1	123.1(6)	C40B	C39B	C38B	120.0
O3	C15A	C16A	111.8(4)	C39B	C40B	C35B	120.0
C17A	C16A	C15A	120.0(4)				

Table 7. Torsion angles [°] for C40 H35 N3 O10.

A	B	C	D	Angle/°	A	B	C	D	Angle/°
O1	C1	C2	O2	70.5(4)	C14A	C12A	C13A	N1	-176.0(11)
O1	C1	C2	C3	-38.3(4)	C15A	O3	C3	C2	73.2(6)
O1	C4	C5	O4	-78.6(4)	C15A	O3	C3	C4	176.6(5)
O1	C4	C5	C6	159.6(4)	C15A	C16A	C17A	C18A	178.1(5)
O1	C4	C9	O2	69.1(4)	C15A	C16A	C25A	C24A	-179.5(5)
O1	C4	C9	C8	-169.9(4)	C16A	C17A	C18A	C19A	-178.6(7)
O2	C2	C3	O3	62.5(5)	C16A	C17A	C18A	C23A	-0.1(10)
O2	C2	C3	C4	-53.0(4)	C17A	C16A	C25A	C24A	-0.4(8)
O3	C3	C4	O1	-176.7(4)	C17A	C18A	C19A	C20A	175.7(7)
O3	C3	C4	C5	63.0(6)	C17A	C18A	C23A	C22A	-177.5(6)
O3	C3	C4	C9	-67.4(5)	C17A	C18A	C23A	C24A	2.5(10)
O3	C15A	C16A	C17A	-105.6(6)	C18A	C19A	C20A	C21A	3.6(12)
O3	C15A	C16A	C25A	73.5(7)	C18A	C23A	C24A	C25A	-3.9(10)
O3	C15B	C16B	C17B	-111.5(15)	C19A	C18A	C23A	C22A	1.0(10)
O3	C15B	C16B	C25B	68.5(15)	C19A	C18A	C23A	C24A	-178.9(7)
O4	C5	C6	C7	-137.0(5)	C19A	C20A	C21A	C22A	-2.5(13)
O4	C26	C27	C28	-168.5(4)	C20A	C21A	C22A	C23A	0.7(12)
O4	C26	C27	C32	8.5(6)	C21A	C22A	C23A	C18A	0.0(11)
O5	C26	C27	C28	11.0(8)	C21A	C22A	C23A	C24A	-180.0(7)
O5	C26	C27	C32	-172.0(5)	C22A	C23A	C24A	C25A	176.1(6)
O6	N3	C30	C29	0.0(8)	C23A	C18A	C19A	C20A	-2.8(11)
O6	N3	C30	C31	-178.1(6)	C23A	C24A	C25A	C16A	2.9(9)
O7	N3	C30	C29	176.9(5)	C25A	C16A	C17A	C18A	-1.0(9)
O7	N3	C30	C31	-1.2(8)	C33A	O10A	C34A	C35A	170.0(5)
N1	C1	C2	O2	-171.1(4)	C33A	N2A	C10A	N1	-171.6(5)
N1	C1	C2	C3	80.1(5)	C33A	N2A	C10A	O8A	8.6(8)
N3	C30	C31	C32	174.7(5)	C33A	N2A	C11A	O9A	-7.9(9)
C1	O1	C4	C3	36.1(4)	C33A	N2A	C11A	C12A	168.7(6)
C1	O1	C4	C5	164.5(4)	C34A	O10A	C33A	N2A	78.8(7)
C1	O1	C4	C9	-70.3(4)	C34A	C35A	C36A	C37A	179.2(5)
C1	N1	C10A	O8A	-2.0(8)	C34A	C35A	C40A	C39A	-179.1(5)
C1	N1	C10A	N2A	178.2(4)	C35A	C36A	C37A	C38A	0.0
C1	N1	C13A	C12A	174.3(10)	C36A	C35A	C40A	C39A	0.0
C1	N1	C10B	O8B	7(3)	C36A	C37A	C38A	C39A	0.0
C1	N1	C10B	N2B	-172.8(12)	C37A	C38A	C39A	C40A	0.0
C1	N1	C13B	C12B	166(5)	C38A	C39A	C40A	C35A	0.0
C1	C2	C3	O3	172.3(4)	C40A	C35A	C36A	C37A	0.0
C1	C2	C3	C4	56.9(4)	O9B	C11B	C12B	C13B	173(6)
C2	O2	C9	C4	1.6(4)	O9B	C11B	C12B	C14B	3(7)
C2	O2	C9	C8	-121.1(4)	O10B	C34B	C35B	C36B	-38(3)
C2	C3	C4	O1	-56.8(4)	O10B	C34B	C35B	C40B	143(3)
C2	C3	C4	C5	-177.0(4)	N2B	C11B	C12B	C13B	-10(7)
C2	C3	C4	C9	52.5(4)	N2B	C11B	C12B	C14B	-180(4)
C3	O3	C15A	C16A	57.8(6)	C10B	N1	C1	O1	-177.1(16)
C3	O3	C15B	C16B	56.0(15)	C10B	N1	C1	C2	69.4(16)
C3	C4	C5	O4	37.3(5)	C10B	N1	C13B	C12B	1(10)

C3	C4	C5	C6	-84.4(5)	C10B	N2B	C11B	O9B	-180(3)
C3	C4	C9	O2	-36.1(4)	C10B	N2B	C11B	C12B	2(5)
C3	C4	C9	C8	84.8(5)	C10B	N2B	C33B	O10B	109(2)
C4	O1	C1	N1	-118.8(4)	C11B	N2B	C10B	N1	7(3)
C4	O1	C1	C2	1.3(4)	C11B	N2B	C10B	O8B	-173(3)
C4	C5	C6	C7	-18.2(7)	C11B	N2B	C33B	O10B	-71(3)
C5	O4	C26	O5	0.4(7)	C11B	C12B	C13B	N1	8(10)
C5	O4	C26	C27	179.9(4)	C13B	N1	C1	O1	18(4)
C5	C4	C9	O2	-169.8(4)	C13B	N1	C1	C2	-95(4)
C5	C4	C9	C8	-48.8(5)	C13B	N1	C10B	O8B	171(4)
C5	C6	C7	C8	3.4(8)	C13B	N1	C10B	N2B	-9(5)
C6	C7	C8	C9	-10.0(7)	C14B	C12B	C13B	N1	178(5)
C7	C8	C9	O2	147.0(4)	C15B	O3	C3	C2	75.1(12)
C7	C8	C9	C4	31.5(6)	C15B	O3	C3	C4	178.5(11)
C9	O2	C2	C1	-71.0(4)	C15B	C16B	C17B	C18B	180.00(4)
C9	O2	C2	C3	33.8(4)	C15B	C16B	C25B	C24B	180.00(5)
C9	C4	C5	O4	161.8(4)	C16B	C17B	C18B	C19B	180.00(5)
C9	C4	C5	C6	40.1(5)	C16B	C17B	C18B	C23B	0.00(9)
C26	O4	C5	C4	155.9(4)	C17B	C16B	C25B	C24B	0.00(9)
C26	O4	C5	C6	-82.4(5)	C17B	C18B	C19B	C20B	180.00(7)
C26	C27	C28	C29	175.7(5)	C17B	C18B	C23B	C22B	180.00(7)
C26	C27	C32	C31	-176.8(5)	C17B	C18B	C23B	C24B	0.00(11)
C27	C28	C29	C30	0.3(8)	C18B	C19B	C20B	C21B	0.00(12)
C28	C27	C32	C31	0.2(7)	C18B	C23B	C24B	C25B	0.00(12)
C28	C29	C30	N3	-175.9(5)	C19B	C18B	C23B	C22B	0.00(12)
C28	C29	C30	C31	2.1(8)	C19B	C18B	C23B	C24B	180.00(8)
C29	C30	C31	C32	-3.3(8)	C19B	C20B	C21B	C22B	0.00(12)
C30	C31	C32	C27	2.0(8)	C20B	C21B	C22B	C23B	0.00(12)
C32	C27	C28	C29	-1.4(7)	C21B	C22B	C23B	C18B	0.00(12)
O9A	C11A	C12A	C13A	-177.8(11)	C21B	C22B	C23B	C24B	180.00(8)
O9A	C11A	C12A	C14A	2.6(12)	C22B	C23B	C24B	C25B	180.00(8)
O10A	C34A	C35A	C36A	178.3(5)	C23B	C18B	C19B	C20B	0.00(12)
O10A	C34A	C35A	C40A	-2.6(8)	C23B	C24B	C25B	C16B	0.00(12)
N2A	C11A	C12A	C13A	5.8(13)	C25B	C16B	C17B	C18B	0.00(5)
N2A	C11A	C12A	C14A	-173.8(7)	C33B	O10B	C34B	C35B	162(2)
C10A	N1	C1	O1	-161.9(4)	C33B	N2B	C10B	N1	-173(2)
C10A	N1	C1	C2	84.6(5)	C33B	N2B	C10B	O8B	7(3)
C10A	N1	C13A	C12A	-8(2)	C33B	N2B	C11B	O9B	0(5)
C10A	N2A	C11A	O9A	169.6(6)	C33B	N2B	C11B	C12B	-178(3)
C10A	N2A	C11A	C12A	-13.8(9)	C34B	O10B	C33B	N2B	-69(3)
C10A	N2A	C33A	O10A	91.0(6)	C34B	C35B	C36B	C37B	-179.2(12)
C11A	N2A	C10A	N1	10.9(8)	C34B	C35B	C40B	C39B	179.2(12)
C11A	N2A	C10A	O8A	-168.9(6)	C35B	C36B	C37B	C38B	0.0
C11A	N2A	C33A	O10A	-91.3(7)	C36B	C35B	C40B	C39B	0.0
C11A	C12A	C13A	N1	4(2)	C36B	C37B	C38B	C39B	0.0
C13A	N1	C1	O1	16.2(11)	C37B	C38B	C39B	C40B	0.0
C13A	N1	C1	C2	-97.3(10)	C38B	C39B	C40B	C35B	0.0
C13A	N1	C10A	O8A	180.0(10)	C40B	C35B	C36B	C37B	0.0
C13A	N1	C10A	N2A	0.2(12)					

Table 8. Atomic Occupancy for C40 H35 N3 O10.

Atom	*Occupancy*	Atom	*Occupancy*	Atom	*Occupancy*
O8A	0.822(5)	O9A	0.822(5)	O10A	0.822(5)
N2A	0.822(5)	C10A	0.822(5)	C11A	0.822(5)
C12A	0.822(5)	C13A	0.822(5)	H13A	0.822(5)
C14A	0.822(5)	H14A	0.822(5)	H14B	0.822(5)
H14C	0.822(5)	C15A	0.822(5)	H15A	0.822(5)
H15B	0.822(5)	C16A	0.822(5)	C17A	0.822(5)
H17A	0.822(5)	C18A	0.822(5)	C19A	0.822(5)
H19A	0.822(5)	C20A	0.822(5)	H20A	0.822(5)
C21A	0.822(5)	H21A	0.822(5)	C22A	0.822(5)
H22A	0.822(5)	C23A	0.822(5)	C24A	0.822(5)
H24A	0.822(5)	C25A	0.822(5)	H25A	0.822(5)
C33A	0.822(5)	H33A	0.822(5)	H33B	0.822(5)
C34A	0.822(5)	H34A	0.822(5)	H34B	0.822(5)
C35A	0.822(5)	C36A	0.822(5)	H36A	0.822(5)
C37A	0.822(5)	H37A	0.822(5)	C38A	0.822(5)
H38A	0.822(5)	C39A	0.822(5)	H39A	0.822(5)
C40A	0.822(5)	H40A	0.822(5)	O8B	0.178(5)
O9B	0.178(5)	O10B	0.178(5)	N2B	0.178(5)
C10B	0.178(5)	C11B	0.178(5)	C12B	0.178(5)
C13B	0.178(5)	H13B	0.178(5)	C14B	0.178(5)
H14D	0.178(5)	H14E	0.178(5)	H14F	0.178(5)
C15B	0.178(5)	H15C	0.178(5)	H15D	0.178(5)
C16B	0.178(5)	C17B	0.178(5)	H17B	0.178(5)
C18B	0.178(5)	C19B	0.178(5)	H19B	0.178(5)
C20B	0.178(5)	H20B	0.178(5)	C21B	0.178(5)
H21B	0.178(5)	C22B	0.178(5)	H22B	0.178(5)
C23B	0.178(5)	C24B	0.178(5)	H24B	0.178(5)
C25B	0.178(5)	H25B	0.178(5)	C33B	0.178(5)
H33C	0.178(5)	H33D	0.178(5)	C34B	0.178(5)
H34C	0.178(5)	H34D	0.178(5)	C35B	0.178(5)
C36B	0.178(5)	H36B	0.178(5)	C37B	0.178(5)
H37B	0.178(5)	C38B	0.178(5)	H38B	0.178(5)
C39B	0.178(5)	H39B	0.178(5)	C40B	0.178(5)
H40B	0.178(5)				

Experimental

Single crystals of $C_{40}H_{35}N_3O_{10}$ [BEN102] were obtained by slow recrystallized from diethyl ether-hexanes. A suitable crystal was selected and mounted on a loop fiber on a Bruker APEX-II CCD diffractometer. The crystal was kept at 100 K during data collection. The structure was solved with the XS [2] structure solution program using Direct Methods and refined with the ShelXL [2] refinement package using Least Squares minimization.

1. Dolomanov, O.V., Bourhis, L.J., Gildea, R.J, Howard, J.A.K. & Puschmann, H. (2009), J. Appl. Cryst. 42, 339-341.
2. Sheldrick, G.M. (2008). Acta Cryst. A64, 112-122.
3. APEX2 (2008), Bruker AXS Inc., Madison, WI 53719-1173.
4. SAINT (2013) V8.34A, Bruker AXS Inc., Madison, WI 53719-1173.
5. XPREP (2013); X-ray data Preparation and Reciprocal space Exploration Program. Bruker AXS Inc., Madison, WI 53719-1173.

Crystal structure determination of $C_{40}H_{35}N_3O_{10}$ (BEN102):

Crystal Data for $C_{40}H_{35}N_3O_{10}$ (M =717.71 g/mol): monoclinic, space group $P2_1$ (no. 4), a = 14.2003(3) Å, b = 7.6452(2) Å, c = 17.2049(4) Å, β = 113.4900(10)°, V = 1713.05(7) Å^3, Z = 2, T = 100.15 K, μ(CuKα) = 0.838 mm^{-1}, $Dcalc$ = 1.391 g/cm^3, 10927 reflections measured (5.6° ≤ 2Θ ≤ 141.364°), 6032 unique (R_{int} = 0.0289, R_{sigma} = 0.0611) which were used in all calculations. The final R_1 was 0.0555 (I > 2σ(I)) and wR_2 was 0.1435 (all data).

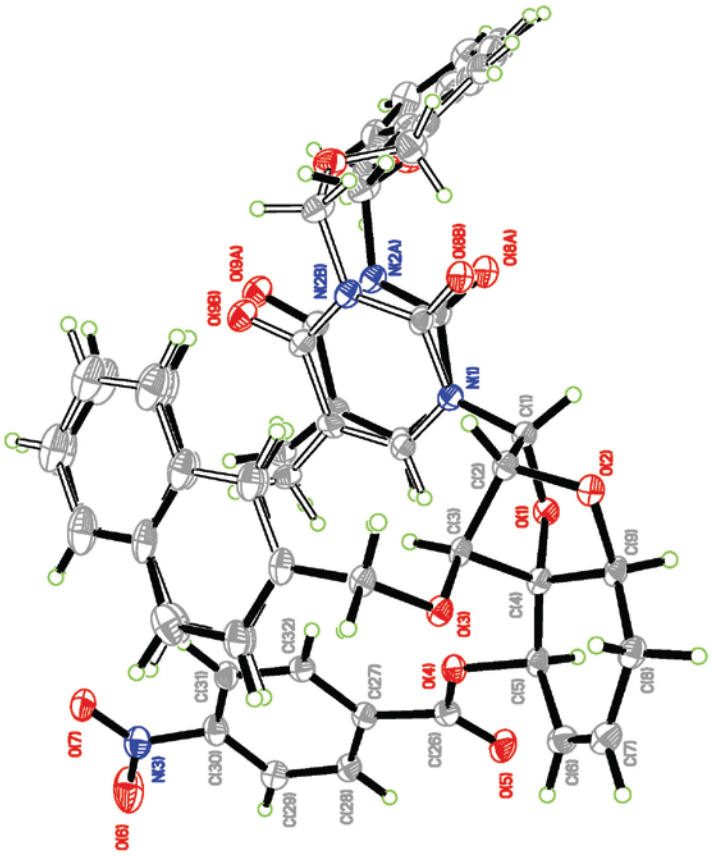

ORTEP view of the C40 H35 N3 O10 compound with the numbering scheme adopted. Ellipsoids are drawn at the 30% probability level. Hydrogen atoms are represented by spheres of arbitrary size.

α-Hydroxy ketone (±)-2.135

Université de Montréal

CRYSTAL AND MOLECULAR STRUCTURE OF

C15 H22 O6 COMPOUND (rober9)

Equipe Hanessian

Département de chimie, Université de Montréal,

C.P. 6128, Succ. Centre-Ville, Montréal, Québec, H3C 3J7 (Canada)

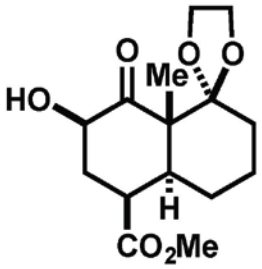

2.135
[X-ray]

Structure solved and refined in the laboratory of X-ray diffraction Université de Montréal by Robert D. Giacometti.

Table 1. Crystal data and structure refinement for C15 H22 O6.

Identification code	rober9
Empirical formula	C15 H22 O6
Formula weight	298.33
Temperature	100K
Wavelength	1.54178 Å
Crystal system	Triclinic
Space group	P-1
Unit cell dimensions	a = 7.5343(1) Å α = 73.554(1)° b = 9.8249(1) Å β = 69.798(1)° c = 10.5007(1) Å γ = 76.004(1)°
Volume	690.615(13)Å^3
Z	2
Density (calculated)	1.435 g/cm^3
Absorption coefficient	0.923 mm^{-1}
F(000)	320
Crystal size	0.08 x 0.04 x 0.02 mm
Theta range for data collection	4.60 to 71.29°
Index ranges	$-9 \le h \le 9$, $-12 \le k \le 12$, $-12 \le \ell \le 12$
Reflections collected	27615
Independent reflections	2581 [R_{int} = 0.020]
Absorption correction	Semi-empirical from equivalents
Max. and min. transmission	0.9817 and 0.9032
Refinement method	Full-matrix least-squares on F^2
Data / restraints / parameters	2581 / 0 / 193
Goodness-of-fit on F^2	1.037
Final R indices [I>2sigma(I)]	R_1 = 0.0344, wR_2 = 0.0906
R indices (all data)	R_1 = 0.0363, wR_2 = 0.0926
Largest diff. peak and hole	0.348 and -0.244 e/Å^3

Table 2. Atomic coordinates (x 10^4) and equivalent isotropic displacement parameters ($Å^2$ x 10^3) for C15 H22 O6.
U_{eq} is defined as one third of the trace of the orthogonalized Uij tensor.

	x	y	z	U_{eq}
O(1)	2956(1)	9446(1)	2644(1)	20(1)
O(2)	272(1)	11784(1)	2614(1)	22(1)
O(3)	-2935(1)	7672(1)	6132(1)	23(1)
O(4)	-4641(1)	7062(1)	5066(1)	18(1)
O(5)	4402(1)	6919(1)	1379(1)	17(1)
O(6)	2354(1)	8325(1)	166(1)	17(1)
C(1)	1466(2)	9263(1)	2563(1)	14(1)
C(2)	-186(2)	10499(1)	2548(1)	17(1)
C(3)	-1864(2)	10003(1)	3813(1)	22(1)
C(4)	-2569(2)	8723(1)	3670(1)	16(1)
C(5)	-1008(2)	7925(1)	2581(1)	14(1)
C(6)	-1471(2)	6509(1)	2546(1)	17(1)
C(7)	-88(2)	5960(1)	1277(1)	20(1)
C(8)	1990(2)	5815(1)	1246(1)	18(1)
C(9)	2459(2)	7198(1)	1358(1)	14(1)
C(10)	1062(2)	7774(1)	2646(1)	13(1)
C(11)	1426(2)	6785(1)	3988(1)	16(1)
C(12)	-3348(2)	7768(1)	5092(1)	15(1)
C(13)	-5582(2)	6152(1)	6359(1)	19(1)
C(14)	5497(2)	7800(1)	159(1)	20(1)
C(15)	4251(2)	8240(2)	-794(1)	21(1)

Table 3. Hydrogen coordinates (x 10^4) and isotropic displacement parameters ($Å^2$ x 10^3) for C15 H22 O6.

	x	y	z	U_{eq}
H(2)	1281	11598	2845	33
H(2A)	-545	10661	1678	21
H(3A)	-2938	10816	3920	26
H(3B)	-1450	9724	4663	26
H(4)	-3677	9138	3286	19
H(5)	-1019	8568	1655	17
H(6A)	-1370	5786	3403	20
H(6B)	-2802	6655	2511	20
H(7A)	-291	6636	421	24
H(7B)	-352	5013	1299	24
H(8A)	2849	5549	367	22
H(8B)	2239	5029	2025	22
H(11A)	2757	6739	3950	24
H(11B)	1195	5819	4076	24
H(11C)	560	7169	4791	24
H(13A)	-4709	5769	6931	28
H(13B)	-5936	5356	6159	28
H(13C)	-6738	6718	6862	28
H(14A)	6749	7249	-263	24
H(14B)	5715	8650	379	24
H(15A)	4470	9181	-1435	25
H(15B)	4486	7511	-1344	25

Table 4. Anisotropic parameters ($Å^2 \times 10^3$) for C15 H22 O6.

The anisotropic displacement factor exponent takes the form:

$$-2\pi^2 [h^2 a^{*2} U_{11} + ... + 2 h k a^* b^* U_{12}]$$

	U11	U22	U33	U23	U13	U12
O(1)	16(1)	23(1)	23(1)	-7(1)	-5(1)	-6(1)
O(2)	22(1)	15(1)	30(1)	-4(1)	-6(1)	-6(1)
O(3)	24(1)	32(1)	16(1)	-6(1)	-3(1)	-14(1)
O(4)	17(1)	21(1)	16(1)	0(1)	-4(1)	-9(1)
O(5)	12(1)	21(1)	16(1)	-1(1)	-2(1)	-2(1)
O(6)	15(1)	21(1)	11(1)	0(1)	-2(1)	-4(1)
C(1)	15(1)	18(1)	9(1)	-2(1)	-1(1)	-5(1)
C(2)	17(1)	14(1)	20(1)	-2(1)	-4(1)	-5(1)
C(3)	18(1)	16(1)	26(1)	-7(1)	3(1)	-5(1)
C(4)	12(1)	15(1)	17(1)	-2(1)	-2(1)	-2(1)
C(5)	12(1)	17(1)	12(1)	-2(1)	-2(1)	-3(1)
C(6)	16(1)	20(1)	16(1)	-3(1)	-4(1)	-7(1)
C(7)	22(1)	24(1)	18(1)	-8(1)	-4(1)	-9(1)
C(8)	19(1)	19(1)	16(1)	-7(1)	-1(1)	-4(1)
C(9)	13(1)	17(1)	12(1)	-2(1)	-3(1)	-2(1)
C(10)	12(1)	15(1)	12(1)	-3(1)	-2(1)	-3(1)
C(11)	15(1)	18(1)	13(1)	-1(1)	-4(1)	-3(1)
C(12)	11(1)	15(1)	17(1)	-6(1)	-1(1)	-1(1)
C(13)	19(1)	19(1)	17(1)	0(1)	-3(1)	-8(1)
C(14)	15(1)	25(1)	17(1)	-2(1)	0(1)	-6(1)
C(15)	17(1)	29(1)	14(1)	-3(1)	1(1)	-7(1)

Table 5. Bond lengths [Å] and angles [°] for C15 H22 O6

O(1)-C(1)	1.2133(15)	O(2)-C(2)-C(3)	111.31(10)
O(2)-C(2)	1.4128(14)	C(1)-C(2)-C(3)	105.69(10)
O(3)-C(12)	1.2085(16)	C(2)-C(3)-C(4)	112.31(10)
O(4)-C(12)	1.3364(15)	C(12)-C(4)-C(3)	110.75(10)
O(4)-C(13)	1.4494(14)	C(12)-C(4)-C(5)	115.03(10)
O(5)-C(9)	1.4291(14)	C(3)-C(4)-C(5)	111.09(10)
O(5)-C(14)	1.4347(15)	C(6)-C(5)-C(10)	112.45(10)
O(6)-C(9)	1.4288(14)	C(6)-C(5)-C(4)	114.12(9)
O(6)-C(15)	1.4353(14)	C(10)-C(5)-C(4)	113.78(10)
C(1)-C(2)	1.5147(17)	C(7)-C(6)-C(5)	110.27(10)
C(1)-C(10)	1.5381(16)	C(6)-C(7)-C(8)	111.12(10)
C(2)-C(3)	1.5401(17)	C(7)-C(8)-C(9)	112.69(10)
C(3)-C(4)	1.5403(17)	O(6)-C(9)-O(5)	106.48(9)
C(4)-C(12)	1.5241(16)	O(6)-C(9)-C(8)	111.43(10)
C(4)-C(5)	1.5616(16)	O(5)-C(9)-C(8)	107.78(10)
C(5)-C(6)	1.5267(16)	O(6)-C(9)-C(10)	106.57(9)
C(5)-C(10)	1.5539(16)	O(5)-C(9)-C(10)	111.69(9)
C(6)-C(7)	1.5258(17)	C(8)-C(9)-C(10)	112.76(9)
C(7)-C(8)	1.5265(18)	C(1)-C(10)-C(11)	106.86(9)
C(8)-C(9)	1.5284(16)	C(1)-C(10)-C(5)	109.20(9)
C(9)-C(10)	1.5561(16)	C(11)-C(10)-C(5)	114.21(9)
C(10)-C(11)	1.5388(16)	C(1)-C(10)-C(9)	109.01(9)
C(14)-C(15)	1.5089(19)	C(11)-C(10)-C(9)	110.06(9)
		C(5)-C(10)-C(9)	107.42(9)
C(12)-O(4)-C(13)	117.44(10)	O(3)-C(12)-O(4)	123.08(11)
C(9)-O(5)-C(14)	108.69(9)	O(3)-C(12)-C(4)	126.22(11)
C(9)-O(6)-C(15)	105.93(9)	O(4)-C(12)-C(4)	110.65(10)
O(1)-C(1)-C(2)	120.02(11)	O(5)-C(14)-C(15)	103.33(10)
O(1)-C(1)-C(10)	122.92(11)	O(6)-C(15)-C(14)	102.47(10)
C(2)-C(1)-C(10)	116.67(10)		
O(2)-C(2)-C(1)	112.24(10)		

Table 6. Torsion angles [°] for C15 H22 O6.

O(1)-C(1)-C(2)-O(2)	0.83(16)	C(2)-C(1)-C(10)-C(5)	4.33(14)
C(10)-C(1)-C(2)-O(2)	173.92(9)	O(1)-C(1)-C(10)-C(9)	-65.71(14)
O(1)-C(1)-C(2)-C(3)	-120.68(12)	C(2)-C(1)-C(10)-C(9)	121.42(11)
C(10)-C(1)-C(2)-C(3)	52.41(13)	C(6)-C(5)-C(10)-C(1)	175.66(9)
O(2)-C(2)-C(3)-C(4)	172.26(10)	C(4)-C(5)-C(10)-C(1)	-52.64(12)
C(1)-C(2)-C(3)-C(4)	-65.63(14)	C(6)-C(5)-C(10)-C(11)	-64.79(13)
C(2)-C(3)-C(4)-C(12)	149.15(11)	C(4)-C(5)-C(10)-C(11)	66.91(13)
C(2)-C(3)-C(4)-C(5)	20.02(15)	C(6)-C(5)-C(10)-C(9)	57.58(12)
C(12)-C(4)-C(5)-C(6)	44.00(14)	C(4)-C(5)-C(10)-C(9)	-170.72(9)
C(3)-C(4)-C(5)-C(6)	170.80(10)	O(6)-C(9)-C(10)-C(1)	-49.71(12)
C(12)-C(4)-C(5)-C(10)	-86.88(12)	O(5)-C(9)-C(10)-C(1)	66.19(12)
C(3)-C(4)-C(5)-C(10)	39.92(14)	C(8)-C(9)-C(10)-C(1)	-172.26(10)
C(10)-C(5)-C(6)-C(7)	-59.63(13)	O(6)-C(9)-C(10)-C(11)	-166.61(9)
C(4)-C(5)-C(6)-C(7)	168.84(10)	O(5)-C(9)-C(10)-C(11)	-50.71(12)
C(5)-C(6)-C(7)-C(8)	55.58(14)	C(8)-C(9)-C(10)-C(11)	70.84(13)
C(6)-C(7)-C(8)-C(9)	-53.33(14)	O(6)-C(9)-C(10)-C(5)	68.49(11)
C(15)-O(6)-C(9)-O(5)	25.52(11)	O(5)-C(9)-C(10)-C(5)	-175.61(9)
C(15)-O(6)-C(9)-C(8)	-91.75(11)	C(8)-C(9)-C(10)-C(5)	-54.06(13)
C(15)-O(6)-C(9)-C(10)	144.87(10)	C(13)-O(4)-C(12)-O(3)	0.41(17)
C(14)-O(5)-C(9)-O(6)	-3.85(12)	C(13)-O(4)-C(12)-C(4)	-177.36(9)
C(14)-O(5)-C(9)-C(8)	115.82(10)	C(3)-C(4)-C(12)-O(3)	-23.82(17)
C(14)-O(5)-C(9)-C(10)	-119.80(10)	C(5)-C(4)-C(12)-O(3)	103.16(14)
C(7)-C(8)-C(9)-O(6)	-66.01(13)	C(3)-C(4)-C(12)-O(4)	153.86(10)
C(7)-C(8)-C(9)-O(5)	177.51(9)	C(5)-C(4)-C(12)-O(4)	-79.16(13)
C(7)-C(8)-C(9)-C(10)	53.78(14)	C(9)-O(5)-C(14)-C(15)	-17.94(12)
O(1)-C(1)-C(10)-C(11)	53.20(14)	C(9)-O(6)-C(15)-C(14)	-35.90(12)
C(2)-C(1)-C(10)-C(11)	-119.67(11)	O(5)-C(14)-C(15)-O(6)	32.73(12)
O(1)-C(1)-C(10)-C(5)	177.21(10)		

Table 7. Bond lengths [Å] and angles [°] related to the hydrogen bonding for C15 H22 O6.

D-H	..A	d(D-H)	d(H..A)	d(D..A)	<DHA
O(2)-H(2)	O(1)	0.84	2.21	2.6690(13)	114.4
O(2)-H(2)	O(3)#1	0.84	2.24	2.9647(13)	144.6

Symmetry transformations used to generate equivalent atoms:

#1 -x,-y+2,-z+1

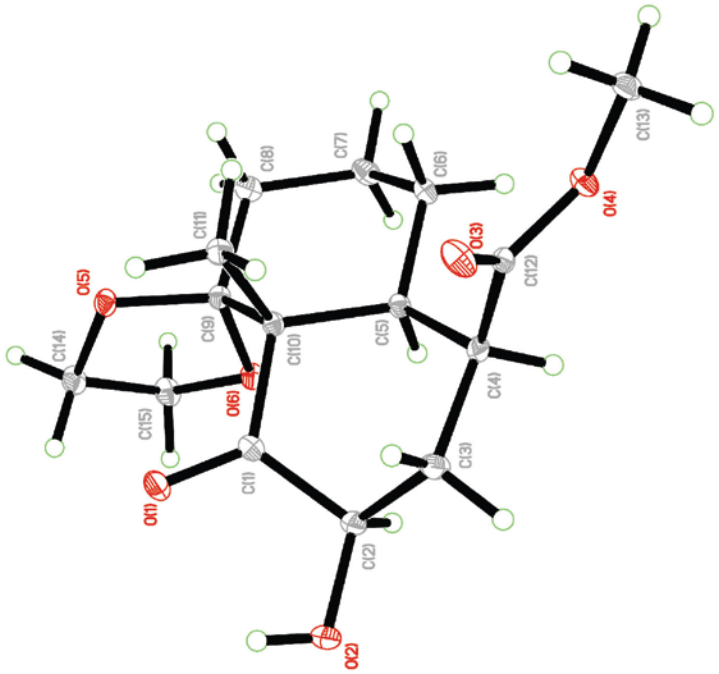

ORTEP view of the C15 H22 O6 compound with the numbering scheme adopted. Ellipsoids drawn at 30% probability level. Hydrogen atoms are represented by sphere of arbitrary size.

REFERENCES

SAINT (2006) Release 7.34A; Integration Software for Single Crystal Data.
Bruker AXS Inc., Madison, WI 53719-1173.

Sheldrick, G.M. (2008). SADABS, Bruker Area Detector Absorption Corrections.
Bruker AXS Inc., Madison, WI 53719-1173.

Sheldrick, G.M. (2008). Acta Cryst. A64, 112-122.

SHELXTL (2001) version 6.12; Bruker Analytical X-ray Systems Inc.,
Madison, WI 53719-1173.

APEX2 (2008) ; Bruker Molecular Analysis Research Tool.
Bruker AXS Inc., Madison, WI 53719-1173.

Spek, A.L. (2008). PLATON, A Multipurpose Crystallographic Tool,
Utrecht University, Utrecht, The Netherlands.

Maris, T. (2004). UdMX, University of Montréal, Montréal, QC, Canada.

XPREP (2008) Version 2008/2; X-ray data Preparation and Reciprocal space
Exploration Program. Bruker AXS Inc., Madison, WI 53719-1173.

Enone 2.144

Université de Montréal

CRYSTAL AND MOLECULAR STRUCTURE OF

C19 H32 O4 Si COMPOUND (ROBE27)

Equipe Hanessian

Département de chimie, Université de Montréal,

C.P. 6128, Succ. Centre-Ville, Montréal, Québec, H3C 3J7 (Canada)

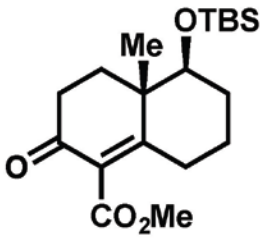

2.144

[X-ray]

Structure solved and refined in the laboratory of X-ray diffraction Université de Montréal by Robert D. Giacometti.

Table 1. Crystal data and structure refinement for C19 H32 O4 Si.

Identification code	robe271
Empirical formula	$C_{19}H_{32}O_4Si$
Formula weight	352.53
Temperature/K	100.15
Crystal system	orthorhombic
Space group	$P2_12_12_1$
a/Å	7.63270(10)
b/Å	12.0186(2)
c/Å	21.6388(3)
α/°	90
β/°	90
γ/°	90
Volume/Å^3	1985.02(5)
Z	4
ρ_{calc}g/cm^3	1.180
μ/mm^{-1}	1.192
F(000)	768.0
Crystal size/mm^3	0.2 × 0.08 × 0.06
Radiation	CuKα (λ = 1.54178)
2Θ range for data collection/°	8.172 to 142.236
Index ranges	$-9 \leq h \leq 9$, $-14 \leq k \leq 14$, $-26 \leq l \leq 26$
Reflections collected	26562
Independent reflections	3830 [R_{int} = 0.0239, R_{sigma} = 0.0152]
Data/restraints/parameters	3830/0/224
Goodness-of-fit on F^2	1.051
Final R indexes [I>=2σ (I)]	R_1 = 0.0317, wR_2 = 0.0850
Final R indexes [all data]	R_1 = 0.0320, wR_2 = 0.0853
Largest diff. peak/hole / e Å^{-3}	0.32/-0.23
Flack parameter	0.040(5)

Table 2. Fractional atomic coordinates ($\times 10^4$) and equivalent isotropic displacement parameters ($Å^2 \times 10^3$) for C19 H32 O4 Si.

U_{eq} is defined as one third of the trace of the orthogonalized Uij tensor.

Atom	x	y	z	U(eq)
Si1	1103.5(6)	1709.3(4)	8273.4(2)	21.41(14)
O2	-2205.4(17)	7595.2(11)	8921.1(6)	22.3(3)
O3	2299(2)	7965.7(11)	8760.3(7)	29.2(3)
O1	-700(2)	8179.6(12)	9750.7(6)	29.7(3)
O4	1344.3(17)	2751.3(10)	8765.9(6)	22.1(3)
C10	1248(2)	4614.1(14)	9159.7(8)	18.5(3)
C9	172(2)	3648.6(15)	8873.3(8)	21.0(4)
C13	-3524(2)	8431.9(16)	9052.9(9)	24.4(4)
C2	3439(2)	6107.7(15)	8826.1(9)	21.7(4)
C1	2609(2)	4982.4(15)	8679.3(8)	20.3(4)
C3	2059(2)	6995.9(15)	8896.6(8)	21.0(4)
C12	-874(2)	7555.0(15)	9322.2(8)	20.8(4)
C4	364(2)	6625.7(16)	9166.6(8)	19.9(3)
C6	-1642(3)	5256.4(16)	9663.2(9)	24.5(4)
C19	3384(3)	297.0(19)	7613.7(12)	40.0(6)
C5	-4(2)	5564.2(15)	9312.3(8)	19.3(4)
C7	-2617(3)	4281.8(17)	9365.7(10)	28.7(4)
C14	-249(3)	2157(2)	7605.2(11)	42.0(6)
C11	2182(3)	4228.4(15)	9754.7(8)	22.6(4)
C17	4208(3)	2310.7(17)	7668.6(11)	33.4(5)
C8	-1388(3)	3293.3(16)	9265.6(10)	26.9(4)
C18	4514(3)	1099(2)	8599.4(11)	42.1(6)
C16	3399(3)	1338.9(16)	8027.5(9)	23.6(4)
C15	36(3)	510.9(18)	8676.3(14)	44.0(6)

Table 3. Hydrogen atom coordinates ($\times 10^4$) and isotropic displacement parameters ($Å^2 \times 10^3$) for C19 H32 O4 Si.

U_{eq} is defined as one third of the trace of the orthogonalized Uij tensor.

Atom	x	y	z	U(eq)
H9	-283	3905	8464	25
H13A	-4040	8288	9460	37
H13B	-4443	8402	8737	37
H13C	-2981	9171	9051	37
H2A	4123	6050	9213	26
H2B	4253	6317	8489	26
H1A	3544	4413	8655	24
H1B	2039	5024	8269	24
H6A	-2431	5910	9681	29
H6B	-1324	5056	10092	29
H19A	4590	90	7509	60
H19B	2731	456	7234	60
H19C	2820	-318	7835	60
H7A	-3601	4053	9635	34
H7B	-3110	4520	8964	34
H14A	-1421	2366	7750	63
H14B	-344	1544	7309	63
H14C	304	2799	7405	63
H11A	2932	4829	9909	34
H11B	2901	3573	9664	34
H11C	1306	4039	10069	34
H17A	4202	2980	7928	50
H17B	3524	2448	7293	50
H17C	5417	2126	7555	50
H8A	-972	3012	9670	32
H8B	-2028	2685	9056	32
H18A	5714	921	8472	63
H18B	4016	466	8825	63
H18C	4526	1755	8868	63
H15A	755	285	9030	66
H15B	-77	-115	8389	66
H15C	-1128	734	8821	66

Table 4. Anisotropic displacement parameters ($Å^2$ x 10^3) for C19 H32 O4 Si.

The anisotropic displacement factor exponent takes the form:
$-2\pi^2[h^2a^{*2}U_{11} + ... + 2hka^*b^*U_{12}]$

Atom	U_{11}	U_{22}	U_{33}	U_{23}	U_{13}	U_{12}
Si1	20.4(2)	18.1(2)	25.7(2)	-2.72(18)	0.82(19)	-1.10(19)
O2	20.8(6)	20.6(6)	25.4(6)	-3.0(5)	-1.8(5)	3.9(5)
O3	26.5(7)	20.5(7)	40.6(8)	5.7(6)	-0.7(6)	-1.4(5)
O1	34.3(8)	27.5(7)	27.3(7)	-7.0(6)	-5.6(6)	7.9(6)
O4	21.5(6)	19.0(6)	26.0(6)	-2.4(5)	-1.4(5)	3.1(5)
C10	17.9(8)	18.6(8)	19.0(7)	0.4(6)	0.5(7)	1.9(7)
C9	20.4(8)	19.0(8)	23.7(8)	-1.8(7)	-1.0(7)	1.2(7)
C13	20.6(8)	21.6(9)	30.9(9)	-0.8(7)	0.0(7)	4.8(7)
C2	19.9(8)	21.9(9)	23.5(8)	-0.9(7)	3.2(7)	-0.2(7)
C1	20.4(8)	20.0(8)	20.4(8)	-1.6(7)	2.5(7)	1.6(7)
C3	21.9(8)	21.8(9)	19.2(8)	-0.8(7)	-2.7(7)	-0.4(7)
C12	22.8(9)	18.2(8)	21.2(8)	1.4(6)	0.0(7)	0.8(7)
C4	21.2(8)	21.2(8)	17.1(7)	-2.3(7)	-2.1(7)	2.1(7)
C6	24.1(9)	22.9(9)	26.5(9)	0.5(7)	6.0(8)	3.4(7)
C19	43.7(13)	29.3(11)	47.2(13)	-12.5(10)	17.1(11)	-1.4(9)
C5	19.1(8)	22.1(9)	16.6(7)	-1.4(7)	-0.9(7)	2.2(7)
C7	20.0(9)	25.8(9)	40.2(11)	-0.8(8)	5.3(8)	-0.8(8)
C14	36.3(12)	52.9(14)	36.7(11)	-11.5(11)	-16(1)	9.8(11)
C11	24.7(9)	21.6(8)	21.7(8)	1.6(7)	-0.8(7)	2.2(7)
C17	34.0(11)	30.3(11)	36.0(11)	-3.6(8)	10.8(9)	-2.0(9)
C8	23.6(9)	20.6(8)	36.5(10)	-1.8(8)	4.7(8)	-2.8(8)
C18	33.9(12)	53.6(15)	38.7(12)	5.2(11)	-1.4(10)	19.6(11)
C16	23.8(9)	23.0(9)	24.0(8)	-3.0(7)	3.6(7)	3.3(7)
C15	42.0(13)	20.2(10)	69.8(16)	-0.2(10)	22.2(12)	-5.8(9)

Table 5. Bond lengths [Å] for C19 H32 O4 Si.

Atom	Atom	Length/Å	Atom	Atom	Length/Å
Si1	O4	1.6546(13)	C9	C8	1.524(3)
Si1	C14	1.856(2)	C2	C1	1.527(2)
Si1	C16	1.8844(19)	C2	C3	1.507(2)
Si1	C15	1.870(2)	C3	C4	1.488(3)
O2	C13	1.451(2)	C12	C4	1.501(2)
O2	C12	1.337(2)	C4	C5	1.344(3)
O3	C3	1.216(2)	C6	C5	1.509(3)
O1	C12	1.200(2)	C6	C7	1.530(3)
O4	C9	1.420(2)	C19	C16	1.539(3)
C10	C9	1.550(2)	C7	C8	1.529(3)
C10	C1	1.535(2)	C17	C16	1.533(3)
C10	C5	1.525(2)	C18	C16	1.529(3)
C10	C11	1.543(2)			

Table 6. Bond angles [Å] for C19 H32 O4 Si.

Atom	Atom	Atom	Angle/°	Atom	Atom	Atom	Angle/°
O4	Si1	C14	110.11(9)	O3	C3	C4	120.84(17)
O4	Si1	C16	104.92(8)	C4	C3	C2	115.82(16)
O4	Si1	C15	109.33(10)	O2	C12	C4	111.07(15)
C14	Si1	C16	111.44(11)	O1	C12	O2	124.24(17)
C14	Si1	C15	110.14(13)	O1	C12	C4	124.68(17)
C15	Si1	C16	110.77(10)	C3	C4	C12	114.39(16)
C12	O2	C13	115.13(14)	C5	C4	C3	123.91(17)
C9	O4	Si1	127.61(11)	C5	C4	C12	121.47(16)
C1	C10	C9	107.67(14)	C5	C6	C7	112.27(15)
C1	C10	C11	109.81(15)	C4	C5	C10	121.93(16)
C5	C10	C9	108.38(14)	C4	C5	C6	121.61(16)
C5	C10	C1	110.79(14)	C6	C5	C10	116.40(16)
C5	C10	C11	109.49(14)	C8	C7	C6	110.88(16)
C11	C10	C9	110.68(14)	C9	C8	C7	109.91(16)
O4	C9	C10	107.48(14)	C19	C16	Si1	110.44(15)
O4	C9	C8	111.76(15)	C17	C16	Si1	109.75(13)
C8	C9	C10	113.63(14)	C17	C16	C19	109.16(16)
C3	C2	C1	111.01(15)	C18	C16	Si1	109.48(14)
C2	C1	C10	113.29(14)	C18	C16	C19	108.74(19)
O3	C3	C2	123.31(18)	C18	C16	C17	109.25(19)

Table 7. Torsion angles [°] for C19 H32 O4 Si.

A	B	C	D	Angle/°	A	B	C	D	Angle/°
Si1	O4	C9	C10	-157.74(12)	C3	C2	C1	C10	-56.0(2)
Si1	O4	C9	C8	76.93(19)	C3	C4	C5	C10	-5.5(3)
O2	C12	C4	C3	106.88(17)	C3	C4	C5	C6	171.60(16)
O2	C12	C4	C5	-78.4(2)	C12	C4	C5	C10	-179.66(15)
O3	C3	C4	C12	-7.2(2)	C12	C4	C5	C6	-2.6(3)
O3	C3	C4	C5	178.19(18)	C6	C7	C8	C9	-56.8(2)
O1	C12	C4	C3	-73.3(2)	C5	C10	C9	O4	-176.89(13)
O1	C12	C4	C5	101.4(2)	C5	C10	C9	C8	-52.68(19)
O4	Si1	C16	C19	174.45(14)	C5	C10	C1	C2	46.7(2)
O4	Si1	C16	C17	-65.16(15)	C5	C6	C7	C8	52.7(2)
O4	Si1	C16	C18	54.74(17)	C7	C6	C5	C10	-50.4(2)
O4	C9	C8	C7	-179.64(15)	C7	C6	C5	C4	132.38(18)
C10	C9	C8	C7	58.5(2)	C14	Si1	O4	C9	28.67(18)
C9	C10	C1	C2	165.08(14)	C14	Si1	C16	C19	-66.41(18)
C9	C10	C5	C4	-134.11(18)	C14	Si1	C16	C17	53.98(17)
C9	C10	C5	C6	48.68(19)	C14	Si1	C16	C18	173.88(17)
C13	O2	C12	O1	-2.9(3)	C11	C10	C9	O4	-56.81(18)
C13	O2	C12	C4	176.87(15)	C11	C10	C9	C8	67.4(2)
C2	C3	C4	C12	170.90(15)	C11	C10	C1	C2	-74.34(18)
C2	C3	C4	C5	-3.7(3)	C11	C10	C5	C4	105.07(19)
C1	C10	C9	O4	63.23(17)	C11	C10	C5	C6	-72.1(2)
C1	C10	C9	C8	-172.57(15)	C16	Si1	O4	C9	148.70(15)
C1	C10	C5	C4	-16.2(2)	C15	Si1	O4	C9	-92.47(17)
C1	C10	C5	C6	166.60(15)	C15	Si1	C16	C19	56.59(18)
C1	C2	C3	O3	-148.34(18)	C15	Si1	C16	C17	176.98(16)
C1	C2	C3	C4	33.6(2)	C15	Si1	C16	C18	-63.12(19)

Experimental

Single crystals of $C_{19}H_{32}O_4Si$ [ROBE27] were obtained by slow recrystallized from diethyl ether-hexanes. A suitable crystal was selected and mounted on a loop fiber on a Bruker APEX-II CCD diffractometer. The crystal was kept at 100 K during data collection. Using Olex2 [1], the structure was solved with the XT [2] structure solution program using Direct Methods and refined with the ShelXL [2] refinement package using Least Squares minimization.

1. Dolomanov, O.V., Bourhis, L.J., Gildea, R.J, Howard, J.A.K. & Puschmann, H. (2009), J. Appl. Cryst. 42, 339-341.
2. Sheldrick, G.M. (2008). Acta Cryst. A64, 112-122.
3. APEX2 (2008), Bruker AXS Inc., Madison, WI 53719-1173.
4. SAINT (2013) V8.34A, Bruker AXS Inc., Madison, WI 53719-1173.
5. XPREP (2013); X-ray data Preparation and Reciprocal space Exploration Program. Bruker AXS Inc., Madison, WI 53719-1173.

Crystal structure determination of $C_{19}H_{32}O_4Si$ (ROBE27):

Crystal Data for $C_{19}H_{32}O_4Si$ (M =352.53 g/mol): orthorhombic, space group $P2_12_12_1$ (no. 19), a = 7.63270(10) Å, b = 12.0186(2) Å, c = 21.6388(3) Å, V = 1985.02(5) Å^3, Z = 4, T = 100.15 K, μ(CuKα) = 1.192 mm^{-1}, $Dcalc$ = 1.180 g/cm^3, 26562 reflections measured (8.172° ≤ 2Θ ≤ 142.236°), 3830 unique (R_{int} = 0.0239, R_{sigma} = 0.0152) which were used in all calculations. The final R_1 was 0.0317 (I > 2σ(I)) and wR_2 was 0.0853 (all data).

Refinement model description

Number of restraints - 0, number of constraints - unknown.
Details:
1. Fixed Uiso
 At 1.2 times of:
  All C(H) groups, All C(H,H) groups
 At 1.5 times of:
  All C(H,H,H) groups
2.a Ternary CH refined with riding coordinates:
 C9(H9)
2.b Secondary CH2 refined with riding coordinates:
 C2(H2A,H2B), C1(H1A,H1B), C6(H6A,H6B), C7(H7A,H7B), C8(H8A,H8B)
2.c Idealised Me refined as rotating group:
 C13(H13A,H13B,H13C), C19(H19A,H19B,H19C), C14(H14A,H14B,H14C), C11(H11A,H11B, H11C), C17(H17A,H17B,H17C), C18(H18A,H18B,H18C), C15(H15A,H15B,H15C)

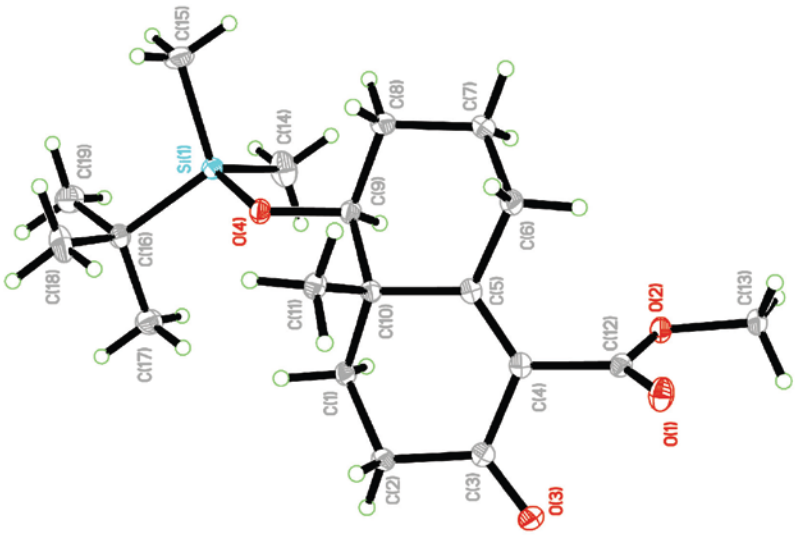

ORTEP view of the C19 H32 O4 SI compound with the numbering scheme adopted. Ellipsoids are drawn at the 30% probability level. Hydrogen atoms are represented by spheres of arbitrary size.

α-Hydroxy ketone (±)-2.145

Université de Montréal

CRYSTAL AND MOLECULAR STRUCTURE OF

C19 H34 O5 Si COMPOUND (robe15)

Equipe Hanessian

Département de chimie, Université de Montréal,

C.P. 6128, Succ. Centre-Ville, Montréal, Québec, H3C 3J7 (Canada)

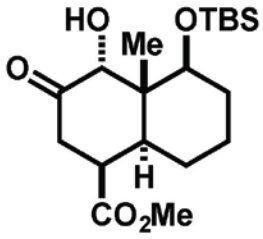

2.145

[X-ray]

Structure solved and refined in the laboratory of X-ray diffraction Université de Montréal by Robert D. Giacometti.

Table 1. Crystal data and structure refinement for C19 H34 O5 Si.

Identification code	robe15
Empirical formula	C19 H34 O5 Si
Formula weight	370.55
Temperature	100K
Wavelength	1.54178 Å
Crystal system	Triclinic
Space group	P-1
Unit cell dimensions	a = 7.0435(1) Å α = 111.405(1)° b = 12.0231(2) Å β = 103.696(1)° c = 13.8411(2) Å γ = 96.886(1)°
Volume	1032.31(3)Å^3
Z	2
Density (calculated)	1.192 g/cm^3
Absorption coefficient	1.205 mm^{-1}
F(000)	404
Crystal size	0.20 x 0.10 x 0.04 mm
Theta range for data collection	3.60 to 71.20°
Index ranges	$-8 \le h \le 8$, $-14 \le k \le 14$, $-16 \le \ell \le 16$
Reflections collected	40258
Independent reflections	3861 [R_{int} = 0.022]
Absorption correction	Semi-empirical from equivalents
Max. and min. transmission	0.9529 and 0.8132
Refinement method	Full-matrix least-squares on F^2
Data / restraints / parameters	3861 / 0 / 234
Goodness-of-fit on F^2	1.070
Final R indices [I>2sigma(I)]	R_1 = 0.0345, wR_2 = 0.0930
R indices (all data)	R_1 = 0.0349, wR_2 = 0.0936
Largest diff. peak and hole	0.365 and -0.315 e/Å^3

Table 2. Atomic coordinates (x 10^4) and equivalent isotropic displacement parameters ($Å^2$ x 10^3) for C19 H34 O5 Si.

U_{eq} is defined as one third of the trace of the orthogonalized Uij tensor.

	x	y	z	U_{eq}
Si(1)	202(1)	5507(1)	8183(1)	17(1)
O(1)	2557(1)	8990(1)	9577(1)	20(1)
O(3)	1197(1)	10953(1)	6843(1)	22(1)
O(2)	-333(1)	10693(1)	8950(1)	22(1)
O(5)	471(1)	6340(1)	7484(1)	17(1)
O(4)	3865(1)	10570(1)	6269(1)	19(1)
C(5)	3966(2)	9143(1)	7765(1)	14(1)
C(12)	2810(2)	10692(1)	6976(1)	16(1)
C(11)	244(2)	8175(1)	6606(1)	15(1)
C(8)	3112(2)	6450(1)	6655(1)	19(1)
C(14)	-1361(2)	3950(1)	7163(1)	22(1)
C(10)	1924(2)	8350(1)	7625(1)	13(1)
C(1)	1196(2)	8964(1)	8616(1)	15(1)
C(13)	2913(2)	10740(1)	5298(1)	23(1)
C(4)	3922(2)	10497(1)	7966(1)	16(1)
C(9)	2297(2)	7094(1)	7585(1)	15(1)
C(3)	3065(2)	11085(1)	8910(1)	19(1)
C(2)	1143(2)	10294(1)	8814(1)	17(1)
C(7)	5098(2)	7240(1)	6780(1)	20(1)
C(6)	4861(2)	8514(1)	6855(1)	17(1)
C(17)	-1797(3)	3113(1)	7739(1)	32(1)
C(19)	-1164(3)	6233(1)	9158(1)	33(1)
C(18)	2711(2)	5403(2)	8926(1)	38(1)
C(16)	-3350(2)	4091(1)	6524(1)	37(1)
C(15)	-228(3)	3354(1)	6365(1)	35(1)

Table 3. Hydrogen coordinates ($\times 10^4$) and isotropic displacement parameters ($Å^2 \times 10^3$) for C19 H34 O5 Si.

	x	y	z	U_{eq}
H(1)	2017	9153	10077	30
H(5)	4911	9181	8447	17
H(11A)	-812	7454	6416	22
H(11B)	796	8056	5997	22
H(11C)	-321	8904	6754	22
H(8A)	2126	6294	5952	22
H(8B)	3321	5650	6654	22
H(1A)	-173	8495	8493	18
H(13A)	1736	10065	4844	34
H(13B)	3867	10751	4887	34
H(13C)	2493	11521	5508	34
H(4)	5347	10957	8201	19
H(9)	3306	7235	8286	18
H(3A)	4075	11243	9606	23
H(3B)	2816	11884	8929	23
H(7A)	5569	6832	6147	24
H(7B)	6121	7322	7445	24
H(6A)	3977	8439	6151	20
H(6B)	6189	9027	6996	20
H(17A)	-2531	3484	8248	47
H(17B)	-528	3013	8140	47
H(17C)	-2609	2309	7196	47
H(19A)	-316	7021	9713	49
H(19B)	-1490	5692	9509	49
H(19C)	-2406	6367	8764	49
H(18A)	3499	5152	8420	57
H(18B)	2535	4796	9235	57
H(18C)	3415	6205	9514	57
H(16A)	-3076	4637	6169	55
H(16B)	-4110	4441	7025	55
H(16C)	-4136	3285	5971	55
H(15A)	-1034	2541	5839	53
H(15B)	1055	3272	6768	53
H(15C)	22	3868	5978	53

Table 4. Anisotropic parameters ($Å^2 \times 10^3$) for C19 H34 O5 Si.

The anisotropic displacement factor exponent takes the form:

$$-2\pi^2 [h^2 a^{*2} U_{11} + ... + 2 h k a^* b^* U_{12}]$$

	U11	U22	U33	U23	U13	U12
Si(1)	19(1)	18(1)	14(1)	8(1)	6(1)	0(1)
O(1)	18(1)	32(1)	11(1)	11(1)	5(1)	6(1)
O(3)	21(1)	30(1)	24(1)	16(1)	10(1)	11(1)
O(2)	24(1)	28(1)	18(1)	9(1)	11(1)	11(1)
O(5)	15(1)	19(1)	19(1)	11(1)	6(1)	0(1)
O(4)	19(1)	27(1)	19(1)	15(1)	8(1)	6(1)
C(5)	12(1)	18(1)	14(1)	9(1)	3(1)	2(1)
C(12)	17(1)	14(1)	16(1)	7(1)	5(1)	1(1)
C(11)	13(1)	19(1)	12(1)	7(1)	3(1)	2(1)
C(8)	19(1)	18(1)	23(1)	11(1)	10(1)	6(1)
C(14)	30(1)	16(1)	19(1)	8(1)	8(1)	4(1)
C(10)	12(1)	17(1)	11(1)	7(1)	4(1)	2(1)
C(1)	13(1)	21(1)	11(1)	8(1)	4(1)	2(1)
C(13)	26(1)	30(1)	20(1)	17(1)	9(1)	8(1)
C(4)	14(1)	17(1)	15(1)	7(1)	3(1)	0(1)
C(9)	13(1)	18(1)	17(1)	10(1)	4(1)	1(1)
C(3)	21(1)	18(1)	15(1)	5(1)	4(1)	2(1)
C(2)	20(1)	22(1)	8(1)	5(1)	5(1)	5(1)
C(7)	17(1)	24(1)	27(1)	14(1)	12(1)	8(1)
C(6)	13(1)	21(1)	20(1)	11(1)	8(1)	4(1)
C(17)	46(1)	20(1)	29(1)	12(1)	13(1)	-1(1)
C(19)	50(1)	23(1)	27(1)	6(1)	25(1)	1(1)
C(18)	27(1)	56(1)	41(1)	39(1)	3(1)	1(1)
C(16)	31(1)	29(1)	37(1)	12(1)	-6(1)	-4(1)
C(15)	64(1)	22(1)	26(1)	9(1)	23(1)	15(1)

Table 5. Bond lengths [Å] and angles [°] for C19 H34 O5 Si

		C(6)-C(5)-C(4)	113.58(9)
Si(1)-O(5)	1.6512(9)	C(6)-C(5)-C(10)	111.97(9)
Si(1)-C(19)	1.8611(15)	C(4)-C(5)-C(10)	113.86(9)
Si(1)-C(18)	1.8661(16)	O(3)-C(12)-O(4)	123.29(11)
Si(1)-C(14)	1.8840(13)	O(3)-C(12)-C(4)	124.77(11)
O(1)-C(1)	1.4318(14)	O(4)-C(12)-C(4)	111.92(10)
O(3)-C(12)	1.2055(15)	C(9)-C(8)-C(7)	110.32(10)
O(2)-C(2)	1.2212(16)	C(15)-C(14)-C(16)	108.96(12)
O(5)-C(9)	1.4283(14)	C(15)-C(14)-C(17)	108.83(11)
O(4)-C(12)	1.3402(15)	C(16)-C(14)-C(17)	109.34(12)
O(4)-C(13)	1.4502(15)	C(15)-C(14)-SI1	109.47(10)
C(5)-C(6)	1.5328(17)	C(16)-C(14)-SI1	109.56(9)
C(5)-C(4)	1.5544(16)	C(17)-C(14)-SI1	110.65(9)
C(5)-C(10)	1.5555(15)	C(11)-C(10)-C(1)	106.99(9)
C(12)-C(4)	1.5222(16)	C(11)-C(10)-C(9)	110.45(9)
C(11)-C(10)	1.5392(15)	C(1)-C(10)-C(9)	108.71(9)
C(8)-C(9)	1.5210(17)	C(11)-C(10)-C(5)	113.74(9)
C(8)-C(7)	1.5280(17)	C(1)-C(10)-C(5)	109.75(9)
C(14)-C(15)	1.532(2)	C(9)-C(10)-C(5)	107.12(9)
C(14)-C(16)	1.534(2)	O(1)-C(1)-C(2)	106.86(9)
C(14)-C(17)	1.5405(18)	O(1)-C(1)-C(10)	109.87(9)
C(10)-C(1)	1.5403(16)	C(2)-C(1)-C(10)	111.19(10)
C(10)-C(9)	1.5464(16)	C(12)-C(4)-C(3)	109.50(10)
C(1)-C(2)	1.5273(17)	C(12)-C(4)-C(5)	115.26(9)
C(4)-C(3)	1.5401(17)	C(3)-C(4)-C(5)	110.92(10)
C(3)-C(2)	1.5060(17)	O(5)-C(9)-C(8)	110.25(10)
C(7)-C(6)	1.5291(17)	O(5)-C(9)-C(10)	109.32(9)
		C(8)-C(9)-C(10)	112.06(9)
O(5)-SI1-C(19)	108.66(6)	C(2)-C(3)-C(4)	112.99(10)
O(5)-SI1-C(18)	110.06(6)	O(2)-C(2)-C(3)	122.98(11)
C(19)-SI1-C(18)	110.53(8)	O(2)-C(2)-C(1)	121.39(11)
O(5)-SI1-C(14)	106.33(5)	C(3)-C(2)-C(1)	115.49(10)
C(19)-SI1-C(14)	109.65(7)	C(8)-C(7)-C(6)	111.10(10)
C(18)-SI1-C(14)	111.49(7)	C(7)-C(6)-C(5)	111.47(10)
C(9)-O(5)-SI1	126.44(7)		
C(12)-O(4)-C(13)	115.58(10)		

Table 6. Torsion angles [°] for C19 H34 O5 Si.

		O(4)-C(12)-C(4)-C(5)	-74.35(13)
C(19)-SI1-O(5)-C(9)	108.81(10)	C(6)-C(5)-C(4)-C(12)	56.52(13)
C(18)-SI1-O(5)-C(9)	-12.34(12)	C(10)-C(5)-C(4)-C(12)	-73.23(13)
C(14)-SI1-O(5)-C(9)	-133.23(10)	C(6)-C(5)-C(4)-C(3)	-178.34(9)
C(13)-O(4)-C(12)-O(3)	-1.71(17)	C(10)-C(5)-C(4)-C(3)	51.91(13)
C(13)-O(4)-C(12)-C(4)	179.97(10)	SI1-O(5)-C(9)-C(8)	102.07(10)
O(5)-SI1-C(14)-C(15)	62.92(10)	SI1-O(5)-C(9)-C(10)	-134.31(9)
C(19)-SI1-C(14)-C(15)	-179.78(10)	C(7)-C(8)-C(9)-O(5)	-178.35(9)
C(18)-SI1-C(14)-C(15)	-57.04(11)	C(7)-C(8)-C(9)-C(10)	59.64(13)
O(5)-SI1-C(14)-C(16)	-56.51(11)	C(11)-C(10)-C(9)-O(5)	-57.10(12)
C(19)-SI1-C(14)-C(16)	60.79(12)	C(1)-C(10)-C(9)-O(5)	60.01(12)
C(18)-SI1-C(14)-C(16)	-176.47(11)	C(5)-C(10)-C(9)-O(5)	178.54(9)
O(5)-SI1-C(14)-C(17)	-177.13(9)	C(11)-C(10)-C(9)-C(8)	65.44(12)
C(19)-SI1-C(14)-C(17)	-59.83(12)	C(1)-C(10)-C(9)-C(8)	-177.45(9)
C(18)-SI1-C(14)-C(17)	62.90(12)	C(5)-C(10)-C(9)-C(8)	-58.92(12)
C(6)-C(5)-C(10)-C(11)	-65.65(12)	C(12)-C(4)-C(3)-C(2)	80.20(12)
C(4)-C(5)-C(10)-C(11)	64.90(13)	C(5)-C(4)-C(3)-C(2)	-48.12(13)
C(6)-C(5)-C(10)-C(1)	174.55(9)	C(4)-C(3)-C(2)-O(2)	-133.76(12)
C(4)-C(5)-C(10)-C(1)	-54.90(12)	C(4)-C(3)-C(2)-C(1)	50.50(14)
C(6)-C(5)-C(10)-C(9)	56.69(12)	O(1)-C(1)-C(2)-O(2)	-109.18(12)
C(4)-C(5)-C(10)-C(9)	-172.76(9)	C(10)-C(1)-C(2)-O(2)	130.92(11)
C(11)-C(10)-C(1)-O(1)	171.53(9)	O(1)-C(1)-C(2)-C(3)	66.63(12)
C(9)-C(10)-C(1)-O(1)	52.23(12)	C(10)-C(1)-C(2)-C(3)	-53.27(13)
C(5)-C(10)-C(1)-O(1)	-64.63(12)	C(9)-C(8)-C(7)-C(6)	-55.78(13)
C(11)-C(10)-C(1)-C(2)	-70.38(12)	C(8)-C(7)-C(6)-C(5)	54.35(14)
C(9)-C(10)-C(1)-C(2)	170.33(9)	C(4)-C(5)-C(6)-C(7)	173.33(10)
C(5)-C(10)-C(1)-C(2)	53.47(12)	C(10)-C(5)-C(6)-C(7)	-55.97(13)
O(3)-C(12)-C(4)-C(3)	-18.52(16)		
O(4)-C(12)-C(4)-C(3)	159.78(10)		
O(3)-C(12)-C(4)-C(5)	107.35(14)		

Table 7. Bond lengths [Å] and angles [°] related to the hydrogen bonding for C19 H34 O5 Si.

D-H	..A	d(D-H)	d(H..A)	d(D..A)	<DHA
O(1)-H(1)	O(2)#1	0.84	1.97	2.8011(12)	169.8

Symmetry transformations used to generate equivalent atoms:

#1 -x,-y+2,-z+2

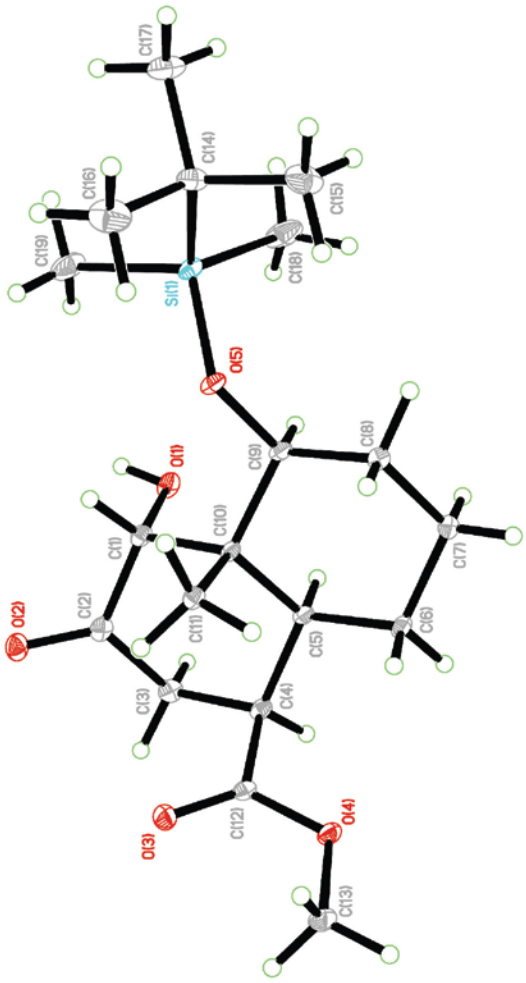

ORTEP view of the C19 H34 O5 Si compound with the numbering scheme adopted. Ellipsoids drawn at 30% probability level. Hydrogen atoms are represented by sphere of arbitrary size.

REFERENCES

SAINT (2006) Release 7.34A; Integration Software for Single Crystal Data.
Bruker AXS Inc., Madison, WI 53719-1173.

Sheldrick, G.M. (2008). SADABS, Bruker Area Detector Absorption Corrections.
Bruker AXS Inc., Madison, WI 53719-1173.

Sheldrick, G.M. (2008). Acta Cryst. A64, 112-122.

SHELXTL (2001) version 6.12; Bruker Analytical X-ray Systems Inc.,
Madison, WI 53719-1173.

APEX2 (2008) ; Bruker Molecular Analysis Research Tool.
Bruker AXS Inc., Madison, WI 53719-1173.

Spek, A.L. (2008). PLATON, A Multipurpose Crystallographic Tool,
Utrecht University, Utrecht, The Netherlands.

Maris, T. (2004). UdMX, University of Montréal, Montréal, QC, Canada.

XPREP (2008) Version 2008/2; X-ray data Preparation and Reciprocal space
Exploration Program. Bruker AXS Inc., Madison, WI 53719-1173.

Ketone 2.152

Université de Montréal

CRYSTAL AND MOLECULAR STRUCTURE OF

C17 H26 O5 Si COMPOUND (ROBE34)

Equipe Hanessian

Département de chimie, Université de Montréal,

C.P. 6128, Succ. Centre-Ville, Montréal, Québec, H3C 3J7 (Canada)

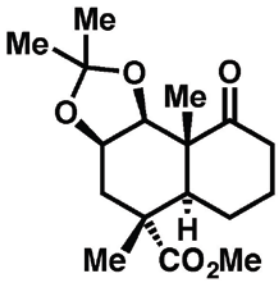

2.152

[X-ray]

Structure solved and refined in the laboratory of X-ray diffraction Université de Montréal by Robert D. Giacometti.

Table 1. Crystal data and structure refinement for C17 H26 O5 Si.

Identification code	robe341
Empirical formula	$C_{17}H_{26}O_5$
Formula weight	310.38
Temperature/K	150.15
Crystal system	monoclinic
Space group	$P2_1$
a/Å	6.4102(3)
b/Å	24.6287(10)
c/Å	10.4569(4)
α/°	90
β/°	90.594(2)
γ/°	90
Volume/Å^3	1650.79(12)
Z	4
ρ_{calc}g/cm^3	1.249
μ/mm^{-1}	0.743
F(000)	672.0
Crystal size/mm^3	0.12 × 0.05 × 0.05
Radiation	CuKα (λ = 1.54178)
2Θ range for data collection/°	7.178 to 139.626
Index ranges	$-7 \le h \le 7$, $-29 \le k \le 23$, $-12 \le l \le 12$
Reflections collected	32981
Independent reflections	5385 [R_{int} = 0.0556, R_{sigma} = 0.0388]
Data/restraints/parameters	5385/1/408
Goodness-of-fit on F^2	1.119
Final R indexes [I>=2σ (I)]	R_1 = 0.0519, wR_2 = 0.1562
Final R indexes [all data]	R_1 = 0.0538, wR_2 = 0.1588
Largest diff. peak/hole / e Å^{-3}	0.32/-0.25
Flack parameter	0.03(11)

Table 2. Fractional atomic coordinates ($\times 10^4$) and equivalent isotropic displacement parameters ($Å^2 \times 10^3$) for C17 H26 O5 Si.

U_{eq} is defined as one third of the trace of the orthogonalized Uij tensor.

Atom	x	y	z	U(eq)
O201	5731(5)	7192.7(13)	11429(3)	43.5(7)
O203	8036(5)	6096.0(13)	11111(3)	46.7(7)
O204	11292(5)	7726.9(15)	7823(3)	54.1(8)
O202	6481(6)	8069.9(14)	10938(3)	54.9(9)
O205	9352(5)	8015.5(16)	6183(3)	54.5(9)
C201	7384(7)	7159.9(18)	10532(4)	38.7(8)
C211	4581(6)	6661(2)	9195(4)	43.6(10)
C205	8297(6)	6895.6(19)	8327(4)	39.1(9)
C208	7915(8)	5731.0(19)	9006(5)	48.5(10)
C210	6941(6)	6734.0(17)	9493(4)	37.6(8)
C217	6089(7)	7389(2)	6594(4)	47(1)
C202	7614(7)	7743.3(18)	10036(4)	41.4(9)
C215	9661(6)	7728.8(18)	7264(4)	39.9(9)
C203	6692(7)	7834.2(18)	8713(4)	41.8(9)
C204	7651(6)	7447.5(18)	7704(4)	39.3(9)
C212	5842(8)	7724.1(19)	11962(4)	49.1(11)
C206	8517(7)	6442(2)	7343(4)	45.2(10)
C209	7670(6)	6177.1(18)	9980(4)	40.4(9)
C207	9361(8)	5922(2)	7935(4)	48.3(10)
C213	7448(11)	7755(3)	13040(5)	67.8(15)
C216	11130(8)	8318(2)	5735(5)	54.3(12)
C214	3706(10)	7885(2)	12399(6)	67.5(15)
O101	5840(5)	5045.1(12)	6342(3)	41.5(7)
O102	5258(5)	4171.4(12)	5769(3)	46.8(7)
O104	-6(5)	4529.9(16)	2801(3)	54.1(9)
O105	1747(5)	4322.1(14)	1035(3)	48.3(7)
O103	3303(5)	6114.2(13)	6164(3)	45.5(7)
C110	4415(6)	5520.7(17)	4469(4)	37.3(8)
C109	3666(6)	6062.2(18)	5025(4)	39.0(9)
C111	6740(7)	5605.7(19)	4148(4)	42.7(9)
C115	1565(6)	4556.4(19)	2183(4)	41.2(9)
C112	5950(7)	4501.4(18)	6809(4)	42.2(9)
C103	4647(6)	4424.3(18)	3589(4)	40.4(9)
C104	3597(6)	4827.5(18)	2633(4)	38.7(9)
C108	3374(8)	6522.5(19)	4100(4)	46.2(10)
C106	2730(7)	5840.2(19)	2363(4)	43.5(10)
C102	3915(6)	4490.1(18)	4958(4)	40.3(9)
C101	4102(6)	5075.3(17)	5479(4)	38.2(9)
C105	2989(6)	5368.8(18)	3309(4)	38.7(9)
C113	4516(9)	4433(2)	7950(5)	54.6(11)
C116	-72(8)	4045(2)	547(5)	52.2(11)
C117	5072(7)	4909(2)	1512(4)	44.8(10)
C107	1901(7)	6352.0(18)	3003(4)	45.9(10)
C114	8205(8)	4386(2)	7104(5)	53.5(11)

Table 3. Hydrogen atom coordinates ($\times 10^4$) and isotropic displacement parameters ($Å^2 \times 10^3$) for C17 H26 O5 Si.

U_{eq} is defined as one third of the trace of the orthogonalized Uij tensor.

Atom	x	y	z	U(eq)
H201	8694	7057	10999	46
H21A	4407	6448	8410	65
H21B	3931	7018	9081	65
H21C	3917	6471	9906	65
H205	9733	6955	8682	47
H20A	6533	5634	8641	58
H20B	8510	5404	9423	58
H21D	5638	7749	6309	70
H21E	4876	7181	6879	70
H21F	6755	7198	5884	70
H202	9119	7850	10047	50
H20C	6941	8215	8453	50
H20D	5165	7776	8740	50
H20E	7138	6368	6946	54
H20F	9469	6563	6659	54
H20G	10779	5986	8287	58
H20H	9457	5636	7271	58
H21G	8812	7640	12721	102
H21H	7027	7515	13739	102
H21I	7542	8129	13354	102
H21J	10705	8547	5011	81
H21K	12219	8066	5462	81
H21L	11673	8548	6428	81
H21M	3790	8232	12857	101
H21N	3157	7605	12970	101
H21O	2776	7924	11655	101
H11A	6851	5830	3377	64
H11B	7400	5253	3998	64
H11C	7444	5788	4864	64
H10A	4351	4048	3305	49
H10B	6177	4478	3568	49
H10C	4741	6630	3749	55
H10D	2782	6840	4550	55
H10E	4096	5921	1973	52
H10F	1756	5730	1669	52
H102	2443	4360	5032	48
H101	2821	5161	5978	46
H105	1572	5305	3671	46
H11D	5041	4652	8667	82
H11E	4478	4050	8202	82
H11F	3106	4553	7716	82
H11G	-514	3770	1164	78
H11H	261	3870	-267	78
H11I	-1202	4308	412	78
H11J	6324	5102	1808	67
H11K	4370	5123	845	67
H11L	5470	4555	1165	67
H10G	489	6282	3342	55
H10H	1795	6649	2367	55
H11M	9053	4481	6362	80
H11N	8378	3999	7298	80
H11O	8654	4602	7843	80

Table 4. Anisotropic displacement parameters ($Å^2$ x 10^3) for C17 H26 O5 Si.

The anisotropic displacement factor exponent takes the form:
$-2\pi^2[h^2a^{*2}U_{11} + ... + 2hka^*b^*U_{12}]$

Atom	U_{11}	U_{22}	U_{33}	U_{23}	U_{13}	U_{12}
O201	56.8(16)	34.8(16)	38.9(14)	-0.1(13)	8.9(12)	-1.7(13)
O203	58.3(17)	41.4(17)	40.5(15)	9.0(13)	-3.6(13)	0.3(14)
O204	43.5(16)	60(2)	58.2(18)	15.1(17)	-2.6(14)	-6.6(14)
O202	89(2)	33.1(17)	43.0(17)	-1.8(13)	17.7(16)	-2.9(16)
O205	51.6(17)	61(2)	50.8(18)	20.9(16)	1.2(14)	-8.7(15)
C201	47(2)	35(2)	33.8(18)	1.2(16)	2.6(15)	-0.8(16)
C211	43(2)	50(3)	37.3(19)	4.4(18)	1.4(16)	-4.7(18)
C205	40.9(18)	43(2)	33.4(18)	1.3(17)	2.1(14)	-2.3(16)
C208	58(3)	34(2)	53(3)	1(2)	8(2)	-3.4(19)
C210	41.7(19)	35(2)	36.0(18)	2.1(16)	1.6(15)	-2.6(16)
C217	47(2)	55(3)	39(2)	2.5(19)	-0.6(17)	-1.9(19)
C202	53(2)	34(2)	37(2)	-0.7(17)	6.5(16)	-3.3(18)
C215	45(2)	35(2)	39(2)	4.5(17)	5.0(16)	0.3(17)
C203	45(2)	38(2)	42(2)	4.8(18)	5.9(16)	2.4(17)
C204	40.9(19)	43(2)	34.4(18)	3.0(17)	2.8(15)	-0.7(17)
C212	72(3)	34(2)	42(2)	-1.9(18)	14(2)	-4(2)
C206	50(2)	47(3)	39(2)	-2.3(18)	4.5(17)	-4.2(19)
C209	43(2)	37(2)	41(2)	0.8(17)	2.2(15)	-4.2(17)
C207	55(2)	42(3)	49(2)	-6.1(19)	8.6(19)	0.5(19)
C213	103(4)	59(3)	42(3)	-9(2)	1(3)	-17(3)
C216	59(3)	54(3)	51(3)	15(2)	9(2)	-7(2)
C214	87(4)	44(3)	72(4)	0(3)	28(3)	4(3)
O101	56.0(16)	31.9(15)	36.6(13)	1.9(12)	-5.5(12)	-0.8(12)
O102	67.2(19)	32.3(16)	40.7(15)	-0.5(12)	-8.5(13)	0.7(13)
O104	45.9(16)	64(2)	52.5(18)	-12.8(16)	5.4(13)	-6.7(15)
O105	53.4(16)	48.9(19)	42.6(15)	-11.7(14)	-0.8(12)	-2.6(13)
O103	56.3(17)	38.9(17)	41.4(15)	-1.8(13)	5.9(12)	0.1(13)
C110	44(2)	33(2)	34.7(18)	-0.8(16)	1.6(15)	-0.4(16)
C109	43.0(19)	33(2)	41(2)	-2.3(17)	1.8(15)	-2.6(16)
C111	46(2)	44(3)	38(2)	1.2(18)	-0.9(16)	-5.4(17)
C115	45(2)	39(2)	39(2)	-2.4(17)	-1.9(16)	0.0(18)
C112	62(2)	30(2)	35(2)	1.8(16)	-2.8(17)	0.1(19)
C103	46(2)	38(2)	37(2)	-2.8(17)	-2.7(16)	3.9(17)
C104	41.7(19)	40(2)	34.1(18)	-4.7(17)	1.4(15)	0.2(17)
C108	59(3)	32(2)	47(2)	2.5(18)	-2.6(18)	-2.6(18)
C106	48(2)	42(3)	40(2)	3.9(18)	-3.2(17)	0.5(18)
C102	45.2(19)	35(2)	41(2)	-2.5(17)	1.2(16)	1.3(17)
C101	44(2)	36(2)	34.9(18)	-1.2(16)	1.7(15)	-3.0(17)
C105	39.7(18)	37(2)	38.9(19)	-2.1(17)	2.1(15)	-1.6(16)
C113	77(3)	44(3)	43(2)	4(2)	6(2)	0(2)
C116	56(3)	50(3)	51(2)	-7(2)	-9.9(19)	0(2)
C117	49(2)	50(3)	36.2(19)	-2.3(18)	3.0(17)	1.4(19)
C107	53(2)	34(2)	50(2)	1.7(18)	-6.2(18)	2.9(18)
C114	62(3)	39(3)	59(3)	3(2)	-6(2)	3(2)

Table 5. Bond lengths [Å] for C17 H26 O5 Si.

Atom	Atom	Length/Å	Atom	Atom	Length/Å
O201	C201	1.424(5)	O101	C112	1.427(5)
O201	C212	1.424(6)	O101	C101	1.429(5)
O203	C209	1.220(5)	O102	C112	1.425(5)
O204	C215	1.192(5)	O102	C102	1.435(5)
O202	C202	1.441(5)	O104	C115	1.204(5)
O202	C212	1.432(5)	O105	C115	1.338(5)
O205	C215	1.346(5)	O105	C116	1.440(6)
O205	C216	1.444(6)	O103	C109	1.223(5)
C201	C210	1.534(6)	C110	C109	1.534(6)
C201	C202	1.535(6)	C110	C111	1.546(6)
C211	C210	1.551(6)	C110	C101	1.537(6)
C205	C210	1.556(5)	C110	C105	1.557(5)
C205	C204	1.562(6)	C109	C108	1.501(6)
C205	C206	1.527(6)	C115	C104	1.533(6)
C208	C209	1.508(6)	C112	C113	1.523(6)
C208	C207	1.535(6)	C112	C114	1.502(7)
C210	C209	1.534(6)	C103	C104	1.558(6)
C217	C204	1.532(6)	C103	C102	1.520(6)
C202	C203	1.516(6)	C104	C105	1.560(6)
C215	C204	1.538(6)	C104	C117	1.527(6)
C203	C204	1.553(6)	C108	C107	1.537(6)
C212	C213	1.521(8)	C106	C105	1.533(6)
C212	C214	1.501(8)	C106	C107	1.525(7)
C206	C207	1.521(7)	C102	C101	1.545(6)

Table 6. Bond angles [Å] for C17 H26 O5 Si.

Atom	Atom	Atom	Angle/°	Atom	Atom	Atom	Angle/°
C212	O201	C201	106.0(3)	C112	O101	C101	107.5(3)
C212	O202	C202	107.9(3)	C112	O102	C102	108.6(3)
C215	O205	C216	115.7(4)	C115	O105	C116	116.4(4)
O201	C201	C210	111.8(3)	C109	C110	C111	105.7(3)
O201	C201	C202	104.1(3)	C109	C110	C101	108.4(3)
C210	C201	C202	114.7(3)	C109	C110	C105	108.7(3)
C210	C205	C204	113.7(3)	C111	C110	C105	115.0(3)
C206	C205	C210	113.4(4)	C101	C110	C111	112.3(3)
C206	C205	C204	112.4(3)	C101	C110	C105	106.5(3)
C209	C208	C207	109.8(4)	O103	C109	C110	121.6(4)
C201	C210	C211	113.2(3)	O103	C109	C108	121.7(4)
C201	C210	C205	106.2(3)	C108	C109	C110	116.7(3)
C211	C210	C205	115.0(3)	O104	C115	O105	122.7(4)
C209	C210	C201	108.8(3)	O104	C115	C104	124.9(4)
C209	C210	C211	104.8(3)	O105	C115	C104	112.4(4)
C209	C210	C205	108.5(3)	O101	C112	C113	110.1(4)
O202	C202	C201	104.5(3)	O101	C112	C114	107.0(4)
O202	C202	C203	108.7(4)	O102	C112	O101	105.1(3)
C203	C202	C201	114.1(4)	O102	C112	C113	110.4(4)
O204	C215	O205	122.3(4)	O102	C112	C114	109.9(4)
O204	C215	C204	125.8(4)	C114	C112	C113	113.9(4)
O205	C215	C204	111.8(3)	C102	C103	C104	113.7(3)
C202	C203	C204	112.1(3)	C115	C104	C103	106.2(4)
C217	C204	C205	113.7(4)	C115	C104	C105	107.2(3)
C217	C204	C215	111.0(3)	C103	C104	C105	111.2(3)
C217	C204	C203	108.2(3)	C117	C104	C115	110.7(3)
C215	C204	C205	107.3(3)	C117	C104	C103	108.0(3)
C215	C204	C203	105.4(3)	C117	C104	C105	113.3(4)
C203	C204	C205	110.8(3)	C109	C108	C107	110.3(4)
O201	C212	O202	105.5(3)	C107	C106	C105	112.2(3)
O201	C212	C213	111.5(4)	O102	C102	C103	108.0(3)
O201	C212	C214	108.7(4)	O102	C102	C101	105.0(3)
O202	C212	C213	109.2(4)	C103	C102	C101	114.1(4)
O202	C212	C214	109.8(4)	O101	C101	C110	111.4(3)
C214	C212	C213	112.0(5)	O101	C101	C102	103.4(3)
C207	C206	C205	112.2(4)	C110	C101	C102	115.7(3)
O203	C209	C208	121.0(4)	C110	C105	C104	114.3(3)
O203	C209	C210	121.5(4)	C106	C105	C110	112.3(4)
C208	C209	C210	117.4(3)	C106	C105	C104	112.4(3)
C206	C207	C208	109.9(4)	C106	C107	C108	109.8(4)

Table 7. Torsion angles [°] for C17 H26 O5 Si.

A	B	C	D	Angle/°	A	B	C	D	Angle/°
O201	C201	C210	C211	30.2(5)	O102	C102	C101	O101	11.8(4)
O201	C201	C210	C205	157.4(3)	O102	C102	C101	C110	133.8(4)
O201	C201	C210	C209	-86.0(4)	O104	C115	C104	C103	76.7(5)
O201	C201	C202	O202	15.0(4)	O104	C115	C104	C105	-42.3(6)
O201	C201	C202	C203	-103.6(4)	O104	C115	C104	C117	-166.3(5)
O204	C215	C204	C205	-38.1(6)	O105	C115	C104	C103	-100.0(4)
O204	C215	C204	C217	-162.9(5)	O105	C115	C104	C105	141.0(4)
O204	C215	C204	C203	80.1(5)	O105	C115	C104	C117	17.0(5)
O202	C202	C203	C204	-173.4(3)	O103	C109	C108	C107	-124.5(5)
O205	C215	C204	C205	145.8(4)	C110	C109	C108	C107	54.7(5)
O205	C215	C204	C217	20.9(5)	C109	C110	C101	O101	-85.8(4)
O205	C215	C204	C203	-96.1(4)	C109	C110	C101	C102	156.6(3)
C201	O201	C212	O202	35.6(5)	C109	C110	C105	C104	179.1(3)
C201	O201	C212	C213	-82.8(4)	C109	C110	C105	C106	49.6(4)
C201	O201	C212	C214	153.3(4)	C109	C108	C107	C106	-55.4(5)
C201	C210	C209	O203	16.0(5)	C111	C110	C109	O103	-107.7(4)
C201	C210	C209	C208	-164.1(4)	C111	C110	C109	C108	73.1(4)
C201	C202	C203	C204	-57.2(5)	C111	C110	C101	O101	30.6(5)
C211	C210	C209	O203	-105.4(4)	C111	C110	C101	C102	-87.0(4)
C211	C210	C209	C208	74.4(4)	C111	C110	C105	C104	60.8(5)
C205	C210	C209	O203	131.2(4)	C111	C110	C105	C106	-68.7(5)
C205	C210	C209	C208	-49.0(5)	C115	C104	C105	C110	144.8(3)
C205	C206	C207	C208	58.3(5)	C115	C104	C105	C106	-85.7(4)
C210	C201	C202	O202	137.6(4)	C112	O101	C101	C110	-152.6(3)
C210	C201	C202	C203	18.9(5)	C112	O101	C101	C102	-27.8(4)
C210	C205	C204	C217	-92.9(4)	C112	O102	C102	C103	130.4(4)
C210	C205	C204	C215	143.9(4)	C112	O102	C102	C101	8.3(4)
C210	C205	C204	C203	29.3(5)	C103	C104	C105	C110	29.1(5)
C210	C205	C206	C207	-55.2(5)	C103	C104	C105	C106	158.6(3)
C202	O202	C212	O201	-25.5(5)	C103	C102	C101	O101	-106.3(4)
C202	O202	C212	C213	94.4(5)	C103	C102	C101	C110	15.8(5)
C202	O202	C212	C214	-142.4(4)	C104	C103	C102	O102	-169.5(3)
C202	C201	C210	C211	-88.1(4)	C104	C103	C102	C101	-53.2(5)
C202	C201	C210	C205	39.1(5)	C102	O102	C112	O101	-25.5(4)
C202	C201	C210	C209	155.7(3)	C102	O102	C112	C113	93.2(4)
C202	C203	C204	C205	30.9(5)	C102	O102	C112	C114	-140.3(4)
C202	C203	C204	C217	156.3(4)	C102	C103	C104	C115	-87.0(4)
C202	C203	C204	C215	-84.9(4)	C102	C103	C104	C105	29.3(5)
C204	C205	C210	C201	-65.5(4)	C102	C103	C104	C117	154.2(4)
C204	C205	C210	C211	60.6(5)	C101	O101	C112	O102	33.8(4)
C204	C205	C210	C209	177.7(3)	C101	O101	C112	C113	-85.2(4)
C204	C205	C206	C207	174.1(4)	C101	O101	C112	C114	150.6(4)
C212	O201	C201	C210	-155.3(4)	C101	C110	C109	O103	12.9(5)
C212	O201	C201	C202	-30.9(4)	C101	C110	C109	C108	-166.3(3)
C212	O202	C202	C201	6.2(5)	C101	C110	C105	C104	-64.2(4)
C212	O202	C202	C203	128.5(4)	C101	C110	C105	C106	166.3(3)
C206	C205	C210	C201	164.5(4)	C105	C110	C109	O103	128.3(4)
C206	C205	C210	C211	-69.4(5)	C105	C110	C109	C108	-50.9(5)
C206	C205	C210	C209	47.6(4)	C105	C110	C101	O101	157.3(3)
C206	C205	C204	C217	37.7(5)	C105	C110	C101	C102	39.7(4)
C206	C205	C204	C215	-85.5(4)	C105	C106	C107	C108	57.8(5)
C206	C205	C204	C203	159.9(3)	C116	O105	C115	O104	1.7(7)
C209	C208	C207	C206	-56.1(5)	C116	O105	C115	C104	178.5(4)
C207	C208	C209	O203	-125.8(4)	C117	C104	C105	C110	-92.8(4)
C207	C208	C209	C210	54.3(5)	C117	C104	C105	C106	36.7(5)
C216	O205	C215	O204	0.4(7)	C107	C106	C105	C110	-55.9(5)
C216	O205	C215	C204	176.8(4)	C107	C106	C105	C104	173.6(3)

Experimental

Single crystals of $C_{17}H_{26}O_5Si$ [ROBE34] were obtained by slow recrystallized from diethyl ether-hexanes. A suitable crystal was selected and mounted on a loop fiber on a Bruker APEX-II CCD diffractometer. The crystal was kept at 150 K during data collection. Using Olex2 [1], the structure was solved with the XT [2] structure solution program using Direct Methods and refined with the ShelXL [2] refinement package using Least Squares minimization.

1. Dolomanov, O.V., Bourhis, L.J., Gildea, R.J, Howard, J.A.K. & Puschmann, H. (2009), J. Appl. Cryst. 42, 339-341.
2. Sheldrick, G.M. (2008). Acta Cryst. A64, 112-122.
3. APEX2 (2008), Bruker AXS Inc., Madison, WI 53719-1173.
4. SAINT (2013) V8.34A, Bruker AXS Inc., Madison, WI 53719-1173.
5. XPREP (2013); X-ray data Preparation and Reciprocal space Exploration Program. Bruker AXS Inc., Madison, WI 53719-1173.

Crystal structure determination of $C_{17}H_{26}O_5Si$ (ROBE34):

Crystal Data for $C_{17}H_{26}O_5Si$ (M =310.38 g/mol): monoclinic, space group $P2_1$ (no. 4), a = 6.4102(3) Å, b = 24.6287(10) Å, c = 10.4569(4) Å, β = 90.594(2)°, V = 1650.79(12) Å^3, Z = 4, T = 150.15 K, μ(CuKα) = 0.743 mm^{-1}, $Dcalc$ = 1.249 g/cm^3, 32981 reflections measured (7.178° ≤ 2Θ ≤ 139.626°), 5385 unique (R_{int} = 0.0556, R_{sigma} = 0.0388) which were used in all calculations. The final R_1 was 0.0519 (I > 2σ(I)) and wR_2 was 0.1588 (all data).

Refinement model description

Number of restraints - 1, number of constraints - unknown.
Details:
1. Fixed Uiso
 At 1.2 times of:
  All C(H) groups, All C(H,H) groups
 At 1.5 times of:
  All C(H,H,H) groups
2.a Ternary CH refined with riding coordinates:
 C201(H201), C205(H205), C202(H202), C102(H102), C101(H101), C105(H105)
2.b Secondary CH2 refined with riding coordinates:
 C208(H20A,H20B), C203(H20C,H20D), C206(H20E,H20F), C207(H20G,H20H), C103(H10A, H10B), C108(H10C,H10D), C106(H10E,H10F), C107(H10G,H10H)
2.c Idealised Me refined as rotating group:
 C211(H21A,H21B,H21C), C217(H21D,H21E,H21F), C213(H21G,H21H,H21I), C216(H21J, H21K,H21L), C214(H21M,H21N,H21O), C111(H11A,H11B,H11C), C113(H11D,H11E,H11F), C116(H11G,H11H,H11I), C117(H11J,H11K,H11L), C114(H11M,H11N,H11O)

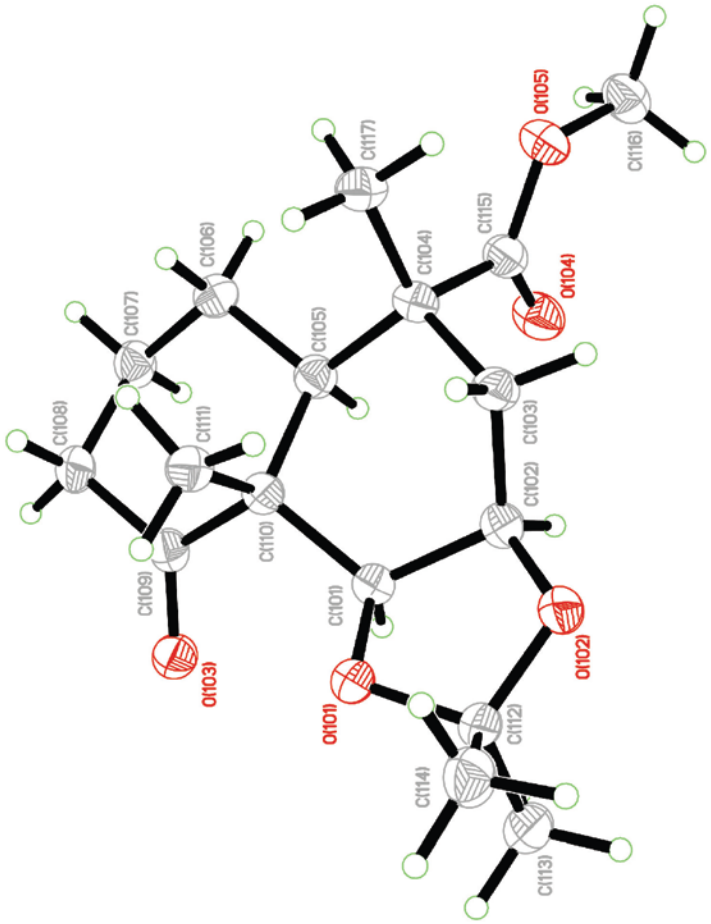

ORTEP view of the C17 H26 O5 Si compound with the numbering scheme adopted. Ellipsoids are drawn at the 30% probability level. Hydrogen atoms are represented by spheres of arbitrary size.

Diol 2.170

Université de Montréal

CRYSTAL AND MOLECULAR STRUCTURE OF

C14 H24 O4 COMPOUND (ROBE43)

Equipe Hanessian

Département de chimie, Université de Montréal,

C.P. 6128, Succ. Centre-Ville, Montréal, Québec, H3C 3J7 (Canada)

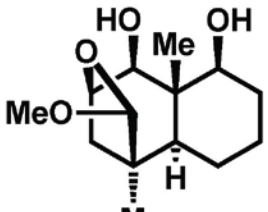

2.170

[X-ray]

Structure solved and refined in the laboratory of X-ray diffraction Université de Montréal by Robert D. Giacometti.

Table 1. Crystal data and structure refinement for C14 H24 O4 Si.

Identification code	robe431
Empirical formula	$C_{14}H_{24}O_4$
Formula weight	256.33
Temperature/K	100.15
Crystal system	orthorhombic
Space group	$P2_12_12_1$
a/Å	6.1688(3)
b/Å	8.6662(4)
c/Å	24.1819(14)
α/°	90
β/°	90
γ/°	90
Volume/Å^3	1292.77(11)
Z	4
ρ_{calc}g/cm^3	1.317
μ/mm^{-1}	0.771
F(000)	560.0
Crystal size/mm^3	0.14 × 0.08 × 0.03
Radiation	CuKα (λ = 1.54178)
2Θ range for data collection/°	7.312 to 141.782
Index ranges	$-7 \leq h \leq 7$, $-10 \leq k \leq 10$, $-29 \leq l \leq 28$
Reflections collected	7744
Independent reflections	2373 [R_{int} = 0.0278, R_{sigma} = 0.0283]
Data/restraints/parameters	2373/0/168
Goodness-of-fit on F^2	1.018
Final R indexes [I>=2σ (I)]	R_1 = 0.0369, wR_2 = 0.0920
Final R indexes [all data]	R_1 = 0.0419, wR_2 = 0.0954
Largest diff. peak/hole / e Å^{-3}	0.19/-0.24
Flack parameter	0.05(8)

Table 2. Fractional atomic coordinates ($\times 10^4$) and equivalent isotropic displacement parameters ($Å^2 \times 10^3$) for C14 H24 O4.

U_{eq} is defined as one third of the trace of the orthogonalized Uij tensor.

Atom	x	y	z	U(eq)
O1	3609(3)	6838.9(19)	2575.0(7)	22.6(4)
O2	4203(3)	5104.7(19)	1509.1(7)	20.9(4)
O3	3756(3)	4185(2)	610.4(7)	22.6(4)
O4	2588(3)	10004.6(19)	2497.6(7)	21.0(4)
C1	2169(4)	6878(3)	2109.7(10)	17.4(5)
C2	2212(4)	5306(3)	1822.9(10)	19.2(5)
C3	459(4)	5227(3)	1383.3(10)	18.4(5)
C4	1529(4)	6241(3)	936.8(10)	17.2(5)
C5	1409(4)	7933(3)	1160.5(10)	17.0(5)
C6	1790(4)	9253(3)	749.4(10)	21.0(5)
C7	1007(4)	10778(3)	1005.7(10)	23.2(5)
C8	1996(4)	11088(3)	1575(1)	22.6(5)
C9	1729(4)	9717(3)	1957.7(10)	18.1(5)
C10	2687(4)	8217(3)	1706.9(9)	16.4(5)
C11	5166(4)	8426(3)	1635.2(10)	20.2(5)
C12	3805(4)	5512(3)	948.7(10)	19.4(5)
C13	5739(4)	3344(3)	615.7(12)	26.5(5)
C14	457(4)	6107(3)	372(1)	22.1(5)

Table 3. Hydrogen atom coordinates ($\times 10^4$) and isotropic displacement parameters ($Å^2 \times 10^3$) for C14 H24 O4.

U_{eq} is defined as one third of the trace of the orthogonalized Uij tensor.

Atom	x	y	z	U(eq)
O1	28.9(10)	17.8(8)	21.2(8)	-0.5(7)
O2	18.6(8)	19.1(8)	25.0(9)	-3.1(7)
O3	20.6(8)	18.7(8)	28.4(9)	-7.1(7)
O4	22.2(8)	19.4(8)	21.5(8)	-3.3(7)
C1	16.6(11)	15.4(10)	20.3(11)	0.7(9)
C2	20.1(12)	16.5(11)	21.1(11)	1.3(9)
C3	16.6(10)	14.3(10)	24.2(12)	0.1(9)
C4	16.2(11)	14.5(10)	20.9(11)	-0.5(9)
C5	16.2(11)	14.7(10)	20.2(11)	-1.1(9)
C6	26.5(12)	17.6(11)	18.9(11)	0.5(10)
C7	29.6(13)	16.4(11)	23.7(12)	4.1(10)
C8	27.4(12)	14.8(10)	25.7(12)	-1.7(10)
C9	17.8(10)	16.6(11)	20(1)	-1.3(9)
C10	14.8(10)	15.1(10)	19.2(11)	-0.3(9)
C11	17.2(11)	18.1(11)	25.2(12)	-2.6(9)
C12	19.6(11)	15.3(10)	23.4(11)	-3.0(9)
C13	23.9(13)	20.6(11)	34.9(13)	-6.0(11)
C14	24.3(12)	18.9(11)	23.1(12)	-0.7(10)

Table 4. Anisotropic displacement parameters ($Å^2$ x 10^3) for C14 H24 O4.

The anisotropic displacement factor exponent takes the form:
$-2\pi^2[h^2a^{*2}U_{11} + ... + 2hka^*b^*U_{12}]$

Atom	U_{11}	U_{22}	U_{33}	U_{23}	U_{13}	U_{12}
O1	28.9(10)	17.8(8)	21.2(8)	-0.5(7)	-4.9(7)	3.1(7)
O2	18.6(8)	19.1(8)	25.0(9)	-3.1(7)	-2.8(7)	5.0(7)
O3	20.6(8)	18.7(8)	28.4(9)	-7.1(7)	0.6(7)	0.6(7)
O4	22.2(8)	19.4(8)	21.5(8)	-3.3(7)	-1.5(7)	-1.8(7)
C1	16.6(11)	15.4(10)	20.3(11)	0.7(9)	-1.4(9)	1.8(9)
C2	20.1(12)	16.5(11)	21.1(11)	1.3(9)	-0.6(9)	0.2(9)
C3	16.6(10)	14.3(10)	24.2(12)	0.1(9)	-0.3(9)	-0.7(9)
C4	16.2(11)	14.5(10)	20.9(11)	-0.5(9)	-1.6(9)	-1.5(9)
C5	16.2(11)	14.7(10)	20.2(11)	-1.1(9)	-0.7(9)	-0.1(9)
C6	26.5(12)	17.6(11)	18.9(11)	0.5(10)	-1.3(9)	-2.5(9)
C7	29.6(13)	16.4(11)	23.7(12)	4.1(10)	-2.3(11)	0.7(10)
C8	27.4(12)	14.8(10)	25.7(12)	-1.7(10)	-0.1(10)	0.2(10)
C9	17.8(10)	16.6(11)	20(1)	-1.3(9)	0.8(9)	1.8(9)
C10	14.8(10)	15.1(10)	19.2(11)	-0.3(9)	0.8(9)	0.0(8)
C11	17.2(11)	18.1(11)	25.2(12)	-2.6(9)	-0.1(10)	-2.5(9)
C12	19.6(11)	15.3(10)	23.4(11)	-3.0(9)	1.1(9)	-2.4(9)
C13	23.9(13)	20.6(11)	34.9(13)	-6.0(11)	5.7(11)	2.7(10)
C14	24.3(12)	18.9(11)	23.1(12)	-0.7(10)	-2.3(10)	-1.5(10)

Table 5. Bond lengths [Å] for C14 H24 O4.

Atom	Atom	Length/Å	Atom	Atom	Length/Å
O1	C1	1.434(3)	C4	C5	1.565(3)
O2	C2	1.454(3)	C4	C12	1.540(3)
O2	C12	1.422(3)	C4	C14	1.522(3)
O3	C12	1.412(3)	C5	C6	1.533(3)
O3	C13	1.424(3)	C5	C10	1.558(3)
O4	C9	1.431(3)	C6	C7	1.538(3)
C1	C2	1.529(3)	C7	C8	1.529(3)
C1	C10	1.549(3)	C8	C9	1.515(3)
C2	C3	1.518(3)	C9	C10	1.551(3)
C3	C4	1.541(3)	C10	C11	1.549(3)

Table 6. Bond angles [Å] for C14 H24 O4.

Atom	Atom	Atom	Angle/°	Atom	Atom	Atom	Angle/°
C12	O2	C2	108.78(17)	C10	C5	C4	114.66(18)
C12	O3	C13	113.18(19)	C5	C6	C7	109.36(19)
O1	C1	C2	108.90(18)	C8	C7	C6	112.84(19)
O1	C1	C10	112.53(19)	C9	C8	C7	111.64(19)
C2	C1	C10	112.28(18)	O4	C9	C8	112.35(19)
O2	C2	C1	110.99(18)	O4	C9	C10	111.20(18)
O2	C2	C3	103.34(18)	C8	C9	C10	112.14(19)
C3	C2	C1	110.20(18)	C1	C10	C5	108.08(18)
C2	C3	C4	99.19(18)	C1	C10	C9	107.66(17)
C3	C4	C5	105.80(19)	C1	C10	C11	111.19(19)
C12	C4	C3	98.26(17)	C9	C10	C5	105.73(18)
C12	C4	C5	114.88(18)	C11	C10	C5	115.01(19)
C14	C4	C3	113.54(19)	C11	C10	C9	108.80(19)
C14	C4	C5	111.18(18)	O2	C12	C4	106.09(19)
C14	C4	C12	112.4(2)	O3	C12	O2	110.70(18)
C6	C5	C4	117.87(19)	O3	C12	C4	107.68(18)
C6	C5	C10	110.76(18)				

Table 7. Bond lengths [Å] and angles [°] related to the hydrogen bonding for C14 H24 O4.

D	H	A	d(D-H)/Å	d(H-A)/Å	d(D-A)/Å	D-H-A/°
O1	H1	O4	0.84	2.15	2.821(2)	136.1
O4	H4	O1 #1	0.84	2.00	2.839(2)	177.3

Symmetry transformations used to generate equivalent atoms:

#1 1-x,1/2+y,1/2-z

Table 8. Torsion angles [°] for C14 H24 O4.

A	B	C	D	Angle/°	A	B	C	D	Angle/°
O1	C1	C2	O2	-74.7(2)	C5	C4	C12	O2	76.4(2)
O1	C1	C2	C3	171.40(19)	C5	C4	C12	O3	-165.04(18)
O1	C1	C10	C5	167.17(18)	C5	C6	C7	C8	53.2(3)
O1	C1	C10	C9	-79.1(2)	C6	C5	C10	C1	178.04(19)
O1	C1	C10	C11	40.0(3)	C6	C5	C10	C9	63.0(2)
O2	C2	C3	C4	-43.6(2)	C6	C5	C10	C11	-57.1(3)
O4	C9	C10	C1	57.6(2)	C6	C7	C8	C9	-51.2(3)
O4	C9	C10	C5	172.92(18)	C7	C8	C9	O4	-178.23(19)
O4	C9	C10	C11	-63.0(2)	C7	C8	C9	C10	55.7(3)
C1	C2	C3	C4	75.1(2)	C8	C9	C10	C1	-175.7(2)
C2	O2	C12	O3	-107.6(2)	C8	C9	C10	C5	-60.3(2)
C2	O2	C12	C4	8.9(2)	C8	C9	C10	C11	63.7(3)
C2	C1	C10	C5	43.9(2)	C10	C1	C2	O2	50.6(2)
C2	C1	C10	C9	157.65(19)	C10	C1	C2	C3	-63.3(2)
C2	C1	C10	C11	-83.3(2)	C10	C5	C6	C7	-60.4(2)
C2	C3	C4	C5	-72.0(2)	C12	O2	C2	C1	-96.0(2)
C2	C3	C4	C12	46.9(2)	C12	O2	C2	C3	22.1(2)
C2	C3	C4	C14	165.85(19)	C12	C4	C5	C6	88.7(2)
C3	C4	C5	C6	-164.1(2)	C12	C4	C5	C10	-44.5(3)
C3	C4	C5	C10	62.7(2)	C13	O3	C12	O2	-60.5(3)
C3	C4	C12	O2	-35.3(2)	C13	O3	C12	C4	-176.08(19)
C3	C4	C12	O3	83.2(2)	C14	C4	C5	C6	-40.4(3)
C4	C5	C6	C7	164.8(2)	C14	C4	C5	C10	-173.61(19)
C4	C5	C10	C1	-45.6(2)	C14	C4	C12	O2	-155.12(19)
C4	C5	C10	C9	-160.61(18)	C14	C4	C12	O3	-36.6(3)
C4	C5	C10	C11	79.3(2)					

Experimental

Single crystals of $C_{14}H_{24}O_4$ [ROBE43] were obtained by slow recrystallized from diethyl ether-hexanes. A suitable crystal was selected and mounted on a loop fiber on a Bruker APEX-II CCD diffractometer. The crystal was kept at 100 K during data collection. Using Olex2 [1], the structure was solved with the XT [2] structure solution program using Direct Methods and refined with the ShelXL [2] refinement package using Least Squares minimization.

1. Dolomanov, O.V., Bourhis, L.J., Gildea, R.J, Howard, J.A.K. & Puschmann, H. (2009), J. Appl. Cryst. 42, 339-341.
2. Sheldrick, G.M. (2008). Acta Cryst. A64, 112-122.
3. APEX2 (2008), Bruker AXS Inc., Madison, WI 53719-1173.
4. SAINT (2013) V8.34A, Bruker AXS Inc., Madison, WI 53719-1173.
5. XPREP (2013); X-ray data Preparation and Reciprocal space Exploration Program. Bruker AXS Inc., Madison, WI 53719-1173.

Crystal structure determination of $C_{14}H_{24}O_4$ (ROBE43):

Crystal Data for $C_{14}H_{24}O_4$ (M =256.33 g/mol): orthorhombic, space group $P2_12_12_1$ (no. 19), a = 6.1688(3) Å, b = 8.6662(4) Å, c = 24.1819(14) Å, V = 1292.77(11) Å^3, Z = 4, T = 100.15 K, μ(CuKα) = 0.771 mm^{-1}, $Dcalc$ = 1.317 g/cm^3, 7744 reflections measured (7.312° ≤ 2Θ ≤ 141.782°), 2373 unique (R_{int} = 0.0278, R_{sigma} = 0.0283) which were used in all calculations. The final R_1 was 0.0369 (I > 2σ(I)) and wR_2 was 0.0954 (all data).

Refinement model description

Number of restraints - 0, number of constraints - unknown.
Details:
1. Fixed Uiso
 At 1.2 times of:
  All C(H) groups, All C(H,H) groups
 At 1.5 times of:
  All C(H,H,H) groups, All O(H) groups
2.a Ternary CH refined with riding coordinates:
 C1(H1A), C2(H2), C5(H5), C9(H9), C12(H12)
2.b Secondary CH2 refined with riding coordinates:
 C3(H3A,H3B), C6(H6A,H6B), C7(H7A,H7B), C8(H8A,H8B)
2.c Idealised Me refined as rotating group:
 C11(H11A,H11B,H11C), C13(H13A,H13B,H13C), C14(H14A,H14B,H14C)
2.d Idealised tetrahedral OH refined as rotating group:
 O1(H1), O4(H4)

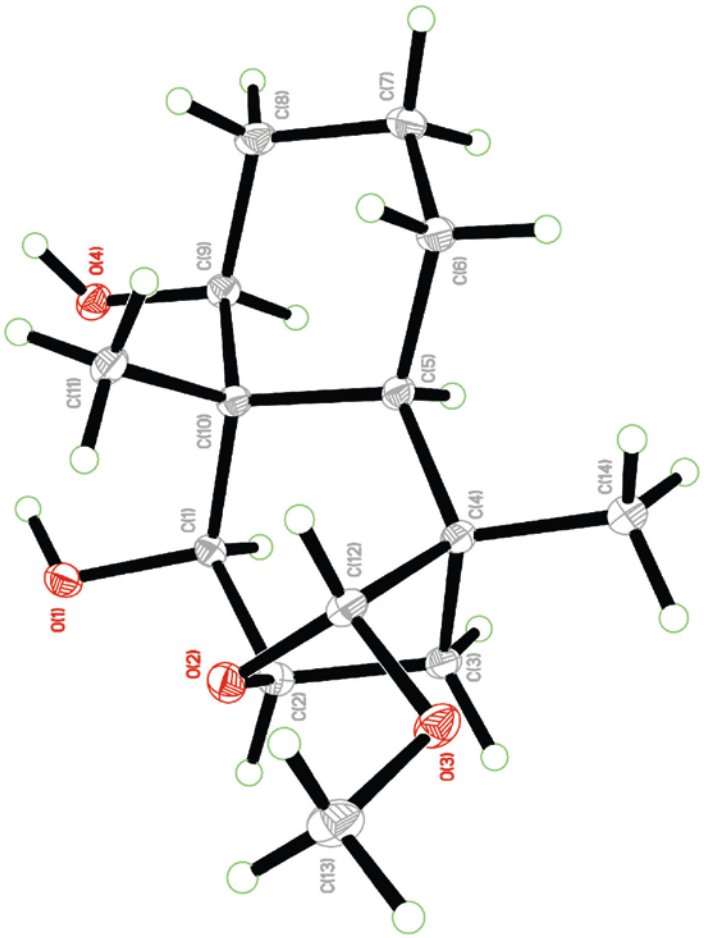

ORTEP view of the C14 H24 O4 compound with the numbering scheme adopted. Ellipsoids are drawn at the 30% probability level. Hydrogen atoms are represented by spheres of arbitrary size.